# Critically derived human neural stem cell line as a potential tool for neuropsychiatric drug discovery

Anderson, Gregory William

*Awarding institution:*
King's College London

# Cortically Derived Human Neural Stem Cell Line as a Potential Tool for Neuropsychiatric Drug Discovery

**Gregory William Anderson**

Institute of Psychiatry, King's College London

Thesis submitted for the degree of PhD

2012

## *Abstract*

Early drug discovery for new psychiatric medicines relies heavily on the use of *in vitro* assays. At present, this work is typically conducted through ectopic expression of human proteins of interest in cells that are often neither human nor neural in origin. As our appreciation of the complexity inherent to receptor pharmacology has increased, these heterologous expression systems have come under increasing scrutiny as a means to evaluate the mode of action of novel neuropsychiatric drug candidates. These limitations likely contribute to the high attrition rate observed as these compounds progress to the clinic. The use of native human neural cells during initial drug development has the potential to overcome some of these problems.

This thesis describes work towards the development of an *in vitro* drug discovery platform using a human, conditionally immortalised, cortically derived, neural stem cell line (CTX0E16/02). Protocols were developed to enable robust and reproducible differentiation of these human neural stem cells into cell-types normally found in the adult cerebral cortex – different GABAergic neuronal subtypes, glutamatergic neurons, astrocytes and potentially oligodendrocytes. Neurons grown under these conditions were also shown to be electrically active. By investigating ligand-induced $Ca^{2+}$ and Erk1/2 signalling, cells within differentiated cortical cultures were shown to express functional receptors, for a range of neurotransmitters, including dopamine, serotonin, glutamate, GABA, histamine, norepinephrine and acetylcholine. Many of these receptors are known targets of currently available neuropsychiatric compounds, making this platform ideal for studying drugs that modulate the activity of the human brain.

Data presented here highlighted the importance of using native neural cells to interrogate the signalling consequences of ligand-receptor interactions. For instance, the reported full 5-$HT_{2A}$-specific agonist – TCB-2 – was shown to demonstrate inverse agonism with respect to intracellular $Ca^{2+}$ accumulation, while cholinergic stimulation was shown to provoke muscarinic receptor-mediated $Ca^{2+}$ influx rather than an expected mobilisation from intracellular stores. Most importantly, however, effects of a therapeutically relevant concentration of the antipsychotic, haloperidol, could be detected using these differentiated CTX0E16/02 cultures. However, this effect was only apparent in the presence of simulated neurophysiological tone. This finding has important implications regarding the way in which the mechanism of action of complex drug-receptor interactions is experimentally investigated *in vitro*.

## *Acknowledgements*

I would sincerely like to thanks – above all – Brenda Williams, without whom none of this would have ever happened and for seemingly allowing me to do whatever I pleased. I've begun to wonder however if this is where her true skill as a supervisor lies – making me think that it was my idea! A big thank you and an apology to Maria Arranz for trying my upmost to do as little genetics as I could possibly manage during this process. I have both of you to thank for giving me this opportunity in the first place, and for this I am eternally grateful! My wife, Babouche, has probably suffered more as a result of this process than anyone. You've been amazing, I love you! A huge thank you to Colin – my work buddy, fry up buddy and personal psychiatrist. I really don't think you appreciate what an incredible support you've been to me over the last few years and really feel I've made a life-long friend, these are so rare. Enormous thanks have to go to David and Stuart at the Wolfon CARD, I think you thought I'd only stick around for a couple of weeks, but you were too helpful and I was compelled to stay! Big thanks too, to my past and current office chums, Zahra, Matt, Lotta, Sophie and Shanas – you've put up with me all this time, congratulations! There are so many more people to thank and I've only left a single page, but here goes: Nick, Dafe, Jon, Steve, Jack, Greame, Andrew, Ed, Doris, Hairy Matt, Angela, Chiara, Ivan, Aaron, Anthony, Leo, Gehan, Saga, Sybille, Sarah, Sandrine – all have helped in some way, shape or form.

I would very much like to thank the Medical Research Council, for funding the research described here and additionally for honouring the contribution of the CASE award partner following their withdrawal.

I'd like to dedicate this thesis to my parents Rotraut and John Anderson – I hope this redeems me after a bit of an uncertain start to my adult life!

## *Table of Contents*


*Abstract* ..... 2

*Acknowledgements* ..... 3

*Table of Contents* ..... 4

*Table of Figures* ..... 8

*Table of Tables* ..... 12

*Abbreviations* ..... 13

*Chapter 1 Introduction* ..... 15

*1.1 Studying the Human Brain* ..... 15

*1.2 ES cells, Neural Stem and Progenitor Cells* ..... 19

*1.3 Induced Pluripotent Stem Cells* ..... 21

*1.4 Induced Neuronal Cells* ..... 23

*1.5 Exploiting the Potential of Pluripotent & Transdifferentiated Cells* ..... 25

*1.6 What's the Problem?* ..... 27

*1.6.1 Schizophrenia* ..... 27

*1.6.2 Antipsychotics* ..... 30

*1.7 G Protein-Coupled Receptors & Antipsychotics* ..... 33

*1.7.1 GPCR Regulation* ..... 35

*1.7.2 Functional Selectivity* ..... 36

*1.7.3 Allosterism* ..... 37

*1.7.4 Receptor Dimerisation* ..... 37

*1.7.5 It's All in the Assay* ..... 39

*1.8 Transcriptomics & Drug Mechanism* ..... 42

*1.9 Pharmacogenetics & Pharmacogenomics* ..... 47

*1.10 Further Applications* ..... 51

*1.11 Aims & Objectives* ..... 52

*Chapter 2 Materials & Methods* ..... 53

*2.1 Cell Culture* ..... 53

*2.1.1 Neural Progenitor Cell Lines* ..... 53

*2.1.2 Neural Progenitor Cell Maintenance* ..... 53

*2.1.3 Neural Progenitor Cell Differentiation* ..... 54

*2.1.4 Primary Neural Stem Cell Culture* ..... 55

*2.2 Immunocytochemistry* ..... 56

*2.2.1 Microscopy* ..... 58

*2.2.2 Cell Counting* ..... 59

*2.3 Gene Expression* ..... 59

2.3.1 Cell Lysis ..... 59
2.3.2 RNA Extraction ..... 60
2.3.3 DNase Treatment of Total RNA ..... 60
2.3.4 First Strand cDNA Synthesis ..... 60
2.3.5 RT-PCR Primer Design ..... 61
2.3.6 Polymerase Chain Reaction (PCR) ..... 61
2.3.7 Polyacrylamide Gel Electrophoresis ..... 61
2.4 Ligand-Induced Pharmacology ..... 62
2.4.1 $Ca^{2+}$ Release Assay ..... 62
2.4.2 $Ca^{2+}$ Release Assay Data Analysis ..... 64
2.4.3 Single Cell $Ca^{2+}$ Imaging ..... 64
2.4.4 Single Cell $Ca^{2+}$ Imaging Data Analysis ..... 65
2.4.5 ERK1/2 Phosphorylayion Assay ..... 65
2.4.6 ERK1/2 Phosphorylayion Assay Data Analysis ..... 67
2.5 Experimental Design ..... 67
Chapter 3 Human NPC Lines Exhibit Divergent Characteristics ..... 68
3.1 Introduction ..... 68
3.2 Results ..... 70
3.2.1 Cortically-Derived Human NPC Lines Demonstrate Robust Differentiation ..... 70
3.2.2 CTX0E03/02 Cells Differentiate into Isolated Clusters of Neurons & Astrocytes ..... 79
3.2.3 CTX0E16/02 Cells Differentiate into Even Monolayer of Neurons & Astrocytes ..... 88
3.2.4 Expression Profile of Proliferative & Differentiated NPC Lines ..... 94
3.2.5 Differentiated Cortical NPC Lines Exhibit Broad Receptor Expression Profile ..... 104
3.2.6 Differentiation & Expression Data Summary ..... 113
Chapter 4 Characterisation of Differentiated CTX0E16/02 Cultures ..... 116
4.1 Introduction ..... 116
4.2 Results ..... 121
4.2.1 Differentiated CTX0E16/02 Cultures Generate Glutamatergic & GABAergic Neurons ..... 121
4.2.2 CTX0E16/02 NPCs Express Functional Neurotransmitter Receptors ..... 125
4.2.3 Differentiated CTX0E16/02 Cultures Demonstrate Attenuated Responses ..... 130
4.2.4 Heterogeneous Ligand-Induced Responses in Proliferative & Differentiated Cultures ..... 133
4.2.5 Promoting Electrical Excitability – Neurosphere Expansion ..... 150
4.2.6 Promoting Electrical Excitability – Increasing PI3K Activity ..... 155
4.2.7 Promoting Electrical Excitability – Influence of Neurotrophic Factors ..... 157
4.2.8 Promoting Electrical Excitability – Is It Just A Waiting Game? ..... 160
4.2.9 Promoting Electrical Excitability – Do We Have To Wait So Long? ..... 164
4.2.10 Promoting Electrical Excitability – Summary ..... 165
4.2.11 Increasing Receptor Expression – Stimulating PKA Activity ..... 168
4.2.12 Increasing Receptor Expression – Use It Or Lose It? ..... 172

*4.2.13 Exploring the Effect of Extended Time in Culture ..... 176*
*4.2.14 Summary ..... 181*
*Chapter 5 Comparison of CTX0E16/02 to Primary NSC Cultures ..... 184*
*5.1 Introduction ..... 184*
*5.2 Results ..... 186*
*5.2.1 Primary Cultures Contain a High Proportion of Neurons ..... 188*
*5.2.2 Primary Cultures Demonstrate Comparable Gene Expression to CTX0E16/02 Cells ..... 189*
*5.2.3 Maintaining Primary Cells in Adherent Culture Alters Ligand-Induced $Ca^{2+}$ Responses ... 193*
*5.2.4 Passaging Number Prior to Differentiation Effects Ligand-Induced $Ca^{2+}$ Responses ..... 196*
*5.2.5 Primary Foetal Neural Cell Cultures Are Electrical Excitable ..... 200*
*5.2.6 Summary ..... 205*
*Chapter 6 Pharmacological Validation & Increasing Assay Sensitivity ..... 212*
*6.1 Introduction ..... 212*
*6.2 Results ..... 214*
*6.2.1 Dopamine-Induced $Ca^{2+}$ Responses in CTX0E16/02 Cultures Prove Difficult to Resolve ... 215*
*6.2.2 5-$HT_{2A}$ Agonist Behaves as Inverse Agonist in Differentiated CTX0E16/02 Cultures ..... 220*
*6.2.3 Acetylcholine Provokes $Ca^{2+}$ Influx Through Metabotropic Receptors ..... 222*
*6.2.4 ERK1/2 Phosphorylation Assay Optimisation ..... 226*
*6.2.5 Dopamine's Complex Pharmacology Is Reflected In ERK1/2 Phosphorylation Profile ..... 231*
*6.2.6 Differentiated CTX0E16/02 Cultures Demonstrate ERK1/2 Phosphorylation In Response To 5-HT, Acetylcholine, Phenylephrine & Histamine ..... 232*
*6.2.7 Haloperidol Behaves As An Inverse-Agonist In Differentiated CTX0E16/02 Cultures ..... 236*
*6.2.8 Differentiated CTX0E16/02 Cultures Express Functional $D_1$, $D_2$ & 5-$HT_{2A}$ Receptors ..... 240*
*6.2.9 Important Considerations for Future Transcriptomic Experiments ..... 244*
*6.2.10 Summary ..... 248*
*Chapter 7 Discussion ..... 253*
*7.1.1 Summary of Discovery for CTX0E16/02 Cells ..... 268*
*7.1.2 Limitations of Methods ..... 268*
*References ..... 270*
*Appendices ..... 300*
*8.1 Media ..... 300*
*8.1.1 Reduced Modified Medium (RMM) ..... 300*
*8.1.2 Human Medium (HM) ..... 300*
*8.1.3 B27 Medium (B27M) ..... 300*
*8.1.4 Supplemented Neurobasal Medium (SNBM) ..... 300*
*8.2 Primers ..... 301*
*8.3 Solutions & Buffers ..... 302*
*8.3.1 $Ca^{2+}$ Release Assay Buffer ..... 302*

*8.3.2 $Ca^{2+}$ Release Loading Buffer ..... 302*

*8.4 Test Compounds ..... 302*

*8.5 Supplementary Data ..... 303*

*8.5.1 Additional Data for Long-Term Continuously Passaged Cultures ..... 303*

*8.6 Supplementary Information ..... 308*

*8.6.1 Personal Communication From Hugo Geerts ..... 308*

## *Table of Figures*

*Figure 1.1 Antipsychotic drugs target various receptors with high affinity ..... 34*

*Figure 2.1 Time course of typical $Ca^{2+}$ release assay experiment ..... 63*

*Figure 2.2 Illustrative diagram of phosphorylated ERK1/2 detection using the Cellul'erk Kit ..... 66*

*Figure 3.1 CTX0E16/02 cells demonstrate robust differentiation into neurons and astrocytes ..... 76*

*Figure 3.2 Bright field images of confluent CTX0E03/02 and CTX0E16/02 cells in proliferative culture 79*

*Figure 3.3 CTX0E03/02 cultures differentiated with RMM supplemented with 1 µM purmorphamine 81*

*Figure 3.4 CTX0E03/02 cultures differentiated in the presence of SNBM ..... 82*

*Figure 3.5 CTX0E03/02 cells readily differentiate into neurons in the presence of SNBM and purmorphamine..... 83*

*Figure 3.6 CTX0E03/02 cells differentiated in the presence of SNBM supplemented with 1 µM purmorphamine..... 84*

*Figure 3.7 Image stack of CTX0E03/02 cells following 28 days of differentiation using SNBM ..... 85*

*Figure 3.8 Flattened stack of CTX0E03/02 cells following 28 day differentiation using SNBM ..... 86*

*Figure 3.9 Image stack of CTX0E03/02 cells following 28 day differentiation using SNBM with purmorphamine..... 87*

*Figure 3.10 Flattened stack of CTX0E03/02 cells following 28 day differentiation in SNBM and purmorphamine..... 88*

*Figure 3.11 CTX0E16/02 cells differentiated in the presence of RMM supplemented with 1 µM purmorphamine..... 89*

*Figure 3.12 CTX0E16/02 cells readily differentiate into neurons in the presence of SNBM ..... 90*

*Figure 3.13 CTX0E16/02 cells differentiate into GABAergic neurons in the presence of SNBM ..... 91*

*Figure 3.14 CTX0E16/02 cells differentiated in the presence of SNBM supplemented with 1 µM purmorphamine..... 92*

*Figure 3.15 CTX0E03/02 cells differentiate into concentrated clumps of neurons while CTX0E16/02 tend to produce a more even monolayer..... 94*

*Figure 3.16 Expression of Various GPCRs and some of their accessory proteins in various human NPC lines..... 99*

*Figure 3.17 Expression of glutamate receptors and receptor subunits in various human NPC lines ... 101*

*Figure 3.18 Expression of genes related to diverse neuropsychiatric disorders in various NSC lines .. 103*

*Figure 3.19 Expression of GPCRs and some of their accessory proteins in differentiated cortical NPCs ..... 106*

*Figure 3.20 Expression of glutamate receptors and receptor subunits in differentiated cortical NPCs 109*

*Figure 3.21 Expression of GPCR accessory proteins and signalling nodes in differentiated cortical NSCs ..... 110*

*Figure 4.1 Diagram to illustrate GPCR-mediated signalling involving regulation of $[Ca^{2+}]$ ..... 121*

*Figure 4.2 Proliferative CTX0E16/02 cultures contain rare $tau^{+}$ and $S100\beta^{+}$ cells..... 122*

*Figure 4.3 Differentiated CTX0E16/02 cells are tripotent..... 124*

*Figure 4.4 Differentiated CTX0E16/02 cultures express markers of GABAergic neuronal subtypes.... 125*

*Figure 4.5 Raw traces of fluorescence intensity changes for a typical FS3 experiment ..... 127*
*Figure 4.6 Dopamine, 5-HT, glutamate and GABA-mediated $Ca^{2+}$ release in proliferative CTX0E16/02 cultures ..... 128*
*Figure 4.7 Phenylephrine, histamine, acetylcholine and carbamoylcholine-mediated $Ca^{2+}$ release in proliferative CTX0E16/02 cultures ..... 129*
*Figure 4.8 Comparison of dopamine, 5-HT, glutamate and GABA-induced $[Ca^{2+}]_i$ changes between proliferative and differentiated CTX0E16/02 cultures ..... 131*
*Figure 4.9 Comparison of phenylephrine, histamine, acetylcholine and carbamoylcholine-induced $[Ca^{2+}]_i$ changes between proliferative and differentiated CTX0E16/02 cultures ..... 132*
*Figure 4.10 Representative bright field images of proliferative and differentiated CTX0E1602 cells . 134*
*Figure 4.11 Raw images of fluorescence intensity changes for typical single cell $Ca^{2+}$-imaging experiments ..... 135*
*Figure 4.12 Cells within differentiated CTX0E16/02 cultures demonstrate dopamine-induced $Ca^{2+}$ oscillations ..... 138*
*Figure 4.13 Proliferative and differentiated CTX0E16/02 cultures demonstrate considerable heterogeneity in response to dopamine, 5-HT and glutamate, but not acetylcholine ..... 139*
*Figure 4.14 Cells within proliferative CTX0E16/02 cultures are capable of 5-HT-induced $Ca^{2+}$ responses ..... 141*
*Figure 4.15 Nature of acetylcholine-induced responses in individual cells of proliferative and differentiated CTX0E16/02 cultures vary considerably ..... 143*
*Figure 4.16 Glutamate–induced responses show greater heterogeneity in differentiated CTX0E16/02 cultures ..... 146*
*Figure 4.17 Small minority of proliferative and differentiated CTX0E16/02 cells capable of KCl-induced depolarisation ..... 147*
*Figure 4.18 Proliferative CTX0E16/02 cultures previously expanded as neurospheres become sensitised to dopamine and glutamate ..... 153*
*Figure 4.19 Pre-aggregation of CTX0E16/02 cultures prior to differentiation alters their response to various ligands ..... 154*
*Figure 4.20 PI3K activation for final 3 days of CTX0E16/02 differentiation increases acetylcholine and glutamate-induced $[Ca^{2+}]_i$ responses ..... 156*
*Figure 4.21 PI3K activation for final 7 days of CTX0E16/02 differentiation increases acetylcholine and glutamate-induced $[Ca^{2+}]_i$ responses ..... 157*
*Figure 4.22 Differentiation of CTX0E16/02 cultures with NGF alters sensitivity to glutamate and acetylcholine ..... 158*
*Figure 4.23 CTX0E16/02 cultures differentiated with BDNF has little effect on ligand-induced $[Ca^{2+}]_i$ 159*
*Figure 4.24 Extended differentiation of CTX0E16/02 cultures alters ligand-induced responses in $[Ca^{2+}]_i$ ..... 161*
*Figure 4.25 Differentiation duration affects ligand-induced $[Ca^{2+}]_i$ responses in CTX0E16/02 cultures 163*
*Figure 4.26 BDNF and $FGF_2$ affects ligand-induced $[Ca^{2+}]_i$ responses in differentiated CTX0E16/02 cultures ..... 165*

*Figure 4.27 Differentiation duration and BDNF promote electrical excitability in CTX0E16/02 cultures ..... 166*

*Figure 4.28 Elevated cAMP in differentiated CTX0E16/02 cultures increases glutamate-induced $[Ca^{2+}]_i$ responses ..... 171*

*Figure 4.29 Elevated cAMP in differentiated CTX0E16/02 cultures modulates ligand-induced $[Ca^{2+}]_i$ responses ..... 172*

*Figure 4.30 Differentiation with glutamate or phenylephrine affects ligand-induced $[Ca^{2+}]_i$ responses ..... 174*

*Figure 4.31 Differentiation with glutamate or phenylephrine affects ligand-induced $[Ca^{2+}]_i$ responses ..... 175*

*Figure 4.32 Long-term continuous passage of CTX0E16/02 cells increases dopamine-induced $[Ca^{2+}]_i$ responses in proliferative and differentiated cultures ..... 178*

*Figure 4.33 Long-term continuous passage of CTX0E16/02 cells increases 5-HT-induced $[Ca^{2+}]_i$ responses in proliferative and differentiated cultures at high concentrations..... 179*

*Figure 4.34 Long-term continuous passage of CTX0E16/02 cells increases acetylcholine-induced $[Ca^{2+}]_i$ responses in differentiated cultures only ..... 180*

*Figure 5.1 Proliferative and differentiated primary cultures include a high proportion of neurons ... 188*

*Figure 5.2 GPCR and GPCR accessory protein gene expression in CTX0E16/02 and primary cultures . 190*

*Figure 5.3 Expression of glutamate receptors and receptor subunits in CTX0E16/02 and primary cultures ..... 191*

*Figure 5.4 Expression of genes related to diverse neuropsychiatric disorders in CTX0E16/02 and primary cultures ..... 192*

*Figure 5.5 Comparison of ligand-induced $Ca^{2+}$ responses between proliferative CTX0E16/02 and primary cultures ..... 194*

*Figure 5.6 Comparison of dopamine-induced $Ca^{2+}$ responses in differentiated CTX0E16/02 and primary NSC cultures ..... 197*

*Figure 5.7 Comparison of 5-HT-induced $Ca^{2+}$ responses in differentiated CTX0E16/02 and primary NSC cultures ..... 197*

*Figure 5.8 Comparison of glutamate-induced $Ca^{2+}$ responses in differentiated CTX0E16/02 and primary NSC cultures ..... 199*

*Figure 5.9 Comparison of acetylcholine-induced $Ca^{2+}$ responses in differentiated CTX0E16/02 and primary NSC cultures ..... 200*

*Figure 5.10 Non-expanded proliferative primary neural cultures are electrically excitable ..... 201*

*Figure 5.11 Primary neural cells maintained in adherent monolayer culture lose electrically excitable ..... 203*

*Figure 5.12 Differentiated primary neural cell cultures exhibit robust electrically excitability..... 204*

*Figure 6.1 Timeline to illustrate the addition of different drugs when using agonists and antagonists ..... 217*

*Figure 6.2 Antagonism of dopamine-induced $Ca^{2+}$ responses in differentiated CTX0E16/02 cultures .. 218*

*Figure 6.3 Relative contribution of 5-HT$_{2A}$-mediated Ca$^{2+}$ responses in differentiated CTX0E16/02 cultures ..... 222*
*Figure 6.4 Acetylcholine-mediated intracellular Ca$^{2+}$ accumulation in differentiated CTX0E16/02 cultures ..... 225*
*Figure 6.5 Functionally distinct GPCRs modulate ERK/MAPK signalling through a range of different mechanisms..... 227*
*Figure 6.6 Optimisation of assay conditions to maximise measured levels of ERK1/2 phosphorylation ..... 228*
*Figure 6.7 ERK1/2 phosphorylation in response to dopamine and 5-HT in differentiated CTX0E16/02 cultures ..... 232*
*Figure 6.8 Acetylcholine & phenylephrine-induced ERK1/2 phosphorylation in differentiated CTX0E16/02 cultures..... 234*
*Figure 6.9 Glutamate & GABA provoke ERK1/2 phosphorylation in differentiated CTX0E16/02 cultures ..... 235*
*Figure 6.10 ERK1/2 phosphorylation in response to histamine and haloperidol in differentiated CTX0E16/02 cultures..... 237*
*Figure 6.11 Proliferative CTX0E16/02 cultures demonstrate low basal levels of ERK1/2 phosphorylation ..... 238*
*Figure 6.12 Influence of dopamine and 5-HT receptor subtype specific agonists on ERK1/2 phosphorylation in differentiated CTX0E16/02 cultures..... 241*
*Figure 6.13 Antagonism of dopamine and 5-HT receptor subtype specific agonist-induced ERK1/2 phosphorylation using specific antagonists in differentiated CTX0E16/02 cultures..... 243*
*Figure 6.14 Influence of haloperidol upon ERK1/2 phosphorylation in differentiated CTX0E16/02 cultures exposed to simulated dopaminergic tone ..... 247*
*Figure 6.15 Diagram of typical plate map for ERK1/2 phosphorylation assays to reduce influence of "edge effect" ..... 251*
*Figure 8.1 Long-term continuous passage of CTX0E16/02 cells increased glutamate-induced [Ca$^{2+}$]$_i$ responses in proliferative and differentiated cultures at high concentrations ..... 303*
*Figure 8.2 Long-term continuous passage of CTX0E16/02 cells increased GABA-induced [Ca$^{2+}$]$_i$ responses in differentiated, but not proliferative cultures at high concentrations..... 304*
*Figure 8.3 Long-term continuous passage of CTX0E16/02 cells increased histamine-induced [Ca$^{2+}$]$_i$ responses in proliferative and differentiated cultures at high concentrations ..... 305*
*Figure 8.4 Long-term continuous passage of CTX0E16/02 cells considerably increased the sensitivity of proliferative, but not differentiated cultures to phenylephrine..... 306*
*Figure 8.5 Long-term continuous passage of CTX0E16/02 cells increases carbamoylcholine-induced [Ca$^{2+}$]$_i$ responses in differentiated, but not proliferative cultures at high concentrations..... 307*

# *Table of Tables*

*Table 1.1 Genome-wide significant variants associated with risk of developing schizophrenia ..... 28*

*Table 2.1 Neural Stem Cell Proliferation & Differentiation Conditions ..... 55*

*Table 2.2 Details of Primary Antibodies ..... 57*

*Table 2.3 Description of use of all antibodies ..... 58*

*Table 3.1 Protocols tested to differentiate the cortically derived NPC lines CTX0E03/02 and CTX0E16/02 ..... 71*

*Table 3.2 Immunoreactivity summary of CTX0E03/02 cultures following 14 day differentiation ..... 72*

*Table 3.3 Immunoreactivity summary of CTX0E03/02 cultures following 21 day differentiation ..... 73*

*Table 3.4 Immunoreactivity summary of CTX0E03/02 cultures following 28 day differentiation ..... 73*

*Table 3.5 Immunoreactivity summary of CTX0E16/02 cultures following 14 day differentiation ..... 74*

*Table 3.6 Immunoreactivity summary of CTX0E16/02 cultures following 21 day differentiation ..... 74*

*Table 3.7 Immunoreactivity summary of CTX0E16/02 cultures following 28 day differentiation ..... 75*

*Table 3.8 List of genes identified as relevant to neuropsychiatric drug action ..... 96*

*Table 3.9 Relative expression of genes encoding GPCRs, their accessory proteins and important signalling molecules in proliferative and differentiated NPCs ..... 111*

*Table 3.10 Relative expression of genes encoding various glutamate receptors or their subunits, and targets relevant to neuropsychiatric drug discovery in proliferative and differentiated NPCs ..... 112*

*Table 4.1 Neurotransmitter receptor primary G protein-coupling partners ..... 120*

*Table 5.1 Culture details for each primary human neural tissue sample ..... 187*

## *Abbreviations*

| Abbreviation | |
|---|---|
| $[Ca^{2+}]_i$ | intracellular $Ca^{2+}$ concentration |
| 4-OHT | (*Z*)-4-hydroxytamoxifen |
| AC | adenylyl cyclase |
| AMPA | (2-amino-3-(5-methyl-3-oxo-1,2- oxazol-4-yl)propanoic acid |
| APD | antipsychotic drug |
| ATP | adenosine-5'-triphosphate |
| B27M | B27 medium |
| BDNF | brain-derived neurotrophic factor |
| bp | base pair |
| BRET | bioluminescence resonance energy transfer |
| cAMP | 3'-5'-cyclic adenosine monophosphate |
| $Ca_V$ | voltage-dependent calcium channels |
| CB | calbindin-D28k |
| CNS | central nervous system |
| CNV | copy number variation |
| CR | calretinin |
| CYP450 | cytochrome P450 |
| DAG | diacylglycerol |
| DAPI | 4',6-diamidino-2-phenylindole dihydrochloride |
| DAPT | *N*-[*N*-(3,5-difluorophenacetyl)-L-alanyl]-S-phenylglycine t-butyl ester |
| DARPP-32 | dopamine and cAMP-regulated phosphoprotein, 32 kD |
| DCX | doublecortin |
| DLPFC | dorsolateral prefrontal cortex |
| DMSO | dimethyl sulfoxide |
| EEG | electroencephalography |
| EGF | epidermal growth factor |
| EPS | extrapyramidal side effects |
| ER | endoplasmic reticulum |
| ERK | extracellular signal-regulated kinase |
| ES | embryonic stem (cell) |
| FACS | fluorescence-activated cell sorting |
| FGF2 | basic fibroblast growth factor |
| fMRI | functional magnetic resonance imaging |
| FRET | fluorescence resonance energy transfer |
| GABA | γ-aminobutyric acid |
| GDNF | glial cell-derived neurotrophic factor |
| GIRK | G-protein-regulated inwardly rectifying K+ channels |
| GPCR | G-protein coupled receptor |
| GRK | G protein-coupled receptor kinases |
| GSK-3b | glycogen synthase kinase 3β |
| GWAS | genome-wide association studies |
| HM | human medium |
| HTS | high-throughput screening |
| IGF-1 | insulin-like growth factor-1 |
| iN | inducible neural (cell) |
| $IP_3$ | inositol 1,4,5-trisphosphate |
| iPS | inducible pluripotent stem (cell) |
| LC | liquid chromatography |

| | |
|---|---|
| LGIC | ligand-gated ion channel |
| mAChR | muscarinic acetylcholine receptor |
| MAP2 | microtubule-associated protein 2 |
| MAPK | mitogen-activated protein kinase |
| MEG | magnetoencephalography |
| MEK1 | mitogen-activated protein kinase kinase 1 |
| mGluR | metabotropic glutamate receptor |
| MRI | magnetic resonance imaging |
| MRS | magnetic resonance spectroscopy |
| MUPP1 | multiple PDZ domain protein |
| nAChR | nicotinic acetylcholine receptors |
| NAM | negative allosteric modulator |
| NB | neurobasal (medium) |
| NGF | nerve growth factor |
| NMDA | *N*-Methyl-D-aspartate |
| NPC | neural progenitor cell |
| NSC | neural stem cell |
| PAM | positive allosteric modulator |
| PANSS | positive and negative syndrome scale |
| PBS | phosphate buffered saline |
| PCR | polymerase chain reaction |
| $PDGF_{BB}$ | homodimer of platelet-derived growth factor subunit B |
| PET | positron emission tomography |
| PI3K | phosphatidylinositol 3-kinase |
| PIP2 | phosphatidylinositol 4,5-bisphosphate |
| PKA | protein kinase A |
| PKC | protein kinase C |
| PLC-β | phospholipase C-β |
| PMA | purmorphamine |
| PSD-95 | postsynaptic density protein 95 |
| PV | parvalbumin |
| RFU | relative fluorescence units |
| RMM | reduced modified medium |
| RT | reverse transcription |
| SERT | 5-HT transporter |
| SNAP-25 | synaptosomal-associated protein of 25 kD |
| SNBM | supplemented neurobasal medium |
| SNP | single nucleotide polymorphism |
| SPECT | single photon emission computed tomography |
| $T_3$ | 3,3',5-triiodo- L-thyronine |
| $T_4$ | L-thyroxine |
| TRP | transient receptor potential (channel) |
| VAMP2 | vesicle-associated membrane protein 2 |
| VDIC | voltage-dependent ion channel |
| vGluT1 | vesicular glutamate transporter 1 |
| vGluT2 | vesicular glutamate transporter 2 |
| WHB | whole human brain |

# *Chapter 1 Introduction*

## *1.1 Studying the Human Brain*

As the most complex known structure, understanding the human brain, and the behavioural repertoire its function produces represents a considerable challenge to science. Not simply because of it's complexity and its relative inaccessibility, but also because of the considerable unmet medical need to help people suffering from diseases of, and damage to, the brain. The pioneering work of Camillo Golgi and Santiago Ramón y Cajal using post mortem tissue provided the foundation for our understanding of the human brain's microscopic anatomy and the cells from which it is composed [1,2]. The analysis of behaviour through controlled studies and changes observed following injury or as a consequence of disease – accessibly described by the likes of Oliver Sacks [3,4] and Vilayanur Subramanian Ramachandran [5] – have provided an intriguing hint of the human brains' inner workings. More recent advances such as the development of non-invasive imaging techniques such as structural and functional magnetic resonance imaging (MRI and fMRI respectively), electroencephalography (EEG), magnetoencephalography (MEG), magnetic resonance spectroscopy (MRS), positron emission tomography (PET) and single photon emission computed tomography (SPECT) have all provided further clues as to the activity of the human brain at a functional level [6].

Neuroscience has also relied heavily on the use of animals both for behavioural experimentation and as a source of live tissue. Animal models as a surrogate to understand the workings of the human brain and the biology of the cells it is composed of have provided a wealth of information – from the first description of the mechanism behind the action potential by Hodgkin and Huxley using the giant squid axon [7] to the development of *Brainbow* mice to facilitate the simultaneous visualisation of numerous proteins within the brain [8]. The use of animals to model the human brain is however not ideal, with limitations perhaps most obvious in the field of psychiatric drug development. The difficulty of using animals to model disorders of aberrant human behaviour such as schizophrenia, depression and anxiety is reflected in the high rate of attrition of drugs designed to target the central nervous system (CNS) once they have progressed into the clinic [9-11]. The value of animals in modelling disorders that are arguably uniquely human is a continuously debated subject, yet their impact has been undeniable and all drugs must demonstrate some sort of efficacy in animals before progressing into man. Indeed, the use of animals can also be pivotal to the identification of biomarkers to indicate such efficacy, the search for which remains one of the greatest challenges of psychiatric drug discovery [12-14].

However, a recent review examining the success rate of nearly 500 compounds entering late stage clinical trial for the treatment of schizophrenia, depression and anxiety found that while preclinical animal models have some utility in predicting overall clinical efficacy and side effect liability, their capacity to predict clinical efficacy above that demonstrated by existing treatments was poor [15]. Crucially, this represents the final stage in the clinical approval process; a stage at which most of the estimated $800 million needed to develop a new drug has been spent [16]. An investigation by Kola and Landis found that of the ten largest pharmaceutical companies operating between 1991 and 2000, the failure rates for compounds developed for the treatment of CNS disorders was a staggering 92% [9].

However, despite demonstrating efficacy in preclinical animal models – a prerequisite for initial testing in humans – the single major reason for the failure of new drugs is a lack of clinical efficacy in man [10,15]. This is exemplified by the development of compounds designed to target the dopamine $D_4$ receptor – L-745,879 and fananserine – in an attempt to relieve symptoms of schizophrenia. While promising pre-clinical efficacy was demonstrated in both whole animal and *in vitro* models, these compounds failed to prove effective once reaching the clinic [15,17,18]. This failure was likely attributable to the limitations of animal models used to predict efficacy relating to complex human behaviour, such as the inhibition of mescaline-induced head twitches, apomorphine-induced climbing or phencyclidine-induced psychomotor effects in rodents as a marker of positive symptom relief in humans [17,18].

In addition to the use of animals as a means to understand the workings of the brain as a whole, much of our current understanding of the physiology and pharmacology of the brain at the cellular and molecular level has similarly come from our use of neural cells derived from animals. Again, these cells have been utilised as a surrogate to understand the workings of the human brain, but as the behaviour of these animals suggests, their brains differ in many ways from our own. It is clear that we have benefitted hugely from the use of animals and their tissues though differences between species can be considerable. An interesting example of this is found in the mongoose, whose radically modified nicotinic receptor subunits render them immune to the α-bungarotoxin contained within the venom of cobra upon which they predate, yet is highly neurotoxic to humans and indeed most other mammals [19]. While this perhaps represents a quirk of evolution, other less obvious differences can have a profound effect such as is illustrated in the case of the arginine vasopressin $V_{1A}$ receptor. This receptor exhibits striking differences between species with regard to its anatomical expression and the behavioural responses its activation provokes [20,21]. Another example is provided by the recent identification of *KCNH2-3.1* – an isoform of an ether-a-go-go (ERG)-family $K^+$ channel that influences neuronal firing [22]. Not only is this channel unique to primates, it is also a high affinity target of several drugs currently used to treat schizophrenia [23], while alleles of this gene have been associated with the risk of developing the disorder [22]. The absence of this channel isoform in lower mammals means that it is impossible to model the effects caused by its modulation *in vivo*, and highlights the difficulties associated with psychiatric drug discovery. As our understanding of neuroscience grows and the techniques available to us to investigate the cellular and molecular basis of the brain become more sensitive, so too has the importance of using not only the relevant tissue but also the correct species. Psychiatric and neurological conditions represent a significant unmet medical need, and with current attrition rates for CNS targeted drugs running so high [9,10], it appears clear that a native tissue system of the human brain would be of great use [24].

The advent of the genomic age brought with it a valuable alternative to the use of isolated tissues and whole animal experiments to investigate pharmacology and physiology – both for basic biology and drug discovery. Molecular cloning provided chimeric human protein expression in surrogate cell lines, facilitating a new level of biochemical characterisation using proteins encoded by human genes [25]. While this facilitated the development of highly selective compounds to target these proteins, it did not

provide the functional insight that a native tissue can deliver. One reason for this is that the human proteins these cell lines were used to express do not act in isolation – they form components of complex signalling cascades and are frequently under the influence of functional regulation by various other molecules that are discretely, differentially expressed in different tissues and cell types [26,27]. Due to the absence of this regulation provided by the complement of signalling molecules found in native tissues, recombinant systems often lack the depth of complexity to accurately portray the true physiological consequence of modulating a particular signalling system. While this reductionist approach has provided a wealth of information – especially when combined with techniques such as site-directed mutagenesis to determine the role of single amino acids within a protein, it has become increasingly clear that these recombinant expression systems cannot be used in isolation to seek a thorough understanding of cell physiology and the molecular components responsible for maintaining it [14].

In contrast to many heterologous expression systems, native tissues not only provide the downstream signalling and regulatory molecules responsible for transducing the effects of a given stimulus in a physiologically meaningful way, they also ensure that the protein being studied is subject to the same post translational modification and – crucially – compartmentalisation of their *in vivo* counterparts. There exist numerous examples whereby functional protein expression – especially for those that show plasma membrane expression *in vivo* – fails due to the absence of the functional machinery or co-chaperones required to facilitate it [28,29]. This is especially true of G protein-coupled receptors (GPCR), particularly those that are members of the odorant receptor family. Indeed, heterologously expressed odorant receptors fail to traffic to the plasma membrane in almost all cell types except mature olfactory neurons [30]. This failure appears to be due to their retention in the endoplasmic reticulum, preventing their export to the Golgi apparatus and subsequently the plasma membrane [31]. This inability to progress though the secretory pathway has been demonstrated for numerous odorant receptors including OR-I3, OR-I7, OR5 OREG and U131 [31,32], and has consequently frustrated attempts to characterise them *in vitro*. This has meant that the majority of odorant receptors have remained orphaned with respect to their natural ligands [33]. However, this problem is not unique; many non-odorant GPCRs also remain orphaned due to the lack of plasma membrane expression, needed to facilitate their *in vitro* characterisation, such as GPCR6A and GPR37 [34,35].

The therapeutic potential of many of these receptors – reflected in the fact that a third of all currently marketed drugs target GPCRs [36] – has meant that considerable work has been dedicated to understanding the mechanisms that control their exit from the endoplasmic reticulum. This has shown that cell surface expression of GPCRs, and indeed other classes of receptors, is under strict regulation and is controlled by a variety of different mechanisms. This has led to the use of various techniques to promote functional receptor expression including the removal of amino acid sequences; as in the case of GPR37 and some odorant receptors [30,34], or the addition of sequences. Indeed this approach was adopted for perhaps the most intensely studied, and first cloned receptor – the $\beta_2$-adrenergic receptor – requiring the addition of a N-terminal cleavable signal sequence to provide sufficient levels of receptor expression to facilitate its study in a recombinant system [37]. Other approaches have involved the co-

expression of receptors with coupling partners – as in the case of $GABA_B$ and several adrenergic receptors [35,38]. Other receptors have been shown to require the presence of accessory proteins for their functional expression, as exemplified by calcitonin receptor-like receptor and its interaction with receptor activity modifying proteins (RAMP)[39]. The use of *in vitro* native tissue models rather than heterologous cell lines circumvents the need for identification and co-expression of molecular chaperones or coupling partners, or indeed the modification of the protein under investigation. In addition, these modifications are likely to alter the functional characteristics of the protein, if not in how it responds to a given stimulus, then in the way it interacts with accessory and regulatory proteins, and is therefore likely to skew our understanding of these proteins' normal function. There exist many reasons why the development of drugs designed to target the brain represents such a challenge – not least simply the chemistry of compounds required to penetrate it – but this endeavour is particularly confounded by a lack of native human tissue with which to perform initial preclinical development [15,24,40].

Although we cannot experiment on humans, the recent surge in our understanding and manipulation of embryonic stem (ES) cells and neural stem cells (NSC), followed by the current developments in inducible pluripotent stem (iPS) cell technology have abruptly made it possible to study human neural cells *in vitro*. Historically, the study of living cells native to the human brain has proven particularly difficult, and is partly due to its predominantly non-regenerative nature. Neurons represent terminally differentiated, post-mitotic cells and as such, are incapable of expansion *in vitro*, meaning mature human neurons can only ever generate primary cultures. Tissue obtained through biopsy is understandably rare, and many regions – especially those encapsulated by the cerebral cortex – are highly inaccessible, restricting the range of cell types available for investigation. In addition, neural biopsy material unsurprisingly tends not to yield healthy brain tissue, but rather cells derived from tumours. These tumorigenic cells may be derived from progenitor cells (neuroblastomas or glioblastomas), astrocytes (astrocytomas), oligodendrocytes (oligodendrogliomas) or ependymal cells (emendymomas)[41], and as a consequence of aberrant expression of oncogenic genes, often have the capacity to be expanded; resulting in the establishment of neural cell lines that can be maintained in the laboratory indefinitely. Such cell lines can either be differentiated into a specific cell type, for example, astrocytes and/or oligodendrocytes in the case of glioblastomas, or neurons in the case of neuroblastoma cell lines (originating from neuroblasts of the sympathetic nervous system, and so are not only of brain origin) like SH-SY5Y [42]. Alternatively cell lines, like NT2 have been generated from teratocarcinomas (germ cell cancers) and have the capacity to generate both neurons and glial cells [43]. Indeed, cell lines such as SH-SY5Y or NT2 has provided important research tools for the *in vitro* study of human nerve cell function [41]. However, due to the tumorigenic origin of these cell lines, any data obtained using them had to be met with a certain degree of caution with respect to the function of normal neurons.

It was not until the late 1990s that clonal neural progenitor cell (NPC) lines were derived from human foetal tissue. These cell lines were initially only capable of giving rise to neurons and astrocytes [44],

though later work demonstrated the full multipotentiality – capacity to generate neurons, astrocytes and oligodendrocytes – of this type of cell line *in vitro* [45,46] and *in vivo* [47]. Therefore, in the absence of available primary human neural tissue, neural stem cells (NSC – cells capable of generating all of the cells types present in the adult brain) or the neural progenitor cells that they generate, represented a renewable and reproducible source of human neural cells. ES cells, NSC and NPCs can each be used to derive mature neural cultures, and each have properties that can make them invaluable tools to the laboratory scientist, as discussed below. However, it is the application for which these cells are to be used that determines those that represent the most appropriate source.

## *1.2 ES cells, Neural Stem and Progenitor Cells*

Stem cells, and the understanding of how to manipulate them, have been widely touted as a potentially revolutionary technology for many neurological conditions. Their clinical use has probably attracted the most attention with promise of cell-replacement therapies for diseases such as Parkinson's, Huntington's and Alzheimer's diseases and even functional repair following stroke or spinal cord injury [48,49]. While embryonic stem (ES) cells are derived from the inner cell mass of the blastocyst and have the capacity to form all cell types of the embryo proper [50], neural stem cells are isolated later in development after formation of the neural tube and as such, have a fate restricted to that of cells of the central nervous system [51]. Importantly, these cells can proliferate indefinitely under appropriate culture conditions and can be stimulated to differentiate into a range of different neural progeny [45,52]. NSCs are also found in the adult human brain but are restricted to the subgranular zone of the dentate gyrus within the hippocampal formation, and the subventricular zone lining the lateral ventricles [53], and are only practically accessible from post-mortem tissue [54]. During development, NSCs generate NPCs that have a more restricted developmental phenotype. These NPCs display positional and temporal specification meaning that their position within the germinal zones of the developing brain dictates the genes they express and hence the types of neurons and glial cells that they generate [55,56]. Isolated NPCs have been shown to retain both their positional and temporal specification and therefore have the advantage of providing neural precursors that have the capability to generate specific neural cell-types. For instance, NPCs of mesencephic origin generate dopaminergic neurons [57], while NPCs isolated from the developing spinal cord generate motor and sensory neurons [58,59]. However, this maintenance of positional specification can be dependent upon culture conditions, for instance, expansion of mouse cortical NPCs in the presence of $FGF_2$ can result in these cells generating GABAergic neurons rather than glutamatergic neurons as they would *in vivo* [60]. Importantly, isolated NPCs retain their capacity for self-renewal, meaning they can be used as an expandable source of cells with which to derive the cells that comprise the adult human brain [55]. Thus NPCs can be isolated from specific brain regions and under appropriate culture conditions will go on to generate appropriate neuronal cell types. This may hold an advantage over using ES cells that first have to be pushed along a neural pathway and then towards a specific neural lineage, making this method of generating neural 'lineage specific' lines much more problematic and time consuming. Therefore, the use of NPCs reduces the amount of differentiation

required to achieve the desired cell type and also reduces the amount of time needed to obtain a specific lineage. In addition, unlike ES cells, due to the positional and temporal assignment NPCs receive, they no longer require the need to be pushed towards a specific lineage. Differentiation can therefore be achieved by simply removing the trophic factors necessary to maintain their self-renewal capacity [45].

Primary samples derived from human neural foetal tissue contain a mixture of cells. The extent of this mix depends both on the neural region and also the gestational period from which the cells are isolated, as different areas of the developing brain mature at different times, with phylogenetically later regions such as the frontal cortex maturing later than those of more phylogenetically ancient structures such as the brainstem. Despite the presence of multipotent NPCs, primary brain samples may also contain terminally differentiated cells such as neurons and oligodendrocytes. Once primary samples are isolated from the developing brain and are expanded *in vitro*, the proportion of each of these different cell types changes due to their varying proliferative capacity, that is; over time, cell types with greater proliferative capacity will begin to dominate and introduce variability to the behaviour of the culture as a whole. Therefore, to reduce the variability observed in such primary human cultures, researchers generate clonal NPC lines, i.e. individual cell lines derived from single precursor cells, as discussed below. Isolation of clonal cell lines can be used as a means to minimise cell type heterogeneity within cultures and generate a population of cells that can be expanded, frozen and thawed. Clonal isolation to produce cell lines also provides the benefit of producing various different types of precursor cells from a primary tissue sample as was recently demonstrated by Hook and colleagues [61].

Initial attempts to develop clonal human NPC lines provided mixed results due to karyotypic instability and loss of self-renewal. While the former appeared to be something that needed to be monitored, it was found the latter could be maintained through conditional immortalisation, involving inducible, ectopic oncogenic gene expression [62,63]. This approach helped to develop cell lines that were less prone to spontaneous differentiation and maintained the proliferative capacity of the original parent cell so that each could be expanded and frozen to generate cell banks that could provide robust and reproducible data [64].

As knowledge regarding the maintenance of NPCs grew, it was realised that conditional immortalisation was not always necessary and the self-renewal properties of certain cells could be maintained indefinitely in the presence of the growth factors EGF and $FGF_2$. A recent study by Hook and colleagues demonstrated the isolation of numerous NPC lines from various human foetal brain regions that relied on first sorting cells based on their expression of cell surface markers known to be associated with self-renewal – CD133 and CD24. Individual colonies were then isolated from cells that demonstrated the greatest proliferative capacity and therefore did not require conditional immortalisation [61]. Due to the variability that can exist between different NPC lines – even for those isolated from the same region and tissue sample – each time new lines are derived they must be individually characterised and compared to existing cell lines. This is a time consuming and laborious process. Another important factor is that the use of well-characterised, established clonal NPC lines prevents the need to obtain further primary tissue samples – a particular concern due to the controversial origin of the cells used to generate these

lines. Many groups are of course fundamentally opposed to the use of foetally derived human cell lines, as the work suggests a condoning of abortion due to these cells originating from terminations of normal pregnancies.

For neuroscience, ES cells, NSC and NPCs represent an invaluable resource both for basic research, and as a potentially revolutionary regenerative therapy. Importantly, each of these types of cell are capable of self renewal, and upon appropriate differentiation; have the capacity to generate cell types that populate the adult human brain. Therefore, they provide an expandable source of cells, with which to study the cellular and molecular mechanisms underpinning the function of the human brain. While ES cells and NSCs have the capacity to generate a broad range of different cell types, this must be achieved through a process of controlled differentiation, and at present, the knowledge relating to how to derive each different neuronal population remains unclear. In contrast, due to positional and temporal specification cues received prior to their isolation, human NPCs demonstrate a cellular fate, which is restricted to that of the region from which they were originally derived [61,65-67]. Consequently, clonal NPC lines do not require the presence of external cues to allow them to differentiate into regionally specified neuronal and glial subtypes. Therefore, NPCs isolated from the cortex should have already been positionally specified so as to generate the specific types of neurons and glia found in this brain area. This potentially makes the derivation of regionally specified neurons and glia easier, and improves the likelihood of obtaining, in culture, cells that more closely resemble those found in the cortex *in vivo*. Unfortunately, the greatest drawback of these types of cells is their controversial origin, as stated above. However, recent advances in our understanding of stem cell biology have brought us to a point where pluripotent stem cells can be created from easily accessible adult human tissues such as skin, hair and blood.

## *1.3 Induced Pluripotent Stem Cells*

A very recent advance that has justifiably attracted considerable interest within the scientific community is the technology behind induced pluripotent stem (iPS) cells – pluripotency being the capacity to derive all somatic lineages [68,69]. This involves the reprogramming of adult somatic cells into pluripotent stem cells through the ectopic expression of various key genes associated with pluripotency. This was first reported by Takahashi and Yamanaka in 2006 through ectopic expression of the transcription factors *Oct3/4*, *Sox2*, *c-Myc*, and *Klf4* in adult mouse fibroblasts under ES cell culture conditions [70]. A year later, the same was achieved using human adult fibroblasts expressing the same four human equivalent genes [71,72]. The resulting cells have been reported to share a similar morphology and other characteristics common to normal ES cells including pluripotency, self-renewal and gene expression pattern, though the field remains very young and for every publication describing the similarities of human iPS cells with ES cells there is another describing their differences [73].

However, these studies were not however the first descriptions of nuclear reprogramming, as this had been achieved previously through somatic and ES cell fusion and the transfer of nuclei from

differentiated cells to enucleated undifferentiated cells [74]. The work by Takahashi and Yamanaka was however the first method described that removed the need for any embryonic cells as a starting material, and therefore circumvented the controversy associated with the use of human ES cells. The field has since developed at an astonishing rate, driven by their relative ease to derive, accessibility and considerable potential. Stem cells have been afforded particular attention with respect to their potential as a source of cells to replace diseased or damaged tissue, such as occurs in neurodegenerative disease, diabetes and stroke or as a consequence of chronic kidney, heart or liver damage. The use of iPS cells for these applications means that pluripotent stem cells can be generated that are genetically identical to those of the desired recipient and would therefore negate the use of immunosuppressive treatment upon engrafting these cells. Another application for which these cells show particular promise is for *in vitro* disease modelling and drug discovery. Indeed, a recent publication from Brennand and colleagues provided an elegant proof of concept for the use of these cells for both applications [75]. They described the generation of pluripotent iPS cells by reprogramming fibroblasts from schizophrenic patients and controls using inducible lentivirus vectors expressing the transcription factor genes *OCT4*, *SOX2*, *KLF4*, *cMYC* and *LIN28* prior to differentiation into neuronal cultures. Neurons derived as a consequence of iPS cell differentiation were morphologically and physiologically representative of primary human neurons and capable of generating spontaneous calcium transients. Neuronal cultures were then compared with respect to morphology and gene expression and significant differences between diseased and control cultures were demonstrated for both. Interestingly, they also demonstrated the reversal of an observed reduction in neuronal connectivity by exposure to the antipsychotic loxapine (but not clozapine, olanzapine, risperidone or thioridazine) during the final stages of neuronal differentiation. This study highlighted the usefulness of iPS cells to model the cellular and molecular characteristics of disease, which is especially important for psychiatric conditions such as schizophrenia, that appear to demonstrate a complex polygenic origin with an ambiguous aetiology. The use of iPS cells in this way also suggests their utility in potentially providing a means to categorise schizophrenic patients based on cellular and molecular criteria, an important step towards personalised treatment for such patients.

While representing an exciting milestone in our understanding and manipulation of cellular pluripotency, iPS cells still require considerable validation with respect to their *in vivo* counterparts, with the same of course true for the differentiated cell types these iPS cells are used to derive. Another consideration for the use of these cells is the significant amount of time, low transformation efficiency and the labour intensiveness of their derivation, consequently incurring considerable cost. The therapeutic potential of iPS cells ensures however that any problems associated with, for example, genomic instability or altered epigenetic signatures (reviewed in detail elsewhere [73,76]) are likely to be tenaciously challenged experimentally to maximise their versatility, which will only serve to enhance our understanding of the cellular mechanisms that underlie pluripotency. Indeed, remarkable progress has already been made in the short time since iPS cells were first described, such as the generation of vector-free iPS cells to prevent the risk of virally-induced teratomas following engraftment [77,78], considerably increased reprogramming efficiencies and the use of alternative cell types to fibroblasts for iPS cell derivation, such as keratinocytes and haematopoietic cells [76,79,80].

The discovery that ectopic expression of specific transcription factors in adult somatic cells could be used as a means to revert them back to their pluripotent origin inspired the idea that cells could be transdifferentiated into any other cell type, assuming the correct combination of transcription factors could be identified. Theoretically, this means that any terminally differentiated cell type could be directly converted to another – eliminating the need for a pluripotent middleman – significantly reducing the time needed to obtain the desired cellular phenotype.

## *1.4 Induced Neuronal Cells*

In 2010, work led by Marius Wernig at Stanford provided the first evidence of direct generation of functional neurons from mouse-derived fibroblasts without first having to revert the cells to a pluripotent state, and with it coining the term induced neuronal (iN) cells [81]. This was achieved through ectopic expression of genes encoding the neurogenic transcription factors *Ascl1*, *Brn2* and *Myt1l*, and considerably reduced the time needed to obtain the desired neuronal phenotype as compared to the generation of iPS cells and subsequent differentiation [82]. This was quickly followed by a series of studies demonstrating that the same could be achieved using human fibroblasts. Pfisterer and colleagues demonstrated that expression of the human equivalent of the same three genes that provoked trans-differentiation in murine cells – *ASCL1*, *BRN2* and *MYT1L* – was also sufficient to produce functional neurons from human fibroblasts [83], though with considerably lower efficiency [84]. This group also demonstrated that the additional expression of *LMX1A* and *FOXA2* – encoding transcription factors associated with a dopaminergic neuronal fate – could direct the resulting cells to a dopaminergic phenotype. Yoo and colleagues then went on to demonstrate that direct human fibroblast to neuronal trans-differentiation could be achieved through ectopic expression of *MIR-9** and *MIR-124* – microRNAs that had been shown to be involved in prescribing cells to a neuronal fate during normal foetal development [85]. It was also demonstrated that the reprogramming efficiency could be significantly enhanced through the expression of *NEUROD2* – encoding a neurogenic transcription factor – and the previously mentioned *ASCL1* and *MYT1L* [86]. In contrast to the earlier report by Pfisterer, Wernig and colleagues stepped in and reported that *ASCL1*, *BRN2* and *MYT1L* expression were insufficient to produce mature functional neurons from human fibroblasts, though these could be obtained through the additional expression of *NEUROD1* (encoding a further neurogenic transcription factor)[87]. Caiazzo and colleagues then showed the generation of functional dopaminergic neurons from mouse and human fibroblasts through inducible lentiviral expression of just three transcription factor genes – *ASCL1*, *NURR1* and *LMX1A* [88]. Finally, Son and colleagues have provided evidence for the direct generation of functional spinal motor neurons from human fibroblasts through virally mediated transduction using *ASCL1*, *BRN2*, *MYT1L*, *LHX3*, *HB9*, *ISL1*, *NGN2* and *NEUROD1* [89]. This was however only achieved using embryonic human fibroblasts, and it remains unclear whether the same is true for their adult equivalents. Taken together, these reports suggest that the only limiting factor in our ability to generate different neuronal subtypes *in vitro*, is knowledge relating to the combination of transcription factors that direct these cellular fates *in vivo*.

The technology behind transdifferentiation of adult somatic cells into pluripotent stem cells (iPS cells) or directly into neurons (iN cells) remains in its infancy, though clearly offers considerable promise. Extensive investigation is however necessary to validate cells derived in this manner with respect to the cells they are claimed to represent, and the field will likely yield a diverse range of methods to derive a broad complement of different cellular subtypes, that faithfully represent their *in vivo* equivalents. At present however, numerous reports have indicated considerable differences between human ES cells and iPS cells. Epigenetic status – a property that defines cell identity through chromatin modification – has been shown in some cases to vary considerably between these two types of cells [90], as have their gene expression profiles [69]. The generation of iPS cells has also been shown to commonly introduce protein-coding point mutations, which were particularly enriched in genes with oncogenic capacity, meaning rigorous screening would be necessary if cells were destined for clinical application to avoid tumour formation [91,92]. Indeed, it has also been suggested that clonal selection may favour cells with tumorigenic capacity [93]. This problem may be avoided through the use of iN cells, though evidence that this is the case is yet to be provided and is limited by the fact that – unlike iPS cells – there is currently no means to expand iN cells [82].

With respect to their utility for the study of basic cellular and molecular mechanisms unique to neural function, iPS and iN cells also have their drawbacks. As mentioned previously, the generation of iPS cells is a time consuming and laborious process and still requires differentiation to provide neurons once pluripotent colonies have been established. The generation of iN cells is considerably faster, though they lack the ability to be expanded once transformed and cannot therefore be used to establish clonal cell lines – potentially increasing variability between experiments. However, if iPS cells truly recapitulate the status of ES cells – those that comprise the inner cell mass of the blastocyst – theoretically they should all be identical, devoid of evidence of their somatic origin and clonal in nature anyway. This has proven however not to be the case, with differences observed between clonal populations of iPS cells derived from the same patient using different somatic tissue sources and indeed when using the same somatic tissue source from a single patient [94-97]. These data suggest the need either for comprehensive screening of iPS cell and iN cells or the development of methods to standardise the cells that are ultimately derived [98].

One of the great advantages of iPS cells and iN cells is that patient-specific cells can be generated meaning they can be used to determine phenotypes relating to disease. While this has been shown to be useful for *in vitro* modelling of complex psychiatric diseases such as schizophrenia [75,99], they provide a less useful system in which to assess the functional consequence of a single gene mutation due to their varied genetic backgrounds and the compensatory effects of non-redundant systems, making this sort of experiment difficult to control. While iN cell generation can be used to produce pure populations of neurons by subsequent fluorescence-activated cell sorting (FACS) to remove untransformed cells, this may actually provide an experimentally misleading culture environment that diverges from that found *in vivo* due to the absence of other neuronal cell types such as astrocytes and oligodendrocytes. Brennand and colleagues demonstrated this when they found that synaptic maturation occurred most robustly

when neurons from differentiated human iPS cells were co-cultured with wild-type astrocytes [75]. This approach was repeated when assessing synapse formation in iN cells from mice [81] and human [87], due to the importance of astrocytes to the process of synaptogenesis [100]. Arguably, this provides a suboptimal disease modelling culture environment as glial cells may play an important part in the pathophysiology of the disease that is attempting to be modelled. Indeed the phenotype associated with a particular disease may actually be restricted to astrocytes meaning no disease-phenotype would be observed in this sort of *in vitro* model. A good example of this is provided in the case of motor neuron degeneration associated with amyotrophic lateral sclerosis, a process that has recently been shown to be largely driven by an astrocytic phenotype [101]. Similarly, due to the supportive role played by astrocytes, the use of wild-type glia could potentially mask neuronal, disease-specific phenotypic characteristics depending on the nature of the abnormality.

Interestingly, a compromise will likely be struck in the near future between the use of time-consuming reprogramming and subsequent differentiation to produce neural cells from iPS cells, and the faster but non-expandable nature of iN cells that lack the capacity to generate glia, following reports of the first transdifferentiation of mouse embryonic fibroblasts to NPC-like cells. Just over a year after the first description of the generation of mouse iN cells, and subsequently the successful generation of human iN cells – the Stanford-based group led by Marius Wernig have demonstrated the generation of cells capable of differentiation into neurons, astrocytes and oligodendrocytes [102]. This was achieved through the ectopic expression of three transcription factors associated with the NPC lineage: *Brn2*, *Sox2* and *FoxG1*. While the generation of these so-called inducible NPCs (iNPCs) still require the use of embryonic tissue, the rate at which this field is progressing means only a small leap of faith is necessary to envisage the generation of iNPCs from adult human somatic cells in the near future.

## *1.5 Exploiting the Potential of Pluripotent & Transdifferentiated Cells*

It is difficult to over estimate the potential that NSC, NPC, ES, iPS and iN cells represent both for the study of neuroscience and the treatment of disease. They provide a virtually limitless source of neural cells that is rapidly changing investigations in the laboratory, by providing *in vitro* models with which to investigate the function of cells native to the human brain, and treatments in the clinic by providing the tools necessary to explore the potential of regenerative medicine. Not only do these technologies replace the use of animals as a source of neural tissue, they arguably provide a cheaper and more faithful representative platform with which to study the cellular and molecular mechanisms of the human brain. Ultimately, it is the desired application that should inform upon the choice of which approach to use. **The original aim of this project was to develop an *in vitro* platform with which to investigate the mechanism of action of antipsychotic medications by evaluating their transcriptional impact**. More specifically, this would involve exposing separate *in vitro* cultures to various different antipsychotic drugs prior to the application of transcriptomic methodologies. The resulting data could then be used to determine changes in gene expression that may inform upon the possible molecular mechanisms responsible for their therapeutic efficacy or side effect liability. For this reason it was

important to develop a human *in vitro* culture system that was highly sensitive, yet provided robustly consistent data, made use of cells that closely resembled those thought to be acted upon by antipsychotic drugs and expressed receptors known to be targeted by these compounds.

The infancy of the field of iPS cell and iN cells ruled out their use at the inception of this study, though the mixed genetic background of individual iPS cell or iN cell lines would have increased background 'noise' for a transcriptomic study meaning larger *n* numbers would be required to determine significant changes in gene expression levels. Due to the high level of multiple statistical testing required to analyse whole genome expression data, this would considerably reduce the sensitivity of the cell culture system and diminish the reproducibility and robustness of the data. To maximise the sensitivity of the platform it was decided to make use of a clonal cell line, ensuring not only a stable genetic background, but – as far as possible – a similar epigenetic profile. This reduced the choice to either a human NSC, NPC or ES cell line and was informed by several factors. The cell line that was to be used would ideally take as little time to differentiate as possible, though it was appreciated that for human neural differentiation this period may still be considerable, be capable of deriving both neurons and glia, and as faithfully as possible represent the cells of the brain that the platform was attempting to model. It should be noted however that this was not an attempt to model disease – a role that would clearly be better served by the use of iPS or iN cells. NPCs were selected based on the fact that while ES cells, NSCs and NPCs can give rise to both neurons and glia, this can be achieved more rapidly by the differentiation of NPCs due to their already restricted fate. In addition, NPCs are isolated at a later gestational stage than ES cells or NSCs, and have therefore spent a longer period of time in their natural developmental environment. This means that NPC have been exposed to the normal succession of embryonic cues that ensure both maximal positional specification and neurogenic capacity; due to the time-point at which they are isolated (this varies according to the neural region from which the NPCs are derived).

Our laboratory had the fortune to have been kindly granted access to a number of clinical grade conditionally immortalised clonal NPC lines by ReNeuron Group plc. These were derived from various regions of the developing human brain including the cortex, hippocampus, striatum, ventral mesencephalon and spinal cord and were conditionally immortalised by retroviral delivery of either a *v*- or *c*-MycER$^{TAM}$ transgene. This technology allows the cells to be maintained in a proliferative state due to the ectopic expression of the *c*-Myc oncogene. As described by Littlewood and colleagues, this was achieved through conjugation of the genes encoding a transcriptionally inactive mutant of the mouse oestrogen receptor, that – while insensitive to endogenous oestrogen – can be activated by a synthetic analogue; 4-hydroxytamoxifen (4-OHT) and human c-Myc. The ectopically expressed protein exists as a cytoplasmic monomer, that upon 4-OHT binding undergoes dimerisation and subsequently translocates to the nucleus where *c*-Myc behaves as an active transcription factor [103]. These cell lines have been shown to be genetically stable with a normal karyotype and have been the subject of several recent publications [63-66,104-110], while one of the cell lines of cortical origin is currently in Phase I clinical trial as a treatment for debilitating stroke [111].

This study therefore begins with a comparison between, and subsequent selection of, one of these NPC lines to further characterise and develop as an *in vitro* platform to assess drug mechanism, in particular antipsychotics, with the possible wider remit of its development as a potential screening tool for novel compounds (see ***Chapter 3***). The reason for developing an *in vitro* model with which to investigate the mechanism of action of antipsychotic medicines is that, despite their widespread use for more than sixty years – the mechanism through which they exert their therapeutic effects remains unclear. This in itself is not a problem, but unfortunately – these therapeutic effects are commonly accompanied by poorly tolerated side effects and they remain ineffective in relieving the symptoms of many of the patients to whom they are prescribed. Although these compounds are used to treat a variety of different conditions, their primary use is in the treatment of schizophrenia.

## *1.6 What's the Problem?*

### *1.6.1 Schizophrenia*

Antipsychotics currently represent the mainstay of treatment for schizophrenia; a severe and complex psychiatric disorder characterised by chronic disturbance of perceptive, emotional and cognitive function. Symptomatic onset typically occurs in late adolescence or early adulthood, though many suffer what are known as prodromal symptoms prior to their first psychotic episode [112-115]. For diagnostic purposes, symptoms are classified into groups – often broadly defined as positive (hallucinations, delusions and disordered thoughts) and negative symptoms (social withdrawal, blunted affect and apathy), which are commonly accompanied by cognitive impairments (for detailed diagnostic criteria see [116,117]). Patients tend to exhibit combinations of these symptoms with varying severity at different times during the course of the illness, which tends to be chronic and progressive [115]. For these reasons, schizophrenia represents a highly disabling disease with 10% of patients eventually committing suicide [118], and the cost to society counted in tens of billions of pounds [119].

The lifetime risk of developing schizophrenia is approximately 1% and transcends gender, culture and race, though risk factors do exist [120-122]. While the aetiology of schizophrenia remains elusive, the influence of genetics as a predisposing factor is firmly established. Data obtained from family, twin and adoption studies have shown the disorder demonstrates a level of heritability approaching 85% [123], with prevalence rising to 6% for patients with an affected parent, 9% with an affected sibling and 48% between monozygotic twins [124]. The risk of developing schizophrenia was first proposed to have a polygenic origin as early as 1967 [125], a supposition supported by the advent of genome-wide association studies (GWAS), though this premise has been concurrently challenged – at least for a proportion of cases – through studies of copy number variations (CNV)[126]. These recent findings have therefore established two diametrically opposed models to describe the genetic origin behind the risk of an individual developing schizophrenia. The first encapsulates the principle of a polygenic heritability for the development of schizophrenia, and points to the combinatorial inheritance of multiple common genetic variants, each conferring low risk, though capable of pushing an individual past a 'threshold of

genetic burden', leading to the presentation of schizophrenia-associated endophenotypes. In contrast, the second implicates the occurrence of single rare, but highly penetrant genetic variants that can occur in a range of different genes and accounts for both isolated sporadic cases and those restricted to narrow gene pools [126].

The first reported GWAS studies of schizophrenia involved hundreds of samples [127-129], which in hindsight unsurprising revealed no loci that managed to reach the estimated genome-wide significance threshold ($p < 7.2 \times 10^{-8}$)[130]. In response to this and other early studies, several collaborative consortia were established to provide the numbers of samples needed to reveal loci with effect sizes relevant to schizophrenia [131]. The most recent GWAS for schizophrenia have involved tens of thousands of pooled samples and yielded several genome-wide significant loci including those in or around genes encoding *ZNF804A*, *NRGN*, *TCF4*, *MIR137*, *PCGEM1*, *CSMD1*, *MMP16*, *CNNM2*, *CCDC68*, *NT5C2*, *STT3A*, *VRK2* and the major histocompatibility complex (MHC) region on chromosome 6p21.3-22.1 (summarised in Table 1.1, below)[132-136]. Many of these genes had not previously been associated with schizophrenia, or even an observed function in the CNS, and between them represent a range of interesting avenues for research.

| Gene | Details |
|---|---|
| *ZNF804A* [133] | Encodes zinc-finger protein 804A (intronic) – evidence suggests it may play a role in neural migration, neurite outgrowth and synapse formation [137] |
| *NRGN* [132] | Encodes neurogranin (upstream) – a calmodulin-binding protein, substrate for protein kinase C and involved in post-synaptic signalling [138] |
| *TCF4* [132,135] | Encodes the E-protein, transcription factor 4 (intronic & upstream respectively) – important for normal brain development [139] |
| VRK2 [135] | Encodes the serine/threonine kinase vaccinia-related kinase 2 (upstream) – thought to influence the inhibition of neuronal apoptosis [135] |
| *MIR137* [134] | Encodes the short non-coding microRNA-137 (intronic) – implicated in regulating adult neurogenesis and neuronal maturation [140,141] |
| *CNNM2* [134] | Encodes cyclin M2 (intronic) – not previously associated with any CNS function |
| *MMP16* [134] | Encodes matrix metallopeptidase 16 (upstream) – not previously associated with any CNS function |
| *CSMD1* [134] | Encodes CUB and Sushi multiple domains 1 (intronic) – not previously associated with any CNS function |
| *PCGEM1* [134] | Encodes the long non-coding RNA prostate cancer gene expression marker 1 (upstream) – not previously associated with any CNS function |
| MHC Region [132,134,142] | Including region surrounding *HIST1H2BJ*, *PRSS16*, *PGBD1*, *NOTCH4*, *TRIM26* and *HIST1H2AG* |

***Table 1.1 Genome-wide significant variants associated with risk of developing schizophrenia***

CNVs have been associated with the risk of developing schizophrenia for some time [143], though several recent studies – again adopting a genome-wide approach – appear to have confirmed this postulate based on the presence of rare, but highly penetrant chromosomal deletions and duplications in various regions, suggesting a heterogeneous origin [126,136,144-146]. These recent leads provided by GWAS and CNV analysis can be added to *NRG1* (neuregulin 1), *DAOA* (D-amino acid oxidase), *RGS4* (regulator of G

protein signalling 4), *DTNBP1* (dysbindin or dystrobrevin-binding protein 1) and *DISC1* (disrupted in schizophrenia 1), which had previously been identified as promising candidates for predicting susceptibility based on numerous lines of evidence, though no risk alleles for any of these genes have as yet been unequivocally identified as causal [147].

The ability to simultaneously interrogate the whole genome to isolate genetic variants that confer an increased risk of developing schizophrenia has paid dividends. Several new lines of investigation have been identified that were not previously associated with the disorder, and will doubtlessly yield an improved understanding of the aetiology of schizophrenia that will hopefully lead to improved and safer medicines in the future. For example, since it's identification as a gene containing an intronic risk allele (rs1344706) for schizophrenia, *ZNF804A* has been shown through RNA knockdown studies to influence the expression of genes associated with cell adhesion, with the authors proposing a role for this protein in neural migration, neurite outgrowth and synapse formation [137]. In addition, Esslinger and colleagues provided evidence of altered functional connectivity in the brains of healthy volunteers carrying the rs1344706 risk allele using fMRI. Their study demonstrated a lack of functional coupling both within the dorsolateral prefrontal cortex (DLPFC) on the same side, and between these areas in each of the two hemispheres in volunteers carrying the rs1344706 risk allele. These same volunteers were also found to exhibit increased coordinated activity between the DLPFC and the hippocampus as compared to those carrying the non-risk allele [148]. Risk alleles do not however represent validated therapeutic targets for antipsychotic drugs, and considerable research attention will be needed to reach this point. Accordingly, well-characterised and widely available *in vitro* human neural tissue models could play a valuable role in the process; both to elucidate the normal role of these genes and the functional consequence of the associated risk alleles, but also for the identification and validation of potential novel drug targets. Indeed a native tissue *in vitro* platform would likely prove useful throughout the drug development process to improve the likelihood of providing efficacy and safety for novel treatments as they progress into the clinic.

The fact that risk alleles for schizophrenia have emerged as significant across the whole genome does not however mean that a "one-drug-fits-all" approach will prove most effective. There remains the possibility that while clinical diagnosis for schizophrenia is reliable, the diagnostic term itself is too nebulous. The emergence of causative alleles beyond highly penetrant CNVs and indeed, common pathophysiology, may therefore be reliant upon the distinction of clinical phenotypes responsible for the component syndromes that together represent the full spectrum of disorders currently described as schizophrenia [149]. Patient-derived, disease-specific iPS and iN cells hold the potential to represent pivotal tools for this avenue of investigation and indeed to model endophenotypes of other disorders that exhibit a polygenic origin.

Paradoxically, recent advances in our understanding of the genetics underpinning susceptibility for developing schizophrenia appear to have – if anything – widened the gap between our knowledge of the disorder's aetiology and our understanding of how to treat it. Several lines of evidence suggest schizophrenia is a product of aberrant *in utero* neural development including at times severe

pathophysiology in the absence of glial scarring and prodromal symptoms [122]. A premise partly supported by recent GWAS findings, in that several of the identified risk alleles are associated with genes involved with normal neural development [126]. How these newly identified risk alleles influence the molecular and cellular landscape of the adult brain is however yet to be determined. An alternative approach to investigate the biochemical environment of the schizophrenic brain is to provide a clearer and more detailed understanding of how currently available antipsychotics exert their action. By identifying the biochemical pathways that these drugs modulate to relieve the symptoms associated with schizophrenia, we may be able to identify alternative targets that can achieve a similar or improved therapeutic efficacy, without the occurrence of poorly tolerated side effects. Indeed, this same approach is being used to identify individual patients that may respond or suffer side effects in response to a specific drug, as discussed in section ***1.9***.

### *1.6.2 Antipsychotics*

Until the 1950s, and the serendipitous discovery of the antipsychotic properties of the phenothiazine, chlorpromazine [150], schizophrenia remained largely untreated. This led to the development of further phenothiazine derivatives, along with butyrophenones (e.g. haloperidol) and thioxanthenes (e.g. chlorprothixene), which together have been termed the typical antipsychotics [151]. While these drugs demonstrated efficacy in relieving the positive symptoms associated with schizophrenia, their ability to treat negative and cognitive symptoms were limited if not absent. Ironically, it was the often, severe side effects elicited by these drugs – movement disturbances resembling that of parkinsonianism – that led Arvid Carlsson to suggest they exert their action through the blockade of dopaminergic transmission [152,153]. It was later shown that the efficacy of antipsychotics was closely correlated with their ability to block dopamine $D_2/D_3$ receptors [154,155], indeed for some patients, treatment exploiting this mechanism appears sufficient, as demonstrated by the selective $D_2$ antagonist; amisulpride [156,157], though this compound has also recently been shown to demonstrate high affinity antagonism of the 5-$HT_7$ receptor [158]. For a time it was widely believed that antipsychotic efficacy was inextricably linked to these movement disturbances – termed extrapyramidal side effects (EPS). This belief was challenged however by the first description of the potent antipsychotic efficacy provided by clozapine, but in the absence of any associated EPS liability [159]. Clozapine's introduction was dogged by reports of it's propensity to provoke agranulocytosis – a potentially life threatening side effect relating to a substantial lowering of circulating leukocytes – and consequently only received approval for general use in the US in 1990 [114]. Not only did clozapine demonstrate improved clinical efficacy when compared to the typical antipsychotics, it also showed a lower propensity to cause EPS and was found to be effective in up to 30% of treatment refractory cases [160-162], and even reduce suicidality [163].

Clozapine's introduction heralded a new era for the treatment of schizophrenia and was closely followed by the introduction of several more chemically related compounds, including risperidone, olanzapine and quetiapine; defining a new class of antipsychotics – the atypicals. These compounds – in

some cases at least – were found to be more potent neuroleptics, showed greater potential in the treatment of negative and positive symptoms and reduced the occurrence of side effects associated with reduced dopaminergic activity, as compared to the typical antipsychotics. They did however bring with them their own repertoire of poorly tolerated side effects such as weight gain, hypercholesterolaemia, postural hypotension, diabetes and seizures [114,164]. This may be attributable to their possessing a more promiscuous pharmacological profile than their first-generation counterparts, with high levels of affinity in some cases reported at various dopaminergic, serotonergic, adrenergic, muscarinic and histaminergic receptors, see Figure 1.1.

Considerable work has been dedicated to determining the origin of atypicality (i.e. antipsychotic efficacy in the absence of EPS), in the hope that this property can be teased from the side effect liability these compounds possess. Meltzer and colleagues proposed that it was the ratio between dopamine $D_2$ and 5-$HT_{2A}$ receptor occupancy that was responsible for 'atypicality' [165], though this was challenged by the fact that this property was shared by the typical antipsychotics chlorpromazine and loxapine [166]. It should be noted that at the time antipsychotic efficacy was first correlated with dopamine receptor occupancy, the only atypical antipsychotic available was clozapine. In addition, Meltzer's hypothesis preceded the identification of further 5-HT receptor subtypes, later facilitated by molecular cloning, which showed that many of the receptors that had accounted for his $D_2$/5-$HT_{2A}$ ratio, were in fact 5-$HT_{2C}$ receptors [167]. Interestingly, a recent study by Richtand and colleagues indicated that while $D_2$ receptor occupancy is correlated with clinical efficacy for typical antipsychotics ($r$ = 0.54, $p$ = 0.046), this does not hold true for the newer atypicals ($r$ = 0.41, $p$ = 0.31)[168]. The same study did however implicate an important role for 5-HT receptor subtypes, suggesting that for typical antipsychotics the 5-$HT_{2C}$/$D_2$ affinity ratio ($r$ = -0.81, $p$ = 0.003) was a better predictor of clinical efficacy than that of $D_2$ or 5-$HT_{2C}$ alone. This inverse relationship suggests that 5-$HT_{2C}$ affinity may be responsible for exacerbating positive symptoms, though the same receptor has been linked with alleviation of $D_2$ blockade-induced EPS [169] and antidepressant properties [170], though also with the development of weight gain [171]. Interestingly, the 5-$HT_{2A}$/$D_2$ affinity ratio was more closely correlated with the clinical efficacy of typical ($r$ = -0.52, $p$ =0.082) than atypical ($r$ = -0.08, $p$ =0.869) antipsychotics, though neither reached significance. Finally, Richtand and colleagues demonstrated that atypical antipsychotic efficacy was strongly correlated with affinity ratios for $D_2$ (5-$HT_{2A}$/5-$HT_{1A}$) ($r$ = 0.80, $p$ = 0.031), and $D_2$ (5-$HT_{2C}$/5-$HT_{1A}$) ($r$ = 0.78, $p$ = 0.038)[168]. The authors of this study did however stress that these data should be treated with some caution for numerous reasons, many of which are discussed in more detail below.

Attempts to recreate the clinical efficacy of antipsychotics without targeting the dopamine $D_2$ receptor have so far failed. Much of this work has been inspired by the pharmacological properties of clozapine and has led to the development, but subsequent failure of compounds targeting $D_4$ (L-745,850), 5-$HT_2$ and $D_4$ (fananserin), 5-$HT_2$ (MDL-100907), and dopamine $D_1$ receptors (SCH-23390) upon reaching the clinic [156]. An alternative theory provided by Kapur and Seeman to explain the antipsychotic efficacy and reduced EPS liability of atypicals is that of fast dissociation from the $D_2$ receptor [166], indeed these authors go on to suggest that if a compound can achieve desirable binding kinetics at the dopamine $D_2$

receptor, binding of other receptors may be superfluous to producing atypical antipsychotic efficacy. Interestingly, the most recently licenced antipsychotic – aripiprazole – dissociates from the $D_2$ receptor at a considerably slower rate than even the typical antipsychotics [172], but is thought to achieve its atypical efficacy through partial agonism at the $D_2$ receptor [173], despite demonstrating a considerably non-specific pharmacology [174]. This is not to say that alternative mechanisms are not being explored as a means to treat schizophrenia. Several compounds are currently in clinical development that exploit mechanistically distinct targets to those of existing antipsychotics including glutamatergic AMPA and NMDA channels, tachykinin $NK_3$ and cannabinoid $CB_1$ receptors and the ER membrane associated receptor $\sigma_1$, though it is currently unclear whether these will provide improved efficacy over existing treatments [175,176]. A description of antipsychotic activity through the affinity of receptors to which they are known to bind at the cell surface would however be a gross over simplification. Upon receptor binding these drugs inevitably modulate a range of intracellular events from transient signalling to lasting transcriptional changes. Elucidation of these effects may well identify targets that can be used to develop novel compounds that demonstrate both greater selectivity and safety.

There are currently more than 20 antipsychotics licenced for use in the UK and that are typically used in the treatment of schizophrenia, though are widely prescribed for numerous other conditions. According to the website of the Medicines and Healthcare products Regulatory Agency (MHRA: www.mhra.gov.uk) – an executive body of the UK government's Department of Health responsible for ensuring that medicines and medical devices work, and are acceptably safe – antipsychotics drugs:

> "…are mainly used to treat mental health conditions such as schizophrenia and other psychoses, agitation, severe anxiety, mania and violent or dangerously impulsive behaviour.
>
> They are also used to treat nausea and vomiting, intractable hiccough and for the management of pain and associated restlessness in palliative care."

The introduction of antipsychotics undoubtedly revolutionised the treatment of schizophrenia and arguably psychiatric treatment in general, yet despite their widespread use both on- and off-label, their mechanism of action remains unclear. This in itself does not constitute a problem, especially when we consider that the mode of action of paracetamol was only recently determined, though was first used clinically in 1887 [177,178]. Unfortunately, many patients remain treatment refractory, with just 50% - 70% of those prescribed antipsychotics experiencing full or adequate symptom relief [179,180]. This represents a significant problem, as patients who remain symptomatic, or suffer adverse affects due to drug treatment are less likely to remain treatment compliant [120]. In addition, the longer the period of inadequate symptom relief, the poorer the long-term prognosis for the patient, especially with regard to the arguably more debilitating negative and cognitive symptoms [115,181,182]. To gain a clearer understanding of the mechanism through which these compounds exert both their therapeutic and adverse effects, it is important to consider the targets with which they interact.

## *1.7 G Protein-Coupled Receptors & Antipsychotics*

As mentioned previously, antipsychotics are known to target a range of different cell surface, membrane spanning receptors though the vast majority of these belong to a family of signal transduction molecules referred to as G-protein coupled receptors (GPCR). Due to the lipophilic nature of these compounds – a property that allows them to gain brain penetrance – the possibility also remains that they could additionally target intracellular targets. Our understanding of these receptors has been enhanced considerably in recent years and as described by Terry Kenakin:

> "…it is clear that, rather than being 'on–off' switches, [GPCRs] are more akin to 'microprocessors' of information." [14]

GRCRs targeted by currently available antipsychotics include dopamine $D_1$, $D_2$, $D_3$, $D_4$ and $D_5$, 5-$HT_{1A, 1B, 1D, 1E, 2A, 2B, 2C, 5, 6}$ and $_7$, adrenergic $\alpha_{1A}$, $\alpha_{1B}$, $\alpha_{1B}$, $\alpha_{2A}$, $\beta_1$ and $\beta_2$, muscarinic acetylcholine $M_1$, $M_2$, $M_3$, $M_4$ and $M_5$, and histamine $H_1$, $H_2$, $H_3$ and $H_4$. In addition they are also known to additionally demonstrate affinity for various transporters and ligand-gated ion channels [174,183,184]. Most, if not all of these receptors demonstrate discrete, cell type-specific expression within the brain, though many are additionally expressed in the periphery and may therefore contribute to the diverse side-effect profile these compounds exhibit. In addition, many of these receptors can exhibit both pre and postsynaptic membrane expression and can therefore alter their functional consequence. GPCRs provide a means for extracellular signals to exert an effect across the cell membrane and consequently provide a method of communication between cells and their external environment – both physical and chemical. The classical view dictates that upon ligand binding, GPCRs undergo a conformational change that initiates signalling via an intracellularly coupled heterotrimeric G protein – so named because of their GTP-dependent activity. In the inactive state heterotrimeric G proteins are comprised of a GDP-bound Gα subunit and a Gβγ subunit complex. The ligand-induced conformational change of the GPCR confers upon it an ability to exchange the Gα subunit-bound GDP for GTP and consequently causes its dissociation from the Gβγ subunit, leaving it free to provoke the activity of various different effector proteins [36]. In humans there exist 16 distinct genes encoding 21 different Gα subunits, 5 genes encoding 6 Gβ subunits and 12 Gγ subunits [185]. The heterotrimers are functionally distinguished into 4 families of which 3 are relevant to receptors targeted by antipsychotics [186]:

- $G\alpha_s$ family (comprising $G\alpha_s$ and $G\alpha_{olf}$) activation leads to a stimulation of adenylyl cyclase (AC) and consequently, an intracellular rise in cAMP, which itself is a regulator of numerous intracellular targets including enzymes and channels (e.g. protein kinase A (PKA) and hyperpolarization-activated cyclic nucleotide-gated channels);
- $G\alpha_i$ family (comprising $G\alpha_i$ and $G\alpha_o$) activation leads to an inhibition of AC and consequently, an intracellular fall in cAMP levels, leading to reduced activity of cAMP-dependent proteins;
- $G\alpha_q$ family (comprising $G\alpha_q$, $G\alpha_{11}$, $G\alpha_{14}$, $G\alpha_{15}$ and $G\alpha_{16}$) activation stimulates the catalytic activity of phospholipase C-β (PLC-β) family proteins, promoting the hydrolytic cleavage of the plasma membrane lipid phosphatidylinositol 4-5-bisphosphate ($PIP_2$) to produce inositol 1,4,5-

trisphosphate ($IP_3$) and diacylglycerol (DAG). $IP_3$ goes on to target receptors found on the surface of the endoplasmic reticulum and causes the release of $Ca^{2+}$ from intracellular stores while DAG causes activation of protein kinase C, leading to activation of Raf1 and initiation of the ERK/MAPK (extracellular signal-regulated kinase/mitogen-activated protein kinase) pathway.

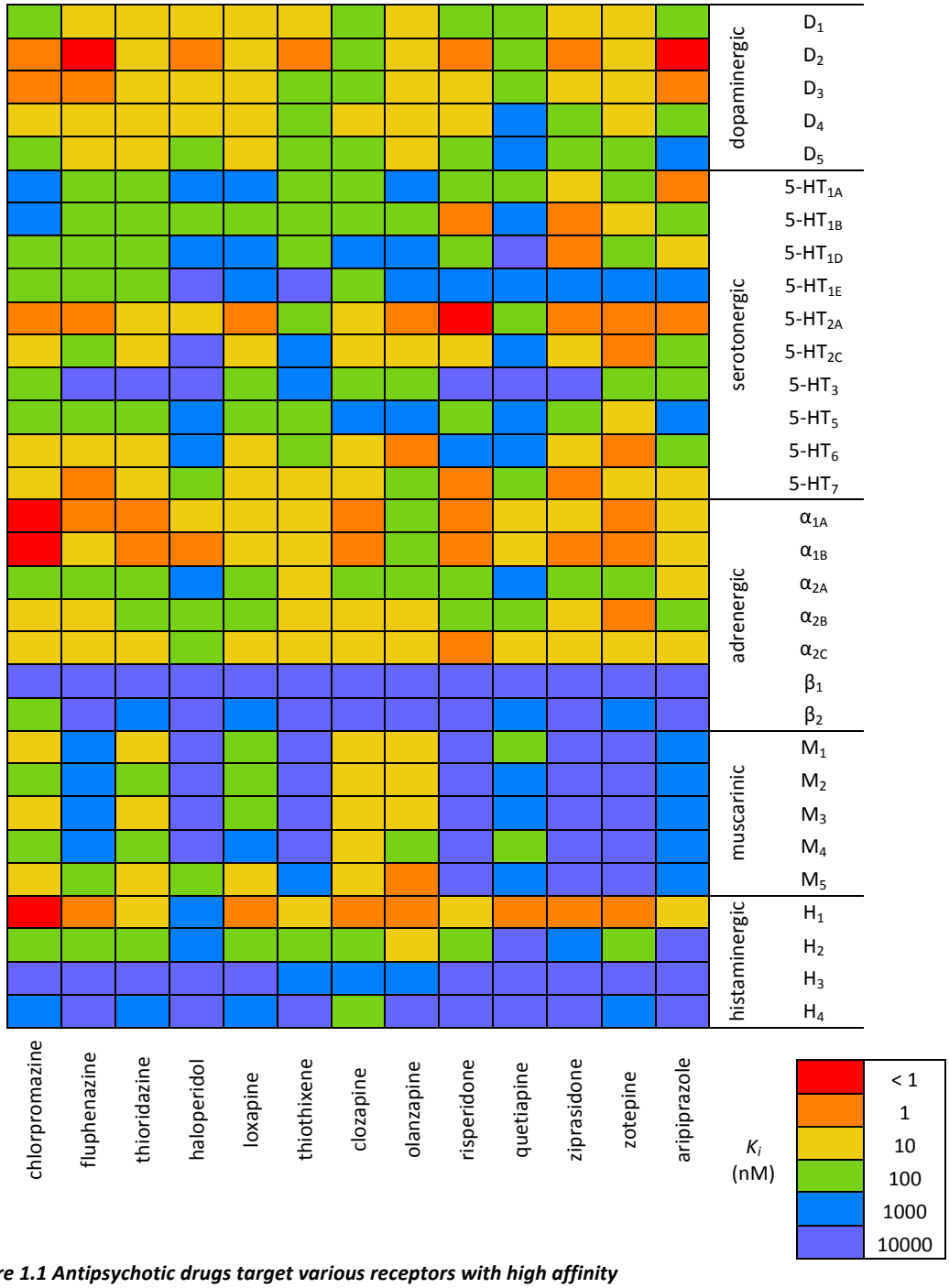


***Figure 1.1 Antipsychotic drugs target various receptors with high affinity***
Heat map showing approximated affinities of different antipsychotic drugs towards a range of neurotransmitter receptor targets. Adapted from [183].

These descriptions however, illustrate a gross over simplification of the functional consequences that ligand binding to these receptors can provoke. In addition to the modulatory effect of $G\alpha_s$ and $G\alpha_i$ upon AC, they have also been shown to modulate the activity of c-Src tyrosine kinases [187]. On the other hand, while the Gβγ subunit complex was originally thought just to exert an inhibitory effect upon the Gα subunit, it has recently been shown to be capable of provoking it's own repertoire of responses. These include stimulation of AC and PLC-β, as seen for the Gα subunits, but they can also modulate activity of inward rectifying $K^+$ channels, $Ca^{2+}$ channels, G protein-coupled receptor kinases (GRK) and PI3Kγ [188-190]. It should be noted that many of these signalling molecules exist as distinct isoforms, though the functional consequence of many of these variants remains unclear. With multiple different receptors expressed by a single cell, and through the discrete expression of signalling molecules responsible for transducing their effects, GPCRs provide cells with a staggeringly complex capacity to respond to a given stimuli. However, ligand binding and the subsequent activation or inhibition of a downstream signalling effector is only the beginning of the story. As mentioned previously, the functional expression of these receptors at the cell surface following *de* novo synthesis is under strict regulation, but similarly precise regulation is exerted at every level of their activity, and that of their downstream effectors. In addition, these molecules cooperate with a range of different cell surface and intracellular molecules – including themselves – to regulate the behaviour of the cells that express them.

### *1.7.1 GPCR Regulation*

GPCRs are also subject to dynamic regulation though the activity of regulator of G protein signalling (RGS) family proteins, 37 of which are encoded by the human genome and exert their action by behaving as GTPase-activating proteins, accelerating the rate of Gα-bound GTP hydrolysis [191]. This allows the Gα and Gβγ subunits to reassociate and therefore attenuate the extent of downstream signalling [36]. Another mechanism through which GPCRs are subjected to regulation occurs via phosphorylation of specific residues on the intracellular loops exposed on the cytoplasmic face of the plasma membrane. This can occur in the absence of bound ligand via the activity of second messenger-dependent protein kinases such as PKA or PKC, and is referred to as heterologous desensitisation [190]. Conversely, homologous desensitisation occurs in ligand occupied receptors through the activity of GRK proteins. The catalytic activity of these enzymes is provoked by receptor activation and also leads to phosphorylation of the intracellular loops of GPCRs. This in turn facilitates the recruitment of β-arrestin-1 or -2, which inhibits the receptor from interacting further with it's associated G protein despite continued agonist-mediated activation of the receptor [189]. β-arrestins can precipitate receptor internalisation by recruiting proteins involved in clathrin-mediated endocytosis and are subsequently returned to the plasma membrane or subjected to endocytic degradation [192]. In addition to their role in desensitisation, β-arrestins have recently been shown to initiate further, G protein-independent signalling by serving as a scaffold protein for additional signalling molecules such as mitogen-activated protein kinases (MAP kinases), Akt and c-Src [191]. Indeed, evidence suggests that these β-arrestin-mediated signalling events are able to continue even after receptor internalisation [193].

### *1.7.2 Functional Selectivity*

To confuse matters further, while antipsychotics modulate the activity of numerous different receptors, the functional consequence of these interactions at any one of those receptors is not necessarily constant. Indeed several of the regulatory mechanisms described above are capable of altering the affinity of a given ligand for a receptor by altering the properties of the receptors binding pocket [192]. In addition, the G protein coupling partner of a given GPCR is not a constant and can be subject to promiscuity. For example, with respect to dopamine receptors – the major target of currently available antipsychotics – while it is widely accepted that dopamine $D_1$ and $D_5$ receptors couple to $G\alpha_s$ and $D_2$, $D_3$ and $D_4$ couple to $G\alpha_i$, it has also been shown that $D_1$ can additionally couple to $G\alpha_{olf}$, and $D_2$, $D_3$ and $D_4$ also couple $G\alpha_o$ and $D_5$ can couple $G\alpha_q$ [191,194]. The ability of a single GPCR to promiscuously couple to different G protein-coupling partners has challenged the traditional pharmacological concept of intrinsic efficacy [195]. Numerous reports of ligands capable of preferentially activating distinct signalling events from a single receptor have now led to the concept of functional selectivity [195,196]. In the most extreme cases this can result in a single ligand exhibiting the characteristics of both an agonist and antagonist at the same receptor. For example, chronic exposure to antagonists is typically associated with receptor upregulation while exposure to agonists is conversely linked to receptor internalisation, a process thought to allow cells to homeostatically regulate the extent to which they can be stimulated [197]. However, some 5-HT antagonists such as loxapine and clozapine have paradoxically been shown to provoke a downregulation of 5-$HT_{2A}$ receptor number both *in vivo* and *in vitro* despite lacking measurable activity at those receptors [198]. This does not however appear to be an isolated quirk of 5-$HT_{2A}$ receptors as certain antagonists of $\beta_2$ adrenergic, μ-opioid, vasopressin $V_2$, cholecystokinin and parathyroid hormone receptors have also been reported to demonstrate this property [195,197,198].

It is likely that functional selectivity – the capacity of a ligand to preferentially provoke one functional response over that of another – may actually lie at the heart of the mechanism of action that some compounds exhibit. Aripiprazole has been shown to demonstrate particularly high affinity and slow dissociation from the dopamine $D_2$ receptor, yet exhibits low hyperprolactinemia and EPS liability [172,173,183]. This effect was shown to be mediated by partial agonism – complete occupancy achieving a submaximal response – of the $D_2$ receptor, but this is only part of the story [199]. By accessing aripiprazole's capacity to provoke $D_2$-mediated cAMP accumulation, ERK1/2 phosphorylation, arachidonic acid release, control of $K^+$ currents and $D_2$ receptor internalisation *in vitro* – this molecule has actually been shown to demonstrate functional selectivity at this receptor [174,200,201]. Ultimately, it is the assay used to assess efficacy of a given ligand that determines whether it is designated as a full agonist, partial agonist or neutral antagonist, leading Kenakin to use the term 'texture' to describe the nature of a compound [14,202]. In an attempt to exploit functional selectivity as a means to maximise antipsychotic efficacy, one group has recently provided evidence of the development of several compounds modelled on aripiprazole that show considerable bias towards β-arrestin-selective signalling over cAMP accumulation via the $D_2$ receptor *in vitro* and promisingly demonstrate antipsychotic-like activity *in vivo* [203]. This novel approach to drug design may provide a means with which to achieve therapeutic efficacy without provoking side effects from the same receptor [196].

### *1.7.3 Allosterism*

Another consideration with respect to determining the activity of drugs at GPCRs is that these receptors represent allosteric systems, an aspect that is often neglected in the way drug activity is assessed [14]. The traditional view of GPCR modulation is that of a drug exerting an effect through its interaction with a receptor's binding pocket, or pharmacophore. A drug acting in this manner is referred to as an orthosteric ligand. Alternatively, an allosteric ligand binds to a site on a receptor that is distinct from that bound by an orthosteric ligand, and can not only modulate the affinity of an orthosteric ligand for the receptor, but also affect its efficacy [204,205]. These allosteric interactions can have both a positive and negative effect and have therefore been termed positive and negative allosteric modulators (PAM and NAM respectively). A useful account to explain both functional selectivity and allosterism is provided by Kenakin and Miller [206]. They describe GPCRs as structurally and energetically disordered molecules, capable of assuming multiple different configurations through which the receptor can constitutively cycle or be forced into. This allows the receptor to either favourably interact with a specific downstream signalling partner or alter the shape of its orthosteric site, consequently altering ligand affinity. Allosterism is not restricted to GPCRs however; this property is exploited in ligand-gated ion channels by benzodiazepine anxiolytics through their positive allosteric modulation of $GABA_A$ receptors [204], while the anticonvulsant lamotrigine is thought to exert its action through positive allosteric modulation of $GABA_A$ receptors and negative allosteric modulation of voltage-gated $Na^+$ channels [207,208]. While no currently available antipsychotics demonstrate allosteric interactions as their primary mechanism, the primary metabolite of clozapine – *N*-desmethylclozapine has been shown to allosterically modulate the activity of the acetylcholine $M_1$ receptor [209]. Interestingly, this brain penetrant clozapine metabolite has also been shown to demonstrate partial agonism at $D_2$ and $D_3$ receptors – similar to that exhibited by aripiprazole and likely contributes to clozapine's superior antipsychotic efficacy in the absence of EPS liability [210]. This, and other observations have led to *N*-desmethylclozapine being pursued as an antipsychotic medication in it's own right [175]. Several allosteric modulators are currently in clinical development and include PAMs targeting $M_1$, $M_4$, mGluR2, mGluR5, AMPA and NMDA [175,176,211].

### *1.7.4 Receptor Dimerisation*

The capacity of GPCRs to form functional oligomers both with themselves (homodimers), other GPCRs, and in some cases ion channels (heterodimers) has functional consequences that are only beginning to be revealed. The ability of GPCRs to form homodimers was first observed for metabotropic glutamate receptors (mGluR) [212] – members of the class C GPCRs, which also includes metabotropic GABA ($GABA_B$) receptors amongst others [213]. Homodimerisation of mGluRs and $GABA_B$ receptors was found to occur constitutively at the cell surface and to be facilitated by the presence of a disulphide bridge linking the large extracellular domains characteristic of this class of GPCRs, together forming the orthosteric binding site [212]. It has also been shown that receptors within this class are capable of heterodimerisation, as in the case of $GABA_{B1}$:$GABA_{B2}$; an interaction necessary for their functional cell surface expression, and

mediated through an intracellular – though in this case, not covalent – interaction between coiled-coil domains located on each receptors carboxyl terminus [189]. In addition, $mGluR_{1A}$:$GABA_B$ heteromers have also been identified in native tissues, which is likely facilitated through interaction with cytoplasmic scaffold proteins, and demonstrate downstream functional diversity as compared to their monomeric counterparts [213,214].

This same phenomenon has more recently been reported to occur between class A GPCRs – of which, the majority of receptors targeted by antipsychotics belong – and also between members of class A and class C receptors. Numerous receptor oligomers have been reported and include: $D_1$:$D_2$, $D_2$:$D_3$, $D_1$:$D_3$, adenosine $A_1$:$D_1$, adenosine $A_{2A}$:$D_2$ [191,215,216], $D_1$:5-$HT_{1B}$ [217], $D_2$:5-$HT_{2A}$ [218,219], $mGluR_2$:5-$HT_{2A}$ [220,221]. There is also a considerable body of evidence to suggest that many GPCRs are often, functionally expressed as homodimers, and include: $D_1$:$D_1$, $D_2$:$D_2$, 5-$HT_{2A}$:5-$HT_{2A}$, 5-$HT_7$:5-$HT_7$ [191,222,223]. The functional consequence of these diverse receptor heterodimers is currently under considerable scrutiny and it has been suggested they can influence virtually every aspect of a given receptors pharmacological properties, from the nature and intensity of second messenger signalling to ligand affinity, selectivity and dissociation [206,215,224], while also influencing receptor expression, trafficking and internalisation [35,36,225]. Much of this work was initially performed in heterologous expression systems and was later confirmed both in native tissues *in vitro* and *in vivo* [214,222]. While much of the early work was performed using techniques such as immunoprecipitation and classical pharmacological approaches, the field has recently been greatly enhanced by the development of techniques such as fluorescence resonance energy transfer (FRET) and bioluminescence resonance energy transfer (BRET), that allow functional interactions between receptors or indeed any proteins that come into close proximity with each other to be observed. This new perspective with respect to the way in which GPCRs function in their native environment has highlighted the need for using native tissue to obtain meaningful pharmacological and physiological data regarding the way in which any pharmacological agent exerts it's effects. This was recently highlighted in a study by Fribourg and colleagues, where they demonstrated the functional consequence of 5-$HT_{2A}$:mGluR2 receptor heterodimers compared to individual receptor monomers in a heterologous expression system following ligand binding to either receptor. They reported a functional integration of ligand-induced response at the receptor level, leading to a subsequent modulation of downstream signalling that could be recapitulated in ex vivo membrane preparations and observed at the behavioural level *in vivo* [221]. This multidimensional approach to investigate what amounts to a ligand-receptor interaction promotes the importance of the assays used to evaluate these properties, and is a perfect example of the concept of 'texture' with respect to ligand response [202].

Either through covalent, electrostatic or accessory protein mediated interactions, many receptors and signalling molecules have been shown to functionally modulate each other's properties and effects. It is important that GPCRs should not be studied in isolation; many of the downstream signalling events initiated by GPCR activation are common to, or potential targets of, alternative cell surface signalling molecules such as tyrosine kinase receptors, integrin receptors, ligand- and voltage-gated ion channels and transient receptor potential (TRP) channels. While much of the pioneering work in this area has

been in the field of cardiovascular medicine, endocrinology and oncology, there is a growing body of evidence suggesting the presence of functionally significant crosstalk between these diverse signalling molecules in neurons and glia [226-230]. One particular example of this type of crosstalk was demonstrated using single isolated, CA1 pyramidal neurons *in vitro* [231]. This study demonstrated that a dopamine $D_4$ receptor-mediated increase in intracellular $Ca^{2+}$ concentration was responsible for a $Ca^{2+}$-dependent inactivation of NMDA receptors. Most interestingly, this dopamine receptor-mediated effect was shown to be dependent upon its ability to transactivate platelet-derived growth factor receptor β (PDGFRβ). Furthermore, while this effect was observed in CA1 pyramidal neurons, it was shown to be absent in cultured hippocampal neurons [231]. This study therefore provided evidence of GPCR-mediated, tyrosine kinase receptor-dependent modulation of ligand-gated ion channels. In addition, the fact that these effects were also shown to be cell type specific only serves to further illustrate the complexity of signalling events associated with GPCRs, and reinforces the need for making use of native tissue models to investigate pharmacological effects *in vitro*. Another mechanism through which functional integration and crosstalk between diverse signalling molecules is known to occur is through so-called signalling nodes such as DARPP-32 and GSK-3 both of which have been implicated as having a role in schizophrenia and antipsychotic action [232-234]

It is clear that individual GPCRs interact either physically or functionally with a range of different receptors and accessory proteins. These have been shown to regulate and modify both the nature and extent of intracellular signalling as a consequence of ligand binding – which itself can be effected. Like GPCRs, the molecules with which they interact have also been shown to demonstrate cell type-specific expression [26,27], meaning that a given receptor can provoke varying responses from the same ligand depending upon the interacting receptors and accessory proteins being expressed by the cell type investigated, as described above for dopamine-induced responses in the hippocampus [231]. This even occurs at the single cell level with compartmentalisation mediated by lipid rafts, caveolae or scaffold proteins creating specific domains at the plasma membrane where proteins such as GPCRs and specific downstream effectors are brought together to ensure a particular response [235-237]. Taken together, this again highlights the importance of using cell types relevant to a native tissue to provide meaningful data with regards to the effect of a particular ligand.

### *1.7.5 It's All in the Assay*

In the knowledge that individual GPCRs are capable of provoking a 'rich' pharmacological response, even from a single ligand – it is important that to investigate them, a similarly diverse range or sufficiently multifarious assay should be used to determine a specific ligands' efficacy. Up until the 1990s, drug development relied heavily upon the use of whole animals and animal-derived, *in vitro* tissue preparations such as guinea pig ileum and rat uterus. These were capable of delivering large amounts of both quantitative and qualitative data though were labour intensive and therefore, very low throughput [14]. The adoption of combinatorial chemistry and a concurrent period of considerable consolidation

within the pharmaceutical industry through mergers and acquisitions meant that compound libraries grew exponentially [238,239]. This necessitated the implementation of techniques such as radioligand binding and biochemical reporter assays, that could be miniaturised and combined with robotics to provide adequate capacity to identify lead compounds from these enormous libraries while trying to keep costs down [240]. These high-throughput screening (HTS) methodologies changed the drug discovery process to a numbers game; with large, diverse libraries more likely to yield promising lead molecules for a given target. However, while increasing capacity, the application of HTS did however compromise the depth of information obtained for a given molecule and is prone to providing considerable levels of false positive 'hits' and false negatives, due to the narrow manner in which they are used to determine efficacy. Cell based assays were also adapted for HTS, to measure ligand-induced second messenger activation, G protein stimulation and $Ca^{2+}$ transients for example – and were powerfully driven by advances in genomics that allowed biochemical targets to be combined with fluorescent reporter systems in robust cellular backgrounds [240].

The fact that single GPCRs can provoke functionally distinct signalling responses, the extent of which can be biased by ligands or the cellular environment means that multiple assays are needed to determine the full functional response of a given compound. The application of FRET and BRET has meant that a staggering number of new assays have recently become available, meaning that instead of measuring, for example, just intracellular concentrations of $Ca^{2+}$ or cAMP, many other second messengers can be measured, or indeed their phosphorylation status. Several companies now even offer bespoke assay development to monitor novel signalling molecules to suit your area of study, while others provide instrumentation to perform automated electrophysiology. The functional readout obtained however is restricted to the assay that is employed, meaning only the effect that is measured can be found. Several new technologies – or the application of old ones – are promising a much richer and/or holistic picture of drug-receptor-cellular response. High content screening can combine both real-time imaging of cellular activities and endpoint evaluation of a given parameter in a high-throughput multiwell format. With the use of different antibodies, these assays can be used to measure a range of different cellular processes including proliferation and migration rate, to neurite outgrowth and synapse formation [241]. These screening platforms can also be used to detect a host of signalling events including GPCR or ion channel activation and protein-protein interactions, with the added advantage that different assays can be multiplexed into a single screen [242,243]. An example of this is provided in the use of the pH-sensitive cyanine dye – CypHer-5 – to monitor GPCR internalisation. CypHer-5 demonstrates little or no fluorescence at pH 7.4, that of the normal extracellular environment, but demonstrates high levels of fluorescence as the surrounding pH drops towards 6.1 – as occurs in endosomal vesicles. CypHer-5-conjugated antibodies can therefore be used to label a GPCR of interest, and exploit the fact that upon agonist binding, most GPCRs are internalised into acidic endosomes. Furthermore, CypHer-5 has the added benefit of demonstrating excitation and emission frequencies at the red end of the spectrum (633 nm and 695 nm respectively), meaning the assay can be integrated to simultaneously monitor, for example, the translocation of GFP-tagged accessory proteins of other receptors [244].

A limiting factor with respect to the assays so far mentioned – even if multiplexed – is that detection is limited to that which the assay seeks to measure. This has led to the development of label-free approaches to evaluate cellular responses to pharmacological agents. The Epic platform, developed by Corning Life Sciences and the CellKey platform, developed by Molecular Devices rely on optical and electrical approaches respectively to measure ligand-induced cellular mass redistribution. They take advantage of the fact that many ligands are capable of provoking either a change in the shape or distribution of molecules that comprise the cells, and provide a readout of the integration of these changes [14]. These instruments can be used to measure characteristically unique patterns of activity that can be linked to specific signalling pathways [245-247]. The label-free approach of both of these techniques removes the need for reporter systems, facilitating a move away from the use of recombinant cell lines and the application of cell types representative of native tissues. Another approach that could facilitate the transition to the use of native tissue cell lines and provide a label-free, and even hypothesis-free means to detect ligand-induced cellular responses is that of mass spectrometry. This technology has been around for decades but has recently benefitted from considerable advances in protein separation, sensitivity, quantitation and throughput, allowing it to be used not only to provide a measure of protein levels but also determine the presence of post translational modifications such as the phosphorylation or ubiquitination status of a given protein [248,249].

The expression of multiple different receptor isoforms for each neurotransmitter allows these chemical messengers to provoke a range of different responses in the various cell types they are exposed to. However, as we have learned, upon ligand binding these receptors do not behave as the simple on/off switches they were once thought to be. Through promiscuous G protein coupling, heterodimerisation, accessory protein recruitment and G protein-independent signalling they are able be elicit a range of different cellular responses, each at varying intensities. Their activity is modulated by a range of different intracellular mechanisms that control everything from the magnitude of the response they can provoke and which downstream effectors they can activate to their affinity for a given ligand or whether the receptor is even available at the cell surface. Through their interaction with different receptor classes and the modulation of signalling nodes they are capable of participating in the integration of signals from various different sources and influence the outcome of various other ligand-receptor interactions. If this were not enough, virtually every protein that is involved at each of these levels of signal transduction and modulation are themselves expressed as different isoforms, and it remains to be seen how these influence ligand-evoked responses. Taken together, this highlights the need for a range of different assays and techniques to achieve a thorough understanding of the pharmacology and physiology of a given molecule. However, when we add to this the discreet expression of different receptors and signalling molecules in different cell types, it becomes clear that to obtain a physiologically meaningful picture of the effects of a given drug, we must also employ the use of physiologically relevant models.

It shouldn't be forgotten however that this bewildering complexity is just an account of normal cell signalling! To understand the mechanism of antipsychotics we must appreciate the effects they exert

through their simultaneous modulation of numerous different receptors. Due to their 'dirty' pharmacology, antipsychotics are likely to influence a vast array of different signalling events in any given cell, and therefore begs the question of which assay(s) should be used to explore their activity to provide a global account of their effects.

## *1.8 Transcriptomics & Drug Mechanism*

Another technique that offers a hypothesis-free approach to investigate drug action is that of transcriptomics. Until recently, this was performed using expression microarrays, an assay platform that allows the extent of each genes' expression to be quantified simultaneously. These tend however to only detect the expression of protein-coding mRNA – the exome, though recent studies have shown that these are not the only types of genes that affect the behaviour of cells – as exemplified by the genetic risk for developing schizophrenia associated with the micro RNA; *MIR137* [134]. In addition, microarrays often lack the sensitivity to detect genes that demonstrate low expression frequency, such as GPCRs. A very recent alternative approach is the use of so called deep or next generation sequencing, which provides the capacity to qualitatively and quantitatively detect all RNA transcripts, regardless of their function, annotation status or expression frequency [250]. Next generation sequencing for transcriptomics – or RNA-Seq – promises to provide a more detailed picture of the intracellular dynamics of the genome by revealing the identity of every expressed transcript, but currently remains relatively expensive and low throughput [251].

Along with provoking or modifying transient signalling events, ligand-receptor interactions are also known to cause sustained cellular responses through changes in gene expression. The most obvious of these are the immediate early genes, several of which are expressed upon sustained activation of the MAPK/ERK pathway – a ubiquitous consequence of GPCR activity – and include *c-Fos, c-Myc* and *Fra1* [252]. Indeed, discreet neural expression of the immediate early genes *c-Fos* and *Arc* has been shown to occur and sometimes indicate efficacy in response to antipsychotic treatment in laboratory animals [253-255]. ERK1/2 activation is also known to cause the phosphorylation of a range of other molecules that themselves have their own transcriptional consequences such as ribosomal S6 kinases (RSKs), Elk-1, Ets-1 and CREB [256]. In parallel with the highly complex pharmacology of antipsychotics, these compounds have also been shown to affect the expression of a wide range of different genes that appear not to be restricted to those expressed as a consequence of ERK1/2 activation. Several different transcriptomic studies have reported gene expression changes in response to various different antipsychotics both in whole animals and *in vitro*. However, while each of these studies have identified a host of different genes that exhibit altered expression in response to antipsychotics – such as ligand- and voltage-gated ion channels, GPCRs, signalling molecules, transcription factors and biosynthetic enzymes [257-263] – few, if any changes have been replicated in any two studies. Like the pharmacological platforms described above; capable of measuring ligand-induced cellular mass redistribution or high content screening, transcriptomics allows the summation of cellular effects provoked by a pharmacological agent to be investigated simultaneously – but additionally allows the component parts to be evaluated individually.

This technique lends itself well to the investigation of antipsychotic mechanism due to their promiscuous and complex pharmacology, which is reflected in their numerous therapeutic effects, and unwanted side effects.

As discussed above, **this study aims to develop an *in vitro*, native tissue-based platform with which to transcriptomically investigate the mechanism of action of antipsychotic medications**. Transcriptomics has now been widely applied as a means to investigate the mechanism of action of antipsychotics – and has been utilised in various different ways. These can be broadly divided into *in vivo* and *in vitro* studies. Several *in vivo* studies have been carried out using post mortem tissue from schizophrenic patients, and have the advantage of representing disease specific tissue. At the same time however, this also represents one of the biggest drawbacks. Obtaining post-mortem tissue of sufficient quality to perform transcriptomic analysis is extremely difficult. Ideally, samples would come from patients that demonstrated minimal disease heterogeneity and demonstrate an absence of psychiatric co-morbidity – a difficulty when much of the available tissue is obtained from suicide victims. The tissue would also need to be sourced from age-matched, antipsychotic treated and drug naïve patients with consistency in how the tissues are collected and in sufficiently high numbers [264-266]. Added to this is the additional confounding problem that changes in gene expression may only be discernible, or perhaps relevant, in discrete cell-types – indeed, little change is seen in neuronal number except for reductions in parvalbumin-positive medium spiny GABAergic interneurons of the cortex. Laser capture microscopy can be used to isolate discrete cell populations to prevent expression changes being diluted by message from more numerous – and perhaps alternatively affected – cell types [267], though this technique is highly labour intensive and it often proves difficult to obtain adequate quantities of material. A recent study demonstrated a perhaps more efficient method to isolate discreet cell populations whereby fluorescence-activated cell sorting (FACS) was used as a means to separate oligodendrocytes from whole rat brain for subsequent microarray analysis [268]. This approach was facilitated by the fact that oligodendrocyte cell surface markers are particularly well characterised as compared to those of neuronal or astrocytic subtypes. FACS on fixed tissue – which is the usual treatment for post mortem human tissue - also presents technically difficulties due to the propensity of cells to poorly segregate and may therefore yield misleading data due to poor sorting. Transcriptomic analysis of human post mortem tissue has been presented as a means to investigate both the pathophysiology of schizophrenia and the mechanism of action of antipsychotics. Attributing observed gene expression changes to a consequence of either one is however difficult, and is perhaps confounded by a masking of markers associated with the underlying pathophysiology as a consequence of antipsychotic treatment [269,270].

Another *in vivo* transcriptomic approach that has been used to investigate the manner in which antipsychotics exert their action makes use of drug treated animals – usually rodents. These studies provide the advantage of controlling many of the factors that generate a source of variability when performing equivalent studies using human post mortem tissue. The treatment regime, including the drug, dose and exposure period can all be standardised along with the genetic background of the animals, their age, weight, diet and provide drug naïve controls. The number of animals used can also be

controlled to ensure sufficient experimental power, as can the method, storage and choice of tissues or brain regions collected. This approach provides the advantages of evaluating antipsychotics in a whole animal environment; including observing effects that may occur as a consequence of active metabolites, a neurochemical network environment that is necessary to observe many of the effects of antagonistic compounds such as pharmacological tone, and a means to assess non central effect that may contribute to side effects such as weight gain and hyperlipidaemia. These studies do however have the obvious drawback of not providing native human tissue and the cellular and physiological differences that are associated with it. Rats for example are known to metabolise pharmacological agents much more rapidly than do humans, meaning that maintaining clinically relevant concentrations of drug in the brain is a particular challenge [271]. In humans it has been shown that the therapeutic efficacy of antipsychotics is only achieved once striatal dopamine $D_2$ receptor occupancy levels rise above approximately 60%, though levels above 80% have been associated with parkinsonian-like side effects [272-275]. Therefore, to accurately model clinically effective antipsychotic drug treatment in animals it may be important to experimentally maintain dopamine $D_2$ receptor occupancy within this same therapeutic window [156]. However, this could be resolved with the use of depot dosing or the use of drug delivery pumps so as to ensure consistent drug exposure, and therefore maintain central receptor occupancy at clinically efficacious levels. Another drawback is the fact that these experiments are conducted in 'normal' animals, i.e. they are not suffering from schizophrenia, and it remains unclear how the effects of antipsychotics may vary when exposed to a 'normal' rather than schizophrenic neurochemical environment. For example, it may be safe to predict that antipsychotics may exert a greater effect in a brain that demonstrates greater dopaminergic tone due to their considerable antagonistic effects at dopamine receptors. However, this consideration may be facile when the differences in the neurochemical environment between species are taken into consideration [269].

As with human post mortem tissue, it may also be desirable to separate out different cell types, so as to improve the likelihood of identifying gene changes that may be unique to neurons, astrocytes or oligodendrocytes. This could be facilitated, as mentioned above, by the use of FACS, though in these rodent studies this could be performed on fresh rather than fixed tissue. The problem of limited cell surface markers with which to sort neurons and astrocytes could also be potentially resolved with the use of bioluminescent genetic constructs, as has been shown previously to isolate different striatal cellular subtypes [276]. Indeed, by combining FACS with a system such as Brainbow – whereby multiple different cell-specific proteins can each be genetically manipulated to form fluorescent fusion protein conjugates [8] – this could provide a powerful means with which to investigate gene expression changes in several groups of discrete cell types or even subtypes from the same animal. To date, *in vivo* transcriptomic experiments in antipsychotic treated animals have identified a handful of novel genes, though none of these have yet been consistently replicated in more than one study, and this is likely to be a consequence of the varying ways in which each were performed, controlled and the strains of animals used [269].

While not providing a neural network environment, an *in vitro* approach to investigate the mechanism of action of antipsychotics provides the benefit of even greater control than can be achieved using animal models. Indeed the very fact that *in vitro* cultures are isolated from a functional neural network means that compensatory mechanisms that may occur as a consequence of drug exposure, such as those previously observed in humans [277], are eliminated. In addition, it is very difficult to control for factors relating to the behaviour of the animals used. For example, rodents are social animals, and the environment within which they are kept and the social interactions that occur between them has been shown to bear a profound influence upon their CNS at the transcriptional and epigenetic level [278]. Indeed, isolation-reared rats have actually been used as a means to model some of the endophenotypes associated with schizophrenia as a tool for the development of novel pharmacological treatments [279]. The added degree of control that can be achieved using *in vitro* experimentation can be used to further eliminate levels of background noise associated with the use of *in vivo* experiments.

Importantly, through the use of differentiated stem cells, *in vitro* experiments now provide the opportunity to use not only human cells that represent those native to the human brain, but also those that are thought to mediate the therapeutic effects of antipsychotics *in vivo*. Several *in vitro* experiments attempting to explore the mechanism of antipsychotics through their transcriptional impact have been previously reported [258,259,280,281]. However, none of these have been performed using cells that have been validated with respect to the functional expression of receptors that are primarily targeted by the compounds they seek to investigate. The first *in vitro* study of this kind was presented by Gunther and colleagues using differentiated primary human neuronal precursor cells [280]. This study was presented as a proof of concept that this approach could be used to transcriptomically distinguish three distinct drug classes: antidepressants, antipsychotics, and opioid receptor agonists, and also as a means to construct a mathematical model that could be used to do this. In presenting the data, the authors focused on the discrimination of the different drug classes by analysing the gene expression profiles induced by each tested drug as a whole, which they referred to as 'efficacy profiles'. The authors provided no detail as to the individual gene expression changes that facilitated their classification of the drug classes tested [280]. This approach was repeated by Lamb and colleagues using a breast cancer cell line; MCF-7, to create a so called 'connectivity map' to link the gene expression induction profiles of numerous different drug classes. No detail of specific gene changes were presented, and instead they proposed a hierarchical clustering-based method as a means of grouping different drug classes based on global 'gene expression signatures' [281]. This study had the obvious drawback of using a cell type that is totally unrelated to the mechanism of action of antipsychotics and therefore draws into question whether they express the proteins necessary for antipsychotics to transduce their effects into the intracellular environment.

The first attempt to use an *in vitro* approach to identify novel genes or underlying mechanisms through which antipsychotics may exert their action was presented by Fernø and colleagues [258]. This group made use of a human glioma cell line and compared the gene expression profiles provoked by exposure to haloperidol and clozapine for 24 hours. Both compounds were shown to cause increased expression of

several genes associated with cholesterol and fatty acid biosynthesis that are known to be controlled by the sterol regulatory element-binding protein (SREBP)[258]. While derived from humans and of neural origin, the glioblastoma multiforme-derived cell line used in this study – GaMg – is an undifferentiated tumorigenic line [282], and does not accurately represent cells of the adult human brain. A more recent study sought to repeat this work using a retinal pigment epithelia cell line – ARPE-19/HPV-16 – and a hypertriploid cell line of glioblastoma origin – H4, but additionally tested a further 16 antipsychotics, again with a 24 hour exposure period [259]. This group confirmed previous findings by Fernø et al., of enhanced expression of genes associated with cholesterol and fatty acid biosynthesis, with both groups converging on altered expression for fatty acid desaturase 1 and 2 (FADS1 and FADS2), fatty acid synthase (FASN), farnesyl diphosphate synthase (FDPS), farnesyl-diphosphate farnesyltransferase 1 (FDFT1) and stearoyl-CoA desaturase (Δ-9-desaturase – SCD). These genes were shown to be upregulated in response to all antipsychotics tested, and were suggested to account for this class of compounds' therapeutic efficacy. Expression changes in genes involving fatty acid biosynthesis have however also been reported to occur in antipsychotic treated Saccharomyces cerevisiae heterozygotes, despite lacking monoamine receptor expression [283]. Interestingly, Polymeropoulos et al., also showed considerable overlap in gene expression induction between antipsychotics and selective oestrogen receptor modulators, and to a lesser extent; antidepressants and antihyperlipidaemics. All these compound classes – to reach their site of action – rely on high lipophilicity. For this reason, it would be interesting to regroup the expression profiles of these drugs based on their physiochemical properties rather than their drug class, to see if similar gene expression groupings occur. This could be performed using a principle component analysis, whereby the observed changes in gene expression induced by each drug treatments are separated based on the factors that confer the greatest degree of variance between samples [284].

It is important to note that in neither of these studies was it shown that the cell lines used, functionally expressed any of the receptors known to be targeted by the antipsychotics tested. In addition, the drug concentrations used for these studies – 10 µM haloperidol and 30 µM clozapine in the first and 10 µM of all tested drugs in the second – were more than 1000 times higher, at least for haloperidol (8 nM), than those found in the brain following a clinically efficacious dose (personal communication from Hugo Geerts). Arguably, any compound demonstrating high lipophilicity exposed to cells at a sufficiently high concentration will provoke gene expression changes – whether these are an indication of their mechanism of action or a consequence of toxicity is unclear. It should also be considered that antipsychotics exert the majority of their action at the receptors they target through antagonism. In a cell culture system of this sort there is no neurotransmission to antagonise; meaning that only the effects of agonism can be discriminated unless affecting receptor-mediated signalling through inhibition of constitutive receptor activity, i.e. inverse agonism.

In an attempt to maximise the physiological relevance of data obtained from an *in vitro* study designed to investigate the mechanism of action of antipsychotic drugs by accessing their transcriptional impact, it is felt that several experimental factors should be taken into consideration. These include:

- The cells used should bear relevance to those that are thought to mediate the effects of antipsychotics *in vivo*. Therefore, they should ideally be of human origin and derived from a neural region involved in mediating the effects of antipsychotics, such as the frontal cortex or striatum;
- The cells used should functionally express the receptors for which antipsychotics exhibit high affinity toward;
- The concentration of drug that cultures are exposed to should reflect that of the concentration achieved in the brain following the administration of therapeutically efficacious doses;
- The period of time that these drug concentrations are exposed to *in vitro* cultures should be optimised so as to enable the observation of physiologically relevant gene expression changes. This may for example involve more than one time point such as 24 hours to identify transient gene expression changes and 7 days to identify more persistent effects;
- The introduction of simulated pharmacological tone should be considered as a means to provide a basal level of receptor activity so that an effect can be observed from compounds that demonstrate neutral antagonism;

The ultimate purpose of developing a cell line to effectively model cells of the adult human brain to transcriptionally investigate the mechanism of action of antipsychotics is two fold. The first is to identify possible novel targets for the development of future antipsychotic medicines that will hopefully provide superior efficacy and reduced side effect liability. The second is not only to make the best use of the compounds we already have, but also as a means to help ensure that new compounds currently in clinical development gain approval and subsequently become available to patients.

## *1.9 Pharmacogenetics & Pharmacogenomics*

Despite the fact that all currently available antipsychotics share a common, primary mechanism of lowering dopaminergic neurotransmission [285,286], how each of these compounds affect individual patients varies enormously; from their ability to relieve symptoms to the type and severity of the side effects they may elicit [287,288]. Together with inconsistent genetic variants, pathophysiology and endophenotype between patients, variability of treatment response has strengthened the view that schizophrenia may represent several biochemically distinct disorders, though this remains to be confirmed [182,289]. It does however leave clinicians in the unenviable position of essentially resorting to conjecture to match individual patients with efficacious pharmacotherapy [288]. For such a complex disorder – or indeed group of disorders – it is perhaps naïve to think that a single drug will ever prove effective for the treatment of all patients labelled with a diagnosis of schizophrenia or even all the symptom domains experienced by an individual patient.

It is clear that better treatments are needed to alleviate the component symptom domains associated with schizophrenia, i.e. positive, negative and cognitive. It currently remains unclear whether this would be most effectively achieved through the development of different drugs to specifically treat each group

of symptoms, or at least involve adjunct treatments, rather than just the current monotherapeutic approach. This has been proposed to be part of the problem with antipsychotic-mediated off-target blockade of dopamine $D_1$ receptors in the prefrontal cortex being linked to an exacerbation of – for some – already debilitating cognitive deficits [290,291]. The extent to which individual patients suffer from each of the different symptom domains is also subject to variability and so different drugs to alleviate the component symptoms would allow each to be independently titrated to tailor a 'personalised' treatment for each patient.

Arguably, to reach the point where we understand the neurochemistry responsible for the presentation of different schizophrenia-related symptoms in individual patients, and develop drugs tailored to treat them would probably require an understanding of the generation of behaviour, personality and consciousness itself, and as such, remains a distant future. In spite of this, many of the compounds currently available have shown promise in discrete groups of patients, though an effective diagnostic criterion to identify these groups remains elusive. An alternative strategy to try and understand the biochemical basis underpinning each patient's disease presentation and treating it accordingly, is to attempt to match each patient with the most effective available treatment. This is the rationale that lies behind pharmacogenetics or pharmacogenomics, an approach that seeks to discover the genetic variants responsible for variability in drug response. While pharmacogenetics was first described in the late 1950s [292-294], the first test with utility in guiding choice of treatment in clinical psychiatry – the Roche AmpliChip R CYP450 Test – was only approved by the FDA in early 2005 [295], and remains the only test approved by the FDA for pharmacogenetic testing in psychiatry [296]. This test is a microarray-based product that distinguishes patients based on their ability to metabolise various antipsychotics and antidepressants by determining which alleles they carry for specific cytochrome P450 (CYP450) enzyme isoforms; assessing 20 alleles and 7 duplications in CYP2D6 and 3 alleles in CYP2C19 [297]. The reason why these isoforms of the cytochrome P450 enzyme are the focus of pharmacogenetic tests for psychiatric medicines is that they represent the primary means of metabolism for these classes of drugs, and therefore dictate the rate at which they are broken down and excreted from the body. Furthermore, these CYP450 isoforms demonstrate considerable genetic heterogeneity with more than 50 known variations in the CYP2D6 isoform alone, with many accounting for functional discrepancy in the rate at which they are able to metabolise their substrates [295]. These 'first-pass' metabolic enzymes were also the focus of the Luminex Tag-It™ Mutation Detection Kit, though more recent, and perhaps more ambitious tests have sought to detect an individual's likelihood of either responding to clozapine (LGC clozapine response test), developing clozapine-induced agranulocytosis (PSxPredict: CLOZAPINE test, PGxHealth) or developing adverse drug reactions (Genomas' PhyzioType system)[297]. Despite their availability these various tests have shown poor clinical uptake due to a lack of supporting data, concern over the interpretation of test results and their considerable expense [296].

The application of pharmacogenetics in the treatment of psychiatric disease remains in its infancy. Individual tests to predict responsiveness to, or side effect susceptibility with specific drugs is clearly beneficial, though it is likely that future tests will need to be more comprehensive to ensure their

widespread clinical application. This suggests the need for more comprehensive genetic testing with respect to a wide range of genes that may influence everything from an individual's potential to therapeutically respond or suffer side effects, to the rate at which they metabolise an individual drug. However, to ensure clinical uptake, these multifactorial tests would need to be accompanied by validated algorithms that provide as an output a simple prediction for each patient, an approach pioneered by Arranz and colleagues to guide the clinical use of clozapine [298]. A test that could direct clinicians towards which of the available drugs would be most appropriate for each patient – to ensure optimal symptom relief, minimal side effect liability and even appropriate dosing – would quickly prove its clinical value. The need for guidance in prescribing medication is arguably also becoming more important as compounds with divergent mechanisms from $D_2$ or 5-$HT_{2A}$ receptor blockade, such as monotherapies exploiting the glutamatergic and cholinergic systems move closer to the clinic [175]. Interestingly, pharmacogenetics also has the capacity to be exploited in the drug development process, possibly as a means of choosing patients for clinical trials to improve the likelihood that these mechanistically novel compounds reach market [299]. This premise has recently been demonstrated as part of a phase II clinical trial seeking to demonstrate the clinical efficacy of a potent and highly selective $mGlu_{2/3}$ receptor agonist (LY404039) being developed as a potential antipsychotic monotherapy by Eli Lilly [300]. LY2140023 is an oral prodrug of LY404039, that has previously been shown to confer significant improvement of schizophrenic symptoms as compared to placebo [301]. As part of the phase II clinical trial, the authors collected genetic information from participating patients and found several single nucleotide polymorphisms (SNPs) associated with improvement in both positive and negative symptoms – as assessed using the positive and negative syndrome scale (PANSS). Interestingly, the majority of these SNPs were in the gene encoding the 5-$HT_{2A}$ receptor, which has been shown not only to form heterodimers with $mGlu_2$ *in vivo* [220], but this complex has also recently been implicated in conferring antipsychotic efficacy [221]. Other SNPs associated with response to LY2140023 were found in NRG1, DRD2, DRD3 and PKHD1.

Phase II clinical trials are performed to establish whether a new drug (or an old drug destined for a novel clinical indication) is significantly better than control in relieving symptoms associated with the indication for which it is being tested. Once established, phase III trials must be conducted to show that the treatment is as effective or better than those currently available. While Liu and colleagues were reporting a phase II trial, they additionally tested LY2140023 alongside placebo and olanzapine – a leading atypical antipsychotic. While the mean level of efficacy of LY2140023 and olanzapine were shown to be roughly similar, once patients were grouped according to genotype for the HTR2A SNP, rs7330461, one homozygous group (T/T) showed numerically better PANSS improvement than the mean for all patients treated with olanzapine, and a three times greater improvement than LY2140023-treated patients that were A/A homozygotes for the same SNP [300]. While only performed in a relatively small group of patients and therefore requiring validation in a larger cohort to determine whether it will reach statistical significance, it does represent a promising find. If confirmed, this would allow the company leading the clinical trial to selectively recruit patients most likely to respond to LY2140023. While this strategy may restrict the size of the market LY2140023 would be approved for use in to only those

patients possessing the rs7330461 T/T genotype, it would ensure that the compound was approved at all, and may provide significant health benefits for those patients – hopefully while lowering side effect liability. Once approved, further clinical trials could then be conducted to demonstrate the compounds efficacy in other groups of patients.

The initial stage in the development of a pharmacogenetic test to guide psychiatric drug treatment is the identification of candidate genes. That is, genes that may demonstrate genetic heterogeneity, the functional consequence of which may be responsible for an individual's likelihood to respond, suffer adverse effects, or influence their ability to metabolise or excrete the drug. These genes will therefore vary according to the property of the drug that the genetic test hopes to address. For example, for the FDA-approved Roche AmpliChip R CYP450 Test, which is used to identify the rate at which an individual will metabolise a particular drug, and therefore guide dosing to achieve and maintain clinical efficacy without provoking side-effects [295], the obvious choice for the candidate genes were those encoding the liver enzymes responsible for their metabolism. Accordingly, to develop a test that hopes to predict response or side effect liability, one must identify genes that influence these clinical outcomes. Therefore, the fact antipsychotic efficacy has been closely correlated with affinity for the dopamine $D_2$ receptor [154], represents a good starting point. In the knowledge that antipsychotics also bind a host of other receptors, these receptors would also represent promising candidates that may influence an individual's likelihood of responding or suffering adverse effects, as would the proteins that transduce these receptors effects. If we look at the genes that Arranz and colleagues identified as influential factors with respect to clozapine's effects [298], we see that they all relate to neurotransmitter systems modulated by clozapine, i.e. dopamine, 5-HT, noradrenaline and histamine. Arguably, the more genes we can identify as playing a role in the mechanism through which antipsychotics exert their therapeutic or unwanted effects, the more comprehensive the resulting genetic test will be, and therefore increase it's capacity to accurately predict clinical outcome.

Once genes have been identified that that influence the effects of antipsychotics, the next stage is to identify genetic variations in the coding or regulatory regions of these genes that may account for variability in how individual patients respond to these drugs. Volunteer patients must then be genotyped for each of the identified genetic variations (SNPs), and these data correlated with how they have responded to different antipsychotics in the past by consulting their medical history. Finally, these correlated data are used to generate algorithms that can be used to predict an individual's likelihood of responding or tolerating a specific drug treatment. While complicated, discoveries in this area are readily susceptible to commercialisation and require far less research and expense than, for example, the development of a new drug, which may cost in excess of $800 million and nearly 12 years to bring to market [16,302].

## *1.10 Further Applications*

The purpose of this study is to identify and characterise a human NPC line that can be used to transcriptomically evaluate the mechanism of action of antipsychotic drugs. However, an NPC line that exhibits the characterististics appropriate for this study would also make it an ideal platform to explore drug effects using various other techniques. For example, epigenomics is a rapidly growing field that has recently benefitted from the emergence of technologies that allow the epigenetic status of the entire genome to be simultaneously scrutinised, such as ChIP-on-chip and ChIP-Seq (chromatin immunoprecipitation combined with either DNA microarrays or next generation sequencing respectively). Broadly speaking, epigenetics represents the study of mechanisms that control how the genome is interpreted beyond the level of the nucleotide sequence. The relevance of epigenetics has recently been implicated in the pathophysiology of schizophrenia, with regard to aberrant control of $GAD_{67}$ and reelin expression in cortical GABAergic neurons by DNA methyltransferase 1 (*DNMT1*) and DNA methyltransferase 3a (*DNMT3a*)[303]. In addition, epigenetic mechanisms have also been suggested to contribute to the effects of antipsychotics. For example, clozapine and sulpiride but not haloperidol or olanzapine have been shown to significantly demethylate the promoter regions of the same two GABAergic genes mentioned above – $GAD_{67}$ and reelin – in Swiss albino mice. Interestingly, this effect was shown to occur in the frontal cortex and striatum, but not the liver of these animals [304]. These data support the idea that antipsychotics may exert some of their actions through chromatin remodeling, though further work is necessary to determine the route through which this is achieved and this could be facilitated by the use of a NPC line as described here.

Another technique that is fast becoming an invaluable tool in many fields of biology is that of mass spectrometry-driven proteomics. Mass spectrometry can be used as a valuable tool to confirm whether changes observed in gene expression identified using microarrays persist at the protein level without the need for specific antibodies that themselves require considerable validation. In addition, it is increasingly proving it's utility in other areas such as the evaluation of cell signalling mechanisms – as exemplified by the emerging field of phospho-proteomics [248]. Reversible phosphorylation of proteins represents one of the most common post translational modifications utilised by signalling molecules to affect the behaviour of their downstream targets. The addition and removal of phosphate groups from serine, threonine, tyrosine or histidine residues – mediated by kinase and phosphatase activity respectively – is a means by which many protein's cellular functions are modulated. For example, the catalytic activity of ERK1 – itself a kinase – is precipitated by it's phosphorylation by MEK1 (mitogen-activated protein kinase kinase 1)[252]. On the other hand, as mentioned previously, the ability of GPCRs to activate their G protein-coupling partners is inhibited by GRK-mediated phosphorylation of amino acid residues exposed within the cytoplasm [189]. Phospho-proteomics makes use of sequential protein separation of biological samples based on the physiochemical properties of its components. The first stage is usually performed by liquid chromatography (LC) and feeds into the second stage, which makes use of a mass spectrometer (MS) to filter proteins based on the presence of a phosphate group into another MS. This second MS then resolves the sequence of each of these proteins. This information is used to generate large databases of information relating to the different phospho-proteins present

within samples, and can be used as a reference against which further samples can be run. Therefore, using the reference database, novel additions and removals of phosphate groups can be identified and attributed to the samples used, e.g. phosphorylations that occur in treated versus untreated samples [248].

Due to the unparalleled specificity and sensitivity offered by MS, it continues to play an ever-increasing role in drug target and biomarker identification and also drug metabolism and toxicity studies using metabolomics [305]. The use of relatively hypothesis free approaches such as those associated with transcriptomics, epigenomics and proteomics has risen exponentially in recent years, as improvements in the scope and accuracy of the facilitating technologies have been accompanied by a parallel drop in price [306]. Biological psychiatry research has recently benefitted from all of these technologies, as exemplified by these three examples relating to the analysis of post-mortem brains from schizophrenia sufferers: microarray-based transcriptomics has been used to identify several genes associated with synaptic function [307] while epigenomics has been used to identify multiple differences in DNA-methylation relating to genes associated with glutamatergic and GABAergic neurotransmission [308]. In the field of proteomics, this has been used to successfully identify proteins whose expression are altered as a result of schizophrenia itself, and the antipsychotics used to treat them [309]. Each of these different approaches could be utilised to considerable effect to investigate mechanisms relating to biological psychiatry with the availability of well-characterised, inexpensive, renewable sources of human neural tissue – as NPC lines and the capacity to differentiate them represent. With controlled genetic backgrounds, the capacity to be experimentally manipulated and the potential to be sourced from regionally specific areas of the human brain, this type of cell line has the potential to provide valuable tools both for basic scientific research and novel drug discovery.

## *1.11 Aims & Objectives*

This project had two specific aims:

- To provide a detailed characterisation of a humal neural progenitor cell line under both proliferative conditions and following differentiation into neurons and glia.
- To use this cell line to develop an *in vitro*, adherent, native tissue-based platform as a tool for the study and development of neuropsychiatric medicines.

# *Chapter 2 Materials & Methods*

## *2.1 Cell Culture*

### *2.1.1 Neural Progenitor Cell Lines*

Human NPC lines were derived from first trimester foetal tissue obtained with consent from King's College Hospital (London, UK) or Advanced Bioscience Resources (Alameda CA, USA) following normal terminations and in accordance with nationally (UK and/or USA) approved ethical and legal guidelines and kindly provided by ReNeuron Group plc. (Guildford, UK). Clonal cell lines from various regions of developing foetal human brain were conditionally-immortalised through ectopic expression of the proto-oncogene *c*-Myc or *v*-Myc under the transcriptional control of mutated oestrogen receptors rendered exclusively sensitive to the synthetic steroid 4-OHT, as described previously [63]. Briefly, these clonal-lines were generated by infection with an amphotropic replication-incompetent retroviral vector (pLNCX-2; Clontech, Mountain View CA, USA) encoding the *c*-MycER$^{TAM}$ or the *v*-mycER$^{TAM}$ (VM cell line only) transgene [63]. Inducible, ectopic expression of the *c*-MycER$^{TAM}$ transgene construct ensures continuous proliferation and stability in the presence of 4-OHT [103,310]. All cell lines used have been confirmed as having a normal karyotype and were maintained at a low passage number for experimentation unless otherwise stated.

Derivation of the cortically derived CTX0E03/02 line has been described previously [63,64] and was performed in parallel with the derivation of another cortically derived line – CTX0E16/02. Both lines were clonally derived from developing embryonic cortex from the same 12-week gestation foetus, obtained from Advanced Bioscience Resources following a normal termination by ectopic expression of the *c*-MycER$^{TAM}$ transgene. The hippocampal and striatal cell lines – HPC03A/07 and STR0C05/08A respectively – were derived from a 12-week gestation foetus and conditionally immortalised using the *c*-MycER$^{TAM}$ transgene [65,66,106]. The two spinal-cord lines (SPC-01 and SPC-04) were derived from a 10-week gestation foetus and conditionally immortalised using the *c*-MycER$^{TAM}$ transgene [67,311]. A ventral mesencephalon-derived clonal cell line (VM or ReNcell VM) was isolated from human 10-week gestation foetal midbrain obtained from King's College Hospital following a normal termination. In contrast to the other 6 cell lines described above, the VM line was immortalized by retroviral transduction of *v*-Myc rather than *c*-Myc to ectopically express the oncogene [104].

### *2.1.2 Neural Progenitor Cell Maintenance*

All cell lines were maintained in serum-free conditions using either ***Reduced Modified Medium*** (RMM) for CTX0E03/02, CTX0E16/02, HPC03A/07, SPC-01 and SPC-04, ***Human Medium*** (HM) for STROC05/08A or ***B27 Medium*** (B27M) for VM supplemented with 10 ngml$^{-1}$ human $FGF_2$ (PeproTech, Rocky Hill, NJ, USA: 100-18B), 20 ngml$^{-1}$ human EGF (PeproTech: AF-100-15) and 100 nM 4-OHT (Sigma: H7904). For media components see Appendices ***8.1.1***, ***8.1.2*** and ***8.1.3*** respectively, on page 300. RMM, HM or B27M supplemented with EGF, $FGF_2$ and 4-OHT is referred to as expansion medium for that cell line.

Cells were seeded from frozen aliquots at approximately 6.5 x $10^4$ cells per $cm^2$ onto laminin-coated (Sigma: L2020 at 0.8 – 1.3 $\mu gcm^{-2}$) Nunc tissue culture EasyFlasks™ (Nunc, Rochester, NY: 156499) and maintained in a humidified atmosphere of 95% air/5% $CO_2$ at 37°C. Cells were routinely expanded as a monolayer with medium replaced every 48 hours. Once 70 – 90% confluent, cells were passaged by incubation with Accutase® (Sigma: A6964) in a humidified atmosphere of 5% $CO_2$/95% air at 37°C for 3 minutes before dilution with non-supplemented DMEM:F12 medium (Sigma: A6421) and centrifuged for 5 minutes at 900 rpm in an ALC PK130 centrifuge equipped with a T535 rotor (ALC, Cologno Monzese, Italy). To maintain growth cells were reseeded at approximately 3 x $10^4$ cells per $cm^2$ while cells used to access $Ca^{2+}$ and ERK1/2 signalling were seeded onto 96-well plates at 3 x $10^4$ cells per well. Cells required for immunocytochemical staining to determine specific protein expression were plated onto poly-D-lysine (PDL, 5 $\mu gml^{-1}$, Sigma: P1149) and laminin-coated (1 $\mu gcm^{-2}$) glass coverslips (VWR, West Chester, PA, USA: 631-0149) at a density of 5 x $10^4$ cells per $cm^2$ and maintained as described above and in section ***2.1.3*** below to obtain proliferative and differentiated cells.

### *2.1.3 Neural Progenitor Cell Differentiation*

Each cell line was differentiated using either published protocols, developed either by colleagues within the Centre for the Cellular Basis of Behaviour (CCBB, Institute of Psychiatry, King's College London) or by ReNeuron (Guildford, UK), or through means developed during the course of this study (for the two cortex derived NPC lines) and are summarised in Table 2.1, below. Optimisation of the differentiation of the two cortically derived neural stem cell lines (CTX0E03/02 and CTX0E16/02) is described in ***Chapter 3***, below. The resultant protocol involved growing the cells to 70% – 90% confluence before washing twice with non-supplemented DMEM:F12 medium and replacing with Supplemented Neurobasal Medium (SNBM) – see Appendices ***8.1.4***, on page 300. The same volume of SNBM added upon initiation of differentiation (10 ml for T75 flask, 100 µl per well for 96-well plates and 1 ml for glass coverslips) was added after 3 days and half again after 7 days. From this point, half the medium was exchanged with fresh SNBM every 7 days, and cells were differentiated for 28 days unless otherwise stated. The hippocampal line – HPC07/03A – was differentiated by growing the cells to 70 – 90% confluence, washing twice with non-supplemented DMEM:F12 medium and replacing with RMM. The cells were not fed again and differentiation was allowed to occur over 7 days. This protocol has been described previously [65]. The two spinal cord lines (SPC-01 and SPC-04) were differentiated by growing cells to 70 – 90% confluence before removing the expansion medium and replacing it with RMM supplemented with the γ-secretase inhibitor *N*-[*N*-(3,5-Difluorophenacetyl)-L-alanyl]-S-phenylglycine t-butyl ester (DAPT, Sigma: D5942)[312], at 10 µM for 48 hours before removing and replacing with RMM for a further 5 days [67]. To differentiate the striatal line (STROC05/08A) cells were plated onto PDL (5 $\mu gml^{-1}$) and laminin-coated (0.8 $\mu gcm^{-2}$) tissue culture plastic. Once cells were 70% – 80% confluent the expansion medium was removed and replaced with HM supplemented with 1 µM purmorphamine (PMA, Calbiochem, Darmstadt, Germany: 540220) – a potent activator of the Hedgehog pathway through activity at the Smoothened receptor [313]. A full medium change was performed every 48 hours and cells were

differentiated for 21 day as described previously [66]. The ventral mesencephalic cell line (VM) was differentiated by growing the cells to 70% – 90% confluence before expansion medium was removed and replaced with B27M. Medium was not replaced and cells were allowed to differentiate for 7 days as described previously [104].

| Cell Line | Laminin Concentration | Expansion Medium | Differentiation Protocol |
|---|---|---|---|
| CTX0E03/02 | 1 $\mu gcm^{-2}$ | RMM | Cells washed twice with DMEM:F12 and replaced with ***Supplemented Neurobasal Medium*** (SNBM) – 28 days |
| CTX0E16/02 | 1 $\mu gcm^{-2}$ | RMM | Cells washed twice with DMEM:F12 and replaced with SNBM – 28 days |
| HPC03A/07 | 0.8 $\mu gcm^{-2}$ | RMM | Cells washed twice with DMEM:F12 and replaced with Reduced Modified Medium (RMM) – 7 days |
| SPC-01 | 1.3 $\mu gcm^{-2}$ | RMM | Expansion medium removed and replaced with RMM supplemented with 10 µM DAPT for 48 hours before replacing with RMM – 7 days |
| SPC-04 | 1.3 $\mu gcm^{-2}$ | RMM | Expansion medium removed and replaced with RMM supplemented with 10 µM DAPT for 48 hours before replacing with RMM – 7 days |
| STROC05/08A | 0.8 $\mu gcm^{-2}$ | HM | Expansion medium removed and replaced with HM supplemented with 1 µM purmorphamine and replaced with fresh medium every 48 hours – 21 days |
| VM | 1 $\mu gcm^{-2}$ | B27M | Expansion medium removed and replaced with B27M – 7 days |

***Table 2.1 Neural Stem Cell Proliferation & Differentiation Conditions***
Expansion medium for each cell line was supplemented with 10 $ngml^{-1}$ human $FGF_2$, 20 $ngml^{-1}$ human EGF and 100 nM 4-OHT.

### *2.1.4 Primary Neural Stem Cell Culture*

Primary neural stem cell cultures were used as reference cultures to compare the expression profiles and pharmacological properties of the neural stem cell lines used in this study to that of the developing human brain. The primary cultures were derived from 7 – 8-week gestation foetal brain samples, obtained with ethical approval from the MRC-Wellcome Trust Human Development Biology Resource (HDBR), Institute of Child Health, London. Primary cell cultures were maintained and differentiated in the same way as the two cortically-derived cell lines – CTX0E03/02 and CTX0E16/02 (see ***2.1.3***, above). On arrival, samples were dissociated by gentle trituration and seeded onto a laminin-coated (1 $\mu gcm^{-2}$) 96-well plates at 30,000 cells per well to evaluate their pharmacological properties under proliferative conditions using a FlexStation® 3 (FS3). Cells were also used to seed PDL (5 $\mu gml^{-1}$) and laminin-coated (1 $\mu gcm^{-2}$) glass coverslips at a density of 5 x $10^4$ cells per $cm^2$ for immunocytochemical analysis and a laminin-coated (1 $\mu gcm^{-2}$) tissue culture flask for further expansion. On the day that these first cultures were assayed using the FS3, proliferative cells grown on coverslips were fixed and cells grown as expanding proliferative cultures were split for further expansion, with a portion dissolved in TRIzol and stored at -80°C for subsequent RNA analysis. Once a sufficient number of proliferative cells were available, these were used to seed a laminin-coated (1 $\mu gcm^{-2}$) 96-well plates at 30,000 cells per well,

PDL (5 μgml$^{-1}$) and laminin-coated (1 μgcm$^{-2}$) glass coverslips at a density of 5 x 10$^4$ cells per cm$^2$ and a laminin-coated (1 μgcm$^{-2}$) tissue culture flask, with each exposed to a normal 28 day differentiation as optimised for the CTX0E16/02 line (see ***2.1.3*** and ***3.2.6***). These cultures were used to determine ligand-induced $Ca^{2+}$ responses, perform phenotypic evaluation using fluorescence immunocytochemistry and for gene expression analysis, respectively in differentiated cultures. Remaining cells were seeded onto a T75 flask set for continued expansion, and split so as to obtain a confluent 96-well plate and a T75 flask of proliferative cells after spending exactly 28 days in adherent culture. The 96-well plate of cells was used to assess ligand-induced $Ca^{2+}$ responses in proliferative cultures using a FS3, while cells from the flask were dissolved in TRIzol and stored at -80°C for RNA analysis.

## *2.2 Immunocytochemistry*

Cells grown on coverslips were washed with PBS (Sigma; P4417) before being fixed using 4% paraformaldehyde (BDH, Hayworth, UK; 294474L) or 4% paraformaldehyde with 0.1% glutaraldehyde (Sigma; G6257)(if staining for presence of glutamate) in PBS for 10 minutes at room temperature followed by three washes in PBS. If staining for internal antigens, cells were then permeabilised using 0.1% Triton X-100 (Sigma; T9284) in PBS for 5 minutes at room temperature before another three PBS washes. To inhibit non-specific staining, coverslips were incubated at room temperature in PBS containing 30% normal goat serum (Sigma, G9023) for 2 hours. Coverslips were then incubated overnight at 4°C in a humidity chamber in the presence of combinations of antibodies raised against, or reported to cross-react with human nestin, doublecortin (DCX), tau, microtubule-associated protein 2 (MAP2), S100β, glutamate, vesicular glutamate transporter 1 and 2 (vGluT1 and vGluT2), parvalbumin, calbindin-D28k, calretinin, vesicle-associated membrane protein 2 (VAMP2 or synaptobrevin 2) or synaptosomal-associated protein of 25 kD (SNAP-25)(for further antibody details see Table 2.2 and Table 2.3, below) in PBS containing 10% normal goat serum. Non-bound primary antibody was removed by three PBS washes prior to a further 1 hour incubation at room temperature in PBS containing 30% normal goat serum. Coverslips were then incubated at room temperature for 1 hour with appropriate fluorescent conjugated secondary antibodies (see Table 2.3, below) diluted in PBS containing 10% normal goat serum, to further minimise non-specific interactions. Three washes in PBS followed, prior to a 2 minute incubation with 4',6-diamidino-2-phenylindole dihydrochloride (DAPI, 1 μgml$^{-1}$, Sigma: D9542) to counter-stain nuclei. Three final PBS washes were performed before mounting coverslips on glass slides using Fluoromount G (Southern Biotech, Birmingham, AL; 0100-01) or ProLong® Gold (Invitrogen: P36930) mounting medium. Slides were stored in the dark at 4°C awaiting image analysis.

When cultures were co-labelled for the cell-surface oligodendrocyte marker; O4, and intracellular antigens, primary antibodies were incubated with cells in two stages. Prior to permeabilising cells with 0.1% Triton X-100, coverslips of cells were exposed to a 2 hour blocking step using PBS containing 30% normal goat serum. Coverslips were then incubated for 2 hours in a humidity chamber with O4 antibody in PBS containing 10% normal goat serum. The fixed cultures were then washed in PBS, permeabilised with Triton X-100 and exposed to a normal staining procedure, as described above, though with only

one further primary antibody applied. Immunocytochemical staining for each antibody combination was repeated on six separate coverslips. Four of these included the normal staining conditions while the other two were used as negative controls. Negative controls were coverslips of cells exposed to the same staining conditions as those described above with the exception of the addition of any primary antibodies or the use of non-specific secondary antibodies (to identify any non-specific interactions between the cells and the secondary antibodies).

| Protein Target | Isotype | Details | Catalogue Number |
|---|---|---|---|
| Nestin | Mouse monoclonal ($IgG_1$) | Immature neural precursor specific intermediate filament protein | Millipore: MAB5326 |
| KI-67 | Rabbit polyclonal (IgG) | Nuclear protein associated with cellular proliferation | Abcam: ab15580 |
| DCX | Rabbit polyclonal (IgG) | Neuronal precursor specific microtubule-associated protein | Abcam: ab18723 |
| Tau | Rabbit polyclonal (IgG) | Neuron specific microtubule-associated protein localised to axons | Dako: A0024 |
| MAP2 | Mouse monoclonal ($IgG_1$) | Neuron specific microtubule-associated protein localised to dendrites | Abcam: ab11267 |
| S100β | Rabbit polyclonal (IgG) | Astrocyte specific $Ca^{2+}$ binding protein localised to cytoplasmic | Dako: M7221 |
| Glutamate | Rabbit polyclonal (IgG) | Glutamatergic neuron specific marker | Sigma: G6642 |
| vGluT1 | Rabbit polyclonal (IgG) | Glutamatergic neuron specific marker (vesicular glutamate transporter 1) | Abcam: ab72311 |
| vGluT2 | Rabbit polyclonal (IgG) | Glutamatergic neuron specific marker (vesicular glutamate transporter 2) | Abcam: ab101756 |
| GABA | Rabbit polyclonal (IgG) | GABAergic neuron specific marker | Sigma: A2052 |
| Parvalbumin | Rabbit polyclonal (IgG) | GABAergic cell type specific $Ca^{2+}$ binding protein | SWant: PV-28 |
| Calbindin-D28k | Rabbit polyclonal (IgG) | GABAergic cell type specific $Ca^{2+}$ binding protein | SWant: CB-38a |
| Calretinin | Rabbit polyclonal (IgG) | GABAergic cell type specific $Ca^{2+}$ binding protein | SWant: 7699/4 |
| VAMP2 | Mouse monoclonal ($IgG_1$) | Synaptic vesicle-associated membrane protein specific marker | Synaptic-Systems: 104 211 |
| SNAP-25 | Mouse monoclonal ($IgG_1$) | Presynaptic membrane specific marker (synaptosomal associated protein of 25 kD) | Synaptic-Systems: 111 011 |
| O4 | Mouse monoclonal (IgM) | Oligodendrocyte specific cell surface marker | Sigma: O7139 |

***Table 2.2 Details of Primary Antibodies***

| Primary Antibody 1 | Secondary Antibody 1 | Primary Antibody 2 | Secondary Antibody 2 |
|---|---|---|---|
| mouse α **nestin** ($IgG_1$, 1:1000) | goat α mouse ($IgG_1$) Alexa fluor 488 (1:1000) | rabbit α **tau** (IgG, 1:1000) | goat α rabbit (IgG) Alexa fluor 594 (1:500) |
| mouse α **nestin** ($IgG_1$, 1:1000) | goat α mouse ($IgG_1$) Alexa fluor 488 (1:1000) | rabbit α **DCX** (IgG, 1:1000) | goat α rabbit (IgG) Alexa fluor 594 (1:500) |
| mouse α **VAMP2** ($IgG_1$, 1:2000) | goat α mouse ($IgG_1$) Alexa fluor 488 (1:1000) | rabbit α **tau** (IgG, 1:1000) | goat α rabbit (IgG) Alexa fluor 594 (1:500) |
| mouse α **VAMP2** ($IgG_1$, 1:2000) | goat α mouse ($IgG_1$) Alexa fluor 488 (1:1000) | rabbit α **DCX** (IgG, 1:1000) | goat α rabbit (IgG) Alexa fluor 594 (1:500) |
| mouse α **SNAP-25** ($IgG_1$, 1:2000) | goat α mouse ($IgG_1$) Alexa fluor 488 (1:1000) | rabbit α **tau** (IgG, 1:1000) | goat α rabbit (IgG) Alexa fluor 594 (1:500) |
| mouse α **SNAP-25** ($IgG_1$, 1:2000) | goat α mouse ($IgG_1$) Alexa fluor 488 (1:1000) | rabbit α **DCX** (IgG, 1:1000) | goat α rabbit (IgG) Alexa fluor 594 (1:500) |
| mouse α **MAP2** ($IgG_1$, 1:500) | goat α mouse ($IgG_1$) Alexa fluor 488 (1:500) | rabbit α **S100ß** (IgG, 1:100) | goat α rabbit (IgG) Alexa fluor 647 (1:500) |
| mouse α **MAP2** ($IgG_1$, 1:500) | goat α mouse ($IgG_1$) Alexa fluor 488 (1:500) | rabbit α **tau** (IgG, 1:1000) | goat α rabbit (IgG) Alexa fluor 647 (1:500) |
| mouse α **MAP2** ($IgG_1$, 1:500) | goat α mouse ($IgG_1$) Alexa fluor 488 (1:500) | rabbit α **CR**, **CB** & **PV** (IgG, 1:10000, 1:20000 & 1:5000) | goat α rabbit (IgG) Alexa fluor 594 (1:1000) |
| mouse α **MAP2** ($IgG_1$, 1:500) | goat α mouse ($IgG_1$) Alexa fluor 488 (1:500) | rabbit α **glutamate** (IgG, 1:2000) | goat α rabbit (IgG) Alexa fluor 594 (1:500) |
| mouse α **MAP2** ($IgG_1$, 1:500) | goat α mouse ($IgG_1$) Alexa fluor 488 (1:500) | rabbit α **CR** (IgG, 1:10000) | goat α rabbit (IgG) Alexa fluor 594 (1:1000) |
| mouse α **MAP2** ($IgG_1$, 1:500) | goat α mouse ($IgG_1$) Alexa fluor 488 (1:500) | rabbit α **CB** (IgG, 1:20000) | goat α rabbit (IgG) Alexa fluor 594 (1:1000) |
| mouse α **MAP2** ($IgG_1$, 1:500) | goat α mouse ($IgG_1$) Alexa fluor 488 (1:500) | rabbit α **PV** (IgG, 1:5000) | goat α rabbit (IgG) Alexa fluor 594 (1:1000) |
| mouse α **MAP2** ($IgG_1$, 1:500) | goat α mouse ($IgG_1$) Alexa fluor 488 (1:500) | rabbit α **GABA** (IgG, 1:2000) | goat α rabbit (IgG) Alexa fluor 594 (1:1000) |
| rabbit α **KI-67** (IgG, 1:1000) | goat α rabbit (IgG) Alexa fluor 488 (1:500) | N/A | N/A |
| rabbit α **S100ß** (IgG, 1:100) | goat α rabbit (IgG) Alexa fluor 488 (1:500) | N/A | N/A |
| mouse α human **O4** (IgM, 1:1000) | goat α mouse (IgM) 488 (1:1000) | N/A | N/A |
| rabbit α **vGluT1** (IgG, 1:1000) | goat α rabbit (IgG) Alexa fluor 488 (1:500) | N/A | N/A |
| rabbit α **vGluT2** (IgG, 1:500) | goat α rabbit (IgG) Alexa fluor 488 (1:500) | N/A | N/A |

***Table 2.3 Description of use of all antibodies***
Abbreviations used are as follows: DCX (doublecortin), VAMP2 (vesicle-associated membrane protein 2), SNAP-25 (synaptosomal-associated protein of 25 kD), MAP2 (microtubule-associated protein 2), CR (calretinin), CB (calbindin-D28k), PV (parvalbumin), vGluT1 (vesicular glutamate transporter 1) and vGluT2 (vesicular glutamate transporter 2)

### *2.2.1 Microscopy*

Immunocytochemistry was used to both qualitatively and quantitatively evaluate proliferative and differentiated cultures of the various cells described in this study. Cultures used for cell counting (see

***2.2.2***, below) were evaluated using a Nikon Eclipse E600 fluorescence microscope (Nikon, Tokyo, Japan), while representative images were taken on a Zeiss Axio Imager Z1, equipped with an ApoTome and an AxioCam MR3 camera running AxioVision 4.7.1 imaging software (Carl Zeiss, Jena, Germany) or a Leica TCS SP5 laser scanning confocal microscope running Leica Application Suite 2.3.5 imaging software (Leica Microsystems, Wetzlar, Germany). Bright field images were captured using a Nikon Eclipse TS100 inverted microscope mounted with a Nikon Digital Sight DS-2Mv colour camera (Nikon, Tokyo, Japan). All images were exported to Adobe Photoshop CS3 for Mac (Adobe Systems Inc., San Jose, CA, USA) for preparation.

### *2.2.2 Cell Counting*

Where staining was quantified, 10 random fields of 60 or more cells were counted per culture, and averaged to determine the percentage of cells expressing each marker within the total population. All counts were averaged from at least three coverslips per condition, and were obtained from at least three different experiments (unless otherwise stated). These values were subsequently used to calculate a mean ± S.E.M. for each condition from the corresponding number of experiments performed. Statistical analysis of counted cells was performed using GraphPad Prism version 5.0d for Mac (GraphPad Software, San Diego, CA, USA).

## *2.3 Gene Expression*

RNA was extracted from proliferative and differentiated cultures of the various cells used in this study to determine the expression of various genes of interest. These included genes encoding various neurotransmitter receptors, intracellular signalling molecules and accessory proteins relevant to the mechanism of action of neuropsychiatric medicines such as antipsychotics, antidepressants and anxiolytics.

### *2.3.1 Cell Lysis*

Proliferative and differentiated cells were grown on tissue culture plastic as described above before being rinsed in PBS and incubated with Accutase® (Sigma: A6964) in a humidified atmosphere of 5% $CO_2$/95% air at 37°C for 3 minutes. The reaction was stopped by dilution with DMEM:F12 medium (Sigma: A6421) before cells were transferred to a 15 ml Falcon tube and centrifuged for 5 minutes at 900 rpm in an ALC PK130 centrifuge equipped with a T535 rotor. Supernatant was removed before the cell pellet was physically disrupted and a sufficient volume of TRIzol® reagent (Invitrogen, Carlsbad, CA, USA: 15596) added with mixing to lyse the cells; typically 1 ml. Dissolved pellets were then stored at -80°C prior to RNA extraction.

### *2.3.2 RNA Extraction*

Samples frozen in TRIzol® were maintained at -80°C until all those required for a single experiment were collected – either replicates of the same condition for NPC cell lines or once all of the samples were collected for work involving primary cultures. Total RNA was then extracted from the samples in batches on the same days to ensure consistency. On the day of extraction frozen cell lysates dissolved in TRIzol® were defrosted at room temperature and left for 5 minutes after they had completely thawed. One millilitre of each sample was transferred to a 1.5 ml nuclease-free microcentrifuge tube along with 200 µl of chloroform (isoamyl alcohol mixture 24:1, Fluka, Buchs, Germany: 25666) and mixed by hand for 10 seconds. The mixture was then transferred to a pre-spun 2 ml heavy phase-lock gel tube (5 Prime, Hamburg, Germany: 2302830) and left to settle at room temperature for 10 minutes before centrifugation at 14,000 rpm using a Hettich EBA 12 R centrifuge with a 1412 rotor (Hettich-Zentrifugen, Tuttlingen, Germany) for 10 minutes at 4°C. Supernatant was transferred to a clean 1.5 ml nuclease-free microcentrifuge tube containing 500 µl of isopropanol (Sigma: I9516), inverted 4 times and left at room temperature for 10 minutes before a further centrifugation at 14,000 rpm for 15 minutes at 4°C. Supernatant was removed and discarded without disturbing the pellet, which was then washed with 1 ml of 75% ethanol (made up with molecular biology grade ethanol (Sigma: E7023) and nuclease-free $H_2O$ (Ambion, Austin, TX, USA: AM9938) and centrifuged at 14,000 rpm for 5 minutes at 4°C. The ethanol supernatant was removed and the pellet left to dry before it was resuspended in nuclease-free $H_2O$. Samples were left on ice for 30 minutes prior to DNase treatment.

### *2.3.3 DNase Treatment of Total RNA*

Potential DNA contamination of total RNA samples was removed using the TURBO DNA-*free*™ Kit (Ambion: AM1907) according to published protocols. In brief, 30 µl of total RNA was mixed with 3.5 µl of 10x TURBO DNase buffer and 2 µl TURBO DNase by gentle trituration in a clean 0.5 ml microcentrifuge tube. The mixture was incubated at 37°C for 30 minutes before addition of 7 µl of resuspended DNase Inactivation Reagent and incubated at room temperature for 2 minutes with 2-3 vortexes during this time. Samples were centrifuged at 10,000 rpm using a Hettich EBA 12 R centrifuge with a 1412 rotor for 90 seconds, the supernatant was transferred to a clean 0.5 ml microcentrifuge tube and stored on ice before the total RNA concentration was assessed using a NanoDrop ND1000 spectrophotometer (Thermo Scientific, Waltham, MA, USA). Samples were then stored at -80°C.

### *2.3.4 First Strand cDNA Synthesis*

Reverse transcription of RNA to cDNA was performed using SuperScript® III Reverse Transcriptase (RT) (Invitrogen: 18080) according to published protocols. In brief, 1.5 µg of sample RNA template was mixed with 2 µl of 50 µM random decamers (Ambion: AM5722G), 1 µl of 40 mM dNTP mix (10 mM each of dATP, dGTP, dCTP and dTTP at neutral pH, Solis Biodyne, Tartu, Estonia: 02-21-00100) and nuclease-free $H_2O$ up to 13 µl. The mixture was incubated at 65°C for 5 minutes before leaving on ice for 1 minute. The

contents of the tube was collected by brief centrifugation and mixed with 4 µl of 5x First-Strand Buffer, 1 µl 0.1 M DTT, 1 µl of SuperScript® III RT (200 units/µl) and 1 µl of nuclease-free $H_2O$ by gentle trituration. Samples were then incubated at 25°C for 5 minutes, 42°C for 60 minutes, 50°C for 30 minutes, then 55°C for 30 minutes before an inactivation step at 70°C for 15 minutes using a GS4 thermal cycler (G-Storm, Byfleet, UK). Reactions were diluted 1 in 7 with nuclease-free $H_2O$ to a final volume of 140 µl and stored at -20°C prior to use as template for PCR amplification reactions.

### *2.3.5 RT-PCR Primer Design*

To determine the expression of specific genes at the mRNA level, primers were designed using published RefSeq sequences sourced from the UCSC Genome Browser website (http://genome.ucsc.edu). Multiple sequence alignments were initially performed for those genes possessing transcript variants using the program; ClustalW2 (http://www.ebi.ac.uk/Tools/msa/clustalw2)[314] to ensure all expressed transcripts of the gene of interest were recognised. Primers were designed, where possible, to span intronic regions of the selected genes to ensure specific amplification of mRNA, even in the presence of DNA contamination, using Primer3Plus (http://www.primer3plus.com)[315]. All primers were designed to produce a product size of 80 – 120 base pairs (bp) with all other settings left as default. This product size was selected so that the same primers could be used for quantitative PCR if required at a later date. Primer pairs were tested to ensure amplicon specificity using the online NCBI Primer Blast tool (http://www.ncbi.nlm.nih.gov/tools/primer-blast)[316]. All primers used are detailed in ***Appendices 8.2***, on page 301.

### *2.3.6 Polymerase Chain Reaction (PCR)*

Individual 12 µl reactions were prepared using 2.4 µl of 5 x HOT FIREPol® Blend Master Mix with 7.5 mM $MgCl_2$ (Solis Biodyne: 04-25-00115), 1 µl each of 2 µM forward and reverse primer (Sigma), 6.0 µl cDNA template and 1.6 µl nuclease-free $H_2O$. Reactions were exposed to the following thermal conditions using a 110°C heated lid: an initial step of 95°C for 15 minutes prior to 35 cycles of 95°C for 40 seconds, the optimum annealing temperature (usually 60°C) for 30 seconds and 72°C for 60 seconds before a final 72°C step for 10 minutes using a GS4 thermal cycler. Samples were then placed on ice before separation using polyacrylamide gel electrophoresis.

### *2.3.7 Polyacrylamide Gel Electrophoresis*

PCR products were separated using gels containing 2.5% (w/v) agarose (Bioline, London, UK: BIO-41025) and 0.0001% ethidium bromide (Merck, Darmstadt, Germany: 111608) in Tris Acetate-EDTA buffer (sigma; T4948) and run at 80 V for 60 – 70 minutes. Gels were visualised using a UVP BioSpectrum® Imaging System running VisionWorks®LS Image Acquisition and Analysis Software (UVP, Upland, CA, USA). Bands were identified using a 100 bp DNA Ladder (Solis Biodyne: 07-11-00050). All experiments

included a no-template negative control and expression was compared to expression seen in cDNA derived from whole human brain RNA (FirstChoice® Human Brain Reference RNA, Ambion: AM6050).

## *2.4 Ligand-Induced Pharmacology*

Proliferative and differentiated cultures of NSC lines and primary foetal tissue were pharmacologically evaluated to compare their ability to respond to various agonist and antagonists by modulating intracellular concentrations of $Ca^{2+}$ or phosphorylation of extracellular-signal-regulated kinase 1/2 (ERK1/2).

### *2.4.1 $Ca^{2+}$ Release Assay*

Cells were plated onto laminin-coated (0.5 µg per well in 50 µl) black-walled, optical-bottomed 96-well plates (Nunc: 165305) at 30,000 cells per well. For experiments using proliferative cells, testing was performed once cells were confluent (48 hours). Experiments using differentiated cells involved allowing the cells to adhere overnight, achieving approximately 80% confluence, before differentiation was initiated. Differentiated cell experiments were typically performed after 28 days of differentiation unless otherwise stated. On the day of the assay all medium was removed and replaced with $Ca^{2+}$ Release Loading Buffer (see Appendices, ***8.3.2***) containing the cell-permeable $Ca^{2+}$-sensitive dye Fura-2 AM at 2.5 µM and the organic anion transporter inhibitor, probenecid at 1 mM. Cells were incubated for 1 hour in a humidified atmosphere of 5% $CO_2$ at 37°C before the loading buffer was removed and cells were washed with $Ca^{2+}$ Release Assay Buffer (see Appendices, ***8.3.1***) to remove any Fura-2 AM dye that had not been absorbed by the cells. This assay buffer was removed and replaced with 50µl of fresh $Ca^{2+}$ Release Assay Buffer per well before the cells were placed in the FlexStation® 3 (Molecular Devices, Sunnyvale, CA, USA) instrument at 37°C for 10 minutes prior to initiation of the assay. Prior to each experiment a reading was taken from all wells to assess the extent and consistency of Fura-2 AM loading. This was determined by comparing emissions at 520 nm following excitation at 380 nm. Readings above 100 relative fluorescence units (RFU) indicated acceptable Fura-2 AM cell loading, though values were typically found to average between 140 – 150 RFU, and correlated with a 340 nm/380 nm ratio of approximately 1.5 – 1.6.

Dose-response relationships for a range of compounds were determined by exposing cells to individual drugs at half logarithmic unit dose intervals to construct dose-response curves for each compound. All drug dilutions were made up in $Ca^{2+}$ Release Assay Buffer at double the required concentration and prepared on the day of the experiment during the loading buffer incubation. Drug additions were made by the liquid-handling robotics of the FlexStation® 3 instrument itself and a 50µl volume was used to achieve the desired drug concentration. Experiments were conducted at 37°C with the fluorophore excited at both 340 nm and 380 nm and detected at 520 nm with a 515 nm cut-off. Unless otherwise stated, a typical experiment consisted of an initial run where each well was exposed to a 180 second

experiment with readings taken every 6 seconds starting at 0 seconds. While readings could be taken slightly more frequently than every 6 seconds, this time was chosen so that the instrument was not under excessive strain for long experiments. Therefore, this frequency was chosen to ensure both the reliability of the instrument and to provide robust reproducible data. A baseline was provided for each well by taking a mean of the first 4 readings. Drug additions were made at 20 seconds to give a final concentration between $10^{-6}$ M and $10^{-3}$ M and followed for a further 100 seconds before 50 µl of $Ca^{2+}$ Release Assay Buffer supplemented with 150 mM KCl was added to increase the KCl concentration by 50 mM. This step was used to determine if the cells were capable of a voltage-dependent $Ca^{2+}$ channel-mediated $Ca^{2+}$ current – a physiological characteristic of mature neurons. Once readings were completed, 100 µl was removed from each well to leave 50 µl, and the plate was returned to the FlexStation® 3 for a further 60 second experiment. Emission, excitation and reading frequency settings remained the same and a baseline was again provided for each well by taking a mean of the first 4 readings. At 20 seconds 50 µl of 20 µM ionomycin in $Ca^{2+}$ Release Assay Buffer was added to expose cells to a final concentration of 10 µM. Ionomycin is an ionophore – produced by the bacterium *Streptomyces conglobatus* [317] – that was used to stimulate a maximal $Ca^{2+}$mediated 340 nm/380 nm emission ratio that was used as a reference for the responses for the cells in each well. Each drug concentration was repeated in triplicate on each 96-well plate. The timing of the above-described experiment is summarised in Figure 2.1 below.

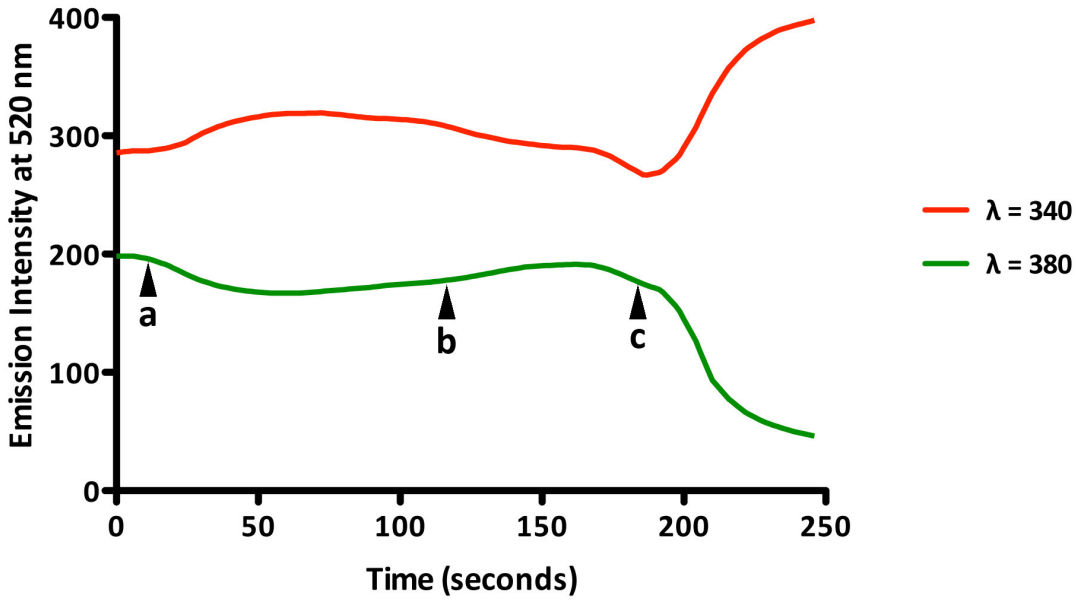


***Figure 2.1 Time course of typical $Ca^{2+}$ release assay experiment***
A mean baseline value was obtained from the first 4 readings before drug was added at 20 seconds (**a**). Intracellular $Ca^{2+}$ accumulation was followed for a further 100 seconds before cells were exposed to 50 mM KCl at 120 seconds (**b**) and monitored for a further 60 seconds. Cells were exposed to ionomycin at 180 seconds (**c**) and followed for a further 60 seconds.

### *2.4.2 $Ca^{2+}$ Release Assay Data Analysis*

All values for each time-point were first expressed as a ratio between the emission observed at 520 nm following excitation at 340 nm and 380 nm for that time-point. A mean was then taken from the first 4 readings (0, 6, 12 and 18 seconds) prior to any drug additions to provide a baseline. The highest 340 nm/380 nm value between 30 – 108 seconds was then taken as the maximal drug-induced $Ca^{2+}$ response and the highest value between 126 – 180 seconds taken as the maximal KCl-induced $Ca^{2+}$ response. The highest value obtained from the second part of each experiment following ionomycin addition was taken as the maximal reference $Ca^{2+}$ response. The baseline value for each well was then subtracted from the same well's maximal drug, KCl and ionomycin-induced value. The drug and KCl-induced value for each well was then expressed relative to that well's ionomycin-induced value. These normalised values for each well were then analysed using GraphPad Prism version 5.0d for Mac, with dose-response curves fitted according to the following three-parameter equation:

$$Y = bottom + \frac{(top - bottom)}{1 + 10^{logEC_{50} - X}}$$

Where Y is the response, X is the agonist concentration, bottom and top are the responses denoting the bottom and top plateaus of the sigmoidal curve respectively, and $logEC_{50}$ is the agonist concentration halfway between bottom and top (logarithm of the effective concentration, 50%). All values were expressed as means ± the standard error of the mean (S.E.M.). Statistical analysis of data was performed where sufficient *n* numbers permitted comparison. Two-way analysis of variance (ANOVA) was used to statistically compare ligand-induced responses between conditions (e.g. proliferative or differentiated, treated or untreated, cell line or primary cultures). In addition, unless otherwise stated, Student's *t*-tests were used to compare individual values such as the level of intracellular $Ca^{2+}$ accumulation provoked by a given concentration of drug in proliferative or differentiated cultures.

### *2.4.3 Single Cell $Ca^{2+}$ Imaging*

Proliferative or differentiated CTX0E16/02 cells grown on PDL (5 $\mu g ml^{-1}$) and laminin-coated (1 $\mu g cm^{-2}$) glass coverslips were incubated in $Ca^{2+}$ Release Loading Buffer (see Appendices, ***8.3.2***) – a physiological saline solution containing 2.5 µM Fura-2 AM and 1 mM probenecid for 1 hour in a humidified atmosphere of 5% $CO_2$ at 37°C. Compounds were diluted in $Ca^{2+}$ Release Assay Buffer and exposed to the cells by continuous local microperfusion through a fine tube placed close to the cells being studied, with experiments performed at 37°C. Images of a group of cells were taken every 2 seconds using 100 x magnification at the 520 nm emission wavelength following excitation at 340 and 380 nm using a microscope-based imaging system (Photon Technology International, Birmingham, NJ, USA). Image analysis of individual cells by emission intensity ratios from 340 nm/380 nm excitation were performed, using the ImageMaster™ software (Photon Technology International).

Once mounted, each coverslip of cells was used to obtain data for a single compound (dopamine, 5-HT, glutamate or acetylcholine), though all were additionally assessed for their ability to respond to KCl.

Each experiment began with 2 minutes of baseline readings to allow cells to settle before the addition of the compound being tested (dopamine, 5-HT, glutamate or acetylcholine) at 1 mM, to which cells were exposed for one minute. Cells were then washed in $Ca^{2+}$ Release Assay Buffer to allow $[Ca^{2+}]_i$ levels to return to baseline before exposing the cells to 50 mM KCl for 1 minute prior to another wash. Once $[Ca^{2+}]_i$ levels had again returned to baseline, the cells were exposed to 1 mM of the test compound plus 50 mM KCl for 1 minute. Finally, cells were washed for a final time in $Ca^{2+}$ Release Assay Buffer to allow $[Ca^{2+}]_i$ levels to return to baseline.

### *2.4.4 Single Cell $Ca^{2+}$ Imaging Data Analysis*

Images captured at 380 nm excitation during initial baseline period for each experiment were used to visualise Fura-2 AM containing cells and used as a guide to encircle 300 cells at random. This value was close to the limit of the ImageMaster™ software though accounted for approximately 80 – 90% of the cells in each field. Higher magnification was not used due to the relatively small number of cells responding to some of the investigated compounds and KCl. Collected data was expressed in two different ways. Firstly, as a mean ± S.E.M. of the maximal responses achieved for each compound or KCl by each cell in all counted fields, relative to the mean level of fluorescence recorded at baseline for that cell. To express the proportion of cells responding to a specific compound or KCl; the percentage of the total number of cells from which recordings were made that showed an increase in fluorescence of > 20%, > 50% or > 100% relative to each cells own baseline were presented. Data analysis and presentation was performed using GraphPad Prism version 5.0d for Mac.

### *2.4.5 ERK1/2 Phosphorylayion Assay*

In response to extracellular stimuli, GPCRs are known to initiate signalling through a range of G-proteins and are also capable of provoking G-protein-independent signalling. Recent evidence suggests that GPCRs can be found to couple to different G-protein signalling partners depending on the cell type within which they are found. Common to all GPCRs however is their ability to modulate the phosphorylation status of ERK1/2. ERK1/2 phosphorylation was therefore used as a means to assess the presence and function of specific GPCRs at the cell surface without having to determine the specific G-protein partner through whom they are primarily signalling. The commercially available Cellul'erk Kit (Cisbio Bioassays, Codolet, France) was used for this study to measure ligand-induced ERK1/2 phosphorylation in CTX0E16/02 cells in response to a range of agonists and antagonists according to published protocols for a two-plate assay. The system makes use of the principle of FRET, whereby a donor chromophore – once excited – can transfer energy to an adjacent donor chromophore through non-radiative dipole-dipole coupling, as illustrated in Figure 2.2, below. This is achieved through a sandwich immunoassay involving an anti-phospho-ERK1/2 antibody (shown in red in the diagram) conjugated to the chromophore d2 and an anti-ERK1/2 antibody conjugated to the chromophore $Eu^{3+}$-cryptate (shown in blue in the diagram). FRET can only occur once the two antibodies are within

approximately 10 nm of each other, and therefore detects the presence of a phosphate group specifically attached to an ERK1/2 molecule.

Cells were plated onto laminin-coated (0.5 µg per well) clear 96-well plates (Nunc: 167008) at 30,000 cells per well. Proliferative and differentiated cells used for experiments were prepared in the same way as cells used for the $Ca^{2+}$ Release Assay described above. On the morning of the experiment, all medium was removed and 50 µl of fresh neurobasal medium supplemented with B27 was added to each well and returned to the incubator for a further 4 hours. Cells were then exposed to a further 50 µl of fresh neurobasal medium supplemented with B27 and additionally containing the compound to be tested at twice the desired concentration. Cells were then incubated at room temperature over a range of time periods to select the optimal time needed to achieve the greatest ERK1/2 phosphorylation response for each ligand. Cell supernatant was removed carefully by aspiration and immediately replaced with 50 µl of lysis buffer supplemented with blocking reagent and incubated for 5 minutes at room temperature with shaking. Cell lysates (16 µl) from each well were then transferred to wells of a 384-well, solid bottom, small volume, white plate (Greiner, Kremsmünster, Austria: 784075) and mixed with 2 µl of each of the two HTRF conjugates (anti-ERK1/2-$Eu^{3+}$-cryptate (donor) and anti-phospho-ERK1/2-d2 (acceptor) – each made up in assay detection buffer) and incubated for 2 hours at room temperature. Each 384-well plate additionally contained 6 wells dedicated to negative (16 µl of blocking reagent-supplemented lysis buffer with 2 µl of anti-ERK1/2-$Eu^{3+}$-cryptate donor conjugate and 2 µl of detection buffer – donor antibody only) and blank (16 µl of blocking reagent-supplemented lysis buffer with 2 µl of each of the donor and acceptor conjugates) controls respectively. Plates were then read using a FlexStation® 3 or Artemis K-101 plate-reader. Readings were made at 620 nm for the donor ($Eu^{3+}$-cryptate) and 665 nm for the acceptor (d2) following excitation at 314 nm. Reading were an average of 50 replicates with a delay and integration time of 100 µseconds.

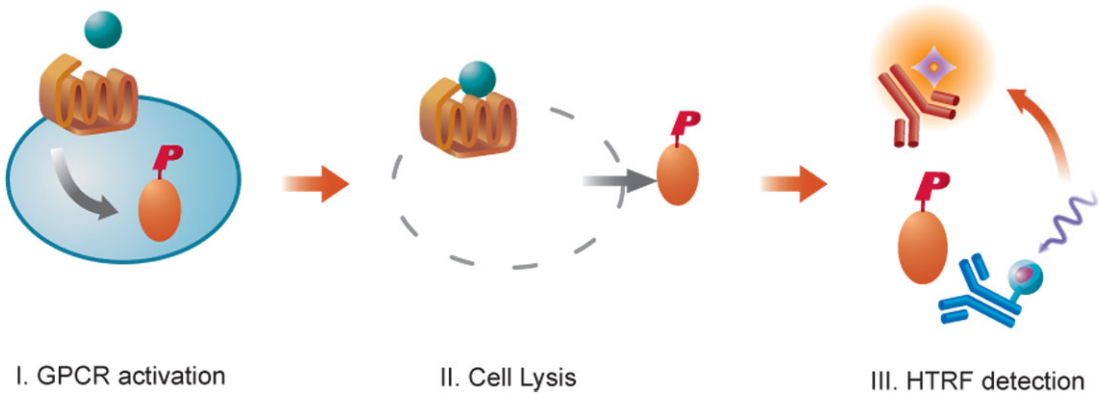


***Figure 2.2 Illustrative diagram of phosphorylated ERK1/2 detection using the Cellul'erk Kit***
Diagram to graphically illustrate the principle behind Cisbio Bioassays Cellul'erk Kit. Diagram used with permission from Cisbio Bioassays Cellul'erk Kit marketing literature.

### *2.4.6 ERK1/2 Phosphorylayion Assay Data Analysis*

A 665 nm/620 nm ratio was calculated for each well/assay and referred to as *R*. A mean *R* value was calculated for the 6 negative control wells on each 384-well plate and referred to as $R_{Neg}$. Values were expressed as *ΔF%* according to the following equation as defined by Albizu and colleagues [318]:

$$\Delta F\% = \frac{R - R_{Neg}}{R_{Neg}} \times 100$$

*ΔF%* values were analysed using GraphPad Prism version 5.0d for Mac (GraphPad Software) with dose-response curves fitted according to the equation shown in ***2.4.2***, above.

## *2.5 Experimental Design*

In all the experimentation described above the following rules were applied. To ensure reliability and consistency between cell culture experiments, seed and working stocks were generated for each of the NPC lines investigated. All cell culture experiments were performed using NPCs exposed to as few passages as possible, and unless otherwise stated, passage number never exceeded 10. As far as was reasonably practicable, cultures were treated as consistently as possible with respect to the conditions they were exposed to whilst proliferating and differentiating. Great care was taken to ensure that cultures demonstrated 'normal' growth characteristics, with any cultures exhibiting a divergent appearance being discarded immediately.

Experiments involving the extraction of RNA and subsequent expression analysis were performed in grouped batches. This included all steps of the process from thawing cellular pellets and extraction of RNA to DNase treatment, measurement of RNA concentration, reverse transcription into cDNA and the PCR reactions themselves. This allowed mixes to be made of as many reaction components as possible so as to minimise variability between individual reactions for different samples.

Functional experiments measuring ligand-induced changes in intracellular $Ca^{2+}$ concentration or ERK1/2 phosphorylation were performed as consistently as possible, with the duration of incubations and washes strictly adhered to. Compounds were always made up immediately prior to experiments, with those sensitive to oxidation, such as dopamine and 5-HT, being made up less than 15 minutes prior to addition to cultures.

# *Chapter 3 Human NPC Lines Exhibit Divergent Characteristics*

Using seven conditionally immortalised NPC lines isolated from various regions of the developing human nervous system as a starting point, this chapter describes a phenotypic and physiological characterisation of these cells in their proliferative and differentiated state. This work aimed to provide a body of data that could inform upon which of these represented the most appropriate *in vitro* model with which to investigate the pharmacological and subcellular mechanism of action of currently available antipsychotic medicines.

## *3.1 Introduction*

Despite sixty years of clinical use, the mechanism of action of antipsychotics as a class of drugs remains poorly understood. Investigation has previously relied upon the use of post mortem tissue from antipsychotic treated schizophrenic patients, non-invasive imaging, animal studies and the use of non-native tissue culture systems. Stem cells – either embryonic or those demonstrating a more restricted neural fate – represent a renewable source of human neural cells that can be differentiated to generate a range of different neural cell-types. The resulting cultures promise considerable potential as a platform that can be used to faithfully model cells that comprise the adult human brain, and therefore a powerful tool with which to investigate neural cell physiology and drugs that impact upon it.

Transcriptomics provides a non-hypothesis driven experimental approach that can be used to compare biological samples based on the differential expression of thousands of genes simultaneously. Depending on the samples compared, this information can be used as a means to indicate genes expression changes that may occur as a consequence of this difference. For example, healthy or diseased, undifferentiated or differentiated, untreated or treated. The value of data obtained from a transcriptomic study is therefore dependent upon the quality of the samples used, with control exerted over as many variables as possible, except for those that are to be measured.

The recent emergence of technology providing the ability to generate neurons from somatic cells of schizophrenic patients through the generation, then differentiation, of iPS cells, or iN cells represents a powerful means with which to investigate aberrant cellular mechanisms attributable to the endophenotypes associated with schizophrenia. However, clonal NPC lines may represent a superior tool to investigate the mechanism of action of drugs used to treat them – especially transcriptomically – because they possess a constant genetic background. By controlling this variable, the sensitivity of the platform can be increased. This means fewer biological replicates are required to see the same effect, while similar numbers of replicates mean that observed changes in gene expression are more likely to reach statistical significance. These are important considerations for transcriptomic experiments due to the multiple statistical testing necessary to interrogate data sets representing the entire genome.

The purpose of this study was to develop an *in vitro* platform that can be used to transcriptomically investigate the mechanism of action of antipsychotic drugs. It is therefore important that this cell

culture system represents the cells upon which these drugs are thought to exert their effects *in vivo*, so as to ensure the validity of any observed gene expression changes. Several characteristics were identified and discussed as being necessary or desirable attributes for an *in vitro* model system to meet the needs of this role in 1.5 above. Criteria for selecting a NPC line for this purpose were identified as:

1. The line should be of human origin, so as to eliminate any species differences in how antipsychotics pharmacologically interact with the cells, such as ligand affinity for a given receptor or signal transduction or regulation as a consequence of ligand binding;
2. The line should demonstrate the capacity to be robustly and reproducibly differentiated into primarily neurons, but also astrocytes. Astrocytes have been shown to play an important supporting role in the functional development of neurons both *in vivo* and *in vitro* [319], from stimulating differentiation [320] to synapse formation [100]. In addition, it is unclear whether antipsychotics exert their mechanism of action exclusively through interaction with neurons, as astrocytes have also recently been implicated as a potential target of these compounds [321]. To this end, future experiments could involve the generation of NPC lines that express neuron, astrocyte or oligodendrocyte specific fluorescent fusion protein conjugates upon differentiation. This would enable the use of FACS to separate constituent cell types from differentiated cultures, and facilitate analysis of changes unique to each cell type. The successful conditional immortalisation of the cell lines used in this thesis demonstrates their capacity to be genetically manipulated. The ability to identify and sort cells in this way also presents the possibility of investigating the effects of antipsychotic on different cell types. For example, experiments could be performed whereby mixed neural cultures could be exposed to antipsychotics and subsequently sorted by FACS, while FACS could also be performed prior to drug exposure – with each set of cells subsequent exposed to transcriptomic analysis. This may allow synergistic and direct effects of antipsychotics in different cell types to be distinguished.
3. Neuronal cells generated should be capable of electrical excitability, as this represents an important physiological feature of this cell type, and therefore has functional consequences;
4. The differentiated cells should express functional receptors known to be targeted by antipsychotic drugs;
5. The line should proliferate and differentiate as an even, adherent monolayer to ensure low signal to noise ratios can be achieved when using high-throughput screening methodologies.

Through a material transfer agreement with the stem cell company ReNeuron, our department has the fortune to have been kindly granted access to a range of their conditionally immortalised NPC lines. The first stage of this process was therefore to select one of these NPC lines that would best fit the above criteria.

Several of the NPC lines available had already proven capable of robust differentiation into neurons and glia and included cell lines derived from the developing striatum (STROC05/08A [66,106]), hippocampus (HPC03A/07 [65,106]), ventral mesencephalon (VM or ReNcell VM [104,322]) and spinal cord (SPC-01 and SPC-04 [67]). With consideration to the pathophysiology related to schizophrenia however, for which

antipsychotics are the primary prescribed treatment, a NPC line derived from the developing cortex was felt to be most appropriate for the purposes of this study. This is due to the fact that considerable evidence points towards aberrant frontal cortical development and activity as a key player in the presentation of schizophrenia and the activity of antipsychotics [115,183,323]. Two cortically derived NPC lines were available – CTX0E03/02 and CTX0E16/02 – of which the first, CTX0E03/02, had previously been shown to be capable of differentiation into neurons and astrocytes [63]. This line had not been shown to be capable of generating electrically excitable cells or oligodendrocytes *in vitro*. Therefore, despite the preference for a cortically derived line, all the NPC lines mentioned above were investigated at this early stage as potential substitutes in the event that the cortically derived NPC lines proved resistant to differentiation or produced cultures bearing characteristics inappropriate for the needs of this study. Any of these cell lines could have potentially expressed the receptors through which antipsychotics are thought to transduce their effects, and may be influenced by the culture environment they are exposed to *in vitro*. Each of these lines were therefore investigated so that an informed decision could be made based on the properties these cells exhibit in an *in vitro* environment.

This chapter details the optimisation of the differentiation of two cortically derived human NPC lines – CTX0E03/02 and CTX0E16/02. Evidence is presented of their ability to be differentiated into both neurons (glutamatergic and GABAergic) and glial cells. The characteristics of differentiated cortical NPC line cultures are assessed with respect to their suitability for pharmacological evaluation using high-throughput screening methodologies measuring ligand-induced intracellular $Ca^{2+}$ accumulation. Finally, a comparison is then made between differentiated cultures from each of the seven NPC lines based on their expression of a range of genes identified as important to the needs of the present study using RT-PCR.

## *3.2 Results*

### *3.2.1 Cortically-Derived Human NPC Lines Demonstrate Robust Differentiation*

Two cortically derived, conditionally immortalised, NPC lines – CTX0E03/02 (currently in clinical trial for the treatment of stroke) and CTX0E16/02 – were tested to determine their ability to differentiate using a variety of methods, and compared to conditions previously described for the differentiation of the CTX0E03/02 line [63]. Protocols that have proven successful to differentiate other ReNeuron NPC lines were investigated along with methods form this laboratory [324-326], and other laboratories [327,328] that have proven successful in differentiating rodent and human-derived NSC and NPC lines.

Both lines were initially propagated under proliferative conditions in Reduced Modified Medium (RMM) supplemented with 10 $ngml^{-1}$ human $FGF_2$, 20 $ngml^{-1}$ human EGF and 100 nM 4-OHT, as described in ***2.1.2***, above. Cells were then seeded onto laminin-coated (0.5 µg per well) black-walled, optical-bottomed 96-well plates at 30,000 cells per well. The following day, once the cultures had reached approximately 70% – 80% confluence, individual wells were washed twice with RMM before being exposed to one of the six differentiation protocols described in Table 3.1, below, for 14, 21 or 28 days.

To determine the success of these initial experiments to promote differentiation of the CTX0E03/02 and CTX0E16/02 lines, cultures were fixed in 4% paraformaldehyde and analysed by immunofluorescence staining, as described in ***2.2***, above. The relative abundance of cells expressing markers indicative of neural progenitor cells (nestin – an intermediate filament protein [329,330]), neuronal precursor cells (doublecortin (DCX) – a microtubule-associated protein [331]), neurons (tau and MAP2 – microtubule-associated proteins localised to axons and dendrites respectively [328,331]) or astrocytes (S100β – a $Ca^{2+}$ binding protein [52]) was assessed. The presence of the synaptic markers VAMP2 and SNAP-25, which are integral membrane proteins of secretory vesicles and presynaptic membranes respectively were also determined. These proteins are both components of the SNARE complex; involved in synaptic vesicle docking enabling neurotransmitter release [332,333].

| Protocol | Description |
|---|---|
| **RMM** | Cells differentiated in RMM – DMEM:F12 with 15 mM HEPES and sodium bicarbonate supplemented with 0.03% human serum, 100 $\mu gml^{-1}$ apo-transferrin, 16.2 $\mu gml^{-1}$ putrescine, 5 $\mu gml^{-1}$ human insulin, 60 $ngml^{-1}$ progesterone, 2 mM L-glutamine and 40 $ngml^{-1}$ sodium selenite |
| **SNBM** | Cells differentiated in neurobasal medium supplemented with 0.03% human serum, 100 $\mu gml^{-1}$ apo-transferrin, 16.2 $\mu gml^{-1}$ putrescine, 5 $\mu gml^{-1}$ human insulin, 60 $ngml^{-1}$ progesterone, 2 mM L-glutamine and 40 $ngml^{-1}$ sodium selenite and B27® supplement |
| **PMA** | Cells differentiated in RMM supplemented with 1 μM purmorphamine (PMA) |
| **DAPT** | Cells exposed to RMM supplemented with the 10 μM of the γ-secretase inhibitor, DAPT for the first 48 hours before being replaced with RMM for the remaining period of the experiment |
| **GDNF** | Cells differentiated in RMM supplemented with 10 $ngml^{-1}$ GDNF |
| **$PDGF_{BB}$** | Cells differentiated in RMM supplemented with 30 $ngml^{-1}$ $PDGF_{BB}$ |

***Table 3.1 Protocols tested to differentiate the cortically derived NPC lines CTX0E03/02 and CTX0E16/02***
Cells were grown under normal proliferative conditions until reaching approximately 70% - 80% confluence before being washed twice in RMM, replaced with one of the culture conditions detailed above and maintained for 14, 21 or 28 days.

In order to evaluate the extent of cellular differentiation for each condition at this early stage of optimisation, an arbitrary scale was established to determine the overall health of the cultures and the relative abundance of each cell type, as indicated by the expression of the cell-type specific markers described above. The relative health of cultures grown under each differentiation condition was determined by assessing the number and density of surviving cells and the abundance of cellular debris across all wells of a given condition, irrespective of the staining combination employed ('-' for no surviving cells up to '+++' for conditions supporting the highest levels of cell survival). To evaluate differentiation, cultures exposed to each condition and at each time point were stained with the following antibody combinations: tau with nestin, MAP2 with S100β, tau with VAMP2 and tau with SNAP-25, with nuclei visualised using DAPI (tau was replaced with DCX for both cell lines at the final time point of 28 days due to a shortage of antibody). Each staining combination was repeated in triplicate and a no-primary antibody control was included to assess specificity. All cultures (individual wells) of a given condition were taken into consideration when scoring the relative abundance of each cell type and were directly compared to those of all other differentiation conditions ('-' for cultures containing no

immunoreactive cells up to '+++' for conditions supporting the highest numbers of immunoreactive cells for the marker in question). Evaluation of this work was performed in a single session with continuous cross-referencing to previous scoring to ensure that the optimum differentiation conditions could be identified for further characterisation. These qualitative data are presented in Table 3.2 to Table 3.7, below. It was recognised that appraisal and comparison of tested differentiation conditions should ideally have been assessed in a blind fashion. However, due to this stage of the optimisation process being performed in 96-well plates and all experimentation being performed by the author, this was not possible.

For CTX0E03/02 cells differentiated for 14 days in Reduced Modified Medium (RMM), survival was robust compared with cells grown in Supplemented Neurobasal Medium (SNBM) or RMM supplemented and PMA (PMA). In SNBM and PMA most surviving cells were found at the edge of wells with little survival in the middle. However, differentiation in RMM and SNBM was similar with few $tau^+$ or $MAP2^+$ neurons, but many $S100\beta^+$ astrocytes and undifferentiated $nestin^+$ cells observed. In contrast, cultures differentiated in PMA had few $nestin^+$ cells remaining but many $tau^+$ and $MAP2^+$ cells. The number of $S100\beta^+$ astrocytes observed was similar to that seen in SNBM and PMA conditions. Cultures exposed to RMM supplemented with DAPT (DAPT) remained healthy, with even growth throughout the well and many $nestin^+$ progenitors, $S100\beta^+$ astrocytes and some $tau^+$ and $MAP2^+$ neurons. GDNF exposed cultures were healthy with many neurons and astrocytes present, while $PDGF_{BB}$ promoted excellent survival with many $S100\beta^+$ astrocytes, but relatively few $tau^+$ and $MAP2^+$ neurons.

| | Nestin | Tau | MAP2 | S100β | VAMP2 | SNAP-25 | Culture Health |
|---|---|---|---|---|---|---|---|
| **RMM** | +++ | + | +/++ | +++ | - | - | +++ |
| **SNBM** | +++ | + | + | +++ | - | - | ++ |
| **PMA** | + | ++ | +++ | +++ | - | - | ++ |
| **DAPT** | +++ | +/++ | + | +++ | - | - | ++ |
| **GDNF** | +++ | ++ | + | ++ | - | - | ++ |
| **$PDGF_{BB}$** | +++ | + | + | +++ | - | - | +++ |

***Table 3.2 Immunoreactivity summary of CTX0E03/02 cultures following 14 day differentiation***

After 21 days, the survival of CTX0E03/02 cells differentiated in RMM had deteriorated with few cells remaining in the middle of wells and now approximately even numbers of $S100\beta^+$ and $tau^+$ cells were present, though few were $MAP2^+$, suggesting that with time, the more mature $MAP2^+$ cells were dying off. For SNBM there was little change in the health of the culture when compared with those at 14 days of differentiation but now there were more $tau^+$ neurons and fewer $nestin^+$ cells present, possibly indicating more neuronal differentiation. However, the numbers of MAP2 expressing cells in the cultures appeared not to have changed, suggesting that neurons had not matured over this time frame. PMA treated cultures were reasonably healthy with some $S100\beta^+$ but few $tau^+$ and $MAP2^+$ cells. Few cells grew in the middle of wells exposed to DAPT, with most of those surviving remaining at the edges. None of these cells expressed MAP2 and few were $tau^+$. Several $S100\beta^+$ cells were present but cultures

were dominated by nestin$^+$ cells that had started to exhibit very long processes. GDNF promoted good healthy cultures but few tau$^+$ and MAP2$^+$ cells were present. As at 14 days, $PDGF_{BB}$ provided excellent cell survival with many S100β$^+$ cells but relatively few tau$^+$ and even less MAP2$^+$ cells.

| | Nestin | Tau | MAP2 | S100β | VAMP2 | SNAP-25 | Culture Health |
|---|---|---|---|---|---|---|---|
| **RMM** | +++ | ++ | -/+ | ++ | - | - | ++ |
| **SNBM** | ++ | ++ | + | +++ | - | - | ++ |
| **PMA** | ++ | + | + | ++ | - | - | ++ |
| **DAPT** | +++ | + | - | ++ | - | - | + |
| **GDNF** | +++ | + | -/+ | ++ | - | - | ++ |
| **$PDGF_{BB}$** | +++ | + | -/+ | +++ | - | - | +++ |

***Table 3.3 Immunoreactivity summary of CTX0E03/02 cultures following 21 day differentiation***

For CTX0E03/02 cells differentiated for 28 days tau staining was replaced with DCX due to a lack of available tau antibody. RMM differentiated cultures were associated with poor survival and large amounts of cell debris. Surviving cells were bunched into small clusters containing no DCX$^+$ neuroblasts, but some MAP2$^+$ neurons and S100β$^+$ astrocytes and many nestin$^+$ cells. Surprisingly, despite no detected VAMP2 immunoreactivity for any conditions at 14 or 21 days, this protein was detected to some extent in all differentiation conditions at 28 days. SNBM differentiated cultures were healthy with many more DCX$^+$ neuroblasts, MAP2$^+$ neurons and S100β$^+$ astrocytes present that seen after 21 days, suggesting further maturation of these cultures. Considerable VAMP2 staining was also present and nestin$^+$ cells had by this time point developed highly elaborate processes. PMA treated cultures demonstrated good healthy growth with few DCX$^+$ neuroblasts present, but many MAP2$^+$ neurons and S100β$^+$ astrocytes and together with cells that expressed diffuse but punctate VAMP2 immunoreactivity. Cultures differentiated using DAPT or GDNF for 28 days produced healthy cultures but were dominated by S100β$^+$ astrocytes and many fewer MAP2$^+$ neurons. DCX was absent while VAMP2 staining was comparable for the two conditions. $PDGF_{BB}$ provided healthy cultures dominated by nestin$^+$ and S100β$^+$ cells. Several MAP2$^+$ cells were present though few cells demonstrated DCX immunoreactivity. Considerable VAMP2 immunoreactivity was also evident. SNAP-25 staining was absent at all tested time points and under any of the tested differentiation conditions.

| | Nestin | Tau | MAP2 | S100β | VAMP2 | SNAP-25 | Culture Health |
|---|---|---|---|---|---|---|---|
| **RMM** | +++ | - | ++ | +++ | +/++ | - | + |
| **SNBM** | +++ | ++/+++ | +++ | +++ | +++ | - | ++ |
| **PMA** | +++ | + | ++/+++ | +++ | ++/+++ | - | ++ |
| **DAPT** | +++ | - | ++ | +++ | ++ | - | ++ |
| **GDNF** | +++ | - | + | +++ | ++/+++ | - | ++ |
| **$PDGF_{BB}$** | +++ | -/+ | ++ | +++ | +++ | - | +++ |

***Table 3.4 Immunoreactivity summary of CTX0E03/02 cultures following 28 day differentiation***

The differentiation of CTX0E16/02 cultures was performed in parallel with that of CTX0E03/02. Differentiating these cells for 14 days in RMM, SNBM or PMA provided good healthy cultures but these included few $tau^+$ or $MAP2^+$ neurons or $S100\beta^+$ astrocytes, with plenty of $nestin^+$ progenitors remaining. Exposure to DAPT was poorly tolerated, leaving few cells though some did show evidence of tau, MAP2 and S100β immunoreactivity. GDNF and $PDGF_{BB}$: provided very healthy cultures with little cell death. GDNF produced few $tau^+$ and $MAP2^+$ cells but a greater number of $S100\beta^+$ cells, while $PDGF_{BB}$ treated cultures produced few $tau^+$, but a greater number of $MAP2^+$ and $S100\beta^+$ cells.

| | Nestin | Tau | MAP2 | S100β | VAMP2 | SNAP-25 | Culture Health |
|---|---|---|---|---|---|---|---|
| **RMM** | +++ | + | + | +/++ | - | - | +++ |
| **SNBM** | +++ | +/++ | +/++ | ++ | - | - | +++ |
| **PMA** | +++ | + | + | + | - | - | +++ |
| **DAPT** | ++ | + | + | + | - | - | + |
| **GDNF** | +++ | + | + | ++ | - | - | +++ |
| **$PDGF_{BB}$** | +++ | + | ++ | +/++ | - | - | +++ |

***Table 3.5 Immunoreactivity summary of CTX0E16/02 cultures following 14 day differentiation***

CTX0E16/02 differentiated for 21 days in RMM provided good healthy cultures with plenty of $S100\beta^+$ astrocytes but less $tau^+$ and even fewer $MAP2^+$ neurons. SNBM produced similarly healthy cultures with comparable S100β staining but greater numbers of $tau^+$ and $MAP2^+$ neurons. PMA produced healthy cultures with plenty of $S100\beta^+$ and $tau^+$ cells but relatively few $MAP2^+$ cells. PMA treated cultures exhibited the lowest level of $nestin^+$ cells at this time point. As with CTX0E03/02, DAPT was not well tolerated with few surviving cells, and few of these expressed markers of neuron or astrocyte directed differentiation. GDNF supported healthy cultures, though produced few $tau^+$ and $MAP2^+$ neurons but greater numbers of $S100\beta^+$ astrocytes. $PDGF_{BB}$ provided excellent healthy cultures with high levels of $S100\beta^+$ astrocytes with some $tau^+$, but fewer $MAP2^+$ neurons.

| | Nestin | Tau | MAP2 | S100β | VAMP2 | SNAP-25 | Culture Health |
|---|---|---|---|---|---|---|---|
| **RMM** | ++ | +/++ | -/+ | +++ | - | - | +++ |
| **SNBM** | ++ | ++ | + | +++ | - | - | +++ |
| **PMA** | +/++ | ++ | -/+ | +++ | - | - | +++ |
| **DAPT** | ++ | + | -/+ | + | - | - | + |
| **GDNF** | +++ | + | -/+ | ++ | - | - | +++ |
| **$PDGF_{BB}$** | ++ | ++ | +/++ | +++ | - | - | +++ |

***Table 3.6 Immunoreactivity summary of CTX0E16/02 cultures following 21 day differentiation***

Exposure of CTX0E16/02 cells for 28 days to RMM or SNBM produced similarly healthy appearing cultures with even monolayer growth. Both cultures demonstrated high levels of $S100\beta^+$ astrocytes and similar numbers of $nestin^+$ progenitors. However, SNBM treated cultures produced higher levels of MAP2 and VAMP2 expressing neurons, while RMM cultures had less of these cell-types but more $DCX^+$

neuroblasts/young neurons, suggesting more pronounced neuronal maturation in the presence of SNBM. PMA produced healthy cultures that demonstrated patches that were highly enriched with $DCX^+$ neuroblasts. $MAP2^+$ neurons were just as numerous but evenly dispersed. Similarly high levels of $nestin^+$ and $S100\beta^+$ cells were detected and some cells exhibited diffuse VAMP2 staining. DAPT treated cultures demonstrated poor survival – as was evident after 14 and 21 days. The majority of those remaining were $S100\beta^+$ astrocytes with few $tau^+$ and $MAP2^+$ neurons present. GDNF produced good healthy cultures with little evidence of cell death and dominated by similarly high numbers of $nestin^+$ progenitors and $S100\beta^+$ astrocytes. More $DCX^+$ than $MAP2^+$ cells suggested the presence of more immature rather than mature neurons at this time point, though considerable VAMP2 staining was observed. After a 28 day exposure to $PDGF_{BB}$ cultures showed relatively poor survival – in stark contrast to that seen at 14 or 21 days. Of the remaining cells, few expressed tau, MAP2 or S100β but many were quite elaborately processed $nestin^+$ cells.

| | Nestin | Tau | MAP2 | S100β | VAMP2 | SNAP-25 | Culture Health |
|---|---|---|---|---|---|---|---|
| **RMM** | ++ | ++ | +/++ | +++ | ++ | - | +++ |
| **SNBM** | ++ | + | ++ | +++ | +++ | - | +++ |
| **PMA** | +++ | ++ | ++ | +++ | ++ | - | +++ |
| **DAPT** | ++ | + | + | +++ | ++ | - | + |
| **GDNF** | +++ | ++ | +/++ | +++ | +++ | - | +++ |
| **$PDGF_{BB}$** | ++ | + | + | + | ++/+++ | - | + |

***Table 3.7 Immunoreactivity summary of CTX0E16/02 cultures following 28 day differentiation***

Through evaluation of these initial experiments it became clear that exposure to either SNBM or 1 µM purmorphamine in RMM proved far more effective than the other tested treatments in terms of the health of the cultures, and the relative number of neurons and astrocytes generated, as determined by analysis of immunocytochemical staining. Interestingly, under all differentiation conditions many of the cells that expressed markers of differentiation also retained expression of nestin. This observation is not unusual following human NPC differentiation and been reported previously [328]. Representative images of immunocytochemically stained CTX0E016/02 cultures differentiated for 28 days using SNBM or 1 µM purmorphamine in RMM – which represented the most effective differentiation conditions – are shown in Figure 3.1. Similarly differentiated CTX0E03/02 cultures showed comparable staining characteristics though cells were less evenly distributed across the growth surface. The ability to generate even, confluent differentiated cultures is however a desirable characteristic for the intended downstream applications of these cells and will therefore influence which cell line is subsequently selected. It should be noted that cultures differentiated in the presence of SNBM were composed of smaller but more numerous cells than were observed in cultures differentiated with purmorphamine supplemented RMM (see Figure 3.1).

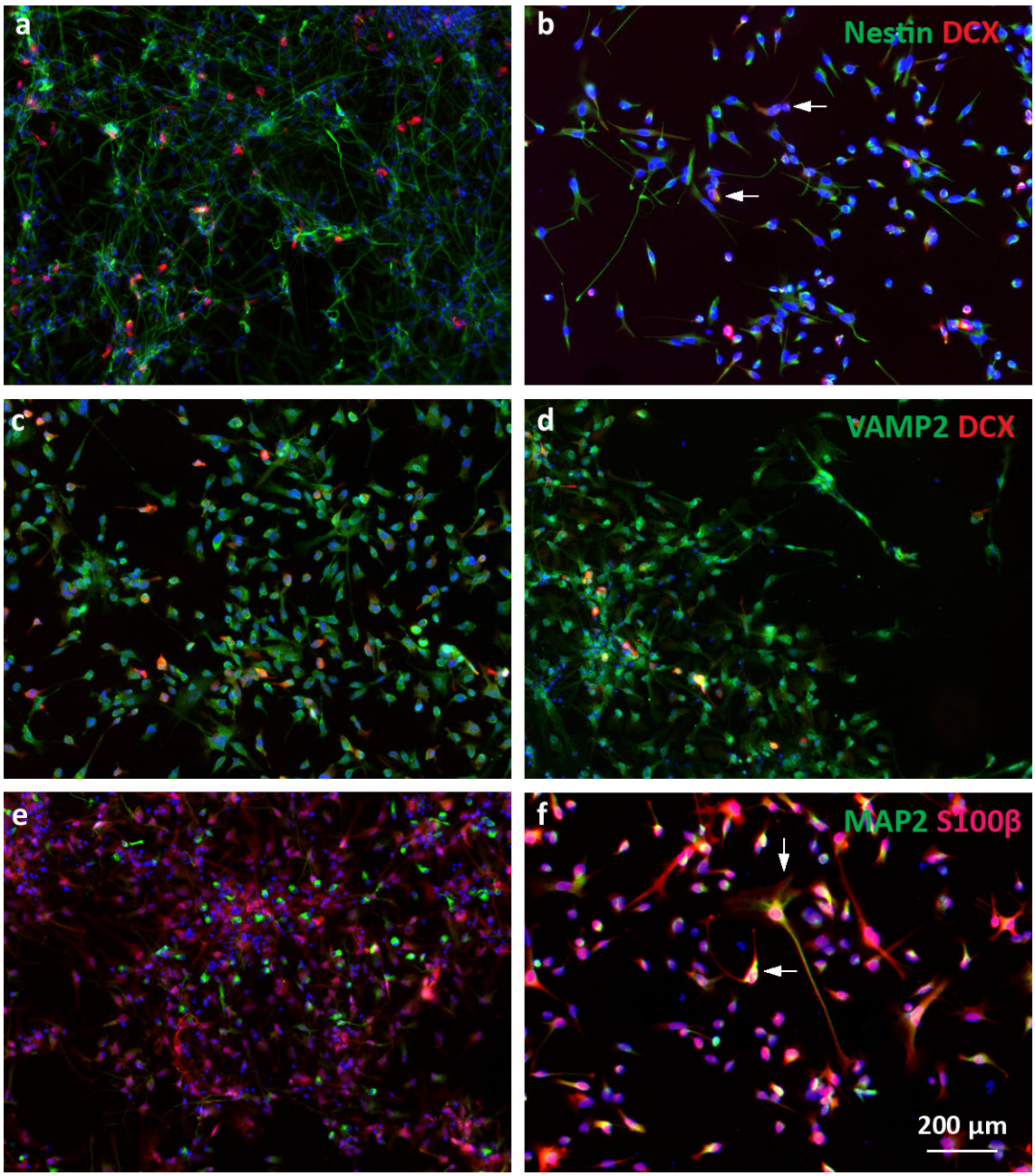


***Figure 3.1 CTX0E16/02 cells demonstrate robust differentiation into neurons and astrocytes***
Panels on the left (a, c and e) show CTX0E16/02 cells differentiated in the presence of SNBM while panels on the right (b, d and f) show CTX0E16/02 cells differentiated in the presence of RMM supplemented with 1 µM purmorphamine for 28 days. Cells differentiated in the presence of SNBM were smaller but more numerous and densely packed than those differentiated with purmorphamine and RMM. Cultures in top panels were stained with nestin (green), DCX (red) and DAPI (a and b), middle panels were stained with VAMP2 (green), DCX (red) and DAPI (c and d) and bottom panels were stained with MAP2 (green), S100β (far red) and DAPI (e and f). Pictures were taken using a Zeiss Axio Imager equipped with an ApoTome.

Several other differences were also apparent between these two differentiation conditions. For example, nestin$^+$ cells were smaller, more numerous and exhibited much more elaborate processes when differentiated using SNBM (Figure 3.1, **a**) as compared to PMA (Figure 3.1, **b**). In addition, the separation of different cellular phenotypes appeared more pronounced for SNBM than for PMA differentiated cultures. For example, a clear distinction could be made between nestin$^+$ and DCX$^+$ cells, labelled in green and red respectively (Figure 3.1, **a**) and MAP2$^+$ and S100β$^+$ cells, labelled in green and far-red respectively (Figure 3.1, **e**) when differentiated with SNBM. However, equivalent images for

cultures differentiated with PMA, show many cells expressing both nestin and DCX (Figure 3.1, **b**) or MAP2 and S100β (Figure 3.1, **f**), examples of which are clearly annotated. It is also interesting to note that for both the CTX0E03/02 and CTX0E16/02 cell lines, VAMP2 expression was provoked by all differentiation conditions tested but only at the latest time point of 28 days (see Figure 3.1, **c** and **d**). Conversely, SNAP-25 immunoreactivity was absent in cultures exposed to all tested conditions. This suggests that while the synaptic vesicle associated protein – VAMP2 – was present after 28 days differentiation, the presynaptic integral membrane protein – SNAP-25 was not. Both of these proteins are necessary to provide cells with the ability to release neurotransmitter and therefore, for the creation of functional synapses. This ability to form functional synapses may be achieved by increasing the amount of time that these cultures are differentiated for, as has been shown previously for neural cultures derived from ES and iPS cells [75,334]. It should be noted that the antibody used to identify the presence of SNAP-25 did not detect the presence of this protein under any of the tested differentiation conditions for the two cortical NPC lines. The antibody used has been shown to work in our laboratory using mouse neural tissue and has been previously reported on for its use in immunocytochemistry using mouse cells [523] and immunohistochemistry using human tissue [524]. The human NPC lines described here have been found through experience to be particularly difficult to immunocytochemically label, and led to the use of extensive blocking to achieve specific staining. Therefore, while a positive control for SNAP-25 immunolabelling could have been provided using human tissue sections or differentiated mouse NPCs, it is still possible that an absence of staining when using differentiated cortical human NPCs could reflect the difficulty in staining these cells rather than a true absence of the protein.

Exposure to SNBM or RMM supplemented with 1 μM purmorphamine were selected as the best conditions with which to differentiate the CTX0E03/02 and CTX0E16/02 cell lines. This choice was based upon the ability of these conditions to support healthy cultures and promote their differentiation into neurons and astrocytes. These two differentiation protocols were therefore chosen to further study the developmental potential of these human NPC lines. This included both further phenotypic characterisation and an analysis in both proliferative and differentiated cultures of the expression of genes encoding proteins that are important for the ability of neuropsychiatric compounds to exert their action (see Table 3.8). In addition, to explore the possibility that the mechanism through which the two chosen conditions precipitated differentiation may show a synergistic effect, a third condition was also included for further study; SNBM with the addition of 1 μM purmorphamine.

To carry out this analysis, proliferative CTX0E03/02 and CTX0E16/02 cells were seeded onto PDL and laminin-coated glass coverslips or laminin-coated tissue culture flasks – as described in ***2.1*** – for subsequent immunofluorescence staining or gene expression analysis respectively. Once cultures had reached 70% - 80% confluence they were washed twice with RMM and then differentiated under one of the following conditions:

- RMM supplemented with 1 μM purmorphamine;
- SNBM;

- SNBM additionally supplemented with 1 µM purmorphamine;

Evaluation of the six initially tested differentiation conditions (described above and summarised in Table 3.1) suggested that while large numbers of S100β$^+$ astrocytes could be generated, differentiations of less than 21 days were insufficient to yield significant numbers of tau$^+$ or MAP2$^+$ neurons. For this reason, separate CTX0E03/02 and CTX0E16/02 cultures were differentiated under each of the three conditions described above for 21, 28 or 35 days. At these time points, cells differentiated on glass coverslips were fixed for immunofluorescence staining as described in ***2.2***, above to determine the presence of the neuronal-specific markers tau and MAP2. Cultures were also stained with a cocktail of antibodies sharing the same isotype to detect the calcium binding proteins calretinin, calbindin-D28k and parvalbumin that recognise subsets of GABAergic neurons [335]. As all tested culture conditions were capable of generating large numbers of S100β$^+$ astrocytes, it was felt that staining for this marker was unnecessary at this stage of protocol optimisation. For gene expression analysis, cultures differentiated in tissue culture flasks were detached, pelleted, dissolved in TRIzol® and stored at -80°C as described in ***2.3.1***. Once all samples had been collected for both cell lines, under each of the tested conditions and at each time point, total RNA was extracted from all samples and DNase treated as a single batch as described in ***2.3.2*** and ***2.3.3***. Equal amounts of RNA for each sample were reverse transcribed to cDNA in duplicate before being pooled and stored at -20°C prior to use as template for PCR reactions to assess the expression of various genes.

Despite the fact the two NPC lines – CTX0E03/02 and CTX0E16/02 – were derived from the same donor and shared the same neural regional origin, the two cell lines showed a strikingly different morphology and pattern of growth. As can be seen in Figure 3.2, the CTX0E03/02 cells extended far more processes than their CTX0E16/02 counterparts. In addition, the CTX0E16/02 grew to cover a greater proportion of the surface area than did the CTX0E03/02 cells, which tended to grow in clusters rather than spread out over the available space. This pattern of growth exhibited by CTX0E03/02 cells resulted in these cultures needing to be passaged long before confluence was reached to avoid the occurrence of high levels of cell death.

Once differentiated, both the CTX0E03/02 and CTX0E16/02 cell lines generated relatively "deep" cultures with the component cells forming layers – this was especially true for differentiated CTX0E03/02 cells. Imaging by conventional fluorescence microscopy was therefore relatively problematic. For this reason, all images shown below were generated using a fluorescence microscopy equipped with an ApoTome or using a scanning confocal microscope. For each differentiation condition, at each time point and for each cell line, four different coverslips were stained with each of two different antibody combinations: MAP2 and tau or MAP2 and a cocktail of parvalbumin (PV), calretinin (CR) and calbindin-D28k (CB). Two coverslips for each condition were additionally included as controls – one stained in the absence of primary antibody and the other using secondary antibodies of different isotypes to the primaries used. Staining on all coverslips was described relative to that exhibited by the corresponding controls. When taking pictures using conventional fluorescence microscopy, equivalent

images were taken of coverslips of cells upon which staining had been performed in the absence of primary antibody. These were taken using both the same objective and exposure settings so as to provide examples of background staining. For images captured using laser scanning confocal microscopy, no primary antibody controls were used to adjust the level of excitation so as to only visualise specific fluorophore-mediated fluorescence.

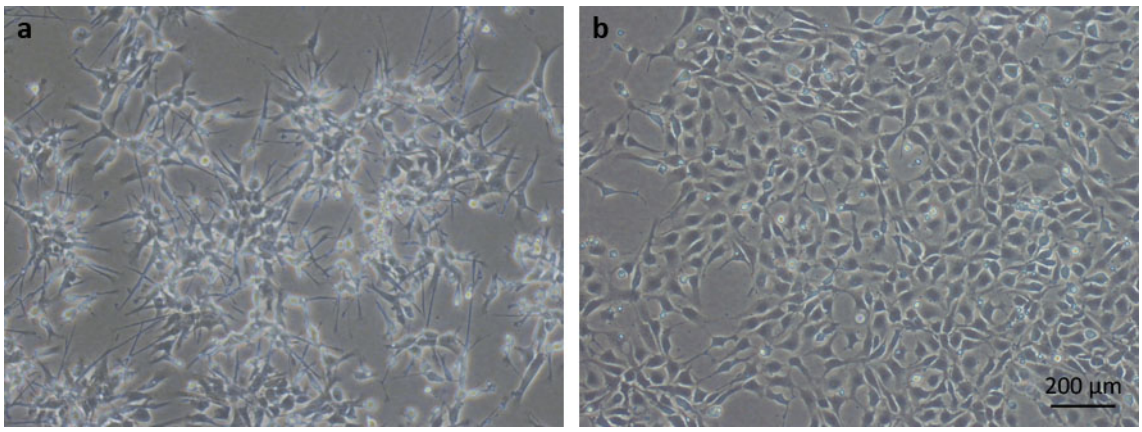


***Figure 3.2 Bright field images of confluent CTX0E03/02 and CTX0E16/02 cells in proliferative culture***
Images illustrative of the different morphologies shown by the two cortically derived human NPC lines used: CTX0E03/02 (a) and CTX0E16/02 (b). CTX0E03/02 cells tended to grow in clumps with the individual cells extending far more processes than cells of the CTX0E16/02 line, which proliferated to form an even monolayer of tessellating cells. Images were taken 3 days after a 1:4 split and captured using an inverted Nikon Eclipse TS100-F fitted with a Y-TV55 Nikon TV lens and a Digital Sight DS-2Mv camera and a 10x objective.

All coverslips for a particular differentiation condition, time point and cell line were primarily evaluated to provide an appraisal of the apparent health of each culture, taking account of the level of confluence and any evidence of cell death. The level of confluence demonstrated by cultures for a particular differentiation condition was particularly important to facilitate further experiments enabling the presence of functional receptors to be assessed. These were to initially involve the use of a FlexStation 3 microplate reader, to monitor ligand-induced intracellular $Ca^{2+}$ mobilisation. This instrument detects levels of fluorescence from fluorophore-loaded live cells grown in 96-well plates, making readings from an average signal across fields that encompass the majority of the area of each well. This system benefits greatly from confluent cultures by minimising background fluorescence caused by reflection of light from the microplate surface and ensures a good signal-to-noise ratio. While this is important for the current study, it would also lend itself to high-throughput screening methodologies that require similar culture characteristics and adds weight to the potential use of a cell line of this as a native tissue screening tool for psychiatric drug development.

### *3.2.2 CTX0E03/02 Cells Differentiate into Isolated Clusters of Neurons & Astrocytes*

**CTX0E03/02 cells differentiated in the presence of RMM supplemented with 1 µM purmorphamine** tended to produce culture dominated by cells with relatively large flat cell bodies and few processes at

all tested time points, as exemplified in Figure 3.3, **c** and **d**. At 21 days the resultant cultures exhibited patches of healthy, evenly distributed cells, as seen in Figure 3.3 panel **c**, though few cells grew between these patches (data not shown). With time in culture less patches of cells were observed and gaps between them were more common. While tau staining remained diffuse, and was less pronounced at later time points (Figure 3.3, **a** and **b**), rare examples of intensely MAP2 stained neurons with long processes could also be found at all time points (see arrows in Figure 3.3, **e** and **f**). To determine whether GABAergic neurons were present in these cultures, a cocktail of antibodies sharing the same isotype, raised against calretinin, calbindin-D28k and parvalbumin was used and visualised using the same secondary antibody. Diffuse staining for GABAergic cell type markers was detected in a few cells after 21 days of differentiation in large flat $MAP2^-$ cells (see arrow in Figure 3.3, **c**), though was less pronounced at 28 days (Figure 3.3, **d**) and was absent at 35 days (data not shown). Few cells remained after 35 days of differentiation, of which, very few were observed to be positive for the neuronal marker tau, while the diffuse MAP2 staining had reduced and a few cells with intensely stained processes were evident (data not shown). It should be noted that only a small minority of cells stained for MAP2, tau or GABAergic cell type markers exhibited a traditional neuronal morphology – rather they resemble undifferentiated cells – with the exception of a few intensely $MAP2^+$ cells. However, this staining was not observed in controls, which suggested this was real.

**CTX0E03/02 cells differentiated in the presence of SNBM** exhibited a strikingly different morphology to those differentiated in the presence of RMM supplemented with 1 µM purmorphamine. An even monolayer of cells was observed after a 21 day exposure to this differentiation condition, with much of the space where cell bodies were absent covered by $tau^+$ and $MAP2^+$ cellular processes (see Figure 3.4, a and c). Areas where cell bodies were present were dominated by large, flat cells demonstrating diffuse tau and MAP2 immunoreactivity and long processes, with smaller cells exhibiting long, intensely stained processes growing over them (Figure 3.4, a (see arrows) and c), with some exhibiting staining for GABAergic cell type markers. This tended to be diffuse and at this stage was restricted to a few large flat cells that were $MAP2^-$. Control staining in the absence of primary antibody suggested this was specific (see arrow in Figure 3.4, **c** and inlayed no primary antibody control). Also present after 21 days, but more pronounced by 28 days were patches or 'clumps' of cells that were enriched with large numbers of the smaller, intensely $tau^+$ and $MAP2^+$ cells growing on top of them. These areas were dominated by dying or dead cells; indicated by fragmented DAPI staining. Conventional fluorescence microscopy was ineffective for capturing images of these clumps and so confocal laser microscopy was employed instead. These areas are described in detail below.

After 28 days there were fewer of the large flat $tau^+$ and $MAP2^+$ cells, though some still remained (see Figure 3.4, b and d). Clumps or patches of cells were now more common and the spaces between these clumps were dominated by $tau^+$ processes linking the clumps (see detailed description below). The number of cells exhibiting intense tau and MAP2 staining had increased and some were now positive for GABAergic cell type markers (see arrows in Figure 3.4, d), though this was not common. Interestingly – unlike cultures differentiated for 21 days – cells exhibiting GABAergic cell type immunoreactivity were

also all MAP2$^+$. The characteristic clumps of cells produced by differentiation with SNBM were also evident at 35 days, though the number of small, intensely stained tau$^+$ and MAP2$^+$ cells had decreased, as had cells stained for MAP2 and GABAergic cell type markers.

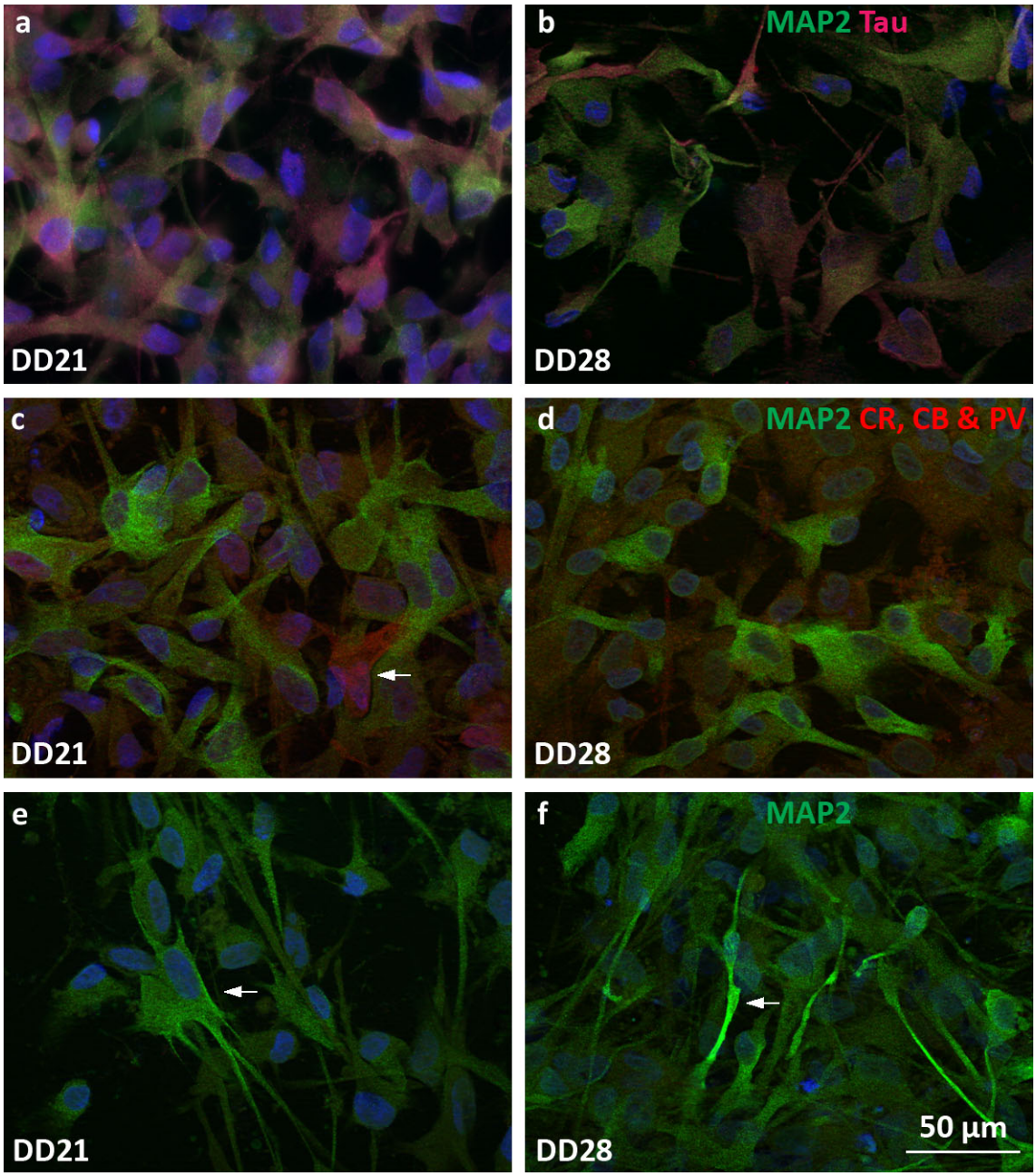


***Figure 3.3 CTX0E03/02 cultures differentiated with RMM supplemented with 1 µM purmorphamine***
Top panels (**a** & **b**) show cells stained with MAP2 (green), tau (far red) and DAPI. Middle panels (**c** & **d**) show cells stained with MAP2 (green), calretinin, calbindin-D28k & parvalbumin (red) and DAPI. Bottom panels show cells stained with MAP2 (green) and DAPI. Pictures were taken using a Zeiss Axio Imager equipped with an ApoTome.

**CTX0E03/02 cells differentiated in the presence of SNBM supplemented with 1 µM purmorphamine** resulted after 21 days in cultures that covered much of the available space with long, process bearing tau$^+$ and MAP2$^+$ cells (see Figure 3.5, **a**). As with cultures differentiated in the presence of SNBM, these cultures exhibited clumps of cells containing large amounts of cell debris – as indicated by fragmented

DAPI staining – that were enriched with tau$^+$ and MAP2$^+$ cells and traversed by numerous tau$^+$ processes. These clumps of cells appeared larger after 28 days of differentiation, and an increase was observed both in the number of tau$^+$ and MAP2$^+$ cells on their surface, and the intensity of staining these cells exhibited (Figure 3.5, **c**). Some clumps at this time point appeared to form long 'tracts' of cells composed of tau$^+$ processes (Figure 3.5, **b**). After 35 days of differentiation, cultures were dominated by these clumps and tracts of cells. However, these accounted for less than half the available area, with few cells growing in the spaces between them. MAP2$^+$ and tau$^+$ positive cells remained enriched within the clumps but less intense immunoreactivity was observed than was seen after 28 days and the cellular processes appeared to be less elaborate (Figure 3.5, **d**).

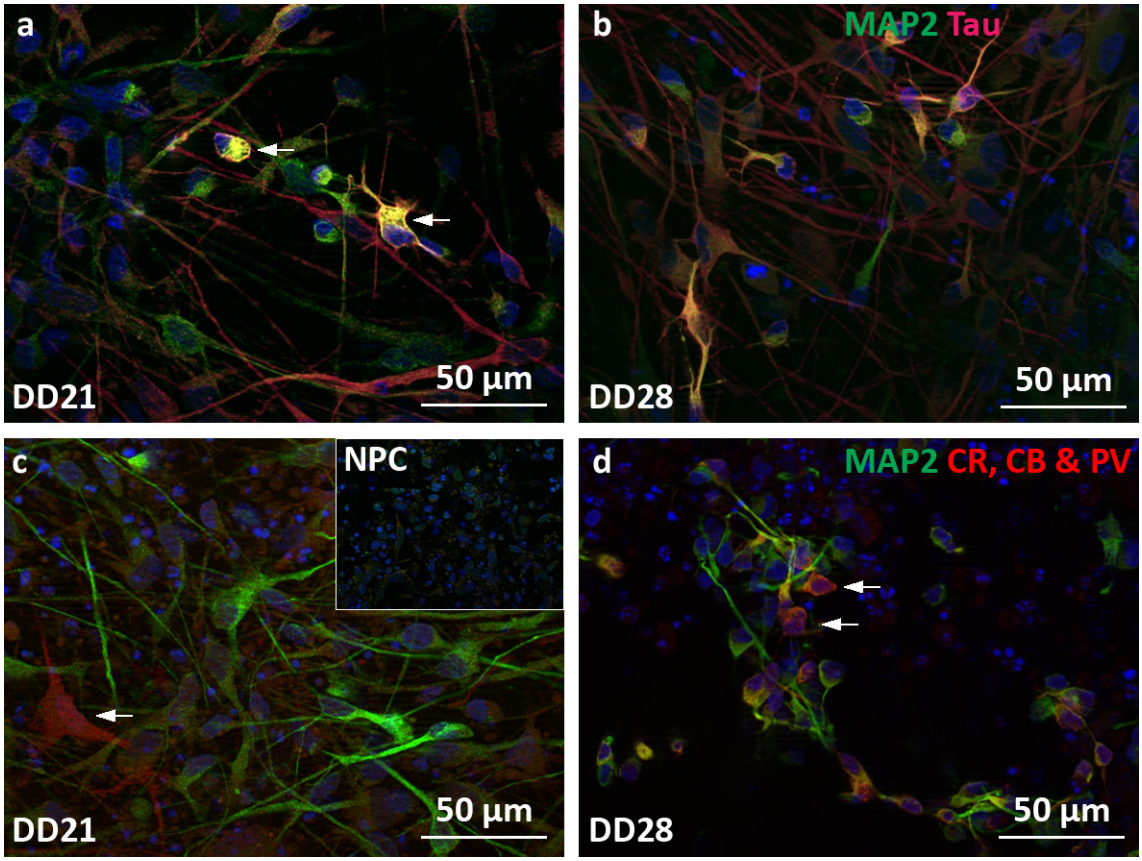


***Figure 3.4 CTX0E03/02 cultures differentiated in the presence of SNBM***
Top panels (**a** & **b**) show cells stained with MAP2 (green), tau (far red) and DAPI, with arrows in panel **a** indicating small intensely tau$^+$ and MAP2$^+$ cells. Bottom panels (**c** & **d**) show cells stained with MAP2 (green), calretinin, calbindin-D28k & parvalbumin (red) and DAPI, with arrow in panel **c** indicating **a** large flat MAP2$^-$ cell, diffusely immunoreactive for GABAergic cell type markers. Arrows in panel **d** show small cells co-labelled for MAP2 and GABAergic cell type markers. Pictures were taken using a Zeiss Axio Imager equipped with an ApoTome.

Cells expressing GABAergic cell type markers were infrequent, but present after 21 days differentiation using SNBM and purmorphamine – and like those seen at 21 days in the presence of SNBM alone – they were not co-labelled with MAP2 and demonstrated a large flat morphology (see arrow in Figure 3.6, **a**). After 28 days of differentiation, small, MAP2$^+$ GABAergic neurons were present that were often located on top of, or near, cellular clumps (see arrow in Figure 3.6, **b**), though large flat cells showing diffuse staining for GABAergic cell type markers were also present (data not shown). After 35 days the number

of small co-labelled cells had reduced considerably with only a few remaining, while the large flat diffusely stained cells had disappeared altogether (data not shown).

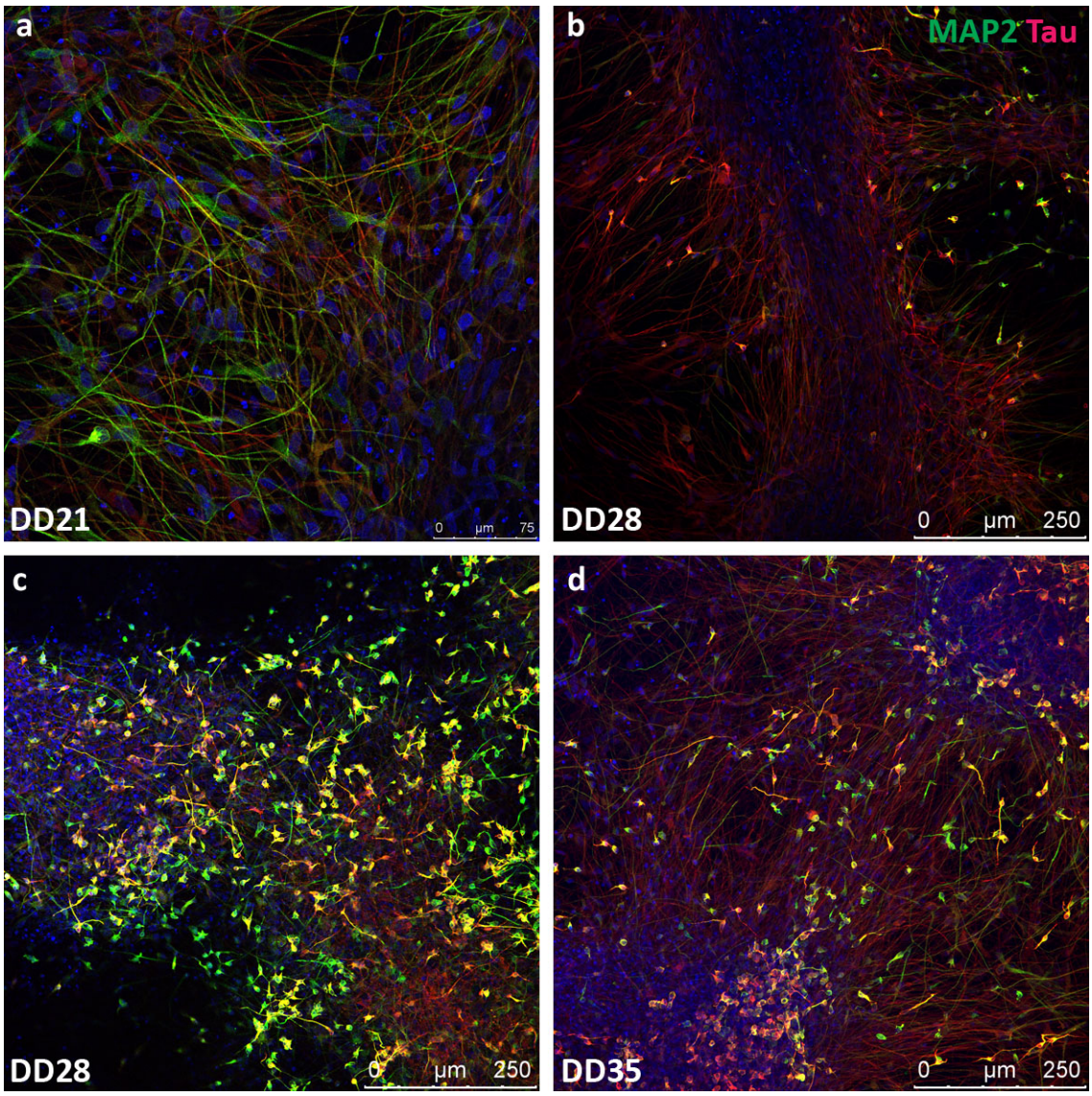


***Figure 3.5 CTX0E03/02 cells readily differentiate into neurons in the presence of SNBM and purmorphamine***
All panels show cells stained using MAP2 (green), tau (far red) and DAPI. Pictures were taken with a Leica TCS SP5 Confocal microscope. Images were captured after non-specific background levels were adjusted for using no primary control stained cells.

A common feature of differentiating the CTX0E03/02 line in the presence of SNBM – with or without purmorphamine – was the presence of clumps of cells containing large amounts of cell debris and enriched with cells exhibiting relatively small soma. These cells were characterised by elaborate or long, intensely tau$^+$ and MAP2$^+$ processes. While not observed after 21 days of differentiation, by 28 days many of these cells were identified as being GABAergic. However, after 35 days of differentiation there were fewer cells labelled in this way, with those remaining demonstrating less intense immunoreactivity than was observed at 28 days. An example of one of these clumps of cells is shown in more detail in Figure 3.7 and Figure 3.8. Due to the depth of this clump (in excess of 50 µm) a scanning confocal

microscope was required to take multiple cross-sectional images of the cells (see Figure 3.7) before the individual images were flattened to provide the image seen in Figure 3.8. By studying the collection of images shown in Figure 3.7 it can be seen that the top of the clump of cells is enriched with a large number of tau$^+$ and MAP2$^+$ cell bodies. Progressing down through the stack shows the large amount of cell debris within the cell clump, as is evident from the fragmented DAPI staining observed. Moreover, the inside of the clump of cells does not appear to contain any tau$^+$ or MAP2$^+$ neurons, though this may be because the antibodies are unable to access this region, or the laser light from the microscope is unable to penetrate here. Tau$^+$ and MAP2$^+$ neurons were also found around the periphery of the clump, though this area was dominated by numerous tau$^+$ processes that appear to descend down the side of the clump and progress across the surrounding area. These form almost a blanket upon which many more tau$^+$ and MAP2$^+$ neurons are found (see Figure 3.8, **c**).

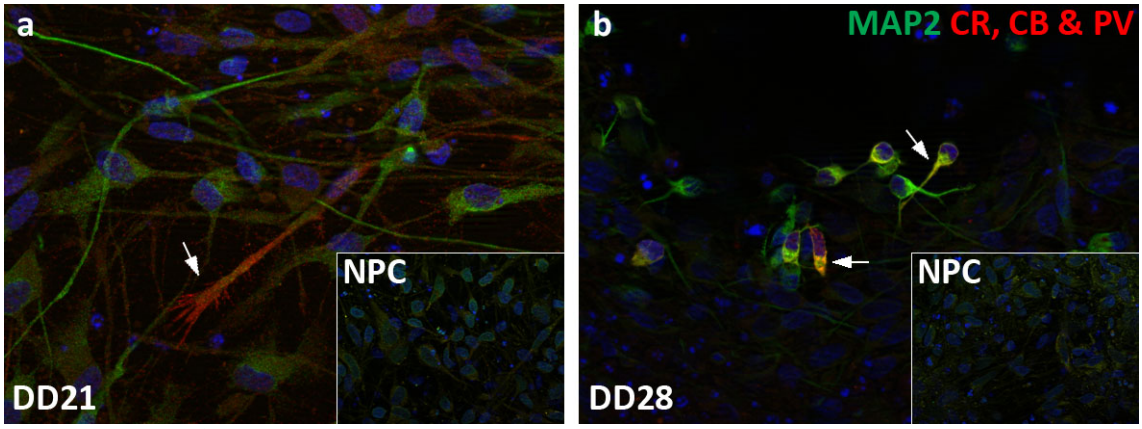


***Figure 3.6 CTX0E03/02 cells differentiated in the presence of SNBM supplemented with 1 µM purmorphamine***
Panels (**a** & **b**) show cells stained with MAP2 (green), calretinin, calbindin-D28k & parvalbumin (red) and DAPI, with the arrow in panel **a** indicating an elaborately processes cell exhibiting immunoreactivity for the GABAergic cell type markers. Arrows in panel **b** show small cells co-labelled for MAP2 and GABAergic cell type markers. Pictures were taken using a Zeiss Axio Imager equipped with an ApoTome.

The tendency of the CTX0E03/02 cells to grow in these characteristic clumps was restricted to those differentiated in the presence of SNBM, and was independent of the presence of 1 µM purmorphamine. To illustrate this, Figure 3.9 and Figure 3.10 show cells differentiated in the presence of SNBM supplemented with 1 µM purmorphamine. These images provide an example of how tau$^+$ neuronal processes appear to link distinct clumps of cells, and appears to provide an environment – other than that found on top of the cellular clumps – for the smaller, intensely tau$^+$ or MAP2$^+$ neurons to thrive. Figure 3.9 depicts a series of cross-sectional images, again captured using a laser scanning confocal microscope, through two adjacent stacks of cells. The images at the top of the stacks show an enrichment of the previously described small-soma, tau$^+$ or MAP2$^+$ neurons. As the images descend through the stack they show these cells enriched on the surface of the clump, along with many tau$^+$ neuronal processes. Towards the bottom of the stack an elaborate network of tau$^+$ processes can be seen linking the two clumps of cells, and appears to provide a good environment for either the survival or appearance of small tau$^+$ or MAP2$^+$ neurons.

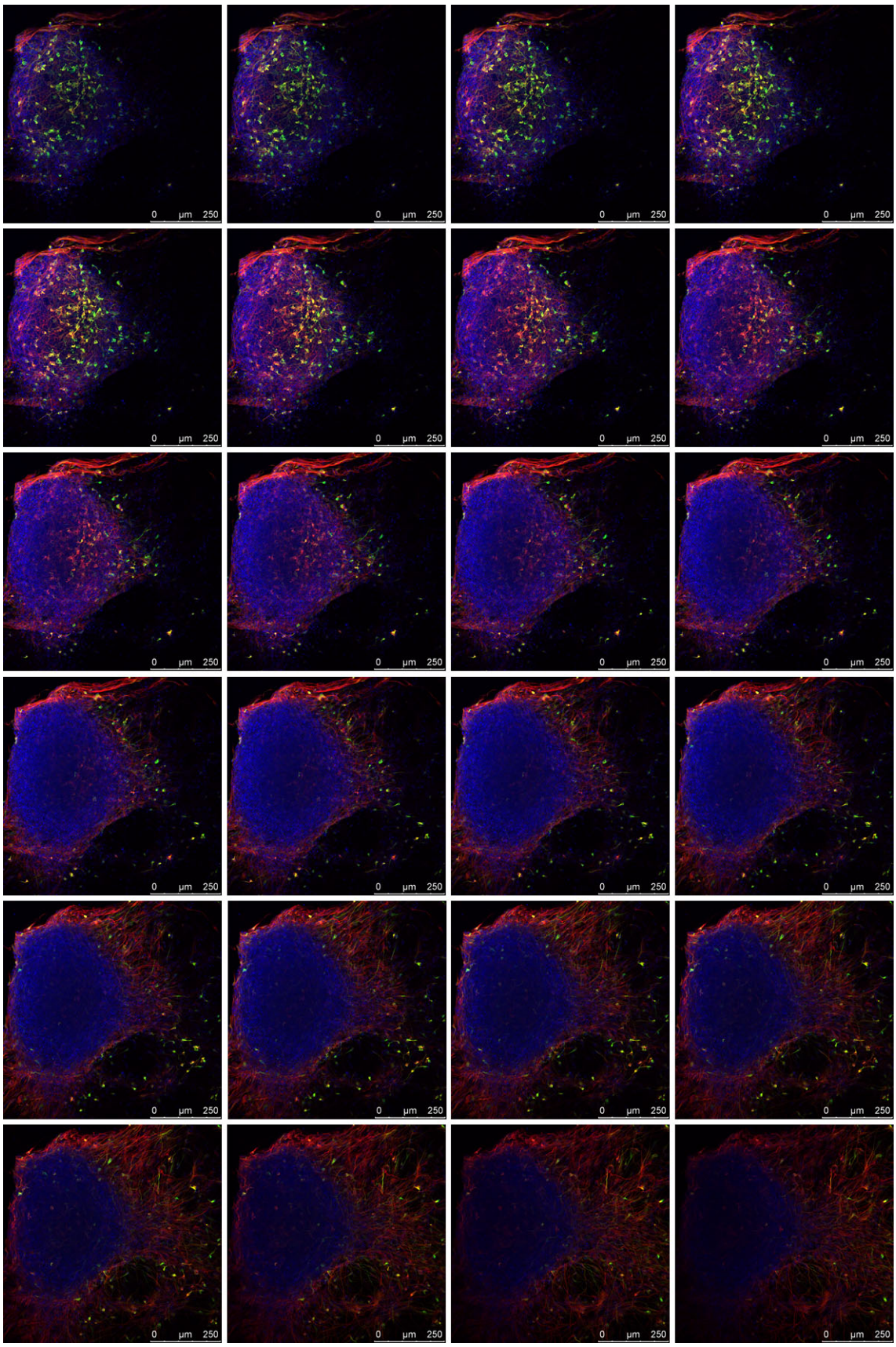


***Figure 3.7 Image stack of CTX0E03/02 cells following 28 days of differentiation using SNBM***
Top left panel shows the top of the stack with the bottom shown in the bottom right panel. MAP2 (green), tau (far red) and DAPI. Pictures were taken with a Leica TCS SP5 Confocal microscope**.**

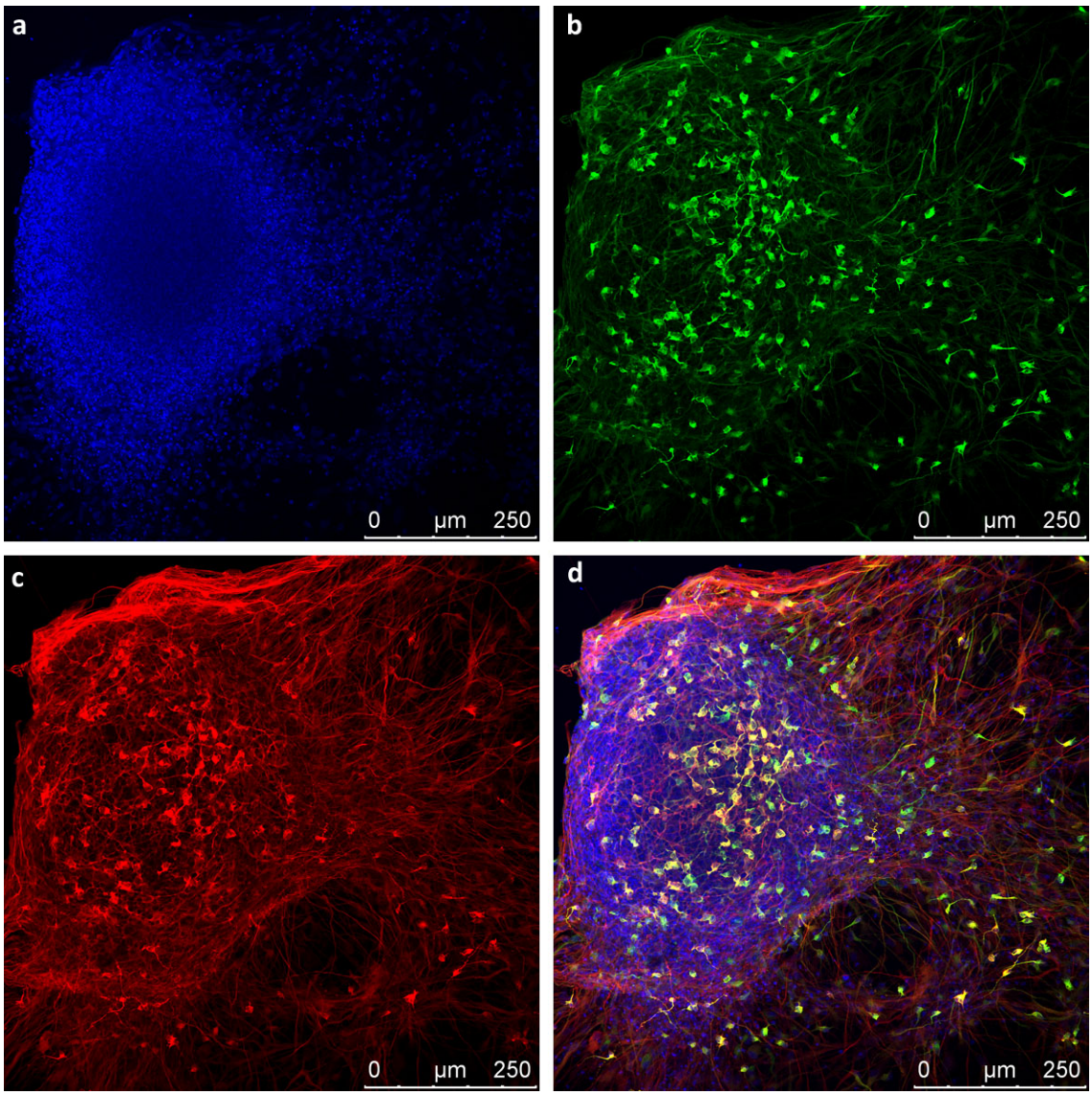


***Figure 3.8 Flattened stack of CTX0E03/02 cells following 28 day differentiation using SNBM***

Panels shows nuclei labelled with DAPI (blue), MAP2 positive cells (green), tau positive cells (far red) and the merged image. Pictures were taken with a Leica TCS SP5 Confocal microscope.

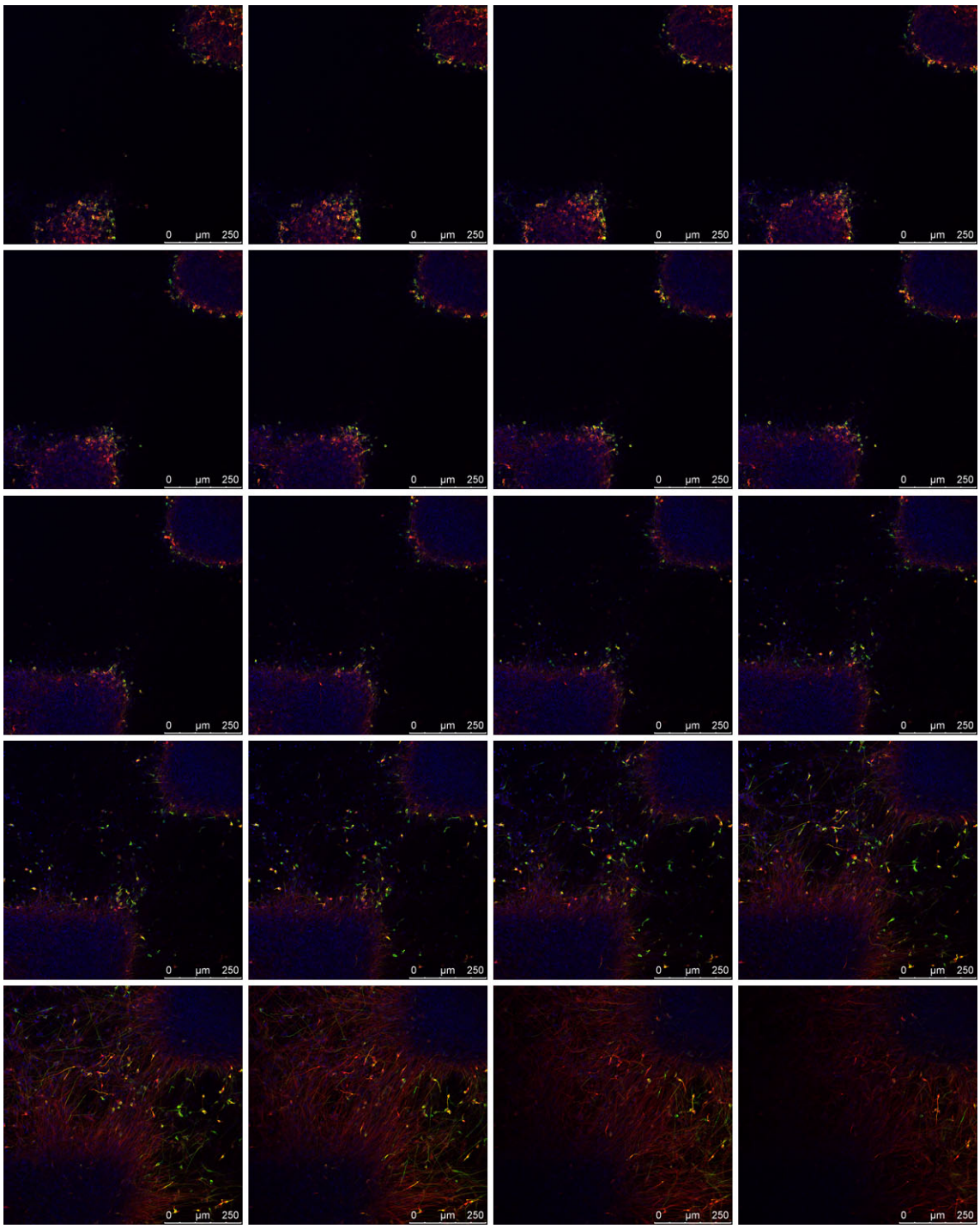


***Figure 3.9 Image stack of CTX0E03/02 cells following 28 day differentiation using SNBM with purmorphamine***
Top left panel shows the top of the stack with the bottom shown in the bottom right panel. MAP2 (green), tau (far red) and DAPI. Pictures were taken with a Leica TCS SP5 Confocal microscope.

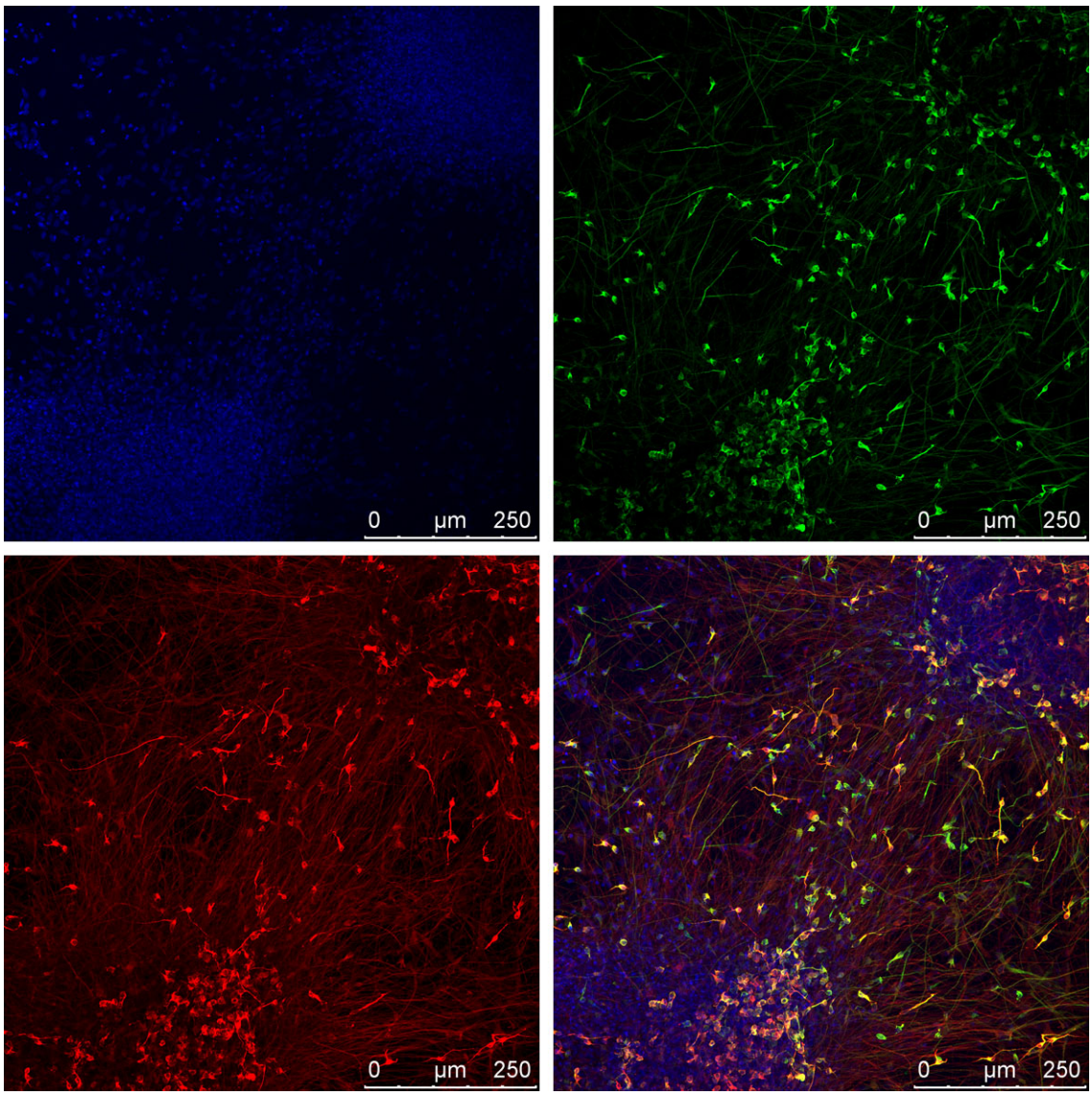


***Figure 3.10 Flattened stack of CTX0E03/02 cells following 28 day differentiation in SNBM and purmorphamine***
Panels shows nuclei labelled with DAPI (blue), MAP2 positive cells (green), tau positive cells (far red) and the merged image. Pictures were taken with a Leica TCS SP5 Confocal microscope.

### *3.2.3 CTX0E16/02 Cells Differentiate into Even Monolayer of Neurons & Astrocytes*

**CTX0E16/02 cells differentiated in the presence of RMM supplemented with 1 µM purmorphamine** for 21 days produced cultures similar in appearance to those observed for the CTX0E03/02 line. The cultures were comprised of a majority of large flat cells diffusely stained with tau and MAP2. In contrast to the CTX0E03/02 line at this stage however, the presence of smaller, elaborately processed, intensely $tau^+$ and $MAP2^+$ neurons were also present (see Figure 3.11, **a**). In some cases, these cells were also stained for GABAergic cell type markers (see arrows in Figure 3.11, **d**). After 28 days of differentiation the cultures represented an even monolayer of cells that was dominated by diffusely stained $tau^+$ and $MAP2^+$ large flat cells (see Figure 3.11, **b**). Surprisingly, fewer of the smaller, intensely $tau^+$ and $MAP2^+$ neurons were present at this stage when compared to cells differentiated for 21 days. There were however more cells expressing GABAergic markers, which tended to be located in isolated patches (see Figure 3.11, **e**). After 35 days of differentiation, the cultures remained healthy with a good monolayer of

cells (see Figure 3.11, **c**), though this was not entirely consistent and patches had emerged where no cells were growing (data not shown). The number of intensely stained tau$^{+}$ and MAP2$^{+}$ neurons was considerably lower than that seen at 28 days, and was restricted to small patches of cells. A greater proportion of GABAergic neurons were evident at this stage (see Figure 3.11, **f**).

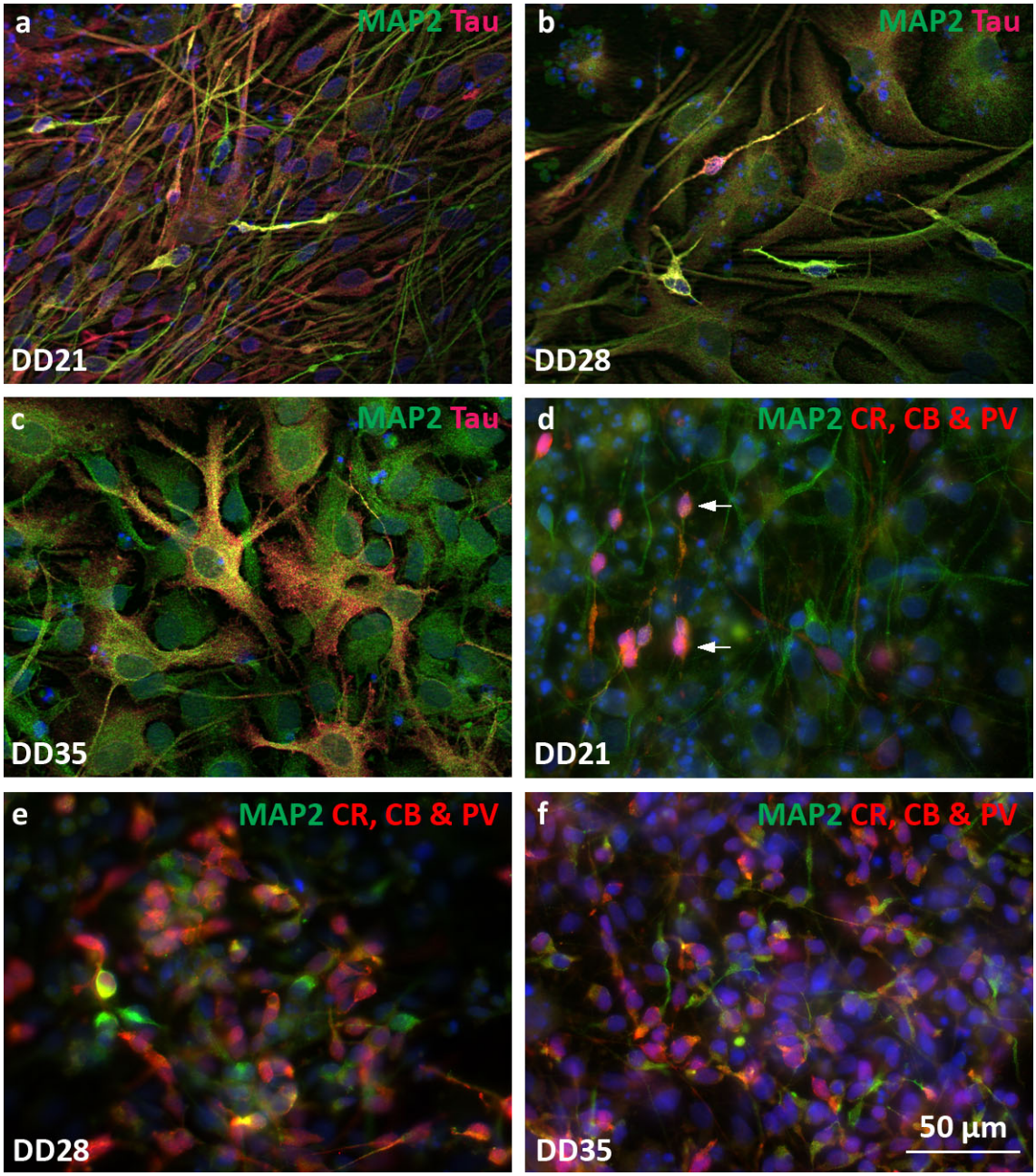


***Figure 3.11 CTX0E16/02 cells differentiated in the presence of RMM supplemented with 1 µM purmorphamine***
Panels **a**, **b** and **c** show cells differentiated for 21, 28 and 35 days respectively and stained with MAP2 (green), Tau (far red) and DAPI. Panels **d**, **e** and **f** show cells differentiated for 21, 28 and 35 days respectively and stained with MAP2 (green), parvalbumin, calretinin & calbindin-D28k (red) and DAPI. Pictures were taken using a Zeiss Axio Imager equipped with an ApoTome.

**CTX0E16/02 cells differentiated in the presence of SNBM** for 21 days produced an even monolayer of cells with an absence of the clumping observed with the CTX0E03/02 line, though cell death – as indicated by fragmented DAPI staining – was present. These differentiation conditions produced an

abundance of both large flat diffusely stained cells and small, elaborately processed, intensely stained cells with respect to tau and MAP2 (see Figure 3.12, **a**). Cells expressing markers indicative of GABAergic neurons were common (Figure 3.12, **b**). After 28 days of differentiation these cultures where dominated by an even monolayer of cells though there were some small patches where cells were absent. The large, flat diffusely tau$^{+}$ and MAP2$^{+}$ cells were less common at this stage and appeared in many cases to have been replaced by an elaborate network of the smaller, elaborately processed, intensely stained tau$^{+}$ and MAP2$^{+}$ neurons (Figure 3.12, **c**).

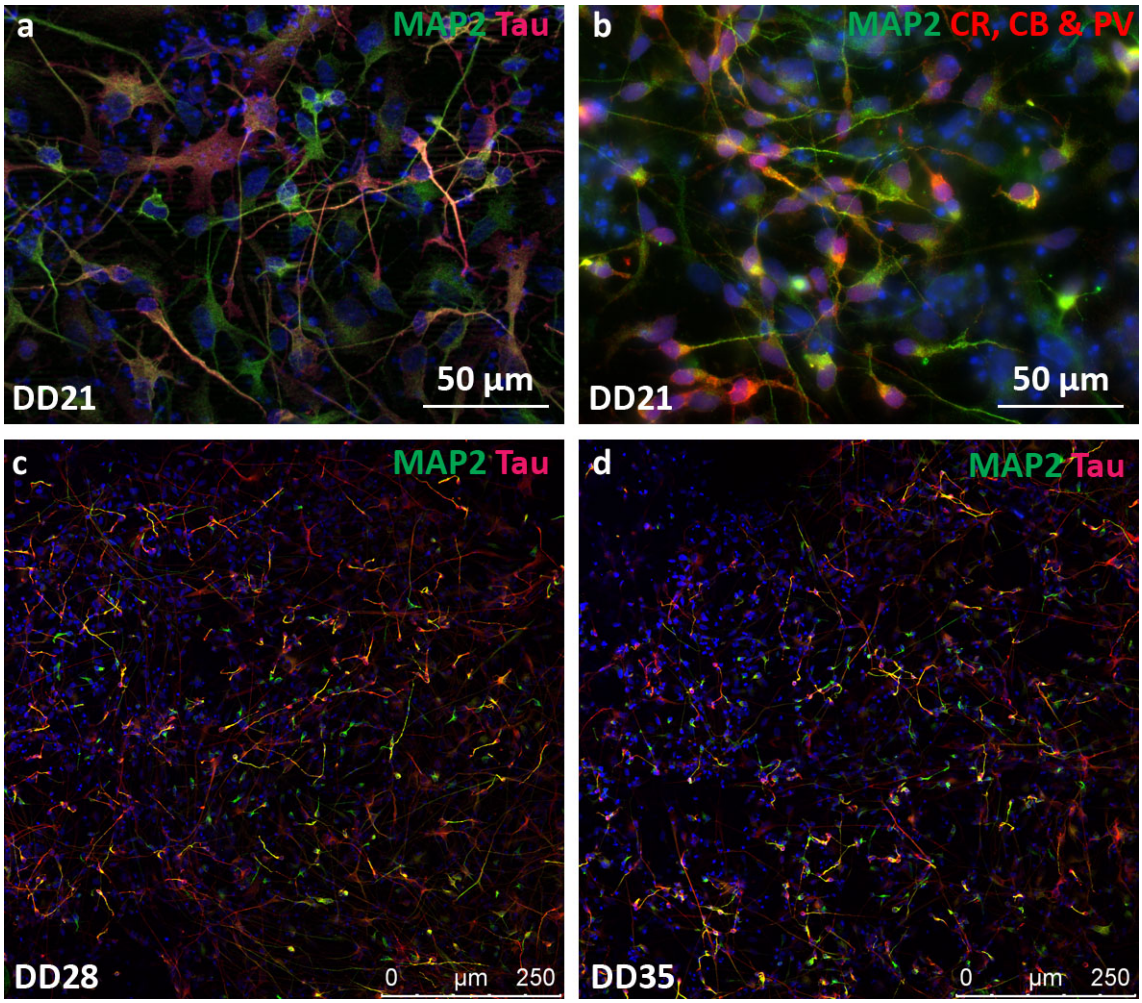


***Figure 3.12 CTX0E16/02 cells readily differentiate into neurons in the presence of SNBM***
Top panels (**a** & **b**) show cells differentiated for 21 days, while panels **c** and **d** show cells differentiated for 28 and 35 days respectively. Panels **a**, **c** and **d** were stained with MAP2 (green), tau (far red) and DAPI while cells in panel b were stained with MAP2 (green), parvalbumin, calretinin & calbindin-D28k (red) and DAPI. Pictures in top panels were taken using a Zeiss Axio Imager equipped with an ApoTome. Pictures in bottom panels were taken with a Leica TCS SP5 Confocal microscope.

Cells expressing GABAergic cellular subtype markers were more common after a 28 day differentiation (see Figure 3.13, **a**) than was seen after 21 days (Figure 3.12, **b**). After 35 days of continuous differentiation the CTX0E16/02 cells demonstrated a healthy monolayer of cells with many elaborately processed cells intensely positive for the neuronal markers tau and MAP2 (Figure 3.12, **d**) and

GABAergic neuronal markers (see Figure 3.13, **b**). There was an absence of the thick clumping observed with the CTX0E03/02 cells, though tau$^{+}$ and MAP2$^{+}$ neurons were enriched in some areas.

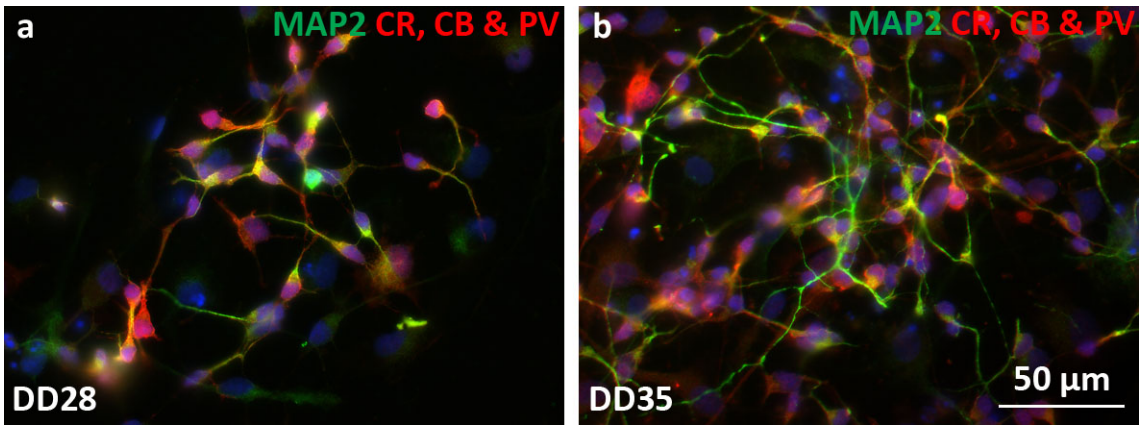


***Figure 3.13 CTX0E16/02 cells differentiate into GABAergic neurons in the presence of SNBM***
Panel **a** show cells differentiated for 28 days, while panels **b** show cells differentiated for 35 days. Cells were stained with MAP2 (green), parvalbumin, calretinin & calbindin-D28k (red) and DAPI. All pictures were taken a Zeiss Axio Imager equipped with an ApoTome.

**CTX0E16/02 cells differentiated in the presence of SNBM supplemented with 1 µM purmorphamine** produced cultures after 21 days that closely resembled those observed after the same period in the presence of SNBM alone. An even monolayer of cells was observed, made up of large flat cells, diffusely stained with tau and MAP2 and cells with smaller cell soma, intensely stained for these neuronal markers (see Figure 3.14, **a**). These smaller neuronal cells were enriched in patches throughout the culture and were often found to be GABAergic (see Figure 3.14, **b**). Following 28 days of differentiation the resultant cultures represented a dense network of cells that appeared healthier than those observed when cells were differentiated in the absence of purmorphamine (see Figure 3.14, **c**). At this stage the number of intensely stained tau$^{+}$ and MAP2$^{+}$ neurons had increased and GABAergic staining had become more distinct (see Figure 3.14, **d**). After 35 days of differentiation there remained a healthy network of cells (see Figure 3.14, **c**), though some clumping was observed – as had been seen in differentiated CTX0E03/02 cultures at this time point. The number of cells expressing GABAergic markers was reduced after this period (see Figure 3.14, **f**).

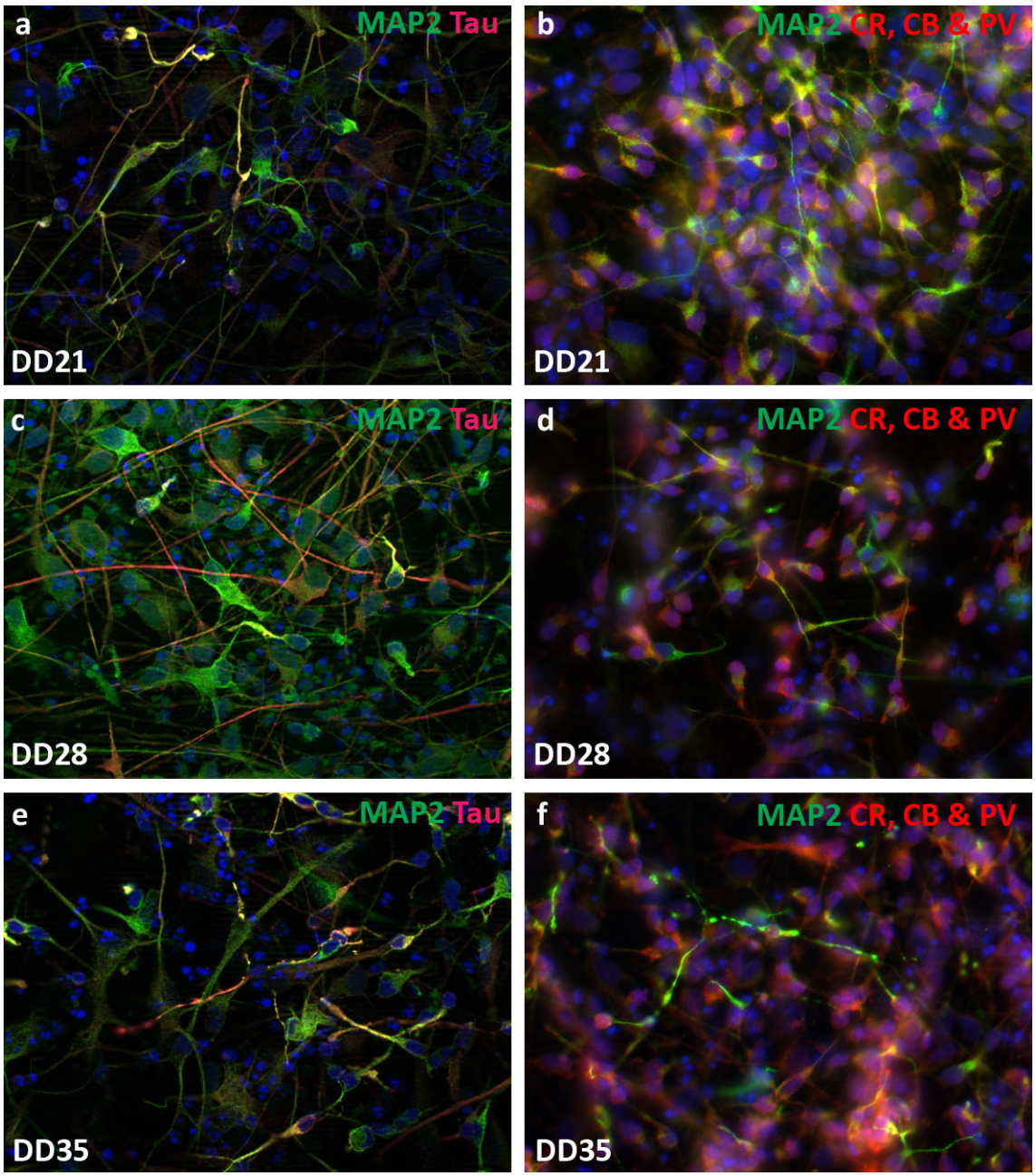


***Figure 3.14 CTX0E16/02 cells differentiated in the presence of SNBM supplemented with 1 µM purmorphamine***
Panels **a** & **b** show cells differentiated for 21 days, panels **c** & **d** show cells differentiated for 28 days and panels **e** & **f** show cells differentiated for 35 days. Panels **a**, **c** & **e** show cultures stained with MAP2 (green), tau (far red) and DAPI. Panels **b**, **d** & **f** show cells stained with MAP2 (green), parvalbumin, calretinin & calbindin-D28k (red) and DAPI. Pictures were taken using a Zeiss Axio Imager equipped with an ApoTome.

**In summary**, when differentiated in the presence of **RMM supplemented with 1 µM purmorphamine**, both the CTX0E03/02 and CTX0E16/02 cell lines produced cultures containing a majority of large, flat cells that stained diffusely for the neuronal markers tau and MAP2. Cells exhibiting small soma, long processes and intense tau and MAP2 immunoreactivity were largely absent though some were found in enriched patches with the CTX0E16/02 line after 21 days of differentiation, though these were less abundant after 28 or 35 days. While GABAergic cells remained absent in the differentiated CTX0E03/02 cells, they were present after 21 days for the CTX0E16/02 line, and their numbers rose steadily with time.

Differentiation of the two cortical lines in **SNBM** produced two distinct cell types – large, flat cells that demonstrated diffuse tau and MAP2 staining and cells with small soma and long, often elaborate cellular processes that exhibited intense tau and MAP2 staining. After 21 days of differentiation the cultures from both cell lines produced a confluent network of cells that covered the available growth area. In both cases the larger, flat cells dominated at this earlier time point though the smaller cells were present and tended to be enriched in patches throughout the culture. For the CTX0E03/02, but not the CTX0E16/02 cells, these patches were often found above clumps of cells. For the CTX0E16/02 line, these patches were also enriched with intensely $tau^+$ and $MAP2^+$ neurons with small cell soma, expressing markers indicative of GABAergic neuronal phenotypes; calretinin, calbindin-D28k and parvalbumin. With an increased period of differentiation, cultures from both cell lines saw a reduction in the number of the larger flat cells and an increase in the proportion of the smaller, elaborately processed, intensely $tau^+$ and $MAP2^+$ neurons. Further enrichment of this cell type was found in clumps (CTX0E03/02) or patches (CTX0E16/02), though while the growth area remained covered for the CTX0E16/02 line, differentiated CTX0E03/02 cultures contained many areas where no cell bodies were present. An increase in the amount of cell debris, as indicated by the presence of fragmented DAPI staining was also observed. Evidence of GABAergic cell type markers also increased with the period of differentiation for the CTX0E16/02 line, though a peak in the expression of these markers appeared to be reached after 28 days for the CTX0E03/02 line, as immunoreactivity was reduced and more diffuse after 35 days.

Cultures resulting from the differentiation of the CTX0E03/02 and CTX0E16/02 lines in **SNBM with 1 μM purmorphamine** were similar to those observed when using SNBM alone. Cultures were however a little more dense for the CTX0E03/02 line with more clumping of cells which contained large amounts of cell debris, as indicated by fragmented DAPI staining. The number of smaller, highly processed, intensely $tau^+$ and $MAP2^+$ cells appeared slightly higher than in cultures where purmorphamine was absent, but the number of cells expressing GABAergic cell type markers were slightly lower when differentiated in these conditions.

When differentiated in the presence of SNBM, independent of the presence of 1 μM purmorphamine, the CTX0E03/02 and CTX0E16/02 cells generated a similar overall number of cells demonstrating a neuronal phenotype (small cell soma with elaborate processes and intense tau and MAP2 immunoreactivity) when considering the whole culture. However, for the CTX0E03/02 line these cells were restricted to small, highly enriches patches (see Figure 3.15, **a**) throughout the culture, with large spaces containing no cell bodies at all. The cultures resulting from differentiation of the CTX0E16/02 cells however produced a more even distribution of these cells throughout the culture – though patches enriched with the smaller cells were present – without the appearance of these clumps (see Figure 3.15, **b**).

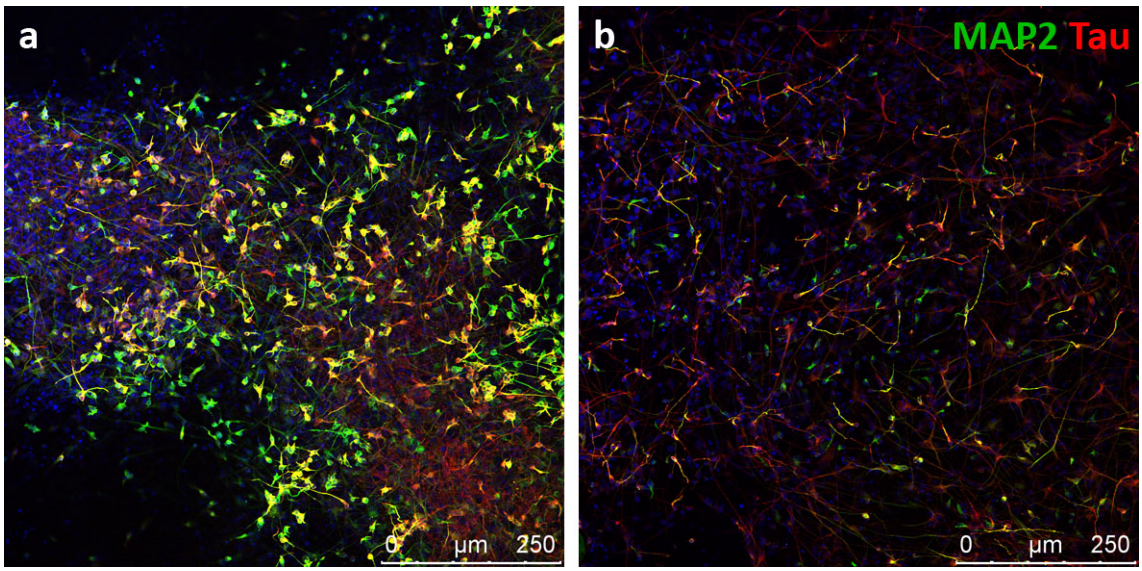


***Figure 3.15 CTX0E03/02 cells differentiate into concentrated clumps of neurons while CTX0E16/02 tend to produce a more even monolayer***

CTX0E03/02 (**a**) and CTX0E16/02 (**b**) differentiated in the presence of neurobasal medium supplemented with B27 for 28 days. Merged images with nuclei labelled blue (DAPI), $MAP2^+$ neurons labelled green and $tau^+$ neurons labelled red. Pictures were taken using a Leica TCS SP5 Confocal microscope.

Taken together, these data suggest that both the CTX0E03/02 and CTX0E16/02 cell lines can be differentiated to produce a high proportion of $tau^+$ and $MAP2^+$ neurons. In addition, under certain conditions cells are also present that express markers indicative of GABAergic neuronal phenotypes. The ability to differentiate is not however the only criteria informing the choice of a cell line for further experimentation, as discussed above. Due to the pharmacological approach of this study, it is also imperative that the cell line that is ultimately chosen for further experimentation is capable of expressing genes encoding proteins required for antipsychotics to exert their action.

### *3.2.4 Expression Profile of Proliferative & Differentiated NPC Lines*

In basic terms, antipsychotics are thought to exert their therapeutic effects through their interactions with various cell surface receptors found within the brain. These receptors allow changes in the chemical environment surrounding these cells to be transduced beyond the surface of the cell. This can occur through various mechanisms, and results in both transient signalling events such as changes in intracellular $Ca^{2+}$ or cAMP concentrations, or more lasting effects such as changes in gene expression. Sensitive techniques such as radioligand binding have identified a host of neurotransmitter receptors that antipsychotic drugs exhibit high affinity towards (and can be found collated on the NIMH Psychoactive Drug Screening Program $K_i$ database (http://pdsp.med.unc.edu/)), while functional pharmacological approaches have identified various accessory proteins that are either necessary for, or influence, the function of these receptors. In addition, many downstream signalling molecules have been identified in various tissues that allow the transduction and integration of signals precipitated by these initial ligand-receptor interactions [233,336]. If a NPC line is to be used to investigate the mechanism of action of antipsychotic drugs, it is important that it expresses as many of the genes encoding these

receptors, accessory proteins and signalling molecules as possible. Using the available literature regarding current understanding of how antipsychotics exert their action, a list of genes was compiled whose expression would be desirable in a cell line used to investigate antipsychotic drug action. Additional genes were also identified that encode proteins essential for normal neuronal function such as CACNA1C – a voltage-gated $Ca^{2+}$ channel – or targeted by compounds used to treat other neuropsychiatric conditions, such as SLC6A4 and GABRA1 – encoding targets for antidepressants (5-HT transporter) and anxiolytics ($GABA_A$ channel subunit), respectively. Genes encoding receptors targeted by compounds currently in clinical development as potentially novel antipsychotic medicines were also included, such as TACR3, GRIA1 and GRIN1 – encoding $NK_3$, AMPA and NMDA receptors respectively. These are detailed in Table 3.8 below.

The experiments described below determined which of the genes detailed in Table 3.8 were expressed in each of the seven human NPC lines described at the beginning of this chapter. This work was performed in parallel with the optimisation of the differentiation of the two cortical NPC lines – CTX0E03/02 and CTX0E16/02. For this reason, initial experiments investigating gene expression were performed using RNA collected from all seven NPC lines in their proliferative state. In addition, for the five NPC lines for which there was an existing differentiation protocol – HPC03A/07, STROC05/08A, VM, SPC-01 and SPC-04 – RNA was also collected from these cells once the relevant differentiation had been performed. Furthermore, the influence upon gene expression of a simple additional step during the differentiation of each cell line was also assessed. This involved each of the differentiating cultures being exposed to a depolarising concentration of $K^+$ (25 mM) at the early stages of neurogenic induction. This was performed based on findings from a previous study suggesting that a depolarising concentration of $K^+$ provided a maturation capacity to differentiating mesencephalic NPCs [337]. The observed effect was shown to occur as a result of membrane depolarisation, as it could be completely inhibited by the presence of tetrodotoxin, which specifically blocks voltage gated $Na^+$ channels. Further investigation showed that the observed effect was mediated through a $Ca^{2+}$-independent mechanism [337].

| Gene | Protein Product |
|---|---|
| *DRD2* | Dopamine $D_2$ receptor (GPCR): high-affinity target for first and second generation antipsychotic drugs and associated with clinical efficacy [154,166,338] |
| *DRD3* | Dopamine $D_3$ receptor (GPCR): high-affinity target for first and second generation antipsychotic drugs, difficult to functionally distinguish from dopamine $D_2$ receptors [191] |
| *HTR2A* | 5-$HT_{2A}$ receptor (GPCR): high-affinity target for second and some first generation antipsychotic drugs, and has been associated with atypicality [165] |
| *CHRM1* | Cholinergic muscarinic $M_1$ receptor (GPCR): mixed-affinity target for range of antipsychotics [183]. Selective compounds under investigated to treat cognitive symptoms and as possible monotherapy [175] |
| *HRH1* | Histamine $H_1$ receptor (GPCR): high-affinity target for first and second generation antipsychotic drugs and associated with weight gain and metabolic side effects [171] |
| *ADRA1A* | Adrenergic $\alpha_{1A}$ receptor (GPCR): high-affinity target for first and second generation antipsychotic drugs and may contribute to efficacy and side effect liability [339] |
| *TACR3* | Tachykinin 3 receptor ($NK_3$, GPCR): target of compounds currently in phase II clinical trial for the treatment of schizophrenia [340] |
| *GRIA2* | Glutamate receptor 2 (AMPA receptor subunit, ionotropic): allosteric modulators of this receptor currently under investigation as possible adjunct treatment for cognitive deficits and monotherapy [175] |
| *GRM1-8* | Metabotropic glutamate receptors 1-8 ($mGluR_{1-8}$, GPCRs): several of these are targeted by compounds currently in clinical and preclinical development for the treatment of schizophrenia – particularly $mGluR_2$, $mGluR_3$ and $mGluR_5$ [175] |
| *GRIN1* | Glutamate receptor, N-methyl D-aspartate (NMDA) 1 (NR1, ionotropic): allosteric modulators currently in phase II clinical trial for the treatment of cognitive and negative symptoms [175] |
| *ARRB2* | β-Arrestin 2 (scaffold and signalling protein): multifunctional scaffolding protein involved in GPCR desensitisation and G-protein independent signalling [341,342] |
| *CAV1* | Caveolin-1 (scaffold protein): Accessory protein involved in GPCR plasma membrane expression and internalisation[235,343,344] |
| *DLG4* | Postsynaptic density protein 95 (PSD-95): Scaffold protein important for GPCR localisation and function [191,345] |
| *MPDZ* | Multiple PDZ domain protein (MUPP1): Scaffold protein important for GPCR localisation and function [190] |
| *CACNA1C* | L-type, voltage-dependent calcium channel $\alpha_{1C}$ subunit: One of the major voltage-dependent $Ca^{2+}$ channel found in the CNS. Recently associated with risk of developing schizophrenia and bipolar disorder [136] |
| *GSK3B* | Glycogen synthase kinase 3β (GSK-3β): Important signalling node for neuronal activity and several neuropsychiatric drugs. Aberrant function has been linked to the schizophrenia [233,234] |
| *PPP1R1B* | Protein phosphatase 1 regulatory subunit 1B (PPP1R1B), also known as dopamine- and cAMP-regulated neuronal phosphoprotein (DARPP-32): Important signalling node for neuronal activity and several neuropsychiatric drugs [233] |
| *SLC6A4* | 5-HT transporter (SERT): Primary target of selective serotonin reuptake inhibitor (SSRI) antidepressants [346] |
| *GABRA1* | GABA receptor subunit $\alpha_1$ (ionotropic): Ubiquitous subunit for all GABA-A receptors – contains binding site for benzodiazepine anxiolytics [347] |
| *AVPR1A* | Arginine vasopressin receptor $V_{1A}$ (GPCR): Current interest as a target for the treatment of autism and schizophreniaReceptor target of novel compounds to treat autism [348] |

***Table 3.8 List of genes identified as relevant to neuropsychiatric drug action***

For the five NPC lines for which differentiation protocols had previously been developed, the conditions used to achieve this varied considerably – both in terms of the culture conditions and the duration of differentiation, as described in ***2.1.3*** and summarised in Table 2.1 above. In consideration of this, and also to minimise disruption to each lines' respective differentiation protocol, a two hour exposure to 25 mM KCl was applied in different ways for each line:

- Normal differentiation of the hippocampal line – HPC03A/07 – involved the removal of expansion medium followed by two washes with blank DMEM:F12 before leaving them in RMM for seven days without a medium change [65]. To account for the possibility that differentiation could be partly mediated through the release of soluble factors into the medium, this conditioned medium was removed and kept. This was immediately replaced with RMM containing a final KCl concentration of 25 mM and maintained under normal incubation conditions for two hours. This medium was then removed and replaced with the conditioned medium. Normally differentiated cells were also exposed to the same procedure using RMM lacking KCl to control for any effect resulting from the medium changes. Differentiations were then continued as previously described;
- Both spinal cord cell lines – SPC-01 and SPC-04 – were differentiated with an initial exposure to RMM supplemented with 10 µM DAPT before changing the medium to unsupplemented RMM for the remaining five days of the differentiation [67]. This medium change was exploited to expose the cells to RMM containing 25 mM KCl for two hours (or a sham medium change for control differentiation cultures), before removal and replacement with RMM for the remaining differentiation period;
- Differentiation of the striatal NPC line – STROC05/08A – involved a longer differentiation period of 21 days and involved the removal of expansion medium (Human Medium (HM – see Appendices, ***8.1.2***), supplemented with EGF, $FGF_2$ and 4-OHT), and replacement with HM supplemented with 1 µM purmorphamine [66]. This was replaced every 48 hours for the duration of the differentiation. Due to the longer differentiation period, it was decided to perform the two hour, $K^+$-induced depolarisation after four rather than two days. This was incorporated into the normal medium change required on this day, with a sham medium change performed on the control differentiation cultures;
- The ventral mesencephalon derived cell line – VM – was differentiated by removal of expansion medium (B27 Medium (B27M – see Appendices, ***8.1.3***), supplemented with EGF, $FGF_2$ and 4-OHT) and replacement with unsupplemented B27M. No further medium change was required for the seven days of the differentiation [104,322]. With a possible role for conditioned medium in this differentiation process, these cells were exposed to 25 mM KCl in the same way as was described for HPC03A/07 above.

Once differentiation under the two conditions (normal and depolarised) for each cell line was complete, the cells were enzymatically detached, pelleted by centrifugation, dissolved in TRIzol® and stored at -80°C as described in ***2.3.1***, above). Total RNA used for subsequent experiments was extracted (see ***2.3.2***, above) from all cell lines on the same day as a single batch, and followed by DNase treatment as detailed in ***2.3.3***. RNA for each sample was then reverse transcribed into cDNA in two separate reactions before being pooled and diluted to a concentration appropriate for PCR analysis (see ***2.3.4***, above). Reverse transcription was also performed in duplicate on the same amount (1.5 µg per reaction) of whole human brain (WHB) control RNA. This was used as a positive control to demonstrate the specificity of the primers that had been designed, but also to facilitate a crude comparison as to the

levels of expression for each gene in adult human brain tissue. Levels of expression of each gene in each RNA sample described below are expressed relative to the level of expression seen in the WHB sample. All reactions for a specific primer pair were exposed to 35 temperature cycles as described in ***2.3.6***, above. Each set of PCR reactions for an individual gene were also accompanied by a negative – no template – control. Each reaction was run in separate lanes of a different 2.5% polyacrylamide gel for each gene, and visualised as detailed in ***2.3.7***, above. Each PCR reaction was performed in duplicate and run in separate gels. Images shown below are representative of both gels (replicate gel images available upon request). In addition to DNase treatment of all RNA samples prior to RT reactions, primers were, as far as possible, designed to amplify intron-spanning regions of the genes of interest. This approach was used to facilitate the detection of possible genomic DNA contamination of cDNA samples. Furthermore, in the case of genes exhibiting alternative transcript variants, multiple sequence alignments were performed prior to primer design to ensure all expressed transcripts of a gene of interest were recognised (see ***2.3.5*** for details).

The GPCR that all currently approved antipsychotics are thought to primarily target in order to exert their therapeutic effects – dopamine $D_2$ (DRD2) – was ubiquitously expressed in all seven NPC lines at levels comparable to that seen in whole human brain (WHB), irrespective of culture conditions (see Figure 3.16). The same was also true of the histamine $H_1$ (HRH1) receptor. Compared to expression levels seen in WHB, dopamine $D_3$ (DRD3) was present at very low levels in the proliferative cortical lines. DRD3 expression was found in all three condition samples for the spinal cord line SPC-01 though its expression only emerged once the second spinal cord line – SPC-04 – was differentiated. Differentiation-induced expression of DRD3 was also a feature of the striatal NSC line, STROC05/08A. While not absent in the proliferative state, DRD3 expression was elevated upon differentiation in the ventral mesencephalic line, VM. In contrast, differentiation caused a reduction in the level of DRD3 expression in the hippocampal cell line, HPC03A/07.

HTR2A – the transcript encoding the 5-$HT_{2A}$ receptor – was expressed at very low levels in proliferative CTX0E03/02 and SPC-04 cells but more so in STROC05/08A. Expression was absent in proliferative CTX0E16/02, SPC-01, HPC03A/07 and VM cultures. HTR2A expression was however robustly induced following differentiation in SPC-01 and intensified in SPC-04 and STROC05/08A. HTR2A expression was virtually absent following differentiation of HPC03A/07 and VM cultures showed some induction following a normal differentiation though very little when additionally exposed to KCl.

CHRM1 – encoding the muscarinic acetylcholine $M_1$ receptor – expression was absent in proliferative CTX0E03/02 cells and showed very low expression levels in proliferative SPC-01, HPC03A/07 and STROC05/08A cultures (see Figure 3.16). Slightly higher expression was seen in proliferative CTX0E16/02, SPC-04 and VM cultures. Both normal and $K^+$ assisted differentiation caused an intensification of CHRM1 expression in SPC-01, SPC-04, STROC05/08A and VM cells while HPC03A/07 showed little or no expression of this gene following differentiation.

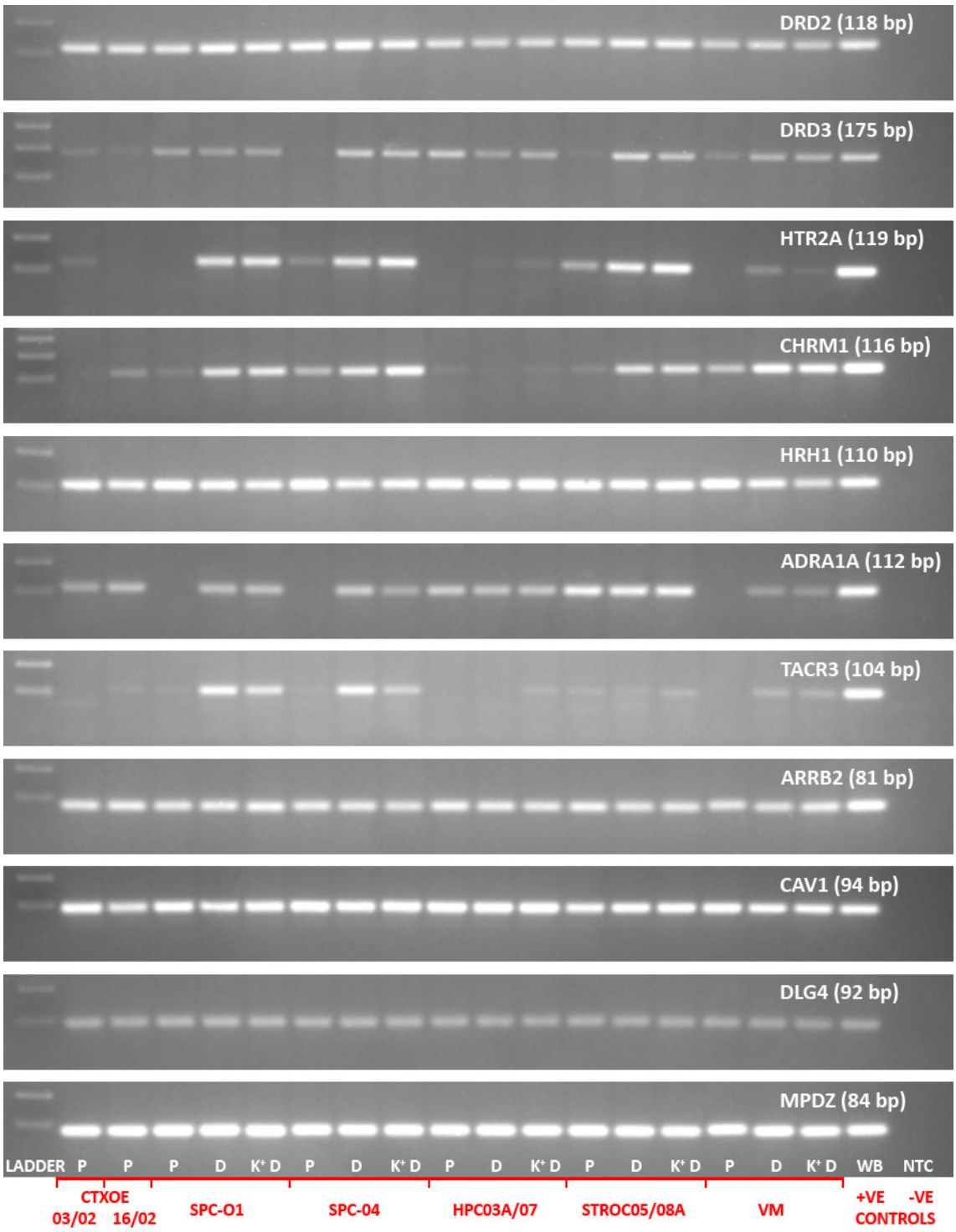


***Figure 3.16 Expression of Various GPCRs and some of their accessory proteins in various human NPC lines***

Semi-quantitative PCR analysis of proliferative and differentiated NPCs with respect to the expression of several GPCRs targeted by currently available and putative antipsychotics: DRD2 and DRD3 encoding dopamine $D_2$ and $D_3$ receptors respectively, HTR2A encoding 5-$HT_{2A}$ receptors, CHRM1 encoding cholinergic muscarinic $M_1$ receptors, HRH1 encoding histamine $H_1$ receptors, ADRA1A encoding adrenergic $\alpha_{1A}$ receptors and TACR3 encoding tachykinin $NK_3$ receptors. The expression of four GPCR accessory proteins are also shown: ARRB2 encoding the scaffold and signalling protein β-arrestin 2, CAV1 encoding the scaffold protein caveolin-1, DLG4 encoding the scaffold protein PSD-95 and MPDZ encoding the scaffold protein MUPP1. Individual lanes represent expression of these genes in proliferative (P), normally differentiated (D) or differentiation with a $K^+$-induced depolarisation step included ($K^+$D). Levels of expression are shown for proliferative CTX0E03/02 and CTX0E16/02 cultures plus SPC-01, SPC-04, HPC03A/07, STROC05/08A and VM under each of the three culture conditions. The expression for each gene, in each of the described culture conditions is accompanied by a WHB cDNA template positive (+ve) control and a no template negative (-ve) control.

Expression of the gene encoding the adrenergic $\alpha_{1A}$ receptor – ADRA1A – was present in proliferative CTX0E03/02, CTX0E16/02, HPC03A/07 and STROC05/08A cultures and was maintained following differentiation of HPC03A/07 and STROC05/08A, whether $K^+$ assisted or not (see Figure 3.16). The expression of ADRA1A was absent in proliferative SPC-01, SPC-04 and VM cells, though both differentiation conditions for each cell line led to the induction of this gene.

The expression of TACR3 (tachykinin $NK_3$ receptor) was absent in proliferative CTX0E03/02, HPC03A/07 and VM cells while showing very low levels in proliferative CTX0E16/02, SPC-01, SPC-04 and STROC05/08A cultures. Normal differentiation provoked robust induction of TACR3 expression in SPC-01 and SPC-04 cells, though was slightly reduced in these lines when exposed to KCl during differentiation. In contrast, expression was only seen in differentiated HPC03A/07 cultures exposed to KCl. The low level of TACR3 expression exhibited by proliferative STROC05/08A cultures was maintained upon differentiation in the presence or absence of added KCl, while low level expression of TACR3 was induced by both differentiation conditions. The expression of genes encoding four different GPCR accessory proteins – ARRB2, CAV1, DLG4 and MPDZ – was also accessed in these various cultures. These genes were all found to be expressed ubiquitously in all tested cultures, at levels comparable to that detected in WHB.

The expression of genes encoding AMPA and NMDA channel subunits plus all metabotropic glutamate receptors was also assessed in the seven NPC lines (see Figure 3.17). GRIA2, encoding the glutamatergic AMPA receptor subunit GluR2 was expressed at vey low levels in proliferative CTX0E03/02 and VM cultures, though was highly expressed in proliferative CTX0E16/02 and STROC05/08A cultures. This high level of expression exhibited by STROC05/08A cells was maintained following differentiation in the presence or absence of KCl. GRIA2 expression was detected in proliferative cultures of both the spinal cord derived NPC lines and was increased to levels comparable to that observed for WHB following differentiation in both of the tested conditions. Comparatively low levels of GRIA2 expression were detected in HPC03A/07 cells, with little difference observed between the different culture conditions tested. In contrast, differentiation of the VM cells caused an increase in GRIA2 gene expression, though this failed to reach levels exhibited by WHB or other cell lines. Expression of the gene encoding the glutamatergic NMDA receptor subunit NR1 – GRIN1 – was barely detectable in proliferative CTX0E03/02, CTX0E16/02, STROC05/08A and VM cultures and was absent in proliferative SPC-01, SPC-04 and HPC03A/07 cultures. Robust induction of this gene was observed following differentiation of the two spinal cord NPC lines using either protocol, though still failed to reach levels detected in WHB. The expression of GRIN1 was induced in both of the differentiated HPC03A/07 cultures, though at barely detectable levels, while the low level of expression observed in proliferative STROC05/08A and VM cultures saw little change following differentiation.

Several of the genes encoding different metabotropic glutamate receptors were expressed to a greater or lesser extent in all NPC lines in all of the tested conditions. These included GRM1, GRM2, GRM4, GRM6, GRM7 and GRM8. Only GRM3 and GRM5 – both encoding receptors targeted by antipsychotics in preclinical development: $mGluR_3$ and $mGluR_5$ respectively – demonstrated discreet expression

between the different tested NPC lines and culture conditions. GRM3 expression was absent in proliferative CTX0E03/02 and CTX0E16/02 cultures and all tested culture conditions for STROC05/08A and VM cultures. However, robust expression was seen in all tested conditions for SPC-01 and SPC-04. In contrast, low expression seen in proliferative HPC03A/07 cultures was enhanced upon differentiation.

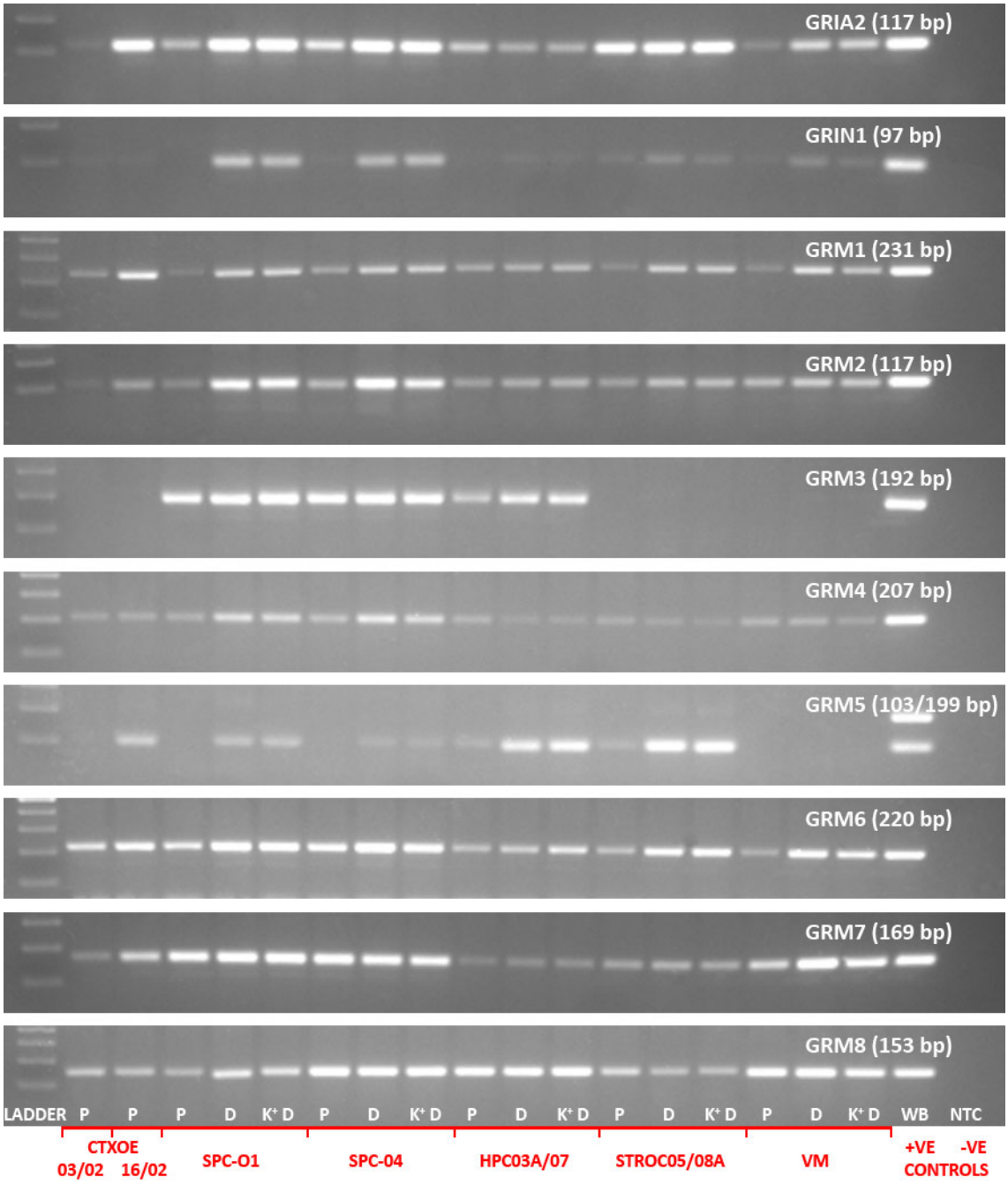


***Figure 3.17 Expression of glutamate receptors and receptor subunits in various human NPC lines***
Semi-quantitative PCR analysis of genes encoding ionotropic glutamate receptor subunits and all metabotropic glutamate receptors in proliferative and differentiated NPCs: GRIA2 encoding the glutamatergic AMPA receptor subunit GluR2, GRIN1 encoding the glutamatergic NMDA receptor subunit NR1, GRM1 – GRM8 encoding the metabotropic glutamate receptors mGluR1 – mGluR8 respectively. Individual lanes represent expression of these genes in proliferative (P), normally differentiated (D) or differentiation with a $K^+$-induced depolarisation step included ($K^+$D). Levels of expression are shown for proliferative CTX0E03/02 and CTX0E16/02 cultures plus SPC-01, SPC-04, HPC03A/07, STROC05/08A and VM under each of the three culture conditions. The expression for each gene, in each of the described culture conditions is accompanied by a WHB cDNA template positive (+ve) control and a no template negative (-ve) control.

Primers used to detect the expression of GRM5 recognised two distinct transcript variants; a and b, with PCR product lengths of 199 and 103 base pairs, respectively. Both transcripts were robustly expressed in WHB control cDNA template, with slightly higher expression of the a variant of the transcript (see Figure 3.17). In contrast, expression of the GRM5 a variant transcript was absent in proliferative cultures from all of the seven NPC lines investigated, and was not detected under any of the tested culture conditions for the SPC-04 or VM lines. Indeed, neither transcript was detected under any of the tested culture conditions for the VM line. GRM5 a variant transcript expression was observed at the limit of detection following differentiation in the presence or absence of KCl for the HPC03A/07 and STROC05/08A lines, though only in the absence of KCl for the SPC-01 line. Expression of this transcript was absent from proliferative CTX0E03/02, SPC-01 and SPC04 cultures, though modest induction of this gene was detected in the two spinal cord derived cell lines following differentiation. Low levels of GRM5 b variant expression were observed in proliferative HPC03A/07 and STROC05/08A cultures, with robust expression – greater than that observed in WHB – detected in both lines following differentiation irrespective of the presence of KCl. Expression of the GRM5 b variant was robustly detected in proliferative CTX0E16/02 cultures.

CACNA1C encodes the $\alpha_{1C}$ subunit of the L-type voltage-gated $Ca^{2+}$ channel, $Ca_v1.2$. The gene has 23 recognised RefSeq transcript variants that were multiply aligned to design the primers used for the detection of the gene in this study. While WHB cDNA template provided a single band corresponding to the expected 90 bp fragment, all tested NPCs also exhibited a second, unexpected band suggesting the additional presence of a fragment of approximately 180 bp (see Figure 3.18). This finding may warrant further investigation but is beyond the scope of this present study. Expression of the 90 bp fragment only will be described here. CACNA1C expression was detected at comparable levels to that seen in WHB in all tested culture conditions for the HPC03A/07, STROC05/08A and VM lines. Lower levels of expression were exhibited by proliferative SPC-01 and SPC-04 cultures, though expression increased upon differentiation, independent of KCl exposure. Proliferative CTX0E03/02 cultures also demonstrated CACNA1C expression, while levels were considerably lower in proliferative CTX0E16/02 cultures.

PPP1R1B encodes the signalling node protein phosphatase 1 regulatory subunit 1B, also known as dopamine and cAMP-regulated neuronal phosphoprotein, 32 kD (DARPP-32), and was expressed in all lines under all tested conditions to some extent. Robust expression, at levels comparable to that seen in WHB were exhibited by proliferative CTX0E03/02 and CTX0E16/02 cultures along with all tested conditions for the SPC-01, HPC03A/07 and STROC05/08A lines. While very low PPP1R1B expression was detected in proliferative VM cultures, once differentiated in the presence or absence of KCl, these levels increased substantially. This was similarly true for SPC-04, though detected expression levels were higher in the proliferative cells than was seen in proliferative VM cultures. GSK3B encodes the signalling node GSK-3$\beta$, and was ubiquitously expressed in all cell lines under all tested conditions at robust levels.

The 5-HT transporter (SERT) – encoded by SLC6A4 – was not expressed at high levels in WHB, but was expressed in all of the tested cell lines regardless of the culture conditions at roughly similar levels with only a few exceptions. SLC6A4 expression levels were slightly lower than those detected in WHB in

proliferative CTX0E03/02, SPC-04 and VM cultures, and also in VM cultures differentiated in the presence of 25 mM KCl. In contrast, the expression of the gene encoding the GABA-A $\alpha_{1A}$ receptor subunit GABRA1, exhibited particularly limited expression while showing high levels in WHB control template. GABRA1 expression was absent in proliferative CTX0E03/02 and CTX0E16/02 cultures and all tested culture conditions for the SPC-01, SPC-04 and VM lines. While expression was absent in proliferative HPC03A/07 and STROC05/08A cultures, it was present in STROC05/08A cells differentiated either in the presence or absence of KCl. Expression was observed, but only at the limit of detection after 35 cycles in cells differentiated in the absence of KCl, and not expressed at all in $K^+$ assisted differentiated HPC03A/07 cultures (see Figure 3.18).

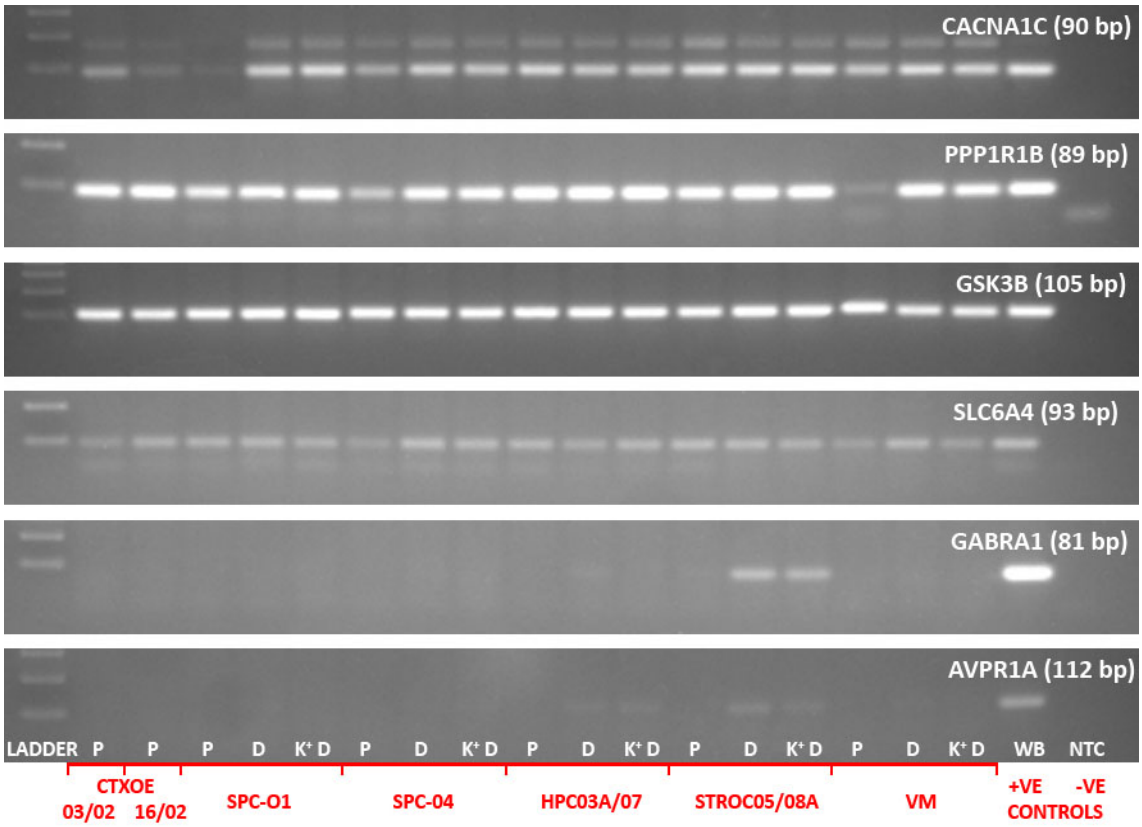


***Figure 3.18 Expression of genes related to diverse neuropsychiatric disorders in various NSC lines***
Semi-quantitative PCR analysis of various genes encoding proteins implicated in the aetiology of and mechanism of drug treatment for different neuropsychiatric disorders in proliferative and differentiated NPCs: CACNA1C encoding the $\alpha_{1C}$ subunit of the L-type voltage-dependent $Ca^{2+}$ channel, $Ca_v1.2$. PPP1R1B and GSK3B encoding the signalling nodes DARPP-32 and GSK-3β respectively, SLC6A4 encoding the 5-HT transporter (SERT), GABRA1 encoding the GABA-A $\alpha_{1A}$ receptor subunit and AVPR1A encoding the arginine vasopressin $AVPR_{1A}$ receptor. Individual lanes represent expression of these genes in proliferative (P), normally differentiated (D) or differentiation with a $K^+$-induced depolarisation step included ($K^+$D). Levels of expression are shown for proliferative CTX0E03/02 and CTX0E16/02 cultures plus SPC-01, SPC-04, HPC03A/07, STROC05/08A and VM under each of the three culture conditions. The expression for each gene, in each of the described culture conditions is accompanied by a WHB cDNA template positive (+ve) control and a no template negative (-ve) control.

AVPR1A – encoding the arginine vasopressin $AVPR_{1A}$ receptor – demonstrated restricted, and if present, weak expression in the seven tested NPC lines. AVPR1A expression was absent in proliferative cultures from each of these seven lines and was absent in all tested conditions for SPC-01, SPC-04 and VM (see

Figure 3.18). Expression was observed at the limit of detection using either normal or $K^+$ assisted differentiation in the SPC-04 and HPC03A/07 lines, though was only detected in normally differentiated cells in the SPC-01 and VM lines. The highest level of AVPR1A expression – though still weak – was detected in differentiated STROC05/08A cultures, though exposure to KCl during differentiation reduced the observed expression of this gene.

Taken together, these data provide evidence of strikingly different expression profiles for each of the different NPC lines tested. This information suggests the retention of some regional and temporal specification – required to produce cellular diversity *in vivo* [349] – following *in vitro* isolation and expansion. Interestingly, this observed diversity in the range and extent of expression of various genes was even evident in NPCs isolated from the same developing neural region from the same patient – as exemplified by CTX0E03/02 and CTX0E16/02, and SPC-01 and SPC-04. This finding was also highlighted by the different morphologies and phenotypic characteristics exhibited by the two cortically derived cell lines described above.

### *3.2.5 Differentiated Cortical NPC Lines Exhibit Broad Receptor Expression Profile*

Initial attempts to differentiate the two NPC lines derived from developing human cortex – CTX0E03/02 and CTX0E16/02 – identified two differentiation conditions that warranted further scrutiny (see ***3.2.1***, above). In addition, to explore the possibility that these two most efficient methods might provide a synergistic capacity to differentiate these cells, a third condition that combined the original two was also investigated. In parallel with CTX0E03/02 and CTX0E16/02 cultures differentiated using these three conditions for phenotypic analysis – as described in ***3.2.2*** and ***3.2.3*** above – cultures were also performed in tissue culture flasks for the purpose of RNA collection. Therefore, CTX0E03/02 and CTX0E16/02 cells were differentiated using either RMM supplemented with 1 µM purmorphamine, SNBM or SNBM supplemented 1 µM purmorphamine for 21, 28 or 35 days. Total RNA was then extracted from each culture and used to generate cDNA to provide template for gene expression analysis. This was performed in exactly the same way as was described above for all other NPC lines. However, RNA was not collected from CTX0E03/02 cells differentiated using SNBM for 28 or 35 days due to poor culture survival. This finding was surprising due to the promise this differentiation condition had shown in generating neurons and astrocytes in preliminary experiments (see ***3.2.1*** and ***3.2.2***). However, differentiation of the CTX0E03/02 line under these conditions had produced very clumped, poorly dispersed cultures exhibiting considerable levels of cell death when grown in 96-well plates and glass coverslips, and may explain their poor survival when grown in tissue culture flasks. Expression of the same genes tested in each of the other NPC lines and summarised in Table 2.1 above, was similarly assessed for each of the collected samples from the differentiated CTX0E03/02 and CTX0E16/02 cultures. This information was used not only to inform the choice of the most appropriate protocol with which to differentiate the CTX0E03/02 and CTX0E16/02 NPC lines with respect to the needs of this study, but also to enable a comparison to be made between the differentiated cortical NPC lines and those derived from other brain regions.

DRD2 – encoding the dopamine $D_2$ receptor – was ubiquitously expressed in both CTX0E03/02 and CTX0E16/02 under all tested differentiation conditions (see Figure 3.19), as was the case for all other NPC lines described previously (see Figure 3.16). The gene encoding the dopamine $D_2$ receptor – DRD3 – was similarly expressed in both cortical lines under all tested conditions, with the only exception being CTX0E03/02 cells differentiated in the presence of purmorphamine supplemented SNBM.

HTR2A – encoding the 5-$HT_{2A}$ receptor – was robustly expressed in both cell lines differentiated in the presence of SNBM alone. This was also the case for both lines differentiated using SNBM supplemented with 1 µM purmorphamine, though the level of expression fell slightly after 35 days of differentiation in CTX0E03/02 cultures. In contrast, while robust HTR2A expression was seen at all tested time points for CTX0E03/02 cells differentiated using purmorphamine supplemented RMM, application of this condition to CTX0E16/02 cells resulted only in weak expression after a 28 day differentiation. Expression was absent at the 21 and 35 day time points.

Expression of the gene encoding the muscarinic acetylcholine $M_1$ receptor – CHRM1 – was absent in CTX0E03/02 cultures differentiated in the presence of SNBM, irrespective of the presence of purmorphamine. While expression was absent after a 21 day differentiation in the presence of purmorphamine supplemented RMM, it was detected after 28 days and had intensified after a 35 day differentiation. CHRM1 expression was detected at all tested time points for CTX0E16/02 cells differentiated using SNBM in the presence or absence of 1 µM purmorphamine. Similar levels of CHRM1 expression were also observed in CTX0E16/02 cultures differentiated in the presence of purmorphamine supplemented RMM after 21 and 28 days, though were absent after 35 days.

HRH1 – encoding the histamine $H_1$ receptor – was robustly expressed by the CTX0E0/03 line under all tested conditions. This was also true of CTX0E16/02 cells differentiated in the presence of RMM supplemented with 1 µM purmorphamine, though expression levels were lower in CTX0E16/02 cultures differentiated using SNBM, irrespective of the presence of purmorphamine or the period of differentiation. Expression of ADRA1A – the gene encoding the adrenergic $\alpha_{1A}$ receptor – was detected in samples from both cortical NPC lines under all tested conditions, though was particularly high in CTX0E16/02 cultures differentiated in the presence of SNBM, with or without 1 µM purmorphamine. The gene encoding the tachykinin $NK_3$ receptor – TACR3 – was weakly expressed in CTX0E03/02 cultures differentiated in the presence of SNBM, with or without purmorphamine. This same low level of expression was also seen in CTX0E03/02 cultures differentiated in the presence of purmorphamine supplemented RMM for 28 and 35 days, though was barely detectable in cultures exposed to this condition for 21 days. Conversely, TACR3 expression was absent in CTX0E16/02 cultures differentiated in the presence of RMM supplemented with purmorphamine. CTX0E16/02 cells differentiated in the presence of SNBM alone saw little expression of TACR3 after 21 days, though showed increased expression after 28 or 35 days of differentiation. In the presence of SNBM supplemented with purmorphamine however, maximal levels of TACR3 expression were seen after 21 days of differentiation, with reduced levels detected at 28 and 35 days.

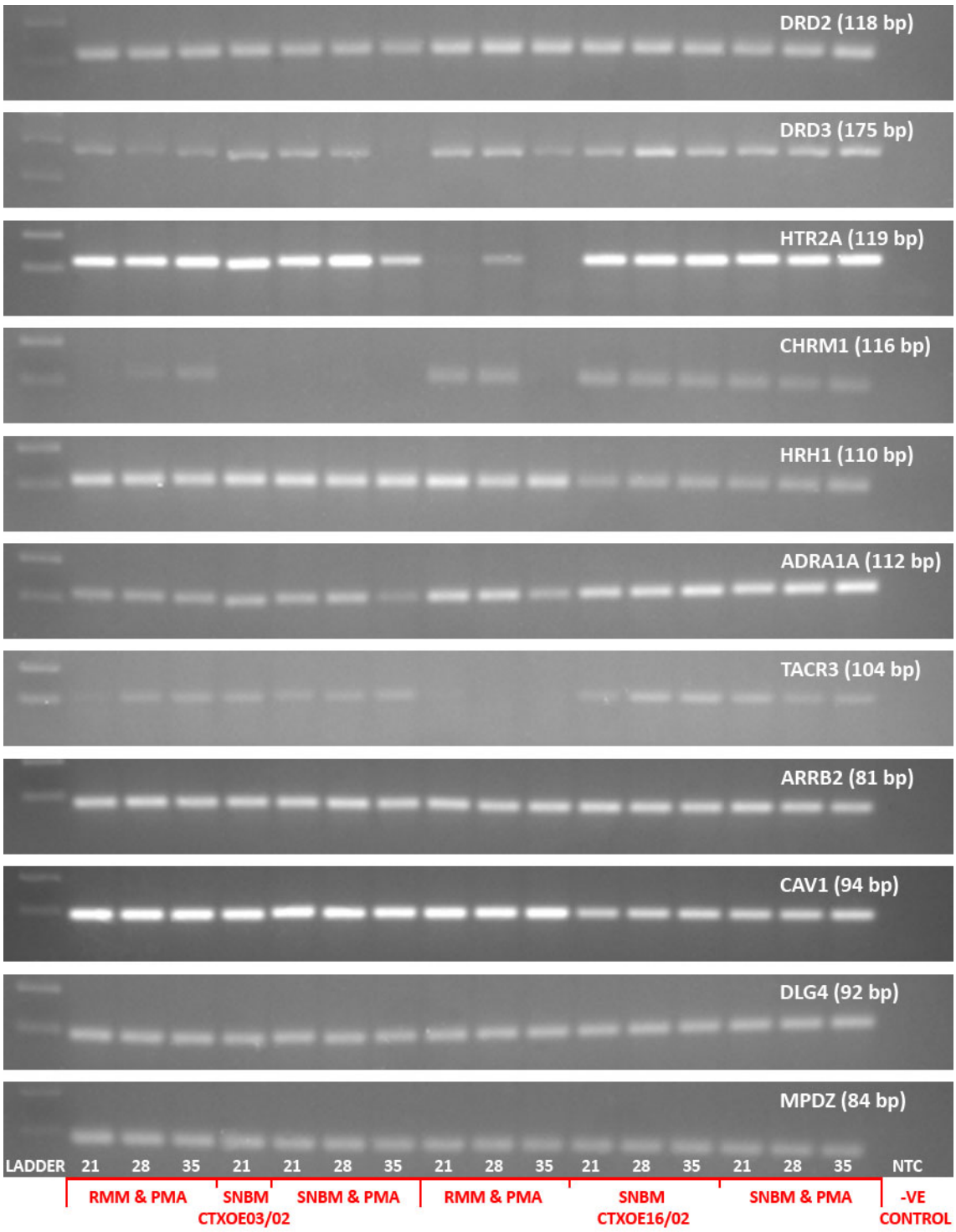


***Figure 3.19 Expression of GPCRs and some of their accessory proteins in differentiated cortical NPCs***

Semi-quantitative PCR analysis of the cortically-derived NPC lines CTX0E03/02 and CTX0E16/02 following differentiation using three different protocols over 21, 28 or 35 days. Panels show expression of several GPCRs targeted by currently available and putative antipsychotics: DRD2 and DRD3 encoding dopamine $D_2$ and $D_3$ receptors respectively, HTR2A encoding 5-$HT_{2A}$ receptors, CHRM1 encoding cholinergic muscarinic $M_1$ receptors, HRH1 encoding histamine $H_1$ receptors, ADRA1A encoding adrenergic $\alpha_{1A}$ receptors and TACR3 encoding tachykinin $NK_3$ receptors. The expression of four GPCR accessory proteins are also shown: ARRB2 encoding the scaffold and signalling protein β-arrestin 2, CAV1 encoding the scaffold protein caveolin-1, DLG4 encoding the scaffold protein PSD-95 and MPDZ encoding the scaffold protein MUPP1. Individual lanes represent expression of these genes in CTX0E03/02 and CTX0E16/02 cells differentiated in the presence of RMM supplemented with 1 µM purmorphamine (PMA), SNBM alone, or SNBM supplemented with 1 µM PMA for 21, 28 or 35 days. Each gel included a no template negative (-ve) control.

Relatively uniform expression was observed between the various tested differentiation conditions for both the CTX0E03/02 and CTX0E16/02 lines, with respect to the four investigated genes encoding proteins associated with GPCR function – ARRB2, CAV1, DLG4 and MPDZ. These genes encode β-arrestin 2, caveolin-1, postsynaptic density protein 95 (PSD-95) and multiple PDZ domain protein (MUPP1) respectively (see Figure 3.19).

GRIA2 – encoding the glutamatergic AMPA receptor subunit GluR2 – demonstrated weak expression in all conditions used to differentiate the CTX0E03/02 line (see Figure 3.20). In contrast, robust expression was observed in all differentiated CTX0E16/02 cultures, with the only exception being those exposed to purmorphamine supplemented RMM for 35 days. CTX0E16/02 cells differentiated using SNBM in the presence or absence of purmorphamine also demonstrated robust expression of the gene encoding the NMDA receptor subunit NR1 – GRIN1 – at all tested time points. For CTX0E16/02 cultures differentiated in the presence of RMM supplemented with purmorphamine, weak expression was observed after 21 days and was further reduced after 28 and 35 days. Weak expression of GRIN1 was detected for all differentiation conditions applied to CTX0E03/02 cultures.

GRM1, GRM4, GRM7 and GRM8; each encoding a corresponding metabotropic glutamate receptor, were ubiquitously expressed to some extent in all tested differentiation conditions for both the CTX0E03/02 and CTX0E16/02 cell lines (see Figure 3.20). Interestingly, these same genes were also expressed in all tested proliferative and differentiated NPC lines described above (see Figure 3.17). Genes encoding the remaining four metabotropic glutamate receptors – GRM2, GRM3, GRM5 and GRM6 demonstrated a more restricted expression profile between the differentiated cortical NPC lines (see Figure 3.20). GRM2 was weakly expressed in CTX0E03/02 cells when differentiated in the presence of purmorphamine supplemented RMM and SNBM alone at all tested time points. Weak expression of this gene was also detected in CTX0E03/02 cultures exposed to SNBM supplemented with purmorphamine at 21 days and 28 days, though was absent after 35 days of differentiation. RMM supplemented with purmorphamine supported expression of GRM2 in CTX0E16/02 cultures at all tested time points though a reduced level was detected after 35 days. GRM2 was also expressed in CTX0E16/02 cultures at all tested time points when differentiated in the presence of SNBM, irrespective of whether it was supplemented with purmorphamine. This was also true of GRM3 expression, though it was not detected in CTX0E16/02 cultures differentiated with purmorphamine supplemented RMM and was absent in all differentiated CTX0E03/02 cultures.

Two distinct transcript variants – a and b, corresponding to 199 and 103 base pair products, respectively – were recognised by the GRM5 primers used in this study. As was the case for the other NPC lines described above, expression of the longer a transcript was poorly expressed in the two cortical NPC lines. Expression of this transcript was absent in all tested differentiation conditions for the CTX0E03/02 line. However, it was expressed at the limit of detection in all tested conditions for the CTX0E16/02 line. In contrast, robust expression of the shorter, b transcript was detected in all tested conditions upon differentiation of CTX0E16/02 cultures. While the GRM5 b transcript expression was absent in CTX0E03/02 cells differentiated for 21 days in the presence of purmorphamine supplemented RMM,

weak expression was detected at the later time points. Weak expression was also detected in samples from CTX0E03/02 cells differentiated in the presence of SNBM alone, and in the presence of purmorphamine, though this was particularly low at the latest time point (see Figure 3.20).

GRM6 was robustly expressed in CTX0E16/02 cultures differentiated in the presence of SNBM irrespective of exposure to purmorphamine. Robust expression was also seen in CTX0E16/02 cells differentiated with purmorphamine supplemented RMM for 21 or 28 days but was considerably weaker after 35 days. GRM6 was also expressed in CTX0E03/02 cultures differentiated in the presence of RMM supplemented with purmorphamine at all tested time points and also after 21 days using SNBM alone. However, while robust expression of GRM6 was detected in CTX0E03/02 cultures differentiated in the presence of purmorphamine supplemented SNBM at 21 and 28 days, it was absent following a 35 day differentiation (see Figure 3.20).

The expression of CACNA1C, PPP1R1B and GSK3B – encoding the L-type voltage-gated $Ca^{2+}$ channel $\alpha_{1C}$ subunit, DARPP-32 and GSK-3$\beta$ respectively – were each robustly expressed in CTX0E03/02 and CTX0E16/02 cultures under all tested differentiation conditions (see Figure 3.21, below). In addition, the gene encoding the 5-HT transporter, SERT – SLC6A4 – was also expressed in both cell lines under all tested conditions. Levels of expression for this gene were however considerably weaker than was seen for other tested genes (Figure 3.21), though was comparable with that observed in WHB and other NPC lines described previously (see Figure 3.18).

Both GABRA1 and AVPR1A – encoding the GABA-A $\alpha_{1A}$ receptor subunit and the arginine vasopressin $AVPR_{1A}$ receptor respectively – showed weak expression in differentiated CTX0E03/02 and CTX0E16/02 cultures (see Figure 3.21). GABRA1 expression was absent in proliferative and purmorphamine supplemented RMM differentiated CTX0E03/02 cultures, though expression was observed in all tested conditions for this cell line when exposed to SNBM, irrespective of purmorphamine exposure. Similarly, GABRA1 expression was also absent from proliferative CTX0E16/02 cultures and those differentiated in the presence of RMM supplemented with purmorphamine. However, weak expression was however observed in CTX0E16/02 cultures exposed to SNBM alone at all tested time points, though was only detectable in cultures differentiated with purmorphamine supplemented SNBM at the latest time of 35 days. AVPR1A expression was absent in proliferative CTX0E03/02 cultures, and those differentiated in the presence of SNBM, with or without purmorphamine – though weak expression was detected at all tested time points when differentiated with purmorphamine supplemented RMM (Figure 3.21). While AVPR1A expression was absent in proliferative CTX0E16/02 cultures, it was robustly expressed in those differentiated in the presence of RMM supplemented with 1 µM purmorphamine for 21 or 28 days. However, expression was absent after a 35 day differentiation. In contrast, the level of AVPR1A expression increased with time when CTX0E16/02 cultures were differentiated in the presence of SNBM, though this effect was more pronounced in the absence of purmorphamine (see Figure 3.21).

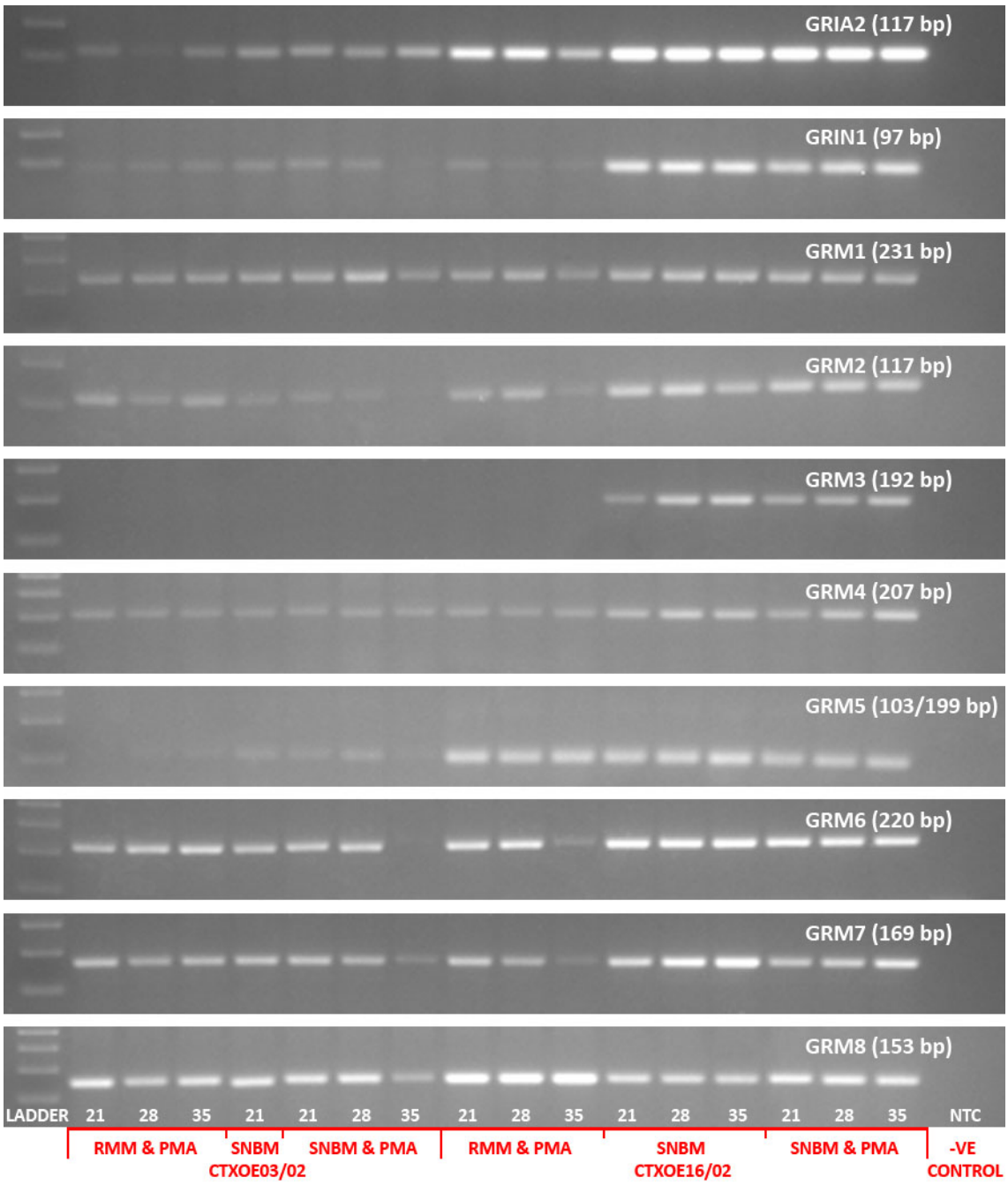


***Figure 3.20 Expression of glutamate receptors and receptor subunits in differentiated cortical NPCs***

Semi-quantitative PCR analysis of genes encoding ionotropic glutamate receptor subunits and all metabotropic glutamate receptors in CTX0E03/02 and CTX0E16/02 cultures following differentiation using three different protocols over 21, 28 or 35 days. Expression was assessed for: GRIA2 encoding the glutamatergic AMPA receptor subunit GluR2, GRIN1 encoding the glutamatergic NMDA receptor subunit NR1, GRM1 – GRM8 encoding the metabotropic glutamate receptors mGluR1 – mGluR8 respectively. Individual lanes represent expression of these genes in CTX0E03/02 and CTX0E16/02 cells differentiated in the presence of RMM supplemented with 1 µM purmorphamine (PMA), SNBM alone, or SNBM supplemented with 1 µM PMA for 21, 28 or 35 days. Each gel included a no template negative (-ve) control.

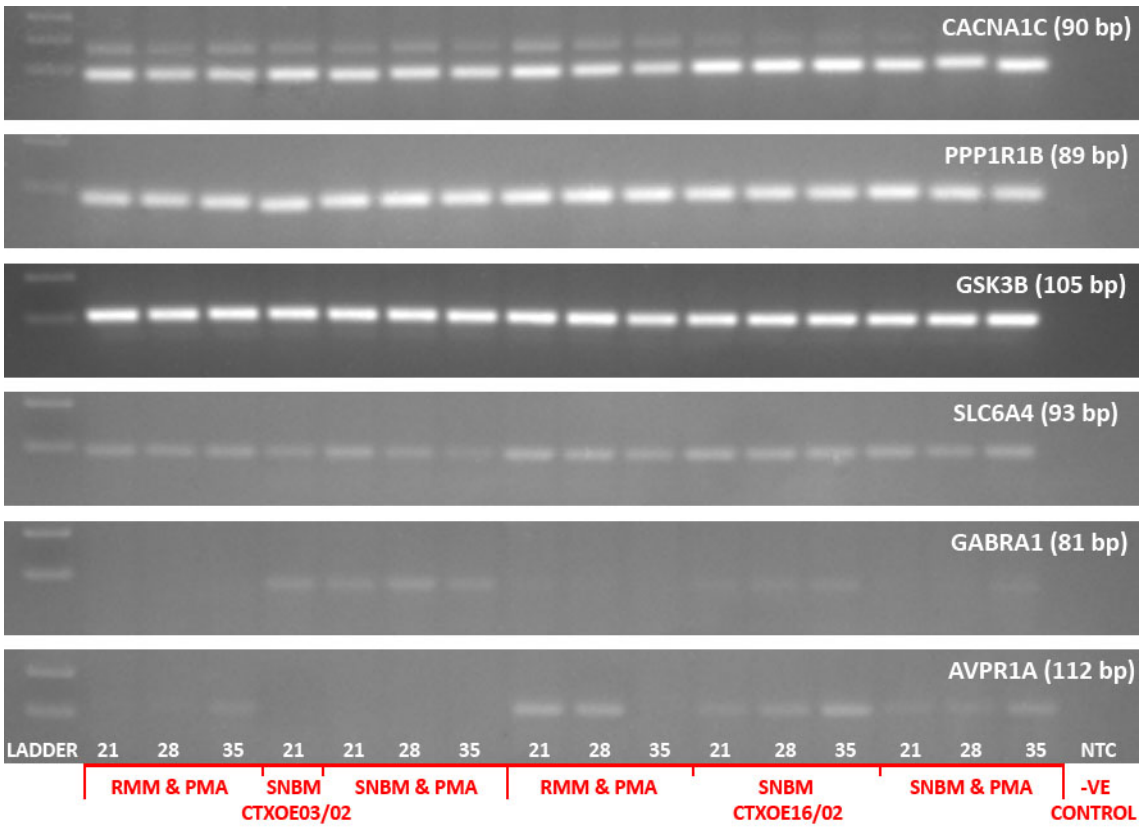


***Figure 3.21 Expression of GPCR accessory proteins and signalling nodes in differentiated cortical NSCs***
Semi-quantitative PCR analysis of the cortically-derived NSC lines CTX0E03/02 and CTX0E16/02 following differentiation using three different protocols over 21, 28 or 35 days. Expression of various genes encoding proteins implicated in the aetiology of and mechanism of drug treatment for different neuropsychiatric disorders in proliferative and differentiated NPCs: CACNA1C encoding the $\alpha_{1C}$ subunit of the L-type voltage-dependent $Ca^{2+}$ channel, $Ca_v1.2$. PPP1R1B and GSK3B encoding the signalling nodes DARPP-32 and GSK-3β respectively, SLC6A4 encoding the 5-HT transporter (SERT), GABRA1 encoding the GABA-A $\alpha_{1A}$ receptor subunit and AVPR1A encoding the arginine vasopressin $AVPR_{1A}$ receptor. Individual lanes represent expression of these genes in CTX0E03/02 and CTX0E16/02 cells differentiated in the presence of RMM supplemented with 1 µM purmorphamine (PMA), SNBM alone, or SNBM supplemented with 1 µM PMA for 21, 28 or 35 days. Each gel included a no template negative (-ve) control.

The expression of each gene was compared between each cell line in each of the tested conditions and scored for relative expression using an arbitrary scale. Scoring was performed on gels where all samples had been run together in two parallel lanes of wells in a single gel. Approximate levels of expression were determined independently for each gene across all samples before assigning a maximal level of expression – '+++' for the gene in question. This method was selected because cDNA from whole human brain did not always exhibit the highest levels of expression across all samples and the maximal level of expression seen for some genes was often very different to that observed for others. These data were combined and presented in Table 3.9 and Table 3.10, below to provide a simple means of comparison between the different tested NPC lines and conditions.

| Cell Sample | DRD2 | DRD3 | HTR2A | CHRM1 | HRH1 | ADRA1A | ARRB2 | CAV1 | DLG4 | MPDZ | GSK3B | PPP1R1B | CACNA1C |
|---|---|---|---|---|---|---|---|---|---|---|---|---|---|
| STROC05/08A: Proliferative | xx | o | xx | xxx | xxx | xxx | xxx | xxx | xxx | xxx | xxx | xxx | xxx |
| STROC05/08A: Differentiated | xxx | xxx | xxx | xxx | xxx | xxx | xxx | xxx | xxx | xxx | xxx | xxx | xxx |
| STROC05/08A: Differentiated with $K^+$ | xxx | xxx | xxx | xxx | xxx | xxx | xxx | xxx | xxx | xxx | xxx | xxx | xxx |
| HPC03A/07: Proliferative | xx | xxx | o | x | xxx | xx | xxx | xxx | xxx | xxx | xxx | xxx | xxx |
| HPC03A/07: Differentiated | xx | xx | x | o | xxx | xx | xxx | xxx | xxx | xxx | xxx | xxx | xxx |
| HPC03A/07: Differentiated with $K^+$ | xx | xx | x | x | xxx | xx | xxx | xxx | xxx | xxx | xxx | xxx | xxx |
| VM: Proliferative | xx | x | o | x | xxx | o | xxx | xxx | xxx | xxx | xxx | x | xx |
| VM: Differentiated | xx | xx | xx | xxx | xxx | x | xxx | xxx | xxx | xxx | xxx | xxx | xxx |
| VM: Differentiated with $K^+$ | xx | xx | x | xxx | xx | x | xxx | xxx | xxx | xxx | xxx | xxx | xxx |
| SPC-01: Proliferative | xxx | xx | o | x | xxx | o | xxx | xxx | xxx | xxx | xxx | xxx | x |
| SPC-01: Differentiated | xxx | xx | xxx | xxx | xxx | xx | xxx | xxx | xxx | xxx | xxx | xxx | xxx |
| SPC-01: Differentiated with $K^+$ | xxx | xx | xxx | xxx | xxx | xx | xxx | xxx | xxx | xxx | xxx | xxx | xxx |
| SPC-04: Proliferative | xxx | o | x | xx | xxx | o | xxx | xxx | xxx | xxx | xxx | xx | xx |
| SPC-04: Differentiated | xxx | xxx | xxx | xxx | xxx | xx | xxx | xxx | xxx | xxx | xxx | xxx | xxx |
| SPC-04: Differentiated with $K^+$ | xxx | xxx | xxx | xxx | xxx | xx | xxx | xxx | xxx | xxx | xxx | xxx | xxx |
| CTX0E03/02: Proliferative | xxx | x | x | o | xxx | xx | xxx | xxx | xxx | xxx | xxx | xxx | xx |
| CTX0E03/02 DD21 RMM & PMM | xxx | xx | xxx | o | xxx | xx | xxx | xxx | xxx | xxx | xxx | xxx | xxx |
| CTX0E03/02 DD28 RMM & PMM | xxx | x | xxx | x | xxx | xx | xxx | xxx | xxx | xxx | xxx | xxx | xx |
| CTX0E03/02 DD35 RMM & PMM | xxx | x | xxx | xx | xxx | xx | xxx | xxx | xxx | xxx | xxx | xxx | xx |
| CTX0E03/02 DD21 NB & B27 | xxx | xx | xxx | o | xxx | xx | xxx | xxx | xxx | xxx | xxx | xxx | xxx |
| CTX0E03/02 DD21 NB, B27 & PMM | xxx | xx | xxx | o | xxx | xx | xxx | xxx | xxx | xxx | xxx | xxx | xx |
| CTX0E03/02 DD28 NB, B27 & PMM | xxx | xx | xxx | o | xxx | xx | xxx | xxx | xxx | xxx | xxx | xxx | xxx |
| CTX0E03/02 DD35 NB, B27 & PMM | xx | o | xx | o | xxx | x | xxx | xxx | xxx | xxx | xxx | xxx | xx |
| CTX0E16/02: Proliferative | xxx | x | o | xx | xxx | xx | xxx | xxx | xxx | xxx | xxx | xxx | x |
| CTX0E16/02 DD21 RMM & PMM | xxx | xx | o | xx | xxx | xxx | xxx | xxx | xxx | xxx | xxx | xxx | xxx |
| CTX0E16/02 DD28 RMM & PMM | xxx | xx | x | xx | xxx | xxx | xxx | xxx | xxx | xxx | xxx | xxx | xx |
| CTX0E16/02 DD35 RMM & PMM | xxx | x | o | o | xxx | xx | xxx | xxx | xxx | xxx | xxx | xxx | xxx |
| CTX0E16/02 DD21 NB & B27 | xxx | xx | xxx | xx | xx | xxx | xxx | xxx | xxx | xxx | xxx | xxx | xxx |
| CTX0E16/02 DD28 NB & B27 | xxx | xxx | xxx | xx | xx | xxx | xxx | xxx | xxx | xxx | xxx | xxx | xxx |
| CTX0E16/02 DD35 NB & B27 | xxx | xx | xxx | xx | xx | xxx | xxx | xxx | xxx | xxx | xxx | xxx | xxx |
| CTX0E16/02 DD21 NB, B27 & PMM | xx | xx | xxx | xx | xx | xxx | xxx | xxx | xxx | xxx | xxx | xxx | xxx |
| CTX0E16/02 DD28 NB, B27 & PMM | xxx | xx | xxx | xx | xx | xxx | xxx | xxx | xxx | xxx | xxx | xxx | xxx |
| CTX0E16/02 DD35 NB, B27 & PMM | xxx | xxx | xxx | xx | xx | xxx | xxx | xxx | xxx | xxx | xxx | xxx | xxx |
| WHB +ve control | xxx | xxx | xxx | xxx | xxx | xxx | xxx | xxx | xxx | xxx | xxx | xxx | xxx |
| No template -ve control | o | o | o | o | o | o | o | o | o | o | o | o | o |

***Table 3.9 Relative expression of genes encoding GPCRs, their accessory proteins and important signalling molecules in proliferative and differentiated NPCs***

| Cell Sample | GRIA2 | GRIN1 | GRM1 | GRM2 | GRM3 | GRM4 | GRM5 (a/b) | GRM6 | GRM7 | GRM8 | TACR3 | SLC6A4 | GABRA1 | AVRP1A |
|---|---|---|---|---|---|---|---|---|---|---|---|---|---|---|
| STROC05/08A: Proliferative | xxx | x | x | xx | o | x | o/x | x | xx | xx | x | xx | o | o |
| STROC05/08A: Differentiated | xxx | x | xxx | xx | o | x | x/xxx | xx | xx | x | x | xx | xx | xx |
| STROC05/08A: Differentiated with $K^+$ | xxx | x | xxx | xx | o | x | x/xxx | xx | xx | x | x | xx | xx | x |
| HPC03A/07: Proliferative | xx | o | xx | xx | x | x | o/x | x | x | xxx | o | xx | o | o |
| HPC03A/07: Differentiated | x | x | xx | xx | xx | x | x/xxx | x | x | xxx | o | xx | o | x |
| HPC03A/07: Differentiated with $K^+$ | x | x | xx | xx | xx | x | x/xxx | xx | x | xxx | x | xx | o | x |
| VM: Proliferative | x | x | x | xx | o | x | o/o | x | xxx | xxx | o | x | o | o |
| VM: Differentiated | xx | x | xxx | xx | o | x | o/o | xx | xxx | xxx | x | xx | o | x |
| VM: Differentiated with $K^+$ | xx | x | xxx | xx | o | x | o/o | xx | xxx | xxx | x | x | o | o |
| SPC-01: Proliferative | x | o | x | x | xx | x | o/o | xx | xxx | x | x | xx | o | o |
| SPC-01: Differentiated | xxx | xx | xxx | xxx | xxx | xx | x/xx | xxx | xxx | xx | xxx | xx | o | x |
| SPC-01: Differentiated with $K^+$ | xxx | xx | xxx | xxx | xxx | xx | o/xx | xxx | xxx | xx | xxx | xx | o | o |
| SPC-04: Proliferative | xx | o | xx | xx | xxx | x | o/o | xx | xxx | xxx | x | x | o | o |
| SPC-04: Differentiated | xxx | xx | xxx | xxx | xxx | xx | o/x | xxx | xxx | xxx | xxx | xx | o | x |
| SPC-04: Differentiated with $K^+$ | xxx | xx | xxx | xxx | xxx | xx | o/x | xxx | xxx | xxx | xx | xx | o | x |
| CTX0E03/02: Proliferative | x | x | x | x | o | x | o/o | xx | x | x | o | x | o | o |
| CTX0E03/02 DD21 RMM & PMM | x | x | xx | xx | o | x | o/x | xx | xx | xx | x | xx | o | x |
| CTX0E03/02 DD28 RMM & PMM | x | x | xx | x | o | x | o/x | xxx | xx | xx | xx | xx | o | x |
| CTX0E03/02 DD35 RMM & PMM | x | x | xx | xx | o | x | o/x | xxx | xx | xx | xx | xx | o | x |
| CTX0E03/02 DD21 NB & B27 | xx | xx | xx | x | o | x | o/x | xx | xx | xx | xx | x | xx | o |
| CTX0E03/02 DD21 NB, B27 & PMM | xx | xx | xx | x | o | x | o/x | xxx | xx | xx | x | xx | xx | o |
| CTX0E03/02 DD28 NB, B27 & PMM | xx | xx | xxx | x | o | x | o/x | xxx | xx | xx | xx | xx | xx | o |
| CTX0E03/02 DD35 NB, B27 & PMM | xx | o | xx | o | o | x | o/x | o | x | x | xx | x | xx | o |
| CTX0E16/02: Proliferative | xxx | x | xxx | xx | o | x | o/xx | xxx | xxx | x | x | xx | o | o |
| CTX0E16/02 DD21 RMM & PMM | xxx | xx | xx | xx | o | x | x/xx | xxx | xx | xxx | o | xx | o | xxx |
| CTX0E16/02 DD28 RMM & PMM | xxx | x | xx | xx | o | x | x/xx | xxx | xx | xxx | o | xx | o | xxx |
| CTX0E16/02 DD35 RMM & PMM | xx | x | x | x | o | x | x/xx | x | x | xxx | o | x | o | o |
| CTX0E16/02 DD21 NB & B27 | xxx | xxx | xxx | xxx | xx | xx | x/xx | xxx | xx | xx | x | xx | x | x |
| CTX0E16/02 DD28 NB & B27 | xxx | xxx | xxx | xxx | xxx | xx | x/xx | xxx | xxx | xx | xx | xx | xx | xx |
| CTX0E16/02 DD35 NB & B27 | xxx | xxx | xxx | xx | xxx | xx | x/xx | xxx | xxx | xx | xx | xx | xx | xxx |
| CTX0E16/02 DD21 NB, B27 & PMM | xxx | xxx | xxx | xxx | xx | x | x/xx | xxx | xx | xxx | x | xx | o | x |
| CTX0E16/02 DD28 NB, B27 & PMM | xxx | xxx | xxx | xxx | xxx | xx | x/xx | xxx | xx | xxx | xx | xx | o | x |
| CTX0E16/02 DD35 NB, B27 & PMM | xxx | xxx | xxx | xxx | xxx | xx | x/xx | xxx | xxx | xxx | xx | xx | x | xx |
| WHB +ve control | xxx | xxx | xxx | xxx | xxx | xxx | xxx/xx | xx | xxx | xxx | xxx | xx | xxx | xxx |
| No template -ve control | o | o | o | o | o | o | o | o | o | o | o | o | o | o |

***Table 3.10 Relative expression of genes encoding various glutamate receptors or their subunits, and targets relevant to neuropsychiatric drug discovery in proliferative and differentiated NPCs***

### *3.2.6 Differentiation & Expression Data Summary*

These data provide evidence that even under proliferative conditions, many of the genes identified as important to the mechanism of action of currently available antipsychotic drugs are expressed in the seven NPC lines tested. In addition, upon differentiation, the range of genes expressed by these cell lines was found to increase and the level of the expression of these genes increased as well. In terms of regional specificity, the cortical lines (CTX0E03/02 and CTX0E16/02) and the striatal line (STROC05/08A) were deemed to be most relevant. This is based upon the fact that aberrant development and activity of various regions of the cortex have been linked to the presentation of endophenotypes associated with schizophrenia, particularly the dorsolateral prefrontal cortex and the entorhinal cortex [115,323]. On the other hand, the striatum contains a particularly high density of dopamine $D_2$ and $D_3$ receptors – the primary neurotransmitter receptor targets through which antipsychotics are thought to exert their therapeutic effects. Indeed, occupancy of striatal $D_2$ and $D_3$ receptors is closely correlated with the clinical efficacy of antipsychotics, as discussed in 1.6.2 above.

The cell lines derived from the hippocampus (HPC03A/07), ventral mesencephalon (VM) and spinal cord (SPC-01 and SPC-04) were included in this investigation to provide alternative options in the event that the cortical lines could not be differentiated, or either the striatal or cortical lines presented properties that would make them difficult to use with high-throughput screening methodologies. Indeed, cells derived from the developing hippocampus or ventral mesencephalon may also provide a model with which to investigate the mechanism of action of antipsychotic drugs as neurons from both regions have been linked in some way with schizophrenia [115,323], though these cell lines were not considered a primary choice. Cells derived from spinal cord NPCs have not been implicated in either the pathophysiology of schizophrenia or as a target for antipsychotics though it was felt that they should be included due to their ability to differentiate both efficiently and rapidly [67]. In addition, it was felt that they still represented a native, human, neural tissue that had the potential to express many of the receptors targeted by antipsychotic drugs.

Initial inspection of the gene expression data summarised in Table 3.9 and Table 3.10, showed that many of the genes investigated were expressed in the seven tested NPC lines – if not when proliferative, then once they had been differentiated. There were a few genes however, that were not commonly expressed in the investigated cell lines, including GABRA1, GRM3 and AVPR1A. With respect to the current study – to investigate the mechanism of action of antipsychotics – GRM3, encoding the metabotropic glutamate receptor $mGluR_3$ was of particular interest. While currently available antipsychotics do not target $mGluR_3$, compounds that act as agonists at this receptor, and $mGluR_2$ are currently in clinical development, and have been shown to demonstrate considerable efficacy in the treatment of schizophrenic symptoms as compared to placebo [301]. Therefore, a transcriptomic comparison of these molecules with currently available antipsychotics may help to identify the presence of a final common signalling pathway in the pharmacological treatment of schizophrenia. Interestingly, the same neuronal pathway that provides the rationale for the potential therapeutic value of $mGluR_{2/3}$ agonists in the treatment of schizophrenia – underactive GABAergic projections from the nucleus

accumbens disinhibiting glutamatergic thalamocortical projections into the prefrontal cortex – also implicate the involvement of $GABA_A$ receptors [183,350]. Many other genes that were investigated demonstrated discrete expression in the various tested lines and differentiation conditions. Ultimately, it was felt that to ensure the maximal versatility of a line chosen for further development both for this study, and it's potential utility for alternative future applications, it was desirable that the line should express as broad a range of relevant genes as possible.

Importantly, the two cortical lines – while demonstrating robust differentiation when determined through their expression of markers of a neuronal or astrocytic phenotype – also provided a broad range of gene expression with respect to the investigated genes. Indeed, differentiation of the CTX0E16/02 line with SNBM for 28 days ensured expression of all the genes investigated to some extent.

In terms of the proportional yield of cells expressing markers indicative of a neuronal or astrocytic phenotype following differentiation, the CTX0E03/02 and CTX0E16/02 cell lines were capable of robust differentiation when exposed to SNBM in the presence or absence of 1 μM purmorphamine. In contrast to the CTX0E16/02 line, which differentiated as an even monolayer, the CTX0E03/02 line was prone to producing patchy cultures with some areas that contained no cells whatsoever, and other patches where cells would grow on top of each other in large clumps. This property may actually be more physiologically relevant to the workings of the brain in that cells would be able to create 3D cultures allowing for rich cell-cell interaction. In addition, recent advances in high-throughput screening methodologies and the use of 3D matrix cultures could allow these properties to be utilised [351,352]. However, screening using this approach is considerably more expensive, would require significant investment by the organisations using these screening methods and remains at a developmental stage. The CTX0E16/02 cell line demonstrated robust differentiation, as determined by immunocytochemical analysis, but these differentiated cells grew as an even monolayer. Virtually all high-throughput screens currently rely on fluorescence assays in 96 to 1536-well plates. The ability of cells to grow as an even, adherent monolayer is a real advantage in this situation as fewer spaces containing no cells ensures a higher signal-to-noise ratio, and therefore, greater sensitivity.

Considering the data presented above, the CTX0E16/02 cell line provides robust differentiation into neurons and astrocytes, and generate evenly distributed, adherent monolayer cultures, thus ensuring good sensitivity using current high-throughput methodologies. Differentiation of the CTX0E16/02 cell line using SNBM additionally provided cultures that expressed all of the genes previously identified as being important for an *in vitro* model to interrogate the mechanism of current neuropsychiatric compounds, or a potential screening tool to develop novel medicines. Differentiation of the CTX0E16/02 line using RMM supplemented with 1 μM purmorphamine resulted in cultures containing far fewer cells positively stained for neuronal or astrocytic markers, and failed to promote the expression of genes such as GABRA1, GRM3 and TACR3. Most importantly however, these cultures lacked the expression of HTR2A – the gene encoding the $5\text{-}HT_{2A}$ receptor – which is thought to contribute to the therapeutic effects of many antipsychotics. With respect to gene expression, differentiation of CTX0E16/02 cultures

with SNBM alone, or SNBM supplemented with 1 µM purmorphamine were virtually identical, with the exception of more pronounced GABRA1 expression in the absence of purmorphamine.

These data suggest that CTX0E16/02 cells differentiated in the presence of SNBM provide the most effective conditions with which to obtain cultures rich in neurons and astrocytes, and additionally exhibit characteristics desirable for a high-throughput screening platform. These data did not support the idea that the use of purmorphamine could provide an additive influence upon SNBM-mediated differentiation and was consequently excluded from further investigation.

When considering the period of differentiation, immunofluorescence analysis suggested that 28 days ensured a greater degree of cellular differentiation than was observed after just 21 days. Little difference was observed however between 28 and 35 days, though slightly more cell death was apparent at the later time point. The range of different genes, whose expression was identified as desirable for an *in vitro* model intended for the investigation of antipsychotic drug activity, was also improved following 28, as compared to 21, days of differentiation using SNBM in the presence or absence of 1 µM purmorphamine. The intensity with which these genes were expressed was also greater after 28 days. With the exception of AVPR1A, none of the investigated genes demonstrated higher expression at 35 days as compared to the 28 day time point. Indeed, in the case of DRD3 and GRM2, the relative expression of these genes was reduced at 35, as compared to 28 days.

While exposure to a depolarising concentration of $K^+$ during the differentiation process was investigated for the striatal, hippocampal, ventral mesencephalic and spinal cord lines, it was decided not to pursue this approach further for the two cortical cell lines. This decision was based on the observation that cultures exposed to this additional $K^+$ exposure step consistently experienced greater levels of cell death. Moreover, exposure to $K^+$ more frequently reduced the level of expression of investigated genes than enhanced them. Another consideration with respect to exposure of cultures to a transient $K^+$-induced depolarisation was that it requires two full medium changes. This posed a problem in that preliminary work had already identified that full medium changes were not well tolerated by either of the two cortical lines (data not shown), especially when followed by a differentiation of 28 or 35 days.

Considering the data provided above, the CTX0E16/02 cell line differentiated for 28 days in SNBM provides cultures most suited to the needs of this study. They differentiate to produce healthy, confluent adherent cultures containing a high proportion of neurons and astrocytes, and are derived from a brain region pertinent to the pathophysiology of schizophrenia, and therefore to the drugs used to treat the disorder. The resultant cultures are well-suited for fluorescence-based pharmacological analysis, additionally making them suitable for commercial drug screening applications, and lend themselves well to the pharmacological characterisation of the cells. This pharmacological evaluation – which is covered in the subsequent chapters – will be essential to the development of this cell line as an *in vitro* platform that can provide the sensitivity to discriminate different neuropsychiatric drugs based on transcriptomic induction that can meaningfully inform upon their mechanism of action.

# *Chapter 4 Characterisation of Differentiated CTX0E16/02 Cultures*

Based on work described in ***Chapter 3*** above, the CTX0E16/02 NPC line was selected for further characterisation as a potential *in vitro* model to investigate the mechanism of action of antipsychotic drugs. It is also recognised that this model may provide considerable utility as a screening platform for the development of novel compounds to treat diverse neuropsychiatric disorders or as a means to assess neurotoxicity. The primary aim of the work described here was to demonstrate that CTX0E16/02 cultures express functional neurotransmitter receptors. This property was assessed in both proliferative and differentiated cultures and serves as a pharmacological characterisation of the cells to determine their suitability as a model to investigate antipsychotic drugs. In addition, this chapter also provides an enhanced phenotypic characterisation of CTX0E16/02 cultures following differentiation using conditions optimised in ***Chapter 3*** and described in ***2.1.3***, above. This addresses the ability of these cultures to generate neurons, and the subtypes that are present, along with astrocytes. Evidence that these standard differentiation conditions could generate oligodendrocytes was also assessed, though this normally requires the use of $T_3$ and $T_4$, and possibly also elevated cAMP of $PDGF_{AA}$ [61,328].

## *4.1 Introduction*

Recent developments in our understanding of receptor pharmacology have highlighted the importance of using native tissues to study the intracellular signalling consequences of ligand binding, as discussed in ***Chapter 1***, above. For neuroscientists this poses a difficult problem. Unsurprisingly, *ex vivo* adult, human neural tissue is difficult to obtain, but added to this is the fact that cells which command the greatest attention – neurons – cannot be expanded due to their post-mitotic nature. In addition, due to the presence of an estimated 2500 – 5000 different neural subtypes within the adult human brain [353], primary tissue samples unsurprisingly tend to be highly heterogeneous. As discussed in ***1.2*** above, foetal-derived human NPCs represent a renewable source of cells that can potentially generate all the different cell-types in the adult CNS. If, as a scientific community we hope to employ differentiated NPCs as *in vitro* platforms with which to interrogate the intracellular mechanisms and signalling pathways underlying neural cell function, it is imperative that these cultures reflect as many of the phenotypic and pharmacological properties of their *in vivo* counterparts as possible. It would be naïve to think that the complexity of human brain function can be accurately recreated in a dish, however, the use of clonal NPC lines that can be used to derive cells native to the adult brain provides an invaluable tool that can be used to study the cells that comprise it. In order to relate the properties of an NPC-based *in vitro* model to that of the human brain however, it is imperative that it should be appropriately characterised.

The cortically derived NPC line – CTX0E16/02 – was selected for further characterisation as it exhibited many of the characteristics that were identified as appropriate for the needs of this study, including robust differentiation into neurons and glia, even adherent monolayer cultures and the expression of genes pertinent to the desired use of these cells, as described in ***3.1***, above. However, due to the variety of different cellular subtypes found within the human cortex, such as glutamatergic pyramidal neurons

or calretinin, calbindin-D28k or parvalbumin expressing GABAergic interneurons, it is important to characterise which of these cells may be present in differentiated CTX0E16/02 cultures, so as to compare their *in vitro* potential to that of their *in vivo* counterparts. This section also aims to provide a functional characterisation of differentiated CTX0E16/02 cultures so as to determine whether or not they represent an appropriate model with which to investigate the effects of antipsychotic drugs

Neurons are by definition excitable cells, a property that confers on them the ability to generate action potentials, and consequently release neurotransmitter to inform neighbouring cells of their activity, or propagate these signals to other relevant parts of the brain or body. This property is mediated by an abundance of various different voltage-dependent ion channels (VDIC) that span the plasma membrane, and therefore make it selectively permeable to the same charge carrying metal ions (primarily $Na^+$, $K^+$, $Cl^-$ and $Ca^{2+}$) that are responsible for the potential difference that exists across their membranes. Of these ions, $Ca^{2+}$ is particularly important due to its parallel role as a signalling molecule [354], causing the activation of numerous different enzymes such as PKC, calcineurin, phosphorylase kinase and nitric oxide synthase to name only a few [355]. Under resting conditions, levels of free cytosolic $Ca^{2+}$ are maintained at very low concentrations. This is achieved though its sequestration by various $Ca^{2+}$ binding proteins or removal – either to the extracellular space or into the endoplasmic reticulum. Specific signals can cause a transient increase in cytoplasmic $Ca^{2+}$ concentration through various different mechanisms. For example, activation of $G\alpha_q$-linked GPCRs leads to $IP_3$ receptor-mediated release of $Ca^{2+}$ from intracellular stores, while activation of glutamatergic NMDA receptors facilitates $Ca^{2+}$ influx from the extracellular space. An important property of neurons, as electrically excitable cells, is their ability to propagate, and therefore amplify these ligand-induced $Ca^{2+}$ transients though the presence of voltage-dependent $Ca^{2+}$ channels [355,356]. To investigate ligand-induced signalling, it is therefore important that neurons generated as a consequence of CTX0E16/02 differentiation are electrically excitable. It is not enough that they just express markers suggestive of a neuronal phenotype such as tau or MAP2.

Another important consideration is that differentiated CTX0E16/02 cultures should express functional receptors known to be high affinity targets for currently available antipsychotic drugs. Data presented in ***3.2.5*** above, established that differentiated CTX0E16/02 cultures express message for a broad range of receptors. Whether this translates as functional receptor expression at the cell surface is yet to be determined, and is one of the aims of the work described in this chapter. Recent evidence has questioned the assumption that cell surface presentation of plasma membrane-localised proteins – such as GPCRs – following *de novo* synthesis is a default process. Indeed, as discussed in 1.1 above, few GPCRs possess the N-terminal signal peptides required for translocation across the ER [344]. Cell surface expression of many receptors is a tightly regulated process and in heterologous expression systems especially, has been shown to require considerable manipulation including protein truncation, co-expression with accessory proteins and other receptors, and the addition of pharmacological chaperones [29,30,34,35]. Pharmacological characterisation of differentiated CTX0E16/02 cultures is therefore necessary to determine the presence of functional receptors at the cell surface. This of course

is far from trivial when we consider the number of different receptors for which currently available antipsychotics exhibit high affinity towards, as discussed in ***1.7*** and summarised in Table 1.1, above.

To provide a broad picture of receptor activity, initial experiments were conducted using dopamine, 5-HT, GABA, glutamate, acetylcholine, histamine, phenylephrine and carbamoylcholine. Receptor function was assessed in both proliferative and differentiated CTX0E16/02 cultures by testing the ability of these ligands to provoke an increase in intracellular $Ca^{2+}$ concentration. Intracellular $Ca^{2+}$ accumulation was used as a measure of receptor activation for several reasons. The first being that it represents a very simple, fast and inexpensive method to initially evaluate receptor-mediated activation of these cultures. The second reason is that it represents one of the most common intracellular second messengers. Modulation of intracellular $Ca^{2+}$ concentration ($[Ca^{2+}]_i$) is utilised as a signalling substrate in all mammalian cells and can be mediated through a variety of different mechanisms, including the activation of many different neurotransmitter receptors. Neurons and astrocytes both express neurotransmitter receptors that upon activation lead to a transient rise in levels of intracellular $Ca^{2+}$. These various neurotransmitter receptors can be broadly split into two categories – ionotropic and metabotropic.

Ionotropic receptors are often referred to as ligand-gated ion channels (LGIC) and as their name suggests, they permit the passive flow of ions through the plasma membrane in response to specific ligands. This is achieved through the organisation of these receptor's membrane-spanning subunits, creating a central pore whose permeability to ions is regulated by ligand-induced conformational changes on the separate subunits. In response to a specific ligand the mechanism through which these receptors may be capable of mediating an elevation of cytosolic $Ca^{2+}$ is two fold. Firstly, the channel itself can be permeable to $Ca^{2+}$, as is seen for NMDA receptors, allowing $Ca^{2+}$ to move rapidly into the cell along its electrochemical gradient upon ligand binding. Alternatively, the receptor may only be permeable to $Na^+$ ions – as is often the case for AMPA receptors. Though, thanks to the presence of another kind of ion channel found in neurons – voltage-dependent ion channels (VDICs) – this influx of $Na^+$ ions causes a depolarisation across the cell membrane and leads to the activation of the more sensitive voltage-dependent $Na^+$ channels. This renewed influx of $Na^+$ ions causes further membrane depolarisation and subsequently causes the opening of voltage-dependent $Ca^{2+}$ channels, and therefore leads to an indirect intracellular rise in $Ca^{2+}$ concentration [357]. LGICs can be either inhibitory or excitatory in nature, a property governed by the ions to which they are selectively permeable. For example, glutamatergic LGICs (NMDA, AMPA and kainite receptors) are excitatory in nature due to their passive permeability to $Na^+$ and $Ca^{2+}$ ions, and thus result in membrane depolarisation. This property is also shared by nicotinic acetylcholine and 5-$HT_3$ receptors [358]. In contrast, GABAergic LGICs ($GABA_A$ receptors) are inhibitory due to their conductance of $Cl^-$ ions into cells, thus causing a repolarisation of the plasma membrane. However, during neural development, $GABA_A$ receptors are also known to cause membrane depolarisation due to an altered $Cl^-$ ion gradient present within cells at this prenatal stage [359].

While the metabotropic class of receptors also includes tyrosine kinases and guanylyl cyclase receptors, the majority of neurotransmitters transduce their effects across the plasma membrane via G-protein

coupled receptors (GPCR). GPCRs represent the major target for currently available antipsychotics and are thought to mediate the majority of their cellular effects (as discussed in ***1.7***, above). Consequently, GPCRs are particularly important with respect to this study. Classically, ligand-induced activation of this class of receptor causes a conformational change that leads to the dissociation of an intracellularly coupled heterotrimeric G protein into an α subunit monomer and a βγ subunit complex – all of which exist as various isoforms. Both of these G protein subunits are capable of provoking further downstream signalling through their interaction with various different downstream effectors such as adenylyl cyclase (AC), phospholipase C-β (PLC-β) or phosphatidylinositol 3-kinase (PI3K). Through their interactions with numerous other signalling molecules, accessory proteins and ion channels, GPCRs are capable of eliciting a staggering range of cellular responses – as outlined in ***1.7***, above – though common to many of them is the ability to provoke a rise in $[Ca^{2+}]_i$.

Perhaps the best understood mechanism that allows GPCRs to elevate levels of cytosolic $Ca^{2+}$ is via specific coupling to $G\alpha_{q/11}$ subunits – which are known to coupled to many of the GPCRs targeted by antipsychotics, and are summarised in Table 4.1, below. Upon ligand binding, the $G\alpha_{q/11}$ subunit dissociates from the Gβγ subunit complex and activates PLC-β, which in turn cleaves phosphatidylinositol 4,5-bisphosphate ($PIP_2$) into diacylglycerol (DAG) and inositol 1,4,5-trisphosphate ($IP_3$). $IP_3$ causes the release of $Ca^{2+}$ from the ER via $IP_3$ receptors while DAG goes on to activate protein kinase C (PKC) – which itself is also activated by a rise in $[Ca^{2+}]_i$. Furthermore, DAG has also been shown to control the influx of $Ca^{2+}$ from the extracellular space via activation of TRP channels [360,361] (as illustrated in Figure 4.1, below). Through various other pathways GPCRs have been shown to modulate the activity of various ion channels and enzymes that in turn often alter intracellular $Ca^{2+}$ concentrations [188,362]. For example, both the $G\alpha_{i/o}$ and the Gβγ subunits have been shown to modulate G-protein-regulated inwardly rectifying $K^+$ (GIRK) channel activity while Gβγ has also been shown to inhibit the activity of P/Q- and N-type voltage-dependent calcium channels ($Ca_V$)[191]. While these non-canonical GPCR-ion channel interactions may lead to a fall in $[Ca^{2+}]_i$ several others have been shown to provoke rises. Using dopamine receptors as an example – while dopamine $D_1$ and $D_2$ receptors are classically thought to couple to $G\alpha_s$ and $G\alpha_i$ respectively – these have been shown to form functional heterodimers both *in vivo* and *in vitro*, capable of provoking intracellular $Ca^{2+}$ accumulation [191]. In addition, the Gβγ subunit complex regulated by $D_2$ has also been shown to be capable of activating PLC-β and consequently causing a rise in $[Ca^{2+}]_i$ [363].

| | Receptor | Gα Subunit Family | Primary Downstream Effector |
|---|---|---|---|
| dopaminergic | $D_1$ | $G\alpha_{s/olf}$ | adenylyl cyclase (stimulation) |
| | $D_2$ | $G\alpha_{i/o}$ | adenylyl cyclase (inhibition) |
| | $D_3$ | $G\alpha_{i/o}$ | adenylyl cyclase (inhibition) |
| | $D_4$ | $G\alpha_{i/o}$ | adenylyl cyclase (inhibition) |
| | $D_5$ | $G\alpha_{s/olf}$ | adenylyl cyclase (stimulation) |
| serotonergic | 5-$HT_{1A}$ | $G\alpha_{i/o}$ | adenylyl cyclase (inhibition) |
| | 5-$HT_{1B}$ | $G\alpha_{i/o}$ | adenylyl cyclase (inhibition) |
| | 5-$HT_{1D}$ | $G\alpha_{i/o}$ | adenylyl cyclase (inhibition) |
| | 5-$HT_{1E}$ | $G\alpha_{i/o}$ | adenylyl cyclase (inhibition) |
| | 5-$HT_{2A}$ | $G\alpha_{q/11}$ | phospholipase C-β (activation) |
| | 5-$HT_{2C}$ | $G\alpha_{q/11}$ | phospholipase C-β (activation) |
| | 5-$HT_5$ | $G\alpha_{i/o}$ | adenylyl cyclase (inhibition) |
| | 5-$HT_6$ | $G\alpha_{s/olf}$ | adenylyl cyclase (stimulation) |
| | 5-$HT_7$ | $G\alpha_{s/olf}$ | adenylyl cyclase (stimulation) |
| adrenergic | $\alpha_{1A}$ | $G\alpha_{q/11}$ | phospholipase C-β (activation) |
| | $\alpha_{1B}$ | $G\alpha_{q/11}$ | phospholipase C-β (activation) |
| | $\alpha_{2A}$ | $G\alpha_{i/o}$ | adenylyl cyclase (inhibition) |
| | $\alpha_{2B}$ | $G\alpha_{i/o}$ | adenylyl cyclase (inhibition) |
| | $\alpha_{2C}$ | $G\alpha_{i/o}$ | adenylyl cyclase (inhibition) |
| | $\beta_1$ | $G\alpha_{s/olf}$ | adenylyl cyclase (stimulation) |
| | $\beta_2$ | $G\alpha_{s/olf}$ | adenylyl cyclase (stimulation) |
| muscarinic | $M_1$ | $G\alpha_{q/11}$ | phospholipase C-β (activation) |
| | $M_2$ | $G\alpha_{i/o}$ | adenylyl cyclase (inhibition) |
| | $M_3$ | $G\alpha_{q/11}$ | phospholipase C-β (activation) |
| | $M_4$ | $G\alpha_{i/o}$ | adenylyl cyclase (inhibition) |
| | $M_5$ | $G\alpha_{q/11}$ | phospholipase C-β (activation) |
| histaminergic | $H_1$ | $G\alpha_{q/11}$ | phospholipase C-β (activation) |
| | $H_2$ | $G\alpha_{s/olf}$ | adenylyl cyclase (stimulation) |
| | $H_3$ | $G\alpha_{i/o}$ | adenylyl cyclase (inhibition) |
| | $H_4$ | $G\alpha_{i/o}$ | adenylyl cyclase (inhibition) |

***Table 4.1 Neurotransmitter receptor primary G protein-coupling partners***
Identifies the family to which the primary Gα subunit-coupling partners of neurotransmitter receptors targeted by currently available antipsychotics belong. Many, if not all, of these receptors are capable of activating alternative signalling consequences depending on their cellular localisation. Table compiled from various sources [191,364-367].

Several neurotransmitter systems – especially the dopaminergic, serotonergic, cholinergic and noradrenergic systems – appear to be important in how antipsychotics their activity, and more are being implicated with the clinical development of novel compounds targeting the glutamate, tachykinin and cannabinoid systems [175,340,350]. This project did not aim to provide an exhaustive list of the effects provoked in CTX0E16/02 cultures by ligands targeting the receptors described above, but instead aimed to determine the presence of receptors for these neurotransmitters at the cell surface. For this reason, it was decided that instead of using a bank of specific ligands for each receptor it would initially be more efficient to determine the presence of receptors using agonists with a broad receptor activity. Experiments were therefore conducted to determine whether a range of different broad specificity agonists were capable of elevating $[Ca^{2+}]_i$ – which was used here as a marker of receptor activation – in CTX0E16/02 cultures. This in itself however poses its own problems when you consider the example of

dopamine induced signalling, where binding to the $D_1$ and $D_5$ receptors causes an activation of adenylyl cyclase and therefore an elevation in cAMP levels through $G\alpha_{s/olf}$ family G proteins, while the remaining dopamine receptors – $D_2$, $D_3$ and $D_4$ – inhibit adenylyl cyclase activity through activation of $G\alpha_{i/o}$ family G proteins. On inspection however, this is a very crude and simplistic portrayal of dopamine signalling, and as explained above, many of the GPCRs that are expressed at the message level in CTX0E16/02 cultures have been shown to modulate multiple different effectors [191,364]. Thus, the work described in this chapter provides a more detailed characterisation of the cells generated through differentiation of the human, cortically derived NPC line – CTX0E16/02. In addition, the expression of functional receptors by these differentiated cells is analysed by determining how they respond to various agonists to receptors known to be targeted by antipsychotics.

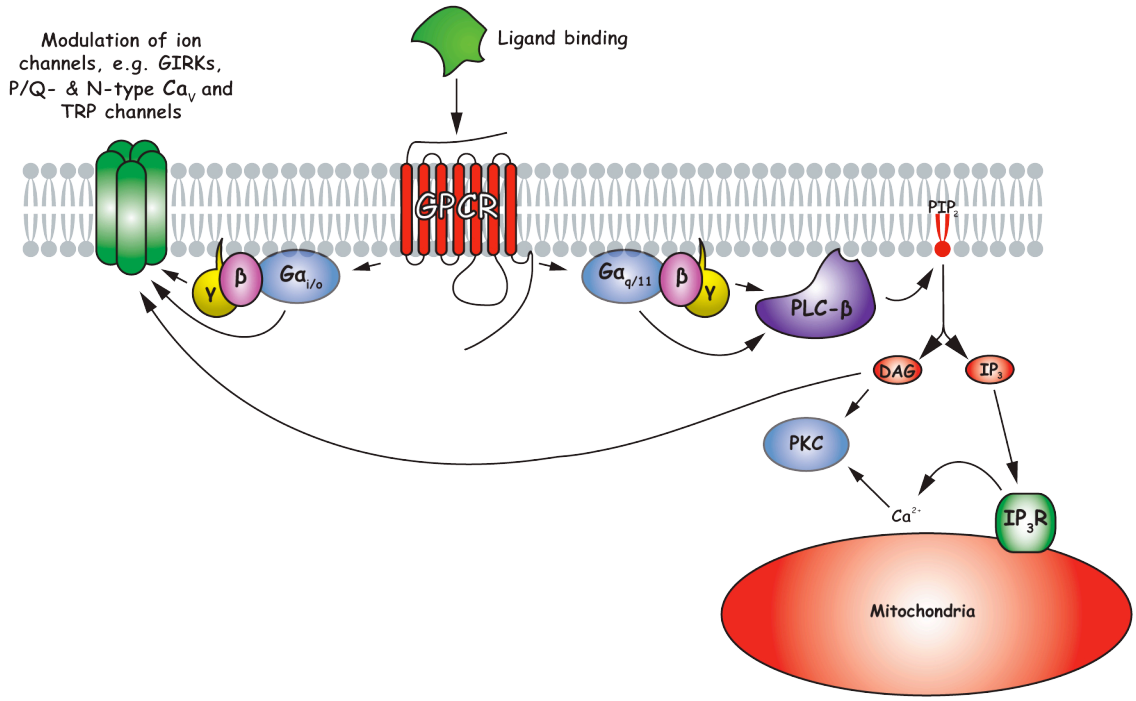


***Figure 4.1 Diagram to illustrate GPCR-mediated signalling involving regulation of [$Ca^{2+}$]***
GPCRs are known to modulate intracellular $Ca^{2+}$ accumulation through a variety of different mechanisms, including $IP_3$-receptor-mediated release from intracellular stores and the modulation of various cell surface ion channels. GPCRs have also been shown to influence other ionic currents across the cell membrane.

## 4.2 Results

### 4.2.1 Differentiated CTX0E16/02 Cultures Generate Glutamatergic & GABAergic Neurons

To investigate the developmental potential of CTX0E16 cells, cultures were grown under differentiation conditions defined in ***2.1.3*** and ***3.2.6*** for 28 days, then fixed and staining using antibodies raised against tau and MAP2 to visualise neurons, S100β to visualise astrocytes and O4 to visualise oligodendrocytes. Staining has previously been shown for VAMP2 to demonstrate evidence of synapse formation (see Figure 3.1, above), while the sub-types of neurons present were further defined using antibodies raised against calcium binding proteins expressed by GABAergic neurons – calretinin, calbindin-D28k and parvalbumin [335], or antibodies against the glutamate transporters, vGluT1 and vGluT2, for glutamatergic

neurons [368]. Evidence is first presented however, to provide a description of the cell types present within proliferative CTX0E16/02 cultures.

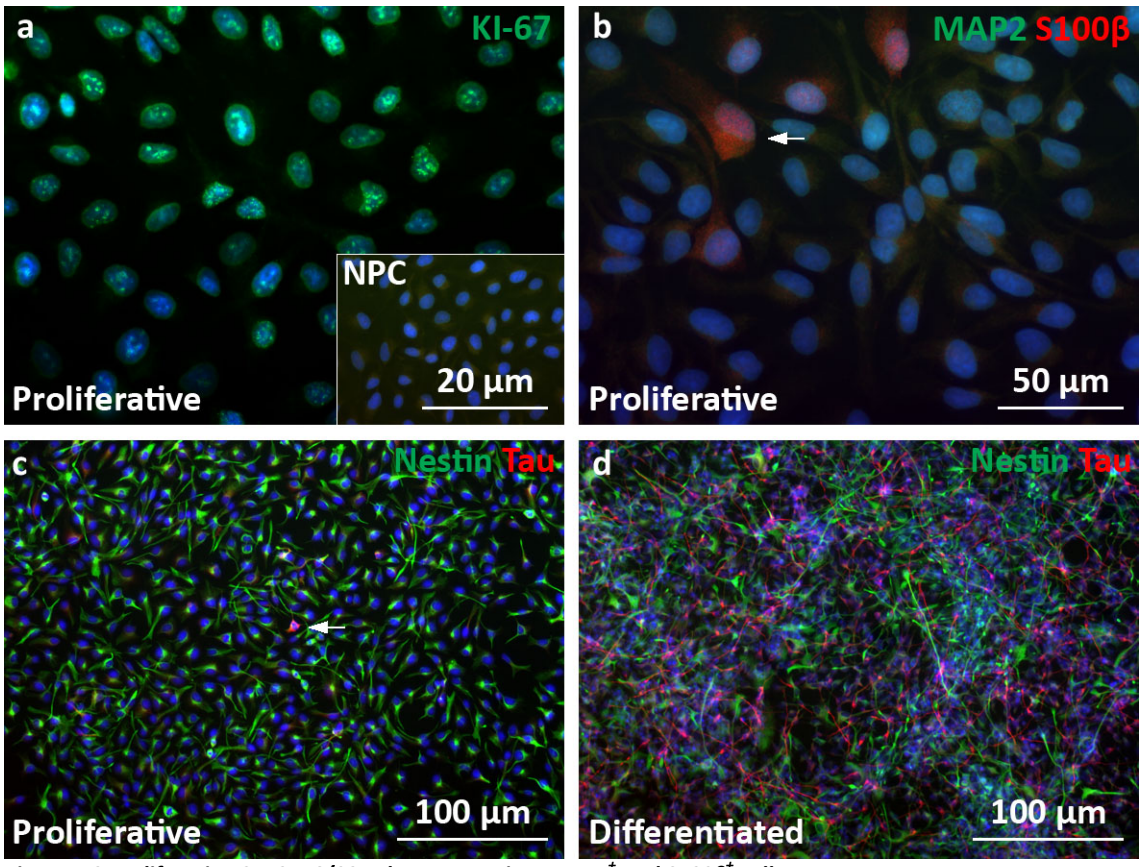


***Figure 4.2 Proliferative CTX0E16/02 cultures contain rare tau$^+$ and S100β$^+$ cells***
Panels **a**, **b** & **c** show proliferative CTX0E16/02 cultures while panel **d** shows differentiated CTX0E16/02 cultures for comparison. Panel **a** is stained with the nuclear proliferation marker KI-67 (green) and DAPI. Panel **b** is stained with MAP2 (green), S100β (red) and DAPI and annotated to show the presence of spontaneously differentiated, diffusely stained S100β$^+$ astrocyte. Panels **c** and **d** are stained with nestin (green), tau (red) and DAPI. Panel **c** is annotated to indicate the presence of a spontaneously differentiated, intensely tau$^+$ neuron. Panel **a** is inlayed with image captured using equivalent microscope settings from cells exposed to staining in the absence of primary antibody. Pictures were taken using a Zeiss Axio Imager equipped with an ApoTome.

Proliferative CTX0E16/02 cultures were dominated by cells expressing the NPC marker; nestin (Figure 4.2, **c**)[61], and the proliferation marker; KI-67 (Figure 4.2, **a**)[369]. Under these proliferative conditions a few neurons, as determined by expression of tau (see arrow in Figure 4.2, **c**), and astrocytes, as determined by expression of S100β (see arrow in Figure 4.2, **b**) were generated. However, the tau expressing cells retained the morphology of NPCs, as did S100β-expressing cells. No cells were found to express the neuronal marker MAP2 (Figure 4.2, **b**). These cells grew to form a confluent monolayer (Figure 4.2, **c**), demonstrated a doubling time of approximately 46 hours and were routinely split 1:3 every three days. Following differentiation, CTX0E16/02 cultures changed dramatically both in their physical appearance and with respect to the proteins they expressed. Upon differentiation, the soma of CTX0E16/02 cells became considerably smaller than their proliferative counterparts, as can be seen when comparing Figure 4.2 **c** and **d**, and Figure 4.10 **a** and **b**. Many differentiated cells continued to express the NPC marker nestin (Figure 4.2, **d** and Figure 4.3, **a**), though this is consistent with previous findings [61]. The

culture conditions described here to differentiate CTX0E16/02 cultures typically favour the generation of cells exhibiting neuronal phenotypes. Indeed, CTX0E16/02 cultures differentiated using SNBM for 28 days contained 53.7% ± 2.8% $tau^+$ and $MAP2^+$ neurons (see Figure 3.12 **c**). $S100\beta^+$ astrocytes were also present, constituting 13.5% ± 1.1% of differentiated cultures, though this is likely an underestimate as these cells tended to bunch together, making it difficult to distinguish individual cells (Figure 4.3 **b** and **d**). The culture conditions used do not however favour the generation of oligodendrocytes, which typically require the addition of factors such as $T_3$, $T_4$, $PDGF_{AA}$ and forskolin. However, very rare examples were found of cells that expressed punctate O4 staining (Figure 4.3 **c**). These cells did not demonstrate the characteristic morphology of oligodendrocytes, but such cells were never visible in controls where primary antibodies were omitted or the wrong class of secondary antibody was used, suggesting that the O4 staining observed was real. It should be noted that the sister line to CTX0E16/02 – CTX0E03/02 – has been shown to generate oligodendrocytes, although this was shown to occur following *in vivo* engraftment into the brains of rats that had previously been subjected to middle cerebral artery occlusion [108]. When differentiated *in vitro*, through simply removing mitogens and 4-OHT, these cells were found only to differentiate into neurons and astrocytes [63].

In addition to expressing the microtubule-associated proteins tau and MAP2, cells within differentiated CTX0E16/02 cultures also expressed neuronal sub-type specific markers. Evidence of the presence of glutamatergic neurons was provided by the detection of the vesicular glutamate transporter proteins vGluT1 and vGluT2 (Figure 4.3, **e**). These molecules are responsible for sequestering glutamate into synaptic vesicles for subsequent exocytosis [368]. As described above (see Figure 3.1, above) the presynaptic vesicle-associated protein – VAMP2 – has also been shown to be robustly expressed in differentiated CTX0E16/02 cultures.

In addition to providing evidence of the presence of glutamatergic neurons, differentiated CTX0E16/02 cultures also contained cells that express the major inhibitory neurotransmitter of the mammalian CNS; GABA (Figure 4.3, **f** and also see ***Chapter 1***) To determine the presence of different GABAergic neuronal subtypes, cultures were stained with antibodies that recognise the $Ca^{2+}$ binding proteins – calretinin, calbindin-D28k and parvalbumin. A large proportion of differentiated CTX0E16/02 cells expressed the GABAergic cell type marker calretinin (Figure 4.4, **a** and **b**), while far fewer cells were found to express calbindin-D28k (Figure 4.4, **c** and **d**). Expression of the GABAergic neuronal subtype marker, parvalbumin was however absent (data not shown).

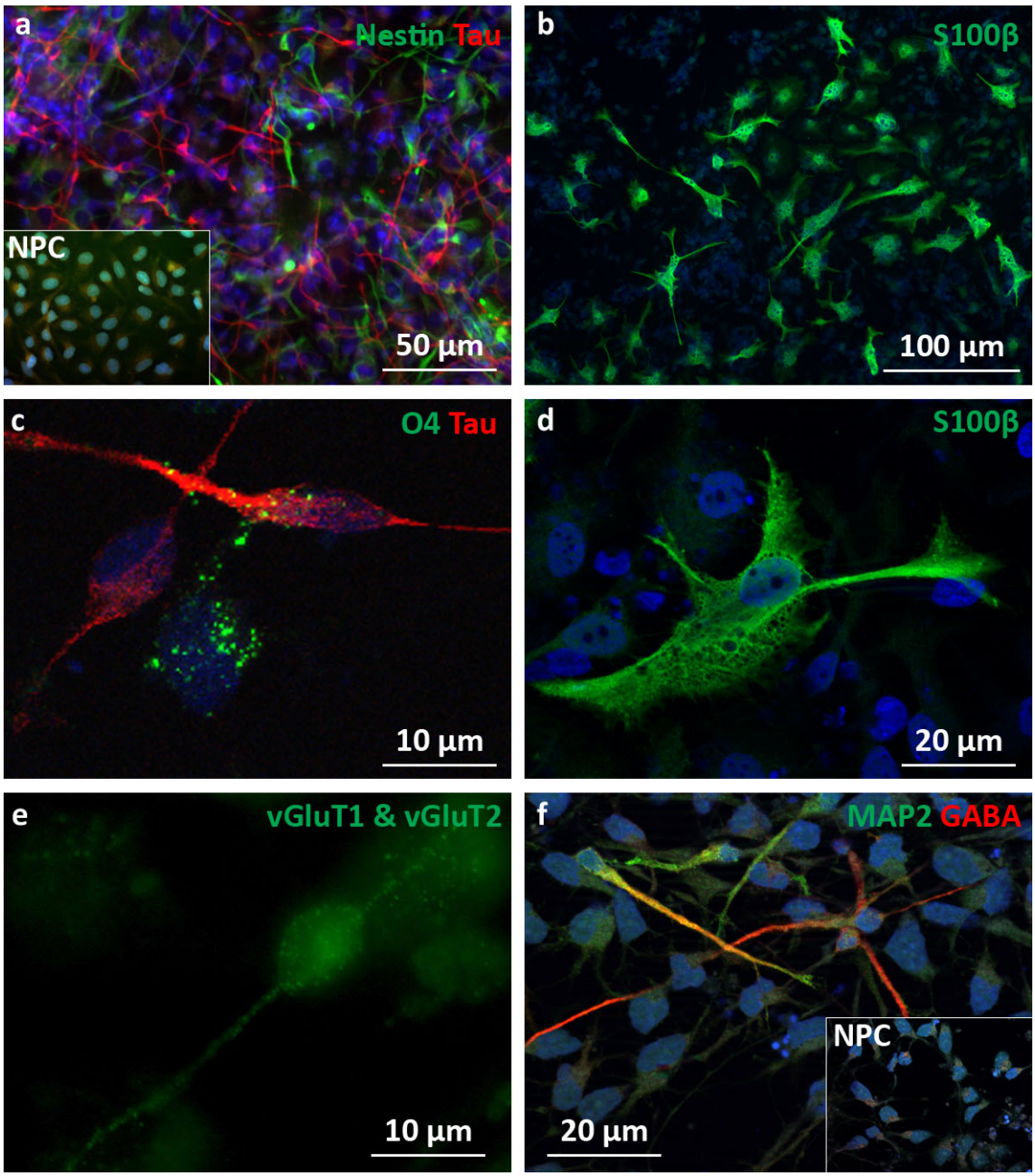


***Figure 4.3 Differentiated CTX0E16/02 cells are tripotent***

All panels show CTX0E16/02 cultures differentiated for 28 days using SNBM. Panel **a** shows cells stained with nestin (green), tau (red) and DAPI with inlayed panel to show level of staining in the absence of primary antibody. Panels **b** and **d** show cells stained for the astrocytic marker S100β (green) and DAPI. Panel **c** shows single cell exhibiting punctate O4 immunoreactivity (green). Panel **e** shows cells demonstrating punctate staining for the presynaptic glutamate transporters vGluT1 and vGluT2 (green). Panel **f** shows cells stained with MAP2 (green), GABA (red) and DAPI, and is inlayed with an image captured using equivalent microscope settings from cells exposed to staining in the absence of primary antibody. Pictures were taken using a Zeiss Axio Imager equipped with an ApoTome.

These data provide evidence of striking phenotypic heterogeneity between cells that comprise differentiated CTX0E16/02 cultures. Following a 28 day differentiation, these NPCs have exhibited the capacity to generate neurons, astrocytes and potentially some oligodendrocytes. Evidence has also been provided demonstrating the expression of the two neurotransmitters glutamate and GABA along with the GABAergic cell type markers calretinin and calbindin-D28k, but not parvalbumin. These cells have also been shown to express markers indicative of the formation of synapses – VAMP2, vGluT1 and vGluT2 – the latter suggesting the presence of excitatory synapses. While these data demonstrate that

differentiated CTX0E16/02 cultures produce cells that express markers indicative of a neuronal phenotype, it remains unclear whether these cells exhibit the functional characteristics of this class of cells – most importantly, electrical excitability. The following section describes some functional characteristics of differentiated CTX0E16/02 cultures with respect to their ability to respond to various different neurotransmitter receptor agonists and their capacity to develop electrical excitability.

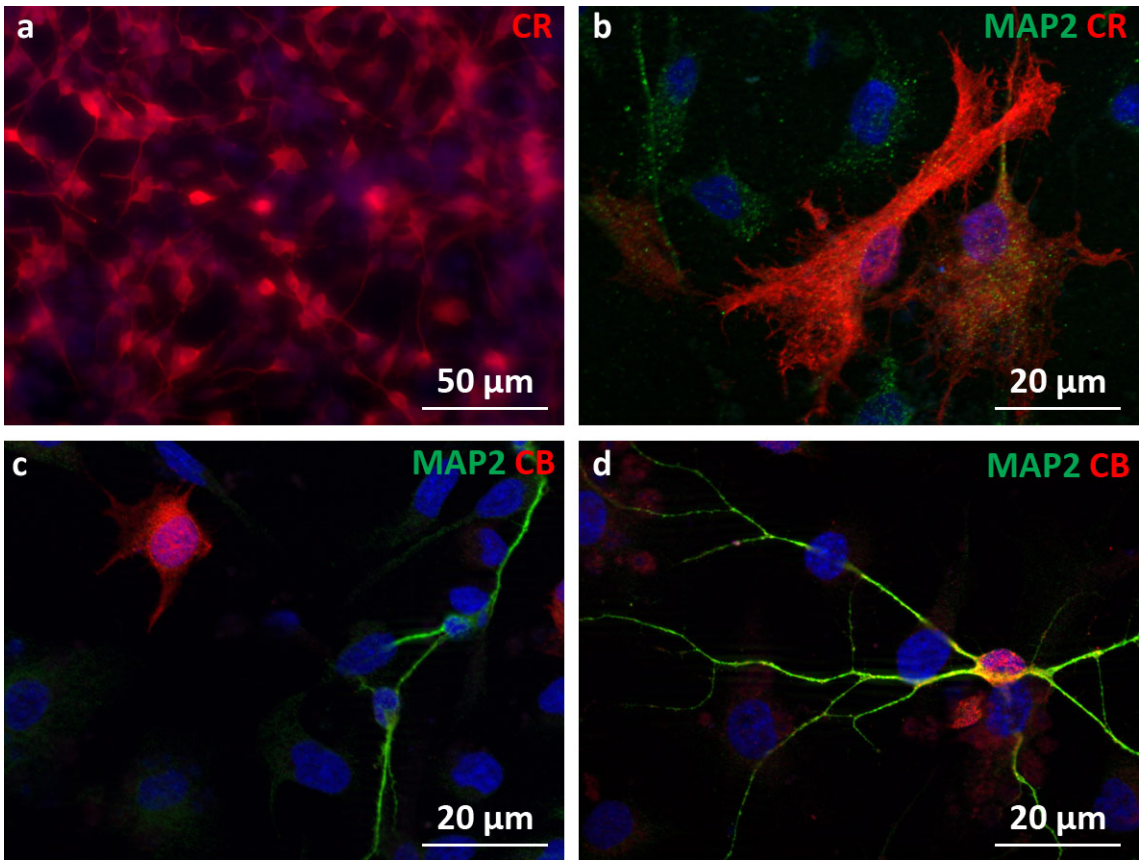


***Figure 4.4 Differentiated CTX0E16/02 cultures express markers of GABAergic neuronal subtypes***
All panels show CTX0E16/02 cultures differentiated for 28 days using SNBM. Panel **a** shows cells stained with calretinin (red) and DAPI, while panels **b** shows cells stained for MAP2 (green), calretinin (red) and DAPI. Panels **c** and **d** show cells stained with MAP2 (green), calbindin-D28k (red) and DAPI. Pictures were taken using a Zeiss Axio Imager equipped with an ApoTome.

### *4.2.2 CTX0E16/02 NPCs Express Functional Neurotransmitter Receptors*

In order for CTX0E16/02 cultures to be useful in the assessment of the mechanism of action of antipsychotics, it is important that they express the receptors that are targeted by these compounds. This is essential to facilitate the investigation of the intracellular signalling consequences following interaction between these receptors and antipsychotic drugs. Work described in ***3.2.5*** above, showed that many of the neurotransmitter receptors targeted by antipsychotics are expressed at the message level, though it remains unclear whether functional receptors are present at the cell surface.

Work described in ***3.2.4*** above, showed that mRNA for many neurotransmitter receptors is expressed in proliferating, undifferentiated CTX0E16/02 cells. It was therefore considered interesting to determine whether these receptors were functional at this developmental stage, as well as to provide a

comparison to what is seen later upon differentiation. In addition, confirmation of the presence of these receptors would suggest that they must serve a potential functional role in the behaviour of NPCs.

Ligand-induced intracellular $Ca^{2+}$ accumulation was investigated in proliferative CTX0E16/02 cultures using the endogenous ligands dopamine, 5-HT, glutamate, GABA, histamine and acetylcholine. The cholinergic agonist carbamoylcholine, which is resistant to cholinesterase activity, and the $\alpha_1$-selective adrenergic agonist phenylephrine, which demonstrates better stability than the native ligand norepinephrine, were also used. Dopamine, 5-HT, acetylcholine, carbamoylcholine, phenylephrine and histamine were selected due to their ability to broadly activate receptors known to be targeted by antipsychotics. On the other hand, glutamate and GABA were selected because of the fundamental roles they play as the major excitatory and inhibitory neurotransmitters of the mammalian brain, respectively. Cultures were loaded with the cell permeable, $Ca^{2+}$-sensitive dye Fura-2 AM (Invitrogen) in the presence of probenecid – an organic anion transporter inhibitor – to prevent the dyes secretion and intracellular sequestration [370]. Cultures were then washed of unincorporated dye and allowed to settle for 10 minutes at 37°C prior to being assayed – as described in ***2.4.1***, above. Cells were exposed to each ligand at half log unit intervals from 1 µM to 1 mM or to assay buffer alone as a negative control to determine the effect of fluid addition. This concentration range was determined to provoke measurable $Ca^{2+}$ influx for all ligands in preliminary experimentation (data not shown). All experiments were conducted in black walled 96-well plates with optically clear bottoms using a FlexStation® 3 (FS3) benchtop multi-mode microplate reader (Molecular Devices). As described in ***2.4.1***, above, cells in each well were excited at 340 nm and 380 nm with emission readings taken at 520 nm every 6 seconds. Each well was exposed to 4 readings prior to addition of any drug to establish baseline fluorescence for each well, against which all other values were quoted as relative fluorescence. Different concentrations of the investigated compounds in assay buffer, or buffer alone were added to each well after 20 seconds using the plate readers own liquid handling robotics, followed by the addition of KCl to a final concentration of 50 mM at 120 seconds to determine whether the cells were electrically active. This was used to determine the presence of cells exhibiting a physiologically mature neuronal phenotype. Cells were then exposed to ionomycin at 210 seconds to obtain a maximal intracellular $Ca^{2+}$ accumulation for each well, against which all fluorescence values for that well were expressed. This reading provides an internal control for cultures in each well so that response values can be reliably compared between different wells, independent of the number of cells in that well. Figure 4.5 has been provided to illustrate the time course of experiments performed on the FS3 as described above. Figure 4.5 **a**, depicts raw traces of proliferative CTXOE16/02 cultures exposed to 1 mM carbamoylcholine after 20 seconds, followed by 50 mM KCl after 120 seconds before the removal of 100 µl from each well at 180 seconds and the addition of 10 µM ionomycin at 210 seconds. Additionally, Figure 4.5 **b**, shows raw traces used to generate a concentration-response curve to carbamoylcholine using proliferative CTXOE16/02 cultures.

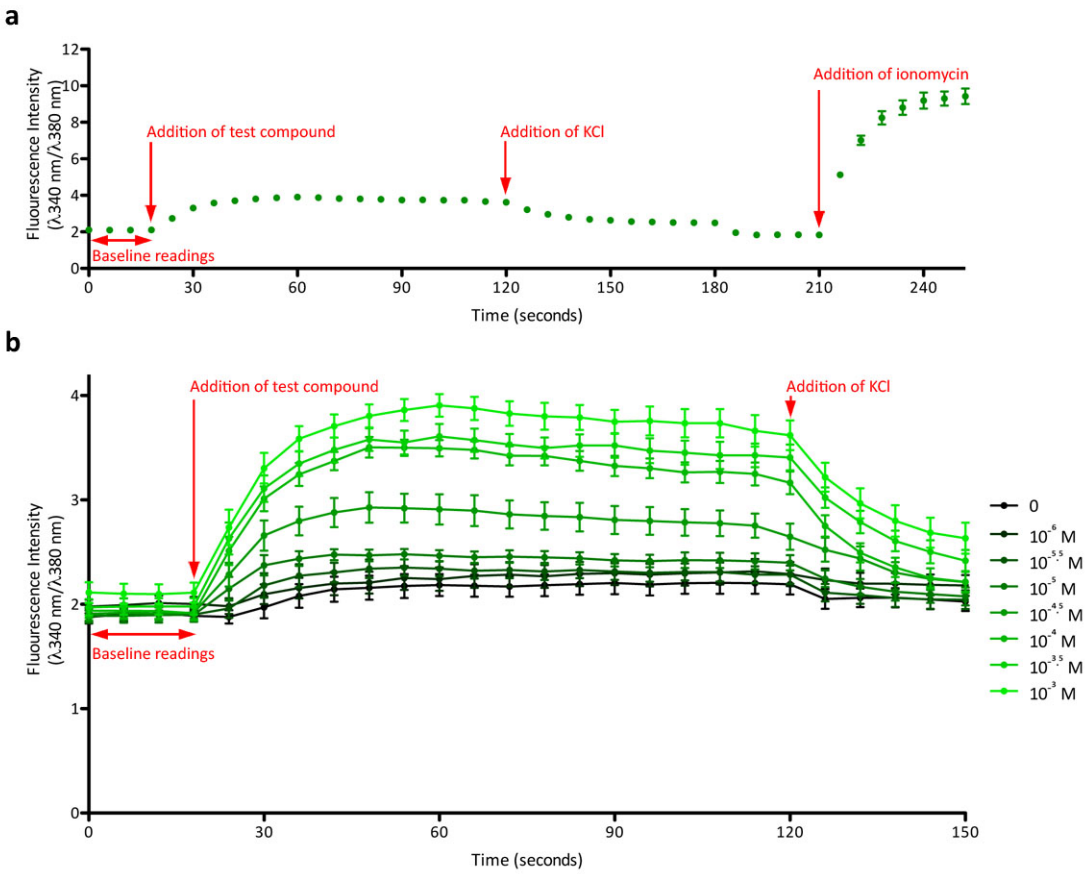


***Figure 4.5 Raw traces of fluorescence intensity changes for a typical FS3 experiment***
Cells were prepared as described in ***2.4.1*** above then incubated for 1 hour in the presence of the cell permeable, $Ca^{2+}$-sensitive fluorescent dye Fura-2 AM. Cells were then washed prior to ligand-induced fluorescence being measured using a FS3. Raw traces are shown for proliferative CTX0E16/02 cells exposed to 1 mM carbamoylcholine followed by 50 mM KCl and 10 µM ionomycin (**a**) and proliferative CTX0E16/02 cells exposed to buffer alone or between 1 µM and 1 mM carbamoylcholine (**b**). Data points represent the mean ± S.E.M. from *n* = 3, with each condition/timepoint being performed in triplicate within each experiment.

Sections ***3.2.4*** and ***3.2.5*** above, demonstrated that many GPCRs targeted by antipsychotics were expressed at the message level by proliferative CTX0E16/02 cultures. However, this did not provide an exhaustive list of all the receptors that may be expressed, and therefore activated by the selected agonists used in these experiments. In addition, several of these agonist are also able to provoke changes in $[Ca^{2+}]_i$ through ionotropic LGICs, such as glutamate and acetylcholine. Thus, these experiments will demonstrate the responsiveness of CTX0E16/02 cells to a range of different neurotransmitter receptor ligands, but are not designed to demonstrate the presence of individual receptor subtypes. For this reason it is difficult to predict how the proliferative CTX0E16/02 cells will respond to each of the tested ligands. Receptors that were shown to be expressed at the message level in these cells were: dopamine $D_2$ and $D_3$, muscarinic $M_1$, histamine $H_1$, adrenoreceptor $\alpha_{1A}$, $mGluR_1$, $mGluR_2$, $mGluR_4$, $mGluR_5$, $mGluR_6$, $mGluR_7$ and $mGluR_8$, plus the glutamatergic NMDA and AMPA channel subunits NR1 and GluR1, respectively.

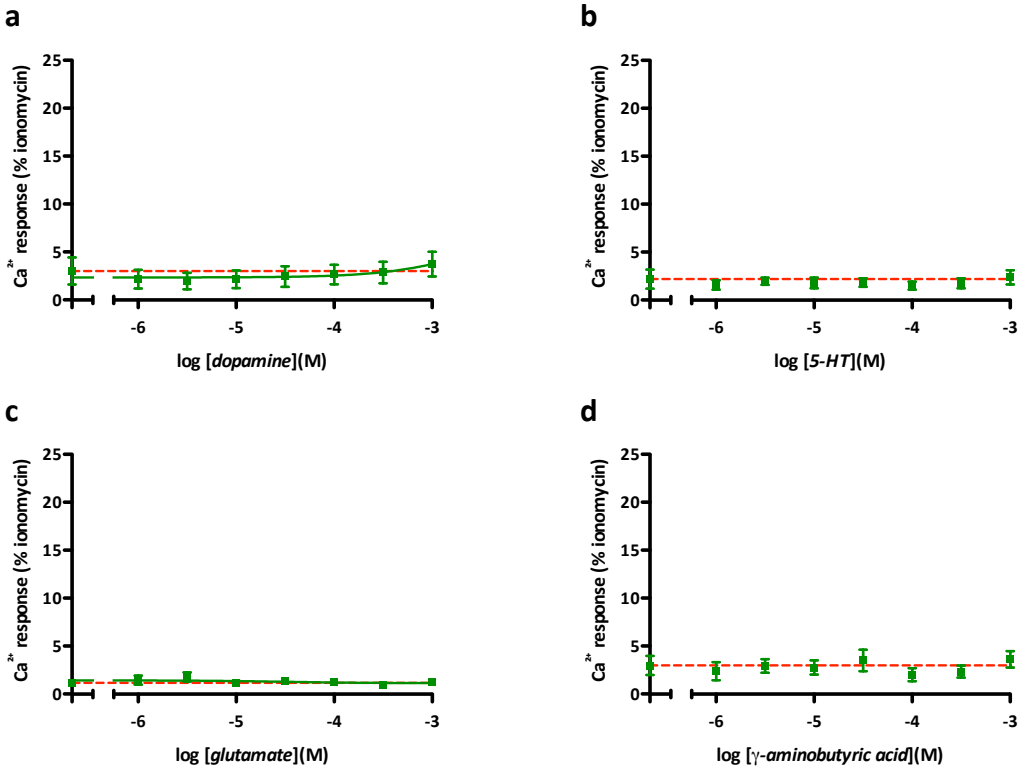


***Figure 4.6 Dopamine, 5-HT, glutamate and GABA-mediated $Ca^{2+}$ release in proliferative CTX0E16/02 cultures***
Cells were prepared as described in ***2.4.1*** above, prior to incubation for 1 hour in the presence of the cell permeable, $Ca^{2+}$-sensitive fluorescent dye Fura-2 AM. Cells were then washed prior to ligand-induced fluorescence being measured using a FS3. Concentration-response curves are shown for dopamine (**a**), 5-HT (**b**), glutamate (**c**) and γ-aminobutyric acid (**d**) in proliferative CTX0E16/02 cells. Data points represent mean ± S.E.M. from *n* = 2, with each performed in triplicate and expressed relative to the positive control, ionomycin. Red lines indicate level of baseline fluorescence observed when buffer in the absence of ligand was added.

Neither dopamine, 5-HT, glutamate or GABA were capable of elevating $[Ca^{2+}]_i$ above baseline in proliferative CTX0E16/02 cells as illustrated in Figure 4.6, above. However, a small but insignificant rise was observed at the highest tested concentration for dopamine. In contrast, proliferative CTX0E16/02 cultures were capable of generating an increase in cytosolic $Ca^{2+}$ concentration in response to phenylephrine, histamine, acetylcholine and carbamoylcholine (see Figure 4.7, panels **a**, **b**, **c** and **d** respectively). Phenylephrine acts as an agonist at $\alpha_1$-adrenergic receptors, of which 3 subtypes exist ($\alpha_{1A}$, $\alpha_{1B}$ and $\alpha_{1D}$) and all couple to $G\alpha_{q/11}$, resulting in $Ca^{2+}$ release from intracellular stores. These receptors also bind most antipsychotics with high affinity. Phenylephrine was capable of provoking a concentration-dependent increase in $Ca^{2+}$ accumulation with an $EC_{50}$ of 5.2 µM – $EC_{50}$ being the concentration of drug that provokes 50% of the observed maximal response (Figure 4.7, **a**). The maximal response achieved was just 5.5% of that observed in response to ionomycin suggesting low receptor expression, inefficient second messenger coupling or a heterogeneous population of cells with respect to response to this ligand. Histamine produced a similarly small effect of 5.3% as compared to ionomycin and an $EC_{50}$ of 47.0 µM (Figure 4.7, **b**). Histamine exerts its actions through four different GPCRs – $H_1$ ($G\alpha_q$-coupled), $H_2$ ($G\alpha_s$-coupled), $H_3$ and $H_4$ ($G\alpha_i$-coupled) with $H_1$ demonstrating ubiquitous expression in all the investigated cell lines detailed in ***3.2.4***, above. $H_1$ is targeted by a range of antipsychotics at nanomolar affinity and has been linked with weight gain in treated patients.

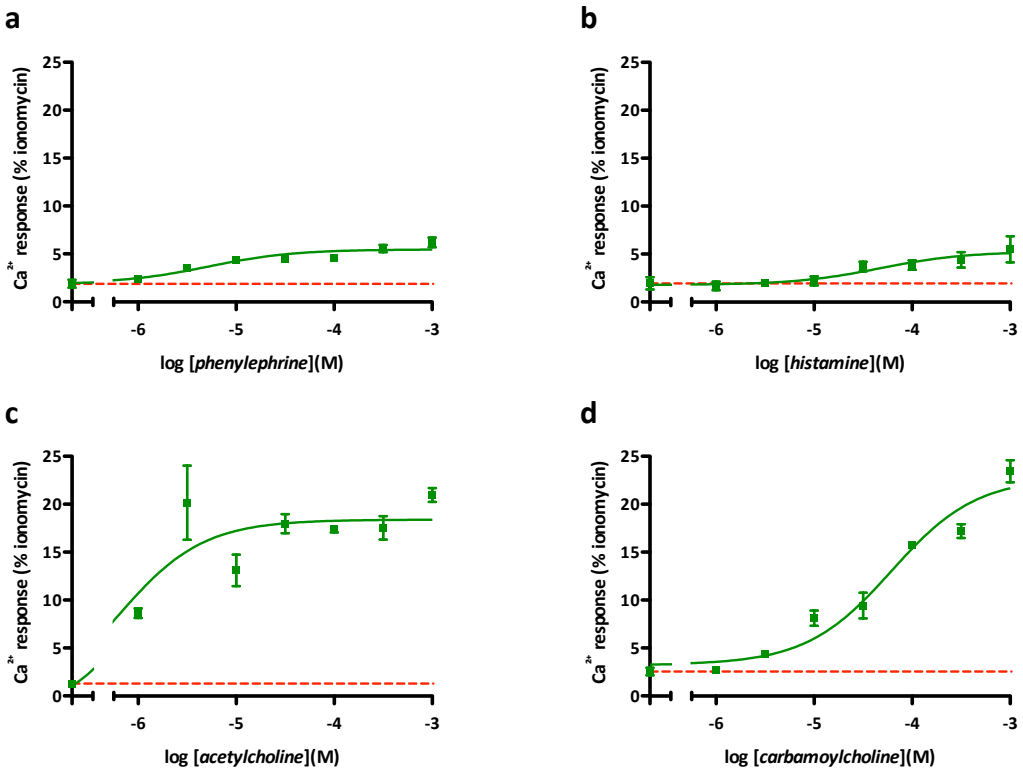


***Figure 4.7 Phenylephrine, histamine, acetylcholine and carbamoylcholine-mediated $Ca^{2+}$ release in proliferative CTX0E16/02 cultures***

Cells were prepared and imaged using a FS3 as described in ***2.4.1***. Concentration-response curves are shown for phenylephrine, $EC_{50}$ = 5.2 µM (**a**), histamine, $EC_{50}$ = 47.0 µM (**b**), acetylcholine (**c**) and carbamoylcholine (**d**) in proliferative CTX0E16/02 cells. Data points represent mean ± S.E.M. from *n* = 2, with each performed in triplicate and expressed relative to the positive control, ionomycin. Red lines indicate level of baseline fluorescence observed when buffer in the absence of ligand was added.

In contrast to phenylephrine and histamine, the cholinergic ligands provoked a far greater $Ca^{2+}$ response in proliferative CTX0E16/02 cultures. Acetylcholine produced what appeared to be a biphasic response that may be caused by distinct responses from several different receptors. Acetylcholine – like glutamate, 5-HT and GABA – binds to both ionotropic (nicotinic) and metabotropic (muscarinic) receptors. Both receptor types are capable of causing a rise in intracellular $Ca^{2+}$ concentrations through distinct mechanisms and may both contribute to the response shown in panel **c** of Figure 4.7, above. Acetylcholine produced a concentration-dependent increase in $[Ca^{2+}]_i$, though the biphasic response made it difficult to estimate an accurate $EC_{50}$ value. A maximal response of 18.4% compared to ionomycin was observed (Figure 4.7, **c**). Carbamoylcholine produced a slightly higher maximal response of 22.8% but saw a rightward shift in potency compared to acetylcholine, though an $EC_{50}$ value could not be accurately obtained as it remained unclear whether a maximal response had been achieved (Figure 4.7, **d**). This may be attributable to a lower efficacy of carbamoylcholine at cholinergic receptors as compared to acetylcholine [371,372]. As expected, none of the proliferative cultures responded to a depolarising $K^+$ challenge suggesting an absence of electrically excitable cells.

Despite the absence of dopamine, 5-HT, glutamate or GABA-induced changes in $[Ca^{2+}]_i$ in proliferative CTX0E16/02 cells, these cells were capable of robust responses to histamine, phenylephrine,

acetylcholine and carbamoylcholine. These data therefore suggest the presence of functional histaminergic, adrenergic and cholinergic receptors in these NPCs.

### *4.2.3 Differentiated CTX0E16/02 Cultures Demonstrate Attenuated Responses*

Ligand-induced intracellular $Ca^{2+}$ accumulation was investigated in differentiated CTX0E16/02 cultures in the same way as was described for proliferative cultures above and according to protocols detailed in ***2.4.1***. CTX0E16/02 cultures were differentiated in 96-well plates for 28 days in SNBM, as detailed in ***2.1.3*** above. After this time, these cultures have been shown to comprise a high proportion of $tau^+$ and $MAP2^+$ neurons, some of which are GABAergic, while others are glutamatergic, and $S100\beta^+$ astrocytes (see ***3.2.3*** and ***4.2.1*** above). At the molecular level, these differentiated CTX0E16/02 cultures were shown to express message for the following receptors or receptor subunits: dopamine $D_2$ and $D_3$, 5-$HT_{2A}$, muscarinic $M_1$, histamine $H_1$, adrenoreceptor $\alpha_{1A}$, $mGluR_{1\text{-}8}$, the $GABA_A$ receptor subunit $\alpha_1$ and the glutamatergic NMDA and AMPA channel subunits NR1 and GluR1, respectively. However, as mentioned previously, this does not detail all of the receptors that may be expressed, and therefore activated by the ligands used. In addition, it is unclear what the GPCRs that may be present are functioned coupled to and so, as with the proliferative cells, it is difficult to predict what responses can be expected from these differentiated cultures.

Responses from proliferative and differentiated cultures exposed to dopamine, 5-HT, glutamate, GABA, histamine, acetylcholine, carbamoylcholine and phenylephrine are shown in Figure 4.8 and Figure 4.9, for comparison. An increase in $[Ca^{2+}]_i$ in responses to dopamine and GABA remained absent following differentiation (Figure 4.8, panels **a** and **d** respectively). This was also the case for 5-HT (Figure 4.9, panel **b**), despite upregulation of the $G\alpha_q$-coupled 5-$HT_{2A}$ receptor following differentiation (see Table 3.10). In contrast, upon differentiation glutamate was able to cause a concentration-dependent increase in $[Ca^{2+}]_i$ and is consistent with previous work using differentiated human NSCs [61]. Glutamate produced a maximal response of 3.5% that of ionomycin with an $EC_{50}$ of 22.0 µM (Figure 4.8, panel **c**), with responses significantly different from those found in proliferative cultures ($p < 0.05$), as determined by two-way ANOVA.

Compounds which were capable of precipitating an increase in $[Ca^{2+}]_i$ in proliferative CTX0E16/02 cultures – phenylephrine, histamine, acetylcholine and carbamoylcholine – all saw their maximal response reduced following differentiation. The maximal response for phenylephrine fell from 5.5% to 1.8% compared to the maximal response provoked by ionomycin, though the $EC_{50}$ remained relatively stable at 5.2 µM and 1.4 µM for proliferative and differentiated cultures respectively (Figure 4.9, **a**). Histamine-induced responses were virtually eliminated, going from a maximal response of 5.3% and an $EC_{50}$ of 47.0 µM in proliferative cultures to a 1.7% maximal response and an $EC_{50}$ of 26.1 µM following differentiation (Figure 4.9, **b**). Cholinergic responses were similarly affected, with acetylcholine-induced responses falling from a high of 18.4% to 8.6% ($p < 0.01$) and accompanied by a considerable rightward shift in potency when comparing proliferative and differentiated cultures respectively. The observed difference

in potency may however be partly attributable to inaccuracy in the extrapolation of the data point at the foot of the curve, as it would appear that acetylcholine is able to provoke increases in $[Ca^{2+}]_i$ at concentrations below the lower limit of 1 µM used in these experiments (Figure 4.9, **c**). Despite this, two-way ANOVA showed that responses to acetylcholine between proliferative and differentiated cultures were significantly different ($p < 0.0001$). Maximal responses for carbamoylcholine fell significantly from 22.8% to 10.2% upon differentiation ($p < 0.05$), while the $EC_{50}$ remained at a similar level – 61.4 µM for proliferative and 50.6 µM differentiated cultures (Figure 4.9, **d**). Following exposure to one of the eight tested ligands or buffer alone, each culture was additionally exposed to a depolarising concentration of $K^+$. Despite four weeks of differentiation, none of these cultures were capable of responding to this challenge with an influx of $Ca^{2+}$. This suggests an absence of electrically excitable cells and therefore, physiologically mature neurons.

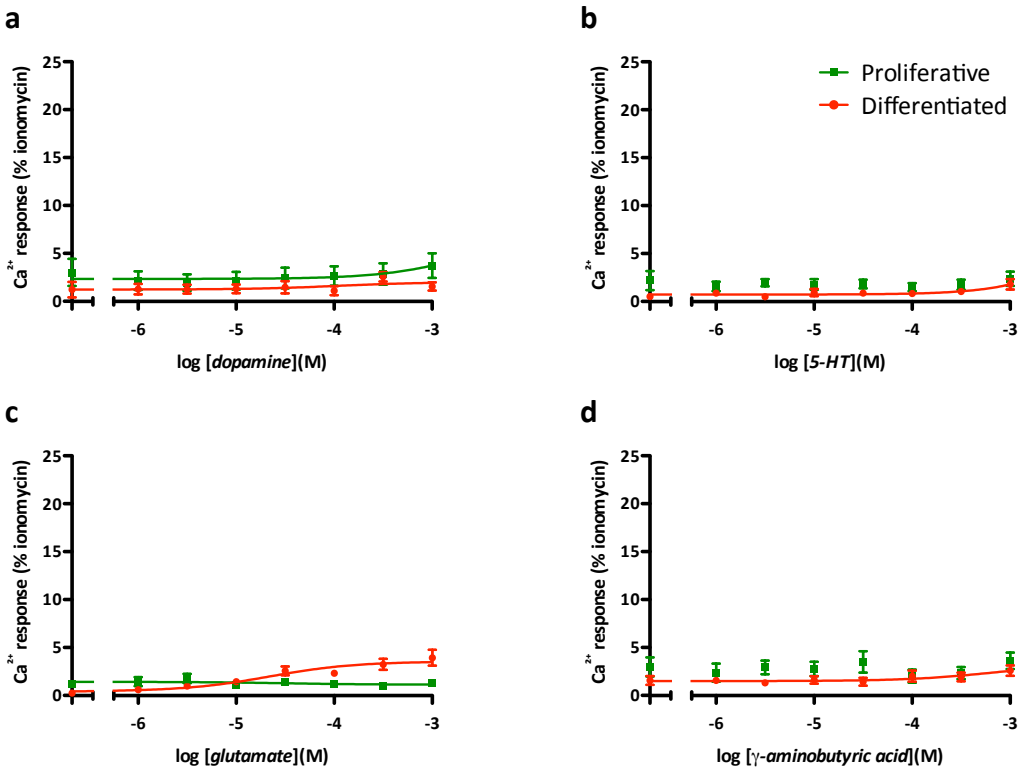


***Figure 4.8 Comparison of dopamine, 5-HT, glutamate and GABA-induced $[Ca^{2+}]_i$ changes between proliferative and differentiated CTX0E16/02 cultures***

Cells were prepared and imaged using a FS3 as described in ***2.4.1***. Concentration-response curves are shown for dopamine (**a**), 5-HT (**b**), glutamate, $EC_{50}$ = 22.0 µM (**c**) and γ-aminobutyric acid (**d**) in proliferative and differentiated (28 days in SNBM) CTX0E16/02 cells. Significant differences between proliferative and differentiated cultures were only observed in response to glutamate ($p < 0.05$), as determined by two-way ANOVA. Data points represent mean ± S.E.M. from $n = 2$, with each performed in triplicate and expressed relative to the positive control, ionomycin.

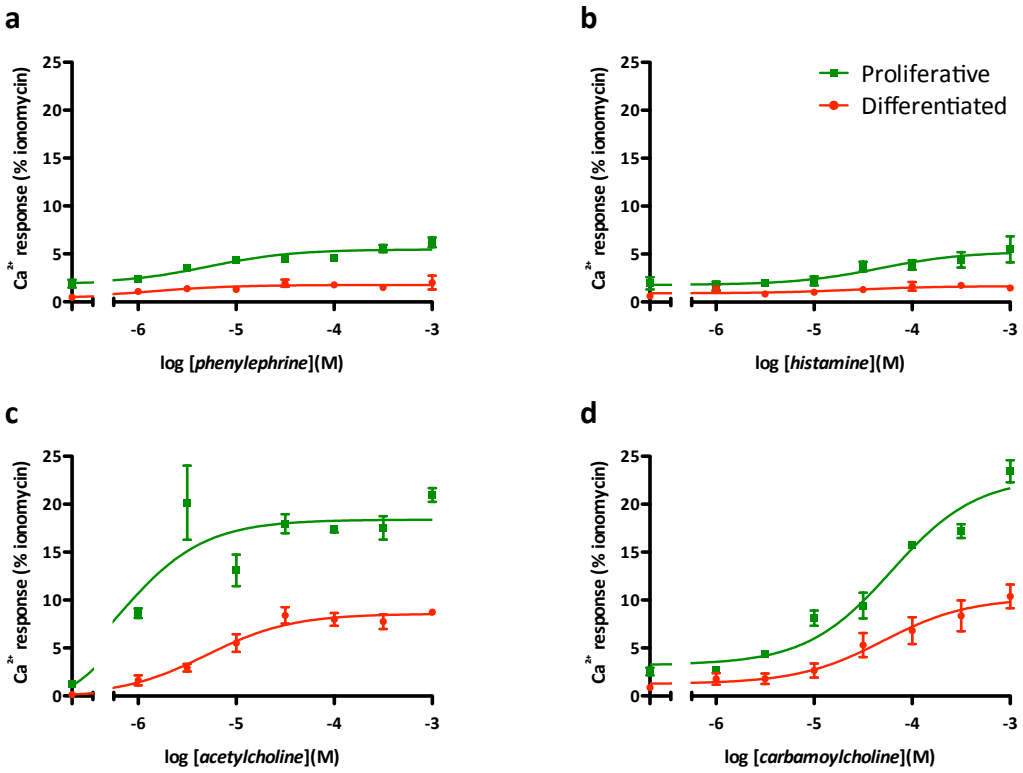


***Figure 4.9 Comparison of phenylephrine, histamine, acetylcholine and carbamoylcholine-induced $[Ca^{2+}]_i$ changes between proliferative and differentiated CTX0E16/02 cultures***

Cells were prepared and imaged using a FS3 as described in ***2.4.1***. Concentration-response curves are shown for phenylephrine, $EC_{50}$ = 5.2 µM and 1.4 µM (**a**), histamine, $EC_{50}$ = 47.0 µM and 26.1 µM (**b**), acetylcholine, $EC_{50}$ = 5.01 µM (**c**) and carbamoylcholine, $EC_{50}$ = 50.6 µM (**d**) in proliferative and differentiated (28 days in SNBM) CTX0E16/02 cells. Significant differences between proliferative and differentiated cultures were observed in response to phenylephrine ($p < 0.0001$), histamine ($p < 0.005$), acetylcholine ($p < 0.0001$) and carbamoylcholine ($p < 0.0001$), as determined by two-way ANOVA. Data points represent mean ± S.E.M. from $n = 2$, with each performed in triplicate and expressed relative to the positive control, ionomycin.

The observed reduction in the maximal $[Ca^{2+}]_i$ provoked by phenylephrine, histamine, acetylcholine and carbamoylcholine following differentiation of CTX0E16/02 cultures seems an interesting finding considering the expression data presented in Table 3.9 and Table 3.10, above. While the expression of not every receptor targeted by these compounds was investigated, the trend for all those that were, was an increase in their expression following differentiation, with the only exception being histamine $H_1$. In addition, with only small variations in the $EC_{50}$ values for each of these compounds following differentiation (except in the case of acetylcholine), it would suggest that the relative contribution of different receptor subtypes to the observed responses had not changed significantly. This is exemplified by the change in the response observed for carbamoylcholine following differentiation, where the maximal response fell significantly from 22.8% to 10.2% while the $EC_{50}$ remained at approximately 50 µM for both proliferative and differentiated cultures.

Paradoxically, despite the fact that upon differentiation of CTX0E16/02 cultures the expression of most receptors increased relative to total RNA at the message level, this was met in nearly all cases with a reduction in the level of ligand-induced intracellular $Ca^{2+}$ accumulation. The possible exceptions being histamine, where a slight fall in receptor expression was observed at the message level, and glutamate,

where no $Ca^{2+}$ response was observed in proliferative cells, while a small dose-dependent response was observed in their differentiated counterparts. This raises several interesting questions, the first being; does an increase in levels of mRNA necessarily relate to an increase in protein? This could be tested with the use of a western blot, but this would only provide an answer as to whether translation of this increased message is occurring. The translation of mRNA encoding receptors does not necessarily equate with the functional expression of these receptors at the cell surface. Therefore, a western blot would not be able to distinguish between receptor present at the cell surface or that which may be trapped within components of the secretory pathway such as the ER or Golgi. The amount of receptor present at the cell surface could however be detected using radioligand binding, though this would have to be performed using intact cells, for the same reasons as those described above, so as not to detect receptors localised to intracellular membranes. This would not be a trivial approach, and it would be difficult to normalise the resulting data due to the differences in the cultures following differentiation, in that the cells that comprise the culture become both smaller and fewer in number. Neither of these approaches would provide a functional explanation at the cellular level however, where dramatic changes are likely to have occurred, especially when we consider the phenotypic changes that occur upon differentiation.

### *4.2.4 Heterogeneous Ligand-Induced Responses in Proliferative & Differentiated Cultures*

Differentiation of the CTX0E16/02 cells altered the appearance of the cultures dramatically, as can be seen in ***Figure 4.10***, below. Following differentiation (***Figure 4.10***, **b**), individual cell body volume reduced considerably, and was accompanied by the extension of numerous cellular processes. While these are difficult to see in the bright phase images in ***Figure 4.10***, they can be clearly observed in the fluorescence immunocytochemistry images in Figure 4.3, above. Cell death was also prevalent in the differentiated cultures, as indicated by the presence of DAPI-stained cell debris, which was largely absent from the proliferative cultures (***Figure 4.10***, **a**). In addition, the proliferative cultures appeared more confluent due to the way the cells tended to tessellate together, while the individual cell bodies in differentiated cultures appeared more isolated; lacking this cell-cell contact. Despite this, the level of basal fluorescence prior to any drug addition between the proliferative and differentiated cultures was very similar. Average emissions from all wells at 520 nm following excitation at 380 nm (a reliable marker of Fura-2 cell loading – see ***2.4.1***, above) were in fact significantly higher in differentiated (147.0 ± 0.95) compared to proliferative (140.8 ± 0.75) cultures. In addition, all fluorescence values were quoted relative to a maximal response elicited by the addition of ionomycin. Taken together, this appears to provide evidence that the reductions observed in the maximal responses provoked by various ligands were not simply due to a reduction in the number or the size of the cells that comprise the culture. Perhaps a more likely explanation for the observed reduction in the ligand-induced maximal responses was that the cultures – upon differentiation – change from a relatively homogeneous pool of cells to a more heterogeneous population. Data presented above supports this supposition at the phenotypic level; where, as NPCs in proliferative culture, the CTX0E16/02 cells are predominantly

nestin$^{+}$, with only a very small proportion of spontaneously generated tau$^{+}$, MAP2$^{+}$ neurons or S100β$^{+}$ astrocytes present (see Figure 4.2, above). In contrast, differentiated CTX0E16/02 cultures were composed of a range of different cell types, for example, GABAergic neurons of different sub-types, glutamatergic neurons and astrocytes. If ligand-induced responses following differentiation are similarly heterogeneous, then this may account for the observed reductions in the maximal responses provoked by phenylephrine, histamine, acetylcholine and carbamoylcholine (see Figure 4.9). For example, in the relatively homogenous cellular pool of proliferative CTX0E16/02 cultures, it may be the case that the majority of cells are capable of responding to a particular ligand, such as acetylcholine, to a similar degree, due to comparable levels of functional acetylcholine receptor being present in these cells. However, differentiation may lead to the restriction of acetylcholine receptor expression in many cells, but a considerable upregulation in others. This would lead to a situation where, while fewer cells are expressing the receptors, those that do are expressing them at a considerably higher frequency. These differentiated cells would therefore be capable of greater responses than those observed from responsive cells in proliferative cultures to the same concentration of ligand. However, the FlexStation® 3 instrument (FS3) used to perform these experiments would not detect these heterogeneous responses, since this instrument provides an average fluorescence reading for a field within each well, it cannot provide data for $[Ca^{2+}]_i$, in individual cells or small groups of cells. Higher 340 nm/38 nm fluorescence ratios in fewer cells may therefore be translated as an overall reduction in the level of fluorescence in response to a particular stimulus. In order to address this issue, single cell $Ca^{2+}$-imaging was used to provide qualitative data at the level of individual cells.

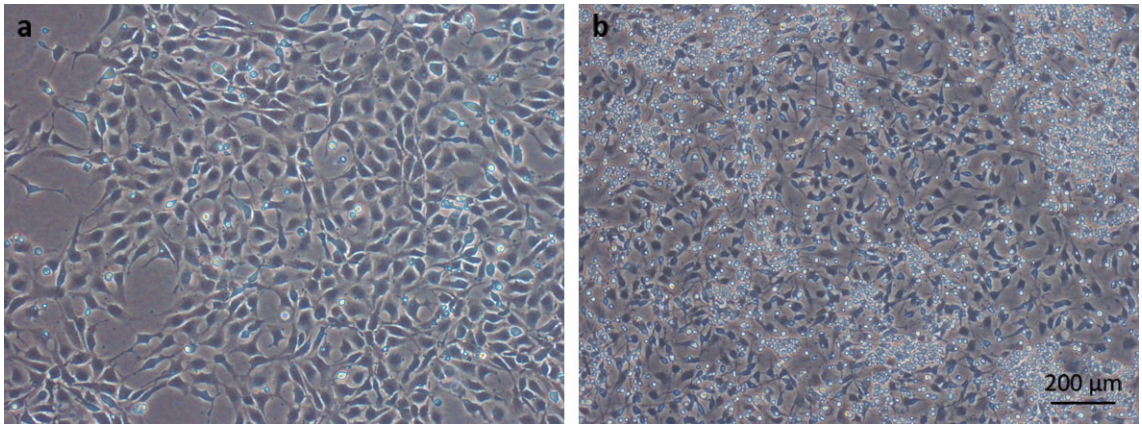


***Figure 4.10 Representative bright field images of proliferative and differentiated CTX0E1602 cells***
Bright field images of CTX0E16/02 cultures when proliferative (a) and following 28 days differentiation in neurobasal medium supplemented with B27 (b). Proliferative CTX0E16/02 cells exhibit noticeably larger cell soma and fewer processes. Considerable quantities of cell debris are present in differentiated cultures indicating a degree of cell death. Images were captured using an inverted Nikon Eclipse TS100-F fitted with a Y-TV55 Nikon TV lens and a Digital Sight DS-2Mv camera and a 10x objective.

CTX0E16/02 cells were grown on PDL and laminin-coated coverslips and imaged as proliferative or differentiated (28 days in SNBM) cultures, as described in ***2.4.3***, above. The method by which CTX0E16/02 cells were both cultured and prepared for single cell $Ca^{2+}$-imaging was kept as consistent as possible with how this was performed for equivalent experiments using the FS3. Individual coverslips of

proliferative or differentiated CTX0E16/02 cells were exposed to either dopamine, 5-HT, acetylcholine or glutamate at 1 mM (the highest tested concentration for experiments using the FS3) for 1 minute. This period was found to be sufficient to observe a maximal response by analysing data obtained using the FS3 (data not shown). Cells were then washed with $Ca^{2+}$ Release Assay Buffer (the same as that used for FS3 experiments) to allow $[Ca^{2+}]_i$ levels to return to baseline before exposing the cells to 50 mM KCl for 1 minute. Figure 4.11 below, shows representative pairs of images of proliferative and differentiated CTX0E16/02 cultures. Each pair of images has been taken from a sequence of images of a single field, either prior to or following exposure to 1 mM acetylcholine to illustrate the level of fluorescence change. These images also show the larger soma of cells found in proliferative cultures as compared to differentiated cultures.

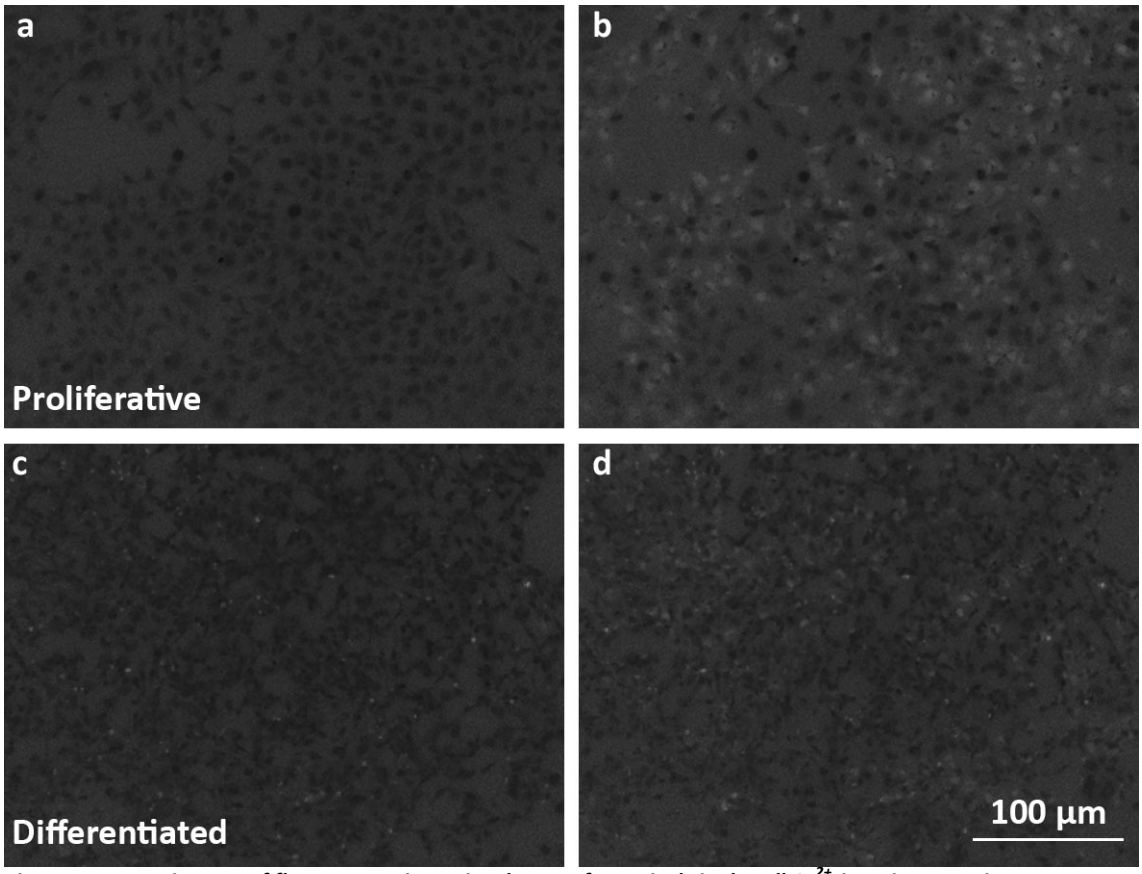


***Figure 4.11 Raw images of fluorescence intensity changes for typical single cell $Ca^{2+}$-imaging experiments***
Panels show representative, derived 340 nm/380 nm still images from single cell $Ca^{2+}$-imaging experiments. Top panels show two images taken from a quantified sequence in which proliferative CTX0E16/02 cultures were exposed first to assay buffer alone (**a**), then assay buffer containing 1 mM acetylcholine (**b**). Lower panels show two images taken from a quantified sequence in which CTX0E16/02 cultures differentiated for 28 days were exposed to assay buffer (**c**) prior to assay buffer containing 1 mM acetylcholine (**d**). Image analysis was performed on individual cells by emission intensity ratios from 340 nm/380 nm excitation using the ImageMaster™ software (Photon Technology International).

Dopamine and 5-HT were incapable of provoking a significant increase in $[Ca^{2+}]_i$ when added at 1 mM to proliferative or differentiated CTX0E16/02 cultures when measured using a FS3 plate reader. This was also true of proliferative cultures exposed to 1 mM glutamate (see Figure 4.8, panels **a**, **b** and **c**).

However, when measuring $Ca^{2+}$ influx at the level of individual cells, it became clear that some cells within proliferative and differentiated CTX0E16/02 cultures were capable of responding to dopamine, 5-HT, glutamate and acetylcholine. However, both the proportion of cells within these cultures that responded, and the extent to which these cells responded was highly variable. In the case of dopamine, the mean maximal response observed across all counted cells was 8.8% ± 0.8% in proliferative cultures (Figure 4.13, **a**) – a value that dropped to 5.9% ± 0.4% in differentiated cultures (Figure 4.13, **c**). While this value takes into consideration the fluorescence observed in the majority of cells in the imaged field, this value does not correlate with that provided by readings made by the FS3 plate reader. The reason for this, as mentioned above, is that the FS3 measures the average level of fluorescence across the whole imaged field – including the spaces between cells. This averaging of fluorescence across the whole field accounts for the reduced level of sensitivity when using the FS3 – in that no fluorescence response was observed when dopamine was applied at 1 mM. A more significant reason for why the FS3 did not detect a measurable increase in $[Ca^{2+}]_i$ following exposure to 1 mM dopamine can be seen when considering the proportion of cells within an imaged field that responded, and also the extent to which each of these cells responded. Just 7.7% of cells within the imaged fields were capable of producing an increase in fluorescence of more that 20% above that which was measured at baseline in response to 1 mM dopamine, while just 3.7% and 0.7% of cells produced responses above 50% or 100% of baseline respectively (Figure 4.13, **b**). These data suggest that considerable heterogeneity exists, even in proliferative cultures, with respect to these cells' ability to respond to 1 mM dopamine. Interestingly, despite an increase in the level of expression of dopamine $D_2$ and $D_3$ receptors following differentiation of CTX0E16/02 cultures (see Table 3.10, above), both the proportion of cells and the magnitude of responses these cells were able to produce in response to 1 mM dopamine was reduced. In differentiated cultures, just 2.5% of cells demonstrated an increase in $[Ca^{2+}]_i$ of more than 20% above baseline, while only 1.0% and 0.2% of cells produced responses above 50% or 100% of baseline respectively (Figure 4.13, **d**).

The most interesting finding regarding dopamine-induced responses was only evident once individual cellular traces were examined. As is clear from Figure 4.13, the majority of cells in both proliferative and differentiated cultures did not respond in any way to the addition of dopamine. However, a small minority of cells were capable of responding to this stimulus. A selection of the raw 340 nm/380 nm traces for some of these are shown in Figure 4.12. While data presented in Figure 4.13 demonstrated that there was considerable heterogeneity within proliferative and differentiated cultures regarding whether individual cells responded or not to 1 mM dopamine, data shown in Figure 4.12 serve to illustrate the considerable heterogeneity that was also observed between these responses. In proliferative CTX0E16/02 cultures both the rate of intracellular $Ca^{2+}$ accumulation and the maximal response achieved in different cells exposed to 1 mM dopamine varied considerably. As can be seen in Figure 4.12, panel **a**, while some cells in proliferative cultures responded very rapidly to dopamine, other cells within the culture responded much more slowly. In addition, while the majority of the traces shown reached a maximal response and plateau at approximately 0.5 RFU (Relative Frequency Units – $\lambda_{340}/\lambda_{380}$) above baseline, some of the cells exhibited responses considerable higher than this.

Interestingly, the cells that demonstrated the larger maximal responses did not immediately plateau, but instead appeared to return to the same level at which the other cells plateau. Upon addition of buffer, all the cells for which traces are shown appear to clear the cytosolic $Ca^{2+}$ at a comparable rate. Interestingly, while none of the cells from proliferative cultures for which traces are shown responded to 50 mM KCl, it's presence did appear to attenuate dopamine-induced increases in $[Ca^{2+}]_i$, by preventing the plateau that was observed in response to continued dopamine exposure. Indeed all traces had returned to baseline levels prior to the addition of the final buffer wash (Figure 4.12, **a**). This finding suggests two broad possibilities; the first being that the system responsible for causing the rise in $[Ca^{2+}]_i$, has been desensitised following the initial addition, meaning that the same concentration of dopamine is incapable of provoking the same magnitude of response. This may indeed be the case, due to the high concentration of dopamine (1 mM) to which the cultures were exposed. This concentration was chosen because no effect was observed in response to dopamine at any tested concentration when measurements were taken using the FS3. Therefore, to increase the chances of seeing any responding cells at the single cell level, it was decided that 1 mM dopamine would be appropriate. The second possibility – which is not mutually exclusive from the first however – is that at least a proportion of the intracellular $Ca^{2+}$ accumulation that occurs in response to 1 mM dopamine, results from an influx from the extracellular space. For example, if the rise in $[Ca^{2+}]_i$ occurred solely as a result of release of $Ca^{2+}$ from intracellular stores, such as through the activation of $G\alpha_q$, and subsequent $IP_3$-mediated release from the ER; the presence of high extracellular $K^+$ would not be expected to alter this effect. However, if a proportion of the observed intracellular $Ca^{2+}$ increase was attributable to passive influx from the extracellular space – probably through non-selective cation channels – this would be expected to be altered in the presence of 50 mM extracellular $K^+$. The rationale for this is that high extracellular $K^+$ would shift the membrane potential from ~-60 mV to approaching 0 mV. This would mean that while $Ca^{2+}$ would still enter the cell along it's chemical gradient, the electrical driving force would no longer be present, and therefore the net flow would be reduced. Likely candidates to mediate these effects are the transient receptor potential (TRP) cation channels – probably those belonging to the TRPC subfamily, to which seven distinct members belong ($TRPC_1$ – $TRPC_7$)[230]. Several of these channels have recently been identified as playing an important role in GPCR-mediated intracellular $Ca^{2+}$ accumulation due to their gating mechanism being under the control of components of the PLC-β pathway. For example, a cleavage product of catalytic PLC-β activity; DAG, has been shown to directly activate $TRPC_2$, $TRPC_3$, $TRPC_6$, and $TRPC_7$ [230,360]. Conversely, PKC – the classical downstream effector of DAG – has also been shown to mediate an inhibitory effect upon the activity of some TRPC channels through direct or indirect phosphorylation [230,361]. This observed effect of a high $K^+$ challenge upon dopamine-mediated intracellular $Ca^{2+}$ accumulation in a minority of proliferative CTX0E16/02 NPCs, suggest that further work is necessary to identify the exact mechanism through which this is thought to occur.

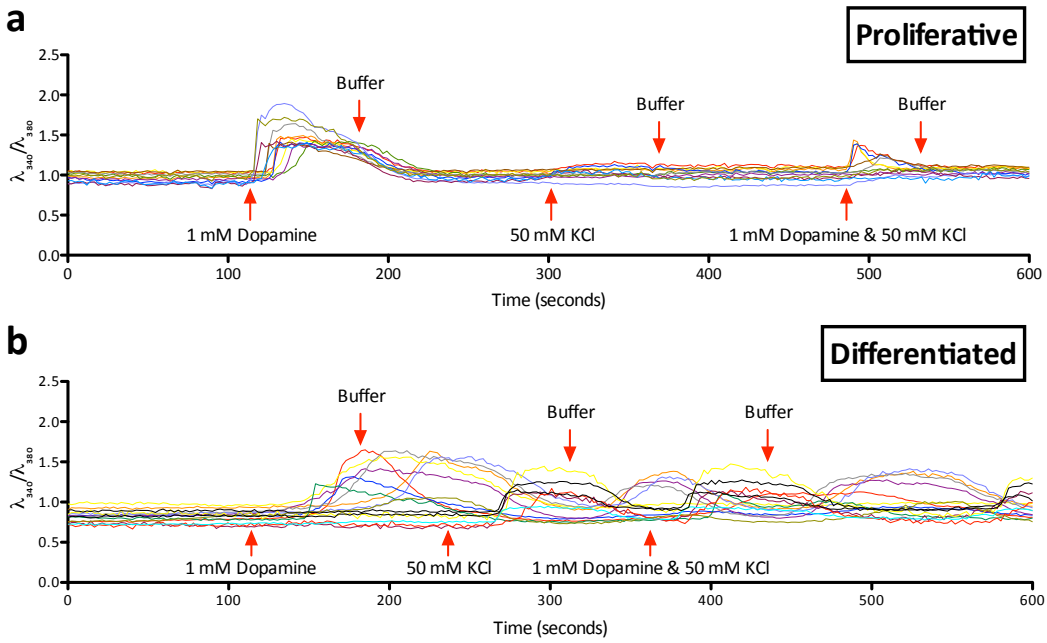


***Figure 4.12 Cells within differentiated CTX0E16/02 cultures demonstrate dopamine-induced $Ca^{2+}$ oscillations***
Proliferative and differentiated CTX0E16/02 cultures were prepared and imaged for single cell $Ca^{2+}$-imaging as described in ***2.4.3***, above. Raw 340 nm/380 nm ($\lambda_{340}/\lambda_{380}$) fluorescence ratio traces are shown for several cells sequentially exposed to 1 mM dopamine, 50 mM KCl and 1 mM dopamine with 50 mM KCl and interceded with buffer washes in proliferative (**a**) and differentiated (**b**) CTX0E16/02 cultures. Timing of additions are indicated using red arrows. Traces for panel **a** were taken from two independent experiments, while traces from panel **b** were all taken from the same experiment.

Responses to 1 mM dopamine in CTX0E16/02 cultures exposed to a 28 day differentiation in the presence of SNBM, were very different to those that were observed in their proliferative counterparts. As discussed previously, and similar to proliferative cultures, very few cells within differentiated cultures responded to dopamine, or indeed KCl in any way at all. Figure 4.12, **b** shows raw traces for some of those cells within these cultures that did appear to respond. However, unlike cells in proliferative cultures which responded immediately to the presence of dopamine, responding cells in differentiated cultures demonstrated a delayed response. In addition, once these cells did start to respond, they appeared unaffected by subsequent washes, KCl or drug additions (see Figure 4.12, **b**). Interestingly, following exposure to dopamine, a minority of cells appeared to exhibit spontaneous $Ca^{2+}$ transients. While this effect was observed in all experiments conducted, all the traces in Figure 4.12, **b** were imaged from the same microscope field. This was to show that the observed $Ca^{2+}$ transients in different cells appeared to be harmonised – though all cells within the observed field did not synchronise together. Indeed, the traces shown in Figure 4.12, **b** appears to provide evidence of two distinct alternately asynchronous populations of cells. The mechanism through which this intracellular $Ca^{2+}$ accumulation is occurring remains unclear and further work is necessary to identify both the source of the $Ca^{2+}$ – whether from inside or outside the cells – and also the mechanism responsible for these cyclic changes in $[Ca^{2+}]_i$. It should be noted however that the appearance of this cyclic intracellular $Ca^{2+}$ accumulation was only observed in the presence of dopamine and glutamate in differentiated cultures. This effect was

absent in all proliferative cultures and was not seen in differentiated cultures exposed to 5-HT or acetylcholine.

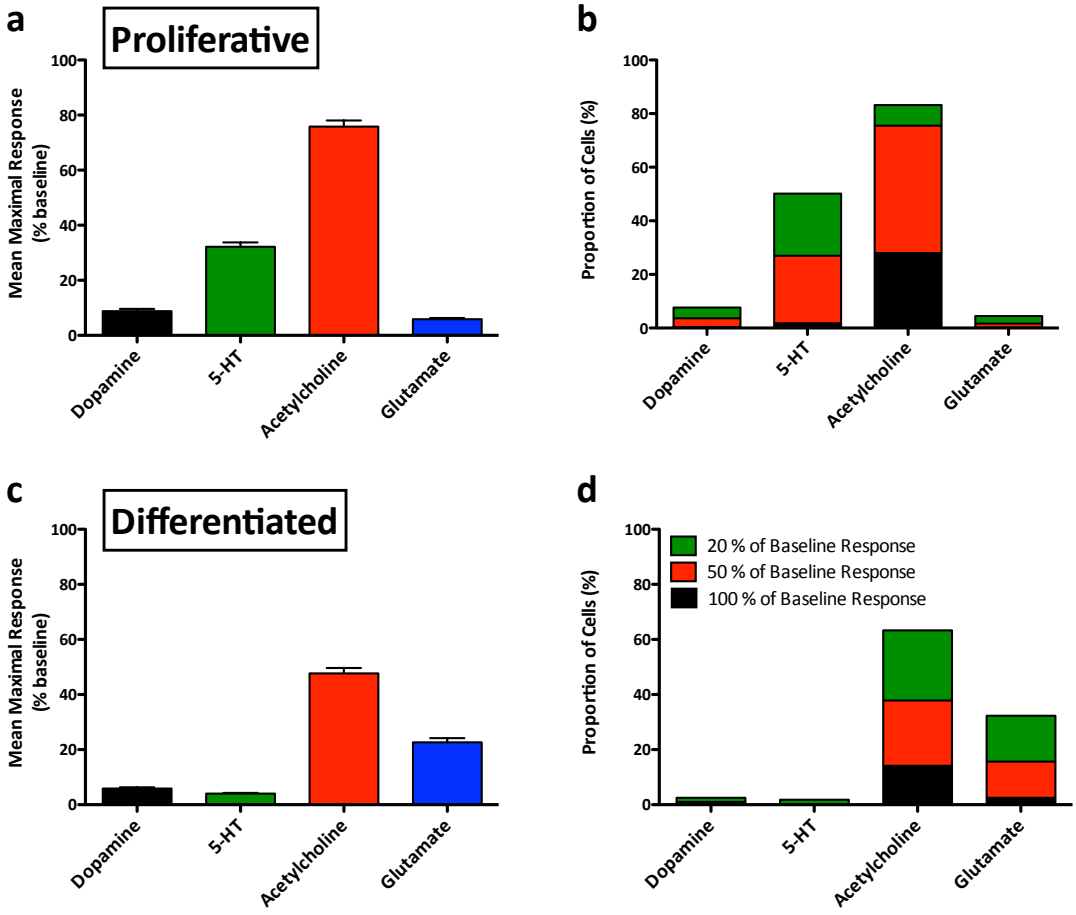


***Figure 4.13 Proliferative and differentiated CTX0E16/02 cultures demonstrate considerable heterogeneity in response to dopamine, 5-HT and glutamate, but not acetylcholine***
Proliferative and differentiated CTX0E16/02 cultures were prepared and imaged for single cell $Ca^{2+}$-imaging as described in ***2.4.3***, above. Data are presented with respect to the mean ± S.E.M. of the maximal response achieved relative to baseline, from all measured cells, from all cultures exposed to each of the four tested neurotransmitter agonists; dopamine, 5-HT, acetylcholine and glutamate in proliferative (**a**) and differentiated (**c**) cultures. Data are also presented that show the proportion of cells within these cultures that demonstrated an increase in fluorescence of > 20%, > 50% or > 100% relative to baseline in response to each of the four tested agonists in proliferative (**b**) and differentiated (**d**) cultures. All values are quoted with respect to a 340 nm/380 nm fluorescence ratio following excitation at 520 nm. Values obtained from the measurement of fluorescence from 300 cells per experiment ($n$ = 2).

As was the case for dopamine, 5-HT was similarly incapable of provoking a measurable increases in $[Ca^{2+}]_i$ in proliferative or differentiated CTX0E16/02 cultures when measured using the FS3 plate reader (see Figure 4.8, panel **b**). However, when measuring $[Ca^{2+}]_i$ in individual cells, it was found that a considerable number in proliferative cultures were capable of responding to 1 mM 5-HT, while few, if any, proved to be responsive in differentiated cultures (Figure 4.13). In proliferative CTX0E16/02 cultures, the mean maximal response observed across all counted cells was 32.2% ± 1.6% (Figure 4.13, **a**), while in differentiated cultures this dropped to 4.0% ± 0.3%, despite the observed appearance of

expression of the gene encoding the $G\alpha_q$-linked 5-$HT_{2A}$ receptor at the message level (see Table 3.9, above) upon differentiation. The absence of the 5-$HT_{2A}$ receptor in proliferative cultures suggests the observed increases in $[Ca^{2+}]_i$ was attributable to other 5-HT receptor subtypes. Considering the absence of measurable 5-HT-induced intracellular $Ca^{2+}$ accumulation in response to 5-HT at any of the tested concentrations (1 µM – 1 mM) when using the FS3, it was surprising to see a relatively high proportion of cells responding to 1 mM 5-HT when analysing single cells. From the cells counted in each experiment, 50.2% responded with a rise in $[Ca^{2+}]_i$ of more that 20% above baseline, while in 27.0% of cells a response of more than 50% above baseline was observed. However, just 1.8% of counted cells saw responses of more that 100% above baseline (Figure 4.13, **b**). Both the proportion and the extent to which the cells responded to 5-HT in differentiated cultures was negligible (Figure 4.13, **d**). With regard to proliferative cultures, heterogeneity was observed in the manner in which responding cells accumulated $Ca^{2+}$ in response to 1 mM 5-HT (Figure 4.14), though this was less pronounced than that observed between responding cells in proliferative cultures exposed to 1 mM dopamine (Figure 4.12, **a**). Cells in proliferative or differentiated cultures were incapable of producing a rise in $[Ca^{2+}]_i$ in response to 50 mM KCl when added alone. Interestingly however, when proliferative cultures were exposed to both 1 mM 5-HT and 50 mM KCl at the same time, responses to 5-HT were either attenuated or eliminated (Figure 4.14) – as was seen in cells exposed to dopamine (Figure 4.12, **a**). In contrast to what was observed in cells exposed to dopamine and KCl, those cells that did respond to 5-HT and KCl were capable of maintaining the rise in $[Ca^{2+}]_i$ that was provoked, though these levels were slightly lower than responses observed in the absence of KCl (Figure 4.14). Again, it is unclear whether this attenuation of the 5-HT response is as a consequence of the presence of KCl, or is simply due to desensitisation mechanisms present within the responding cells.

Acetylcholine was capable of provoking robust intracellular $Ca^{2+}$ accumulation in both proliferative and differentiated CTX0E16/02 cultures when measured using the FS3, though these responses were considerably attenuated in differentiated cultures (Figure 4.9, panel **c**). Similarly robust maximal responses were also observed in response to carbamoylcholine, though a considerable rightward shift in potency was observed when compared to acetylcholine with $EC_{50}$ values of 0.62 µM and 61.38 µM respectively in proliferative cells, and 5.01 µM and 50.64 µM for acetylcholine and carbamoylcholine respectively in differentiated cells. This difference may be partly attributable to carbamoylcholine's lower efficacy at nicotinic acetylcholine receptors (nAChR), as this compound demonstrates some selectivity for muscarinic acetylcholine receptors (mAChR)[373,374]. It is hoped that by analysing intracellular $Ca^{2+}$ accumulation in individual cells within these cultures, this may provide evidence as to why considerably lower responses are observed in differentiated as compared to proliferative cultures. The most likely explanation for this is a reduction in receptor number following differentiation. The expression of just one cholinergic receptor – the mAChR $M_1$ – was determined in proliferative and differentiated cultures, and this was shown to remain relatively constant between the two different culture types at the message level (see Table 3.9, above). However, the expression of every other receptor investigated – with the exception of histamine $H_1$ – was increased following differentiation. This does not however exclude the possibility that other cholinergic receptors may be down-regulated

upon differentiation, and therefore account for the observed reduction in response to both acetylcholine and carbamoylcholine.

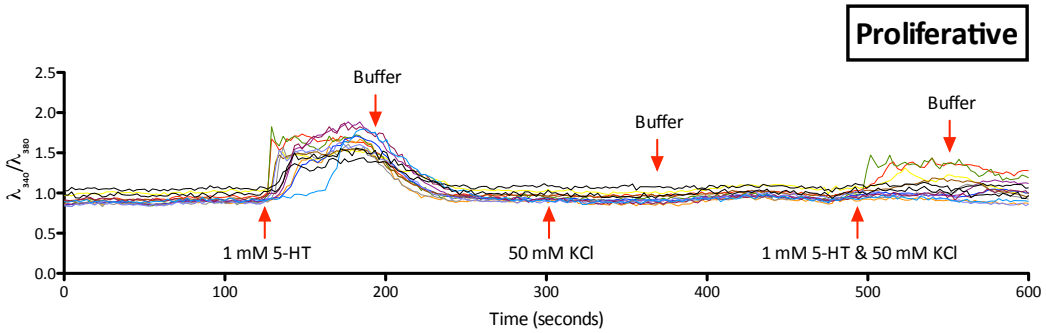


***Figure 4.14 Cells within proliferative CTX0E16/02 cultures are capable of 5-HT-induced $Ca^{2+}$ responses***
Proliferative CTX0E16/02 cultures were prepared and imaged for single cell $Ca^{2+}$-imaging as described in ***2.4.3***, above. Raw 340 nm/380 nm ($\lambda_{340}/\lambda_{380}$) fluorescence ratio traces are shown for several cells sequentially exposed to 1 mM 5-HT, 50 mM KCl and 1 mM 5-HT with 50 mM KCl and interceded with buffer washes in proliferative CTX0E16/02 cultures. Timing of additions are indicated using red arrows. Traces were taken from two independent experiments.

Thus, measurement of changes in $[Ca^{2+}]_i$ at the level of individual cells in proliferative and differentiated CTX0E16/02 cultures showed that both the proportion of cells, and the extent to which these cells were responding was greater in proliferative cultures. The mean maximal response observed across all counted cells was 75.8% ± 2.2% in proliferative cultures (Figure 4.13, **a**) – a value that dropped to 47.7% ± 2.0% in differentiated cultures (Figure 4.13, **c**). Taken together with the fact that cells within differentiated cultures exhibited smaller cell soma than those in proliferative cultures – as can be seen in Figure 4.10 and Figure 4.11 above – it is clear why fluorescence readings were lower in differentiated as compared to proliferative cultures when measured using the FS3. One suggestion for the reduced levels of fluorescence detected in differentiated cultures using the FS3, is that a lower proportion of cells respond, due to the cells within the culture becoming differentiated into a range of different cell types. It was also proposed that the cells within the differentiated cultures that remained responsive would demonstrate higher ligand-induced intracellular $Ca^{2+}$ accumulation. This was suggested to account for a concurrent increase in the expression of receptor mRNA following differentiation. Upon inspection of measured increases in $[Ca^{2+}]_i$ in individual cells following exposure to 1 mM acetylcholine, it was indeed found that fewer cells within differentiated cultures were capable of responding. In proliferative cultures, 83.2% of cells were capable of responding to acetylcholine with a response of at least 20% above baseline (Figure 4.13, **b**), as compared with just 63.3% of cells in differentiated cultures (Figure 4.13, **d**). However, the extent to which responding cells in differentiated cultures reacted was actually lower than that seen in proliferative cultures. The majority of responding cells within proliferative cultures were capable of $[Ca^{2+}]_i$ rises of more than 50% above their respective baseline. Of the cells measured in proliferative cultures, 75.5% were capable of responses of more than 50% of their baseline, while 28% were capable of responses of more than 100% of their baseline (Figure 4.13, **b**). This

compared to 37.8% of cells in differentiated cultures capable of responses above 50% of their baseline and 14.2% capable of more than 100% of their baseline (Figure 4.13, **d**).

Examination of raw traces, revealing changes in $[Ca^{2+}]_i$ in individual cells provided further evidence of differences between responses to acetylcholine in proliferative and differentiated cultures (Figure 4.15). Exposing proliferative cultures to acetylcholine provoked characteristically sustained responses that appeared unchanged in response to the addition of buffer (Figure 4.15, **a**). Responding cells quickly achieved a maximal $[Ca^{2+}]_i$ before slowly beginning to decrease. However, the rate at which $[Ca^{2+}]_i$ fell appeared unchanged when acetylcholine was removed and cells were exposed only to buffer. Interestingly, it was only upon addition of 50 mM KCl that fluorescence levels quickly returned to those observed at baseline. It should be noted that the scale on the graph representing traces in proliferative cultures exposed to acetylcholine (Figure 4.15, **a**) is 33% longer than the scale used in the graph representing differentiated cultures (Figure 4.15, **b**). The reason for this is that cells within proliferative cultures took considerably longer to return towards levels of baseline fluorescence than their differentiated counterparts. This effect of KCl in proliferative CTX0E16/02 cultures following exposure to acetylcholine was also observed when performing equivalent experiments using the FS3 (data not shown); suggesting that at least some of the cytosolic $Ca^{2+}$ accumulation that occurs in response to acetylcholine in proliferative cultures results from an influx from the extracellular space. The reason for this is that if $Ca^{2+}$ conductive, VDIC channels were present then the addition of 50 mM KCl would be expected to increase the $[Ca^{2+}]_i$, though the opposite is seen to occur. In contrast, if all of the intracellular $Ca^{2+}$ accumulation occurred as a result of release from intracellular stores then this would not be expected to be affected by a high $K^+$ challenge in cells where VDIC are absent. However, if the rise in $[Ca^{2+}]_i$ was partly due to the influx of $Ca^{2+}$ through non-selective cation channels such as nAChR, or the previously mentioned TRPC channels, then exposure of these cells to 50 mM KCl would shift the membrane potential towards 0 mV and consequently remove the electrical driving force supporting $Ca^{2+}$ entry into these cells. The reason for the rapid fall in $[Ca^{2+}]_i$ following exposure to KCl may therefore be explained by a reduced strain upon the cells' normal capacity to remove $Ca^{2+}$ from the cytoplasm, as mediated through the activity of $Na^+/Ca^{2+}$ exchangers and $Ca^{2+}$-ATPases in the plasma membrane and $Ca^{2+}$-ATPases and $Ca^{2+}$-uniporters in the ER [355]. Further investigation would be needed to identify the exact mechanism through which this effect occurs.

Simultaneous exposure of proliferative cells to 1 mM acetylcholine and 50 mM KCl, reduced the maximal response achieved when acetylcholine was added alone earlier in the experiment (Figure 4.15, **a**). However, as discussed previously, this may simply be a consequence of desensitisation within the system. Interestingly though, washing cultures in buffer after exposure to acetylcholine and KCl caused an increase in $[Ca^{2+}]_i$, before levels begin to fall again towards those observed at baseline. It is not clear what is responsible for this rise, though considering the sustained effect of acetylcholine on $[Ca^{2+}]_i$ at the beginning of the experiment, it is tempting to think that the removal of KCl – and acetylcholine – towards the end of the experiment, allows acetylcholine's residual effect to be observed. This is

probably due to the re-establishment of the electrochemical gradient that allows $Ca^{2+}$ to passively enter the cell.

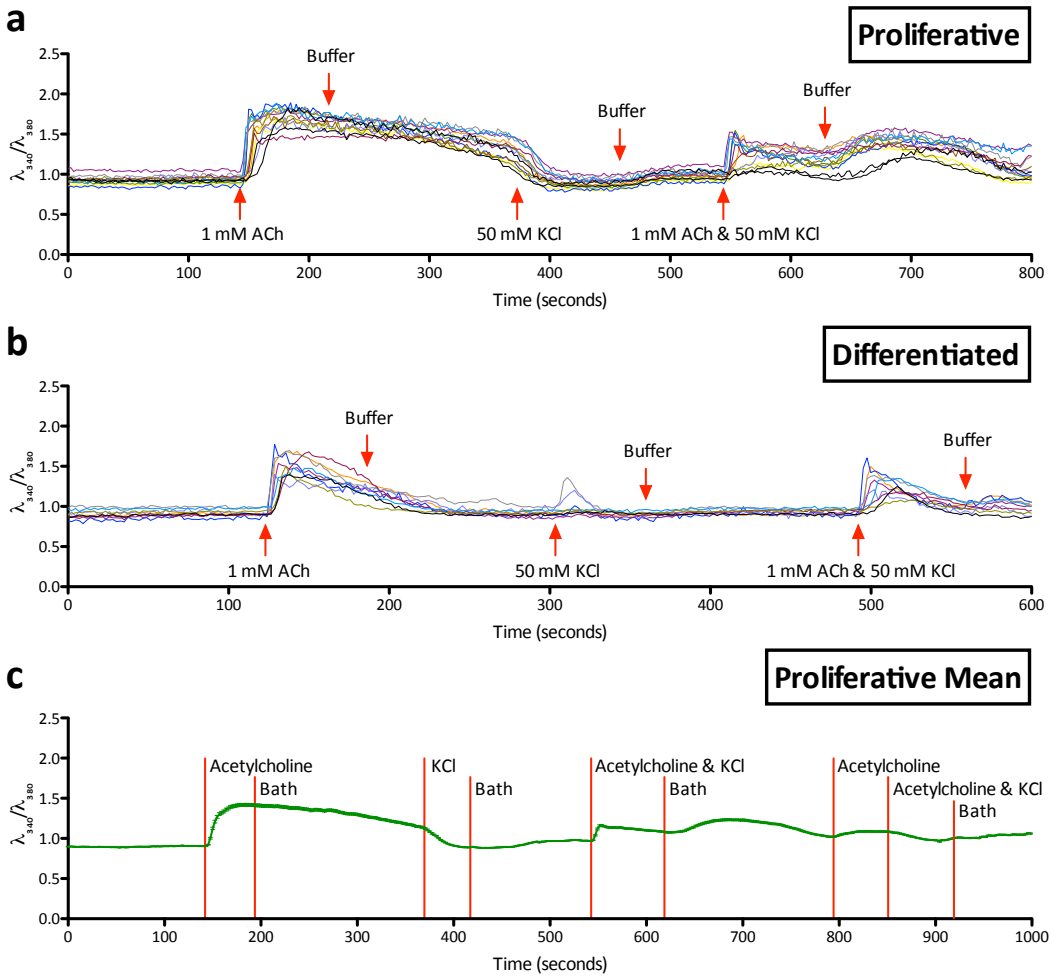


***Figure 4.15 Nature of acetylcholine-induced responses in individual cells of proliferative and differentiated CTX0E16/02 cultures vary considerably***

Proliferative and differentiated CTX0E16/02 cultures were prepared and imaged for single cell $Ca^{2+}$-imaging as described in ***2.4.3***, above. Raw 340 nm/380 nm ($\lambda_{340}/\lambda_{380}$) fluorescence ratio traces are shown for several cells sequentially exposed to 1 mM acetylcholine (ACh), 50 mM KCl and 1 mM acetylcholine with 50 mM KCl and interceded with buffer washes in proliferative (**a**) and differentiated (**b**) CTX0E16/02 cultures. Panel **c** shows the mean ± S.E.M. of raw traces for all counted cells from a single experiment. Timing of all additions are indicated using red arrows or red lines. Traces for panels **a** and **b** were taken from two independent experiments.

The sustained $[Ca^{2+}]_i$ increase observed in response to acetylcholine in proliferative CTX0E16/02 cultures was not present in differentiated cells. Upon exposure to 1 mM acetylcholine, differentiated CTX0E16/02 cultures saw a sharp rise in $[Ca^{2+}]_i$, before rapidly dropping towards levels observed at baseline. The rate of this decrease seemed unaffected by the subsequent buffer wash. Surprisingly, some cells responded to the addition of 50 mM KCl alone, though this was not unique to cells previously exposed to acetylcholine, as is discussed later. Simultaneous exposure of differentiated cultures to acetylcholine and KCl produced responses that were lower than that observed when acetylcholine was added alone though this is thought to be partly attributable to desensitisation. This desensitising effect

can be clearly seen in Figure 4.15 **c**, which represents a mean of the raw traces from all 300 counted cells from a single experiment where proliferative cultures were exposed to acetylcholine. Following successive additions of acetylcholine, KCl and acetylcholine with KCl – each interceded with buffer washes – the cultures were again exposed to acetylcholine at approximately 790 seconds. The subsequent response is substantially lower than that seen when acetylcholine was initially added after 140 seconds, and suggests that some sort of desensitisation has occurring within the system. The nature of this desensitisation is unclear however, but may be partly due to activity-dependent changes such as receptor phosphorylation. Cellular leakage over the course of the experiment of the Fura-2 AM dye, responsible for the visualisation of intracellular $Ca^{2+}$, is also likely to contribute to this observed effect.

Despite the presence of desensitisation within the experimental system, it is clear that KCl exerts its own effect when exposed to cells in conjunction with acetylcholine. This effect was most obviously observed in proliferative cultures; where the removal of acetylcholine and KCl with a buffer wash caused a rise in $[Ca^{2+}]_i$ (Figure 4.15, **a**). While small, this effect was also observed in some cells within differentiated cultures (Figure 4.15, **b**).

Exposure of proliferative CTX0E16/02 cultures to glutamate was incapable of provoking a measurable rise in $[Ca^{2+}]_i$ at any tested concentrations (1 µM – 1 mM), though a small concentration-dependent response was observed in differentiated cultures when measured using the FS3 (Figure 4.8, **c**). This was reflected in data obtained from analysis of intracellular $Ca^{2+}$ accumulation in individual cells, though the improved sensitivity of this platform additionally facilitated the detection of a minority of responsive cells in proliferative cultures. The mean maximal response observed across all counted cells in proliferative CTX0E16/02 cultures was 5.9% ± 0.5% (Figure 4.13, **a**). Just 4.5% of all counted cells (*n* = 2, 300 cells per experiment) were capable of producing a response of more than 20% above its own baseline. Only 1.7% were capable of a response of more than 50% above baseline, while 0.2% produced a response of more than 100% above baseline (Figure 4.13, **b**). These values are surprisingly low when we consider that the expression of both AMPA and NMDA channel subunits were detected at the message level in proliferative CTX0E16/02 cultures, along with all mGluRs except $mGluR_3$ (see Table 3.10, above). Both AMPA and NMDA channels are capable of $Ca^{2+}$ permeability, and $mGluR_1$, $mGluR_2$ and $mGluR_5$ are all $G\alpha_q$-linked GPCRs; and should therefore be capable of releasing $Ca^{2+}$ from intracellular stores [357]. This suggests these receptors are either not translated, or do not reach the cell surface. Upon differentiation of CTX0E16/02 cultures; expression was detected for all tested glutamate receptors or receptor subunits at the message level – including $mGluR_3$. In addition, with respect to that seen in proliferative cultures, the level of expression for each of these transcripts was either maintained or intensified (Table 3.10). This increased receptor expression would account for the appearance of detectable increases in $[Ca^{2+}]_i$ in differentiated CTX0E16/02 cultures when measured using the FS3 (see Figure 4.8, **c**). This effect was also observed when measuring levels of glutamate-induced fluorescence in individual cells, with the detection of a mean maximal response across all tested cells of 22.6% ± 1.6% above baseline (Figure 4.13, **c**). With respect to all counted cells (*n* = 2, 300 cells per experiment); 32.3% were capable of responses of more than 20% above their baseline level of fluorescence. In addition,

15.7% were capable of responses of more than 50% above baseline and 2.5% produced a response of more than 100% above baseline (Figure 4.13, **d**). These values represent a considerable increase compared to equivalent data obtained from proliferative cultures exposed to 1 mM glutamate.

While few cells within proliferative CTX0E16/02 cultures were capable of responding to 1 mM glutamate, those that did tended to show relatively heterogeneous responses. This is illustrated in Figure 4.16 **a**, which shows 340 nm/380 nm fluorescence ratio traces for selected individual cells within proliferative cultures. Responses to glutamate in proliferative cultures were characteristically rapid, with respect both to the rate at which a maximal response was achieved, and how quickly fluorescence levels returned to those observed at baseline. In contrast, responses to 1 mM glutamate in differentiated cultures were much more heterogeneous in nature (Figure 4.16, **b**). Some cells retained the rapid $Ca^{2+}$ mobilisation kinetics observed in proliferative cells, while others demonstrated a much slower and sustained level of intracellular $Ca^{2+}$ accumulation. Interestingly, in contrast to what was observed in cells exposed to dopamine, 5-HT and acetylcholine, the presence of 50 mM KCl exerted little effect upon glutamate-induced responses in many cells in both proliferative and differentiated cultures (Figure 4.16). This suggests that the reason for reduced intracellular $Ca^{2+}$ accumulation observed in cells exposed to dopamine, 5-HT and acetylcholine is less likely to be attributable to the leakage of Fura-2 AM dye from the cells over the course of the experiment. This therefore implicates either desensitisation within the system or a direct effect of KCl as discussed above. However, the possibility remains that the mechanism through which glutamate provokes an increase in $[Ca^{2+}]_i$ is less likely to allow Fura-2 AM to leave the cell as compared to that seen for other tested neurotransmitter agonists. Another interesting feature of glutamate's influence upon $[Ca^{2+}]_i$ was the presence of cells capable of producing apparently spontaneous $Ca^{2+}$ transients in differentiated cultures, as was discussed previously for differentiated cells exposed to dopamine. Figure 4.16 **b**, shows two cells that demonstrated this property (light blue and orange traces), though it is unclear what causes this effect or what type of cells these are. Finally, the traces shown in Figure 4.16 clearly illustrate the presence of cells in both proliferative and differentiated cultures that are capable of responding to 50 mM KCl. This was a particularly surprising finding; as data obtained using the FS3 had suggested the absence of electrically excitable cells, even after a 28 day differentiation (data not shown). The presence of cells capable of intracellular $Ca^{2+}$ accumulation in response to a 50 mM $K^+$ challenge was not unique however to cultures exposed to glutamate. In order to assess the prevalence of electrically excitable cells in proliferative and differentiated CTX0E16/02 cultures, all individual cellular traces from each experiment were analysed using a similar method to that used to characterise ligand-induced responses, as is graphically represented in Figure 4.13, above. However, rather than using the original level of baseline fluorescence recorded at the beginning of the experiment, an average 340 nm/380 nm baseline fluorescence was instead derived from the mean of the 30 seconds preceding the addition of KCl in each experiment. This was done for two reasons; the first was to ensure that responses to KCl were not misreported due to the level of fluorescence not returning to baseline following exposure to neurotransmitter ligand – as was the case for acetylcholine in proliferative cultures (Figure 4.15, **a**). The second reason was to account for cells that demonstrated spontaneous $Ca^{2+}$ transients, as these may not have shown baseline

fluorescence levels at the point when KCl was added. KCl-induced responses were also analysed as groups, according to the neurotransmitter agonist they were previously exposed to. This was done to identify whether prior exposure to each of the tested ligands may influence the excitability of cells within each culture.

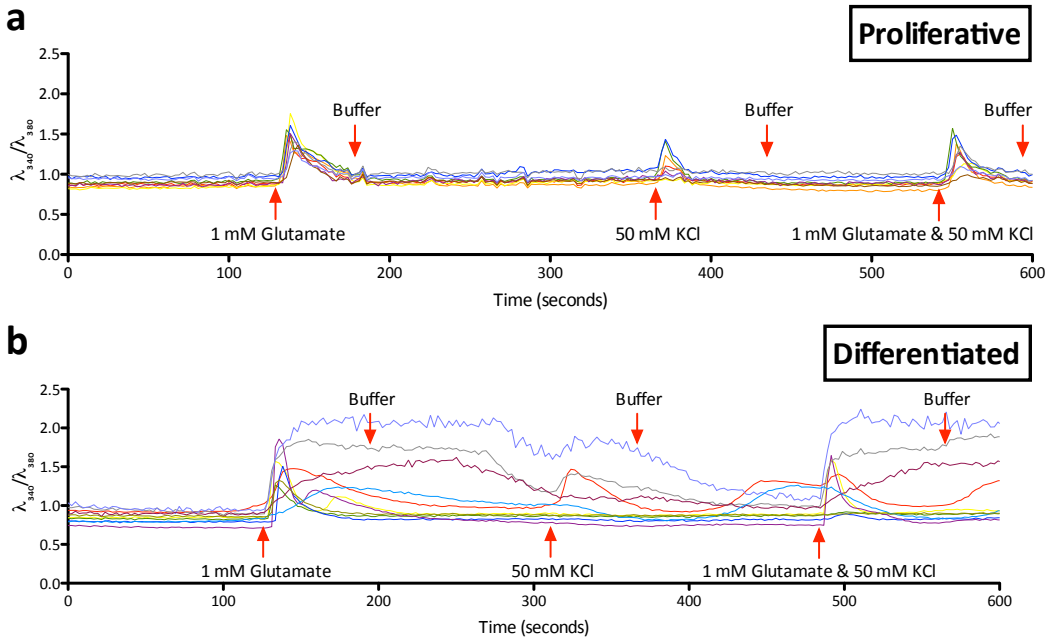


***Figure 4.16 Glutamate–induced responses show greater heterogeneity in differentiated CTX0E16/02 cultures***
Proliferative and differentiated CTX0E16/02 cultures were prepared and imaged for single cell $Ca^{2+}$-imaging as described in ***2.4.3***, above. Raw 340 nm/380 nm ($\lambda_{340}/\lambda_{380}$) fluorescence ratio traces are shown for several cells sequentially exposed to 1 mM glutamate, 50 mM KCl and 1 mM glutamate with 50 mM KCl and interceded with buffer washes in proliferative (**a**) and differentiated (**b**) CTX0E16/02 cultures. Timing of additions are indicated using red arrows. Traces for both panels were taken from two independent experiments.

The mean maximal response to 50 mM KCl across all counted cells in proliferative CTX0E16/02 cultures, with respect to baseline fluorescence was relatively consistent between cells previously exposed to dopamine, 5-HT and glutamate, with respective values of 5.1% ± 0.4%, 3.7% ± 0.4% and 4.6% ± 0.3%. In contrast, proliferative cells previously exposed to acetylcholine saw a fall in fluorescence of -6.3% ± 0.3% (Figure 4.17, **a**). This is attributable to the fact that fluorescence levels in proliferative cells exposed to acetylcholine did not return to baseline prior to exposure to KCl. Indeed – as discussed previously – the presence of KCl caused the $[Ca^{2+}]_i$ to quickly return to baseline in these cells (Figure 4.15, **a**). The extent to which individual cells within proliferative cultures responded to KCl was also relatively consistent. No cells were capable of a response of more than 100% above baseline, while 0.3%, 0.3% and 0.2% of cells were capable of responses of more than 50% above baseline to KCl following exposure to dopamine, 5-HT or glutamate, respectively. The greatest variation, though this was still small, was seen in the number of cells capable of producing a response greater than 20% above baseline. These values were 4.5%, 2.5% and 2.5%, for cells previously exposed to dopamine, 5-HT or glutamate, respectively (Figure 4.17, **b**).

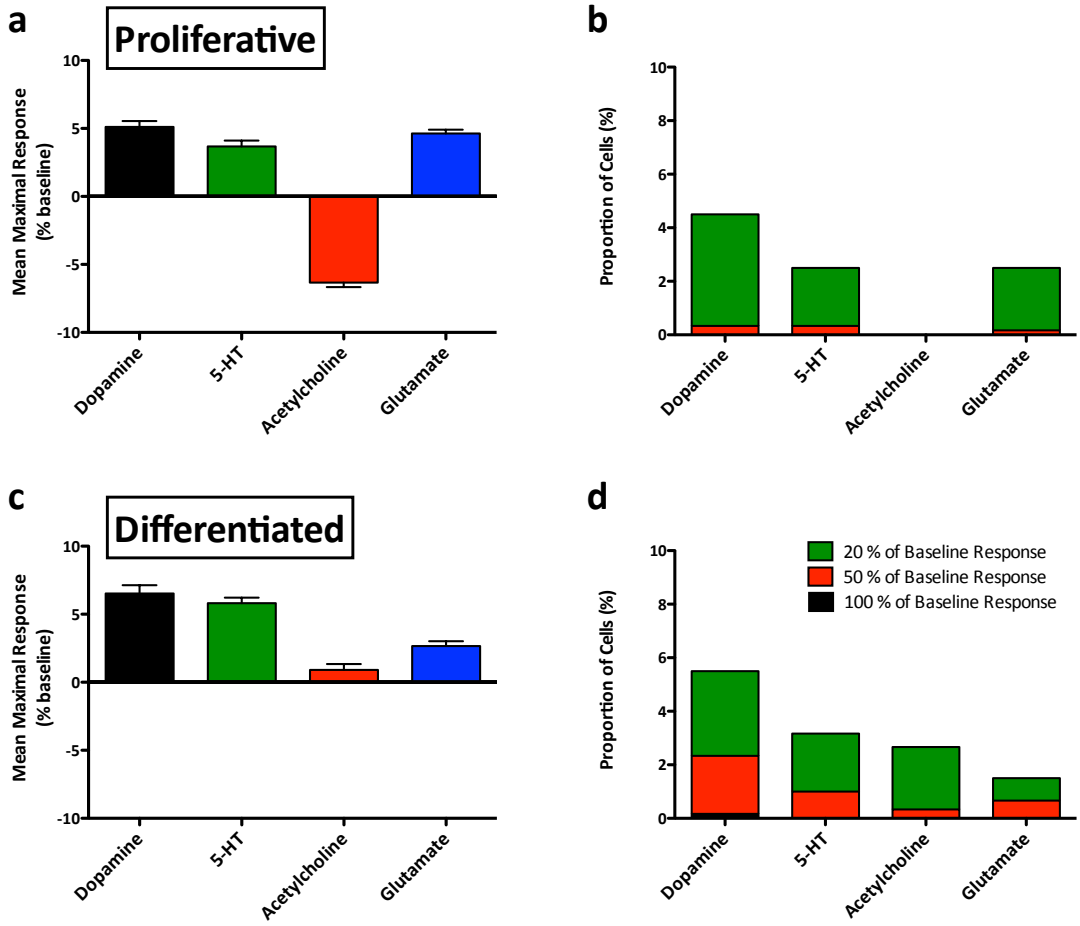


***Figure 4.17 Small minority of proliferative and differentiated CTX0E16/02 cells capable of KCl-induced depolarisation***

Proliferative and differentiated CTX0E16/02 cultures were prepared and imaged for single cell $Ca^{2+}$-imaging as described in ***2.4.3***, above. Data are presented with respect to the mean ± S.E.M. of the maximal response achieved relative to baseline, from all measured cells, from all cultures exposed to KCl after each of the four tested neurotransmitter agonists; dopamine, 5-HT, acetylcholine and glutamate in proliferative (**a**) and differentiated (**c**) cultures. Data are also presented that show the proportion of cells within these cultures that demonstrated an increase in fluorescence of > 20%, > 50% or > 100% relative to baseline in response to KCl in proliferative (**b**) and differentiated (**d**) cultures. All values are quoted with respect to a 340 nm/380 nm fluorescence ratio following excitation at 520 nm. Values obtained from the measurement of fluorescence from 300 cells per experiment ($n$ = 2).

Variation was also observed in how cells within differentiated CTX0E16/02 cultures responded to a 50 mM $K^+$ challenge following exposure to each of the four tested neurotransmitter agonists. The mean maximal responses to KCl across all counted cells in differentiated cultures, with respect to baseline fluorescence were 6.5% ± 0.6%, 5.8% ± 0.4%, 0.9% ± 0.4% and 2.7% ± 0.4% when previously exposed to either dopamine, 5-HT, acetylcholine or glutamate, respectively (Figure 4.17, **c**). Upon closer inspection it was found that while no tested cells that were previously exposed to 5-HT, acetylcholine or glutamate were capable of producing responses of more than 100% above baseline in response to KCl, just 0.2% of cells previously exposed to dopamine were (Figure 4.17, **d**). Differentiated cells previously exposed to all tested ligands were however capable of producing smaller KCl-induced responses. Cells previously exposed to dopamine presented the greatest number of cells capable of responses of more than 50% above baseline following exposure to KCl with 2.3%, this value was 1% after 5-HT, 0.3% after

acetylcholine and 0.7% after glutamate. For cells capable of a response of more than 20% above baseline in response to 50 mM KCl, these values rose to 5.5%, 3.2%, 2.7% and 1.5% for dopamine, 5-HT, acetylcholine and glutamate, respectively (Figure 4.17, **d**).

In summary, these data clearly demonstrate the improved sensitivity of using low throughput, single cell $Ca^{2+}$ imaging as compared to that provided using a FS3. However, in order to measure concentration dependent changes in response to a variety of different ligands, it is difficult not to make the compromise in favour of higher throughput and lower sensitivity, especially when it is considered that many of the tested ligands exhibited desensitisation within the assay platform, as discussed above. Therefore, in order to accurately generate concentration-dependent data, a different coverslip of cells would likely have to be used to test each ligand at each concentration. These would also have to be repeated subsequently to provide mean values across multiple biological replicates, and as such is experimentally impractical. Measuring ligand- and KCl-induced intracellular $Ca^{2+}$ accumulation responses at the level of individual cells has however provided a wealth of qualitative information regarding the nature of cells within proliferative and differentiated CTX0E16/02 cultures. Interestingly, these data have shown that a small minority of cells within both proliferative and differentiated cultures are capable of producing an increase in $[Ca^{2+}]_i$ in response to 50 mM KCl, suggesting the presence of electrically excitable cells. Surprisingly, the number of cells that demonstrated this electrical excitability were roughly similar in the two different types of culture.

The purpose of investigating ligand-induced changes in $[Ca^{2+}]_i$ in individual cells, was to address the observation that despite an increase in the expression of many receptors relevant to the transduction of signals provoked by the tested ligands at the message level, this was met with a reduction in the level of ligand-induced $Ca^{2+}$ accumulation. These data support the hypothesis proposed above that cells in differentiated cultures demonstrate more functional heterogeneity with respect to changes in $[Ca^{2+}]_i$, provoked by a range of agonists than cells in proliferative cultures. This heterogeneity was seen both in the number of cells that responded, and also in the kinetics of the responses observed between different cells. However, it was not the case that cells within differentiated cultures were capable of higher levels of intracellular $Ca^{2+}$ accumulation in response to the same ligand when compared to proliferative cells. Indeed, the opposite was in fact true; that cells in proliferative cultures exhibited larger rises in $[Ca^{2+}]_i$ in response to the same concentration of ligand.

Taken together, these data suggest several reasons for the observed decrease in 340 nm/380 nm fluorescence ratio levels detected in differentiated as compared to proliferative cultures in response to dopamine, 5-HT and acetylcholine, but not glutamate. The first is that a smaller proportion of cells within differentiated cultures are capable of responding to the same concentration of these three agonists. The second is that cells that do respond in differentiated cultures exhibit less pronounced increases in $[Ca^{2+}]_i$. Finally, another factor which is likely to contribute to the lower levels of fluorescence detected, at least when using the FS3, is that the size of cell soma are considerably smaller in differentiated cultures as compared to those found in proliferative cultures – as is clear from (***Figure 4.10***, panels **a** and **b**). It was also considered that another reason for the observed reduction in ligand-

induced fluorescence may be attributable to the presence of fewer cells in differentiated cultures due to the presence of considerable quantities of cellular debris in these cultures. However, when performing data analysis for single cell $Ca^{2+}$ imaging experiments, it was found that a similar number of cells were found within each visualised field, irrespective of the culture conditions used (data not shown).

These data do not therefore resolve the issue relating to the observed decrease in ligand-induced intracellular $Ca^{2+}$ accumulation in differentiated cultures, despite an increase in the expression of nearly all tested receptors at the message level. Indeed, considerably higher levels of intracellular $Ca^{2+}$ accumulation were observed in cells of proliferative compared to differentiated cultures in response to 1 mM 5-HT (see Figure 4.13, above), yet expression of the $G\alpha_q$-coupled, $5\text{-}HT_{2A}$ receptor – known to elevate $[Ca^{2+}]_i$ – was absent in proliferative cultures and robustly expressed at the message level in differentiated cultures (see Table 3.9, above). It is clear that the expression of all receptors capable of transducing the effects of, for example, dopamine, 5-HT and acetylcholine – which each saw a reduction in their capacity to provoke changes in $[Ca^{2+}]_i$ in differentiated cultures – have not been investigated. It is therefore conceivable that the expression of these other receptors may have decreased, and therefore account for the reduced responsiveness of cells within differentiated cultures. However, this would be against the overwhelming trend of an increase in the expression of neurotransmitter receptors at the message level following differentiation of the CTX0E16/02 cultures (see Table 3.9 and Table 3.10, above). While it may be expected that increased levels of mRNA expression would result in increased levels of corresponding protein, this does not necessarily mean functional protein. For example, as was discussed previously, many GPCRs when expressed in heterologous expression systems do not present as functional receptors at the cell surface. In many cases, these receptors are translated but remain trapped within the membranes of components of the secretory pathway, such as the ER and Golgi – as in the case of the $\beta_2$-adrenergic receptor [37]. Until relatively recently, *de novo* synthesis of GPCRs was assumed to result in ubiquitous presentation at the cell surface as a default mechanism. Unsurprisingly however, recent work in this area has shown that like almost every aspect of these receptors' function, their initial plasma membrane expression following translation is a strictly regulated process [375,376].

The data presented above suggest that this phenomenon is not restricted to GPCRs. For example, a considerable increase was observed in the expression of the gene encoding for the L-type voltage-dependent $Ca^{2+}$ channel subunit $\alpha_{1C}$ (CACNA1C) following differentiation of CTX0E16/02 cultures (see Table 3.9), yet this was not accompanied by a rise in electrical excitability (Figure 4.17). Previous reports have shown that – as is the case for GPCRs – plasma membrane expression of functional L-type voltage-dependent $Ca^{2+}$ channels is a tightly regulated process both in heterologous expression systems and neurons [377-379]. In an attempt to address the issue of apparently low levels of functional receptor and ion channel expression at the plasma membrane of differentiated CTX0E16/02 cells, the following sections describes several different strategies that were tested to improve both electrical excitability and ligand sensitivity in these cultures.

### *4.2.5 Promoting Electrical Excitability – Neurosphere Expansion*

A brief search of the available literature provides descriptions of a wide range of techniques that have been used to promote electrical excitability following differentiation of NPCs, from simply extending the period of differentiation and the use of various growth factors, to exposure to low frequency magnetic fields. For the purposes of this study, but also bearing in mind that differentiated CTX0E16/02 cells may represent a very useful screening tool, it was considered important to identify a method to promote electrical excitability in the differentiated CTX0E16/02 cultures that would not adversely affect cell survival, would ideally be scalable to suit HTS methodologies and produce electrical excitability as quickly as possible. With respect to this final point, it was felt that rapid development of electrical excitability was an important consideration as this would mean that experiments could be conducted in a shorter period of time, consequently leading to greater throughput and reduced costs.

Using similar conditionally-immortalised NPCs, Donato and colleagues have previously demonstrated the successful precipitation of electrical excitability in differentiated cells by first expanding the undifferentiated NPCs as neurospheres – referred to by the authors as 'pre-aggregation differentiation' [104]. Neurospheres are free-floating clusters of NPCs that form under *in vitro* culture conditions when grown on a non-adherent substrate in the presence of mitogens (EGF and $FGF_2$)[380]. These experiments were performed using the ventral mesencephalon derived NPC line (VM or ReNcell VM) described in ***3.2.4*** above, plus a cortex derived cell line (ReNcell CX)[66,104]. Cells were expanded as neurospheres on uncoated tissue culture plastic for one week prior to plating onto laminin-coated dishes as undisrupted neurospheres. Cells were propagated for a further 3-4 days as proliferative cultures, allowing the cells time to migrate away from the neursphere to form a confluent monolayer, prior to differentiation for 1 week by the removal of growth factors. However, this protocol only proved successful in promoting electrical excitability in the ReNcell VM line [104]. The differentiation protocol developed for the two cortically derived NPC lines described above was shown to be considerably more effective in promoting the appearance of neurons and astrocytes than simply removing growth factors and 4-OHT, as used by Donato and colleagues. As it is neurons that exhibit electrical excitability, it would therefore be expected that culture conditions that generate more cells exhibiting a neuronal phenotype would also generate more cells exhibiting electrical excitability. Indeed, Donato and colleagues show that the cultures exposed to 'pre-aggregation differentiation', that go on to reveal electrical excitability, produced considerably more cells exhibiting a neuronal phenotype – as indicated by the degree of immunoreactivity for the neuronal marker, βIII-tubulin [104]. If, as this study suggests, the environment within neurospheres promotes the appearance of a more functional neuronal phenotype, then the reason why the cortically derived cell line (ReNcell CX) was more resistant to the development of electrical excitability may have been that the single week for which they were propagated as neurospheres was insufficient. Numerous reports in the literature suggest that not only is considerably more time needed to differentiate human NPCs into functional neurons as compared to those derived from animals, but this also appears to be true of NPCs derived from more phylogenetically recent structures within the human brain [57,58,61,324,327,328,337]. Therefore, in an attempt to increase the number of electrically excitable cells in differentiated CTX0E16/02 cultures, the 'pre-aggregation differentiation'

protocol described by Donato et al., was integrated with the optimised culture conditions for the differentiation of CTX0E16/02 cells described above (28 day exposure to SNBM). However, rather than growing the CTX0E16/02 cells as neurospheres for just a single week prior to differentiation, this was extended to see whether 2 weeks or 6 weeks may yield a greater number of electrically excitable cells.

Previous experiments have shown that single cell $Ca^{2+}$ imaging is considerably more sensitive for the detection of intracellular $Ca^{2+}$ accumulation than that provided by the FS3. However, robust electrical excitability, as exhibited by functionally mature neurons, should be detectable using the FS3 (Personal communication: Professor Stuart Bevan, Wolfson Centre for Age Related Diseases, King's College London), and additionally provides a much more rapid means to perform these experiments. In addition, data presented above suggested that prior exposure to either dopamine, 5-HT, acetylcholine or glutamate may affect the extent to which cells within differentiated cultures are capable of responding to a 50 mM $K^+$ challenge (see Figure 4.17, **c** and **d**). Therefore, measurement of intracellular $Ca^{2+}$ accumulation in CTX0E16/02 cultures, differentiated in 96-well plates for the FS3, additionally provided the capacity to test for the effect of prior exposure to these four neurotransmitter agonists on KCl-induced changes in $[Ca^{2+}]_i$ in a single experiment. Furthermore, this approach also provided the opportunity to test whether 'pre-aggregation' exerted any influence upon dopamine-, 5-HT-, acetylcholine- or glutamate-induced changes in $[Ca^{2+}]_i$ – this possibility was tested in both proliferative and differentiated cultures.

CTX0E16/02 cells were expanded as neurospheres for either 14 or 42 days prior to plating onto laminin-coated 96-well plates. Neurospheres were then maintained under proliferative conditions to allow them to form a confluent monolayer, as described by Donato and colleagues [104]. Cultures were then either immediately analysed for their ability to respond to a range of different neurotransmitter receptor agonists or differentiated for 28 days in SNBM (see 2.1.3). Proliferative and differentiated cultures were assayed as described in ***2.4.1*** above, whereby individual wells of cells were first exposed to assay buffer or concentrations of dopamine, 5-HT, glutamate or acetylcholine between 1 µM and 1 mM at half log unit intervals in triplicate. Cultures were then exposed to KCl, to a final concentration of 50 mM, to determine whether electrically excitable cells were present, prior to the addition of ionomycin to precipitate maximal intracellular $Ca^{2+}$ accumulation. All values from each well were expressed relative to the ionomycin-induced $[Ca^{2+}]_i$ for that well.

Expansion of cells as neurospheres for either 14 or 42 days prior to differentiation did not promote measurable electrical excitability in these cultures, irrespective of whether they were previously exposed to dopamine, 5-HT, glutamate or acetylcholine. This was determined by whether they were capable of exhibiting an increase in $[Ca^{2+}]_i$ in response to a 50 mM KCl challenge (data not shown). Interestingly however, expansion of CTX0E16/02 cells as neurospheres did alter the way the resulting cultures responded to the various agonists tested. With respect to proliferative cells, pre-expansion as neurospheres sensitised the cultures to dopamine in a time dependent manner (Figure 4.18, **a**). While normal proliferative cultures did not respond to dopamine by elevating $[Ca^{2+}]_i$, cultures that were pre-expanded as neurospheres developed a concentration-dependent response which was more pronounced

after an extended period of pre-expansion as neurospheres. A 14-day pre-expansion as neurospheres produced an $EC_{50}$ of 153 µM and a maximal response of 5.9% of that produced by ionomycin. Following 42 days of expansion as neurospheres, the potency remained relatively similar with an $EC_{50}$ of 107 µM while the maximal response increased to 10.7% of ionomycin's. It is difficult to ascribe these responses to any particular receptor due to the numerous ways in which dopamine has been shown to cause increases in $[Ca^{2+}]_i$, both with respect to the receptor and the downstream mechanism [191]. A small change was also observed when proliferative cultures were exposed to 5-HT (Figure 4.18, **b**), with an $EC_{50}$ of 227 µM after a 42 day expansion as neurospheres, while a measurable response was only observed at the highest tested 5-HT concentration in cultures exposed to a 14 day expansion as neurospheres. These responses remain considerably lower than what would be expected based on the potency of 5-HT acting on its endogenous human receptors [364]. As was observed in normal proliferative CTXO16/02 cultures, cells exposed to a 14 day expansion as neurospheres were incapable of responding to glutamate by increasing $[Ca^{2+}]_i$. However, cultures did became sensitised to glutamate after 42 days of pre-aggregation, demonstrating an $EC_{50}$ of 14 µM, but with a maximal response of just 4.9% of that of induced by ionomycin (Figure 4.18, **c**). In response to acetylcholine, normal proliferative CTX0E16/02 cultures and those exposed to pre-aggregation demonstrated relatively similar maximal responses, though a considerable rightward shift in potency was observed for the two neurospheres conditions – moving from a baseline $EC_{50}$ for normal proliferative cultures of 0.6 µM to 7 µM and 11 µM for 14 day and 42 day pre-aggregation respectively (Figure 4.18, **b**). However, the leftward shift in potency exhibited by normal proliferative cultures is largely attributable to the comparatively large response evoked by 3.2 µM acetylcholine. While variable in magnitude, this characteristically large response at this lower concentration was present in all experiments, suggesting it was not an artefact. It should be noted that observed responses are the summed effect from all receptors activated by each tested ligand. Therefore, this large response evoked by 3.2 µM acetylcholine, may be attributable to a particular receptor whose expression is less pronounced in cultures expanded as neurospheres.

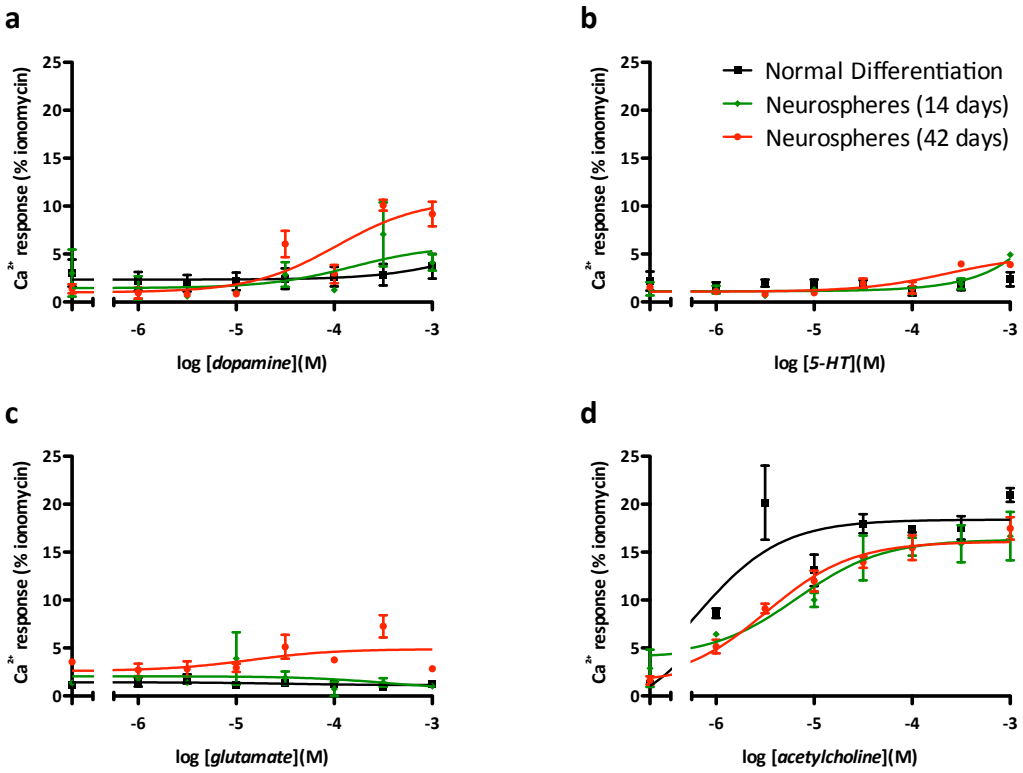


***Figure 4.18 Proliferative CTX0E16/02 cultures previously expanded as neurospheres become sensitised to dopamine and glutamate***

CTX0E16/02 cells were expanded as neurospheres for 14 or 42 days prior to plating on laminin coated plates. Once confluent, cells were incubated for 1 hour in the presence of the cell permeable, $Ca^{2+}$-sensitive fluorescent dye Fura-2 AM. Cells were then washed prior to ligand-induced fluorescence being measured using a FS3. Concentration-response curves are shown for dopamine, $EC_{50}$ = 153 µM and 107 µM (**a**), 5-HT, $EC_{50}$ = 227 µM (**b**), glutamate, $EC_{50}$ = 14 µM (**c**) and acetylcholine, $EC_{50}$ = 0.6 µM, 7 µM and 11 µM (**d**) in normal (for comparison), 14 day pre-expanded neurosphere and 42 day pre-expanded neurosphere proliferative CTX0E16/02 cells. Data points represent mean ± S.E.M. from *n* = 2, each with 3 technical replicates and expressed relative to the positive control, ionomycin.

Expansion of cultures as neurospheres prior to differentiation similarly affected cultures' responses to neurotransmitter receptor agonists. While a 14 day pre-aggregation left cells unresponsive to dopamine with respect to its ability to elevate $[Ca^{2+}]_i$ (as was seen for cultures following a normal differentiation), cultures exposed to a 42 day expansion as neurospheres responded with an $EC_{50}$ of 7 µM, but a maximal response of just 4.2% that of ionomycin. However, this maximal response achieved in response to the highest tested concentration of dopamine (1 mM) was not found to be significantly different from control (Figure 4.19, **a**). Unlike cultures exposed to a normal differentiation, 5-HT was also able to provoke an increase in $[Ca^{2+}]_i$, following a 42 day expansion as neurospheres, though not after 14 days. This response was however only apparent at the highest tested concentration of 1 mM, though was significantly different from control ($p < 0.05$)(Figure 4.19, **b**). Responses to glutamate were also affected, though when considering the elevated fluorescence ratio level recorded at baseline (the effect caused by the addition of buffer alone) for cultures expanded as neurospheres for 14 days, these values were in fact quite similar, with $EC_{50}$ values of 22 µM and 99 µM respectively for normally differentiated cells and those expanded as neurospheres for 14 days. Cultures expanded as neurospheres for 42 days prior to differentiation exhibited an $EC_{50}$ of 3.6 µM, though this leftward shift in potency is largely attributable to

the response observed at 10 µM, which inevitably skewed the non-linear regression. This large response was only seen in one of the experiments however, and may therefore be an experimental artefact (Figure 4.19, **c**). Finally, acetylcholine-induced $[Ca^{2+}]_i$ responses were also modified by expansion of cells as neurospheres prior to differentiation. While normally differentiated cultures demonstrated an $EC_{50}$ of 5 µM, those expanded as neurospheres for 14 days demonstrated a 4-fold rightward shift in this value to 21 µM. However, the maximal response achieved from cultures expanded as neurospheres for 14 days – 20.5% – was more than double that of normally differentiated cultures, at 8.6% of ionomycin-induced responses. The maximal response provoked by acetylcholine was also higher in cells expanded for 42 days as neurospheres prior to differentiation, and was accompanied by a further rightward shift in potency. This meant that the $EC_{50}$ could not be resolved from the range of acetylcholine concentrations tested (Figure 4.19, **d**).

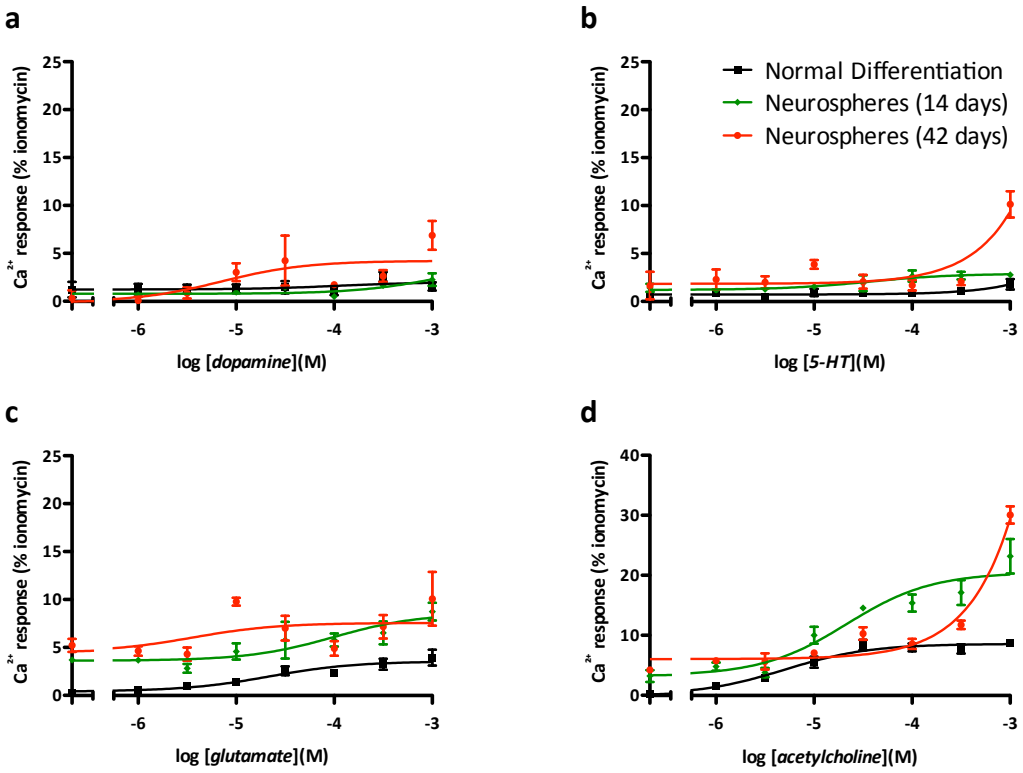


***Figure 4.19 Pre-aggregation of CTX0E16/02 cultures prior to differentiation alters their response to various ligands***
CTX0E16/02 cells were expanded as neurospheres for 14 or 42 days before being differentiated for 28 days in the presence of SNBM. On the day of the experiment, cells were incubated for 1 hour in the presence of the cell permeable, $Ca^{2+}$-sensitive fluorescent dye Fura-2 AM. Cells were then washed prior to ligand-induced fluorescence being measured using a FS3. Concentration-response curves are shown for dopamine, $EC_{50}$ = 7 µM (**a**), 5-HT, $EC_{50}$ = 36 µM (**b**), glutamate, $EC_{50}$ = 22 µM, 99 µM and 4 µM (**c**) and acetylcholine, $EC_{50}$ = 5 µM and 21 µM (**d**) in normal (for comparison), 14 day pre-expanded neurosphere and 42 day pre-expanded neurosphere differentiated CTX0E16/02 cells. Data points represent mean ± S.E.M. from *n* = 2, each with 3 technical replicates and expressed relative to the positive control, ionomycin.

While ineffective in precipitating electrical excitability, these data clearly demonstrate that by changing culture condition, the response of these cells to various neurotransmitter receptor agonists can be

manipulated. Expansion of the CTX0E16/02 cells as neurospheres conferred not only an effect in proliferative cultures tested only a couple of days after transition to adherent cultures, but effects were also observed to persist after a 28 day differentiation. Despite these being just qualitative observations, further work could conceivably yield an array of different culture conditions that could each be employed to facilitate the investigation of specific receptor systems by promoting the responsiveness of the cultures to the transmitter system of interest, as is discussed later.

### *4.2.6 Promoting Electrical Excitability – Increasing PI3K Activity*

The plasma membrane expression of many receptors and ion channels is highly regulated, allowing cells to modulate their own behaviour in response to various different signals. Recent work has demonstrated that this is also the case for voltage-dependent calcium channels ($Ca_V$), providing cells the ability to modulate their excitability. Viard and colleagues demonstrated that phosphatidylinositol 3-kinase (PI3K) plays a key role in plasma membrane expression of $Ca_V$, leading to enhanced $Ca_V$-mediated currents [378], an effect mediated by the serine/threonine kinase Akt, also known as protein kinase B. PI3K-mediated enhancement of $Ca_V$ currents has been demonstrated *in vitro* in primary rat vascular myocytes [377], cerebellar granule neurons [381], dorsal root ganglion neurons, and the African green monkey kidney fibroblast cell line – COS-7 [378]. Increasing neuronal activity of PI3K in these studies was achieved though the use of the tyrosine kinase receptor ligand, insulin-like growth factor-1 (IGF-1)[378]. However, IGF-1 has been implicated as playing a role both in the pathophysiology of schizophrenia [382] and in the mechanism of action of antipsychotics [383]. For this reason, it was felt that using IGF-1 may complicate any experimental findings when investigating the effects of different antipsychotics downstream. Direct activation of PI3K represented a more specific approach to enhance cell surface expression of $Ca_V$, and was achieved in the aforementioned studies either by heterologous expression of mutant enzymes or intracellular infusion of purified proteins known to activate PI3K due to their lack of cell permeability [377,378]. Neither of these approaches suit the needs of this study as they would modify the cells in such a way that data resulting from a transcriptomic study may become misleading.

In an attempt to provoke electrically excitability in differentiated CTX0E16/02 cultures and to avoid the complications described above, the cell-permeable, recombinant peptide 740 Y-P was employed. 740 Y-P works by activating the endogenous pool of PI3K, by directly binding the p85 regulatory subunit and consequently stimulating the catalytic activity of the p110 PI3K subunit leading to Akt phosphorylation [384]. Williams and Doherty demonstrated a 740 Y-P-mediated dose-dependent survival response in primary rat cerebellar granule neurons maintained in defined medium lacking insulin with a significant increase in survival reported at 0.05 $\mu gml^{-1}$ [385]. Therefore, to explore the possibility that the 740 Y-P peptide may be able to provoke electrical excitability in CTX0E16/02 cultures; CTX0E16/02 cells were differentiated for 28 days in 96-well plates in the presence of SNBM, and exposed to 740 Y-P at 0.05 $\mu gml^{-1}$, 0.5 $\mu gml^{-1}$, 5 $\mu gml^{-1}$ or 25 $\mu gml^{-1}$ for the final 3 or 7 days of differentiation. These periods were chosen to determine whether, 740 Y-P could be used to sustain the presence of $Ca_V$ at the cell surface, rather than just provoke a transient increase in $Ca_V$ plasma membrane presentation through its action

on PI3K. Cultures were then assayed using the FS3 to first assess their ability to respond to acetylcholine and glutamate by elevating $[Ca^{2+}]_i$ – as these ligands were previously identified as providing robust responses in differentiated cultures, and so changes would be easier to discern – before challenging the cells with 50 mM KCl.

Exposure to 740 Y-P for the final 3 or 7 days of a 28 day differentiation did not promote electrical excitability in CTX0E16/02 cultures (data not shown). The PI3K activating peptide did however alter acetylcholine and glutamate-induced $[Ca^{2+}]_i$ (Figure 4.20 and Figure 4.21, below). With respect to acetylcholine, exposure of cells to 740 Y-P for the final 3 or 7 days of differentiation had little impact on $EC_{50}$ values, however, it did exert an influence upon the maximal $[Ca^{2+}]_i$ achieved, though this was found not to be a concentration-dependent relationship with respect to 740 Y-P. The greatest observed increases in maximal response from acetylcholine were however observed when cells were exposed to the highest dose of 740 Y-P tested – 25 $\mu gml^{-1}$ – for the final 7 days of differentiation, with the best-fit value 125.9% higher than for normally differentiated cells (see Figure 4.21, **a**) after subtracting baseline values.

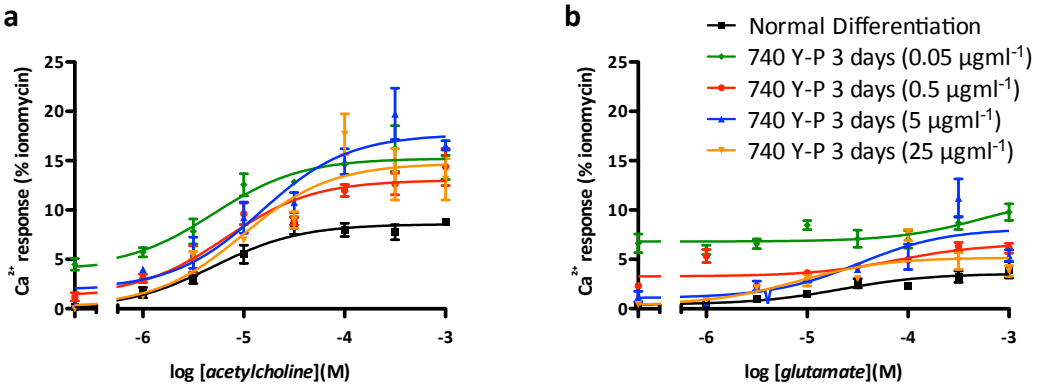


***Figure 4.20 PI3K activation for final 3 days of CTX0E16/02 differentiation increases acetylcholine and glutamate-induced $[Ca^{2+}]_i$ responses***
CTX0E16/02 cells were differentiated for 28 days using SNBM. For the final 3 days the cultures were additionally exposed to the PI3K activating peptide – 740 Y-P – at 0.05 $\mu gml^{-1}$, 0.5 $\mu gml^{-1}$, 5 $\mu gml^{-1}$ or 25 $\mu gml^{-1}$. On the day of the experiment, cells were incubated for 1 hour in the presence of the cell permeable, $Ca^{2+}$-sensitive fluorescent dye Fura-2 AM. Cells were then washed prior to ligand-induced fluorescence being measured using a FS3. Concentration-response curves are shown for acetylcholine, $EC_{50}$ = 5 µM, 5 µM, 7 µM, 15 µM and 10 µM (**a**) and glutamate, $EC_{50}$ = 22 µM, 79 µM, 33 µM and 8 µM (**b**) in normally differentiated cells (for comparison), and cells exposed to 740 Y-P at 0.05 $\mu gml^{-1}$, 0.5 $\mu gml^{-1}$, 5 $\mu gml^{-1}$ or 25 $\mu gml^{-1}$ for the final 3 days of differentiation. Data points represent mean ± S.E.M. from $n$ = 1 ($n$ = 2 for normal differentiation), with 3 technical replicates and expressed relative to the positive control, ionomycin.

A similar pattern was seen for glutamate-induced $[Ca^{2+}]_i$ responses, with 5 $\mu gml^{-1}$ 740 Y-P causing an increase of 125.0% and 123.7% in the maximal response respectively for cells exposed for 3 or 7 days, despite little change in the $EC_{50}$ value. These data should however be considered carefully as the primary objective of the experiments was to determine whether the PI3K activating peptide – 740 Y-P – was capable of conferring electrical excitability upon differentiated CTX0E16/02 cultures. Two 96-well plates of cells were seeded from independent cultures for each of the two 740 Y-P exposure time points –

therefore providing *n* = 2, each with 3 technical replicates for each of the 740 Y-P concentrations to demonstrate the presence of electrical excitability (addition of assay buffer alone, followed by KCl). However, to investigate ligand-induced responses, one of these two plates was used to examine the effects of acetylcholine, while the second was used to examine glutamate. This meant that at each of the tested concentrations of 740 Y-P, only 3 technical replicates (*n* = 1) were performed for each tested concentration of either acetylcholine or glutamate, and were therefore underpowered.

It remains unclear whether the highest tested concentration of 740 Y-P was capable of producing a maximal effect in differentiated CTX0E16/02 cultures. The concentration of this factor could therefore have been titrated to determine whether a higher concentration may have been able to provoke electrical excitability in differentiated CTX0E16/02 cells. However, due to the expense of this peptide, it was decided that the use of 740 Y-P at any higher concentration would have precluded its use when considering the cell culture system as a scalable platform. In spite of this, data presented here suggests that modulation of PI3K activity can exert an influence upon ligand-induced $[Ca^{2+}]_i$ responses, though the mechanism for this increased ligand sensitivity is unclear.

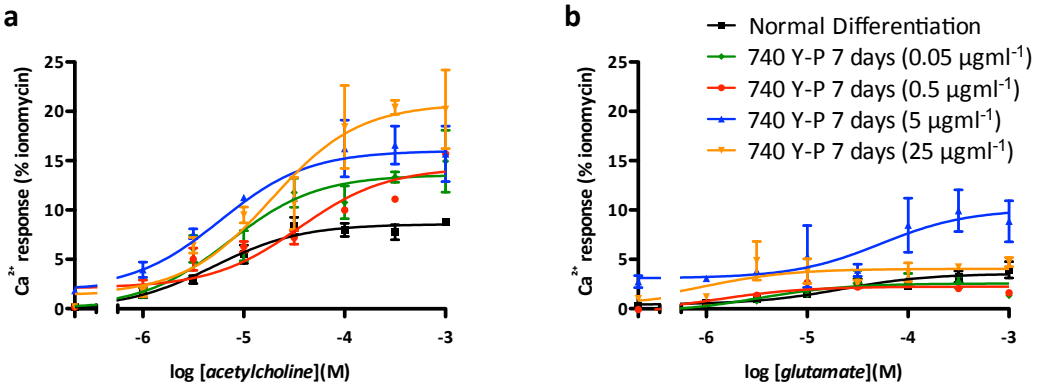


***Figure 4.21 PI3K activation for final 7 days of CTX0E16/02 differentiation increases acetylcholine and glutamate-induced $[Ca^{2+}]_i$ responses***
CTX0E16/02 cells were differentiated for 28 days using SNBM. For the final 7 days the cultures were additionally exposed to the PI3K activating peptide – 740 Y-P – at 0.05 µgml$^{-1}$, 0.5 µgml$^{-1}$, 5 µgml$^{-1}$ or 25 µgml$^{-1}$. On the day of the experiment, cells were incubated for 1 hour in the presence of the cell permeable, $Ca^{2+}$-sensitive fluorescent dye Fura-2 AM. Cells were then washed prior to ligand-induced fluorescence being measured using a FS3. Concentration-response curves are shown for acetylcholine, $EC_{50}$ = 5.01 µM, 7 µM, 36 µM, 6 µM and 19 µM (**a**) and glutamate, $EC_{50}$ = 22 µM, 3 µM, 1 µM, 54 µM and 1 µM (**b**) in normally differentiated cells (for comparison), and cells exposed to 740 Y-P at 0.05 µgml$^{-1}$, 0.5 µgml$^{-1}$, 5 µgml$^{-1}$ or 25 µgml$^{-1}$ for the final 3 days of differentiation. Data points represent mean ± S.E.M. from *n* = 1 (*n* = 2 for normal differentiation), with 3 technical replicates and expressed relative to the positive control, ionomycin.

### *4.2.7 Promoting Electrical Excitability – Influence of Neurotrophic Factors*

Another mechanism whereby cells have been shown to develop neuronal excitability in vitro is through exposure to neurotrophins – particularly nerve growth factor (NGF) and brain-derived neurotrophic factor (BDNF) – via their actions at Trk and p75 tyrosine kinase receptors. As early as 1977, Dichter and colleagues demonstrated that NGF provides the capacity to increase electrical excitability in the rat

pheochromocytoma cell line – PC12 [386], and was later shown to induce $Na^+$-channel expression [387,388] via cAMP-dependent activation of PKA [389]. In various studies, NGF and BDNF have been shown to promote $Na^+$, $Ca^{2+}$ and $K^+$ currents via changes in channel expression and density at the cell surface of several different neuronal cell types [390-395]. For this reason, a series of experiments were conducted exposing cells to NGF and BDNF to determine whether they could precipitate electrical activity in differentiated CTX0E16/02 cultures. CTX0E16/02 cells were first differentiated in 96-well plates for 28 days in SNBM supplemented with 100 $ngml^{-1}$ NGF. This concentration was used based on published work showing it can both stimulate differentiation and reduce levels of cell death [396]. Experiments were then performed using a FS3, to test whether these cultures exhibited the capacity to elevate $[Ca^{2+}]_i$ in response to a 50 mM $K^+$ challenge. The ability of dopamine, 5-HT, glutamate and acetylcholine to provoke intracellular $Ca^{2+}$ accumulation in these cultures was also tested.

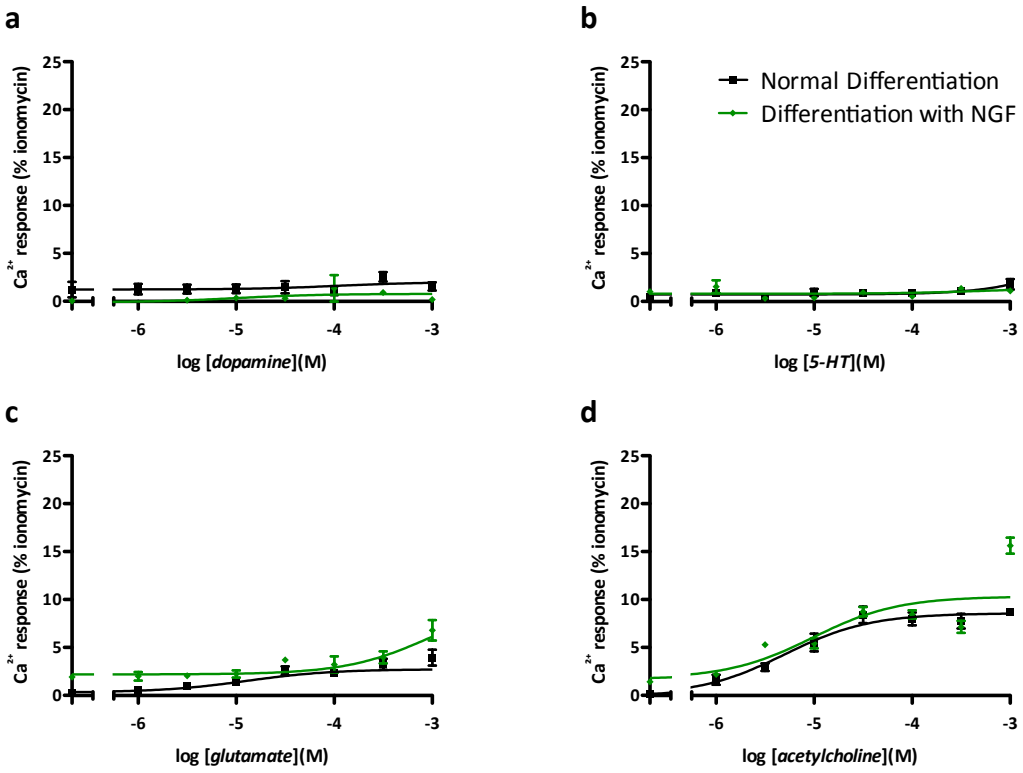


***Figure 4.22 Differentiation of CTX0E16/02 cultures with NGF alters sensitivity to glutamate and acetylcholine***
CTX0E16/02 cells were differentiated for 28 days using SNBM supplemented with 100 $ngml^{-1}$ NGF. On the day of the experiment, cells were incubated for 1 hour in the presence of the cell permeable, $Ca^{2+}$-sensitive fluorescent dye Fura-2 AM. Cells were then washed prior to ligand-induced fluorescence being measured using a FS3. Concentration-response curves are shown for dopamine (**a**), 5-HT (**b**), glutamate (**c**) and acetylcholine (**d**) in normal (for comparison) and NGF differentiated CTX0E16/02 cultures. Data points represent mean ± S.E.M. from *n* = 2, each with 3 technical replicates and expressed relative to the positive control, ionomycin.

Exposure to 100 $ngml^{-1}$ NGF over the course of a 28-day differentiation was insufficient to provoke electrical excitability in these cultures and no change was observed for dopamine or 5-HT-induced $[Ca^{2+}]_i$ responses (Figure 4.22, **a** and **b**). In contrast, while responses to glutamate and acetylcholine at concentrations between 1 µM ($10^{-6}$ M) and 316.2 µM ($10^{-3.5}$ M) were very similar, the highest concentration (1

mM) of each ligand provoked a response considerably higher than when cells were differentiated in the absence of NGF (Figure 4.22, **c** and **d**). For acetylcholine at least, this finding is consistent with previous findings [386], though this work was conducted in the PC12 cell line.

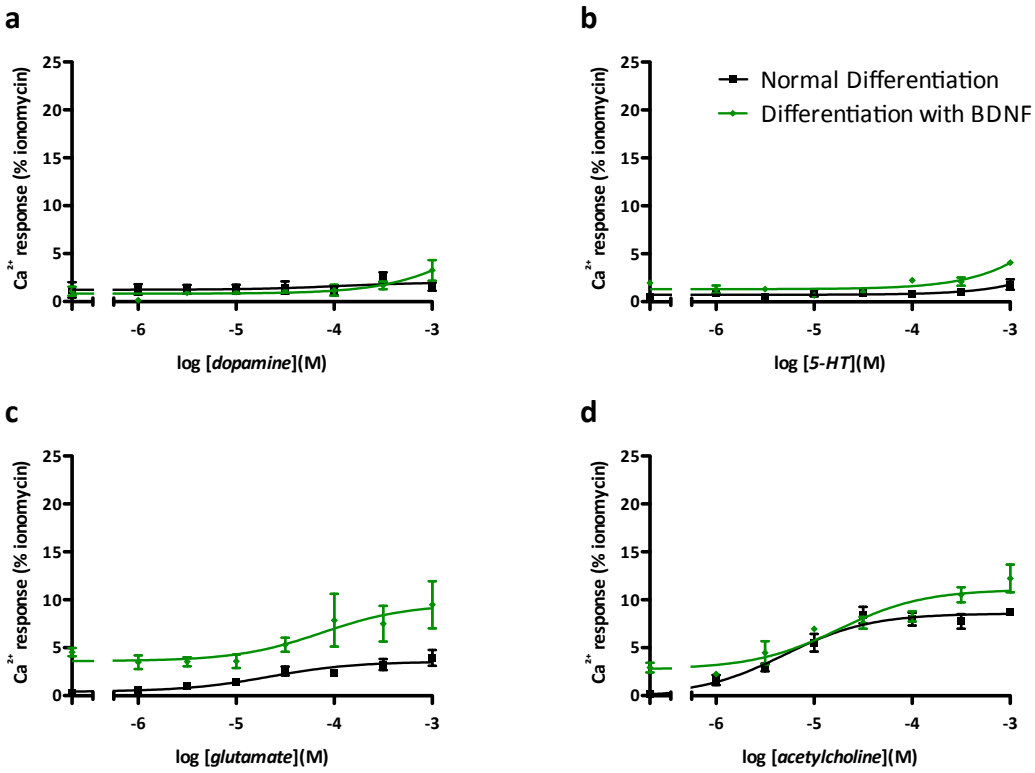


***Figure 4.23 CTX0E16/02 cultures differentiated with BDNF has little effect on ligand-induced $[Ca^{2+}]_i$***
CTX0E16/02 cells were differentiated for 28 days using SNBM supplemented with 10 ngml$^{-1}$ BDNF. On the day of the experiment, cells were incubated for 1 hour in the presence of the cell permeable, $Ca^{2+}$-sensitive fluorescent dye Fura-2 AM. Cells were then washed prior to ligand-induced fluorescence being measured using a FS3. Concentration-response curves are shown for dopamine (**a**), 5-HT (**b**), glutamate, $EC_{50}$ = 22 µM and 75 µM (**c**) and acetylcholine, $EC_{50}$ = 5 µM and 18 µM (**d**)) in normal (for comparison) and BDNF differentiated CTX0E16/02 cultures. Data points represent mean ± S.E.M. from *n* = 2, each with 3 technical replicates and expressed relative to the positive control, ionomycin.

In contrast to differentiation in the presence of 100 ngml$^{-1}$ NGF, CTX0E16/02 cultures differentiated for 28 days in the presence of SNBM supplemented with 10 ngml$^{-1}$ BDNF were capable of demonstrating electrical excitability, as determined by intracellular $Ca^{2+}$ accumulation in response to the addition of 50 mM KCl (data not shown). The concentration of BDNF used was selected based on published work showing it can enhance membrane potentials in both rodent hippocampal neurons and *Xenopus* motor neurons [397,398]. This effect was however neither consistent nor robust with only a small $Ca^{2+}$ accumulation observed in a minority of wells. In addition, this effect was only observed in cultures that were previously exposed only to assay buffer before addition of KCl. No well that was first exposed to assay buffer containing dopamine, 5-HT, glutamate or acetylcholine responded to KCl with an increase in $[Ca^{2+}]_i$. Exposure to 10 ngml$^{-1}$ BDNF during a 28 day differentiation had little effect upon ligand-induced intracellular $Ca^{2+}$ accumulation as compared to a 28 day differentiation in the absence of BDNF.

Responses to dopamine and 5-HT (Figure 4.23, **a** and **b**) remained absent while responses to glutamate and acetylcholine (Figure 4.23, **c** and **d**) were of similar magnitude once increased baseline fluorescence was accounted for, and demonstrated only slight changes in $EC_{50}$ values. In the presence of 10 $ngml^{-1}$ BDNF, the $EC_{50}$ value for glutamate shifted to 75 μM from 22 μM in its absence while for acetylcholine the $EC_{50}$ value was 18 μM in the presence of BDNF and 5 μM in its absence.

### *4.2.8 Promoting Electrical Excitability – Is It Just A Waiting Game?*

The ability of neuronal cultures derived from human embryonic or neural stem cells to develop electrical excitability has been described previously [61,334,399]. Work led by Susanna Narkilahti has demonstrated the formation of spontaneously active neural networks *in vitro* from human embryonic stem cells. These studies showed that electrical excitability developed within the first week following neural differentiation, though differed from experiments described here with respect to the type of cells used and the additional use of a human feeder cell layer [334,399]. Furthermore, these studies employed a more sensitive, electrophysiology-based approach, recording all electrical activity. Indeed, these studies only demonstrated the presence of voltage-dependent $Na^+$ channel-mediated currents, and it remains unclear whether currents mediated by voltage-dependent $Ca^{2+}$ channels were present in their culture system. Hook and colleagues demonstrated the development of electrical activity using a much more comparable experimental paradigm – non-immortalised human NPCs – though these took 4 to 5 months of differentiation before cells responded substantially to $K^+$-induced depolarisation [61].

To explore the possibility that a longer differentiation period would be sufficient to promote electrical excitability in differentiated CTX0E16/02 cultures, these cells were differentiated for 42 or 56 day using SNBM. Cultures were then tested for their ability to elevate $[Ca^{2+}]_i$ in response to dopamine, 5-HT, glutamate, GABA, histamine, acetylcholine, carbamoylcholine and phenylephrine before being challenged with 50 mM KCl. As discussed above, CTX0E16/02 cultures differentiated for 28 days were unable to respond to $K^+$-induced depolarisation by elevating $[Ca^{2+}]_i$. This was also the case at 42 days, with the exception of cultures previously exposed to high concentrations of dopamine ($10^{-3.5}$ or $10^{-3}$ M), despite the fact that these concentrations of dopamine did not themselves precipitate elevated $[Ca^{2+}]_i$ (data not shown). This represents an interesting finding when we consider data presented above regarding intracellular $Ca^{2+}$ accumulation in individual cells. Data presented above showed that in both proliferative and differentiated CTX0E16/02 cultures, prior exposure to dopamine allowed a higher proportion of cells to respond to a 50 mM $K^+$ challenge. In addition, the extent to which these cells were capable of responding was also increased as compared to those previously exposed to 5-HT, acetylcholine or glutamate (see Figure 4.17, above). After a 56 day differentiation, CTX0E16/02 cultures were able to respond to $K^+$-induced depolarisation by elevating $[Ca^{2+}]_i$, though the magnitude of these responses was limited and was eliminated if cells were pre-treated with any of the tested compounds at all concentrations, with the exception of dopamine (see Figure 4.25, **a**). Similarly to data from cells differentiated for 42 days, dopamine was able to sensitise cells to the depolarising effects of 50 mM KCl, though this effect was observed at all tested doses of dopamine after a 56 day differentiation and

responses were more pronounced at the higher concentrations, despite the fact that dopamine alone was incapable of increasing $[Ca^{2+}]_i$ (Figure 4.27, **a**). The mechanism through which dopamine exerts this effect is unclear, but recent advances in dopamine pharmacology have shown that this neurotransmitter demonstrates staggering complexity – especially when considering these effects are mediated through just five, relatively similar endogenous receptors (for detailed review see [191]).

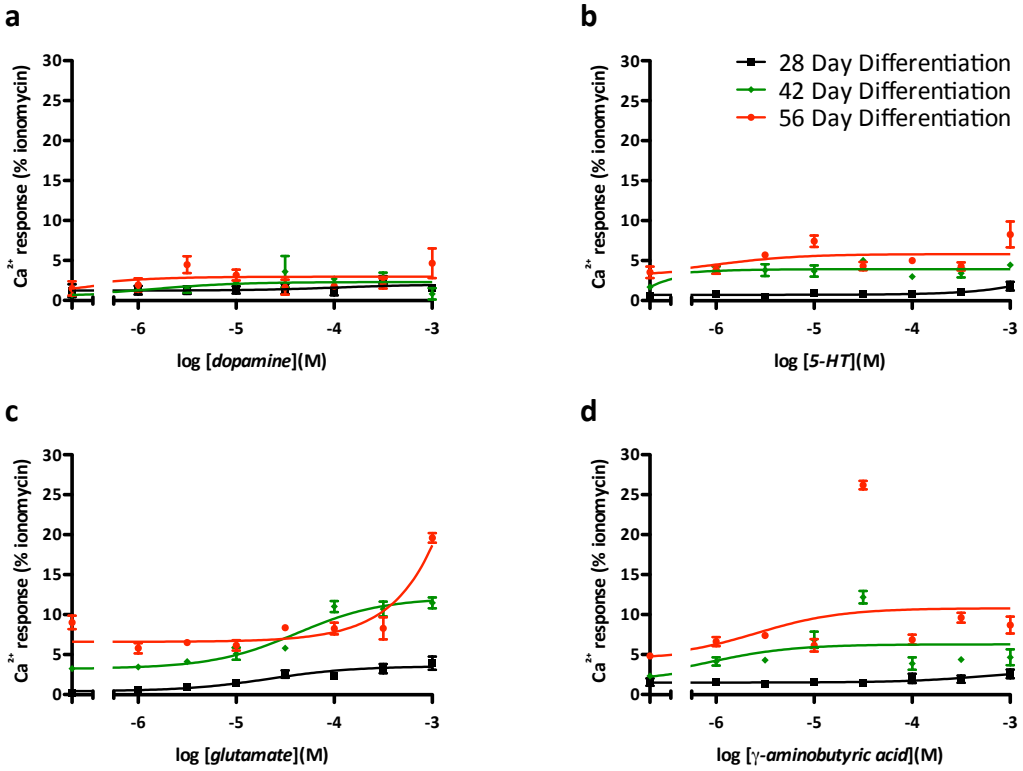


***Figure 4.24 Extended differentiation of CTX0E16/02 cultures alters ligand-induced responses in $[Ca^{2+}]_i$***
CTX0E16/02 cells were differentiated for 28, 42 or 56 days using SNBM. On the day of the experiment, cells were incubated for 1 hour in the presence of the cell permeable, $Ca^{2+}$-sensitive fluorescent dye Fura-2 AM. Cells were then washed prior to ligand-induced fluorescence being measured using a FS3. Concentration-response curves are shown for dopamine (**a**), 5-HT (**b**), glutamate, $EC_{50}$ = 22 µM and 42 µM (**c**) and γ-aminobutyric acid, $EC_{50}$ = 1 µM and 3 µM (**d**)) in CTX0E16/02 cultures differentiated for 28, 42 and 56 days. Data points represent mean ± S.E.M. from *n* = 2, each with 3 technical replicates and expressed relative to the positive control, ionomycin.

Dopamine's ability to sensitise cells to the depolarising effect of $K^+$ definitely warrants further investigation. Indeed, exposure to dopamine during differentiation may itself be a candidate for promoting the occurrence of electrical excitability and will be discussed later. Extending the period of differentiation from 28 days to 42 or 56 days, also influenced some ligand-induced increases in $[Ca^{2+}]_i$. Dopamine-induced responses remained constant, with little or no change in $[Ca^{2+}]_i$ following exposure to any of the tested concentrations (Figure 4.24, **a**). Similarly, responses to 5-HT were virtually absent if we consider the elevated baseline due to small buffer-evoked changes in $[Ca^{2+}]_i$ (Figure 4.24, **b**). In response to glutamate, CTX0E16/02 cultures demonstrated a greater maximal response at higher concentrations, and a rightward shift in potency as the period of differentiation increased (Figure 4.24, **c**). While no elevation in $[Ca^{2+}]_i$ was observed in response to GABA after a 28 day differentiation,

responses were observed after 42 or 56 days (Figure 4.24, **d**). Most interesting was a spike in intracellular $Ca^{2+}$ accumulation when cultures were exposed $10^{-4.5}$ M GABA, which was not seen at concentrations above this up to 1 mM. As mentioned previously, this effect may be attributable to the combination of receptors activated by a neurotransmitter like GABA, which has varying affinity for several different endogenous receptors with diverse downstream signalling events that can in some cases, cancel out the effects of others.

The maximal response to phenylephrine following 42 days of differentiation was higher than those observed after 28 days, but were only observed at the highest concentrations tested due to a considerable rightward shift in potency (Figure 4.25, a). In contrast, after 56 days of differentiation the efficacy of phenylephrine was almost identical to that observed after 28 days with $EC_{50}$ values of 1.4 µM and 3.0 µM for 28 and 56 day differentiations respectively. Maximal responses were also slightly higher after 56 days of differentiation as compared to that observed after 28 days. Changes in response to histamine-induced $[Ca^{2+}]_i$ responses with increased differentiation duration were comparable to those observed in response to glutamate. At 42 days, maximal histamine-induced $[Ca^{2+}]_i$ responses were slightly more pronounced than those seen at 28 days, while the $EC_{50}$ values remained consistent at 26.1 µM and 1.4 µM for 28 and 42 day differentiations respectively (Figure 4.25, **b**). Considering the level of baseline fluorescence at 56 days, responses to histamine were very similar to that observed at 28 days though responses at 1 mM were considerably higher at 56 compared to 28 days. Levels of intracellular $Ca^{2+}$ accumulation in response to acetylcholine were slightly higher at 42 days as compared to 28 days differentiation while the $EC_{50}$ value shifted from 5 µM to 23 µM with the increased differentiation. When considering the elevated level of baseline fluorescence observed at 56 days there was very little response at all to acetylcholine after this differentiation period (Figure 4.25, **c**). For the other tested cholinergic ligand – carbamoylcholine – maximal responses were slightly higher after a 42 day differentiation as compared to 28 days with comparable $EC_{50}$ values of 51 µM and 33 µM for 28 and 42 day differentiations respectively. Following a 56 day differentiation, $[Ca^{2+}]_i$ responses provoked by concentrations of carbamoylcholine below 100 µM were all but absent - as was the case for acetylcholine. In contrast to acetylcholine however, doses of 100 µM or higher provoked considerably greater responses than those seen after 28 or 42 days (Figure 4.25, **d**) (note the different y-axis scale used for acetylcholine and carbamoylcholine graphs as compared to phenylephrine and histamine). This increased activity of carbamoylcholine may be attributable to it's resistance to acetylcholinesterase as compared to the endogenous ligand. This could be tested using an acetylcholinesterase inhibitor such as rivastigmine.

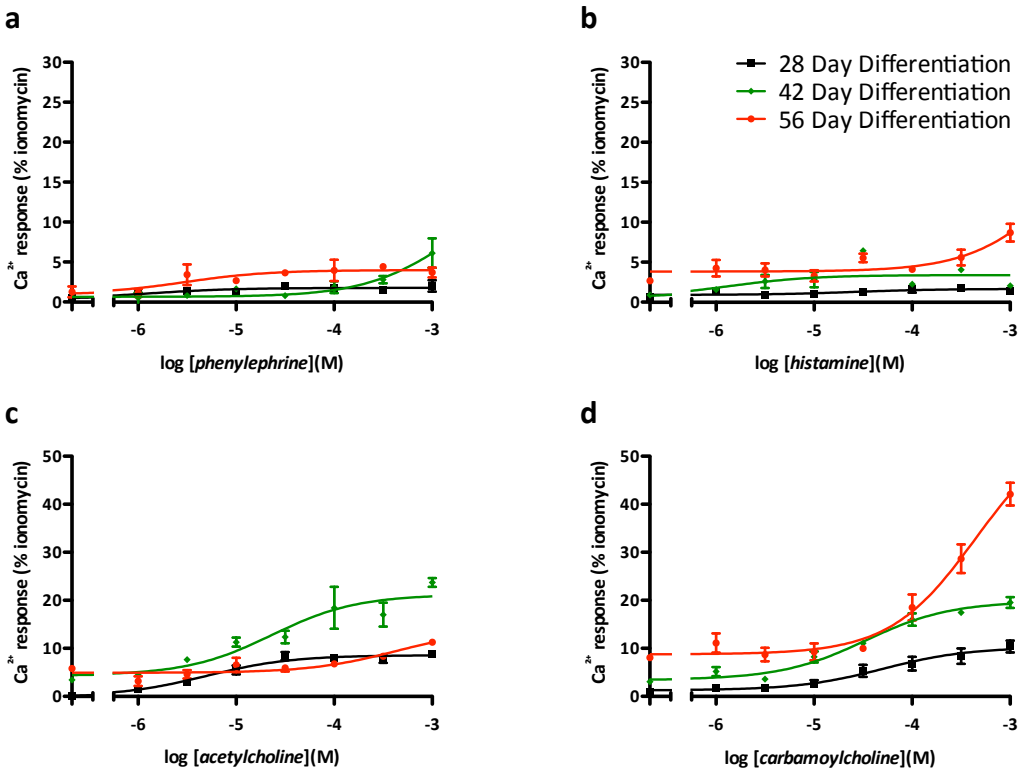


***Figure 4.25 Differentiation duration affects ligand-induced $[Ca^{2+}]_i$ responses in CTX0E16/02 cultures***
CTX0E16/02 cells were differentiated for 28, 42 or 56 days using SNBM. On the day of the experiment, cells were incubated for 1 hour in the presence of the cell permeable, $Ca^{2+}$-sensitive fluorescent dye Fura-2 AM. Cells were then washed prior to ligand-induced fluorescence being measured using a FS3. Concentration-response curves are shown for phenylephrine, $EC_{50}$ = 1.4 µM and 3.0 µM (**a**), histamine, $EC_{50}$ = 26.1 µM and 1.4 µM (**b**), acetylcholine, $EC_{50}$ = 5 µM, and 23 µM (**c**) and carbamoylcholine, $EC_{50}$ = 51 µM and 33 µM (**d**) in CTX0E16/02 cultures differentiated for 28, 42 and 56 days. Note different y-axis scale used for acetylcholine and carbamoylcholine. Data points represent mean ± S.E.M. from *n* = 2, each with 3 technical replicates and expressed relative to the positive control, ionomycin.

Taken together these data show that differentiated CTX0E16/02 cells have the capacity to become electrically excitable cultures either through increasing the duration of the differentiation or via trophic stimulation. Consistent with previously published work however, these $K^+$-induced depolarisations remain minimal even after 8 weeks of differentiation [61] or a 4 week differentiation in the presence of BDNF. Longer differentiation periods unfortunately introduce several drawbacks, including an increased likelihood of infection (especially when cells are grown without the use of antibiotics), increased levels of cell death and greater cost due to the use of more reagents and man-hours to maintain the cultures. To explore whether the magnitude of $K^+$-induced depolarisations could be increased without having to significantly increase the duration of differentiations, experiments were conducted whereby cells were exposed to a 42 day differentiation with the addition of trophic support from either BDNF or $FGF_2$. Previous experiments have shown that minimal electrical excitability can be detected in CTX0E16/02 cultures when differentiated for 56 days in the presence of SNBM or 28 days in the presence of SNBM supplemented with 10 $ngml^{-1}$ BDNF. These two culture conditions have therefore been integrated to determine whether greater electrical excitability can be provoked in less time (42 days), but with the addition of trophic support. $FGF_2$ was investigated based on its ability to promote survival during longer differentiation periods. Interestingly, as $FGF_2$ has been shown to mediate this effect through the

activation of PI3K [385], it was hoped that it might also provoke electrical excitability, or at least not prevent it due to its ability to maintain pluripotency [400,401]. Although 10 ngml$^{-1}$ $FGF_2$ has been used, as described above in proliferative cultures as a mitogen, it has previously been shown to additionally promote the differentiation of murine cortical NPCs towards a mixed population of neurons and glia. Interestingly, $FGF_2$ concentrations of 0.1 or 1 ngml$^{-1}$ were shown to push these cells toward a neuron only fate [402], though a mixed neuron-glial fate was desired for this study for reasons described above.

### *4.2.9 Promoting Electrical Excitability – Do We Have To Wait So Long?*

Differentiation of CTX0E16/02 cultures in the presence of 10 ngml$^{-1}$ BDNF for 42 days was capable of promoting electrical excitability in response to 50 mM KCl. While this effect was observed previously in cultures differentiated under the same conditions but for the shorter period of 28 days, it was not a consistent finding, in that not every well of cells was capable of generating a measurable increase in $[Ca^{2+}]_i$. In addition, this effect was only observed in cultures that had not been previously stimulated with either dopamine, 5-HT, acetylcholine or glutamate. In contrast, differentiation of CTX0E16/02 cells with 10 ngml$^{-1}$ BDNF for 42 days led to a consistent increase in $[Ca^{2+}]_i$ following a 50 mM $K^+$ challenge in cultures that had not been previously exposed to a neurotransmitter agonist. In addition, at this later time point, while cultures previously exposed to acetylcholine or glutamate were incapable of increasing $[Ca^{2+}]_i$ following a 50 mM $K^+$ challenge, those exposed to dopamine or 5-HT were (Figure 4.27, **c** and **d**).

In the case of cells differentiated in the presence of $FGF_2$ for 42 days, no electrical excitability was observed in wells exposed to assay buffer alone. However, as with cells exposed to a 56 day differentiation in the absence of trophic support, or a 42 day differentiation in the presence of 10 ngml$^{-1}$ BDNF, cells pre-treated with dopamine did demonstrate electrical excitability (Figure 4.27, **b**). When comparing ligand-induced responses in cells differentiated for 42 days, little change was observed in responses to dopamine or 5-HT between cultures exposed to a normal differentiation or those additionally exposed to BDNF or $FGF_2$, none of the three conditions demonstrated appreciable levels of intracellular $Ca^{2+}$ accumulation (Figure 4.26, **a** and **b**). In the case of glutamate however, cells differentiated in the presence of $FGF_2$ responded with a very similar $EC_{50}$ value of 24 µM as compared to 42 µM for cells exposed to a normal 42 day differentiation, though the maximal response was reduced. In contrast, cells differentiated in the presence of BDNF showed a considerable rightward shift in potency though maximal response at the highest tested glutamate concentration of 1 mM was considerably higher (Figure 4.26, **c**). The opposite was the case for cells exposed to acetylcholine where differentiation with $FGF_2$ resulted in a considerable increase in maximal response at the highest tested concentration in parallel with a rightward shift in potency. Differentiation with BDNF for 42 days left cells with a similar $EC_{50}$ for acetylcholine; 64 µM as compared to 23 µM for cells exposed to a normal differentiation while the maximal response was reduced (Figure 4.26, **d**).

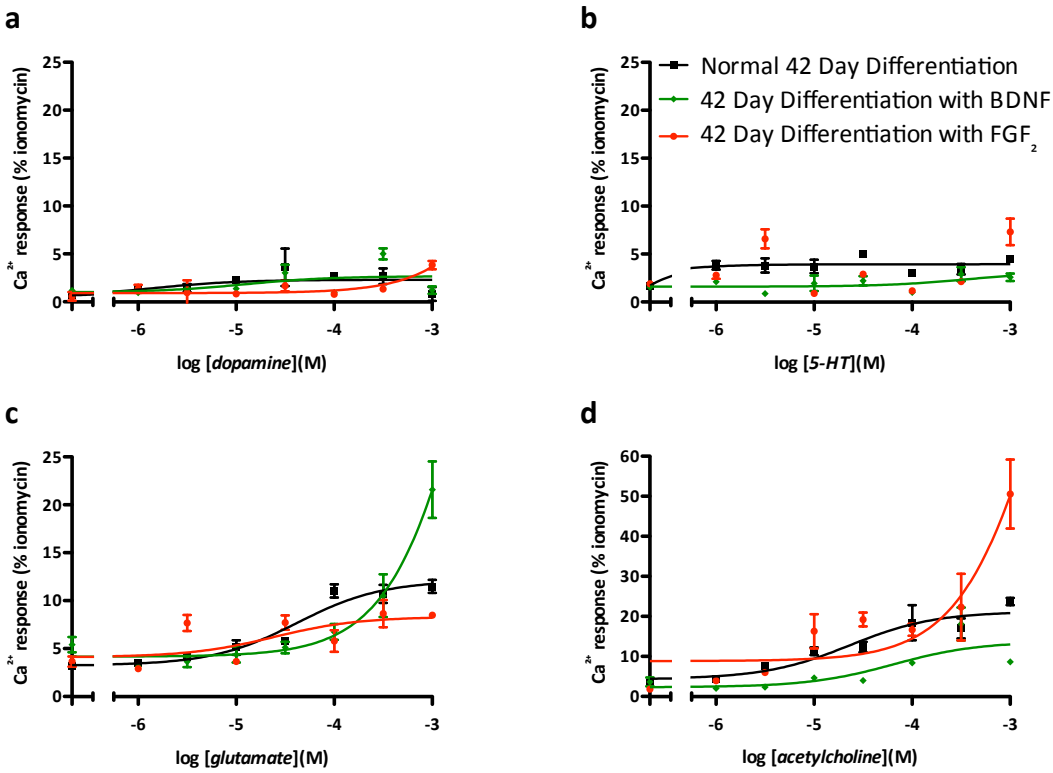


***Figure 4.26 BDNF and $FGF_2$ affects ligand-induced $[Ca^{2+}]_i$ responses in differentiated CTX0E16/02 cultures***
CTX0E16/02 cells were differentiated for 42 days using SNBM alone, or additionally supplemented with 10 $ngml^{-1}$ BDNF or 10 $ngml^{-1}$ $FGF_2$. On the day of the experiment, cells were incubated for 1 hour in the presence of the cell permeable, $Ca^{2+}$-sensitive fluorescent dye Fura-2 AM. Cells were then washed prior to ligand-induced fluorescence being measured using a FS3. Concentration-response curves are shown for dopamine (**a**), 5-HT (**b**), glutamate, $EC_{50}$ = 42 µM and 24 µM (**c**) and acetylcholine, $EC_{50}$ = 23 µM and 64 µM (**d**) in CTX0E16/02 cultures differentiated for 42 days as normal or supplemented with 10 $ngml^{-1}$ BDNF or 10 $ngml^{-1}$ $FGF_2$. Data points represent mean ± S.E.M. from *n* = 2, each with 3 technical replicates and expressed relative to the positive control, ionomycin.

### *4.2.10 Promoting Electrical Excitability – Summary*

Differentiation of the CTX0E16/02 NPC line for 28 days using SNBM was found to generate cells exhibiting both neuronal and glial phenotypes, as determined by immunocytochemical analysis (see ***4.2.1***, above). However, upon initial investigation of the physiological properties of these cultures using a FS3 plate reader, it was found they were incapable of responding to a 50 mM $K^+$ challenge by elevating $[Ca^{2+}]_i$ (see ***4.2.3***, above). Further investigation, monitoring intracellular $Ca^{2+}$ accumulation in individual cells, showed that a small proportion of cells within both proliferative and differentiated CTX0E16/02 cultures were capable of $K^+$-induced electrical excitability (see ***4.2.4***, above). However, not only did very few cells respond (far less than the proportion that were found to be either $tau^+$ or $MAP2^+$), the extent of intracellular $Ca^{2+}$ accumulation in those cells that did, was deemed not to be characteristic of cells demonstrating a mature neuronal phenotype. Neurons are by definition excitable cells, though as discussed above, this property is not only important to confer upon them the ability to generate action potentials and subsequently release neurotransmitter, allowing them to communicate to other cells. This property also has important implications regarding how neurons translate the signals they receive from their environment due to the dualistic role played by $Ca^{2+}$ ions in both contributing to membrane potential and acting as an intracellular second messenger. The aim of this study was to develop a native

tissue *in vitro* platform with which to investigate the mechanism of action of antipsychotic medications, and as such, it is therefore important that it is capable of as faithfully as possible, reproducing the signalling consequences resulting from the interaction of these drugs with their cellular targets.

Consequently, several different approaches have been investigated as a means to precipitate electrical activity in differentiated CTX0E16/02 cultures including the expansion of cultures as neurospheres prior to differentiation, extending the duration of culture differentiation, and pharmacological manipulation through the use of trophic factors and the stimulation of PI3K activity.

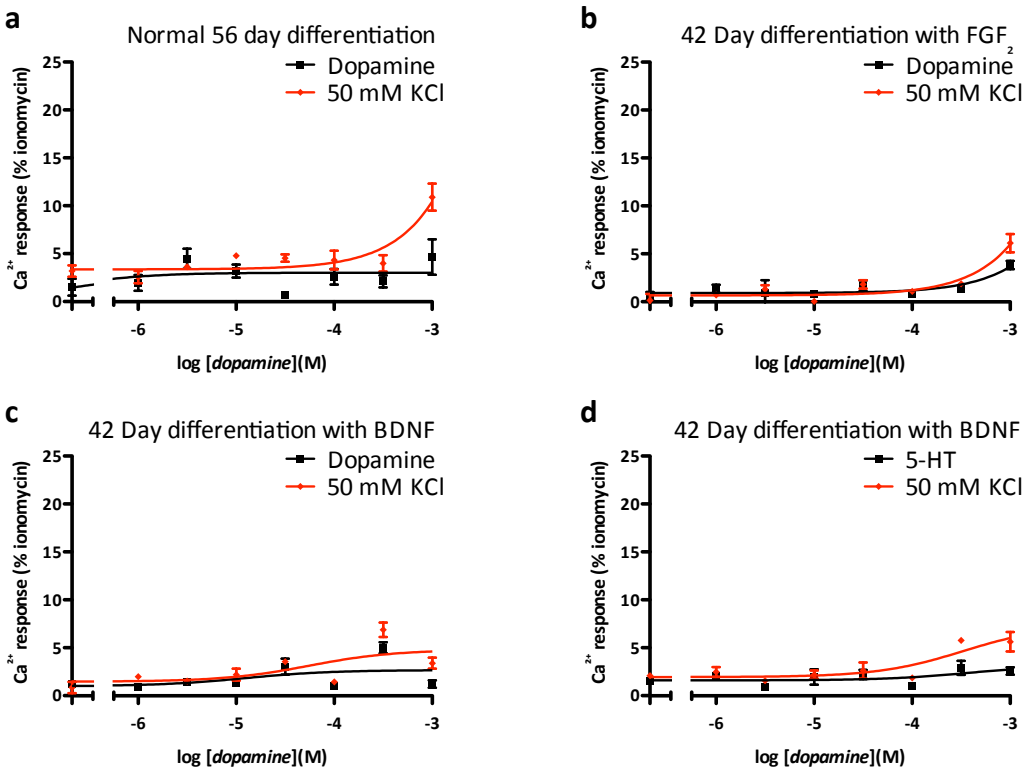


***Figure 4.27 Differentiation duration and BDNF promote electrical excitability in CTX0E16/02 cultures***
CTX0E16/02 cells were differentiated for 56 days using SNBM or for 42 days using SNBM supplemented with 10 $ngml^{-1}$ BDNF or 10 $ngml^{-1}$ $FGF_2$. On the day of the experiment, cells were incubated for 1 hour in the presence of the cell permeable, $Ca^{2+}$-sensitive fluorescent dye Fura-2 AM. Cells were then washed prior to dopamine or 5-HT-induced fluorescence being measured using a FS3. Each well was subsequently exposed to 50 mM KCl to test electrical excitability of cultures. Data points represent mean ± S.E.M. from *n* = 2, each with 3 technical replicates and expressed relative to the positive control, ionomycin

The expansion of human NPCs, derived from the ventral mesencephalon but not the cortex, as neurospheres for one week prior to differentiation was previously reported to generate cultures containing electrically excitable cells [104]. The reason why this technique was not successful in cortically derived cells, was hypothesised to be due to an insufficiently long duration of pre-aggregation. Experiments were therefore performed whereby CTX0E16/02 cells were expanded as neurospheres for either 14 or 42 days prior to a normal differentiation – as defined in ***3.2.6***, above. This approach did not however result in the detection of electrically excitable cells (see ***4.2.5***, above).

The next approach tested was based on findings by Viard and colleagues, showing that PI3K plays a key role in the plasma membrane expression of $Ca_V$, leading to enhanced $Ca_V$-mediated currents [378]. Expression analysis of differentiated CTX0E16/02 cultures had already shown that a gene encoding the L-type type $Ca^{2+}$ channel subunit $\alpha_{1C}$ (CACNA1C) was robustly expressed in these cells (see Table 3.9, above), suggesting that cell surface expression may be all that was required to precipitate electrical excitability. Endogenous PI3K activity was therefore stimulated using the cell-permeable, recombinant activating peptide 740 Y-P [384]. Unfortunately, this approach also failed to promote electrical excitability in differentiated cultures, and may be due to PI3K only being capable of exerting a transient effect upon cell surface expression of voltage-dependent $Ca^{2+}$ channels (see 4.2.6 above).

Several trophic factors have been implicated in the maturation process of developing neurons. For this reason, the capacity of both NGF and BDNF were tested to determine whether their presence could provoke electrical excitability in differentiated CTX0E16/02 cultures. NGF did not exert a measurable effect upon electrical excitability when used as a supplement to the normal differentiation procedure. However, BDNF was found to promote electrical excitability, as determined by a rise in $[Ca^{2+}]_i$ following a 50 mM $K^+$ challenge. This effect was not observed in all experiments, and could not be detected in cultures previously exposed to the neurotransmitter agonists; dopamine, 5-HT, acetylcholine or glutamate (see 4.2.7 above).

While BDNF was shown to exert an effect upon the excitability of CTX0E16/02 cultures differentiated for 28 days, it was found to be both weak and inconsistent with regard to the extent of the observed response. Several published reports have however suggested that the differentiation of human cortical NPCs to produce electrically excitable cultures takes considerably longer than the four weeks originally employed in this study [61,334,399]. Therefore, to explore this possibility, CTX0E16/02 cultures were differentiated for either six or eight weeks to see whether this was sufficient to detect the robust electrical excitability. CTX0E16/02 cultures differentiated for 42 days were found to be incapable of producing a rise in $[Ca^{2+}]_i$ in response to 50 mM KCl, unless previously stimulated with high concentrations of dopamine, despite exerting no influence upon intracellular $Ca^{2+}$ accumulation in their own right. In contrast, cultures differentiated for 56 days were capable of responding to a $K^+$-induced depolarisation by elevating $[Ca^{2+}]_i$, though this effect was small, and was abolished if cultures were previously exposed to any of the tested concentrations of dopamine, 5-HT, acetylcholine or glutamate (see 4.2.8 above).

These data suggested that extending the period of differentiation can be successfully used as a strategy to promote electrical excitability in differentiating CTX0E16/02 cultures. However, additional time in culture presents several drawbacks including concomitantly reduced throughput, higher cost and greater risk of infection. Therefore, due to the detectable, but weak effect that trophic support was shown to provide in promoting electrical excitability, this strategy was integrated with an increase in the duration of differentiation, to determine whether CTX0E16/02 cultures could be stimulated to become robustly excitable following a differentiation of less than 56 days. The capacity of both BDNF and $FGF_2$ were tested to determine whether they could effectively increase electrical excitability in CTX0E16/02

cultures differentiated for 42 days. BDNF was shown to promote electrical excitability, and could be observed in all cultures that were exposed only to 50 mM KCl. In addition, these cultures were also capable of demonstrating an increase in $[Ca^{2+}]_i$ following exposure to either dopamine or 5-HT, but not acetylcholine or glutamate. In contrast, while $FGF_2$ did not precipitate electrical excitability in CTX0E16/02 cultures differentiated for 42 days – as determined by measuring changes in $[Ca^{2+}]_i$ following exposure to KCl alone – this condition was shown to allow cells previously stimulated with high concentrations of dopamine to accumulate intracellular $Ca^{2+}$ (see 4.2.9 above).

These data show that CTX0E16/02 cells are capable of generating differentiated cultures containing electrically excitable cells. This has been shown to be promoted by either increasing the period of differentiation, or providing appropriate trophic stimulation. In addition, it has been shown that these two different strategies can be combined to achieve the same level of excitability in a shorter space of time. This does not however eliminate the possibility that the other tested conditions for promoting culture excitability – while not exerting an effect on their own – could also deliver an additive influence. Another interesting finding was that dopamine, and to lesser extent 5-HT, appear to have the capacity to sensitise cells to the depolarising effects of KCl. Further work is required to explore the mechanism through which this occurs, and whether it can be blocked with the use of specific antagonists.

### *4.2.11 Increasing Receptor Expression – Stimulating PKA Activity*

Differentiated CTX0E16/02 cultures express a broad range of neurotransmitter receptors at the message level and show a trend of increased receptor expression as compared to their proliferative precursors. However, with the exception of glutamate, responses to tested ligands are severely attenuated in differentiated as compared to proliferative cultures. Data presented above exploring putative strategies to precipitate electrical excitability in these cultures have shown that ligand-induced responses to various compounds are highly plastic and were affected in some way by all of the tested approaches. The observed changes in response could be attributable to several factors including altered cell surface receptor expression [225,403,404], changes in signalling efficiency [336], promiscuous signalling partners [342,405], upregulation of receptor accessory proteins and changes in the regulation of the signalling molecules concerned [36,186,197,230]. As discussed previously, receptor expression at the cell surface is highly regulated and indeed, many receptors have been shown to require considerable modification or manipulation in order to permit their ectopic expression in non-native cells [34,35]. The CTX0E16/02 cell line does represent a native neural cell type, though while considerable receptor expression can be detected at the message level (see Table 3.9 and Table 3.10, above), this is not reflected in their functional responses, suggesting little receptor expression at the cell surface. The following experiments were conducted to explore the possibility that receptors can be pharmacologically stimulated to increase their cell surface expression or signalling efficiency.

A recent study by Nicolson and colleagues demonstrated that pre-treatment of primary rat dorsal root ganglion (DRG) neurons with the prostaglandin, $PGE_2$ was able to sensitise the cells to histamine, as

measured by its ability to evoke a concentration-dependent rise in $[Ca^{2+}]_i$. This effect was shown to be mediated through a rise in intracellular cAMP levels leading to PKA activation [406]. It is not clear from the study how enhanced PKA activity leads to increased sensitivity to histamine, however PKA may exert it's effect by increasing receptor number at the cell surface or by enhancing the sensitivity of the receptors already located there. In addition to this, and as previously mentioned, increased intracellular cAMP levels have additionally been shown to induce $Na^+$-channel expression through activation of PKA [387-389]. Therefore, it was proposed that through elevating intracellular cAMP concentrations, it may be possible to increase the sensitivity of differentiated CTX0E16/02 cultures to various ligands. Due to it's influence upon $Na^+$-channel expression, this approach was also considered as a possible means to promote electrical excitability, as has been discussed above. To address the influence of elevated cAMP on differentiated CTX0E16/02 cultures, experiments were performed whereby cultures were differentiated for 28 days in SNBM supplemented with the cell-permeable analogue of cAMP – dibutyryl-cAMP (1 mM), and the phosphodiesterase inhibitor – 3-Isobutyl-1-methylxanthine (IBMX, 0.5 mM) for the final 3 hours, 3 days or 7 days of differentiation. IBMX was used to prevent the catalytic metabolism of cAMP by intracellular phosphodiesterase, while the concentrations of dibutyryl-cAMP and IBMX used were selected based on previous studies showing these were capable of provoking $Na^+$-channel expression and neurite outgrowth in PC12 cells [389]. Cultures were then loaded with Fura-2 AM and assayed for their ability to respond to various ligands by elevating $[Ca^{2+}]_i$, before being tested for their ability to respond to a depolarising $K^+$ challenge.

Following a normal 28 day differentiation, dopamine was incapable of causing an increase in $[Ca^{2+}]_i$ at any of the concentrations tested, and was mirrored by cultures exposed to 1 mM dibutyryl-cAMP and 0.5 mM IBMX for the final 3 hours or 3 days of differentiation. If exposed to dibutyryl-cAMP and IBMX for the final 7 days of differentiation however, cultures were capable of producing a dopamine-induced rise in $[Ca^{2+}]_i$, though only at the highest tested doses (Figure 4.28, **a**). This is perhaps surprising when it is considered that dopamine receptors are classically thought of as either $G\alpha_s$ ($D_1$ and $D_5$) or $G\alpha_i$-linked ($D_2$, $D_3$ and $D_4$), though there is growing evidence that dopamine receptors are also capable of modulating PLC activity through $G\alpha_q$ coupling, and therefore capable of elevating $[Ca^{2+}]_i$. Various studies have attributed this effect to $D_1$ [407-410], $D_2$ [363] or $D_5$ [411,412] receptors or functional $D_1/D_2$ or $D_5/D_2$ receptor heteromers [413,414], though the exact mechanism remains unclear [191]. Different dopamine-mediated mechanisms may be responsible for changes in $[Ca^{2+}]_i$ observed in different tissues, and this only reinforces the assertion that it is important to make use of native cells when investigating the intracellular signalling consequences of drug exposure. Based on the available literature it is clear that further work would be necessary to determine the mechanism responsible for this observed increase in $[Ca^{2+}]_i$. Intracellular $Ca^{2+}$ accumulation in response to 5-HT remained absent, despite exposure to dibutyryl-cAMP and IBMX, as was observed when CTX0E16/02 cultures were exposed to a normal 28 day differentiation (Figure 4.28, **b**). This was however – as seen for dopamine – with the exception of cultures exposed to dibutyryl-cAMP and IBMX for the final 7 days of differentiation, where a small response was observed at the highest tested concentrations. Changes in $[Ca^{2+}]_i$ induced by glutamate were more pronounced following exposure to dibutyryl-cAMP and IBMX (Figure 4.28, **c**). If exposed for

just the final 3 hours prior to the assay then no change was observed in glutamate-induced responses when compared to cells exposed to a normal 28 day differentiation. The appearance of slightly different $EC_{50}$ values of 22 μM and 10 μM for normally differentiated cultures and those exposed to dibutyryl-cAMP and IBMX for 3 hours respectively, appear largely attributable to normally differentiated cells exhibiting a slightly lower maximal response (Figure 4.28, **c**). If exposed to dibutyryl-cAMP and IBMX for 3 days however, there was a considerable rightward shift in potency but a far greater maximal response, while exposure for 7 days caused an even further reduction in potency, but a reduced maximal response compared to that seen after a 3 day exposure (Figure 4.28, **c**). In contrast, while responses to GABA were largely absent in normally differentiated cultures and also those exposed to dibutyryl-cAMP and IBMX for 3 or 7 days, a small rise in $[Ca^{2+}]_i$ was seen from cultures in response to the highest tested GABA concentrations when exposed to dibutyryl-cAMP and IBMX for just 3 hours (Figure 4.28, **d**).

Cultures exposed to a normal 28 day differentiation showed only a slight concentration-dependent response to phenylephrine with an $EC_{50}$ of 1 μM and a maximal response of just 1.8% of that produced by ionomycin (Figure 4.29, **a**). On exposure to dibutyryl-cAMP and IBMX, phenylephrine-induced responses were all but absent when compared to baseline measurements except at the highest tested concentration of 1 mM, where responses were elevated for cultures exposed to dibutyryl-cAMP and IBMX for 3 hours, 3 days or 7 days. A similar response profile was also observed for cells exposed to histamine with only the highest doses capable of eliciting an increase in $[Ca^{2+}]_i$. (Figure 4.29, **b**). This is in contrast to the study that inspired this approach, where elevated levels of cAMP led to increased histamine sensitivity [406]. This study was however performed using primary rat DRG neurons that harbour a physiological reason to be able to be sensitised to histamine due to their peripheral projections. In addition, the study by Nicolson and colleagues used a transient stimulation of PKA activity – just 5 minutes prior to the addition of histamine. This shorter time point was not considered as it would not be able to show sustained - if any - effects upon receptor activity.

Responses to acetylcholine were relatively unchanged by exposure to dibutyryl-cAMP and IBMX (Figure 4.29, **c**). When exposed to dibutyryl-cAMP and IBMX for just 3 hours, the maximal response and $EC_{50}$ (8.4% of ionomycin and 8 μM respectively) for acetylcholine were virtually identical to that seen for cultures exposed to a normal differentiation (8.6% of ionomycin and 5 μM). When exposed to dibutyryl-cAMP and IBMX for 3 days there was an apparent rightward shift in potency with an $EC_{50}$ of 26 μM, though the maximal response achieved was very similar once the elevated baseline fluorescence ratio was taken into account (Figure 4.29, **c**). This trend continued when cultures were exposed to dibutyryl-cAMP and IBMX for the longer 7 day period, showing a further rightward shift in potency with a predicted (the curve had not reached a plateau by 1 mM) $EC_{50}$ value of 133 μM, though the maximal response achieved was again comparable with the other tested conditions once baseline fluorescence was accounted for (Figure 4.29, **c**). Interestingly, the other tested cholinergic ligand – carbamoylcholine – exhibited a very different effect in response to dibutyryl-cAMP and IBMX, to that seen for acetylcholine. Cultures exposed to dibutyryl-cAMP and IBMX for 3 or 7 days saw a considerable rightward shift in potency with respect to their ability to accumulate intracellular $Ca^{2+}$ in the presence of

carbamoylcholine when compared to normally differentiated cells. The maximal responses achieved at the highest tested concentrations were however considerably larger (Figure 4.29, **d**). Surprisingly, while a 3 hour exposure to dibutyryl-cAMP and IBMX had little effect upon acetylcholine-induced responses, and indeed lower tested concentrations of carbamoylcholine, when exposed to the highest tested concentration of carbamoylcholine a maximal response was observed that was approximately 4 times that seen in normally differentiated cultures (Figure 4.29, **d**).

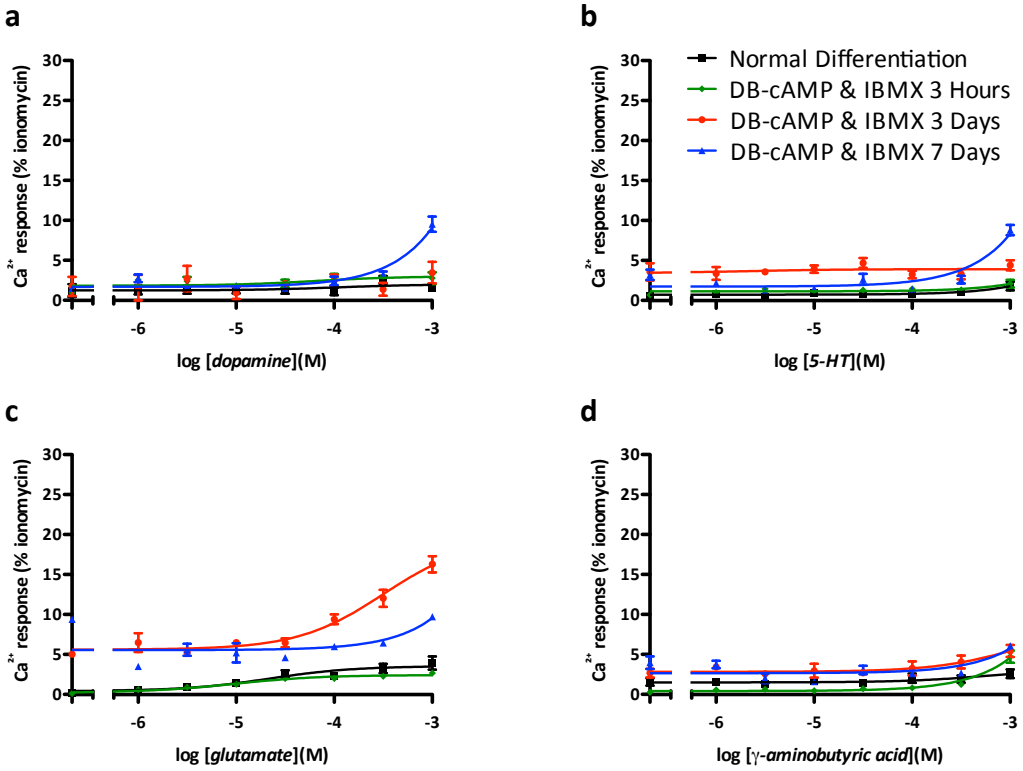


***Figure 4.28 Elevated cAMP in differentiated CTX0E16/02 cultures increases glutamate-induced $[Ca^{2+}]_i$ responses***
CTX0E16/02 cells were differentiated for 28 days using SNBM and supplemented with 1 mM dibutyryl-cAMP and 0.5 mM IBMX for the final 7 days, 3 days or 3 hours of differentiation. On the day of the experiment, cells were incubated for 1 hour in the presence of the cell permeable, $Ca^{2+}$-sensitive fluorescent dye Fura-2 AM. Cells were then washed prior to ligand-induced fluorescence being measured using a FS3. Concentration-response curves are shown for dopamine (**a**), 5-HT (**b**), glutamate, $EC_{50}$ = 22 µM and 10 µM (**c**) and γ-aminobutyric acid (**d**) in normally differentiated cells (for comparison), and cells exposed to 1 mM dibutyryl-cAMP and 0.5 mM IBMX for the final 3 hours, 3 days or 7 days of differentiation. Data points represent mean ± S.E.M. from *n* = 1 (*n* = 2 for normal differentiation), with 3 technical replicates and expressed relative to the positive control, ionomycin.

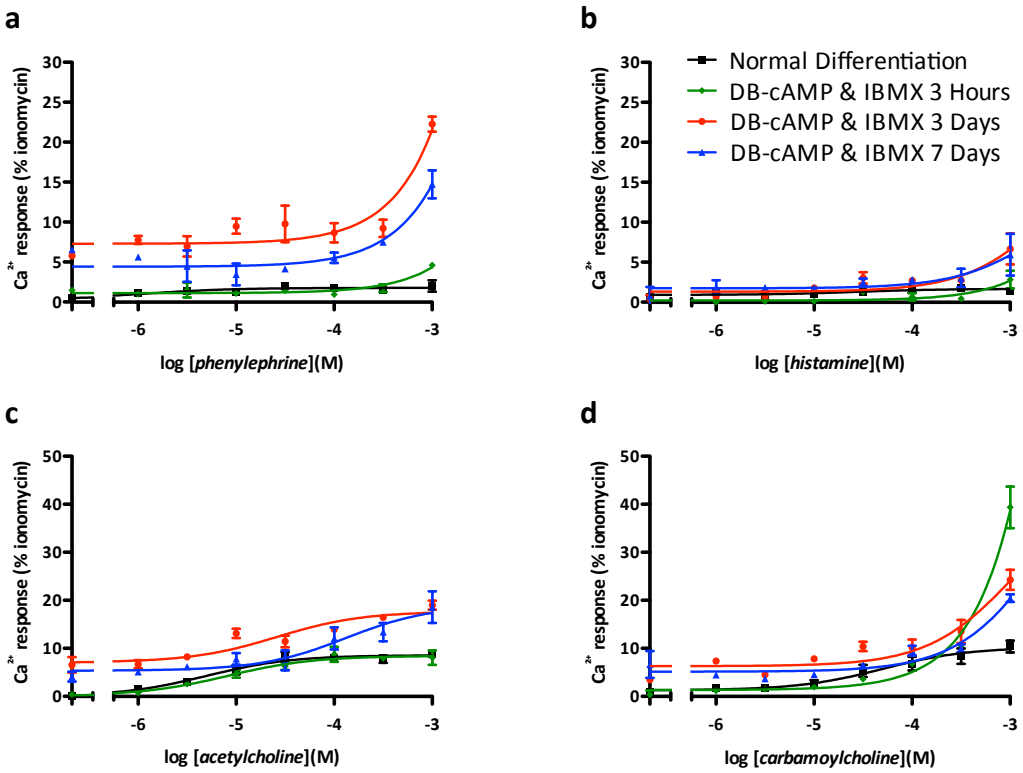


***Figure 4.29 Elevated cAMP in differentiated CTX0E16/02 cultures modulates ligand-induced $[Ca^{2+}]_i$ responses***
CTX0E16/02 cells were differentiated for 28 days using SNBM and supplemented with 1 mM dibutyryl-cAMP and 0.5 mM IBMX for the final 7 days, 3 days or 3 hours of differentiation. On the day of the experiment, cells were incubated for 1 hour in the presence of the cell permeable, $Ca^{2+}$-sensitive fluorescent dye Fura-2 AM. Cells were then washed prior to ligand-induced fluorescence being measured using a FS3. Concentration-response curves are shown for phenylephrine, $EC_{50}$ = 1 µM (**a**), histamine, $EC_{50}$ = 26 µM (**b**), acetylcholine, $EC_{50}$ = 5 µM, 8 µM and 26 µM (**c**) and carbamoylcholine, $EC_{50}$ = 51 µM (**d**) in normally differentiated cells (for comparison), and cells exposed to 1 mM dibutyryl-cAMP and 0.5 mM IBMX for the final 3 hours, 3 days or 7 days of differentiation. Data points represent mean ± S.E.M. from *n* = 1 (*n* = 2 for normal differentiation), with 3 technical replicates and expressed relative to the positive control, ionomycin.

Elevation of intracellular levels of cAMP through the addition of a cell permeable analogue and IBMX to prevent its breakdown did not as hoped, increase the sensitivity of CTX0E16/02 cultures to the eight tested ligands. While increases were observed in the maximal $[Ca^{2+}]_i$ achieved in response to dopamine, glutamate, phenylephrine and carbamoylcholine this was in every case accompanied by a rightward shift in potency. It appears likely that the effect observed by Nicolson and colleagues with respect to an increase in the sensitivity of DRG neurons to histamine [406], by elevating intracellular cAMP concentrations may either be cell type-specific or only capable of exerting a transient effect. If the sensitising effect mediated by cAMP is indeed a transient one, this would make this strategy to increase receptor expression unfeasible for the present study.

### *4.2.12 Increasing Receptor Expression – Use It Or Lose It?*

An alternative approach to stimulate cell surface receptor expression was inspired by simple Hebbian synaptic plasticity, a mechanism still thought to be central to the development and maturation of the nervous system. Simply speaking, once a synaptic connection between two cells has been established,

the efficiency of this connection can be modulated based on its level of activity. The more the synapse is used, the more efficient it becomes and is thought to be brought about through changes at both the pre- and post-synaptic terminals [415]. In an attempt to test whether this theory can be adopted for *in vitro* cultures, CTX0E16/02 cultures were differentiated for 28 days in SNBM supplemented with glutamate, acetylcholine or phenylephrine. These compounds were selected based on their ability to elicit robust intracellular $Ca^{2+}$ accumulation either in proliferative or differentiated CTX0E16/02 cultures. The concentration at which each of these compounds was added to the differentiating cultures was determined by the responses they had provoked when tested in proliferative and 28 days differentiated cultures (see ***4.2.2*** and ***4.2.3***, above). For phenylephrine and acetylcholine the concentration chosen was the $EC_{50}$ exhibited for each of these compounds by CTX0E16/02 cultures in their proliferative state in preliminary experiments (see Figure 4.7 **a** and **c**, above) – 3 µM for both compounds. These concentration were chosen to ensure a robust but not a maximal response so as not to expose the cells to excessive $[Ca^{2+}]_i$ that may prove toxic. Glutamate was incapable of provoking a rise in $[Ca^{2+}]_i$ in proliferative cells so the $EC_{50}$ exhibited by differentiated CTX0E16/02 cultures in preliminary experiments was instead employed – 40 µM (see Figure 4.8, **c**).

Unfortunately, cultures exposed to 3 µM acetylcholine did not survive the full 28 day differentiation. These cultures exhibited considerable signs of cell death in the first 7 days and were completely dead by the end of the second week of culture; probably attributable to toxicity from elevated $[Ca^{2+}]_i$. In contrast, the health of cultures exposed to 40 µM glutamate or 3 µM phenylephrine over the course of a 28 day differentiation appeared unaffected. CTX0E16/02 cultures exposed to a normal 28 day differentiation were unable to respond to dopamine at any tested concentrations by elevating $[Ca^{2+}]_i$ (see Figure 4.8, **a**). However, if differentiated in the presence of 40 µM glutamate or 3 µM phenylephrine, the cultures were capable of a slight concentration-dependent response to dopamine with $EC_{50}$ values of 7 µM and 20 µM respectively (Figure 4.30, **a**). Levels of intracellular $Ca^{2+}$ accumulation provoked by 5-HT in these cultures were also minimal, and only observed at the highest tested concentration of 1 mM (Figure 4.30, **b**). A similar profile was observed for responses to glutamate in cultures differentiated in the presence of glutamate or 3 µM phenylephrine. While CTX0E16/02 cultures exposed to a normal 28 day differentiation were capable of a concentration dependent increase in $[Ca^{2+}]_i$, with an $EC_{50}$ of 22 µM, cultures differentiated with 40 µM glutamate or 3 µM phenylephrine saw a considerable rightward shift in potency, though maximal responses were greater, even once levels of baseline fluorescence were taken into account (Figure 4.30, **c**). Exposure to glutamate or phenylephrine during differentiation did not alter GABA-induced changes in $[Ca^{2+}]_i$. As with normally differentiated cultures, GABA was incapable of provoking a rise in $[Ca^{2+}]_i$, at any tested concentration (Figure 4.30, **d**).

Phenylephrine-induced $[Ca^{2+}]_i$ responses were affected by exposure to glutamate and phenylephrine during cellular differentiation. Compared to cultures exposed to a normal differentiation, which showed an $EC_{50}$ of 1 µM, cells differentiated in the presence of 40 µM glutamate saw a considerable rightward shift in potency with responses over baseline only observed at 1 mM, while cultures exposed to 3 µM phenylephrine saw a shift in $EC_{50}$ to 48 µM but an enhanced maximal response (Figure 4.31, **a**).

Differentiation in the presence of 40 µM glutamate had no influence upon histamine-induced $[Ca^{2+}]_i$ responses providing an $EC_{50}$ of 21 µM as compared to 26 µM for normally differentiated cells. If differentiated in the presence of 3 µM phenylephrine however, an increase in histamine potency was observed with an $EC_{50}$ of 3 µM and an enhanced maximal response (Figure 4.31, **b**). In response to acetylcholine, cells differentiated in the presence of 40 µM glutamate saw similar levels of intracellular $Ca^{2+}$ accumulation to that observed for cells exposed to a normal differentiation except that the maximal response at 1 mM was considerably higher (Figure 4.31, **c**). In contrast, cells exposed to 3 µM phenylephrine during differentiation exhibited a very similar $EC_{50}$ of 1 µM as compared to 5 µM for normally differentiated cells. Once the elevated baseline observed for cells differentiated with phenylephrine was taken into account, the maximal response was also very similar at approximately 9% of that provoked by ionomycin (Figure 4.31, **c**). Similar to observations for acetylcholine, carbamoylcholine-induced responses in cells differentiated with 40 µM glutamate were almost identical to those seen for normally differentiated cells, with the exception of responses at the highest concentration of 1 mM, where responses were slightly higher. For cells differentiated with 3 µM phenylephrine, there was a large rightward shift in potency while the maximal response was increased (Figure 4.31, **d**).

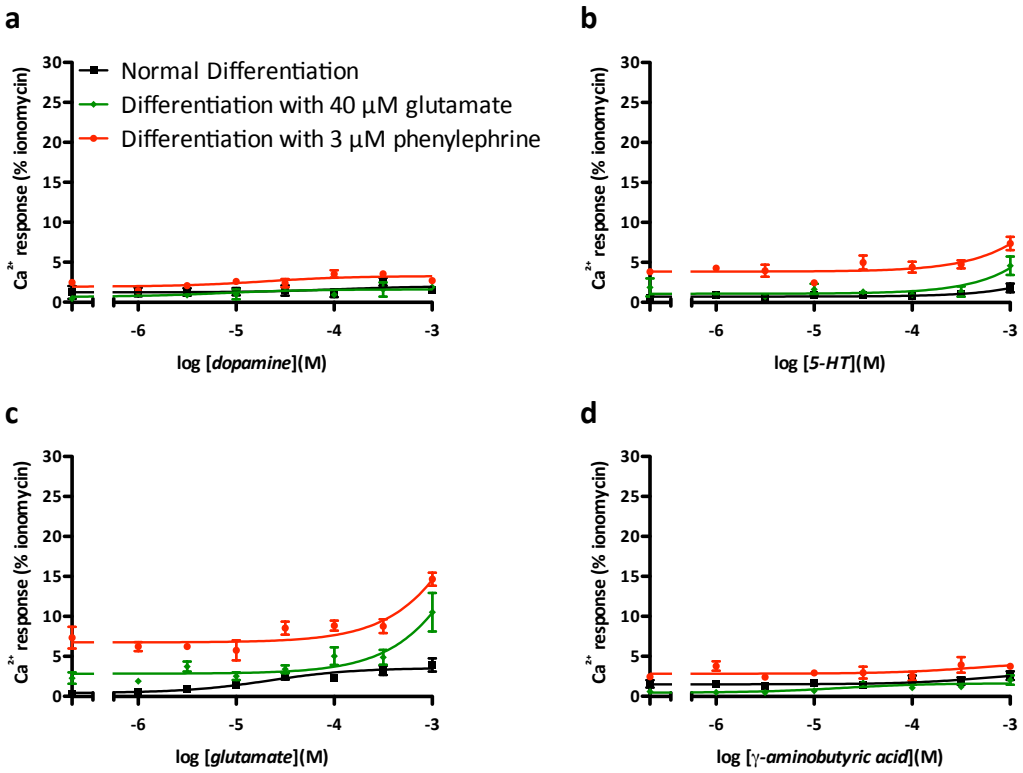


***Figure 4.30 Differentiation with glutamate or phenylephrine affects ligand-induced $[Ca^{2+}]_i$ responses***
CTX0E16/02 cells were differentiated for 28 days using SNBM supplemented with either 40 µM glutamate or 3 µM phenylephrine. On the day of the experiment, cells were incubated for 1 hour in the presence of the cell permeable, $Ca^{2+}$-sensitive fluorescent dye Fura-2 AM. Cells were then washed prior to ligand-induced fluorescence being measured using a FS3. Concentration-response curves are shown for dopamine, $EC_{50}$ = 7 µM and 20 µM (**a**), 5-HT (**b**), glutamate, $EC_{50}$ = 22 µM (**c**) and γ-aminobutyric acid (**d**) in normally differentiated cells (for comparison), and cells differentiated in the presence of 40 µM glutamate or 3 µM phenylephrine. Data points represent mean ± S.E.M. from *n* = 2, each with 3 technical replicates and expressed relative to the positive control, ionomycin.

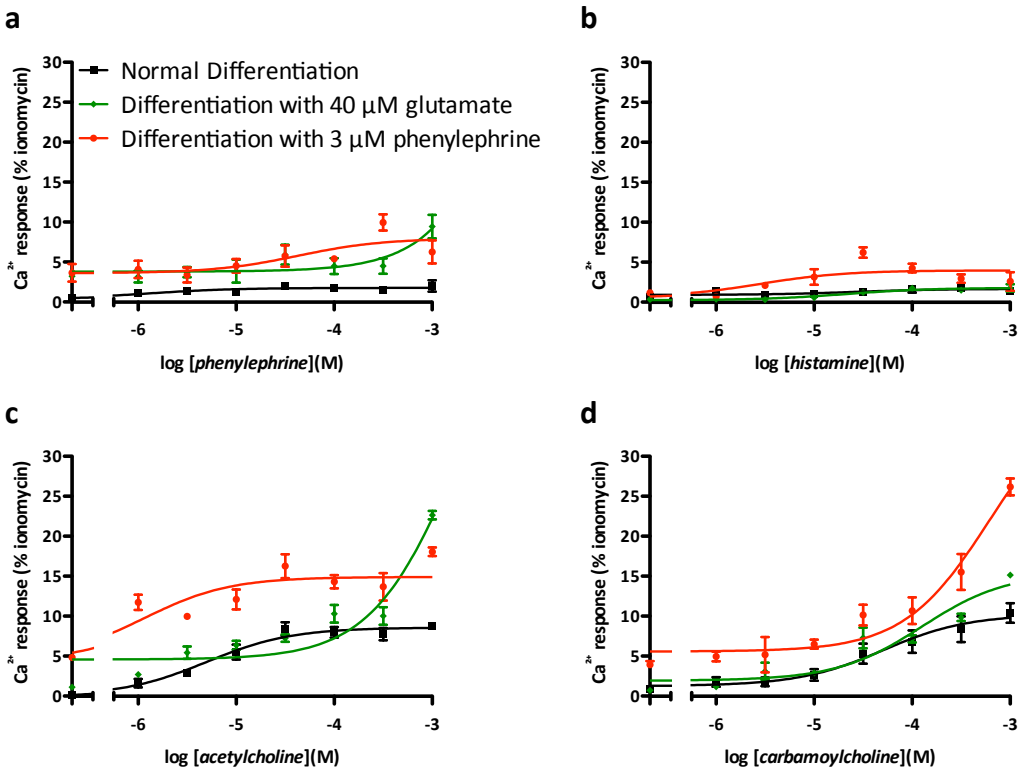


***Figure 4.31 Differentiation with glutamate or phenylephrine affects ligand-induced $[Ca^{2+}]_i$ responses***
CTX0E16/02 cells were differentiated for 28 days using SNBM supplemented with either 40 µM glutamate or 3 µM phenylephrine. On the day of the experiment, cells were incubated for 1 hour in the presence of the cell permeable, $Ca^{2+}$-sensitive fluorescent dye Fura-2 AM. Cells were then washed prior to ligand-induced fluorescence being measured using a FS3. Concentration-response curves are shown for phenylephrine, $EC_{50}$ = 1 µM and 43 µM (**a**), histamine, $EC_{50}$ = 26 µM, 21 µM and 3 µM (**b**), acetylcholine, $EC_{50}$ = 5 µM and 1 µM (**c**) and carbamoylcholine, $EC_{50}$ = 51 µM (**d**) in normally differentiated cells (for comparison), and cells differentiated in the presence of 40 µM glutamate or 3 µM phenylephrine. Data points represent mean ± S.E.M. from *n* = 2, each with 3 technical replicates and expressed relative to the positive control, ionomycin.

Exposure of CTX0E16/02 cultures to either glutamate or phenylephrine during the process of differentiation was investigated as a potential strategy to increase receptor expression by means of use-dependency. However, as discussed above, many of the different approaches explored as a means of provoking electrical excitability in differentiating CTX0E16/02 cultures also exert diverse effects upon ligand-induced responses. For this reason, the effect of exposure to glutamate or phenylephrine during the process of differentiation was investigated with respect to ligand-induced responses to a variety of different agonists, not just glutamate and phenylephrine. Contrary to what was hoped, differentiation in the presence of glutamate did not sensitise cells to this ligand. Indeed, a considerable rightward shift in potency, though a marginally increase in the response from the highest tested concentration of glutamate, was observed as compared to normally differentiated cells. Interestingly, this same effect of glutamate was also observed in cultures exposed to phenylephrine and acetylcholine, and to a lesser extent for carbamoylcholine – a rightward shift in potency but a greater maximal response. The effect of exposure of differentiating cultures to phenylephrine was similarly not restricted to phenylephrine-induced responses. In common with cultures differentiated with glutamate, phenylephrine commonly caused a rightward shift in potency accompanied by greater maximal responses. This effect was observed for intracellular $Ca^{2+}$ accumulation in response to glutamate, carbamoylcholine and

phenylephrine itself. In contrast however, cultures differentiated with phenylephrine were sensitised to histamine and acetylcholine, showing both a slight leftward shift in potency, and a greater maximal responses. These data suggest that rather than increasing the sensitivity of cells to glutamate or phenylephrine when exposed to these ligands during differentiation, the opposite is in fact the case. It is likely that this occurs through receptor downregulation or desensitisation through homeostatic mechanisms to prevent over stimulation of cells, though this would require further investigation to confirm. However, the fact that exposure to these ligands during differentiation also effected responses to other tested agonists, highlights the plastic nature of these cells and their sensitivity to external stimuli. The plastic nature of CTX0E16/02 cultures is also exemplified in the sections above, showing that many different types of external stimulus can bear an influence upon the resulting differentiated cells. However, responses were found to be consistent within tested culture treatments, whereby, cultures exposed to the same differentiation protocol in independent experiments, provided reproducible ligand-induced responses. Reproducibility will be imperative to a successful *in vitro* platform employed for either basic science or drug discovery. While it has been shown that differentiated CTX0E16/02 cultures can be manipulated in many different ways to alter the pharmacological responsiveness of differentiated cultures, it is important that these changes are consistent. An important factor to consider with respect to the reproducibility of data obtained from CTX0E16/02 cultures is how their properties change with time in culture. The following section explores the influence of extended time in culture upon the pharmacological behaviour of CTX0E16/02 cultures.

### *4.2.13 Exploring the Effect of Extended Time in Culture*

Proliferative and differentiated CTX0E16/02 cultures demonstrate good reproducibility with respect to ligand-induced intracellular $Ca^{2+}$ accumulation in response to various compounds, as is clear from standard error values recorded between technical and biological replicates (see Figure 4.8 and Figure 4.9, above). The body of data presented above provides considerable evidence to demonstrate the sensitivity of CTX0E16/02 cells to their environment as indicated by their ligand-induced $[Ca^{2+}]_i$ responses. It should be noted however that all of the data presented above was obtained from CTX0E16/02 cells exposed to between 16 and 22 passages. For a cell line to be adopted either for use as a basic research tool or as a drug screening platform it is important to understand how the behaviour of these cells may change following extended periods in culture as a monolayer. To address whether continuous passage of CTX0E16/02 cultures influences ligand-induced $[Ca^{2+}]_i$ responses, CTX0E16/02 cells were raised from a $13^{th}$ passage frozen stock and continuously expanded to 50 passages. After 30, 40 and 50 passages CTX0E16/02 cultures were plated out onto 96-well plates and assayed either as proliferative cells or exposed to a normal 28 day differentiation before being assayed for $[Ca^{2+}]_i$ responses provoked by various ligands. After 50 passages the CTX0E16/02 cells were frozen in liquid $N_2$ before being raised and re-assayed after a single passage (passage 51). This was performed to determine whether freezing cells influenced their pharmacological properties. Unfortunately, cells seeded onto 96-well plates after 50 passages, to be assayed as proliferative and differentiated cultures suffered due to a

problem with a poor batch of medium. Due to time restraints and the considerable amount of time required to complete this experiment, no data were obtained from cells exposed to 50 continuous passages.

Proliferative and differentiated CTX0E16/02 cultures were tested for their ability to respond to dopamine, 5-HT, glutamate, GABA, histamine, phenylephrine, acetylcholine and carbamoylcholine by measuring $[Ca^{2+}]_i$. As with previous experiments, cultures were additionally exposed to a depolarising 50 mM KCl challenge following the addition of any test compound to determine whether cultures contained electrically excitable cells. Cultures were then exposed to the ionophore ionomycin, to provide a relative fluorescence reading for each experimental well. Data are presented for proliferative and differentiated cultures as either "low passage", which includes mean data from two 96-well plates (one passage 15 and one passage 16 – original experiments for proliferative and differentiated cultures, as seen in Figure 4.8 and Figure 4.9) or "all passages", which includes mean data from the "low passage" plates, along with data from a passage 30, 40 and 51 plate. Data are also presented for ligand-induced $[Ca^{2+}]_i$ responses at each of the passages tested. These experiments generated a particularly large amount of data and so only dopamine, 5-HT and acetylcholine-induced responses are shown below. Responses from these neurotransmitters are discussed because of their relevance to this study, but also because they represent interesting data regarding how the pharmacological properties of these cells change with time in culture. Data for cells exposed to glutamate, GABA, histamine, phenylephrine and carbamoylcholine can however be found in the Appendices – see Supplementary Data ***8.5.1***.

Proliferative CTX0E16/02 cultures did not respond to dopamine at low passages (Figure 4.32, **a**). This remained the case after 30 passages but increased substantially following 40 passages (17 continuous passages – Figure 4.32, **b**). Interestingly, intracellular $Ca^{2+}$ accumulation in response to dopamine was significantly reduced after cells were exposed to a freeze/thaw cycle after 50 passages, though these cells did retain the ability to respond to dopamine in a concentration-dependent manner, as had been observed after 40 passages, but not after 30 passages or lower (Figure 4.32, **b**). Differentiated CTX0E16/02 cultures were also incapable of responding to dopamine by elevating $[Ca^{2+}]_i$ at low passages (Figure 4.32, **c**). Similar to observations from proliferative cultures, this remained the case after 30 passages, while 40 passages produced an increased responsiveness at concentrations greater than 100 µM (Figure 4.32, **d**). In contrast to what was observed in proliferative cultures however, exposing cells to a freeze/thaw cycle after 50 passages, did not reduce dopamine-induced responses compared to those observed after 40 passages (or 17 continuous passages – Figure 4.32, **d**).

Intracellular $Ca^{2+}$ accumulation in responses to 5-HT in proliferative CTX0E16/02 cultures remained largely unchanged with increased time in culture (Figure 4.33, **a** and **b**). Low passage proliferative cultures did not respond to 5-HT, though as the passages increased the cultures were capable of responding to 5-HT, though only at the highest tested concentration of 1 mM (Figure 4.33, **b**). Following freezing however, 5-HT-induced $[Ca^{2+}]_i$ responses dropped back to the levels observed in low passage cultures (Figure 4.33, **b**). In differentiated CTX0E16/02 cultures, responses again increased at the highest

tested concentrations of 5-HT with increased time in culture, and fell back to the levels observed for low passage cultures following freezing (Figure 4.33, **d**).

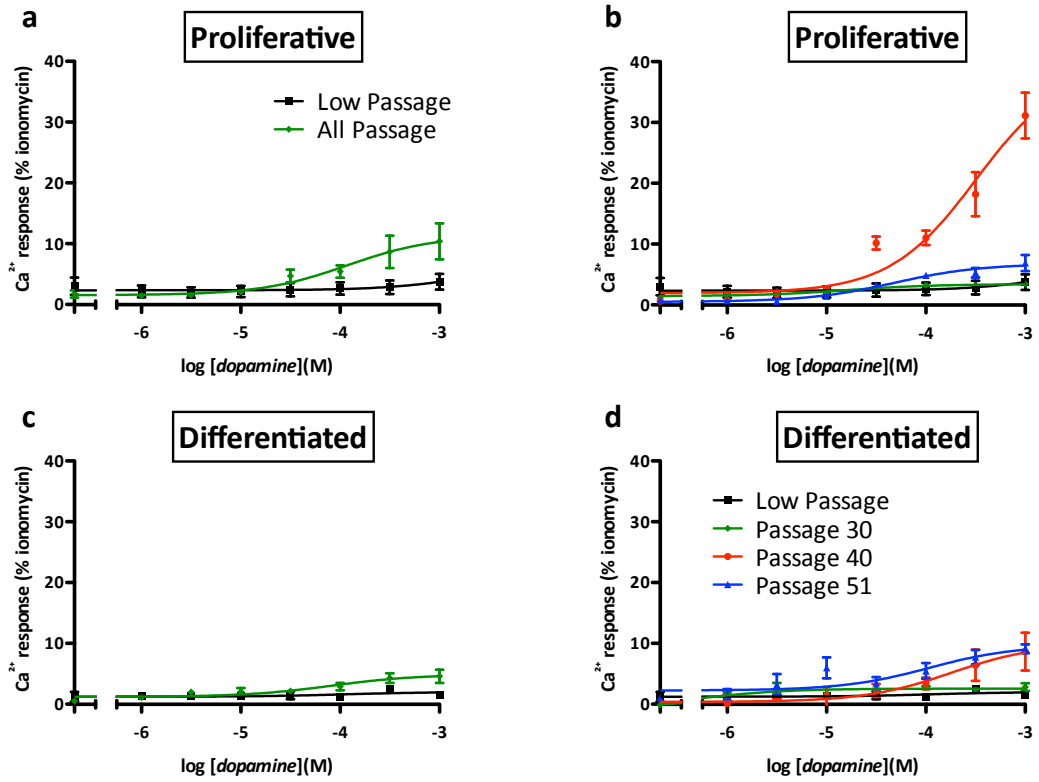


***Figure 4.32 Long-term continuous passage of CTX0E16/02 cells increases dopamine-induced $[Ca^{2+}]_i$ responses in proliferative and differentiated cultures***
Proliferative and differentiated CTX0E16/02 cultures were tested for their ability to respond to dopamine by measuring intracellular $Ca^{2+}$ accumulation. Baseline data or "low passage" (black curves) represents the mean and S.E.M. from two biological replicates (two different frozen cell stocks), each including 3 technical replicates. Higher passage data was the product of continuously expanded CTX0E16/02 cultures with data collected at passage 30 and passage 40. Cells were continuously expanded to passage 50 before being frozen, re-raised and tested at passage 51. Data from all tested passages were pooled to provide the "all passage" category. On the day of the experiment, cells were incubated for 1 hour in the presence of the cell permeable, $Ca^{2+}$-sensitive fluorescent dye Fura-2 AM. Cells were then washed prior to dopamine-induced fluorescence being measured using a FS3. Concentration-response curves are shown for proliferative (**a** & **b**) and differentiated (**c** & **d**) cultures. Panel **b**, $EC_{50}$ = 16 µM and 48 µM. Panel **c**, $EC_{50}$ = 83 µM. Panel **d**, $EC_{50}$ = 1 µM, 180 µM and 108 µM. Data points represent mean ± S.E.M. from *n* = 1 (*n* = 2 for "low passage"), with 3 technical replicates and expressed relative to the positive control, ionomycin.

Once levels of intracellular $Ca^{2+}$ accumulation in response to acetylcholine in proliferative CTX0E16/02 cultures from multiple passages were plotted together, very little variation was observed compared with that seen from low passage cultures (Figure 4.34, **a**). Low passage cells demonstrated an $EC_{50}$ of 1 µM and a maximal response of 18.4% of that evoked by ionomycin, while data from all passages combined exhibited an $EC_{50}$ of 2 µM and a maximal response of 17.1%. These data perhaps belie the changes in acetylcholine-induced intracellular $Ca^{2+}$ accumulation in proliferative CTX0E16/02 cultures at each of the tested passages (Figure 4.34, **b**). With reference to low passage cultures, after 30 passages the $EC_{50}$ was only slightly reduced to 2 µM from 1 µM while the maximal response rose from 18.4% to 23.6%. In contrast, after 40 passages the maximal response was almost identical to that seen from low passage

cultures while the efficacy of acetylcholine to produce an increase in $[Ca^{2+}]_i$ reduced considerably with an $EC_{50}$ of 11 µM (Figure 4.34, **b**). Following further passages and a freeze/thaw cycle, the $EC_{50}$ of acetylcholine-induced responses remained at the level observed after 40 passages (10 µM), though a considerable drop was observed in the maximal response (Figure 4.34, **b**). Intracellular $Ca^{2+}$ accumulation in differentiated CTX0E16/02 cultures in response to acetylcholine changed little at low concentrations while at concentrations above 100 µM the maximal response achieved increased considerably, greatly altering the shape of the two curves (Figure 4.34, **c**). When looking at responses from separate passages (Figure 4.34, **d**), it became clear that there is a considerable rightward shift in potency at higher passages – an effect that does not seem to be reversed by a freeze/thaw cycle of the cells (Figure 4.34, **d**).

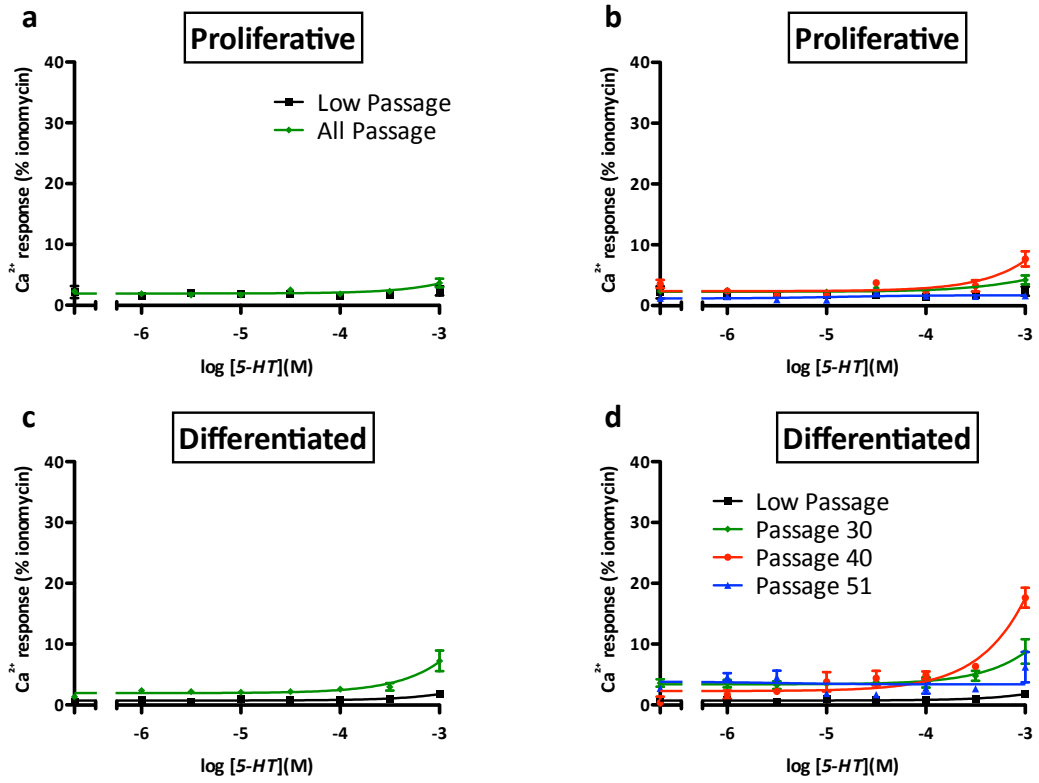


***Figure 4.33 Long-term continuous passage of CTX0E16/02 cells increases 5-HT-induced $[Ca^{2+}]_i$ responses in proliferative and differentiated cultures at high concentrations***

Proliferative and differentiated CTX0E16/02 cultures were tested for their ability to respond to 5-HT by measuring intracellular $Ca^{2+}$ accumulation. Baseline data or "low passage" (black curves) represents the mean and S.E.M. from two biological replicates (two different frozen cell stocks), each including 3 technical replicates. Higher passage data was the product of continuously expanded CTX0E16/02 cultures with data collected at passage 30 and passage 40. Cells were continuously expanded to passage 50 before being frozen, re-raised and tested at passage 51. Data from all tested passages were pooled to provide the "all passage" category. On the day of the experiment, cells were incubated for 1 hour in the presence of the cell permeable, $Ca^{2+}$-sensitive fluorescent dye Fura-2 AM. Cells were then washed prior to 5-HT-induced fluorescence being measured using a FS3. Concentration-response curves are shown for proliferative (**a** & **b**) and differentiated (**c** & **d**) cultures. Data points represent mean ± S.E.M. from $n = 1$ ($n = 2$ for "low passage"), with 3 technical replicates and expressed relative to the positive control, ionomycin.

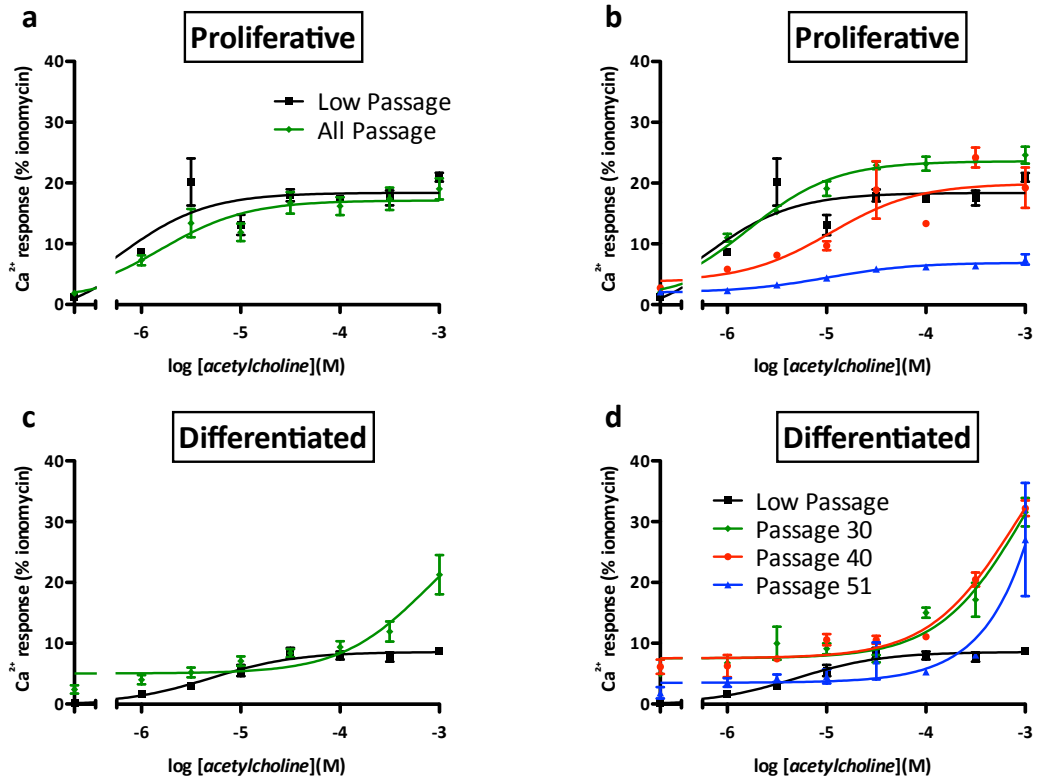


***Figure 4.34 Long-term continuous passage of CTX0E16/02 cells increases acetylcholine-induced $[Ca^{2+}]_i$ responses in differentiated cultures only***

Proliferative and differentiated CTX0E16/02 cultures were tested for their ability to respond to acetylcholine by measuring intracellular $Ca^{2+}$ accumulation. Baseline data or "low passage" (black curves) represents the mean and S.E.M. from two biological replicates (two different frozen cell stocks), each including 3 technical replicates. Higher passage data was the product of continuously expanded CTX0E16/02 cultures with data collected at passage 30 and passage 40. Cells were continuously expanded to passage 50 before being frozen, re-raised and tested at passage 51. Data from all tested passages were pooled to provide the "all passage" category. On the day of the experiment, cells were incubated for 1 hour in the presence of the cell permeable, $Ca^{2+}$-sensitive fluorescent dye Fura-2 AM. Cells were then washed prior to acetylcholine-induced fluorescence being measured using a FS3. Concentration-response curves are shown for proliferative (**a** & **b**) and differentiated (**c** & **d**) cultures. Panel **a**, $EC_{50}$ = 1 µM and 2 µM. Panel **b**, $EC_{50}$ = 1 µM, 2 µM, 11 µM and 10 µM. Panel **c**, $EC_{50}$ = 5 µM. Panel **d**, $EC_{50}$ = 5 µM. Data points represent mean ± S.E.M. from *n* = 1 (*n* = 2 for "low passage"), with 3 technical replicates and expressed relative to the positive control, ionomycin.

Changes in intracellular $Ca^{2+}$ accumulation in response to dopamine, 5-HT and acetylcholine following continuous expansion demonstrated similar characteristics to those observed for glutamate, GABA, histamine, phenylephrine and carbamoylcholine (see Supplementary Data, ***8.5.1***). Rising passage number tended to be associated with an increase in $Ca^{2+}$ accumulation at the higher concentrations tested while freezing cells at high passage appeared in many cases to bring ligand-induced $[Ca^{2+}]_i$ responses back towards that exhibited by low passage cultures. This was not however the case for all compounds. Histamine and phenylephrine, for example, saw a rise in responses from proliferative cells following a freeze/thaw cycle after 50 passages (see ***8.5.1***, Figure 0.3 and Figure 0.4). What does seem clear from these data is that responses from CTX0E16/02 cultures appear to "mature" following continuous expansion, with very little response from many ligands at very low passage that appears to increase with time in culture. An ideal situation may be that cultures should be expanded continuously for 10 to 15 passages from thawing before any testing is performed to allow receptor numbers at the cells surface to

stabilise. For high-throughput applications this would be necessary anyway to obtain sufficient numbers of cells for an assay. Changes in ligand-induced responses following continuous expansion *in vitro* are not confined to conditionally-immortalised NPC lines however. Indeed, heterologous cell lines "stably" expressing receptors for experimental purposes are also commonly affected by changes in responsiveness [14,240].

Taken together, these data show that time in culture does influence the way CTX0E16/02 cultures respond to pharmacological stimulation with respect to their ability to provoke increases in $[Ca^{2+}]_i$. In addition, this is also the case when cells are exposed to freeze/thaw cycles. Arguably, this in itself is not a problem, as long as it is ensured that experiments are performed after the same number of passages after a freeze/thaw cycle. For many of the tested agonists, it appears that performing experiments following at least ten passages in continuous adherent culture, may actually be preferable to performing experiments after less than five passages, as most of the experiments described above were. Indeed measurable responses to dopamine, 5-HT, glutamate and phenylephrine were only observed in proliferative cultures after longer periods in continuous culture. Similarly, longer culture periods were also required to detect measurable responses to dopamine, 5-HT, GABA and histamine in differentiated cultures. The maximal responses observed for many ligands tended to become more robust following multiple passages, though was frequently accompanied by a rightward shift in potency. What is perhaps required is that CTX0E16/02 cultures should be optimised so as to identify an ideal period of continuous culture that provides the greatest sensitivity to the greatest range of ligands. This period could then be used for further downstream experiments. Fortunately, it appears from these preliminary data, that at least ten consecutive passages would be needed to reach this point, meaning that sufficient numbers of cells would be able to be generated, even for very large experiments. For example, from a single vial of cells raised into a T75 flask, a conservative split of 1:3 for ten continuous passages would yield more than 59,000 T75 flasks of cells.

It should be noted that increased time in continuous culture did not lead to the appearance of detectable electrical excitability in proliferative or differentiated cultures. However, based on the data presented above, it may be desirable to attempt to provoke the appearance of this property after further time in passage. It would appear from these data that more functional receptors are found at the plasma membrane after longer periods in culture – as indicated by the appearance of larger ligand-induced increases in $[Ca^{2+}]_i$ – a property that may also translate to the appearance of VDIC at the cell surface.

### *4.2.14 Summary*

This chapter has provided evidence detailing the multipotent nature of CTX0E16/02 NPCs with respect to their capacity to be differentiated into neurons and astrocytes, with some evidence provided of cells capable of expressing markers indicative of oligodendrocytes – though these lacked characteristic morphology. In addition, evidence has been presented showing that these cultures generate both

glutamatergic and GABAergic neuronal subtypes (***4.2.1***). We have seen that both proliferative and differentiated CTX0E16/02 cultures express functional neurotransmitter receptors through their ability to modulate $[Ca^{2+}]_i$ in response to both endogenous and synthetic ligands. Considerable differences were observed between proliferative and differentiated cultures with respect to their responsiveness to these tested ligands. Single cell $Ca^{2+}$ imaging was used to demonstrate that these differences were partly attributable to an increase in the heterogeneity of cells within differentiated cultures, with respect to their ability to respond to different ligands. This analysis also showed that differentiated cells were capable of relatively modest ligand-induced intracellular $Ca^{2+}$ accumulation compared to their proliferative counterparts. Through the manipulation of proliferative and differentiated CTX0E16/02 cultures in various different ways, it has been shown that ligand-induced responses are remarkably plastic. However, it was also found that individual manipulations of the culture system, effected different neurotransmitter systems in different ways; shifting potency and maximally evoked responses in either direction, depending upon the ligand tested.

By accessing levels of intracellular $Ca^{2+}$ accumulation in individual cells it was shown that a small number of cells in both proliferative and differentiated CTX0E16/02 cultures were capable of demonstrating electrical excitability. This was determined by their ability to flux $Ca^{2+}$ in response to a depolarising $K^+$ challenge, though the levels observed were not indicative of a mature neuronal phenotype. Several different strategies were tested for their capacity to precipitate electrical excitability, and it was found that this could be achieved either though simply extending the period of differentiation or by the addition of trophic support. Furthermore, it was found that combining these two approaches exerted an additive influence upon electrical excitability. Finally, it was found that through continuously passaging CTX0E16/02 cells in adherent culture, cultures became more sensitive to many of the investigated ligands. This indicated that pharmacological experiments should be performed after at least ten passages after thawing to ensure that sufficient signals are transduced to the intracellular environment in order to detect measurable responses.

Data presented in this chapter illustrates the sensitivity and plasticity of the CTX0E16/02 cell line. Ligand-induced intracellular $Ca^{2+}$ accumulation in response to a variety of compounds was profoundly affected by differentiation of the cells. These responses have proven malleable by extending the period of differentiation, expanding the cells as neurospheres prior to differentiation or exposing differentiating cultures to a variety of trophic factors and pharmacological agents. Through these various forms of manipulation, the CTX0E16/02 cells have proven capable of exhibiting voltage-dependent $Ca^{2+}$ responses, and the ability to modulate intracellular $Ca^{2+}$ accumulation in response to various different ligands. While single cell Ca2+-imaging data has shed light upon why some of these changes occur at the level of the whole culture, what is less clear are the changes that occur within cells, that are responsible for these changes. Could an increase in dopamine-induced $[Ca^{2+}]_i$ following repeated in vitro expansion be due to a simple increase in receptor number or the product of promiscuity of downstream signalling events? Could increased phenylephrine responsiveness following exposure to dibutyryl-cAMP and IBMX be attributable to simple amplification through signalling crosstalk, or is it a

product of post-translational modification of adrenergic receptors by PKA? These data appear to have raised more questions than have been sufficiently answered, and at this stage it seems unclear whether the responses observed are in any way consistent with the situation in vivo – what this cellular platform ultimately seeks to model. A particular difficulty in this respect is the paucity of available data from similar cell lines to make comparisons with. Almost no data regarding this avenue of research are available in the literature. Surprisingly, not a single publication describing the pharmacological properties of immortalised human NPC lines could be found through PubMed searches. For non-immortalised NPCs, only reports relating to responses to acetylcholine appear to exist [61]. To address this situation, it was decided to compare the characteristics of the CTX0E16/02 cell line with primary human neural foetal tissue. ***Chapter 5*** provides a pharmacological comparison of both proliferative and differentiated CTX0E16/02 cultures with equivalent cultures from primary human neural foetal tissue.

# *Chapter 5 Comparison of CTX0E16/02 to Primary NSC Cultures*

In attempting to develop a model system to explore intracellular signalling in native human cells, it is important to ensure that the system is as representative as possible of the cells we hope to model. Ultimately, it is hoped that the CTX0E16/02 cell line – as described above – can be used to investigate the mechanism of action of antipsychotic medicines. This cell line was isolated from the developing human cortex, an area which – in adulthood – is implicated both in the pathophysiology associated with schizophrenia and as a substrate through which antipsychotics are thought to exert, at least a portion of, their therapeutic effects [114,115,323]. Data presented in ***Chapter 3*** showed that CTX0E16/02 cells are capable of robust and reproducible differentiation into neurons and glial cells. Upon differentiation these cells were shown to express mRNA for genes encoding a broad range of receptors, accessory proteins and signalling molecules, identified as important with respect to how antipsychotics are currently thought to transduce their effects to the intracellular environment (see Table 3.9 and Table 3.10, above). Furthermore, evidence has also been provided in ***Chapter 4*** showing that differentiated CTX0E16/02 cultures contain cells capable of functionally responding to endogenous neurotransmitter ligands, many of whose cognate receptors are known to be targeted by antipsychotic drugs [183]. A direct *in vitro* comparison between differentiated CTX0E16/02 cultures and the cells that comprise the adult human cortex is made difficult for the same reasons that have led the neuroscience community to embrace the use of NPCs in the first place, primarily the scarcity of primary tissue and the non-expandable nature of neurons – as detailed in ***1.1*** and 1.2 above.

It is important, however, to ensure that the cellular characteristics observed for differentiated CTX0E16/02 cultures are comparable to those exhibited by similar cells from the *in vivo* environment from which they originate. This is especially important, since the CTX0E16/02 cells have been conditionally immortalised using a c-mycER$^{TAM}$ transgene, a genetic modification for which the influence on the physiological behaviour of these cells remains unclear, though such conditionally immortalised lines are now in clinical trials for the treatment of stroke [111]. To address these concerns, this chapter provides a comparison between the observed characteristics of CTX0E16/02 cultures and those derived from primary human embryonic neural tissue samples.

## *5.1 Introduction*

Recent developments in our understanding of receptor pharmacology have highlighted the limitations of heterologous expression systems, and emphasised the importance of using native tissues to study the intracellular signalling consequences of ligand binding – as discussed in ***1.1***. For neuroscientists this poses a difficult problem. Unsurprisingly, *ex vivo* human neural tissue is difficult to source and upon expansion often results in an enrichment of glial cells due to the post-mitotic nature of neurons. It has been shown that NPCs can, however, be isolated from post-mortem adult human brain, though yields are low, especially from regions other than the dentate gyrus and the sub-ventricular zone of the lateral ventricles, and the proliferative capacity of these cells appears to diminish as the age of the donor

increases [54,416]. On the other hand, NPCs isolated from embryonic tissue demonstrate a less restricted proliferative capacity, and can theoretically be isolated from all regions of the developing human brain [46,51]. They bring with them however, considerable ethical and societal concerns, problems that have been partially circumvented through the use of conditional immortalisation – as was used in the generation of the CTX0E16/02 line – by removing the need to source further embryonic tissue [62], or more recently through the generation of iPS and iN cells [71,75,81,87].

Use of the CTX0E16/02 cells as a model system to help elucidate the mechanism of action of antipsychotics is just that – a model. We cannot hope to recapitulate the complexity of the human brain in a dish, and this is not what is attempting to be achieved in this study. Indeed, what we wish to generate is a simplified model that allows the transcriptional consequences provoked by the interaction of antipsychotics with various cell surface receptors to be examined.

Neurons are a heterogeneous group of cells that can differ with respect to their size, shape, location, connectivity, excitability and receptor expression diversity, density and associated signalling partner coupling [417]. For example, large glutamatergic cortical pyramidal neurons of the cortex are known to project to a range of different locations including the striatum, hippocampus, spinal cord and contralateral hemisphere, while the projections of their neighbouring, small GABAergic interneurons are restricted within the cortex. Each of these cell types must be capable of decoding signals from a variety of other types of neurons, which themselves release different neurotransmitters [335,418,419]. This does not however prevent receptors from being characterised based on the responses they provoke, neurons from being categorised into subtypes based on their physiological properties or grouping of neurons based on their role within a circuit. The same is of course true when describing receptor pharmacology. Heterologous expression of a receptor of interest in lines such as HEK and COS-7 cells have provided relatively exact information regarding the affinity of a receptor for a ligand or the potency of a ligand to provoke a specific response. However, this approach is perhaps too Spartan when considering the effect of a ligand at the transcriptional level. Receptor activation provokes a series of signalling events and the nature and magnitude of this response – in the case of GPCRs – is dictated by a range of different factors including the type of receptor activated, the state of the receptor (active or inactive), the G-protein coupling partner present, and the type and number of downstream signalling molecules containing relevant signalling domains to permit their activation. This rendition is crudely simplistic, but highlights why the use of native tissues is desirable when attempting to investigate transient signalling and the subsequent transcriptional consequences of ligand binding at the cell surface. While differentiated NPCs – such as those derived from CTX0E16/02 cultures – cannot hope to exactly recapitulate the signalling complexity of the whole human brain, they may represent a happy median. These cells represent a system where receptor expression and downstream signalling pathways are more representative of the native tissues they seek to model, compared with the situation where a single receptor is expressed in a non-neural cell type, and therefore represent a valuable research tool.

During development the brain is generated from the neural tube comprising a single cell layer of neural stem cells, called neuroepithelial cells. Through a battery of intrinsic and extrinsic cues [331,417], these

neural stem cells generate different populations of progenitor cells that in turn generate the cell types required to generate the different brain regions and hence a functional brain. The CTX0E16/02 cell line represents an immortalised, clonal, population of neural progenitor cells isolated from the developing human cortex. To further validate the use of the CTX0E16/02 cell line, research described in this chapter determines how faithfully this line reflects the phenotypic and pharmacological properties of primary human foetal tissue. This was pursued through a series of experiments describing the phenotypic and transcriptional characteristics of primary NPCs when grown under proliferative and differentiation conditions, and comparing these finding to those obtained for CTX0E16/02 cells grown under similar conditions. A comparison of primary human foetal tissue and CTX0E16/02 cultures' ligand-induced $Ca^{2+}$ signalling and electrical properties are also provided.

## *5.2 Results*

Primary human foetal tissue was obtained from the MRC-Wellcome Trust Human Development Biology Resource (HDBR) at the Institute of Child Health, London, in accordance with UK ethical and legal guidelines. All cultures were derived from 7 – 8-week gestation whole foetal brain samples, and therefore represented a mixed cell population, unlike the clonal CTX0E16/02 line, though were the closest representative primary NPC source available. While the CTX0E16/02 cell line was derived from 12-week gestation foetal brain, 7 – 8-week gestation was the latest time point from which tissue was available. Both of these time points are however dominated by proliferation of NSCs/NPCs – a process that continues at an aggressive rate up until 25-weeks of gestation [420].

On arrival, tissue samples were dissociated through gentle trituration and plated directly onto either laminin-coated flasks for expansion, PDL and laminin-coated coverslips for immunostaining, or laminin-coated 96-well plates to determine ligand-induced $Ca^{2+}$ responses in proliferative cultures (see ***2.1.4***). Once cultures grown in 96-well plates had reached confluence, and were therefore ready to be assayed using the FS3, cultures grown on coverslips were fixed and cultures set aside for expansion were split; with a fraction dissolved in TRIzol and stored at -80°C for subsequent gene expression analysis. In this way, cells were cultured in the same environment – as proliferative, adherent cultures on laminin-coated tissue culture plastic – for the same period of time, and were therefore used to investigate and correlate gene expression with observed ligand-induced $Ca^{2+}$ responses and phenotypic characteristics. Depending on the primary tissue sample, confluence within 96-well plates was reached between 6 to 16 days. This period was influenced both by the amount of sourced tissue and the rate of growth of the cultures. The cells that remained from the split used to obtain material for gene expression analysis – as described above – were seeded onto a laminin-coated flask for further expansion. Once a sufficient number of these cells were available they were seeded onto a 96-well plate, glass coverslips and a T75 flask, and differentiated for 28 days under conditions optimised for the CTX0E16/02 line (see ***2.1.3*** and ***3.2.6***). These cultures were used to determine ligand-induced $Ca^{2+}$ responses, perform phenotypic evaluation using immunofluorescence and for gene expression analysis, respectively in differentiated cultures. The time needed to generate sufficient cells for differentiation varied between samples and

ranged from 20 (2 samples, 3 passages) to 22 days (3 samples – 3 passages for 1 sample and 5 passages for 2 of these samples, see Table 5.1). Remaining cells were set aside for continued expansion, and split so as to obtain a confluent 96-well plate and a T75 flask of proliferative cells after spending exactly 28 days in adherent, monolayer (ML) culture. This 96-well plate of cells was used to assess ligand-induced $Ca^{2+}$ responses in proliferative cultures using a FS3, while cells from the flask were dissolved in TRIzol and stored at -80°C for RNA analysis to determine expression levels of relevant genes following 28 days of proliferative growth as an adherent monolayer. Different samples demonstrated variable doubling periods, and in some cases required additional passages to provide the number of cells required for each experiment. Information regarding the time taken for each sample to reach each assay milestone are summarised in Table 5.1, below.

| Sample | 1 | 2 | 3 | 4 | 5 |
|---|---|---|---|---|---|
| Dissociation & seeding | Day 0 | Day 0 | Day 0 | Day 0 | Day 0 |
| Initial proliferative: FS3 assay & RNA | Passage 0 Day 6 | Passage 0 Day 6 | Passage 0 Day 9 | Passage 0 Day 16 | Passage 0 Day 12 |
| Split for differentiation | Passage 5 Day 22 | Passage 5 Day 22 | Passage 4 Day 22 | Passage 3 Day 20 | Passage 3 Day 20 |
| Initiation of differentiation | Passage 5 Day 23 | Passage 5 Day 23 | Discarded | Passage 3 Day 22 | Passage 3 Day 22 |
| 28 Day monolayer (ML) proliferative: FS3 assay & RNA | Passage 7 Day 28 | Passage 7 Day 28 | Passage 6 Day 28 | Passage 5 Day 28 | Passage 5 Day 28 |
| Differentiated: FS3 assay, RNA & fix coverslips | Passage 5 Day 51 | Passage 5 Day 51 | Discarded | Passage 3 Day 50 | Passage 3 Day 50 |

***Table 5.1 Culture details for each primary human neural tissue sample***

Proliferative and differentiated CTX0E16/02 cultures were compared with those derived from primary human neural tissue samples by assessing the phenotypic characteristics, gene expression and ligand- and KCl-induced $Ca^{2+}$ responses. As described above, proliferative primary human neural cultures were assessed at two time points; the first being cultures that had reached confluence following plating immediately after dissociation of the primary tissue samples. The second time point represented cultures that had been in continuous culture as an adherent monolayer for 28 days, in an attempt to more accurately mimic proliferative CTX0E16/02 cultures, by enriching the number of NPCs, while also exposing them to the same culture conditions. Following initial dissociation of the primary tissue samples, all subsequent tissue culture methods were performed in exactly the same way as for the CTX0E16/02 line. This included the use of 4-OHT, despite the primary cultures not containing the conditionally immortalising c-mycER$^{TAM}$ transcript, as it was felt this would ensure a more controlled experimental paradigm by enabling the influence of any off-target effects of 4-OHT to be eliminated from the comparison. While the c-mycER$^{TAM}$ transcript encodes a mutated oestrogen receptor that is not activated by oestrogen, this does not eliminate the possibility that 4-OHT may exert an influence upon endogenous oestrogen receptors that may be expressed in these cells [421,422].

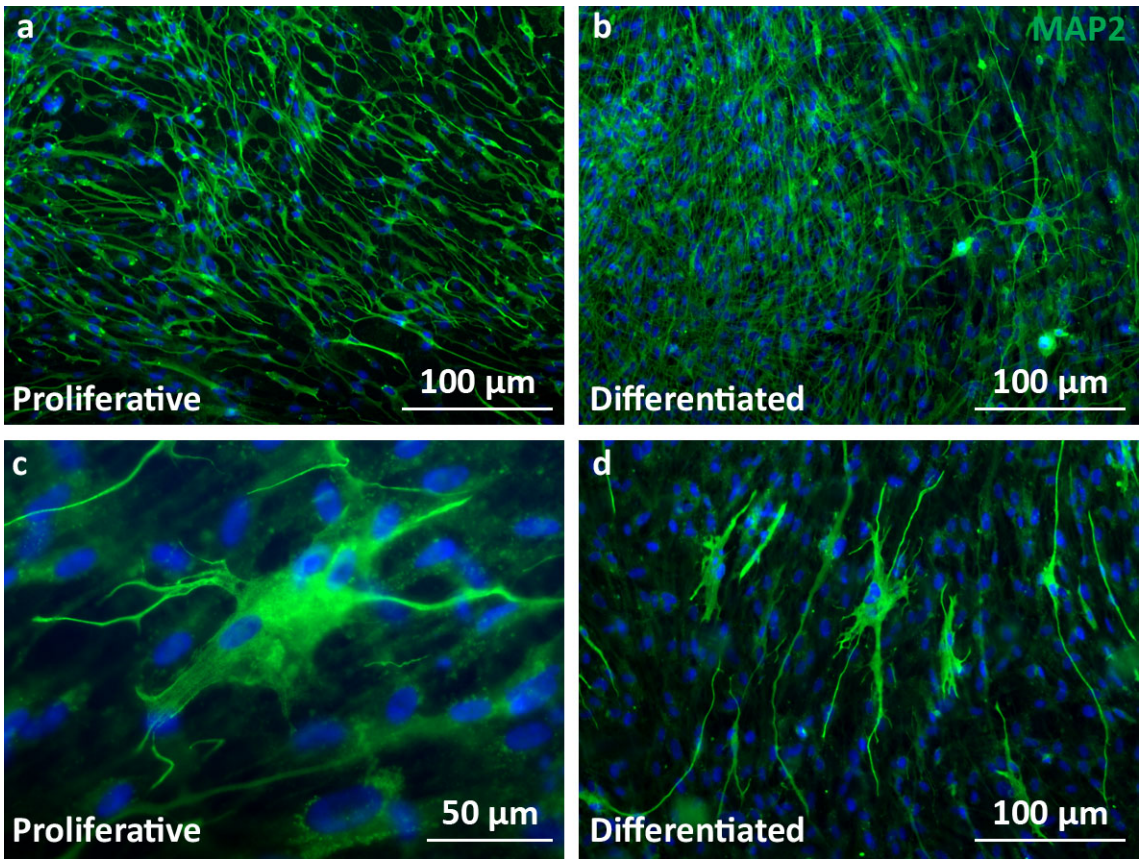


***Figure 5.1 Proliferative and differentiated primary cultures include a high proportion of neurons***
Representative images of proliferative and differentiated primary cultures. Panels **a** & **c** show proliferative primary cultures, while panels **b** and **d** show primary cultures differentiated using SNBM for 28 days. All cultures were stained for the neuronal marker MAP2 (green) and DAPI to label cell nuclei. Pictures were taken using a Zeiss Axio Imager equipped with an ApoTome.

### *5.2.1 Primary Cultures Contain a High Proportion of Neurons*

Proliferative and differentiated cultures derived from primary human embryonic neural tissue samples were prepared as described above. Cultures were then fixed and stained for the neuronal marker MAP2, with nuclei counterstained using DAPI. Surprisingly, both proliferative and differentiated cultures contained a high proportion of $MAP2^{+}$ neurons, as is clear from the representative images shown in Figure 5.1. Broadly speaking, proliferative cultures tended to be comprised of neuronal cells with larger cell bodies and shorter processes (Figure 5.1, **a** and **c**), while neuronal cells within differentiated cultures tended to have smaller cell bodies with longer, more elaborate processes (Figure 5.1, **b** and **d**). However, the appearance of proliferative and differentiated cultures – with respect to the number of MAP2 expressing neurons appeared strikingly similar. This is in contrast to that observed for CTX0E16/02 cultures, where MAP2 immunoreactivity was absent in proliferative cultures. This is attributable however, to the fact that CTX0E16/02 cells represent a clonal NPC line while these data provide evidence that even at this early stage in human neural development (7 – 8 weeks gestation), a considerable number of neurons have already differentiated. This is consistent with a previous report from Bystron and colleagues, who provided evidence of the appearance of neurons as early as 31 days gestation in human foetal forebrain [423].

### *5.2.2 Primary Cultures Demonstrate Comparable Gene Expression to CTX0E16/02 Cells*

Total RNA was extracted from each of five, primary human neural tissue samples to correspond with equivalent cultures in 96-well plates that were used to assess ligand-induced intracellular $Ca^{2+}$ accumulation. These experiments were performed on each primary tissue sample that had been dissociated and plated on day of collection and grown under proliferative, adherent conditions until confluent (designated 'P' for proliferative), or after they had been in continuous, adherent monolayer expansion for 28 days (designated 'ML' for monolayer). RNA was also extracted from these primary cultures after they had been differentiation for 28 days (designated 'D' for differentiated), as described in ***3.2.6***. Expression was tested for the same genes that were assessed previously in a range of conditionally immortalised NPCs, as summarised in Table 3.9 and Table 3.10, above. For direct comparison, the expression of each gene was also tested in proliferative and differentiated CTX0E16/02 cultures, with PCR products run alongside those for primary cultures in the same gels.

As was the case for all of the NPC lines tested previously (see Table 3.9), both the dopamine $D_2$ and the histamine $H_1$ receptor were ubiquitously expressed at the message level in all conditions for all primary tissue samples (Figure 5.2). The same was true of the four tested GPCR accessory proteins: β-arrestin 2, caveolin-1, PSD-95 and MUPP1 (Figure 5.2). The gene encoding the 5-$HT_{2A}$ receptor (*HTR2A*) was also expressed to some extent in all tested conditions for the primary cultures, though weak expression was observed in expanded cultures (ML). Expression of genes encoding some of the tested GPCRs exhibited a definite pattern between the different culture conditions for the primary samples. For example, the expression of *CHRM1*, *ADRA1A* and *TACR3* had high levels of expression in non-expanded proliferative cultures (P), while expression of these genes was either absent or very weak in expanded proliferative cultures (Figure 5.2). Upon differentiation, the expression of these three genes either remain absent, or were expressed at a level below that seen in the non-expanded proliferative cultures (P). Expression of the gene encoding the dopamine $D_3$ receptor was seen to some extent in all conditions for all primary samples, though very weak expression was detected in non-expanded proliferative cultures for sample one (Figure 5.2).

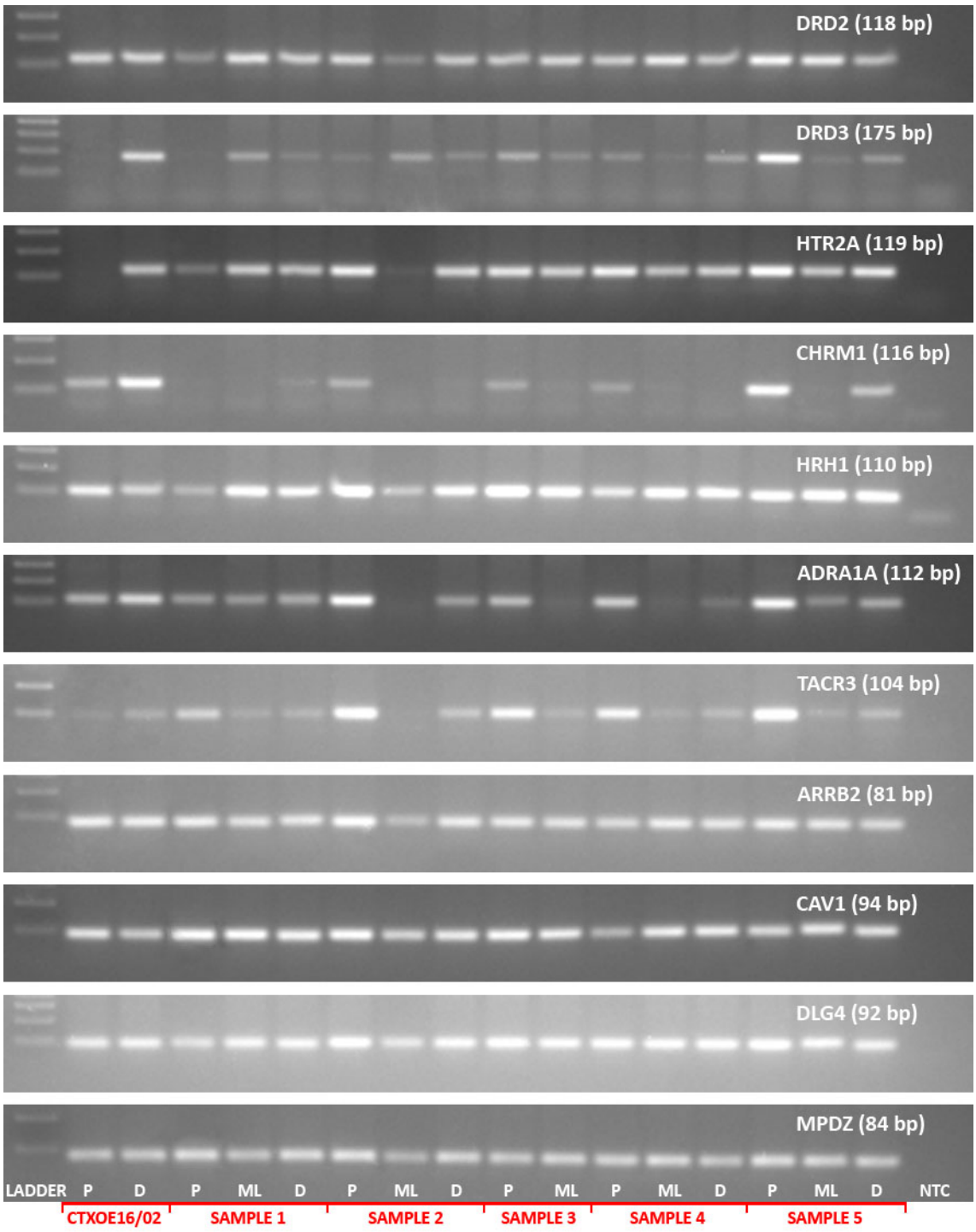


***Figure 5.2 GPCR and GPCR accessory protein gene expression in CTX0E16/02 and primary cultures***

Semi-quantitative PCR analysis of CTX0E16/02 and primary NPC cultures with respect to the expression GPCRs targeted by currently available and putative antipsychotics: DRD2 and DRD3 encoding the dopamine $D_2$ and $D_3$ receptors, HTR2A encoding 5-$HT_{2A}$, CHRM1 encoding cholinergic muscarinic $M_1$, HRH1 encoding histamine $H_1$, ADRA1A encoding adrenergic $\alpha_{1A}$ and TACR3 encoding tachykinin $NK_3$ receptors. The expression of four GPCR accessory proteins are also shown: ARRB2 encoding β-arrestin 2, CAV1 encoding caveolin-1, DLG4 encoding PSD-95 and MPDZ encoding MUPP1. Individual lanes represent expression of these genes in proliferative (P) or normally differentiated (D) CTX0E16/02 cultures or five different primary cultures as proliferative cultures as soon as they had reached confluence after initially being seeded as adherent proliferative cultures (P), after 28 days in adherent monolayer culture (ML) or following differentiation (D). Each gel included a no template negative (-ve) control.

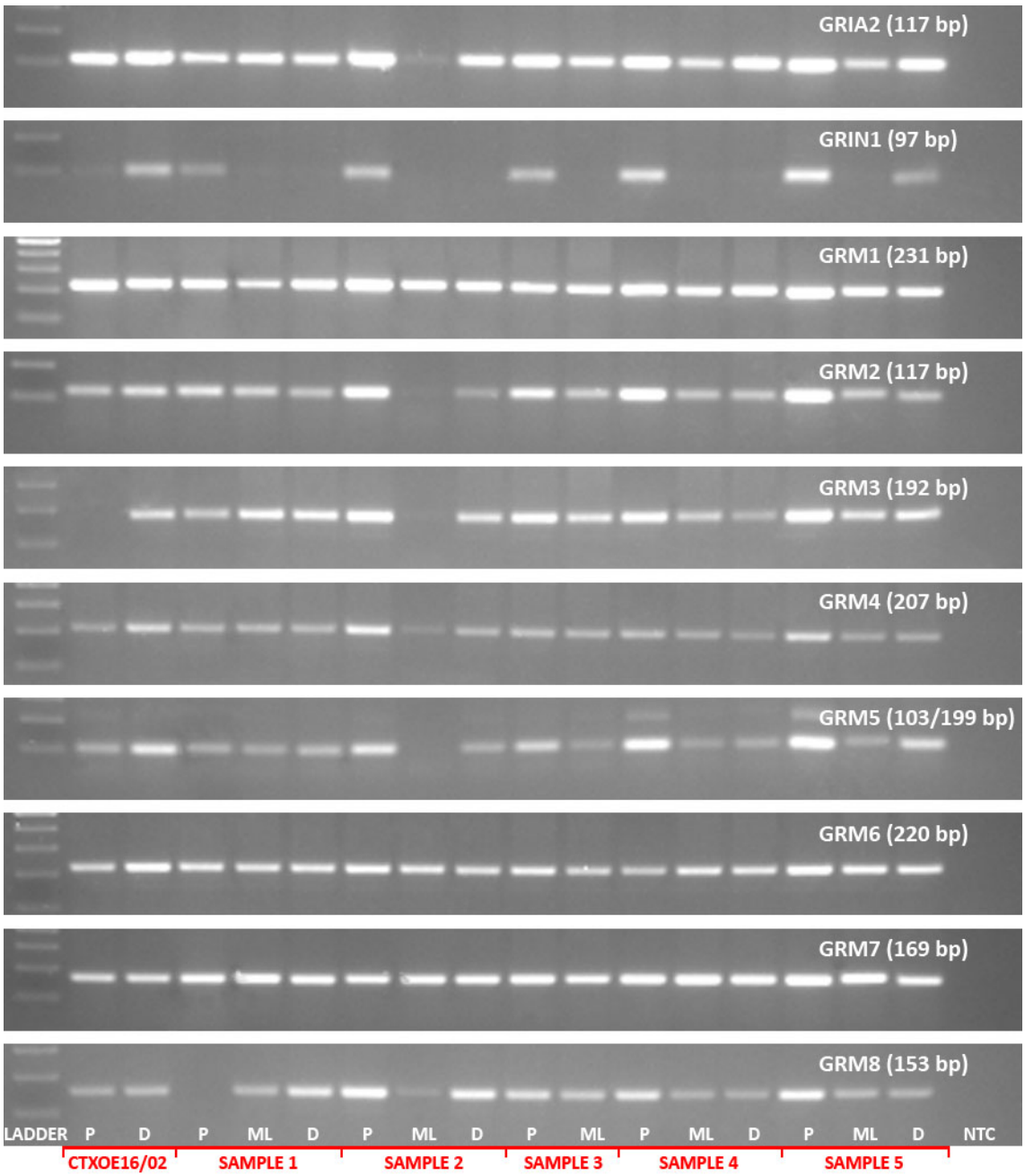


***Figure 5.3 Expression of glutamate receptors and receptor subunits in CTX0E16/02 and primary cultures***
Semi-quantitative PCR analysis of CTX0E16/02 and primary NPC cultures with respect to genes encoding ionotropic glutamate receptor subunits and all metabotropic glutamate receptors: GRIA2 encoding the AMPA receptor subunit GluR2, GRIN1 encoding the NMDA receptor subunit NR1, GRM1 – GRM8 encoding the metabotropic glutamate receptors mGluR1 – mGluR8 respectively. Individual lanes represent expression of these genes in proliferative (P) or normally differentiated (D) CTX0E16/02 cultures or five different primary cultures as proliferative cultures as soon as they had reached confluence after initially being seeded as adherent cultures (P), after 28 days in adherent monolayer culture (ML) or following differentiation (D). Each gel included a no template negative (-ve) control.

With respect to genes encoding ionotropic glutamate receptor subunits; while the AMPA receptor subunit GluR2 was expressed to some extent in all tested conditions for all primary samples, the NMDA receptor subunit, NR1 was only expressed in non-expanded proliferative cultures (P) with the exception of the differentiated cultures (D) from sample five (see Figure 5.3). The expression of this gene was not seen in any expanded proliferative primary cultures. Genes encoding the metabotropic glutamate receptors $mGluR_1$, $mGluR_6$ and $mGluR_7$ were robustly expressed in all conditions for all samples (Figure

5.3). Similarly, $mGluR_2$, $mGluR_3$ and $mGluR_4$ were expressed in all samples, though weak expression was observed for each of these genes in sample two after proliferative expansion (ML). Expression of $mGluR_5$ was also present in each tested sample with the exception of sample two after proliferative expansion (ML), where the expression of this gene was absent. As was described previously for the expression of *CHRM1*, *ADRA1A* and *TACR3*, the highest levels of expression for most of the metabotropic glutamate receptors was seen in non-expanded proliferative cultures, with lower or absent expression in differentiated cultures or expanded proliferative cultures (Figure 5.3).

Expression was detected to some degree in all primary samples under each of the tested conditions for the genes encoding the $\alpha_{1C}$ subunit of the L-type $Ca_v$ channel, DARPP-32 and GSK-3β (see Figure 5.4). Expression of the $GABA_A$ $\alpha_{1A}$ receptor subunit and the 5-HT transporter (SERT) exhibited a similar pattern of expression to several of the GPCRs described above – that of high expression in non-expanded proliferative cultures (P), and either very low or absent expression in differentiated cultures (D) or expanded proliferative cultures (ML) (see Figure 5.4). In contrast, expression of the arginine vasopressin $AVPR_{1A}$ receptor did not show a set pattern of expression between the tested culture conditions for the five primary samples (see Figure 5.4).

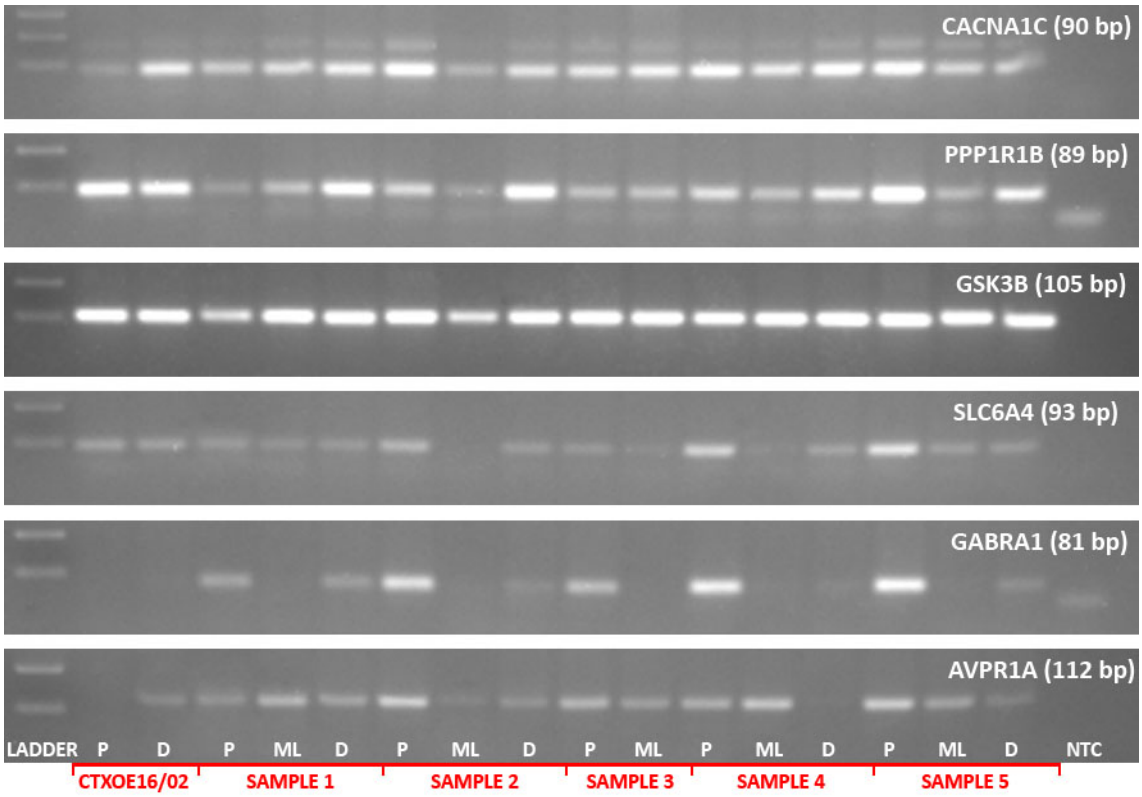


***Figure 5.4 Expression of genes related to diverse neuropsychiatric disorders in CTX0E16/02 and primary cultures***
Semi-quantitative PCR analysis of CTX0E16/02 and primary NPC cultures with respect to genes encoding proteins implicated in the aetiology of and mechanism of drug treatment for different neuropsychiatric disorders: CACNA1C encoding the $\alpha_{1C}$ subunit of the $Ca_v1.2$ channel. PPP1R1B and GSK3B encoding DARPP-32 and GSK-3β respectively, SLC6A4 encoding the 5-HT transporter (SERT), GABRA1 encoding the $GABA_A$ $\alpha_{1A}$ subunit and AVPR1A encoding the arginine vasopressin $AVPR_{1A}$ receptor. Individual lanes represent expression of these genes in proliferative (P) or normally differentiated (D) CTX0E16/02 cultures or five different primary cultures as proliferative cultures as soon as they had reached confluence after initially being seeded as adherent cultures (P), after 28 days in adherent monolayer culture (ML) or following differentiation (D). Each gel included a no template negative (-ve) control.

Differentiation of the seven NPC lines described in ***Chapter 3*** above, was accompanied by an increase in the range of the different genes that these cells expressed. With respect to the 27 genes for which expression was examined, only in a few cases was reduced gene expression observed following differentiation (*DRD3* and *CHRM1* in HPC03A/07, *GRM8* in STROC05/08A and *HRH1* in CTX0E16/02 cells, see Table 3.9 and Table 3.10). If expression was detected in proliferative cultures this tended to be intensified following differentiation, and for many genes that were not expressed in proliferative cultures, expression appeared following differentiation. In no case was a gene expressed in proliferative cultures but not in differentiated cultures of the same cell line. This trend was also reflected in cultures derived from primary neural tissue samples – as shown in Figure 5.2, Figure 5.3 and Figure 5.4, above. Primary cultures expanded for 28 days as proliferative cultures (to mimic proliferative NPC cultures by enriching cells capable of self renewal) tended to demonstrated a limited range of expression with respect to the genes tested. However, differentiation of these primary cultures saw an increase in both the range of the different genes expressed and also the intensity. Rare exceptions did appear, but were not consistent across all primary samples with the exception of *AVPR1A*, and may reflect differences in the cells that comprised the primary samples as the neural region from which these were derived may not have been consistent. Interestingly, the breadth and intensity of different genes expressed was often highest in cultures that were immediately plated following sample dissociation. This is perhaps unsurprising however, when we consider the high proportion of neurons present within these cultures (see Figure 5.1).

### *5.2.3 Maintaining Primary Cells in Adherent Culture Alters Ligand-Induced $Ca^{2+}$ Responses*

Levels of intracellular $Ca^{2+}$ accumulation in response to dopamine, 5-HT, glutamate or acetylcholine were measured in proliferative primary cultures (both non-expanded and expanded for 28 days) using a FS3 plate reader. Observed responses were compared to those exhibited by proliferative CTX0E16/02 cultures. In general, non-expanded, primary proliferative samples demonstrated some differences in their responses to ligands when compared to proliferative CTX0E16/02 cultures, however, the response of expanded primary cultures were strikingly similar. Neither non-expanded, or expanded proliferative primary cultures were capable of elevating $[Ca^{2+}]_i$ in response to dopamine – as was observed in proliferative CTX0E16/02 cultures (see Figure 5.5, **a**). However, all three cultures appeared to show a slight increase in $[Ca^{2+}]_i$ in response to dopamine at the highest tested concentration of 1 mM, though this failed to reach significance in each case. Non-expanded, primary proliferative cultures demonstrated a small concentration-dependent increase in $[Ca^{2+}]_i$ in response to 5-HT with a predicted $EC_{50} \approx 190$ µM. This represents a rightward shift in potency from what might be expected based on the nM affinity of 5-HT for most of it's endogenous receptors [424], though this reduced efficacy may be due to the maximal response remaining so low (just 3% with respect to ionomycin-evoked responses above baseline), suggesting the assay was insufficiently sensitive to detect receptor mediated $Ca^{2+}$ accumulation at lower concentrations. Once the cells had been expanded as a monolayer for 28 days prior to testing however, this concentration-dependent increase in $[Ca^{2+}]_i$ from 100 µM and above was

replaced by a response only at the highest tested concentration of 1 mM, similar to that exhibited by proliferative CTX0E16/02 cultures (Figure 5.5, **b**). This effect was mirrored by glutamate-induced $Ca^{2+}$ responses (Figure 5.5, **c**). While small, concentration-dependent, intracellular $Ca^{2+}$ accumulations were observed in response to glutamate in non-expanded cultures, this was eliminated following expansion, as was observed in CTX0E16/02 cultures. For glutamate – unlike 5-HT – no response at the highest tested concentrations of 1 mM was observed in expanded primary, or proliferative CTX0E16/02 cultures (Figure 5.5, **c**).

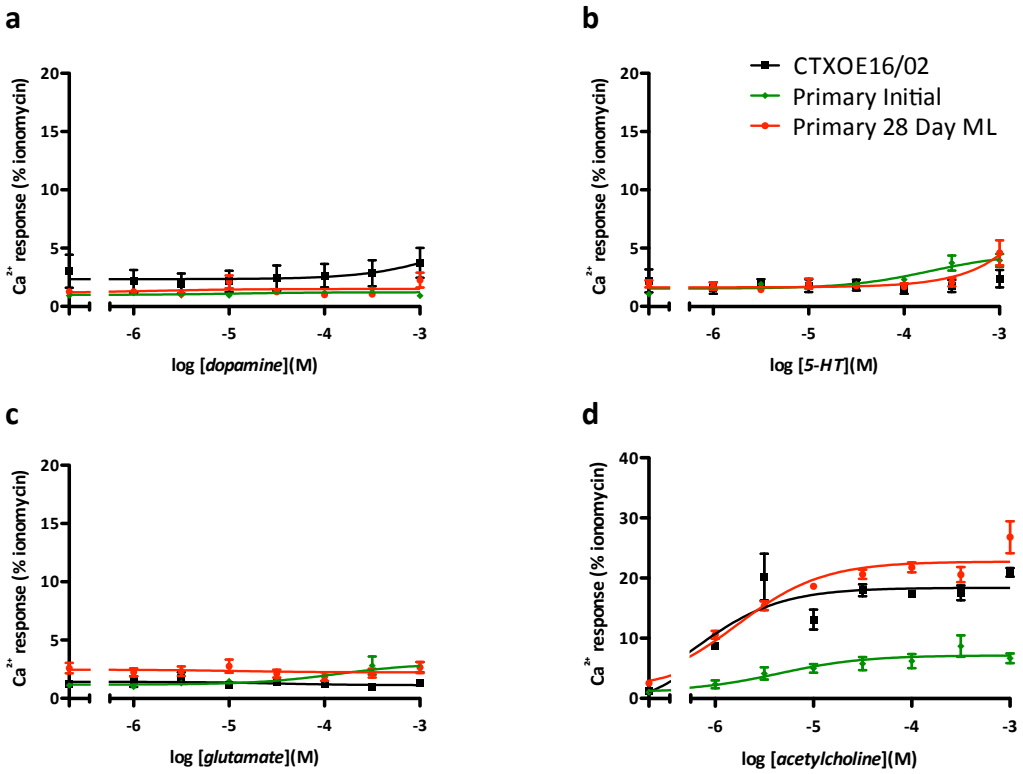


***Figure 5.5 Comparison of ligand-induced $Ca^{2+}$ responses between proliferative CTX0E16/02 and primary cultures***
CTX0E16/02 cells were seeded onto laminin-coated 96-well plates at 3 x $10^4$ cells per well following passage, while primary cultures were either plated directly onto laminin-coated 96-well plates following dissociation (Primary Initial) or expanded as a monolayer (ML) for 28 days prior to seeding (Primary 28 Day ML) at the same density as CTX0E16/02 cells where possible (sometimes limited for immediately plated cultures due to the amount of available primary tissue). Cultures were then grown to confluence prior to incubation for 1 hour in the presence of the cell permeable, $Ca^{2+}$-sensitive fluorescent dye Fura-2 AM. Cells were then washed prior to ligand-induced fluorescence being measured using a FS3. Concentration-response curves are shown for dopamine (**a**), 5-HT, $EC_{50}$ ≈ 190 µM (**b**), glutamate (**c**) and acetylcholine, $EC_{50}$ = 0.6 µM, 4.4 µM and 1.7 µM (**d**). Significant differences were observed between the two types of proliferative primary cultures for 5-HT ($p < 0.005$) and acetylcholine ($p < 0.0001$) but not dopamine or glutamate, as determined by two-way ANOVA. Data points represent mean ± S.E.M. from $n = 2$ for CTX0E16/02 cultures and $n = 5$ for primary cultures, each with 3 technical replicates and expressed relative to the positive control, ionomycin. N.B. scale for acetylcholine-induced responses is twice as large as for dopamine, 5-HT and glutamate.

Both primary and CTX0E16/02 proliferative cultures exhibited robust, concentration-dependent increases in $[Ca^{2+}]_i$ in response to acetylcholine (Figure 5.5, **d**). For non-expanded primary cells this response demonstrated a maximal response of just 6.0% relative to ionomycin-evoked responses, and an $EC_{50}$ of 4.4 µM. The magnitude of this response to acetylcholine was comparable to that observed in

differentiated CTX0E16/02 cultures (see Figure 4.9), and may be attributable to the high proportion of neurons in these cultures (see Figure 5.1). Indeed, reduced responses to acetylcholine have been reported previously for NPC cultures following differentiation, i.e. when a higher proportion of neurons are present [61]. Following expansion, the maximal response to acetylcholine rose to a baseline-corrected value of 21.0%, while the $EC_{50}$ remained relatively constant at 1.7 µM. These values are strikingly similar to those observed in proliferative CTX0E16/02 cultures, which demonstrated a baseline-corrected maximal response of 20.2% and an $EC_{50}$ of 0.6 µM (Figure 5.5, **d**). Indeed, responses to acetylcholine were not statistically different between proliferative CTX0E16/02 cultures and expanded primary cultures, yet pronounced differences were observed between non-expanded and expanded primary cultures ($p < 0.0001$), as determined by two-way ANOVA.

The time taken for non-expanded, proliferative primary cultures, used to measure ligand-induced $Ca^{2+}$ responses to reach confluence, varied considerably between different samples, as is clear from Table 5.1 above. This period varied from between 6 to 16 days for the five primary samples tested. Surprisingly however, this discrepancy had little influence upon the magnitude of ligand-induced $Ca^{2+}$ response between samples – or coincidentally, the proportion of $MAP2^+$ neurons within these cultures (data not shown). This would suggest that differences observed in ligand-induced $Ca^{2+}$ responses between non-expanded and expanded proliferative primary cultures, were more likely attributable to the process of passaging the cells rather than the actual period in culture. This is in contrast to the electrical excitability of these cultures as is discussed in section ***5.2.5*.**

These data provide an interesting perspective regarding ligand-induced $Ca^{2+}$ responses in proliferative primary human foetal tissue cultures. While levels of intracellular $Ca^{2+}$ accumulation in response to 5-HT, glutamate and acetylcholine (for dopamine they were absent) differed considerably between CTX0E16/02 and non-expanded proliferative primary cultures, these levels resembled those seen for CTX0E16/02 cultures once the cells had been expanded for 28 days. This effect appears to be attributable to the process of passaging the cells, as mentioned above. In general, as shown in Figure 5.5 above, while ligand-induced $Ca^{2+}$ responses were different to those exhibited by proliferative CTX0E16/02 cells in non-expanded proliferative primary cultures, they closely resembled each other once they had ben expanded in a similar way to CTX0E16/02 cells (in adherent monolayer culture). A likely reason for the difference observed between non-expanded and expanded proliferative primary cultures is the presence of early born neurons in these cultures (see Figure 5.1, above). Passaging would be expected to reduce the proportion of neurons within these cultures as self-renewing NPCs proliferate. This suggestion is supported by gene expression data presented above, in that differentiated samples – for the seven conditionally immortalised NPC lines (see Table 3.9 and Table 3.10, above) and the primary samples – demonstrated a broader gene expression pattern to that observed by expanded proliferative, primary cultures (see Figure 5.2, Figure 5.3 and Figure 5.4, above). As mentioned previously, a similarly broad, and in many cases more intense level of gene expression was observed in primary proliferative cultures that were not expanded. This suggestion could be tested using

immunocytochemical analysis to examine the phenotypic characteristics of primary cultures that were expanded as proliferative adherent cultures.

In summary, non-expanded proliferative primary cultures resemble differentiated CTX0E16/02 cultures with respect to gene expression and their ligand-induced $Ca^{2+}$ responses, and is likely attributable to the high proportion of neurons present within these cultures. However, once cells derived from primary samples were expanded as adherent cultures, they exhibited both gene expression profiles and ligand-induced $Ca^{2+}$ responses that were strikingly similar to that of proliferative CTX0E16/02 cultures. These data therefore support that fact that CTX0E16/02 cells represent a valid model of primary NPCs.

### *5.2.4 Passaging Number Prior to Differentiation Effects Ligand-Induced $Ca^{2+}$ Responses*

After expansion primary proliferative cultures were seeded onto a tissue culture flask, glass coverslips or a 96 well plate and differentiated for 28 days (see ***2.1.3*** and ***3.2.6***) for subsequent gene expression analysis, phenotypic characterisation and ligand-induced $Ca^{2+}$ response analysis, respectively. While five different samples were tested for proliferative primary cultures, one of these primary samples failed to survive the full differentiation period, and consequently, data shown in panel **a** of Figure 5.6, Figure 5.7, Figure 5.8 and Figure 5.9 below, represent the means and S.E.M. for the four remaining samples. It should also be noted that due to the variable behaviour of the cultures derived from each primary tissue sample, while the amount of time that each spent in proliferative culture prior to the initiation of differentiation was virtually the same (either 22 or 23 days), the number of passages performed varied between three and five. This information is detailed in Table 5.1, above. Unlike proliferative cultures derived from primary tissue samples, where the number of passages prior to seeding for analysis exerted little influence upon ligand-induced $Ca^{2+}$ responses, the same was not true for differentiated cultures. For this reason, data for ligand-induced $Ca^{2+}$ responses in differentiated primary cultures are also presented for each tested ligand as pairs, based on the number of passages these cultures underwent prior to plating cultures for differentiation (see panel **b** of Figure 5.6, Figure 5.7, Figure 5.8 and Figure 5.9, below).

Evidence of intracellular $Ca^{2+}$ accumulation in response to dopamine was absent when data for differentiated primary cultures derived from all four samples were pooled together (Figure 5.6, **a**). However, a small response at the highest tested concentration of 1 mM was observed in differentiated samples exposed to just three passages – though this failed to reach significance (Figure 5.6, **b**). An absence of intracellular $Ca^{2+}$ accumulation in response to dopamine in differentiated primary cultures was consistent with that observed in differentiated CTX0E16/02.

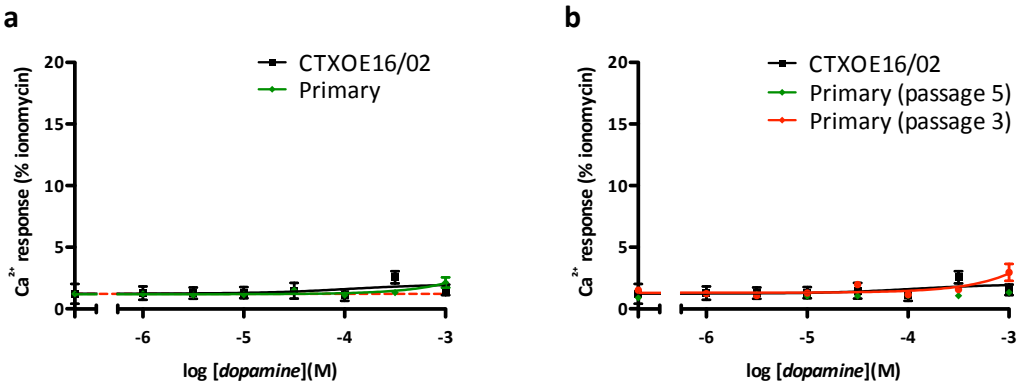


***Figure 5.6 Comparison of dopamine-induced $Ca^{2+}$ responses in differentiated CTX0E16/02 and primary NSC cultures***
CTX0E16/02 and primary cells were seeded onto laminin-coated 96-well plates at 3 x $10^4$ cells per well following passage. Cultures were then grown to approximately 80% confluence prior to exposure to a normal 28 day differentiation in SNBM. On the day of the experiment, cultures were incubated for 1 hour in the presence of the cell permeable, $Ca^{2+}$-sensitive fluorescent dye Fura-2 AM. Cells were then washed prior to ligand-induced fluorescence being measured using a FS3 instrument. Dopamine concentration-response curves exhibited by differentiated CTX0E16/02 (*n* = 2) and pooled primary tissue samples (*n* = 4)(**a**), and differentiated CTX0E16/02 (*n* = 2) and paired primary tissue samples exposed to either 5 (*n* = 2) or 3 (*n* = 2) passages prior to differentiation (**b**). Data points represent mean ± S.E.M. with 3 technical replicates provided for each biological replicate and expressed relative to the positive control, ionomycin. Dashed red line in panel **a** indicates baseline fluorescence for pooled primary cultures.

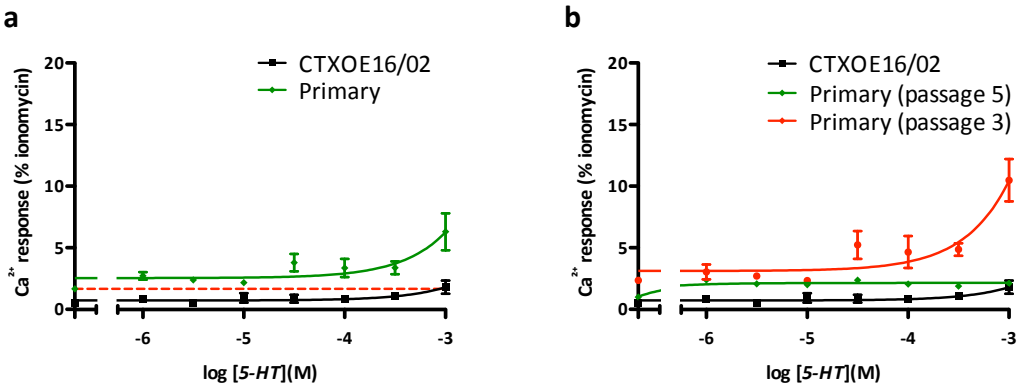


***Figure 5.7 Comparison of 5-HT-induced $Ca^{2+}$ responses in differentiated CTX0E16/02 and primary NSC cultures***
CTX0E16/02 and primary cells were seeded onto laminin-coated 96-well plates at 3 x $10^4$ cells per well following passage. Cultures were then grown to approximately 80% confluence prior to exposure to a normal 28 day differentiation in SNBM. On the day of the experiment, cultures were incubated for 1 hour in the presence of the cell permeable, $Ca^{2+}$-sensitive fluorescent dye Fura-2 AM. Cells were then washed prior to ligand-induced fluorescence being measured using a FS3 instrument. 5-HT concentration-response curves exhibited by differentiated CTX0E16/02 (*n* = 2) and pooled primary tissue samples (*n* = 4)(**a**), and differentiated CTX0E16/02 (*n* = 2) and paired primary tissue samples exposed to either 5 (*n* = 2) or 3 (*n* = 2) passages prior to the establishment of the cultures (**b**). Data points represent mean ± S.E.M. with 3 technical replicates provided for each biological replicate and expressed relative to the positive control, ionomycin. Dashed red line in panel **a** indicates baseline fluorescence for pooled primary cultures.

Responses induced by 5-HT in differentiated CTX0E16/02 cells were absent except for a small response at the highest tested concentration of 1 mM (Figure 5.7, **a**). In contrast, small responses were observed for 5-HT, even at the lowest tested concentration of 1 µM when all differentiated primary data were combined, though as the concentration was increased the responses did not follow a simple sigmoidal dose response curve. This may be attributable to conflicting signalling responses contributed by various

different 5-HT receptors (see Table 4.1, above)[364]. A further increase in $[Ca^{2+}]_i$ was also observed at the highest tested concentration of 5-HT (1 mM) when all differentiated primary data were combined, mirroring responses seen in differentiated CTX0E16/02 cells (Figure 5.7, **a**). When dissecting responses from primary cultures that underwent three or five passages before being plated for differentiation, however, it would appear that after five passages a maximal response was evident at the lowest tested concentration of 1 µM and was of a similar level to the maximal response obtained for CTX0E16/02 cultures at 1 mM (Figure 5.7, **b**). Thus, when these data were combined (see Figure 5.7, **a**), the elevation in $[Ca^{2+}]_i$ response at 1 mM was attributable to primary cultures exposed to three passages.

Intracellular $Ca^{2+}$ accumulation in differentiated primary cultures in response to glutamate when data from all samples were combined saw a considerable rightward shift in potency when compared to differentiated CTX0E16/02 cells (Figure 5.8, **a**). For combined primary data, no response was observed to glutamate until the concentration reached 100 µM, while the $EC_{50}$ for glutamate in differentiated CTX0E16/02 cultures was lower than this at 22.02 µM (Figure 5.8, **a**). Due to this rightward shift, it was not clear whether a maximal response to glutamate was achieved for differentiated primary cultures at the highest tested concentration. Once the elevated best-fit baseline value was taken into account for the combined primary data however, the response observed to 1 mM glutamate was comparable to that observed in differentiated CTX0E16/02 cultures (Figure 5.8, **a**). A different picture emerged when primary samples were separated based on the number of passages they went through prior to the initiation of differentiation. For the two samples exposed to three passages there was a higher level of baseline fluorescence and responses were only observed at concentrations of 31.6 µM and above (Figure 5.8, **b**). In addition, there was considerable variability in the magnitude of responses where they occurred above baseline – as can be seen by the size of the error bars in Figure 5.8, **b**. It was the primary cultures that had just three passages rather than five that accounted for the observed rightward shift in potency when primary sample response data for glutamate were combined. In contrast, primary cultures that underwent five passages exhibited more homogenous levels of intracellular $Ca^{2+}$ accumulation in response to glutamate (Figure 5.8, **b**). If the hypothesis proposed above is true – that the continuous passaging of primary cultures causes an enrichment of NPCs, reducing the proportion of post mitotic cells such as neurons – this may account for the more homogenous responses to the same stimulus in cultures that underwent five passages. Responses to glutamate in primary cultures that went through five passages were strikingly similar to those observed for CTX0E16/02 cells; sharing an almost identical maximal response, though revealing a leftward shift in potency with an $EC_{50}$ of 5.63 µM as compared to 22.02 µM for CTX0E16/02 cultures. This was in contrast to observations for primary cultures that underwent just three passages, which exhibited a rightward shift in potency (Figure 5.8, **b**).

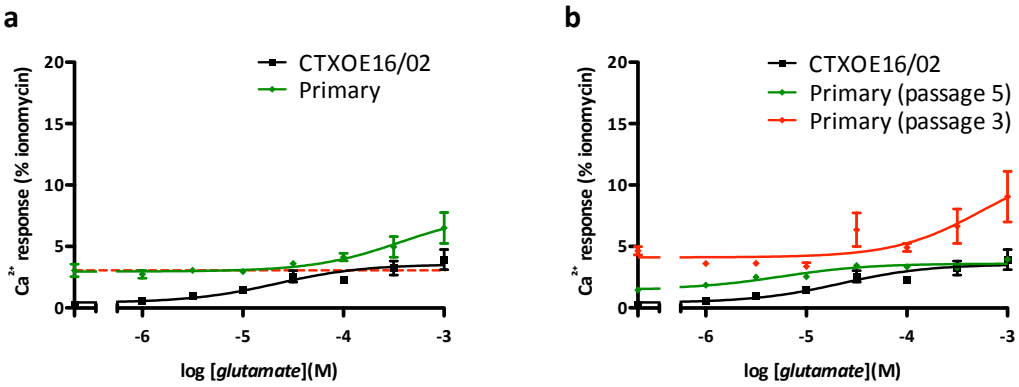


***Figure 5.8 Comparison of glutamate-induced $Ca^{2+}$ responses in differentiated CTX0E16/02 and primary NSC cultures***
CTX0E16/02 and primary cells were seeded onto laminin-coated 96-well plates at 3 x $10^4$ cells per well following passage. Cultures were then grown to approximately 80% confluence prior to exposure to a normal 28 day differentiation in SNBM. On the day of the experiment, cultures were incubated for 1 hour in the presence of the cell permeable, $Ca^{2+}$-sensitive fluorescent dye Fura-2 AM. Cells were then washed prior to ligand-induced fluorescence being measured using a FS3 instrument. Glutamate concentration-response curves exhibited by differentiated CTX0E16/02 ($EC_{50}$ = 22.0 µM, *n* = 2) and pooled primary tissue samples (*n* = 4)(**a**), and differentiated CTX0E16/02 ($EC_{50}$ = 22.0 µM, *n* = 2) and paired primary tissue samples exposed to either 5 ($EC_{50}$ = 5.6 µM, *n* = 2) or 3 (*n* = 2) passages prior to the establishment of the cultures (**b**). Data points represent mean ± S.E.M. with 3 technical replicates provided for each biological replicate and expressed relative to the positive control, ionomycin. Dashed red line in panel **a** indicates baseline fluorescence for pooled primary cultures.

Differences in intracellular $Ca^{2+}$ accumulations in response to acetylcholine between primary samples exposed to either three or five passages were even more pronounced than they were for glutamate, though followed a similar trend. When primary data was combined for all four differentiated samples, there was considerable variability between responses at each tested concentration, as is evident from the level of standard error (Figure 5.9, **a**). Combined data from differentiated primary cultures demonstrated responses to acetylcholine at the lowest tested concentration of 1 µM. With no plateau following the steep portion of the curve, this indicated a considerable rightward shift in potency compared to an $EC_{50}$ of 5.0 µM for CTX0E16/02 cultures (Figure 5.9, **a**). A different story emerges when primary samples were grouped according to the number of passages they underwent prior to differentiation. Responses to acetylcholine in primary samples that went through five passages prior to differentiation were virtually absent, with only minimal responses detected, but recorded an $EC_{50}$ of 4.4 µM – almost identical to that seen for CTX0E16/02 cultures at 5.0 µM (Figure 5.9, **b**). A reduction in sensitivity to acetylcholine or other cholinergic ligands following differentiation is consistent with that observed for CTX0E16/02 cultures and other tested NPC lines [61], though not previously to this extent. In primary cultures that underwent just 3 passages, responses were both greater and more variable in magnitude, with considerable responses observed at the lowest tested concentration of 1 µM and provided an $EC_{50} \approx 140$ µM, a considerable rightward shift in potency when compared to the other primary or CTX0E16/02 cultures (Figure 5.9, **b**).

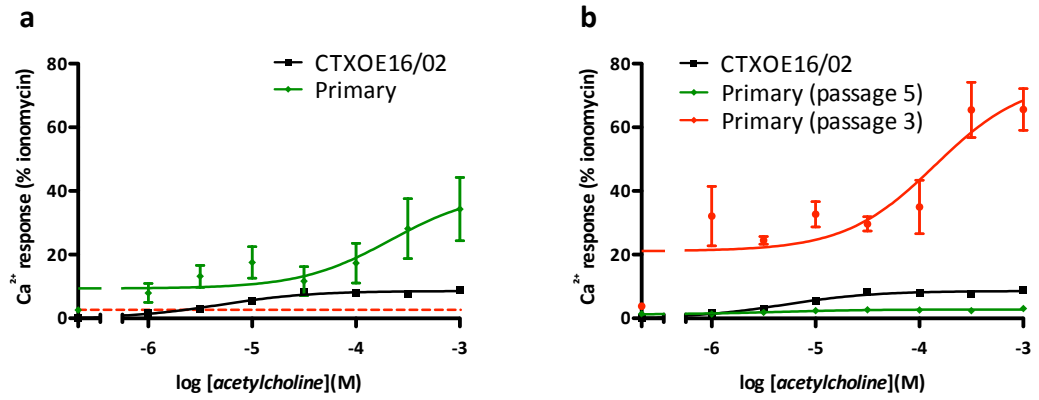


***Figure 5.9 Comparison of acetylcholine-induced $Ca^{2+}$ responses in differentiated CTX0E16/02 and primary NSC cultures***

CTX0E16/02 and primary cells were seeded onto laminin-coated 96-well plates at 3 x $10^4$ cells per well following passage. Cultures were then grown to approximately 80% confluence prior to exposure to a normal 28 day differentiation in SNBM. On the day of the experiment, cultures were incubated for 1 hour in the presence of the cell permeable, $Ca^{2+}$-sensitive fluorescent dye Fura-2 AM. Cells were then washed prior to ligand-induced fluorescence being measured using a FS3 instrument. Acetylcholine concentration-response curves exhibited by differentiated CTX0E16/02 ($EC_{50}$ = 5.0 µM, *n* = 2) and pooled primary tissue samples (*n* = 4)(**a**), and differentiated CTX0E16/02 ($EC_{50}$ = 5.0 µM, *n* = 2) and paired primary tissue samples exposed to either 5 ($EC_{50}$ = 4.4 µM, *n* = 2) or 3 ($EC_{50}$ ≈ 140 µM, *n* = 2) passages prior to the establishment of the cultures (**b**). Data points represent mean ± S.E.M. with 3 technical replicates provided for each biological replicate and expressed relative to the positive control, ionomycin. Dashed red line in panel **a** indicates baseline fluorescence for pooled primary cultures. N.B. scale for acetylcholine-induced responses is four times as large as for dopamine (Figure 5.6), 5-HT (Figure 5.7) or glutamate (Figure 5.8).

In summary, ligand-induced $Ca^{2+}$ responses were appreciably different between proliferative CTX0E16/02 cultures and non-expanded primary cultures (see Figure 5.5). Once cultures derived from each primary sample had been expanded in adherent, monolayer culture for 28 days (5 – 7 passages, see Table 5.1) however, responses were strikingly similar to those exhibited by proliferative CTX0E16/02 cultures. In contrast, greater disparity was observed between ligand-induced $Ca^{2+}$ responses exhibited by primary and CTX0E16/02 cultures following differentiation (see Figure 5.6, Figure 5.7, Figure 5.8 and Figure 5.9). However, the data presented above suggest that by increasing the number of passages that cultures derived from each primary sample underwent prior to their differentiation, ligand-induced $Ca^{2+}$ responses become more comparable to those exhibited by differentiated CTX0E16/02 cultures (see panel **b** of Figure 5.6, Figure 5.7, Figure 5.8 and Figure 5.9). Following experiments to determine levels of intracellular $Ca^{2+}$ accumulation in response to dopamine, 5-HT, glutamate or acetylcholine in the different types of culture derived from primary neural samples, experiments were also performed to determine whether cells within these cultures were electrically excitable. This was determined by assessing their ability to elevate $[Ca^{2+}]_i$ in response to a 50 mM $K^+$ challenge.

### *5.2.5 Primary Foetal Neural Cell Cultures Are Electrical Excitable*

In order to determine whether cultures derived from primary tissue samples contained electrically excitable cells, following the addition of either assay buffer or assay buffer containing dopamine, 5-HT, glutamate or acetylcholine to Fura-2 AM loaded cells (the results of which are detailed above), cultures

were subsequently exposed to 50 mM KCl. In support of phenotypic data presented above (see Figure 5.1), non-expanded, proliferative primary cultures were found to be electrically excitable, as determined by their ability to mobilise intracellular $Ca^{2+}$ in response to a 50 mM KCl challenge (see Figure 5.10), showing that functional neurons were present within these cultures. Interestingly, the magnitudes of KCl-induced intracellular $Ca^{2+}$ accumulations were affected by the time taken for the cultures to reach confluence. Cultures from 2 samples that took just 6 days to reach confluence and demonstrated considerable KCl-induced intracellular $Ca^{2+}$ accumulation, while for a sample that took 9 days this level was severely attenuated. The two remaining samples that took 12 and 16 days respectively to reach confluence were unable to demonstrate electrical excitability when tested.

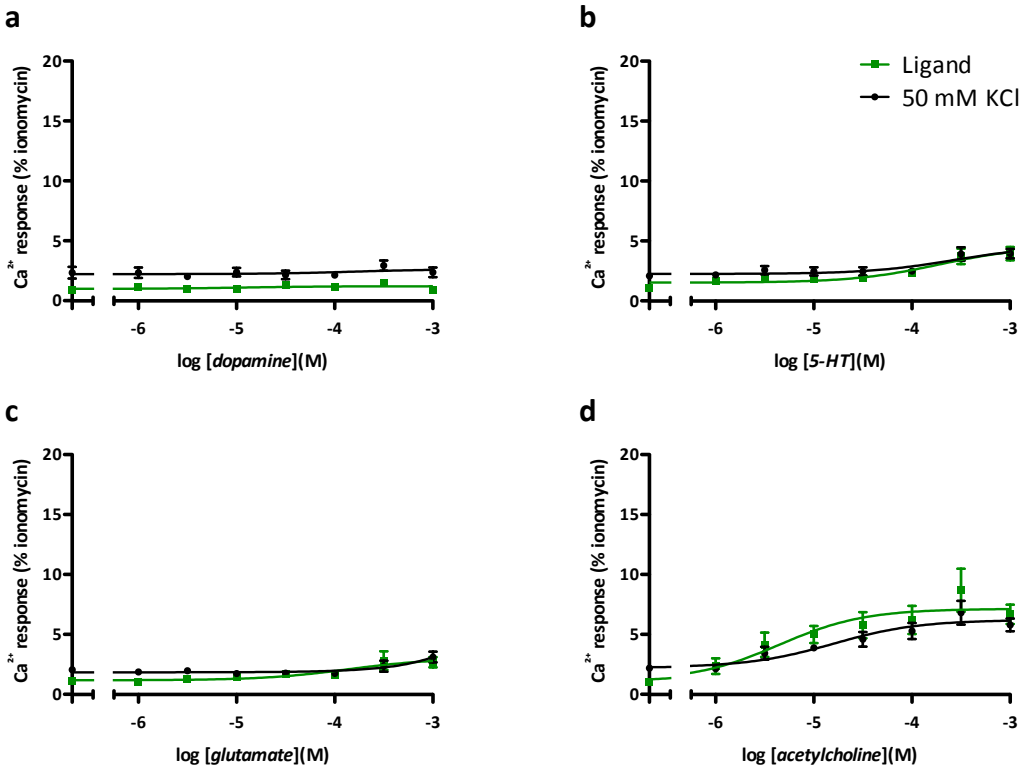


***Figure 5.10 Non-expanded proliferative primary neural cultures are electrically excitable***
Cultures were established by dissociating cells of primary neural embryonic tissue samples and plating them immediately onto laminin-coated 96-well plates. Cultures were then maintained under proliferative conditions until reaching confluence. On the day of the experiment, cultures were incubated for 1 hour in the presence of the cell permeable, $Ca^{2+}$-sensitive fluorescent dye Fura-2 AM. Cells were then washed prior to ligand-induced fluorescence being measured using a FS3. Following the addition of either assay buffer or assay buffer containing dopamine, 5-HT, glutamate or acetylcholine, cultures in each well were exposed to KCl to a final concentration of 50 mM. Concentration-response curves are shown for dopamine (**a**), 5-HT, $EC_{50}$ = 187 µM (**b**), glutamate (**c**) and acetylcholine, $EC_{50}$ = 4.4 µM (**d**). Level of intracellular $Ca^{2+}$ accumulation provoked by subsequent addition of KCl following the addition of each of these ligands is represented by solid black circles. Data points represent mean ± S.E.M. from *n* = 5, each with 3 technical replicates and expressed relative to the positive control, ionomycin.

Data presented in Figure 5.10 shows combined data from all non-expanded, proliferative primary cultures of changes in $[Ca^{2+}]_i$ provoked by 50 mM KCl when added after each tested ligand. Responses to KCl are still detectable even after averaging data from all cultures – irrespective of the period they took

to become confluent (Figure 5.10). It should be noted however that if cultures were previously exposed to a concentration of ligand that itself provoked intracellular $Ca^{2+}$ accumulation, then responses to KCl were not detected. For example, dopamine was incapable of provoking an increase in $[Ca^{2+}]_i$ at any tested concentration. In this case, subsequent exposure to KCl caused similar levels of intracellular $Ca^{2+}$ accumulation, irrespective of the concentration of dopamine previously added (see Figure 5.10, **a**). In contrast, both 5-HT and glutamate were capable of provoking small increase in $[Ca^{2+}]_i$ at higher tested concentrations. When KCl was added to wells where the concentration of ligand was incapable of provoking an appreciable response, a small increase in $[Ca^{2+}]_i$ was observed, while no increase in $[Ca^{2+}]_i$ was observed in wells where the prior addition of ligand had provoked a response (see Figure 5.10, **b** and **c**). On the other hand, acetylcholine was capable of provoking comparably robust, concentration-dependent increases in $[Ca^{2+}]_i$. In this case, the subsequent addition of KCl actually caused the $[Ca^{2+}]_i$ to fall with respect to the level that had been achieved previously in response to acetylcholine (Figure 5.10, **d**). This effect has been described previously for CTX0E16/02 cultures, and is likely attributable to membrane depolarisation, and the consequent removal of the electrical gradient supporting $Ca^{2+}$ entry into cells (see Figure 4.15).

Bearing in mind that intracellular $Ca^{2+}$ accumulation in response to a 50 mM $K^+$ challenge in proliferative cultures derived from primary samples was only observed in those that had spent nine days or less in adherent culture, it is perhaps unsurprising that the same $K^+$ challenge was incapable of precipitating increases in $[Ca^{2+}]_i$ in any of the five primary samples following 28 days expansion in monolayer culture (see Figure 5.11). These data do not provide direct evidence that cultures that took longer to reach confluence ever contained cells capable of KCl-induced intracellular $Ca^{2+}$ accumulations, though the time-dependent decrease in response magnitude would suggest that they did, and is supported by the fact that all these primary cultures demonstrated similar numbers of $MAP2^+$ neurons. If we therefore presume that all the primary tissue samples contained electrically excitable cells upon initial dissociation, there would appear to be a couple of possibilities that may account for this loss of function. The loss of electrical excitability may be attributable to neuronal death, though visible levels of cell death in these cultures were minimal (data not shown). A perhaps more likely explanation is that maintaining these cells in adherent, proliferative culture reduces their capacity to exhibit electrical excitability. It remains unclear however, whether the observed loss of electrical excitability is attributable to the fact the cultures are maintained as adherent cultures or as proliferative cultures – or occurs as a consequence of both. If it is the case that rather than dying, cells initially capable of responding to a $K^+$ challenge lose this capacity, the mechanism responsible for this also remains unclear. This may perhaps occur as a consequence of $Ca_V$ internalisation, though the gradual reduction in the magnitude of $K^+$-induced intracellular $Ca^{2+}$ accumulation over several days may simply implicate a loss of *de novo* synthesis of these channels.

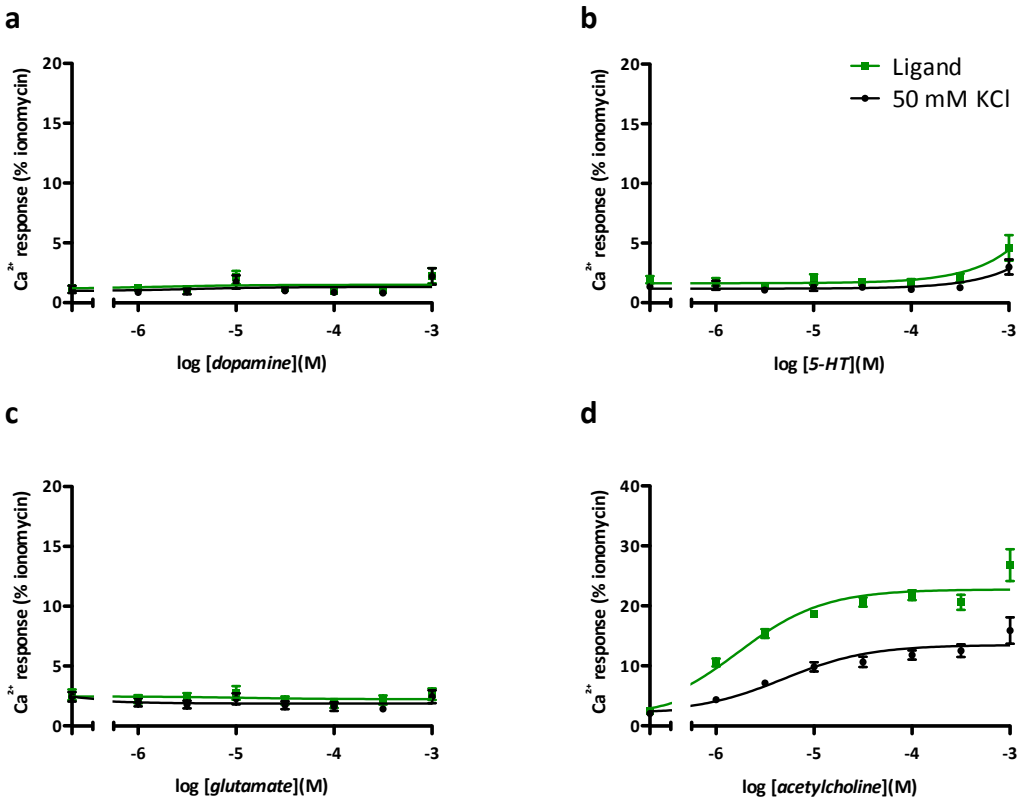


***Figure 5.11 Primary neural cells maintained in adherent monolayer culture lose electrically excitable***
Primary neural embryonic tissue samples were dissociated and maintained as proliferative, adherent cultures and plated onto laminin-coated 96-well plates so as to be confluent 28 days after their initial dissociation. On the day of the experiment, cultures were incubated for 1 hour in the presence of the cell permeable, $Ca^{2+}$-sensitive fluorescent dye Fura-2 AM. Cells were then washed prior to ligand-induced fluorescence being measured using a FS3. Following the addition of either assay buffer or assay buffer containing dopamine, 5-HT, glutamate or acetylcholine, cultures in each well were exposed to KCl to a final concentration of 50 mM. Concentration-response curves are shown for dopamine (**a**), 5-HT (**b**), glutamate (**c**) and acetylcholine, $EC_{50}$ = 1.7 µM (**d**). Level of intracellular $Ca^{2+}$ accumulation provoked by subsequent addition of KCl following the addition of each of these ligands is represented by solid black circles. Data points represent mean ± S.E.M. from *n* = 5, each with 3 technical replicates and expressed relative to the positive control, ionomycin. N.B. scale for acetylcholine-induced responses is twice as large as for dopamine, 5-HT or glutamate.

In contrast to CTX0E16/02 cultures, all primary cultures demonstrated the ability to respond to a $K^+$ challenge by elevating $[Ca^{2+}]_i$ following a normal 28 day differentiation (see Figure 5.12). Interestingly, the magnitude of responses from differentiated primary cultures was related to the number of passages rather than the time each sample had spent in monolayer culture, with greater responses from cultures that underwent fewer passages. In addition, the samples that were electrically excitable as proliferative cultures were not the cultures showing the larger responses in differentiated cultures. The two samples that demonstrated robust KCl-induced $Ca^{2+}$ influx as non-expanded proliferative cultures demonstrated considerably smaller responses once differentiated than did other differentiated samples. These two samples were maintained under proliferative culture conditions for the same period of time prior to differentiation as other primary samples, though underwent five passages prior to differentiation, rather than just three for the two samples that took 12 and 16 days respectively to reach confluence. Thus, differentiated cultures derived from samples exposed to the fewest passages produced the largest KCl-induced intracellular $Ca^{2+}$ accumulations. Data shown in Figure 5.12 represent means of KCl-induced

$Ca^{2+}$ accumulation in all samples following exposure to varying concentration of dopamine 5-HT, glutamate or acetylcholine. As was the case in proliferative cultures that were immediately plated following sample dissociation, little rise in $[Ca^{2+}]_i$ was observed in samples that had been previously stimulated with concentrations of ligand that themselves provoked an increase in $[Ca^{2+}]_i$, as can be seen at the highest tested concentrations for 5-HT and glutamate (see Figure 5.12, **b** and **c**). The $[Ca^{2+}]_i$ response provoked by even the lowest tested concentration of acetylcholine could not be surmounted by the addition of 50 mM KCl however. Following exposure to acetylcholine, the addition of KCl always provoked a reduction in the observed level of $[Ca^{2+}]_i$ (Figure 5.12, **d**).

In summary, non-expanded proliferative primary cultures demonstrated the ability to elevate $[Ca^{2+}]_i$ in response to a 50 mM $K^+$ challenge, though progressively lost this capacity with time in culture. In contrast, expanded primary cultures did not show electrical excitability in response to KCl. However, upon differentiation, all primary culture were capable of demonstrating KCl-induced increases in $[Ca^{2+}]_i$, though these responses were more pronounced in primary cultures that had been exposed to fewer passages, prior to the initiation of differentiation.

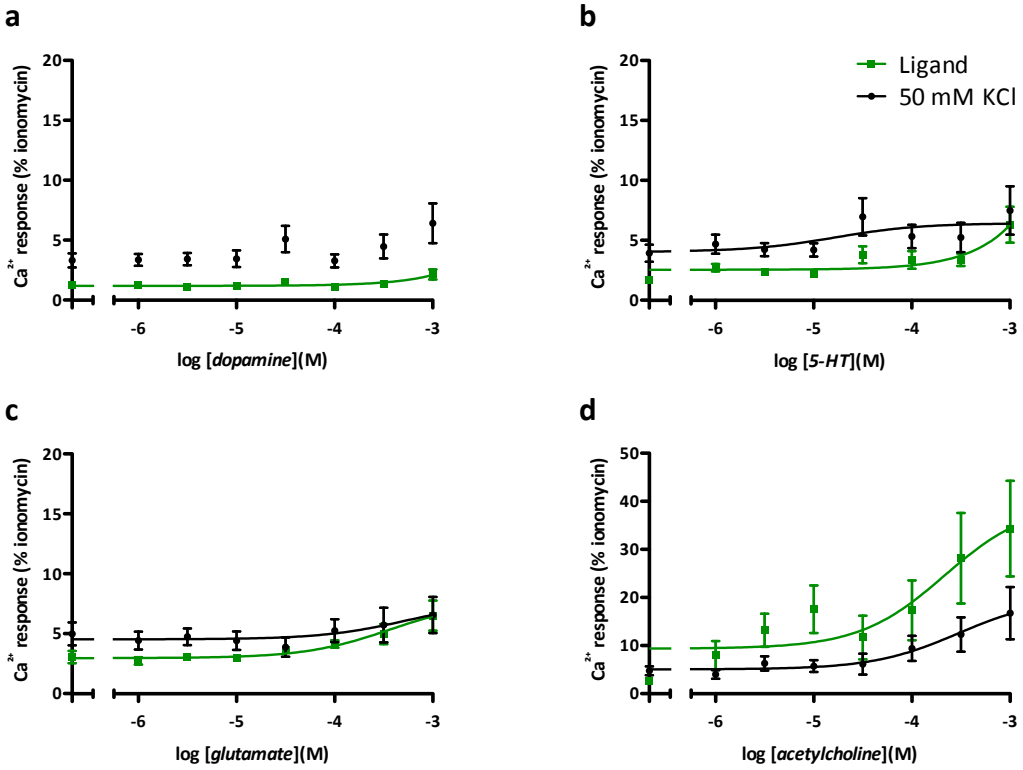


***Figure 5.12 Differentiated primary neural cell cultures exhibit robust electrically excitability***
Primary neural embryonic tissue samples were dissociated and expanded as proliferative, adherent cultures prior to plating onto laminin-coated 96-well plates and differentiated for 28 days using SNBM. On the day of the experiment, cultures were incubated for 1 hour in the presence of the cell permeable, $Ca^{2+}$-sensitive fluorescent dye Fura-2 AM. Cells were then washed prior to ligand-induced fluorescence being measured using a FS3. Following the addition of either assay buffer or assay buffer containing dopamine, 5-HT, glutamate or acetylcholine, cultures in each well were exposed to KCl to a final concentration of 50 mM. Concentration-response curves are shown for dopamine (**a**), 5-HT (**b**), glutamate (**c**) and acetylcholine (**d**). Level of intracellular $Ca^{2+}$ accumulation provoked by subsequent addition of KCl following the addition of each of these ligands is represented by solid black circles. Data points represent mean ± S.E.M. from *n* = 4, each with 3 technical replicates and expressed relative to the positive control, ionomycin. N.B. scale for acetylcholine-induced responses is larger than that for dopamine, 5-HT or glutamate.

### *5.2.6 Summary*

Taken together, these data show that cultures derived from 7 – 8 week gestation, primary human embryonic neural samples already contain a considerable proportion of $MAP2^+$ neurons (see Figure 5.1) and the capacity to elevate $[Ca^{2+}]_i$ in response to a 50 mM $K^+$ challenge (see Figure 5.10). These cultures also demonstrated expression profiles indicative of a neuronal phenotype, in that – for the genes tested – these cultures expressed a broad range of genes, often with considerable intensity (see Figure 5.2, Figure 5.3 and Figure 5.4) and comparable to that seen in differentiated CTX0E16/02 cultures. In addition, these cultures also demonstrated ligand-induced $Ca^{2+}$ responses that were more comparable to those seen in differentiated rather than proliferative CTX0E16/02 cultures (Figure 5.5). Once primary neural cell cultures had been expanded for 28 days using the same conditions that proliferative CTX0E16/02 cultures were routinely maintained under, their characteristics were strikingly similar to those exhibited by proliferative CTX0E16/02 cultures. For example, they lost their observed sensitivity to 5-HT and glutamate and gained sensitivity to acetylcholine with respect to these compounds' capacity to provoke intracellular $Ca^{2+}$ accumulation (see Figure 5.5, **b**, **c** and **d**). These cultures also demonstrated a more restricted expression profile, similar to that seen in proliferative cultures of the seven NPC lines described above (see Table 3.9 and Table 3.10). Furthermore, genes for which expression was retained in expanded proliferative cultures, tended to demonstrate a considerable attenuation in intensity compared to non-expanded proliferative cultures (see Figure 5.2, Figure 5.3 and Figure 5.4). In addition, expanded proliferative primary cultures also lost their capacity to elevate $[Ca^{2+}]_i$ in response to a 50 mM $K^+$ challenge (see Figure 5.11) – as was observed in proliferative CTX0E16/02 cultures.

The broad expression profile exhibited by non-expanded, proliferative cultures, and lost after expansion, returned following differentiation (see Figure 5.2, Figure 5.3 and Figure 5.4), a characteristic also shared with differentiated CTX0E16/02 cultures. These differentiated cultures contained a large number of $MAP2^+$ neurons (see Figure 5.1), and elevated $[Ca^{2+}]_i$ in response to a 50 mM $K^+$ challenge (see Figure 5.12). Changes were also observed with respect to levels of intracellular $Ca^{2+}$ accumulation in response to different ligands. Variability was observed between samples that underwent either three or five passages prior to differentiation, though these data served to show that cultures that went through additional passages demonstrated ligand-induced $Ca^{2+}$ responses that were more similar to those observed in differentiated CTX0E16/02 cultures. When considered together, these data suggest that the CTX0E16/02 cultures closely resemble those of equivalent primary cultures, with respect to the characteristics tested here.

Clearly it would have been preferable to perform these experiments using primary tissue derived from both the same gestational period and neural region as the CTX0E16/02 cell line. For example, the CTX0E16/02 cell line was isolated from developing human foetal cortex at 12 weeks gestation, while the primary neural cell cultures used in experiments described above were isolated from samples of whole brain, at 7 – 8 weeks gestation. This was unfortunately not possible for this study due to later gestation primary neural tissue samples not being available, and the samples being provided in such a way so to make it difficult to isolate cells comprising only the cortex. In addition, had it been possible to isolate

cells from just the developing cortex, there would have been insufficient quantities of cells to perform experiments described here using non-expanded cultures. However, despite the differences between the origin of the CTX0E16/02 line and the primary samples used here, the similarity between the two types of cultures with respect to ligand-evoked $Ca^{2+}$ responses and gene expression were strikingly similar when maintained under comparable culture conditions. In addition, had primary cultures been exposed to similar numbers of passages and freeze/thaw cycles as were the CTX0E16/02 cells prior to experimentation, these differences may conceivably be even less evident, and suggest that the difference between cultures as a result of their gestational origin are less pronounced than that conferred by the culture condition they are exposed to.

Despite the caveats mentioned above, it is felt that the data provides evidence that pharmacologically, the CTX0E16/02 cell line behaves in a manner comparable to primary tissue, and as such represents an appropriate model. The possibility remains however, that the reason why primary cultures come to share characteristics exhibited by CTX0E16/02 cells is due to the fact that they have been expanded and differentiated in exactly the same way. This possibility could perhaps be addressed by comparing primary cultures with the behaviour of the other six NPC lines described in ***Chapter 3***, above. Primary cultures could then be maintained and differentiated in the same way as each of the different NPC lines and used to determine whether this 1) changes the behaviour of the primary cultures with respect to the data generated here, and 2) if changes are observed – would the primary cultures then behave in a manner more akin to the NPC line whose culture conditions have been adopted. This would however represent a large body of work and outside the remit of the present study. It should be noted however that the cultures derived from primary embryonic neural samples described above represent a mixed population of cells, both with respect to NPCs and neurons, but also regarding their region of origin with the brain. Therefore, cultures that were derived by seeding cells immediately following sample dissociation were likely to contain neurons from diverse areas of the developing brain, each of which may demonstrate variable characteristics with respect to how they respond to the neurotransmitter agonists tested. This cellular heterogeneity may also contribute to the differences observed between these non-expanded primary cultures and proliferative CTX0E16/02 cultures. However – as described above – once the primary cultures were expanded, a process which would be expected to enrich the number of NPCs within these cultures, both the gene expression and ligand-induced pharmacological responses were surprisingly similar. This is of course despite the fact that the resulting primary cultures would still be expected to contain a mixed population of NPCs with respect to their region of origin within the developing brain. In general, it appeared that with increased time in adherent monolayer culture under the same conditions that CTX0E16/02 cultures are grown, the characteristics of primary cultures became more comparable to this conditionally immortalised cell line. Had more time been available, it would also be interesting to investigate the effect of freezing and thawing upon primary cultures, a process which the CTX0E16/02 cell line has been exposed to several times during their initial isolation and banking of the line. It is proposed that this procedure would also be likely to influence the characteristics of primary cultures, as has been shown above for CTX0E16/02 cells following long term continuous culture (see ***4.2.13***).

Interestingly, what did differ considerably between the primary cultures and that of the CTX0E16/02 cell line was the electrical properties they exhibited. Taken together, the data presented above show that 7 – 8-week gestation foetal brain tissue already contain electrical excitable neurons. A finding that is consistent with those of Bystron and colleagues who confirmed the appearance of a population of neurons in human foetal cerebral cortex as early as 31 days gestation [423], though this was only assessed using immunohistochemistry and did not provide functional evidence showing that these cells were electrically excitable. The earliest stage of human neural development from which provoked electrical currents have been recorded is 16 weeks [425], with the first spontaneous firing recorded at 20 weeks [426]. Both of these previous studies concentrated on cells of the developing cortex however, and did not eliminate the possibility that neurons in other more phylogenetically ancient areas of the brain develop electrical excitability at an earlier stage, such as the brain stem or subcortical cortical ganglia [427]. Due to the fact the primary cultures used in this study were derived from whole brain samples, the electrical excitability observed could be as a consequence of early born neurons from these evolutionarily older regions of the brain rather than the cerebral cortex. It should be added however that data presented here showing electrical excitability in primary culture was obtained after cells were already grown in adherent culture for a minimum of 6 days to enable them to reach confluence before any recordings were made. Consequently, the possibility exists that electrical excitability developed within these cultures following sample dissociation and culturing. However, the fact that the magnitude of KCl-induced intracellular $Ca^{2+}$ accumulations decreased between samples in a manner dependent upon the time it took to reach confluence suggests a progressive loss of excitability rather than a gain. This could of course be resolved through electrophysiological techniques immediately following sample collection, as has been performed elsewhere [425,427].

If electrically excitable neurons are already present within human foetal neural tissue as early as 7 – 8-week gestation, this would suggest that culture conditions used in experiments detailed above to maintain proliferative cultures stimulate a loss of this property. The factors influencing this loss of electrical excitability appear to be either the medium constituents, the maintenance of cultures in adherent monolayers or a combination of the two. It remains unclear from the data presented above whether the process of passaging cells or exposing them to freeze/thaw cycles may also contributes to this effect, though may additionally help to account for the relative resistance to developing this property that the CTX0E16/02 cultures exhibit.

Expansion of primary cells in adherent cultures may deprive cells of signals they normally received *in vivo* through cell-cell adhesion or through interactions with components of the extracellular matrix. These signals have been shown to be transduced to the intracellular environment through cell surface receptors such as integrins, and more recently, adhesion GPCRs [428-430]. While all cultures were propagated on laminin, this is not the only ligand recognised by integrins, and the use of molecules such as fibronectin or collagens may help to maintain electrical excitability. In addition, normal paracrine signalling between cells may also be disrupted when tissue samples are dissociated and seeded for monolayer culture or when passaged. Cells seeded for monolayer culture are much further apart than

they are *in vivo* and the volumes of medium required would instantly cause dilution of any secreted paracrine signalling molecules. These questions could perhaps be addressed by propagation of cells as neurospheres prior to differentiation. However, the fact that primary cultures grown on adherent substrates quickly regained electrical excitability following differentiation, would suggest that it may be the presence (or absence) of chemical components within the proliferative medium used that play a key role in the observed loss.

It is interesting to note that while the CTX0E16/02 cell line took at least eight weeks to develop electrical excitability under 'normal' differentiation conditions (exposure to SNBM), all primary cultures demonstrated robust intracellular $Ca^{2+}$ accumulation in responses to 50 mM KCl after just four weeks in the presence of SNBM. Primary cultures were found to be electrically excitable when initially plated following sample dissociation – a property that is likely attributable to the presence of functional neurons in these cultures – though progressively lost this property with time in culture. This raises the question of what is responsible for the loss of this property. This could be attributable to the death of the neuronal cells that were initially responsible for providing the cultures with this property, though little evidence of cell death was evident in these cultures. An alternative explanation is that the VGICs responsible for providing neurons with this capability are internalised when they are grown under proliferative condition in adherent cultures. Further work would be required to establish of this were the case. Indeed, if cells within primary cultures lose their electrical excitability though simply internalising the ion channels that provide this capacity, this may also help to explain the more rapid development of electrical excitability in these cultures following differentiation – by representing existing channels in the plasma membrane. Data presented above suggest that different populations of neural cells do not demonstrate the same capacity to generate electrical excitability, or at least develop this property at the same rate. For example, the CTX0E16/02 cell line was derived from 12-week gestation cortical tissue, while primary cultures were derived from 7 – 8-week gestation primary cultures tissue samples. This would perhaps suggest that CTX0E16/02 cells should become electrically active more rapidly than those derived from 7 – 8-week gestation tissue. The possibility remains however that due to the CTX0E16/02 line being derived from the phylogenetically recent cortex, that progenitor cells from this region require longer to reach physiological maturity. With the origin of the primary cultures used in this study being whole brain tissue samples however, the rapid ability to become electrically excitable may be attributable to the presence of NPCs which represent precursors to more ancient brain regions. This would be consistent with previously published data showing that while robust electrical excitability could be provoked in NPCs derived from the ventral mesencephalon, cortical cells remained resistant [104], while other recent reports have suggested that 2 – 4 months are required to functionally differentiated human NPCs [61,328]. Another possibility is that the transfection and subsequent selection methodology used to derive the CTX0E16/02 clonal cell line favoured cells with a reduced capacity to rapidly develop physiological neuronal properties upon differentiation. Postmitotic cells are known to be resistant to the introduction and expression of exogenous genetic constructs [431,432]. If for arguments sake, the efficiency of introducing an exogenous construct is on a sliding scale; with the least differentiated cells exhibiting the greatest potential, then the cells most likely to be

transformed would statistically be those that are least differentiated or most multipotential, and may therefore take longer to reach functional maturity when differentiated.

When considering the magnitude of KCl-induced $Ca^{2+}$ accumulations in differentiated primary cultures however, it would appear that the process of passaging cells cumulatively reduces the potential of cells within those cultures to become electrically excitable, as described above. This may be the cause of the CTX0E16/02 cultures' relative resistance to develop electrical excitability, as the earliest passages used for this cell lines was 15. This resistance to generate electrically excitable differentiated cultures is consistent with previous findings using a clonal cell line derived from 14-week gestation human cortex that was conditionally immortalised by an identical process to that of the CTX0E16/02 cell line [104]. All experiments in this study conducted by Donato and colleagues were carried out on cells exposed to 15 to 30 passages. These data beg the question of whether the cultures that were used to derive the CTX0E16/02 cell line were electrically excitable when initially acquired, or indeed whether any 12 week gestation cortical human tissue sample contain electrically excitable cells. With this in mind, it would be interesting to culture primary NPCs through increasing numbers of passages to determine how readily they are capable of differentiating after increasing time in adherant culture following exposure to the same culture conditions as described above. This may identify whether the observed resistance to differentiation of CTX0E16/02 cells is as a consequence of their exposure to this type of culture environment, or whether this is a normal property of NPCs from the cortex rather than from more primitive brain regions. It would also be interesting to address this same question in neuronal cultures derived from non-immortalised NPC cultures or indeed those derived from ES or iPS cells, as these would not have been expected to be electrically active at any point. In addition, ES or iPS cells could also be used to generate neurons from different neuronal lineages to determine whether those representative of the cortex take longer to functionally mature than one derived from those representative of the spinal cord for example.

Another factor that may contribute to the relative resistance to developing a mature – electrically excitably – neuronal phenotype may be the process of freezing cells. The CTX0E16/02 cell line would have been exposed to at least 3 freeze/thaw cycles prior to the experiments described above being performed. The experiments described above using primary NSC cultures were all performed with continuous passage. It would be interesting to see whether primary cell cultures become more resistant to the development of electrical excitability following single or multiple freeze/thaw cycles. While this may identify a contributory factor though, it is unfortunately unavoidable for a clonal NSC line such as CTX0E16/02.

The data presented above clearly raise several questions about the factors influencing the development of electrical excitability in adherent, differentiated NPC cultures. For the purposes of this study however – to explore the development of a human, cortically-derived NPC line for both basic research and screening purposes – there are certain factors which may influence the potential of differentiated cells to develop electrical excitability that cannot be avoided when developing a neural stem cell line. These include freezing and thawing cells, multiple passages and monolayer culture. Previously published work

has also highlighted several other approaches to stimulate electrical excitability or accelerate neuronal differentiation of NPCs but have been excluded for their relative impracticality with respect to the desired application of these cultures:

- Recent work has demonstrated promise for the use of nanoscale engineered surfaces or 3D matrices. These novel cell culture substrates seek to more faithfully mimic the arrangement of ECM components *in vivo*. With respect to NPCs, these growth substrates have been shown to provide superior conditions to conventional ECM component-coated plasticware for both expansion and differentiation [433-437]. While commercial products are now available, they remain the vanguard, and as such are prohibitively expensive.
- Exposure of cells to a depolarising concentration of KCl during differentiation has also been shown to promote neuronal differentiation and maturation [438-441]. This approach is both simple and inexpensive though unfortunately it was not well tolerated by the CTX0E16/02 cell line, and failed to provoke electrical excitability after a normal 28 day differentiation (data not shown).
- Grassi and colleagues demonstrated the efficacy of extremely low-frequency (50 Hz) electromagnetic fields in promoting plasma membrane expression of voltage-gated $Ca^{2+}$ channels in neuroendocrine cells [442]. More recently, the same group demonstrated that this approach could be applied to promote neural differentiation *in vitro* [443] and *in vivo* [444]. This approach is relatively non-invasive, but may prove difficult to control the uniformity of intensity of the electromagnetic field each different cultures was exposed to if propagating multiple cultures. This approach would additionally require the purchase of specific hardware.
- Primary culture conditioned medium has also been shown to demonstrate utility in promoting or accelerating differentiation of NPCs *in vitro* [320,445]. This approach would however require the continued use of primary cells, making work of this sort labour intensive and would precludes it's use for high-throughput screening. Work to identify the secreted factors responsible for this affect will certainly improve our ability to manipulate neuronal differentiation in the future.
- In an attempt to provide an ECM environment similar to that found *in vivo*, and provide cells with relevant paracrine signalling, the use of co-cultures have been widely used [446]. These often employ the use of mouse embryonic fibroblasts as a feeder cell layer to either support the maintenance or differentiation of various types of stem cell. Recent work has also identified the advantages of human derived feeder cell layers [447]. Unfortunately, while effective, this approach technically complicates experiments and for the purposes of transcriptomic studies and compound screening may provide misleading data that would be impossible to distinguish.

The soluble factors contained within medium exert a critical influence on the maintenance and differentiation of NPCs. If the ultimate goal of deriving clonal NPC lines is that they are capable of providing an expandable source of mature neurons and glia, then further work may be necessary to define factors used during the isolation process that not only provide multipotentiality and a normal karyotype, but also allow for the most rapid development of electrically excitable mature neuron. It

would therefore be of interest to investigate factors used in the derivation of NPC lines that may be either superfluous or inhibit the development of physiologically mature neural phenotypes.

# *Chapter 6 Pharmacological Validation & Increasing Assay Sensitivity*

A considerable body of data has been presented in the preceding chapters regarding the pharmacological responsiveness of proliferative and differentiated CTX0E16/02 cultures to various neurotransmitter receptor agonists. These ligand-induced responses have been measured using a $Ca^{2+}$-dependent fluorescence approach. As discussed previously, receptor-mediated intracellular $Ca^{2+}$ accumulation can occur through a variety of different mechanisms (see ***4.1***), but with respect to the activation of GPCRs this is primarily thought to occur through coupling to the heterotrimeric G-protein subunit, $G\alpha_{q/11}$ [362]. This induces the catalytic activity of the phospholipid cleavage enzyme phospholipase C-β (PLC-β), which cleaves membrane-bound phosphatidylinositol 4,5-bisphosphate ($PIP_2$) into diacylglycerol (DAG) and inositol 1,4,5-trisphosphate ($IP_3$). While DAG goes on to activate PKC, $IP_3$ causes the release of $Ca^{2+}$ from intracellular stores through its action at it's cognate, $IP_3$ receptor [188,336,362]. Many of the receptors targeted by antipsychotics demonstrate $G\alpha_{q/11}$ coupling such as 5-$HT_{2A}$, $M_1$ and $H_1$. In contrast however, arguably the most important receptor with regard to facilitating the effects of antipsychotics, the dopamine $D_2$ (and functionally similar dopamine $D_3$) receptor has been shown to mediate it's effects through it's canonical pathway beginning with the activation of the $G\alpha_i$ subunit. This leads to inhibition of adenylyl cyclase and subsequently a reduced conversion of ATP to cAMP, resulting in reduced PKA activity. Under certain conditions however, the dopamine $D_2$ receptor has also been shown to be capable of precipitating intracellular $Ca^{2+}$ accumulation. For example, $D_2$ has been shown to form functional heterodimers with $D_1$ or 5-$HT_{2A}$ receptors, facilitating promiscuous $G\alpha_{q/11}$ coupling, while it is also capable of provoking Gβγ-mediated activation of PLC-β [191,221]. Dopamine has also been shown to mediate increases in $[Ca^{2+}]_i$ in this study in both CTX0E16/02 and primary human embryonic neural cultures (see 4.2.2 above). This chapter explores receptor-mediated intracellular $Ca^{2+}$ accumulation in CTX0E16/02 cultures in response to dopamine, 5-HT and acetylcholine, using a range of specific agonists and antagonists, in an attempt to identify receptor subtypes responsible for the observed response. This chapter also details the use of a more reliable and sensitive surrogate for receptor activation in the form of ERK1/2 phosphorylation.

## *6.1 Introduction*

Measurement of intracellular $Ca^{2+}$ accumulation represents a simple and relatively inexpensive means to determine receptor-mediated activation, as well as providing an uncomplicated method to determine electrical excitability of cultures. It does not however reflect the full extent of receptor-mediated activity within a cell. Arguably the most important receptor with regards to antipsychotic activity is the dopamine $D_2$ receptor. This is due to affinity for this receptor being directly correlated with clinical efficacy for this class of drug [154]. The canonical pathway for the dopamine $D_2$ receptor, indeed for all dopamine receptors, involves the modulation of adenylyl cyclase (AC) through their coupling with either the $G\alpha_s$ ($D_1$ and $D_5$) or $G\alpha_i$ ($D_2$, $D_3$ and $D_4$) subunits, and does not involve intracellular $Ca^{2+}$ accumulation. Dopamine receptor pharmacology is far from simple though, and is certainly not restricted to modifying the rate of intracellular cAMP production. Indeed, several mechanisms have been implicated through

which dopamine is capable of modulating intracellular $Ca^{2+}$ concentrations, as discussed in ***4.1***, and reviewed in detail elsewhere [191]. Dopamine has been shown to be capable of provoking elevations in $[Ca^{2+}]_i$ in both proliferative and differentiated CTX0E16/02 cultures above (see 4.2.2 above). In addition, data has been provided showing intracellular $Ca^{2+}$ accumulations in response to 5-HT, glutamate, GABA, histamine, acetylcholine, phenylephrine and carbamoylcholine under certain conditions (see ***Chapter 4***). While robust changes in $[Ca^{2+}]_i$ were observed in responses to cholinergic ligands, glutamate and phenylephrine (see Figure 4.9), changes have remained more moderate in response to dopamine and 5-HT, requiring relatively large concentrations of drug to provoke a response (see Figure 4.18). In addition, due to the use of non-selective – and in many cases – neurotransmitter ligands, it remains unclear what contribution each of the receptors targeted by these ligands contribute to the observed changes in levels of intracellular $Ca^{2+}$ accumulation. This chapter will examine both the origin and specificity of some of these ligand-induced changes in $[Ca^{2+}]_i$ with the use of specific antagonists and the manipulation of experimental conditions, as a means to confirm that observed responses are indeed due to ligand binding and not as a consequence of non-specific interactions.

Many of the compounds (mostly neurotransmitters) tested on CTX0E16/02 cultures are known to bind receptors that are thought to directly modulate $[Ca^{2+}]_i$ such as histamine $H_1$ and 5-$HT_{2A}$ through $G\alpha_{q/11}$ subunit coupling, or $Ca^{2+}$-permeable ionotropic receptors to glutamate, 5-HT or acetylcholine [171,357,364,374]. For this reason, measurement of $[Ca^{2+}]_i$ represents a versatile and robust means to examine receptor activity. To more closely investigate the ligand-induced activity of dopamine receptors however, a more obvious choice would be to monitor adenylyl cyclase (AC) activity through measurement of intracellular cAMP levels, as mentioned above. Currently, the most accessible method to do this experimentally is through the use of antibodies raised against cAMP, and kits to perform this work are now commercially available but remain very expensive. Another factor to consider when looking for a surrogate marker of receptor activity is that measurement of cAMP levels is unfortunately limited to activation of $G\alpha_s$ and $G\alpha_i$-coupled GPCRs. In addition, to investigate $G\alpha_i$ activation – which inhibits AC activity – pre-stimulation of the enzyme with, for example forskolin is required, which necessitates optimisation and introduces an artificial component to the normal activity of the enzyme, and therefore the cells themselves. Unlike changes in the intracellular concentration of $Ca^{2+}$ or cAMP, modulation of the MAPK/ERK pathway is ubiquitous to all GPCRs [252,448], as discussed in 1.8 above. For this reason, the phosphorylation status of ERK1/2 provides a universal indicator of GPCR activity and as such, represents a relevant surrogate marker to investigate the presence of active receptors important for antipsychotic activity, since GPCRs represent their major targets.

ERK1 and ERK2 are both examples of MAP kinases that show considerable sequence homology and are activated upon phosphorylation of adjacent threonine and tyrosine residues arranged in a TXY motif within their respective activation loops [449]. Phosphorylation of ERK1 occurs at Thr202/Tyr204 while phosphorylation of ERK2 occurs at Thr185/Tyr187. These residues represent the only known subtrates for the dual-specificity protein kinases MEK1 and MEK2 [252]. MEK1 and MEK2 are activated through phosphorylation by B-Raf or c-Raf1, which are serine/threonine protein kinases, and it at the point of

Raf activation that integration occurs from the distinct GPCR signalling cascade families ($G\alpha_{i/o}$, $G\alpha_q$ and $G\alpha_s$) implicated in antipsychotic efficacy [228].

Levels of ERK1/2 phosphorylation can be monitored by several methods including the use of western blots [450], transgenic reporter systems [451], fluorescence resonance energy transfer (FRET) based assays [448,452], mass spectrometry and nuclear magnetic resonance spectroscopy [453]. Each approach has it's benefits and shortcomings, but with respect to a high-throughput environment as is required here due to the shear number of assays needing to be performed, a FRET based approach was most appropriate [454]. Several kit based FRET assays have become available in recent years to resolve levels of phosphorylated ERK1/2 *in vitro*. Perhaps the most widely used by industry for HTS applications is AlphaScreen®SureFire® technology, that requires the use of both special lighting facilities to perform the assay and Alpha assay-specific plate reading equipment to resolve data. Lacking access to either of these resources it was decided to opt for an alternative FRET based system – HTRF® technology – that could be used both in ambient light and using plate-reading facilities kindly made available by Dr Andrew Beavil, within the Randall Division of Cell and Molecular Biophysics, King's College London.

Due to the poor levels of intracellular $Ca^{2+}$ accumulation provoked by ligands such as dopamine and 5-HT in many of the experiments presented above, ERK1/2 phosphorylation will instead be used as a means to determine the extent to which CTX0E16/02 cultures respond to these ligands. Dopamine and 5-HT are considered as particularly important due to their known function in the transduction of the effects of antipsychotics. Through further scrutiny of ligand-induced intracellular $Ca^{2+}$ accumulation and an evaluation of ligand-induced ERK1/2 phosphorylation, the work described in this chapter provides a more detailed description of cellular responses provoked through receptors for which antipsychotics demonstrate high affinity. Levels of ligand-induced ERK1/2 phosphorylation will be used to supplement data already obtained through measurement of ligand-induced $Ca^{2+}$ accumulation, to provide a more detailed picture of the pharmacological responsiveness of differentiated CTX0E16/02 cultures. These data are then used to identify important considerations for the use of native human cells – as represented by the CTX0E16/02 line – in basic science and drug discovery. The feasibility of using differentiated CTX0E16/02 cultures to investigate the mechanism of action of antipsychotic medicines is addressed, and identifies important factors that must be considered when using them as an *in vitro* tool to interrogate the mode of action of psychiatric medicines.

## *6.2 Results*

Data presented in ***Chapter 4*** detailed intracellular $Ca^{2+}$ accumulations in response to various ligands in CTX0E16/02 cells grown under proliferative and a variety of different differentiation conditions. This section provides further evidence regarding the nature of some of these responses to generate a more detailed picture of the signalling event(s) responsible for the observed ligand-induced changes in $[Ca^{2+}]_i$. Owing to time restraints, the work described in the following sections focus upon dopamine, 5-HT and acetylcholine-induced responses in differentiated CTX0E16/02 cultures. Dopamine and 5-HT-induced

responses were selected for further scrutiny due to the established role that their cognate receptors play in the transduction of the effects of antipsychotics to the intracellular environment [156,166,455,456]. Acetylcholine was additionally investigated due to its ability to provoke consistently robust, concentration-dependent intracellular $Ca^{2+}$ responses, thus providing a broad dynamic range of activity within which the effects of pharmacological manipulation could more readily be discerned. In addition, the cholinergic system is also implicated in the action of antipsychotic drugs through their reported affinity for a range of different muscarinic receptors [183,209,457]. Indeed, the muscarinic $M_1$ receptor is currently being explored as a target to treat the various symptom domains of schizophrenia as a monotherapy, and also as an adjunct to relieve cognitive symptoms [175] – an indication which is additionally attempting to be addressed through the use of compounds targeted cholinergic nicotinic receptors [157,176].

While changes in $[Ca^{2+}]_i$ have been observed in response to dopamine, 5-HT and acetylcholine in CTX0E16/02 cells under various culture conditions (see ***Chapter 4***), it remains unclear which of the dopamine receptors are responsible for transducing these effects. With a view to using these cells to investigate the mechanism of action of antipsychotic medicines, there was particular interest in the relative contribution to these changes in $[Ca^{2+}]_i$ provoked by dopamine and 5-HT from $D_2$ and 5-$HT_{2A}$ receptors. In addition, it also remained unclear whether intracellular $Ca^{2+}$ accumulation provoked by acetylcholine is attributable to its action at muscarinic or nicotinic receptors, or a combination of the two. The following sections will therefore be use to investigate the source of the observed increases in $[Ca^{2+}]_i$ in response to dopamine, 5-HT and acetylcholine.

### *6.2.1 Dopamine-Induced $Ca^{2+}$ Responses in CTX0E16/02 Cultures Prove Difficult to Resolve*

Neither dopamine or 5-HT were capable of precipitating large increases in $[Ca^{2+}]_i$ in differentiated CTX0E16/02 cultures. Of the various differentiation conditions tested, exposure to 1 mM dibutyryl-cAMP and 0.5 mM IBMX for the final 7 days of differentiation facilitated the largest response above baseline to either dopamine or 5-HT (see Figure 4.28, above). The responses observed did not however appear to follow a concentration-dependent relationship; with intracellular $Ca^{2+}$ accumulation only occurring at the highest tested concentration (1 mM for both dopamine and 5-HT). These small changes in $[Ca^{2+}]_i$ could be explained in various ways, for instance, low receptor expression, inefficient G-protein coupling or alternative downstream signalling events such as cAMP accumulation. However, at present it remains unclear which of the dopamine or 5-HT receptors are responsible for transducing the effects observed. With a particular interest in using the CTX0E16/02 cells to study the action of antipsychotic medicines, as mentioned above, responses to dopamine and 5-HT were interrogated through the use of antagonist known to selectively block the dopamine $D_2$ and 5-$HT_{2A}$ receptors.

To investigate the relative contribution of the different receptors responsible for the observed increase in $[Ca^{2+}]_i$ when differentiated CTX0E16/02 cultures were exposed to dopamine, cultures were first incubation with the selective competitive $D_2/D_3$ receptor antagonist raclopride ($K_i$ values: 1.8, 3.5, 2400

and 18000 for $D_2$, $D_3$, $D_4$ and $D_1$ receptors respectively with $D_5$ receptor affinity tending to reflect that of $D_1$ for dopamine antagonists [458]) or the $D_1/D_5$ receptor antagonist SCH39166 ($K_i$ values: 5.0, 4.4, 3751.8, >1000 and 5934.1 for $D_1$, $D_5$, $D_2$, $D_3$ and $D_4$ receptors respectively [459,460]), before exposure to dopamine. SCH39166 was selected in place of the standard selective $D_1$-selective antagonist SCH23390 because it is a potent agonist at 5-$HT_{1C}$ receptors ($K_i$ = 6.3 nM *in vitro* [461]). Due to the high affinity that raclopride and SCH39166 demonstrate at the receptors of interest – $D_2/D_3$ and $D_1/D_5$ respectively – it was decided that they would be tested at concentrations between 0.1 nM and 100 nM. These concentrations were tested for their ability to eliminate increases in $[Ca^{2+}]_i$ provoked by 1 mM dopamine (the highest tested concentration from previously described experiments).

CTX0E16/02 cultures were differentiated for 28 days in SNBM, with 1 mM dibutyryl-cAMP and 0.5 mM IBMX added for the final 7 days of differentiation (as described in ***4.2.11***), as these conditions were found to produce the most robust $[Ca^{2+}]_i$ increases in response to dopamine and 5-HT. Cultures were then prepared for intracellular $Ca^{2+}$ mobilisation assays as described in 2.4.1 above. Previously described experiments investigating ligand-induced intracellular $Ca^{2+}$ accumulation involved cultures being exposed to agonists dissolved in $Ca^{2+}$ Release Assay Buffer prior to a 50 mM KCl challenge. However, to investigate the action of an agonist in the presence of an antagonist, it is important that the antagonist is first allowed to reach equilibrium receptor binding prior to the addition of agonist (personal communication from Professor Stuart Bevan). This approach has the additional benefit of establishing whether the antagonist itself is capable of provoking a response and therefore serves as a control. With this in mind, and consistent with industry standard drug screening methodologies (personal communication from Professor Stuart Bevan), experiments on each well were performed as described in 2.4.1 above, only with a change in the timing when each compound was added. Briefly, these experiments were performed at 37°C with the Fura-2 AM dye excited at both 340 nm and 380 nm and detected at 520 nm with a 515 nm cut-off. Each well initially contained 50 µl of $Ca^{2+}$ Release Assay Buffer and was exposed to an initial 180 second experiment with readings taken every 6 seconds starting at 0 seconds. A baseline was provided for each well by taking a mean of the first 4 readings. To investigate dopamine-induced changes in $[Ca^{2+}]_i$; after 20 seconds, cultures were exposed to either raclopride ($D_2/D_3$ antagonist), SCH39166 ($D_1/D_5$ antagonist) or both raclopride and SCH39166. Compounds were made up at twice the required concentration with 50 µl of each compound/concentration added to individual wells to achieve a final concentration of between 0.1 nM and 100 nM at half log unit intervals. Following a 100 second exposure to antagonist, cultures were then exposed to a final dopamine concentration of 1 mM. This was achieved by adding 20 µl of 6 mM dopamine to each well. This of course slightly diluted the concentration of antagonist each well was exposed to but, as stated above, is an industry standard method to explore antagonist activity. Final readings were taken after 60 seconds exposure to dopamine and 180 seconds after the start of the experiment. At this point, 70 µl was removed from each well to leave 50 µl and a second stage of the experiment was performed. This involved a 60 second experiment with readings taken every 6 seconds using the same parameters as those described above. At 20 seconds 50 µl of 20 µM ionomycin in $Ca^{2+}$ Release Assay Buffer was added to each well to expose cells to a final concentration of 10 µM. This was

used to provoke a maximal response for each well, against which all previous readings were provided as a relative value. The timing of drug additions are summarised in Figure 6.1, below. Two separate 96-well plates were used for these experiments, each containing differentiated CTX0E16/02 cultures that were derived from separate frozen cell aliquots and exposed to at least 3 passages prior to seeding. These data therefore represented an *n* of 2 with 3 technical replicates for each biological replicate.

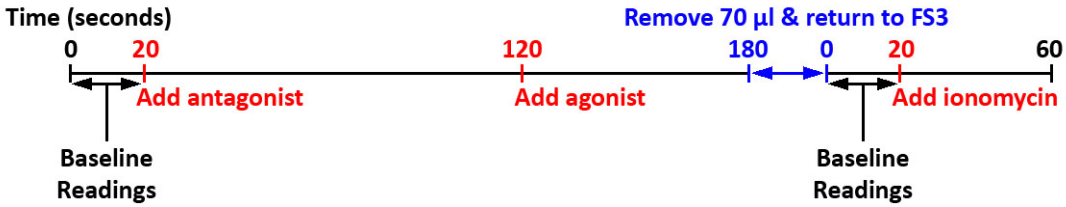


***Figure 6.1 Timeline to illustrate the addition of different drugs when using agonists and antagonists***

Data obtained from experiments looking at the effect of dopamine antagonists on dopamine-induced increases in $[Ca^{2+}]_i$ proved difficult to interpret and were far from what might have been expected. When added alone, the selective $D_2/D_3$ antagonist raclopride did not alter $[Ca^{2+}]_i$ as compared to baseline, where only $Ca^{2+}$ Release Assay Buffer was added (Figure 6.2 **a**, below). On addition of 1 mM dopamine however, a small reduction was observed in $[Ca^{2+}]_i$ at all tested concentrations of raclopride. This effect was not observed in cultures where assay buffer containing no raclopride was added, suggesting the observed effect was not as a consequence of the addition of fluid to the wells. If antagonism of the $D_2/D_3$ receptors was occurring, then responses observed should be as a consequence of dopamine's activity at other dopamine receptors expressed by the differentiated CTX0E16/02 cells. These data indicate that raclopride was only capable of reducing $[Ca^{2+}]_i$ once dopamine was added and appears counter-intuitive considering dopamine itself, in the absence of any raclopride did not elevate $[Ca^{2+}]_i$. Had dopamine exerted an effect upon $[Ca^{2+}]_i$ though stimulation of $D_2/D_3$ receptors, this would be expected to be observed in the presence of lower concentrations of raclopride, and indeed in the absence of raclopride, with a reduction in $[Ca^{2+}]_i$ as the concentration of raclopride increased. The reduction in $[Ca^{2+}]_i$ in the presence of raclopride following the addition of dopamine was not concentration-dependent and suggests either that these data are artifactual or that measurement of $[Ca^{2+}]_i$ as a marker of dopamine's activity on differentiated CTX0E16/02 cultures is insufficiently sensitive. Based on data showing dopamine's ability to elevate levels of ERK1/2 phosphorylation, the latter is thought to be the case.

These data highlight the difficulties of using cells with a broad receptor expression profile to investigate detailed pharmacology *in vitro*, using a relatively crude marker such as $[Ca^{2+}]_i$. The reasons for this are several-fold; firstly, the levels of $[Ca^{2+}]_i$ observed in response to 1 mM dopamine are very low (indeed, in this experiment they were absent – despite showing an effect under the same conditions in previous experiments), and therefore represents a very narrow dynamic range to observe any changes. This was highlighted when investigating intracellular $Ca^{2+}$ accumulation in single cells, where small responses

were observed in relatively few cells within each culture (see section ***4.2.2***). With respect to dopamine receptors, it is also unclear what intracellular mechanism is responsible for any observed rise in intracellular $Ca^{2+}$. Various reports have demonstrated the capacity of dopamine receptors to modulate $[Ca^{2+}]_i$ through promiscuous $G\alpha_q$ coupling by $D_1/D_5$ receptors [407,411,462], $D_2$ receptor-mediated activation of PLC via their associated $G\beta\gamma$ subunit [363], $D_2$ receptor-mediated modulation of L and N-type $Ca^{2+}$ channels [363,463] and even the ability of $D_1/D_2$ heterodimers to couple directly to $G\alpha_q$ [413]. However, the exact mechanism (s) through which dopamine is capable of modulating $[Ca^{2+}]_i$ remains controversial and is likely to be tissue and cell type specific [191].

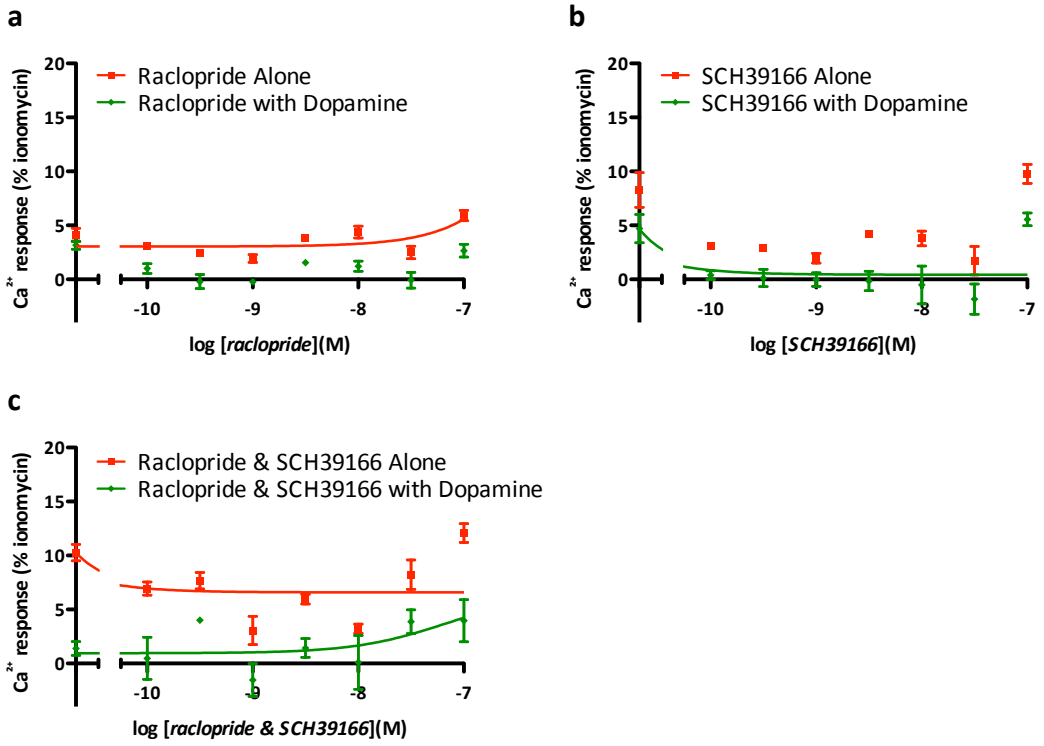


***Figure 6.2 Antagonism of dopamine-induced $Ca^{2+}$ responses in differentiated CTX0E16/02 cultures***
CTX0E16/02 cells were seeded onto laminin-coated 96-well plates at 3 x $10^4$ cells per well and differentiated for 28 days using SNBM that was additionally supplemented with 1 mM dibutyryl-cAMP and 0.5 mM IBMX for the final 7 days of differentiation. Cultures were incubated for 1 hour in the presence of the cell permeable, $Ca^{2+}$-sensitive fluorescent dye Fura-2 AM, before being washed prior to ligand-induced fluorescence being measured using a FlexStation 3. Cultures were first exposed to raclopride, SCH39166 or both raclopride and SCH39166 to a final concentration of between 0.1 nM to 100 nM. All cultures were then exposed to dopamine to a final concentration of 1 mM. Concentration-response curves are shown for raclopride (**a**), SCH39166 (**b**) and raclopride & SCH39166 (**c**). Red squares show effect of antagonist alone while green diamonds indicate responses observed after the addition of dopamine to the same well. Data points represent mean ± S.E.M. from *n* = 2, each with 3 technical replicates and expressed relative to the positive control, ionomycin.

Intracellular $Ca^{2+}$ accumulations observed in differentiated CTX0E16/02 cultures exposed to the selective $D_1/D_5$ antagonist SCH39166 were equally as difficult to interpret. Due to a relatively high level of baseline fluorescence, when added alone SCH39166 appeared to cause a reduction in $[Ca^{2+}]_i$, but this effect was not concentration-dependent. In addition, at the highest tested concentration of SCH39166 (100 nM), levels of $[Ca^{2+}]_i$ returned to the same levels observed at baseline (Figure 6.2, panel **b**). As with

raclopride, addition of dopamine caused an apparent reduction in $[Ca^{2+}]_i$. This reduction in $[Ca^{2+}]_i$ was similar at all tested concentrations of SCH31966 and in contrast to that seen in the experiment with raclopride was also observed in cultures exposed to no antagonist, suggesting this effect was perhaps a consequence of the drug addition itself, and therefore likely to be non-specific. A similar trend was observed when differentiated CTX0E16/02 cultures were exposed to both raclopride and SCH39166 in combination. No concentration-dependent effect was observed, and exposure to dopamine caused a further reduction in $[Ca^{2+}]_i$. Greater variability between responses was also observed upon addition of dopamine, as is clear from the size of the error bars (Figure 6.2, panel **b**). There was concern that the observed effects were simply due to the cells demonstrating poor adherence to the tissue culture plastic upon which they were differentiated, and the addition of compounds by the FS3 liquid handling robotics were responsible for the observed fluctuations. Upon investigation with phase contrast microscopy however there was no evidence of poor adherence. Taken together, these data suggest that the measurement of $[Ca^{2+}]_i$ as a marker to examine the effect of dopamine upon CTX0E16/02 cells is insufficiently sensitive. A premise that was highlighted when examining increases in $[Ca^{2+}]_i$ at the level of individual cells (see ***4.2.2*** and Figure 4.12).

Another factor affecting ligand-induced intracellular $Ca^{2+}$ accumulations was that of an observed "edge-effect". This emerged from retrospective analysis of raw data from individual wells, though while this effect was minimal for some experiments, it appeared to me more pronounced in experiments where differentiated CTX0E16/02 cells were exposed to challenging conditions such as long periods in culture, or in this case, an elevation of cAMP-mediated activity. This "edge-effect" meant that cultures in wells surrounding the edge of each 96-well plate tended to demonstrate higher basal fluorescence ratios, and often presented outlying values – skewing readings above that detected in wells away from the edge of plates but exposed to the same condition, such as drug concentration. There exist various potential causes for these observations that will be explored in the Discussion below, with a series of recommendations to improve and hopefully prevent this influence for further experimentation using the CTX0E16/02 cell line. When performing $Ca^{2+}$ mobilisation assays, the wells to which both the highest tested concentration of drug used in each experiment and assay buffer alone (negative control) was added were always locate at the edge of plates. For many of the experiments described previously in ***Chapter 4*** and ***Chapter 5***, this was less of an issue when a clear trend was observable from robust responses, or the differentiation protocol did not affect basal fluorescence ratios within the cultures. Due to the low magnitude of intracellular $Ca^{2+}$ accumulations observed in the experiments illustrated in Figure 6.2 above, the influence of this "edge-effect" appeared to significantly affect the sensitivity of this assay to resolve accurate responses in the presence of antagonists.

These data indicate that the measurement of intracellular $Ca^{2+}$ accumulation in differentiated CTX0E16/02 cultures using a FS3 plate reader provides insufficient sensitivity to detect dopamine-induced responses. Data presented below showing dopamine-induced ERK1/2 phosphorylation suggests that dopamine's effects are mediated through an alternative second messenger – presumably cAMP.

### *6.2.2 5-HT$_{2A}$ Agonist Behaves as Inverse Agonist in Differentiated CTX0E16/02 Cultures*

Experiments were also performed to investigate increases in $[Ca^{2+}]_i$ provoked by 5-HT and the relative contribution of this signal made by 5-HT$_{2A}$ receptors. As described previously, intracellular $Ca^{2+}$ accumulation in response to 5-HT – like those to dopamine – was most pronounced when CTX0E16/02 cells were differentiated for 28 days in the presence of SNBM, with 1 mM dibutyryl-cAMP and 0.5 mM IBMX being added for the final 7 days of differentiation. Cultures were prepared and assayed in the same way as described for experiments designed to elucidate the relative contribution of different dopamine receptors. However, since broadly selective 5-HT antagonists are not currently available, and due to the considerable diversity of 5-HT receptors compared to those for dopamine, it was felt that the number of different compounds needed to try and block a 5-HT-induced response would yield data impossible to interpret. This is confounded by the fact that many of the "specific" 5-HT receptor subtype antagonists available also show affinity for structurally similar GPCRs such as those targeted by catecholamines. Unlike experiments where heterologous systems are used to express a single cloned receptor of interest, the CTX0E16/02 cells express a wide range of receptors and so it is difficult to determine non-specific responses to a particular compound. This can be performed in heterologous expression systems by simply exposing the compound of interest to receptor-null cells. Therefore, cultures were instead exposed to the 5-HT$_{2A}$-specific antagonist, MDL11939 in the presence of 1 mM 5-HT, in an attempt to determine the relative contribution of 5-HT$_{2A}$-receptors to the observed increase in $[Ca^{2+}]_i$ provoked by 5-HT. This receptor was of particular interest due to its reported role in mediating the effects of antipsychotic drugs [286]. Individual wells of 96-well plates were therefore exposed to varying concentrations of the 5-HT$_{2A}$-selective antagonist MDL11939 to provide a concentration-response curve between 0.1 nM and 100 nM prior to the addition of 5-HT to all wells to a final concentration of 1 mM.

As with experiments investigating dopamine antagonism above, these cultures demonstrated relatively high basal fluorescence ratios when exposed only to $Ca^{2+}$ Release Assay Buffer (see Figure 6.3, **a**). With the addition of the 5-HT$_{2A}$-specific antagonist, MDL11939 there appeared to be a non-concentration dependent reduction in $[Ca^{2+}]_i$ at all except the highest tested concentration of 100 nM when an increase in $[Ca^{2+}]_i$ was observed. This may be attributable to the same "edge effect" that was described above. In contrast to experiments looking at dopamine antagonism however, subsequent exposure to 5-HT caused an increase in intracellular $Ca^{2+}$ accumulation – as would be expected of an agonist. However, this effect was also observed in cultures exposed to high concentrations of the 5-HT$_{2A}$-specific antagonist, MDL11939 (Figure 6.3, **a**). When compared to the original experiments looking at 5-HT-induced responses in similarly differentiated cultures however, these responses were considerably larger than those seen in response to 1 mM 5-HT (see Figure 4.12), suggesting little contribution of 5-HT$_{2A}$ receptors to the observed increase in $[Ca^{2+}]_i$. Using an alternative approach to determine 5-HT$_{2A}$-mediated responses, differentiated cells were exposed to the 5-HT$_{2A}$-receptor-specific agonist, 4-Bromo-3,6-dimethoxybenzocyclobut en-1-yl)methylamine (TCB-2). On the same 96-well plates used to determine the effect of MDL11939 on 5-HT-induced responses, cells were exposed to varying concentrations TCB-2 to construct a concentration response curve from 1 µM to 1 mM, these data are

shown in ***Figure 6.3***, panel **b**. While more potent and better-characterised 5-$HT_{2A}$-specific agonists exist – such as lysergic acid diethylamide (LSD) or 2,5-dimethoxy-4-iodoamphetamine (DOI) – these are very difficult to obtain due to their potent hallucinogenic properties, and are consequently controlled under the UK Misuse of Drugs Act 1971.

In contrast to expectations, TCB-2 demonstrated a concentration-dependent reduction in intracellular $Ca^{2+}$ accumulation (Figure 6.3 panel b, below). As a full agonist at the typically $G\alpha_q$-coupled 5-$HT_{2A}$ receptor, TCB-2 was expected to elicit a concentration-dependent increase in $[Ca^{2+}]_i$. Indeed, using NIH3T3 cells stably expressing rat 5-$HT_{2A}$ receptors, TCB-2 was shown to demonstrate functional selectivity by producing a 65-fold preference for the activation of the PLC pathway ($EC_{50}$ = 18 nM for $IP_3$ accumulation) rather than the $PLA_2$ pathway ($EC_{50}$ = 1180 nM for arachidonic acid release)[464], thus favouring intracellular $Ca^{2+}$ accumulation. In addition, TCB-2 was shown to display particularly high affinity for 5-$HT_{2A}$ receptors, with a $K_i$ of 0.35 nM and 0.26 nM at rat and human 5-$HT_{2A}$ receptors respectively when stably expressed in NIH3T3 cells [464], and was capable of provoking considerable levels of ERK1/2 phosphorylation at 1 nM in HEK293 cells stably expressing the human form of the receptor [465]. *In vivo*, TCB-2 has also been shown to demonstrate equal potency in drug discrimination assays in rats to the most potent known phenethylamine hallucinogens, which represent highly efficacious agonists at this receptor subtype [466], and elicit parallel behavioural responses in mice to the potent 5-$HT_{2A/2C}$ agonist, DOI [467]. Further work is required to determine the root of the observed concentration-dependent decrease in $[Ca^{2+}]_i$ in response to TCB-2 in differentiated CTX0E16/02 cultures. The effect exerted by TCB-2 upon CTX0E16/02 cultures – a concentration-dependent decrease in $[Ca^{2+}]_i$ in the absence of stimulation – is that of an inverse agonist. However, it remains unclear which receptor(s) this effect is mediated through, and no reports in the existing literature have implicated TCB-2 as being capable of exerting this property.

TCB-2 has not been widely studied to date, with it's synthesis and initial characterisation only being described as recently as 2006 [464]. Indeed, much of the work so far reported using this compound have been with respect to its affinity and activity at 5-$HT_{2A}$ receptors. It's specificity for this receptor is highlighted by the ability of MDL11939 to block 5-$HT_{2A}$-associated behavioural responses provoked by TCB-2 in mice [467] or altanserin (a 5-$HT_{2A}$ specific antagonist) to block TCB-2-mediated behavioural responses in rats [468], though this in itself does not preclude it's activity at other cellular signalling targets. Indeed, specificity for 5-$HT_{2A}$ receptors does not itself eliminate the possibility that TCB-2 may be capable of provoking distinct signalling events in differentiated CTX0E16/02 cultures to those observed when 5-$HT_{2A}$ receptors are heterologously expressed in NIH3T3 or HEK293 cells. Recent reports have described the ability of 5-$HT_{2A}$ receptors to form functional heterodimers with dopamine $D_2$ receptors when co-expressed in HEK293T cells [219], or mGluR2 receptors in HEK293T cells or Xenopus oocytes [220,221] *in vitro*. In each case a functional consequence was observed in response to known ligands that targeted either of the receptors in the heteromer. Evidence of physical association of 5-$HT_{2A}$ and mGluR2 receptors has also been demonstrated in *ex vivo* human and mouse cortex [220]. Collectively, these data only highlight the usefulness and relevance of exploring receptor pharmacology in native

expression systems such as the CTX0E16/02 cell line. These data appear to show that – as was the case for dopamine – measurement of $[Ca^{2+}]_i$ in differentiated CTX0E16/02 cultures is an insufficiently sensitive approach to evaluate the effects of 5-HT, and ascribe these to individual receptor subtypes. In contrast however, this strategy was able to detect an apparently novel effect of TCB-2 in a native tissue model. These experiments indicate that a different functional marker may be needed to explore the effects transduced by dopamine and 5-HT receptors in CTX0E16/02 cells, though suggest that this should be used in conjunction with the measurement of $[Ca^{2+}]_i$ rather than as a replacement. Indeed, as discussed in 1.7.2 above, only through the measurement of a range of different functional endpoints can the full 'texture' of ligand-receptor interaction be perceived. This in itself highlights the importance of using *in vitro* native tissue models to explore the pharmacological effects of a given ligand.

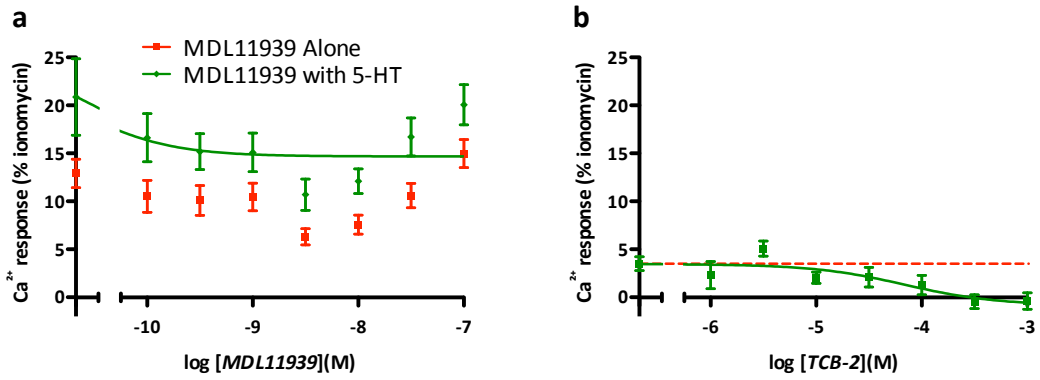


***Figure 6.3 Relative contribution of 5-HT$_{2A}$-mediated $Ca^{2+}$ responses in differentiated CTX0E16/02 cultures***
CTX0E16/02 cells were seeded onto laminin-coated 96-well plates at 3 x $10^4$ cells per well and differentiated for 28 days using SNBM that was additionally supplemented with 1 mM dibutyryl-cAMP and 0.5 mM IBMX for the final 7 days of differentiation. Cultures were incubated for 1 hour in the presence of the cell permeable, $Ca^{2+}$-sensitive fluorescent dye Fura-2 AM, before being washed prior to ligand-induced fluorescence being measured using a FlexStation 3. (**a**) cultures were first exposed to MDL11939 to a final concentration of between 0.1 nM to 100 nM. All cultures were then exposed to 5-HT to a final concentration of 1 mM. Red squares show effect of MDL11939 alone while green diamonds indicate responses observed after the addition of 5-HT to the same well. (**b**) concentration-response curve for the 5-HT$_{2A}$-selective agonist TCB-2 between 1 µM and 1 mM. Data points represent mean ± S.E.M. from *n* = 2, each with 3 technical replicates and expressed relative to the positive control, ionomycin.

### *6.2.3 Acetylcholine Provokes $Ca^{2+}$ Influx Through Metabotropic Receptors*

Acetylcholine was capable of consistently producing robust increases in $[Ca^{2+}]_i$ in both proliferative and differentiated CTX0E16/02 cultures, and therefore represents a greater dynamic range of activity to try and determine the specificity of evoked signals – a problem that has been described above for dopamine and 5-HT-induced rises in $[Ca^{2+}]_i$. Acetylcholine's effects can be transduced through either metabotropic muscarinic receptors ($M_1$ to $M_5$)[366] or ionotropic nicotinic receptor, of which several subunit combinations exist within the CNS [374]. $M_1$, $M_3$ and $M_5$ have all been shown to couple to $G\alpha_q$ and can therefore elevate $[Ca^{2+}]_i$ via release from intracellular stores upon activation. Nicotinic receptors on the other hand are non-selective cation channels that are permeable to $Na^+$ and $K^+$, though some subunit combinations can also render these channels permeable to $Ca^{2+}$ [469]. With respect to

antipsychotic activity, the muscarinic $M_1$ receptor is of particular interest due to several currently available antipsychotics showing relatively high affinity there, and also represents a target for novel therapies, particularly with respect to relief of cognitive symptoms [175,176]. To determine the relative contribution of different receptors to the observed rise in $[Ca^{2+}]_i$ following exposure of differentiated CTX0E16/02 cultures to acetylcholine, a series of experiments were performed using both nicotinic and muscarinic antagonists, and removal of $Ca^{2+}$ from the assay buffer to establish whether the source of $Ca^{2+}$ accumulations was from intracellular stores or due to $Ca^{2+}$ influx. All experiments using cholinergic antagonists were performed in the presence of 10 μM acetylcholine, as this was shown to produce approximately 80% of a maximal response in differentiated CTX0E16/02 cultures and was therefore on the log phase of the acetylcholine concentration-response curve (see Figure 4.9 **c**). This concentration would therefore provide a robust response without receptor saturation and facilitate the appearance of receptor inhibition.

To determine the origin of intracellular $Ca^{2+}$ following exposure of differentiated CTX0E16/02 cultures to increasing concentrations of acetylcholine, this experiment was repeated using $Ca^{2+}$ Release Assay Buffer lacking $Ca^{2+}$ and additionally supplemented with the $Ca^{2+}$ chelating agent, EGTA at 1 mM ($Ca^{2+}$-free assay buffer contained: 140 mM NaCl, 5 mM KCl, 1 mM $MgCl_2$, 10 mM HEPES, 10 mM glucose and 1 mM EGTA). Acetylcholine was only capable of eliciting a minimal concentration-dependent rise in $[Ca^{2+}]_i$ in the presence of $Ca^{2+}$-free assay buffer containing EGTA (see Figure 6.4 **a**, below). These data suggested that the majority of intracellular $Ca^{2+}$ accumulation observed in response to acetylcholine originated from the extracellular environment rather than intracellular stores, thus implicating the activity of $Ca^{2+}$-permeable nicotinic acetylcholine receptors. Mecamylamine represents a non-competitive, non-selective neuronal nicotinic receptor antagonist with μM affinity for α3/β2, α4/β2, α2/β4, α3/β4, α4/β and α7 nicotinic receptors [469]. This compound was used to determine the extent of acetylcholine-mediated intracellular $Ca^{2+}$ accumulation attributable to nicotinic receptors, representing a non-selective antagonist with considerable affinity for a whole range of neuronal nicotinic receptor subtypes [469]. Alternative available competitive antagonists tended to be specific for certain nicotinic receptor subtypes, or in the case of d-tubocucarine was too non-specific, with considerable affinity for 5-$HT_3$ and $GABA_A$ receptors [470,471]. When administered alone, mecamylamine produced no effect on normally differentiated CTX0E16/02 cultures, but was also incapable of preventing the rise in $[Ca^{2+}]_i$ with subsequent exposure to 10 μM acetylcholine (Figure 6.4, **b**). In conflict with the previous experiment to determine the effect of $Ca^{2+}$-free assay buffer, these data suggest that nicotinic receptors contribute little to the rise in $[Ca^{2+}]_i$ observed in differentiated CTX0E16/02 cultures following exposure to 10 μM acetylcholine. There remains the possibility however that nicotinic receptors not targeted by mecamylamine are also present on differentiated CTX0E16/02 cells and account for part of the observed $Ca^{2+}$ flux. Further characterisation with multiple specific antagonists would be required for this to be determined. Taken together, these data suggest that the majority of intracellular $Ca^{2+}$ accumulation observed in response to 10 μM acetylcholine is attributable to an effect at muscarinic rather than nicotinic receptors. It also suggests however, that the increase in $[Ca^{2+}]_i$ does not solely arise through $G\alpha_q$-mediated activation of PLC-β and subsequent release of $Ca^{2+}$ from intracellular stores, and

implicates $Ca^{2+}$ influx as a contributory factor. The mechanism through which this occurs remains unclear, though could be caused by muscarinic receptor mediated opening of $Ca^{2+}$ permeable TRPC channels, as discussed in ***4.1*** and ***4.2.2***.

To explore the contribution of muscarinic receptors to the observed acetylcholine-induced rise in $[Ca^{2+}]_i$ in differentiated CTX0E16/02 cultures, the influence of the muscarinic antagonists, biperiden and telenzepine were investigated. Biperiden is a relatively non-selective but high affinity, competitive muscarinic receptor antagonist ($K_i$ = 0.48 nM, 6.3 nM, 3.9 nM, 2.4 nM and 6.3 nM for $M_1$, $M_2$, $M_3$, $M_4$ and $M_5$ receptors respectively [472]), while telenzepine is a competitive and relatively $M_1$-selective antagonist ($K_i$ = 0.94 nM and 17.8 nM for $M_1$ and $M_2$ receptors respectively [473]). When added alone, neither biperiden or telenzepine provoked a rise in $[Ca^{2+}]_i$ (see Figure 6.4, **c** and **d**). Upon addition of 10 µM acetylcholine, biperiden demonstrated a concentration-dependent inhibition of intracellular $Ca^{2+}$ accumulation with an $IC_{50}$ of 5 nM though appeared not to fully eliminate acetylcholine-induced $Ca^{2+}$ accumulation (Figure 6.4, **c**). Telenzepine was capable of completely eliminating $Ca^{2+}$ accumulation in response to 10 µM acetylcholine though showed a lower $IC_{50}$ of 63 nM (Figure 6.4, panel **d**). Biperiden has been shown to demonstrate nanomolar affinity for all five muscarinic receptor subtypes and is especially high for the muscarinic $M_1$ receptor at 0.5 nM [472]. The $IC_{50}$ of 5 nM for biperiden in differentiated CTX0E16/02 is therefore consistent with these values though it is unclear why there was not a complete elimination of the acetylcholine-induced rise in $[Ca^{2+}]_i$, as was observed for telenzepine. Telenzepine itself was less potent in eliminating acetylcholine-induced intracellular $Ca^{2+}$ accumulation ($IC_{50}$ = 63 nM) though was capable of completely eliminating this response at 1 µM. Telenzepine demonstrates slightly lower affinity for the $M_1$ and $M_2$ receptors and data for the remaining muscarinic receptors remains undetermined [473]. These data would therefore suggest that telenzepine either demonstrates relatively high affinity for all five muscarinic receptor subtypes or that acetylcholine-induced intracellular $Ca^{2+}$ accumulation is largely mediated through $M_1$ and $M_2$ receptors alone. The former is however the more likely explanation as muscarinic receptors exhibit particularly high sequence homology [366], and this has so far hampered the development of subtype-specific ligands [474]. Although further work is required to fully characterise the acetylcholine-induced increases in $[Ca^{2+}]_i$ observed in differentiated CTX0E16/02 cultures. The work described above suggests that the majority of the observed intracellular $Ca^{2+}$ accumulation provoked by acetylcholine is attributable to its action at muscarinic receptors. However, due to the fact that the observed rise in $[Ca^{2+}]_i$ occurs as a consequence of $Ca^{2+}$ influx (see Figure 6.4 **a**, below), this eliminates $IP_3$-mediated release of $Ca^{2+}$ from intracellular stores due to $G\alpha_q$-mediated activation of PLC-β and subsequent $PIP_2$ cleavage as a possible mechanism. This does not eliminate $G\alpha_q$-mediated activation of PLC-β from the picture however. As discussed previously, PLC-β-mediated cleavage of $PIP_2$ leads to the intracellular accumulation of both $IP_3$ and DAG, while $IP_3$ is known to release $Ca^{2+}$ from intracellular stores through binding to its cognate receptor, increasing evidence suggests that DAG can control $Ca^{2+}$ entry through its action on TRPC channels [360,361,475].

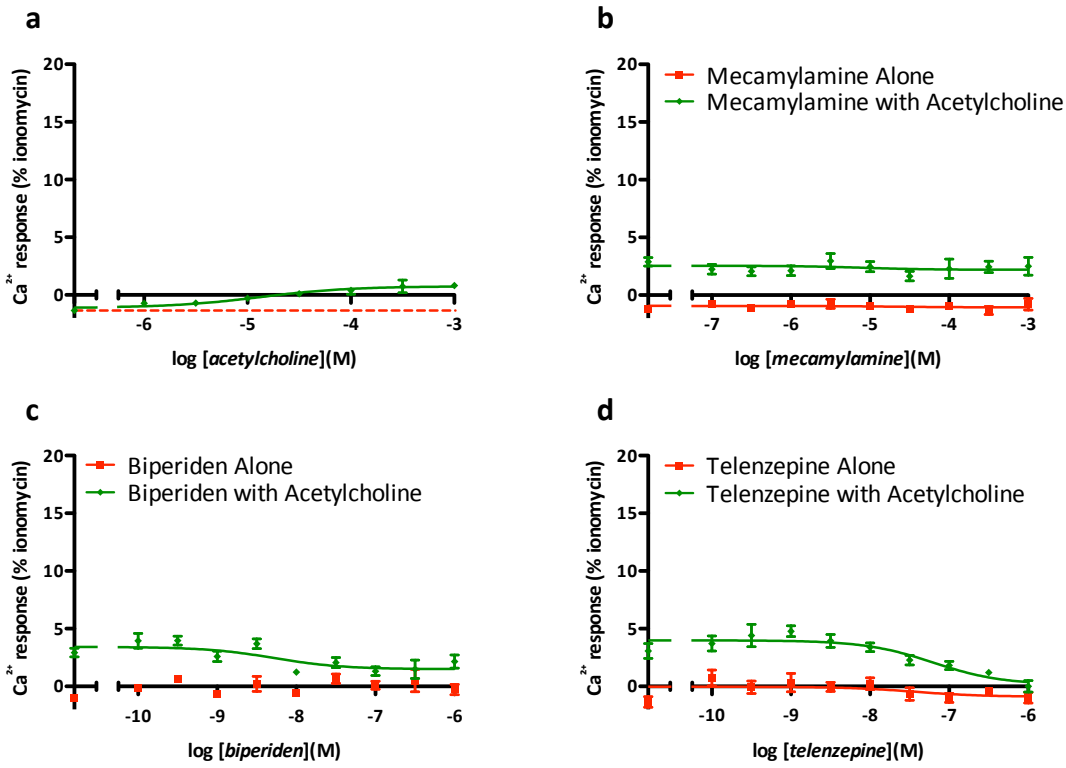


***Figure 6.4 Acetylcholine-mediated intracellular $Ca^{2+}$ accumulation in differentiated CTX0E16/02 cultures***
CTX0E16/02 cells were seeded onto laminin-coated 96-well plates at 3 x $10^4$ cells per well and differentiated for 28 days using SNBM. Cultures were incubated for 1 hour in the presence of the cell permeable, $Ca^{2+}$-sensitive fluorescent dye Fura-2 AM, before being washed prior to ligand-induced fluorescence being measured using a FlexStation 3. (**a**) concentration-response curve for acetylcholine between 1 µM and 1 mM in the presence of $Ca^{2+}$-free assay buffer – dotted red line indicates level of fluorescence in the absence of acetylcholine ($EC_{50}$ = 13 µM). Other cultures were first exposed to (**b**) mecamylamine ([final] = 100 nM to 1 mM), (**c**) biperiden ([final] = 0.1 nM to 1 µM, $IC_{50}$ = 5 nM) or (**d**) telenzepine ([final] = 0.1 nM to 1 µM, $IC_{50}$ = 63 nM), before all these cultures were exposed to acetylcholine to a final concentration of 10 µM. Red squares show effect of antagonist alone while green diamonds indicate responses observed after the addition of acetylcholine to the same well. Data points represent mean ± S.E.M. from *n* = 2, each with 3 technical replicates and expressed relative to the positive control, ionomycin.

While these data implicate muscarinic rather than nicotinic receptors as the source of the observed rise in $[Ca^{2+}]_i$ in response to acetylcholine in differentiated CTX0E16/02 cultures, and show that this change occurs as a consequence of $Ca^{2+}$ influx, they do not indicate which of the muscarinic receptors are involved. As mentioned above, the TRPC channels that are likely to mediate these effects can be activated by DAG, resulting from the catalytic activity of PLC-β, which can be provoked by $G\alpha_q$-coupled GPCRs. Of the five muscarinic receptors subtypes that have been identified, three have been shown to demonstrate this coupling: $M_1$, $M_3$ and $M_5$ [366], however, despite the fact the remaining $M_2$ and $M_4$ receptors couple to $G\alpha_i$, these are also known to activate PLC-β through their associated Gβγ subunits [362]. Further experiments are required both to confirm that the observed increase in $[Ca^{2+}]_i$ in response to acetylcholine, occurs via TRPC-mediated $Ca^{2+}$ influx, and that this arises via a DAG-dependent mechanism. Experiments that could be easily performed using antagonists of TRPC and PLC-β, such as SKF96365 and U73122, respectively [476,477]. In addition, further work is also necessary to identify the relative contribution of the different muscarinic receptors to the observed intracellular $Ca^{2+}$ accumulation in differentiated CTX0E16/02 cultures in response to acetylcholine.

While the measurement of $[Ca^{2+}]_i$ has provided a robust means with which to investigate acetylcholine-induced responses in differentiated CTX0E16/02 cultures, this approach has been found to be insufficiently sensitive to investigate dopamine and 5-HT receptor-mediated effects. Experiments described in ***4.2.2*** examining intracellular $Ca^{2+}$ accumulation in individual cells showed that while cells within proliferative and differentiated CTX0E16/02 cultures are capable of responding to dopamine and 5-HT, these are both few in number and exhibit minimal responses. However, measurement of intracellular $Ca^{2+}$ accumulation at the single cell level represents an impractical strategy when seeking to pharmacologically characterise cultures with respect to the activity of a broad range of receptors, as is the case in this study. Therefore, in order to provide a more detailed description of ligand-induced responses in differentiated CTX0E16/02 cultures, a more sensitive approach is required. This issue will be addressed in the following section.

### *6.2.4 ERK1/2 Phosphorylation Assay Optimisation*

As mentioned previously, ERK1/2 phosphorylation is a ubiquitous consequence of GPCR activation – at least for the $G\alpha_{i/o}$, $G\alpha_q$ and $G\alpha_s$ family members [252,448], which encompass all of the known GPCR targets of currently available antipsychotics [183]. Each of the G protein α-subunit families leads to activation of distinct signalling pathways and therefore provoke ERK1/2 phosphorylation via separate mechanisms, as illustrated in Figure 6.5, below. This 'final common pathway' has been exploited here in an attempt to investigate the activation of GPCRs that do not demonstrate significant signalling through a $Ca^{2+}$-dependent mechanism. In addition, the detection of ERK1/2 phosphorylation has been explored as a potentially more sensitive means with which to investigate the activation of receptors pertinent to antipsychotic efficacy. All experiments examining receptor-mediated ERK1/2 phosphorylation were performed using the commercially available Cellul'erk kit (Cisbio Bioassays, Codolet, France). The principle of the system is that live cultures can be activated – by a specific ligand for example – before medium is removed from the cells and replaced with a lysis buffer. Once lysed, a proportion of this lysate is mixed with an α-ERK1/2 antibody conjugated to a fluorescent donor moiety and an α-phospho-ERK1/2 antibody conjugated to a fluorescent acceptor moiety. The assay relies on a sandwich immunoassay principle and levels of phosphorylated ERK1/2 are derived from the relative level of FRET occurring between the donor and acceptor fluorescent moieties. This principle of this assay is illustrated in Figure 2.2, above.

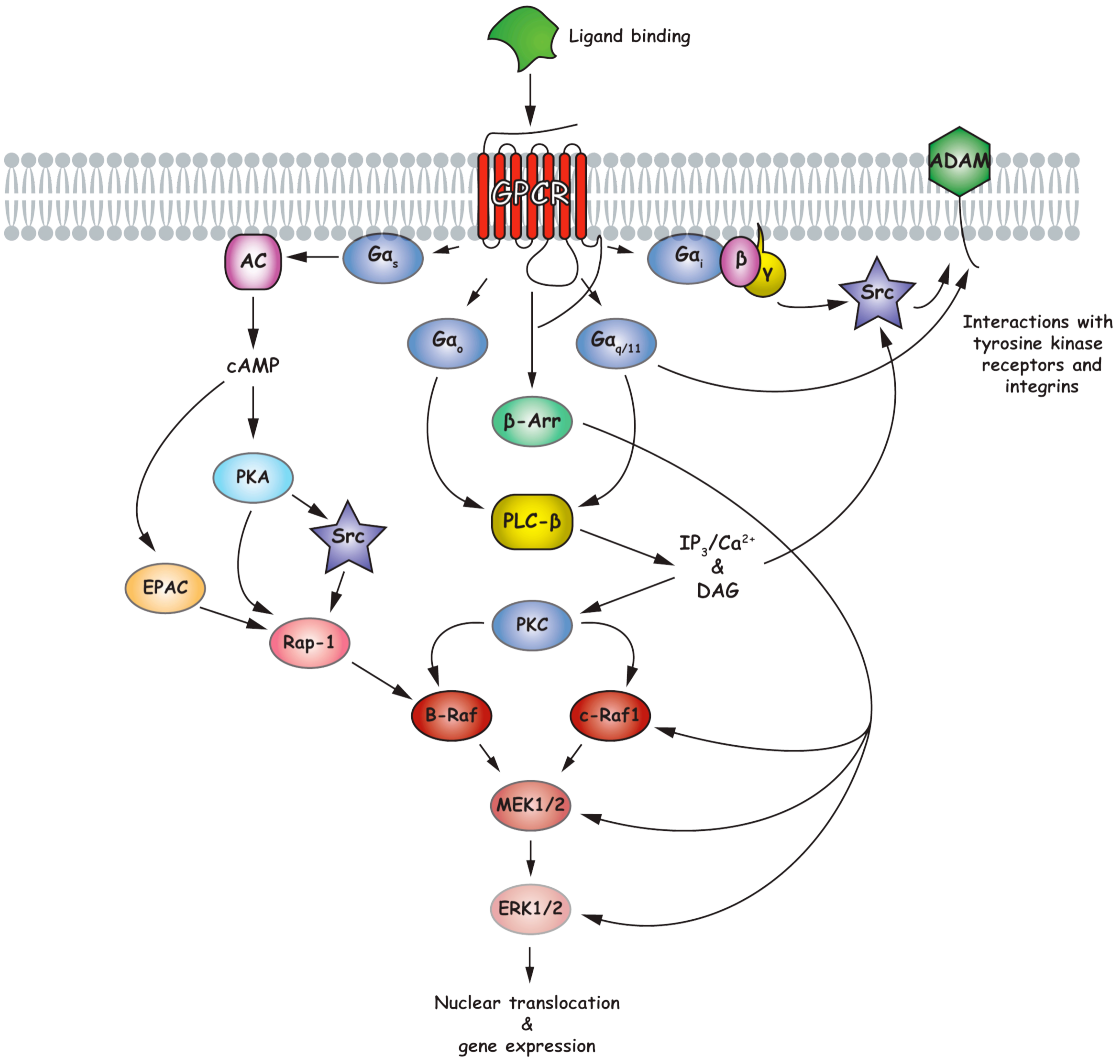


***Figure 6.5 Functionally distinct GPCRs modulate ERK/MAPK signalling through a range of different mechanisms***
Despite the activation of divergent signalling pathways upon neurotransmitter-induced, GPCR-mediated signalling via different G protein coupling partners, all of the four α subunit families are capable of leading to modulation of the phosphorylation status of ERK1/2. These signalling mechanisms also facilitate crosstalk with concomitant tyrosine kinase and integrin signalling. Modified from excellent reviews by Luttrell [228] and Osmond and colleagues [448].

Initial experiments were conducted to optimise conditions for use of the Cellul'erk kit with the CTX0E16/02 cell line. In the knowledge that both proliferative and differentiated CTX0E16/02 cultures were capable of robust, largely GPCR-mediated response to acetylcholine (as shown in Figure 4.9, Figure 4.13, Figure 4.15 and Figure 6.4), this was utilised as a positive control to determine the optimum cell lysis period following ligand-induced stimulation to ensure maximal FRET detection. This same experiment was also used, as a means to determine the optimal period of time cultures should be exposed to acetylcholine prior to lysis, to ensure the measurement of maximal levels of ERK1/2 phosphorylation. This first experiment was performed using proliferative, rather than differentiated CTX0E16/02 cultures, as these were known to demonstrate larger acetylcholine-induced responses and therefore served as a positive control for the optimisation of the assay. Proliferative CTX0E16/02 cultures were exposed to 1 mM acetylcholine for 1, 3, 5, 10, 15, 20, 30, 45 or 60 minutes prior to a 3, 5 or 10 minute lysis period. At most of the drug exposure time-points, a 5 minute cell lysis was found to

provide an optimal level of ERK1/2 phosphorylation as compared to lysis periods of 3 and 10 minutes (see Figure 6.6, **a**) and was therefore used as the lysis period for all experiments described in this chapter.

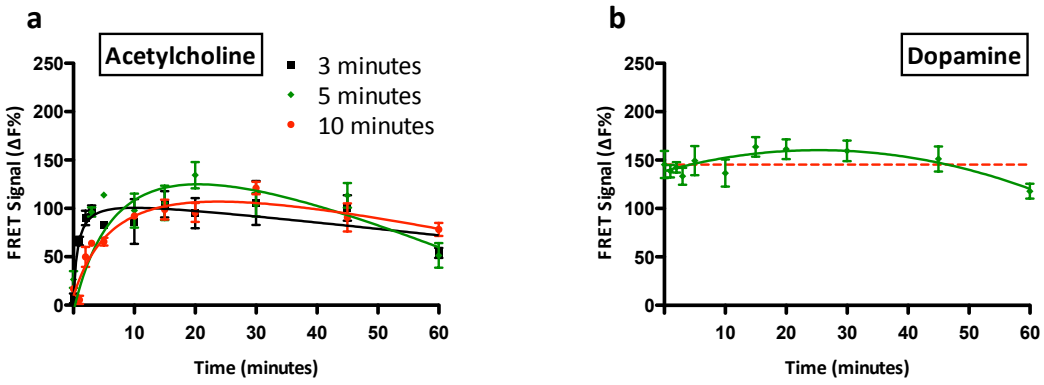


***Figure 6.6 Optimisation of assay conditions to maximise measured levels of ERK1/2 phosphorylation***
CTX0E16/02 cells were seeded onto laminin-coated 96-well plates at 3 x $10^4$ cells per well. (**a**) Confluent, proliferative CTX0E16/02 cultures were exposed to 1 mM acetylcholine for 1, 3, 5, 10, 15, 20, 30, 45 or 60 minutes prior to removal of medium and lysis for 3, 5 or 10 minutes. Lysates were then used to measure levels of ERK1/2 phosphorylation using Cellul'erk kit components. (**b**) CTX0E16/02 cultures were exposed to a normal 28 day differentiation before being exposed to 1 mM dopamine for 1, 3, 5, 10, 15, 20, 30, 45 or 60 minutes prior to removal of medium and lysis for 5 minutes. Lysates were used to determine ERK1/2 phosphorylation levels using Cellul'erk kit components according to published protocols. Red dashed line shows levels of ERK1/2 phosphorylation in differentiated CTX0E16/02 cultures not exposed to ligand. Data points represent mean ± S.E.M. from 3 technical replicates (*n* = 1) and are expressed relative to donor-only fluorescence levels.

All further experiments measuring ligand-induced ERK1/2 phosphorylation levels were conducted on CTX0E16/02 cultures exposed to a normal 28 day differentiation. Dopamine was selected as the first ligand with which to optimise assay conditions, due to its known importance to antipsychotic efficacy. This involved determining a time-course of ERK1/2 phosphorylation in response to 1 mM dopamine, to identify the exposure period that provided maximal detection of ERK1/2 phosphorylation. This experiment was conducted as described above in proliferative cultures for acetylcholine, with differentiated cultures exposed to 1 mM of dopamine for 1, 3, 5, 10, 15, 20, 30, 45 or 60 minutes prior to a previously optimised (Figure 6.6, **a**), 5 minute lysis. Exposure of differentiated CTX0E16/02 cultures to 1 mM dopamine failed to provoke a large increase in ERK1/2 phosphorylation, with levels only rising above baseline after 15 minutes – which also represented the peak level of activity – and had returned to baseline after 45 minutes (Figure 6.6, **b**).

Interestingly, levels of ERK1/2 phosphorylation following exposure to acetylcholine in proliferative cultures and exposure to dopamine in differentiated CTX0E16/02 cultures demonstrated an initial rise before falling back towards baseline levels despite the source of stimulation remaining. The reason why levels of ERK1/2 phosphorylation are not sustained despite continued ligand exposure is unclear, though could involve receptor desensitisation at the cell surface, receptor internalisation – preventing further stimulation, different receptors demonstrating divergent signalling kinetics pushing ERK1/2

phosphorylation in different directions, ligand metabolism or a combination of these factors [252]. This finding is however consistent with existing literature regarding GPCR-mediated phosphorylation of ERK1/2 [448,452,478].

ERK1/2 phosphorylation assays were introduced to this study to facilitate investigation of GPCRs that stimulated little or no rise in $[Ca^{2+}]_i$ in response to ligand binding. Due to its pivotal role in antipsychotic activity, dopamine-mediated signalling was of particular interest, yet despite robust expression of the genes encoding the dopamine $D_2$ and $D_3$ receptors (DRD2 and DRD3) at the mRNA level in differentiated CTX0E16/02 cultures, relatively little ERK1/2 phosphorylation was observed in response to 1 mM dopamine (see Figure 6.6, **b**). As a catecholamine, dopamine – like epinephrine and norepinephrine – is readily susceptible to oxidisation and is therefore often stabilised experimentally with the use of the reducing agent; ascorbic acid [479]. Several reports have suggested however that ascorbic acid can itself exert an effect on cultured cells [480-483]. While investigating dopamine's ability to precipitate intracellular $Ca^{2+}$ concentrations, the addition of ascorbic acid was used in an attempt to amplify any dopamine-mediated responses. This did not prove successful in elevating dopamine-induced $Ca^{2+}$ accumulations, though did identify that ascorbic acid was itself capable of elevating intracellular $Ca^{2+}$ concentrations at doses above 20 µM (data not shown). In an attempt to maximise dopamine-induced ERK1/2 phosphorylation, while minimising any non-specific effects, ascorbic acid was added to cultures along with dopamine to a final concentration of 20 µM, in a repeat of the experiment shown in Figure 6.6, **b**.

Interestingly, in the presence of 20 µM ascorbic acid, 1 mM dopamine was capable of provoking a far greater level of ERK1/2 phosphorylation (Figure 6.7, **a**) than was seen when it was not used (see Figure 6.6, **b**). It is not clear however whether this is due to the anti-oxidative effect of ascorbic acid or an effect at the dopamine receptor itself and would require further work to determine. Levels of ERK1/2 phosphorylation were elevated just 1 minute after exposure to 1 mM dopamine, and continued to rise with a peak activity occurring at 45 minutes before beginning to drop back towards pre-stimulation levels at 60 minutes (Figure 6.7, **a**).

In attempting to account for this observed increase in sensitivity to dopamine, further research revealed that ascorbic acid may actually have an effect on the dopamine receptor itself, acting almost as a positive allosteric modulator to facilitate ligand binding [484,485]. Indeed, ascorbic acid has even been proposed to play a physiological role *in vivo* by assisting dopamine-mediated signalling [485,486] and demonstrates relatively homogenous distribution throughout the human brain [487]. Downstream experiments planned for the CTX0E16/02 cell line involve the investigation of antipsychotic activity, a class of drugs that are known to primarily target the dopaminergic system. However, antipsychotics, like almost all clinically approved pharmacological agents, exert their action through antagonism. Despite not mediating an effect in their own right, neutral antagonists exert their action by binding to a receptor and preventing its cognate ligand from activating it. Therefore, the effect of an antagonist can only be detected in the presence of an agonist. For this reason, future experiments to explore the effects of antipsychotic drugs will be optimised so as to simulate physiological activation of receptors – referred to as pharmacological or physiological tone. Because antipsychotics are known to behave as antagonists at

a range of different neurotransmitter receptors, this will involve exposing CTX0E16/02 cultures to a range of different agonists. This subject will be covered in more detail later, however, because these downstream experiments will involve exposing CTX0E16/02 cultures to dopamine (along with other neurotransmitter receptor agonists) to observe the effects of antipsychotics, and due to the observed effect of ascorbic acid upon dopamine-induced signalling, it is planned that this will be used as an adjunct in future experiments. Consequently, when each of the different agonists are added to CTX0E16/02 cultures to simulate neural physiological tone, they too will have to be exposed to ascorbic acid. For this reason, all further experiments described here investigating the effect that various compounds have upon levels of ERK1/2 phosphorylation have involved the addition of 20 µM ascorbic acid. This step was taken as a means of control so that if ascorbic acid exerts an effect on any other neurotransmitter system, this effect will have been observed prior to the execution of any downstream experiments. In addition, as several of the neurotransmitter agonists used in this study are also susceptibly to oxidisation such as 5-HT, histamine and also phenylephrine – which itself was used rather than norepinephrine because of its instability – the presence of a physiologically relevant antioxidant, as represented by ascorbic acid is likely to be beneficial.

Having established a time course of ERK1/2 phosphorylation in response to 1 mM dopamine, similar experiments were performed for 5-HT, acetylcholine and histamine, as is described below. The level of FRET produced in these initial experiments were resolved using a FlexStation 3 plate reader, though this was found not to offer maximal sensitivity for this particular application. Therefore, in a further attempt to improve ERK1/2 phosphorylation detection sensitivity, we changed to using an Artemis K-101 (Berthold Technologies GmbH & Co., Bad Wildbad, Germany) plate reader (access kindly granted by Dr Andrew Beavil, Randall Division of Cell and Molecular Biophysics, King's College London). These instruments are purpose built to provide maximal sensitivity for HTRF®-based assays such as the Cellul'erk kit, and was therefore used for further experimentation. Its improved sensitivity was reflected in an increase in detected FRET signal units, as is clear by comparing Figure 6.8, **c** and **d**.

The preliminary experiments described above identified an optimal period of cell lysis so as to ensure maximal detection of ERK1/2 phosphorylation levels. In addition, this section has described the need for the use of ascorbic acid in all subsequent experiments, and the use of more sensitive instrumentation to further improve detection of ERK1/2 phosphorylation. The following section describes a series of experiments where dopamine, 5-HT, acetylcholine, phenylephrine and histamine were each tested at 1 mM in differentiated CTX0E16/02 cultures to determine a time course of ERK1/2 phosphorylation. Once the duration of drug exposure that provoked a maximal level of ERK1/2 phosphorylation was identified, this was used to determine a concentration-response profile for each compound. Along with data describing ligand-induced intracellular $Ca^{2+}$ accumulation in differentiated CTX0E16/02 cultures, this information was used to determine whether these cells functionally express the wide variety of neurotransmitter receptors targeted by antipsychotics. These data will help establish the putative usefulness of the CTX0E16/02 cell line as a platform with which to interrogate the mechanism of action

of antipsychotic drugs, while providing a further pharmacological characterisation of differentiated CTX0E16/02 cultures.

### *6.2.5 Dopamine's Complex Pharmacology Is Reflected In ERK1/2 Phosphorylation Profile*

Having established that dopamine provoked a peak level of ERK1/2 phosphorylation after 45 minutes of exposure to differentiated CTX0E16/02 cultures, this time point was used to generate a dose-response relationship for concentrations of dopamine between 31.6 pM ($10^{-10.5}$ M) and 100 μM ($10^{-4}$ M). Levels of ERK1/2 phosphorylation in response to dopamine were found not to exhibit a simple sigmoidal concentration-response relationship with an apparent peak in activity at 3.16 nM ($10^{-8.5}$ M) and again at 100 nM ($10^{-7}$ M) and 3.16 μM ($10^{-5.5}$ M)(Figure 6.7, **b**). This complex response may be attributable to the influence of different dopamine receptor subtypes that affect the phosphorylation status of ERK1/2 in different ways. For example, dopamine is known to demonstrate varying affinity for each of its cognate receptors [458], while each of these may demonstrate different ERK1/2 phosphorylation kinetics. This is perhaps a likely scenario when we consider that the mechanism through which ERK1/2 phosphorylation occurs as a consequence of dopamine activating each of it's different receptors is variable [191]. This is before we even consider that dopamine receptors may also exist in differentiated CTX0E16/02 cultures as functional heteromers with other receptors. As the experiment shown in Figure 6.7 **b**, is a snapshot of ERK1/2 phosphorylation at a single time point (45 minutes), and each of the receptors may provoke ERK1/2 phosphorylation to varying degrees, and with different time courses, this may account for the observed response exhibited by dopamine. To confuse matters, ligand affinity for dopamine receptors is not a constant property, as they are capable of readily adopting both high and low-affinity agonist binding states [458]. For example, the $D_2$ receptor can exist in a high-affinity state ($D_2^{High}$) – capable of binding dopamine at low nanomolar concentrations – and a low-affinity state ($D_{2Low}$), reducing dopamine's affinity for the receptor to the high micromolar range [338,488]. The relative affinity of dopamine for its endogenous receptors, each in their high-affinity state has been reported to be 0.9 nM, <0.9 nM, ~7 nM, ~4 nM and ~30 nM in cloned human $D_1$, $D_2$, $D_3$, $D_4$ and $D_5$ receptors respectively [458]. It is unclear from this work what proportion of each different dopamine receptor is in each of the high or low-affinity states in differentiated CTX0E16/02 cultures, or how binding to receptors in these different states may affect signal transduction. It may however provide a rationale for the concentration-response relationship for dopamine observed here. Non-linear regression analysis of dopamine-induced ERK1/2 phosphorylation described here provided an estimated $EC_{50}$ of 0.5 nM. This value would appear consistent with activation of dopamine receptors – particularly $D_1$ and $D_2$ – in their high-affinity state, assuming affinity ($K_i$) can be correlated with levels of ERK1/2 phosphorylation [458]. These data show that differentiated CTX0E16/02 cultures express functional dopamine receptors, though it remains unclear which subtypes may be responsible for the observed effect.

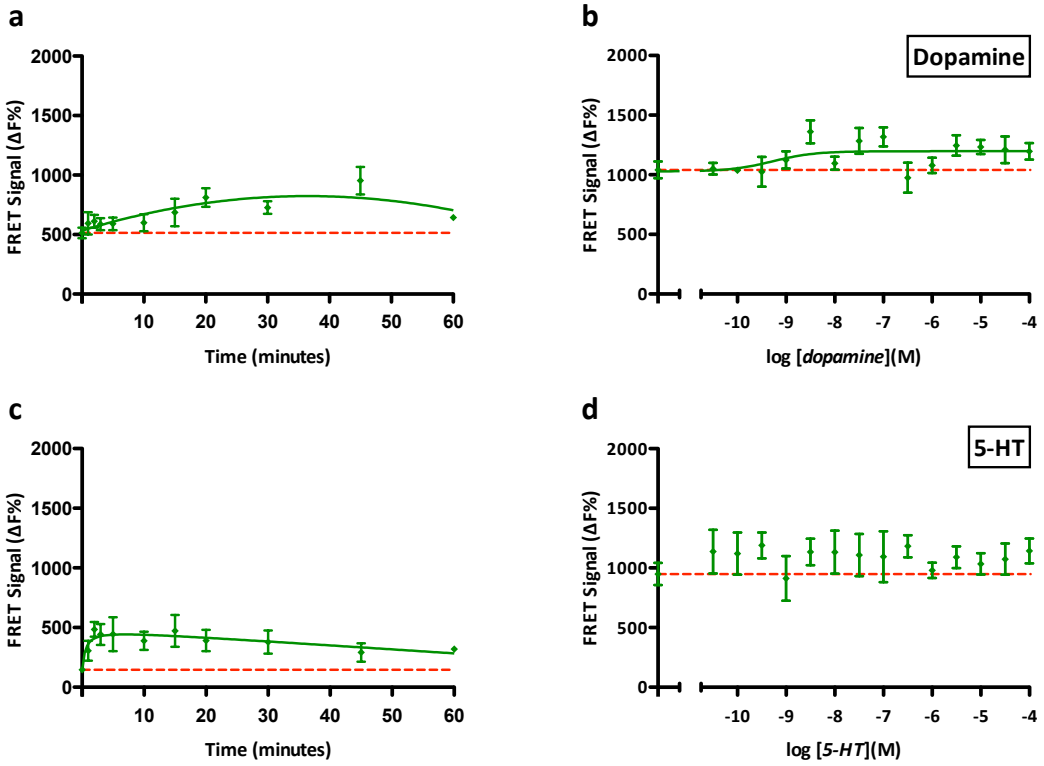


***Figure 6.7 ERK1/2 phosphorylation in response to dopamine and 5-HT in differentiated CTX0E16/02 cultures***
CTX0E16/02 cells were seeded onto laminin-coated 96-well plates at 3 x $10^4$ cells per well and differentiated for 28 days using SNBM. On the day of the experiment all medium was removed and replaced with fresh medium 4 hours prior to addition of either dopamine or 5-HT. For time-course experiments, CTX0E16/02 cultures were exposed to 1 mM dopamine in the presence of 20 µM ascorbic acid (**a**) or 1 mM 5-HT (**c**) for 1, 3, 5, 10, 15, 20, 30, 45 or 60 minutes prior to removal of medium and lysis for 5 minutes. Data points represent mean ± S.E.M. from 3 technical replicates (*n* = 1) and are expressed relative to donor-only fluorescence levels. For concentration-response experiments, differentiated CTX0E16/02 cultures were exposed to dopamine (**b**) or 5-HT (**d**) at 31.6 pM ($10^{-10.5}$ M) to 100µM ($10^{-4}$ M) at half log-unit intervals for 45 or 15 minutes for dopamine ($EC_{50}$ = 0.5 nM) and 5-HT respectively. Lysates were used to determine ERK1/2 phosphorylation levels using Cellul'erk kit components according to published protocols. Data points represent mean ± S.E.M. from 3 technical replicates (*n* = 2) and are expressed relative to donor-only fluorescence levels. Red dashed line shows levels of ERK1/2 phosphorylation in differentiated CTX0E16/02 cultures not exposed to ligand.

### *6.2.6 Differentiated CTX0E16/02 Cultures Demonstrate ERK1/2 Phosphorylation In Response To 5-HT, Acetylcholine, Phenylephrine & Histamine*

5-HT provoked rapid phosphorylation of ERK1/2 when added at 1 mM, with a relatively high level occurring after just 3 minutes, and was sustained around this level until a maximal level of ERK1/2 phosphorylation was detected at 15 minutes (see Figure 6.7 **c**). This time-point was therefore selected for the subsequent concentration-response experiment). Levels of ERK1/2 phosphorylation dropped slowly from the observed peak after a 15 minute 5-HT exposure, though levels remained above baseline when differentiated CTX0E16/02 cultures had been exposed to 5-HT for 60 minutes – the final tested time point (Figure 6.7, **c**). When exposing differentiated CTX0E16/02 cultures to different concentrations of 5-HT, a less clear picture emerged. A clear concentration-response relationship was not observed for 5-HT, with considerable variation in ERK1/2 phosphorylation recorded at most concentrations as indicated by the size of error bars (see Figure 6.7, **d**). As with dopamine, this variation may be attributable to the various different receptors targeted by 5-HT and further work to characterise 5-HT

receptor-mediated responses in these cells will probably necessitate the use of specific 5-HT receptor agonists, and/or a combination of agonists and antagonists.

While acetylcholine provoked the largest increases in $[Ca^{2+}]_i$ of all tested compounds in differentiated CTX0E16/02 cultures (see Figure 4.7), its ability to provoke ERK1/2 phosphorylation was minimal – especially when compared to that evoked by phenylephrine (see Figure 6.8 **b** and **d**). Levels of ERK1/2 phosphorylation were found to be lower than that observed in cultures exposed to no acetylcholine, if exposed to 1 mM acetylcholine for less than 10 minutes (see Figure 6.8 **a**, below). Levels only rose above baseline once cultures had been exposed to acetylcholine for at least 15 minutes. A similarly low level of ERK1/2 phosphorylation was detected in cultures exposed to acetylcholine for 20, 30 or 45 minutes, with this final time point representing a marginal peak in activity – and was therefore used to determine a dose-response relationship for this ligand. After 60 minutes exposure to acetylcholine, ERK1/2 phosphorylation levels returned to those seen for cultures exposed to no drug at all (Figure 6.8, **a**). While responses to acetylcholine were small, it exhibited a clear sigmoidal concentration-dependent response with an $EC_{50}$ of 0.6 µM (Figure 6.8, **b**). This represented a leftward shift in potency by an order of magnitude when compared to acetylcholine's ability to provoke intracellular $Ca^{2+}$ accumulation, for which it demonstrated an $EC_{50}$ of 5 µM. This disparity may be caused by a number of different factors, though would together point towards a greater signalling efficiency with respect to ERK1/2 phosphorylation compared to $Ca^{2+}$ accumulation. The seemingly lower efficacy of acetylcholine with respect to $Ca^{2+}$ mobilisation may simply be attributable to the superior sensitivity of the ERK1/2 phosphorylation assay.

Levels of ERK1/2 phosphorylation in response to 1 mM phenylephrine were considerably greater than those observed for any other compound tested here. Increased ERK1/2 phosphorylation was detected after just 1 minute and continued to rise, with peak activity recorded from a 20 minute drug exposure. Levels of ERK1/2 phosphorylation then slowly declined, though remained well above baseline at the final tested drug exposure time point of 60 minutes (Figure 6.8, **c**). Maximal ERK1/2 phosphorylation in differentiated CTX0E16/02 cultures was observed following a 20 minute exposure to phenylephrine, which was used to demonstrated a clear sigmoidal concentration-response relationship, with an $EC_{50}$ of 3.7 µM for this ligand. This value was consistent with previously published work [489,490]. This was almost identical to the $EC_{50}$ value of 1.4 µM recorded for phenylephrine-induced $Ca^{2+}$ accumulation, though the magnitude of response was far greater with respect to ERK1/2 phosphorylation (Figure 6.8, **d**). This is perhaps surprising when we consider that phenylephrine is an $\alpha_1$-adrenoceptor subtype selective agonist, with $\alpha_{1A}$, $\alpha_{1B}$, and $\alpha_{1D}$ all typically coupled to $G\alpha_q$, and therefore associated with increases in $[Ca^{2+}]_i$, though appears to highlight the sensitivity of the ERK1/2 phosphorylation assay and therefore validate its use as an appropriate surrogate of receptor activity. It should be noted that previously published work has described a synergistic effect or $\alpha_{1A}$ and $\alpha_{1B}$-adrenoceptors with respect to phenylephrine-induced ERK1/2 phosphorylation when the cloned human receptors were co-expressed in HEK 293 cells. This phenomenon was postulated to be attributable to these receptor subtypes

forming functionally-enhanced heteromers [490]. Further work would be required to demonstrate this phenomenon in the ***in vitro*** system used here.

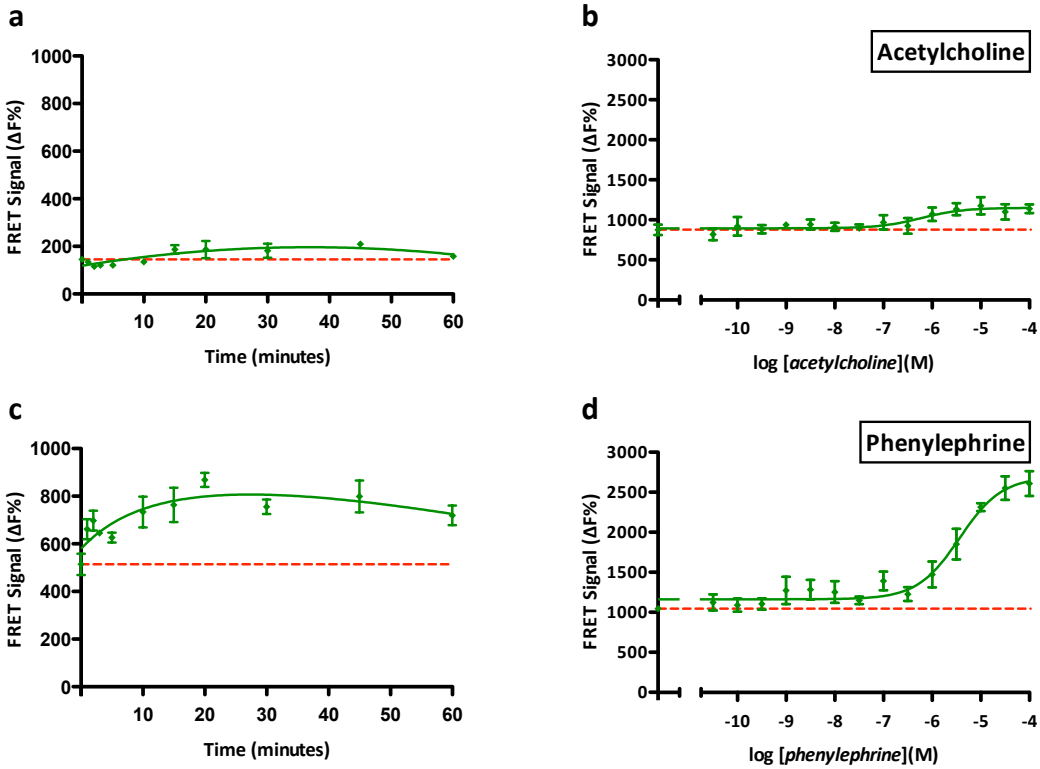


***Figure 6.8 Acetylcholine & phenylephrine-induced ERK1/2 phosphorylation in differentiated CTX0E16/02 cultures***
CTX0E16/02 cells were seeded onto laminin-coated 96-well plates at 3 x $10^4$ cells per well and differentiated for 28 days using SNBM. On the day of the experiment all medium was removed and replaced with fresh medium 4 hours prior to addition of either acetylcholine or phenylephrine. For time-course experiments, CTX0E16/02 cultures were exposed to 1 mM acetylcholine (**a**) or 1 mM phenylephrine in the presence of 20 µM ascorbic acid (**c**) for 1, 3, 5, 10, 15, 20, 30, 45 or 60 minutes prior to removal of medium and lysis for 5 minutes. Data points represent mean ± S.E.M. from 3 technical replicates (*n* = 1) and are expressed relative to donor-only fluorescence levels. For concentration-response experiments, differentiated CTX0E16/02 cultures were exposed to acetylcholine (**b**) or phenylephrine (**d**) at 31.6 pM ($10^{-10.5}$ M) to 100µM ($10^{-4}$ M) at half log-unit intervals for 45 or 20 minutes for acetylcholine ($EC_{50}$ = 0.6 µM) and phenylephrine ($EC_{50}$ = 3.7 µM) respectively. Lysates were used to determine ERK1/2 phosphorylation levels using Cellul'erk kit components according to published protocols. Data points represent mean ± S.E.M. from 3 technical replicates (*n* = 2) and are expressed relative to donor-only fluorescence levels. Red dashed line shows levels of ERK1/2 phosphorylation in differentiated CTX0E16/02 cultures not exposed to ligand.

Similar to responses observed for 5-HT and phenylephrine, 1 mM histamine provoked an immediate phosphorylation of ERK1/2, rising to a peak after just 15 minutes exposure. ERK1/2 phosphorylation then dropped, with a return to levels observed in the presence of no drug after just 45 minutes. After a 60 minute exposure to histamine, ERK1/2 phosphorylation levels were actually lower than that detected in cultures exposed to no drug at all (Figure 6.10, **a**). A clear concentration-dependent relationship for histamine was not evident, with high variability between responses at each of the tested concentrations, though all provoked ERK1/2 phosphorylation levels were higher than that observed at baseline; in the absence of drug (Figure 6.10, **b**). Non-linear regression provided an $EC_{50}$ of 22 pM though this suggests an efficacy far greater than available data would suggest, with published $K_i$ values

for cloned human histamine receptors in HEK 293 cells determined as 7,010 nM, >10,000 nM, 2.61 nM and 39.8 nM for histamine $H_1$, $H_2$, $H_3$ and $H_4$ respectively [491]. The apparent potency of histamine would therefore appear to be an artefact caused by the highly variable levels of ERK1/2 phosphorylation recorded at each tested concentration. These data suggest that differentiated CTX0E16/02 cultures are capable of responding to histamine, though further work using histamine receptor subtype-specific agonists is required to provide a clearer picture of how these cells respond.

These data provide evidence that differentiated CTX0E16/02 cultures express functional receptors for all of the major neurotransmitter systems targeted by currently available antipsychotic drugs, namely, dopaminergic, serotonergic, cholinergic, adrenergic and histaminergic. However, it currently remains unclear which of the receptor subtypes targeted by these neurotransmitters are expressed in differentiated CTX0E16/02 cells. These data support previous findings presented in ***Chapter 4*** showing that receptors for these neurotransmitter systems were also capable of provoking increases in intracellular $Ca^{2+}$ accumulation in response to agonist-induced activation. In addition, by measuring ERK1/2 phosphorylation in differentiated CTX0E16/02 cultures exposed to 1 mM glutamate or 1 mM GABA for between 1 and 60 minutes, the presence of receptors targeted by these neurotransmitters was also confirmed (see Figure 6.9). While glutamate had previously been shown to be capable of triggering a concentration-dependent increase in $[Ca^{2+}]_i$ in differentiated CTX0E16/02 cultures (see Figure 4.8, c), this approach had failed to detect an effect of the inhibitory neurotransmitter, GABA.

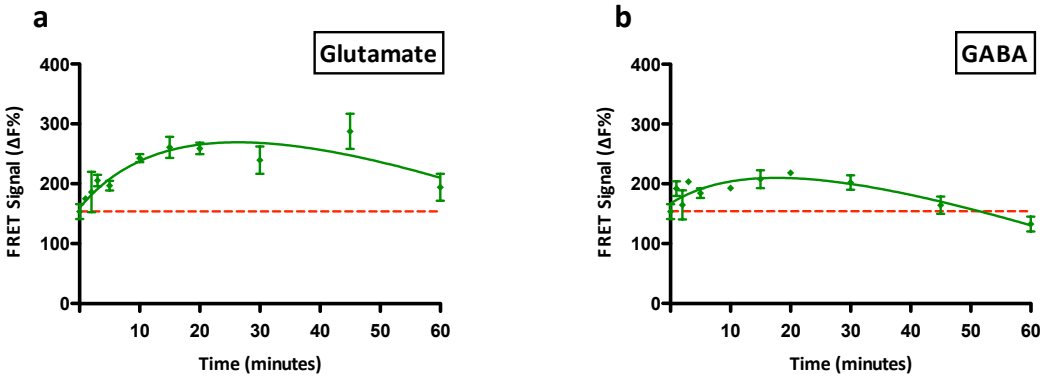


***Figure 6.9 Glutamate & GABA provoke ERK1/2 phosphorylation in differentiated CTX0E16/02 cultures***
CTX0E16/02 cells were seeded onto laminin-coated 96-well plates at 3 x $10^4$ cells per well and differentiated for 28 days using SNBM. On the day of the experiment all medium was removed and replaced with fresh medium 4 hours prior to the addition of either 1 mM glutamate or 1 mM GABA for 1, 3, 5, 10, 15, 20, 30, 45 or 60 minutes prior to removal of medium and lysis for 5 minutes. Lysates were used to determine ERK1/2 phosphorylation levels using Cellul'erk kit components according to published protocols. Red dashed line shows levels of ERK1/2 phosphorylation in differentiated CTX0E16/02 cultures not exposed to ligand. Data points represent mean ± S.E.M. from 3 technical replicates ($n$ = 1) and are expressed relative to donor-only fluorescence levels.

These data demonstrate that the detection of ligand-induced ERK1/2 phosphorylation represents a high-throughput and sensitive means with which to determine receptor activation in CTX0E16/02 cultures. In addition, a comparison of the increases in $[Ca^{2+}]_i$ and ERK1/2 phosphorylation in response to acetylcholine and phenylephrine in differentiated CTX0E16/02 cultures (see Figure 4.9 **a** and **c**, and

Figure 6.8 **b** and **d**) provides evidence of functional selectivity between these two signalling events from the same ligands. These data highlight the importance of examining multiple functional endpoints in order to pharmacologically characterise a ligand in an *in vitro* model and reinforces the premise that 'intrinsic efficacy' is an obsolete pharmacological concept. Measurement of ERK1/2 phosphorylation therefore represents a sensitive means by which further characterisation of differentiated CTX0E16/02 cultures can be pursued.

### *6.2.7 Haloperidol Behaves As An Inverse-Agonist In Differentiated CTX0E16/02 Cultures*

The purpose of this study was to characterise the CTX0E16/02 cell line, so as to provide an experimental platform with which to transcriptomically investigate the mechanism of action of antipsychotic drugs. In order to do this, it is vitally important that these compounds are exposed to cultures at a physiologically relevant concentration. This will ensure that observed changes in gene expression relate to the mechanism through which these compounds exert their therapeutic effects, or indeed their side effects, and do not reflect cellular toxicity induced by these compounds. This consideration is especially important when investigating the mechanism of drugs that exert their effects in the CNS, as to reach their target, they must achieve brain penetrance. This property, for antipsychotics at least, is conferred through high lipophilicity. However, while this physiochemical attribute allows these compounds to traverse the blood brain barrier, and therefore enter the brain, it also means that they can traverse, and accumulate within the lipid membranes of cells in culture and effect intracellular targets [492]. Arguably, if a sufficiently high concentration of any drug is added to cells in cultures, a transcriptional effect is likely to be observed – this does not however ensure that these changes are relevant to the action of the drug *in vivo*. In an attempt to explore the concentration of antipsychotic drugs required to exert an effect *in vitro*, the effect of haloperidol upon ERK1/2 phosphorylation levels in differentiated CTX0E16/02 cultures was examined.

Haloperidol is a typical or first generation antipsychotic that represented the most frequently prescribed compound for the treatment of psychosis throughout the 1980s and early 1990s [493]. While its use has declined in recent years it remains clinically useful and for this reason has been extensively studied since its introduction in 1959 [494]. Like all other compounds in its class, haloperidol demonstrates high affinity for a broad range of neurotransmitter receptors (see Figure 1.1, above), many of which are expressed by differentiated CTX0E16/02 cells. Experiments described above were performed to assess the influence of various receptor agonists on levels of ERK1/2 phosphorylation. Haloperidol was chosen as a compound representative of antipsychotics and was tested in exactly the same manner as were agonists, to determine its influence upon transient cellular signalling using levels of ERK1/2 phosphorylation as a surrogate marker. In contrast to the effect exerted by the agonists, 1 mM haloperidol (this concentration was only used for optimisation) caused a rapid and sustained reduction in levels ERK1/2 phosphorylation in differentiated CTX0E16/02 cultures. Maximal inhibition of ERK1/2 phosphorylation was achieved following a 45 minutes exposure, and remained at this level in cultures exposed to haloperidol for 60 minutes – the latest time point tested (Figure 6.10, **c**). It would be

interesting to see whether this level of inhibition was sustained continually or whether – as seen for agonists above – levels returned to baseline after an extended period of time. When added to differentiated CTX0E16/02 cultures at varying concentrations – using a 45 minute incubation, as this was sufficient to obtain a maximal response – haloperidol did not provoke any effect until it was added at a final concentration of 3.16 µM ($10^{-5.5}$ M), from which point it steadily reduced observed levels of ERK1/2 phosphorylation (Figure 6.10, **b**) in a concentration-dependent manner up to the highest tested concentration of 100 µM.

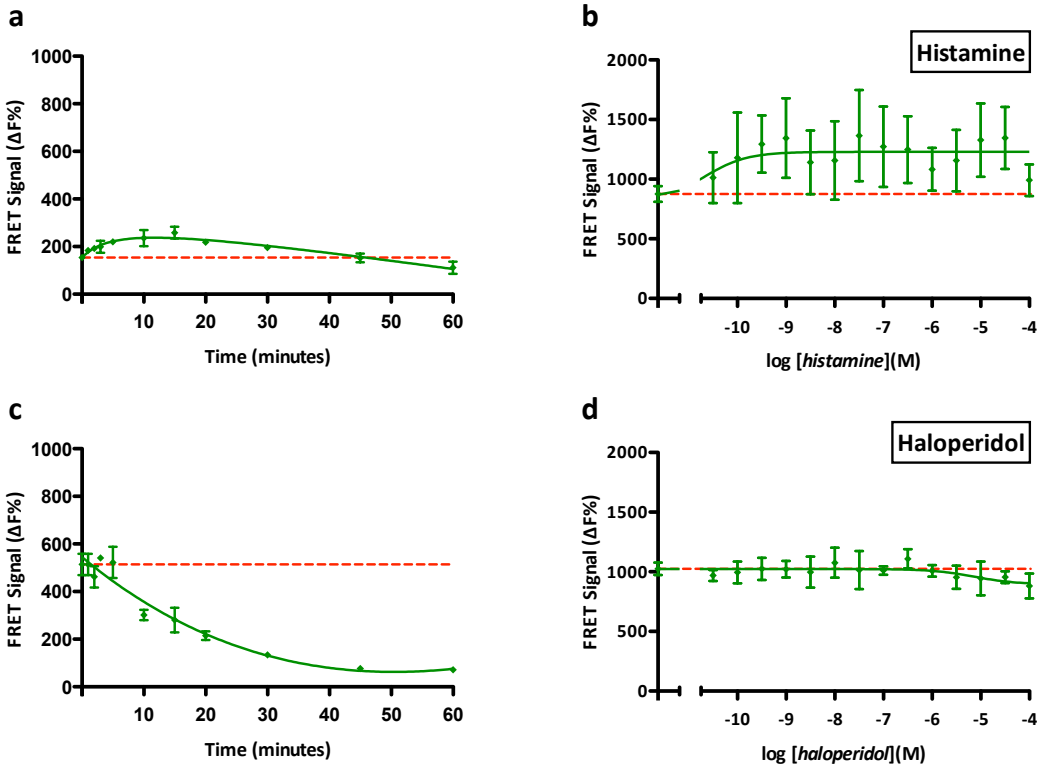


***Figure 6.10 ERK1/2 phosphorylation in response to histamine and haloperidol in differentiated CTX0E16/02 cultures***

CTX0E16/02 cells were seeded onto laminin-coated 96-well plates at 3 x $10^4$ cells per well and differentiated for 28 days using SNBM. On the day of the experiment all medium was removed and replaced with fresh medium 4 hours prior to addition of either histamine or haloperidol. For time-course experiments, CTX0E16/02 cultures were exposed to 1 mM histamine (**a**) or 1 mM haloperidol in the presence of 20 µM ascorbic acid (**c**) for 1, 3, 5, 10, 15, 20, 30, 45 or 60 minutes prior to removal of medium and lysis for 5 minutes. Data points represent mean ± S.E.M. from 3 technical replicates (*n* = 1) and are expressed relative to donor-only fluorescence levels. For concentration-response experiments, differentiated CTX0E16/02 cultures were exposed to histamine (**b**) or haloperidol (**d**) at 31.6 pM ($10^{-10.5}$ M) to 100µM ($10^{-4}$ M) at half log-unit intervals for 15 or 45 minutes for histamine ($EC_{50}$ = 22 pM) and haloperidol respectively. Lysates were used to determine ERK1/2 phosphorylation levels using Cellul'erk kit components according to published protocols. Data points represent mean ± S.E.M. from 3 technical replicates (*n* = 2) and are expressed relative to donor-only fluorescence levels. Red dashed line shows levels of ERK1/2 phosphorylation in differentiated CTX0E16/02 cultures not exposed to ligand.

These data raise several interesting questions regarding the both the nature of ERK1/2 activity in differentiated CTX0E16/02 cultures and the influence of haloperidol. The considerable decrease in levels of ERK1/2 phosphorylation in response to 1 mM haloperidol – greater than any increase provoked by any of the agonists tested, with the exception of phenylephrine – demonstrates that differentiated

CTX0E16/02 cultures exhibit significant levels of constitutive ERK1/2 activity (see Figure 6.10, **c**). It remains unclear however, how this level of constitutive ERK1/2 phosphorylation compares to that of other cell types. However, preliminary experiments investigating levels of ERK1/2 phosphorylation in response to 1 mM acetylcholine or 1 mM 5-HT in proliferative CTX0E16/02 cultures showed that basal levels of ERK1/2 phosphorylation were close to zero, as can been seen in Figure 6.11, below. These data, along with that obtained from other initial experiments using proliferative CTX0E16/02 cultures (data not shown) demonstrated that levels of ERK1/2 phosphorylation (or level of FRET detection) remained close to zero in un-stimulated cells. This raises the question of why there is a higher level of ERK1/2 constitutive activity in differentiated rather than proliferative CTX0E16/02 cultures and whether this phenomenon is common to other differentiated cell types? What is clear is that elevated basal levels of ERK1/2 phosphorylation would create a greater dynamic range or ERK1/2 activity within which cells would be capable of responding. For example, if levels of ERK1/2 phosphorylation in proliferative CTX0E16/02 cells are homeostatically maintained at a level close to zero, this means that they are only capable of increasing this level to stimulate intracellular signalling. However, in the case of differentiated CTX0E16/02 cells, with an elevated level of basal ERK1/2 activity, this allows the enzyme's activity to be modulated in either direction and therefore increases it's signalling capacity. In addition, levels of ERK1/2 phosphorylation observed in response to phenylephrine (see Figure 6.8, **d**) show that the basal level of ERK1/2 activity in differentiated cells are far from the maximal levels that can be achieved. Whether this elevated homeostatic regulation of ERK1/2 activity is physiologically relevant to neuronal cultures remains unclear, though certainly warrants further investigation.

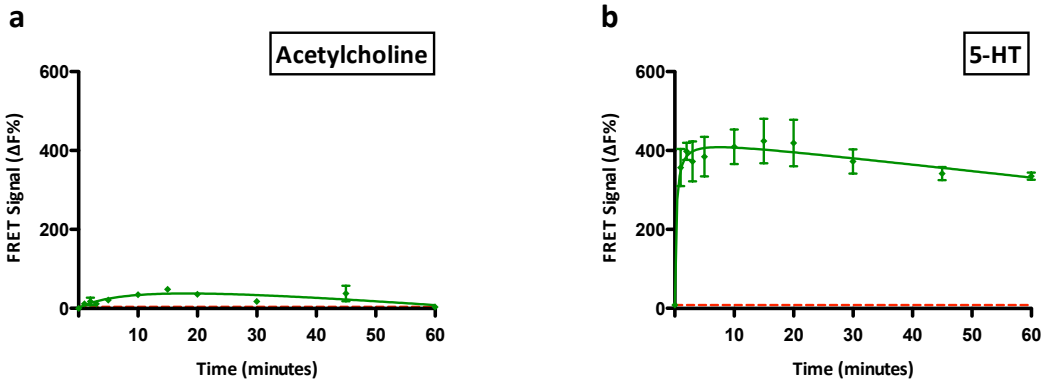


***Figure 6.11 Proliferative CTX0E16/02 cultures demonstrate low basal levels of ERK1/2 phosphorylation***
CTX0E16/02 cells were seeded onto laminin-coated 96-well plates at 3 x $10^4$ cells per well and maintained under proliferative conditions until reaching confluence. On the day of the experiment all medium was removed and replaced with fresh medium 4 hours prior to the addition of either 1 mM acetylcholine or 1 mM 5-HT for 1, 3, 5, 10, 15, 20, 30, 45 or 60 minutes prior to removal of medium and lysis for 5 minutes. Lysates were used to determine ERK1/2 phosphorylation levels using Cellul'erk kit components according to published protocols. Red dashed line shows levels of ERK1/2 phosphorylation in differentiated CTX0E16/02 cultures not exposed to ligand. Data points represent mean ± S.E.M. from 3 technical replicates ($n$ = 1) and are expressed relative to donor-only fluorescence levels.

With respect to what is responsible for maintaining higher basal levels of ERK1/2 phosphorylation in differentiated, as compared to proliferative cultures; the observed effect of haloperidol may provide us

some insight in this regard. Figure 6.10 showed that haloperidol is capable of robustly reducing levels of ERK1/2 phosphorylation in differentiated CTX0E16/02 cultures – when added at 1 mM at least – though lower concentrations also showed this effect, if to a lesser extent. If it is assumed that haloperidol exerts this effect through its action at various receptors found at the cell surface, and it is through this action at these receptors that haloperidol is capable of reducing levels of ERK1/2 phosphorylation, this would suggest that elevated levels of ERK1/2 activation occurs as a consequence of constitutive GPCR activity in differentiated cultures. It is unclear however what is responsible for this increased level of constitutive GPCR activity and whether this is a normal characteristic of neural cultures. What it does tell us however, is that rather than being a neutral antagonist, haloperidol appears instead to be an inverse agonist. This result is consistent with previous findings where it has been shown that haloperidol exerts its action through $D_2$ and $D_3$ dopamine receptors via inverse agonism [210,495], though this is the first time it has been shown in a native human neural tissue. However, it is noteworthy that the extent of the reduction in levels of phosphorylated ERK1/2 in response to 1 mM haloperidol was considerable greater than levels of ERK1/2 phosphorylation in response to 1 mM dopamine. It may be the case that haloperidol is also capable of behaving as an inverse agonist at the other receptors it is known to demonstrate high affinity for, though this remains unclear from the data presented here. It should be noted however that haloperidol demonstrates nanomolar affinity for most of it's receptor targets, yet ERK1/2 inhibition in response to haloperidol was only observed once the concentration reached 3.16 µM ($10^{-5.5}$ M)(see Figure 6.10 **d**), and significant levels of ERK1/2 inhibition were only really demonstrated with its use at 1 mM (Figure 6.10, **c**); representing a very high dose. This raises the question of whether haloperidol's action is restricted to its activity at cell surface receptors or whether it can exert other effects when used at high concentrations. As mentioned previously, haloperidol demonstrates high lipophilicity, and so a direct mechanism though interaction with intracellular signalling molecules cannot be ruled out as a possible mechanism to explain haloperidol's ability to reduce levels of phosphorylated ERK1/2.

Another consideration regarding the observed effect of haloperidol is that rather than – or as well as – reducing the level of constitutive activity of GPCRs in differentiated CTX0E16/02 cultures, it may be modulating network activity within these cultures. Data presented in Chapter 3 and Chapter 4 showed that differentiated CTX0E16/02 include both glutamatergic and GABAergic cell types. However, it was not tested whether cells within these cultures may also generate neurons capable of releasing other neurotransmitters; whose action at their cognate receptors could be modulated by the presence of haloperidol. The possibility that differentiated CTX0E16/02 cells form functional networks may also explain the relatively high levels of basal ERK1/2 phosphorylation detected in these cultures. However, this earlier work also clearly showed that only a very small minority of cells within CTX0E16/02 cultures, differentiated for 28 days were capable of demonstrating electrical excitability, a property necessary to allow neurons to release vesicle-bound neurotransmitter. Indeed, the relative proportion of cells capable of elevating $[Ca^{2+}]_i$ in response to a 50 mM challenge in differentiated cultures was strikingly similar to that observed in proliferative cultures (see Figure 4.17, above), where little, if any basal ERK1/2 activity was detected (Figure 6.11). Therefore, even if the cells within differentiated CTX0E16/02

cultures are making neurotransmitters, they are incapable of releasing them; suggesting pharmacological tone is not responsible for the elevated level of ERK1/2 activity.

The work presented above demonstrates that ERK1/2 phosphorylation can be induced in differentiated CTX0E16/02 cultures following exposure to dopamine, 5-HT, acetylcholine, histamine, phenylephrine, glutamate and GABA. In addition, it has also been shown that at high concentrations, haloperidol behaves as an inverse agonist with respect to ERK1/2 phosphorylation. However, all of these ligands are highly non-selective with regard to the receptors they are capable of activating – or inhibiting, in the case of haloperidol. The following section will therefore investigate the presence of receptor subtypes for the neurotransmitter systems that are thought to be most important in mediating the effects of currently available antipsychotics.

### *6.2.8 Differentiated CTX0E16/02 Cultures Express Functional $D_1$, $D_2$ & 5-$HT_{2A}$ Receptors*

Both dopamine and 5-HT – receptors for which are arguably the most important to antipsychotic action – induced ERK1/2 phosphorylation in a pattern that was difficult to interpret and suggested a combinatorial influence of several of their receptor subtypes. To provide a more detailed picture of the influence of different dopamine and 5-HT receptor subtypes upon ERK1/2 phosphorylation, experiments were performed to determine levels of ERK1/2 phosphorylation in response to receptor-subtype specific agonists and antagonists. Quinpirole, a dopamine $D_2$-specific agonist ($K_i$ = 1900 nM, 4.8 nM, ~24 nM and ~30 nM in cloned human $D_1$, $D_2$, $D_3$ and $D_4$ receptors respectively, in their high-affinity state [458]), was used to determine the level of $D_2$-mediated ERK1/2 phosphorylation in differentiated CTX0E16/02 cultures. Initial experimentation sought to determine the optimal period of exposure to quinpirole to obtain a maximal level of ERK1/2 phosphorylation by exposing cultures to 100 µM quinpirole for between 1 and 60 minutes. A high concentration of quinpirole was used for this initial optimisation experiment so as to ensure a response could be observed. Quinpirole provoked a sharp initial rise in ERK1/2 phosphorylation with peak activity being reached after just 10 minutes and sustained for the remainder of the experiment (Figure 6.12 **a**, below). This is in contrast to that seen for dopamine, which caused a slow rate of ERK1/2 phosphorylation that peaked at 45 minutes but remained above baseline at 60 minutes (see Figure 6.7 **a**, above). Quinpirole demonstrated a concentration-dependent increase in ERK1/2 phosphorylation following a pre-optimised exposure of 10 minutes with an $EC_{50}$ of 31 nM (Figure 6.12, **b**). This is slightly lower than a previously published value of 9.05 nM, though this was achieved using $D_{2S}$-expressing CHO cells and is difficult to accurately compare with responses from a native tissue such as the CTX0E16/02 cell line [496].

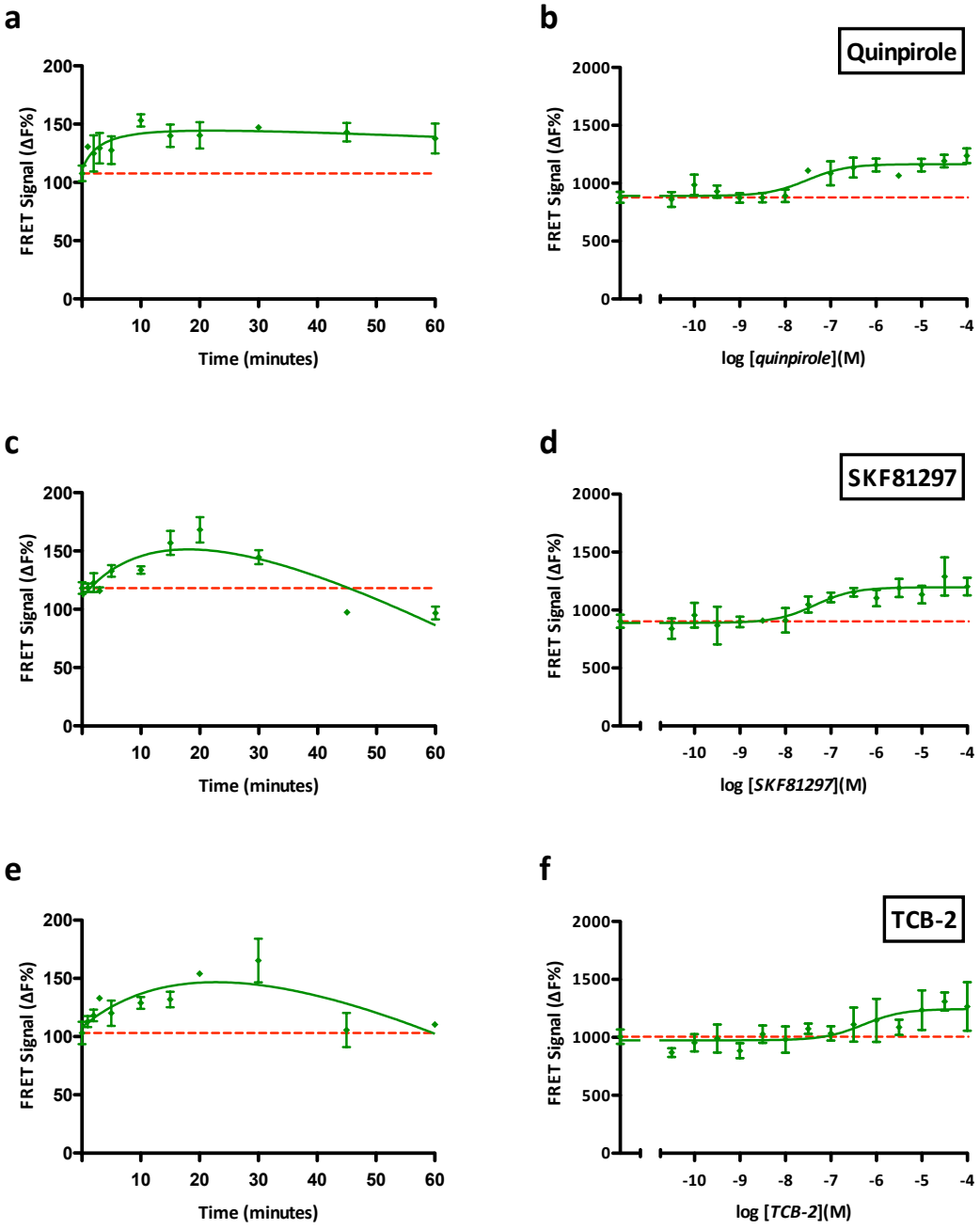


***Figure 6.12 Influence of dopamine and 5-HT receptor subtype specific agonists on ERK1/2 phosphorylation in differentiated CTX0E16/02 cultures***

CTX0E16/02 cells were seeded onto laminin-coated 96-well plates at 3 x $10^4$ cells per well and differentiated for 28 days using SNBM. On the day of the experiment all medium was removed and replaced with fresh medium 4 hours prior to addition of either quinpirole ($D_2$-selective agonist), SKF81297 ($D_1$-selective agonist) or TCB-2 (5-$HT_{2A}$-selective agonist). For time-course experiments, CTX0E16/02 cultures were exposed to 100 µM quinpirole in the presence of 20 µM ascorbic acid (**a**), 100 µM SKF81297 in the presence of 20 µM ascorbic acid (**c**) or 100 µM TCB-2 (**e**) for 1, 3, 5, 10, 15, 20, 30, 45 or 60 minutes prior to removal of medium and lysis for 5 minutes. Data points represent mean ± S.E.M. from 3 technical replicates (*n* = 1) and are expressed relative to donor-only fluorescence levels. For concentration-response experiments, differentiated CTX0E16/02 cultures were exposed to quinpirole (**b**), SKF81297 (**d**) or TCB-2 (**f**) at 31.6 pM ($10^{-10.5}$ M) to 100µM ($10^{-4}$ M) at half log-unit intervals for 10, 20 or 30 minutes for quinpirole ($EC_{50}$ = 31 nM), SKF81297 ($EC_{50}$ = 45 nM) and TCB-2 ($EC_{50}$ = 516 nM) respectively. Lysates were used to determine ERK1/2 phosphorylation levels using Cellul'erk kit components according to published protocols. Data points represent mean ± S.E.M. from 3 technical replicates (*n* = 2) and are expressed relative to donor-only fluorescence levels. Red dashed line shows levels of ERK1/2 phosphorylation in differentiated CTX0E16/02 cultures not exposed to ligand.

SKF81297 is a dopamine $D_1$-selective agonist with $K_i$ of 1.9 nM, 1272 nM and >10000 nM at $D_1$, $D_2$ and $D_3$ in cloned human receptors respectively (no binding data available for $D_2$ and $D_3$ receptors) [497]. Time-course exposure of differentiated CTX0E16/02 cultures to 100 µM SKF81297 demonstrated rapid ERK1/2 phosphorylation with a peak in activity after 20 minutes followed by a rapid decline – dropping below baseline by 45 minutes and remaining there until the end of the experiment at 60 minutes. Using 20 minutes at the optimal exposure period, differentiated CTX0E16/02 cultures were exposed to SKF81297 at concentrations between 31.6 pM ($10^{-10.5}$ M) and 100 µM ($10^{-4}$ M) at half log-unit intervals in the presence of 20 µM ascorbic acid. SKF81297 provoked a concentration-dependent increase in ERK1/2 phosphorylation with an $EC_{50}$ of 45 nM. Taken together, these data indicate the presence of both dopamine $D_1$ and $D_2$ receptors, and based on nanomolar $EC_{50}$ values, suggests at least some of these receptors are present in their high-affinity state. These data suggest at least $D_1$ and $D_2$ receptors contribute to the rise in ERK1/2 phosphorylation precipitated by exposure to dopamine (see Figure 6.7 **a** and **b**, above).

The 5-$HT_{2A}$-specific agonist TCB-2 ($K_i$ = 0.75 nM) was used to determine whether this receptor contributed to the elevation in ERK1/2 phosphorylation observed in response to 5-HT (Figure 6.7 **c** and **d**). TCB-2 at 100 µM provoked a rapid rise in ERK1/2 phosphorylation that peaked at 30 minutes but returned quickly to baseline by 45 minutes and remained there until the end of the experiment. Using 30 minutes as the optimum exposure period, TCB-2 was capable of exhibiting a concentration-dependent increase in ERK1/2 phosphorylation with an $EC_{50}$ of 516 nM. This is considerably lower than a previous report using HEK 293 cells stably expressing cloned human 5-$HT_{2A}$ receptors, though levels of receptor expression were likely to be significantly higher in this recombinant system [465].

In order to determine the specificity of ERK1/2 phosphorylation in response to quinpirole, SKF81297 and TCB-2, experiments were conducted using corresponding receptor-specific antagonists – raclopride, SCH39166 and MDL11939 for dopamine $D_2$, $D_1$ and 5-$HT_{2A}$ respectively – in an attempt to block these responses. These experiments were performed by exposing differentiated CTX0E16/02 cultures to increasing concentrations of a specific antagonist, in the presence of the corresponding agonist at a concentration that provoked approximately 80% of maximal ERK1/2 phosphorylation. Therefore, to interrogate ERK1/2 phosphorylation in response to dopamine $D_2$ receptor activation, differentiated CTX0E16/02 cultures were exposed to the $D_2$-specific antagonist raclopride, at concentrations between 31.6 pM ($10^{-10.5}$ M) and 100 µM ($10^{-4}$ M) at half log-unit intervals in the presence of 20 µM ascorbic acid and the $D_2$-specific agonist quinpirole at 316.2 nM ($10^{-6.5}$ M). For dopamine $D_1$-mediated responses, a concentration response curve was constructed in the same manner using the specific antagonist SCH39166 in the presence of the specific agonist SKF81297 at 316.2 nM ($10^{-6.5}$ M) and a final concentration of 20 µM ascorbic acid. In the case of the 5-$HT_{2A}$ receptor, increasing blockade was evaluated using the specific antagonist MDL11939 with receptor stimulation provided by 1 µM ($10^{-6}$ M) TCB-2.

As expected, raclopride delivered a concentration-dependent reduction in the level of ERK1/2 phosphorylation provoked by 316.2 nM quinpirole with an $IC_{50}$ of 460 nM (Figure 6.13 **a**). These data

would therefore suggest that ERK1/2 phosphorylation observed following exposure of differentiated CTX0E16/02 cultures to quinpirole is a dopamine $D_2$ receptor-specific response.

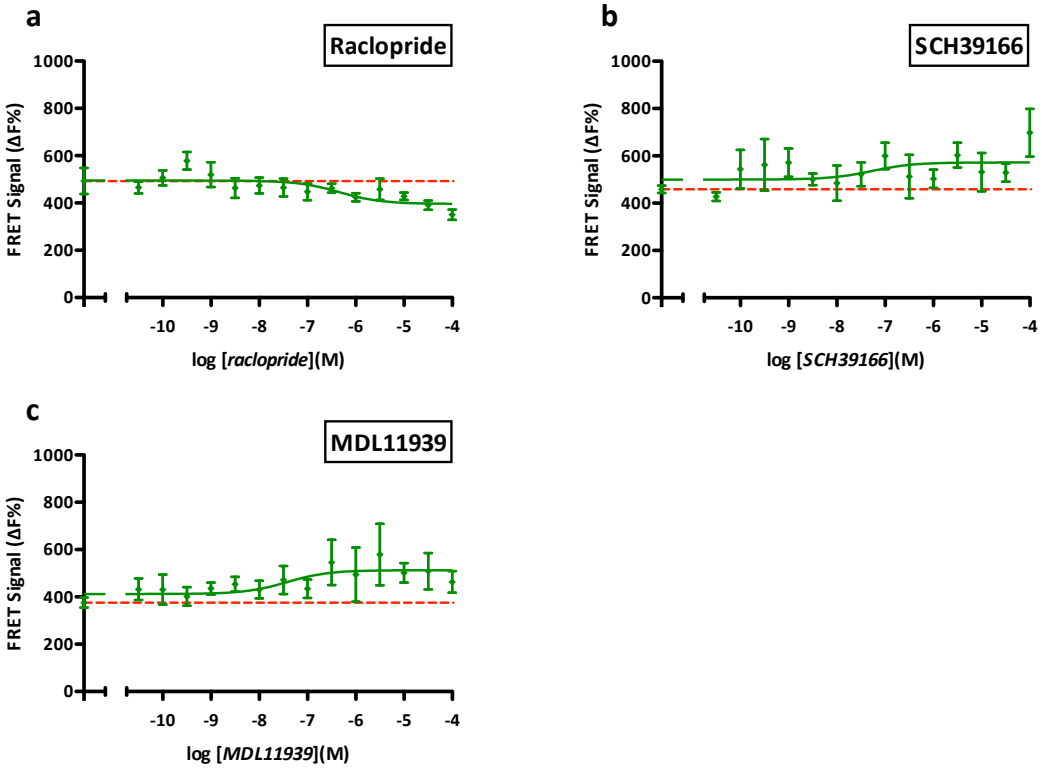


***Figure 6.13 Antagonism of dopamine and 5-HT receptor subtype specific agonist-induced ERK1/2 phosphorylation using specific antagonists in differentiated CTX0E16/02 cultures***
CTX0E16/02 cells were seeded onto laminin-coated 96-well plates at 3 x $10^4$ cells per well and differentiated for 28 days using SNBM. On the day of the experiment all medium was removed and replaced with fresh medium 4 hours prior to addition of compounds. Differentiated CTX0E16/02 cultures were exposed to (**a**) raclopride ($D_2/D_3$-selective antagonist) at 31.6 pM ($10^{-10.5}$ M) to 100µM ($10^{-4}$ M) at half log-unit intervals for 10 minutes in the presence of 316.2 nM ($10^{-6.5}$ M) quinpirole ($D_2$-selective agonist) and 20 µM ascorbic acid ($IC_{50}$ = 460 nM), (**b**) SCH39166 ($D_1/D_5$-selective antagonist) at 31.6 pM ($10^{-10.5}$ M) to 100µM ($10^{-4}$ M) at half log-unit intervals for 20 minutes in the presence of 316.2 nM ($10^{-6.5}$ M) SKF81297 ($D_1/D_5$-selective agonist) and 20 µM ascorbic acid ($EC_{50}$ = 53 nM) and (**c**) MDL11939 (5-$HT_{2A}$-selective antagonist) at 31.6 pM ($10^{-10.5}$ M) to 100µM ($10^{-4}$ M) at half log-unit intervals for 30 minutes in the presence of 1 µM ($10^{-6}$ M) TCB-2 (5-$HT_{2A}$-selective agonist, $EC_{50}$ = 38 nM). Lysates were used to determine ERK1/2 phosphorylation levels using Cellul'erk kit components according to published protocols. Data points represent mean ± S.E.M. from 3 technical replicates (*n* = 2) and are expressed relative to donor-only fluorescence levels. Red dashed line shows levels of ERK1/2 phosphorylation in differentiated CTX0E16/02 cultures exposed to agonist alone.

In contrast to raclopride, antagonists to the dopamine $D_1$ (SCH39166) and the 5-$HT_{2A}$ (MDL11939) receptors both caused a concentration-dependent increase in levels of ERK1/2 phosphorylation in differentiated CTX0E16/02 cultures that had been co-stimulated by agonist (SKF81297 and TCB-2 respectively) concentrations that were shown to provoke a slightly sub-maximal response (see Figure 6.13 **a** and **b**, above). SCH39166 has been shown to potently displace the classic $D_1/D_5$-specific antagonist, SCH23390 from cloned human receptors suggesting they both bind the same site of these receptors [459]. While behavioural differences have been observed between SCH39166 and SCH23390, these have been attributed to SCH23390s affinity for the 5-$HT_{2C}$ receptor [498]. Recent advances in GPCR

pharmacology have however highlighted that both functional selectivity and receptor dimerization may play a key role in dopamine receptor signalling [195,216,223,499,500]. [145] This finding appears to corroborate the importance of using native tissue rather than heterologous expression systems to accurately characterise receptor pharmacology.

5-$HT_{2A}$ receptors have also been shown to demonstrate functional selectivity and receptor dimerization [195,218,220,222], which may also help to explain the apparent potentiation of TCB-2-mediated ERK1/2 phosphorylation by MDL11939, and the previously mentioned TCB-2-mediated concentration-dependent reduction in intracellular $Ca^{2+}$ concentration (Figure 6.3 **b**, above). When considering data obtained from intracellular $Ca^{2+}$ accumulation and ERK1/2 phosphorylation experiments using these same ligands to dopamine and 5-HT receptors, it appears clear that further work is necessary to more fully understand the nature of these interactions and their signalling consequences. The CTX0E16/02 cell line may therefore represent an ideal native tissue platform with which to interrogate the complex pharmacology associated with various neurotransmitter receptors.

### *6.2.9 Important Considerations for Future Transcriptomic Experiments*

Use of an *in vitro* paradigm to reveal gene expression changes following exposure to antipsychotic drugs does not represent a novel approach in itself. Several published studies have applied this approach over the course of the past decade though consistent findings have remained elusive [258,259,280,281,501]. In addition, few genes other than those that were already identified as obvious candidates have been identified and these tend not to correspond with similar gene expression studies performed using post mortem tissue from schizophrenic patients. Of these studies, none of them verified the expression of receptors known to be targeted by antipsychotics in their respective cellular systems – at the level of message or functional protein at the cell surface. Indeed, one of these studies made use of a cell line that is known not to express the primary target of antipsychotics – dopamine receptors [281,502]. Another technical consideration that is likely to influence gene expression changes following exposure to antipsychotics *in vitro* is the concentration of drug exposed to cultures. Of those publications using this approach to interrogate the mechanism of action of antipsychotics, doses of haloperidol for example have ranged from 0.2 µM to 50 µM, concentrations which are described as 'pharmaceutically' or 'physiologically' relevant [259,280,281]. PET imaging data from schizophrenic patients receiving clinically efficacious doses of haloperidol suggest this value to be 8 nM – a value arrived at by Dr Hugo Geerts of In Silico Biosciences and Associate Professor at the University of Pennsylvania (Personal Communication). By integrating a large array of clinical and preclinical data from the available literature, "In Silico Biosciences build mechanistic mathematical models of physiological systems of CNS diseases such as schizophrenia". The accuracy of their mathematical models therefore rely on the accuracy of the biological data they use [503,504]. This means that, of currently published *in vitro* studies, concentrations of haloperidol exposed to cultures have ranged from 25 to over 6250 times that of what is achieved in the brain following therapeutic dosing [456,505,506].

As discussed previously, an imperative of antipsychotics is that they are brain penetrant, and are therefore required to show considerable lipophilicity. In a cell culture environment, this means that antipsychotic compounds are capable of transcending the plasma membrane, allowing them to interact with intracellular biological molecules. The extent to which this occurs *in vivo* is open to debate, though its likelihood would inevitably be enhanced as concentration increases *in vitro*. Indeed, some antipsychotic have been identified as capable of interacting with intracellular targets such as cyclooxygenases and lipoxygenases at higher concentrations and may therefore yield misleading or wholly incorrect gene expression changes with respect to their mechanism of action [502,507].

Classically, antipsychotic clinical efficacy is thought to be achieved through antagonism of cell surface receptors – with the exception perhaps of clozapine through its major circulating metabolite *N*-desmethylclozapine, which has been shown to behave as a muscarinic $M_1$ partial agonist [209,457] and the newer generation antipsychotic aripiprazole, that has been shown to behave as a partial agonist at dopamine $D_2$ and $D_3$ receptors *in vitro* [174,199]. Interestingly however, due to the presence of cholinergic or dopaminergic physiological tone, these compounds would therefore behave as antagonists *in vivo*. Data have been provided here to suggest that haloperidol exerts an effect upon levels of ERK1/2 phosphorylation characteristic of inverse agonism (see Figure 6.10, **c** and **d**), though the receptor through which this was achieved remains unclear, and the potency of the observed effect was considerably below what may be expected when considering the low nM affinity this compound exhibits to the majority of the receptors it is known to target (see Figure 1.1, above). Published data has also suggested that many antipsychotics – including haloperidol – may act as inverse agonists at dopamine $D_2$ and $D_3$ receptors [210,508]. These findings should however be considered with caution, due to the use in these studies of heterologous systems expressing constitutively active mutant receptors. It remains unclear whether antipsychotics exert this action *in vivo*, though warrants further investigation. Importantly, antagonists, and indeed partial agonists and inverse agonists require the presence of physiological tone for their true pharmacological characteristics to be determined. For example, as mentioned previously, while aripiprazole behaves as a $D_2$ partial agonist *in vitro*, this effect would be interpreted in the presence of physiological tone as antagonism, as its occupancy of $D_2$ receptors would prevent the full agonist activation by its cognate ligand – dopamine. An *in vitro* cell culture system that provides physiological tone – especially for the range of neurotransmitters found in the adult brain – is yet to be described. Perhaps the closest example of this at present is a study describing the formation of spontaneously active neuronal networks derived from human embryonic stem cells, data from which support the suggestion of functional glutamatergic and GABAergic synapse formation [334].

In the absence of physiologically relevant levels of pharmacological tone *in vitro*, it could be postulated that the concentration of an antagonist required to provoke a physiological response may be far higher than would be required in its presence. Indeed, for neutral antagonists – if the concentration is increased to a level so as to provoke a response at all, then these are likely to be as a result of off-target or toxic interactions, or through inhibition of constitutive receptor activity. With respect to highly lipophilic, brain penetrant compounds such as those utilised for the treatment of various

neuropsychiatric conditions, as the concentration of *in vitro* exposure increases, so too would the likelihood of a cellular response. Even in the absence of off-target intracellular interactions, these compounds may still affect the liquidity of membrane at the cell surface and that of the organelles they contain. If the purpose of an *in vitro* transcriptomic experiment is to provide a simple paradigm with which to explore the mechanism of action of antipsychotic medicines, then the concentration of drug used should ideally mirror that to which the medicated brain is exposed, so as to reduce the occurrence of false positives. As described above, differentiated CTX0E16/02 cultures exposed to haloperidol demonstrated a reduction in ERK1/2 phosphorylation as concentrations began to reach 10 μM (see Figure 6.10 **d**). Phosphorylation of ERK1/2 represents a primary mechanism though which GPCR-mediated signalling can lead to gene expression changes, as it confers upon it the ability to translocate into the nucleus to induce immediate early gene expression and therefore amplify the effect of the initial signal (reviewed in detail elsewhere [256,509]).

To determine whether an effect of haloperidol could be observed at therapeutically relevant concentrations *in vitro*, differentiated CTX0E16/02 cultures were exposed to increasing concentrations of haloperidol in the presence of simulated dopaminergic tone. Pharmacological tone itself is an abstract concept that is used to describe an average level of activity – the summation of activity at billions of synapses. The concentration of neurotransmitter at any one synapse *in vivo* may involve periods with little or no activity associated with low-frequency tonic firing that contrast greatly with periods of burst activity [510]. Release of neurotransmitter is both pulsatile and focal – with the exception of leakage from the synaptic cleft [510]. It is also subject to various clearance mechanisms including reuptake and enzymatic degradation [7]. This level of complexity cannot of course be simulated and, if it were possible, would never be financially viable for a study of this kind. Dopamine was instead added in the same manner as haloperidol – as a supplement to the medium surrounding the cultures. Although a clear sigmoidal concentration-response relationship with respect to ERK1/2 phosphorylation in response to dopamine in differentiated CTX0E16/02 cultures was not observed, there did appear to be two early peaks of activity at 3.16 nM ($10^{-8.5}$ M) and 100 nM ($10^{-7}$ M)(see Figure 6.7 **b**, above). These two concentrations were therefore used in two separate experiments to determine the effect of haloperidol in the presence of dopamine. Differentiated CTX0E16/02 cultures were exposed to haloperidol at concentrations between 31.6 pM ($10^{-10.5}$ M) and 100 μM ($10^{-4}$ M) at half log-unit intervals in the presence of dopamine at either 3.16 nM ($10^{-8.5}$ M) or 100 nM ($10^{-7}$ M) and 20 μM ascorbic acid for 45 minutes (incubation period associated with maximal dopamine-mediated ERK1/2 phosphorylation). Cultures were then lysed and levels of phosphorylated ERK1/2 determined using Cellul'erk kit components.

In the absence of dopaminergic 'tone', a concentration-dependent decrease in levels of ERK1/2 phosphorylation starting at approximately 3.16 μM, though had failed to plateau once the highest tested concentration of 100 μM was reached (see Figure 6.10 **d**, above). In contrast, in the presence of simulated dopaminergic tone of 3.16 nM ($10^{-8.5}$ M), haloperidol demonstrated a concentration-dependent decrease in ERK1/2 phosphorylation starting at approximately 0.1 nM and exhibited an $IC_{50}$

of 0.9 nM (Figure 6.14 **a**). In the presence of 100 nM ($10^{-7}$ M) dopamine, this curve was subject to a rightward shift, with haloperidol demonstrating an $IC_{50}$ of 59 nM (Figure 6.14, **b**). As expected, due to dopamine receptor stimulation, an effect of haloperidol could be observed at a considerably lower concentration than when it was exposed to differentiated CTX0E16/02 cultures alone. In the presence of simulated dopaminergic tone of 3.16 nM, a similar level of effect from haloperidol with respect to ERK1/2 phosphorylation, was observed, though demonstrated a leftward shift in potency of approximately four orders of magnitude, while this value was reduced to approximately two orders of magnitude in the presence of 10 nM dopamine.

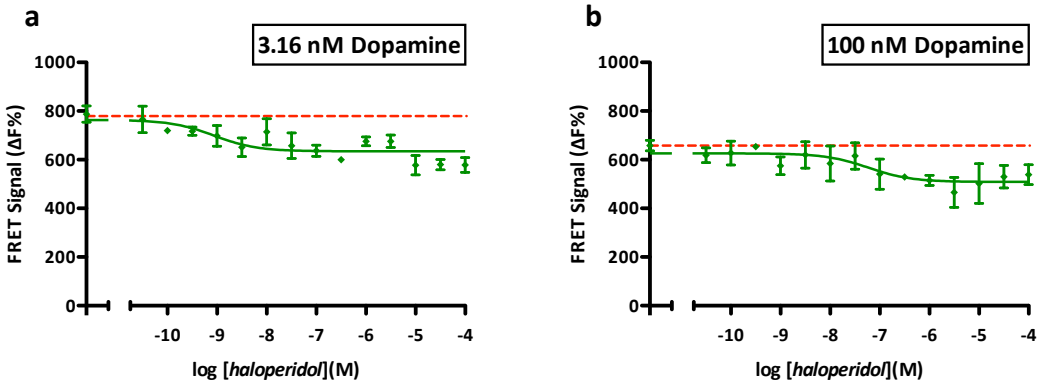


***Figure 6.14 Influence of haloperidol upon ERK1/2 phosphorylation in differentiated CTX0E16/02 cultures exposed to simulated dopaminergic tone***
CTX0E16/02 cells were seeded onto laminin-coated 96-well plates at 3 x $10^4$ cells per well and differentiated for 28 days using SNBM. On the day of the experiment all medium was removed and replaced with fresh medium 4 hours prior to addition of compounds. Differentiated CTX0E16/02 cultures were exposed to haloperidol at 31.6 pM ($10^{-10.5}$ M) to 100µM ($10^{-4}$ M) at half log-unit intervals for 45 minutes in the presence of 20 µM ascorbic acid and either (**a**) 3.16 nM dopamine ($IC_{50}$ = 0.9 nM) or (**b**) 100 nM dopamine ($IC_{50}$ = 59 nM). Lysates were used to determine ERK1/2 phosphorylation levels using Cellul'erk kit components according to published protocols. Data points represent mean ± S.E.M. from 3 technical replicates (*n* = 2) and are expressed relative to donor-only fluorescence levels. Red dashed line shows levels of ERK1/2 phosphorylation in differentiated CTX0E16/02 cultures exposed to 3.16 nM dopamine (**a**) or 100 nM dopamine (**b**) alone.

This finding in itself is far from novel, with haloperidol's blockade of dopamine receptors first proposed by Carlsson & Lindqvist as early as 1963 [152]. Intense scrutiny of the pharmacology behind antipsychotic efficacy has persisted, and it is now firmly established that all available antipsychotics possess high affinity for a range of different receptors [183]. Interaction with the majority of these receptors was thought to be exerted through antagonism, though as our understanding of GPCR pharmacology has grown, so too have the description of these compound's receptor interactions. For example, many antipsychotics – haloperidol amongst them – have now been described as behaving as inverse agonists rather than neutral antagonists at the dopamine $D_2$ receptor [508,511]. Haloperidol has also been described as an inverse agonist at dopamine $D_3$ receptors [210,512], a property that may have contributed to haloperidol's ability to reduce levels of ERK1/2 phosphorylation in the absence of dopaminergic tone, as described above (Figure 6.10, **c** and **d**). Whether haloperidol also behaves as an inverse agonist at other receptors for which it demonstrates high affinity is however yet to be established.

The fact that levels of ERK1/2 phosphorylation can be used as a marker to reveal an effect of haloperidol at therapeutically relevant concentrations when added in conjunction with dopamine does however highlight a shortcoming of the use of *in vitro* systems as an experimental platform to interrogate the mechanism of action of antipsychotic medicines. In the absence of pharmacological tone, the effect of only full agonists, partial agonists and inverse agonists can be detected. By definition, the influence of a neutral antagonist could not be discriminated. This does not however illustrate the full picture, as the behaviour of all these pharmacological entities would be altered in the presence of tone, and does not begin to provide an appreciation for compounds that may demonstrate allosteric receptor interactions. These data provide evidence that the presence of physiological tone is an important prerequisite of being able to detect the activity of haloperidol. These finding have important implications with respect to experiments that hope to elucidate the mechanism of any drug in an *in vitro* environment, as is discussed in more detail in Chapter 7 below.

### *6.2.10 Summary*

This chapter built on work presented in ***Chapter 4*** to provide a detailed pharmacological characterisation of the pharmacological properties demonstrated by differentiated CTX0E16/02 cultures. Ligand-induced intracellular $Ca^{2+}$ accumulation has been described in CTX0E16/02 cultures exposed to various methods of differentiation in response to dopamine, 5-HT, glutamate, GABA, acetylcholine, histamine, phenylephrine and carbamoylcholine. The nature and specificity of these increases in intracellular $Ca^{2+}$ concentration were explored here in further detail for dopamine, 5-HT and acetylcholine. Robust responses from acetylcholine facilitated a detailed dissection of the relative contribution of ionotropic nicotinic receptors and metabotropic muscarinic receptors, though further work would be necessary to determine the influence of individual receptor subtypes upon observed levels of $Ca^{2+}$ accumulation. Less pronounced responses mediated by dopamine and 5-HT were more difficult to corroborate with regard to their specificity. This may have been attributable both to the narrow dynamic range provided by minimal responses from these ligands, by the lack of selectivity these ligands demonstrate, and the conflicting influence of distinct signalling pathways precipitated by different receptors that affect intracellular $Ca^{2+}$ concentration through divergent mechanisms, as discussed in ***4.1*** and graphically summarised in Figure 4.1. Surprisingly, this work also insinuated an apparent inverse agonistic effect of the 5-$HT_{2A}$-specific agonist, TCB-2 in differentiated CTX0E16/02 cultures with respect to intracellular $Ca^{2+}$ accumulation. This represents a novel finding, and is in contrast to it's observed behaviour as an agonist with respect to ERK1/2 phosphorylation in the same cultures.

Limitations associated with the use of intracellular $Ca^{2+}$ concentration as a surrogate for GPCR activity led to experiments that exploited the ubiquitous ability of GPCRs to modulate levels of ERK1/2 phosphorylation. These experiments were particularly informative with regard to the pharmacological nature of differentiated CTX0E16/02 cultures due to it's considerably higher detection sensitivity

compared to the measurement $[Ca^{2+}]_i$. Measurement of levels of ERK1/2 phosphorylation in CTX0E16/02 cultures showed that:

- Differentiated CTX0E16/02 cultures demonstrated considerable higher basal levels of phosphorylated ERK1/2 than their proliferative counterparts, as indicated by significantly higher levels of detected FRET. This may however be attributable to a greater overall level of ERK1/2 expression in differentiated as compared to proliferative cultures. This highlights a drawback of this type of high-throughput detection method, as absolute levels of ERK1/2 cannot be determined as each experimental well is exposed to the same amount of each antibody, and no discrimination can be made between bound and unbound antibody. This finding clearly warrants further investigation, as variations in the basal level of ERK1/2 phosphorylation would allow different responses to be derived from the same ligand, even if the receptor population was the same. Using haloperidol's apparent inverse agonistic effect with respect to ERK1/2 phosphorylation in differentiated CTX0E16/02 cultures as an example, little or no response would be expected to be observed in proliferative cultures exhibiting an absence of basal ERK1/2 phosphorylation. This finding therefore highlights the importance of using a native tissue system to investigate ligand pharmacology, as an *in vitro* system lacking basal ERK1/2 activity would be incapable of observing these responses, including proliferative CTX0E16/02 cultures.
- The method of detection used to determine levels of ERK1/2 phosphorylation provided a considerably more sensitive means by which GPCR activity could be monitored, though as an endpoint assay, lacks the temporal resolution provided by measurement of intracellular $Ca^{2+}$ concentrations. High-throughput assays are now available to assess the phosphorylation status of a broad range of signalling molecules though remain very expensive when compared to the that used to measure $Ca^{2+}$ concentration.
- Levels of ERK1/2 phosphorylation did not correlate with levels of intracellular $Ca^{2+}$ accumulation in response to a given compound or concentration. Indeed, while acetylcholine consistently provoked the most robust increases in $[Ca^{2+}]_i$, it provoked amongst the lowest levels of ERK1/2 phosphorylation (see Figure 4.9, **c** and Figure 6.8, **b**). In contrast, while differentiated CTX0E16/02 cultures demonstrated minimal intracellular $Ca^{2+}$ accumulation in response to phenylephrine, this ligand was capable of provoking the highest detected levels of ERK1/2 phosphorylation (see Figure 4.9, **a** and Figure 6.8, **d**). This inverse functional selectivity demonstrated by acetylcholine and phenylephrine with respect to intracellular $Ca^{2+}$ accumulation and ERK1/2 phosphorylation have not been described elsewhere and as such represent a novel finding.
- Levels of ligand-induced intracellular $Ca^{2+}$ accumulation or ERK1/2 phosphorylation cannot therefore be used to accurately estimate levels of functional receptor expression at the cell surface. The most reliable way to approach this would be to perform radioligand binding using intact cells, though is technically demanding and requires considerable optimisation. However,

this could perhaps be performed through a fluorescence-based strategy with the recent introduction of fluorescent GPCR ligands for this purpose by Abcam and Tocris.

- The time-course of ERK1/2 phosphorylation induced by each different tested ligand varied considerably. This may partly explain how the same signal from different receptors can be discriminated.
- Different ligands also provoked very different levels of variability between cultures. For example, dopamine, phenylephrine and acetylcholine produced comparably consistent levels of ERK1/2 phosphorylation between cultures, while responses to 5-HT and histamine varied considerably from one well to another, as indicated by the size of error bars for each of these experiments. Considering the sensitivity demonstrated by this method of detection for ERK1/2 phosphorylation, this may be due to heterogeneity within differentiated CTX0E16/02 cultures with respect to the number of cells that demonstrate ERK1/2 phosphorylation in response to these ligands, as was found to be the case for cells capable of responding to dopamine or 5-HT by elevating $[Ca^{2+}]_i$ (see Figure 4.13, **c**). For example, if individual cells within these cultures are capable of producing robust, measurable increases in ERK1/2 phosphorylation, though only few of these cells are present within each culture, a small difference in the number of these responding cells could potentially result in a relatively large difference in the level of phosphorylated ERK1/2 detected.
- Use of specific $D_1$-like and $D_2$-like agonists demonstrated the presence of both of these receptor subtypes in differentiated CTX0E16/02 cultures. Interestingly, despite having opposing effects upon adenylyl cyclase, and consequently cAMP levels, both receptor types caused an increase in ERK1/2 phosphorylation.
- While raclopride was capable of reversing levels of ERK1/2 phosphorylation observed in response to quinpirole, SCH39166 and MDL11939 appeared to potentiate increases in ERK1/2 phosphorylation provoked by SKF81297 and TCB-2 respectively. Further work is required to determine the cause of this apparent anomaly, as both SCH39166 and MDL11939 are thought to be full antagonists at dopamine $D_1$-like and 5-$HT_{2A}$ receptors respectively. Data presented here suggests these compounds may be capable of behaving as positive allosteric modulators. This again highlighted the importance of using native tissues to study *in vitro* pharmacology.
- As was observed when investigating ligand-induced changes in $[Ca^{2+}]_i$, variability also tended to be greater when using antagonists to inhibit agonist-induced ERK1/2 phosphorylation. However, this was not always the case, as raclopride's inhibition of quinpirole-induced responses yielded particularly consistent data, while SCH39166 and MDL11939's inhibition of SKF81297 and TCB-2's respective responses were less tight.
- While the Cellul'erk kit yielded valuable data, it should be noted that this assay would greatly benefit from the use of robotics to perform any liquid handling. All experiments described above using this assay were performed manually, though due to the use of 384-well small volume plates, the transfer of very small (but identical) volumes and the importance of timing

(to ensure consistent lysis periods between wells and minimal exposure of reagents to light), it is felt that the use of robotics would greatly improve the accuracy of data obtained.

- It was mentioned that when performing experiments to measure levels of ligand-induced intracellular $Ca^{2+}$ accumulation it became clear that resultant data was subject to an apparent "edge effect". This was thought to be as a consequence of cells – differentiated in 96-well plates – remaining in culture for extended periods of time, and wells closer to the edge of plates inevitably being subject to greater levels of media evaporation. Higher evaporation therefore leading to changes in the concentration of solutes within each wells' medium. In an attempt to partially address this issue for the more sensitive ERK1/2 phosphorylation assays, the arrangement of drug concentration exposures were varied across the plate. This was employed to try and ensure that technical replicates of the same experimental condition were as far as possible, not both at the edge of a plate. An example of one of the plate maps used is shown in Figure 6.15, below.

| | 1 | 2 | 3 | 4 | 5 | 6 | 7 | 8 | 9 | 10 | 11 | 12 |
|---|---|---|---|---|---|---|---|---|---|---|---|---|
| **A** | -10.5 | -10 | -9.5 | -9 | -8.5 | -8 | -7.5 | -7 | -6.5 | -6 | -5.5 | -4 |
| **B** | C | -10 | -9.5 | -9 | -8.5 | -8 | -7.5 | -7 | -6.5 | -6 | -5.5 | -5 |
| **C** | -4.5 | -4.5 | -10.5 | -9.5 | -8.5 | -7.5 | C | C | -10.5 | -4 | -5 | C |
| **D** | -4.5 | -4.5 | -10.5 | -9.5 | -8.5 | -7.5 | -6.5 | -6 | -5.5 | -5 | C | C |
| **E** | -4 | -4 | -10 | -9 | -8 | -7 | -6.5 | -6 | -5.5 | -5 | C | C |
| **F** | -4.5 | -4.5 | -10 | -9 | -8 | -7 | C | C | -10.5 | -4 | -5 | C |
| **G** | C | -10 | -9.5 | -9 | -8.5 | -8 | -7.5 | -7 | -6.5 | -6 | -5.5 | -5 |
| **H** | -10.5 | -10 | -9.5 | -9 | -8.5 | -8 | -7.5 | -7 | -6.5 | -6 | -5.5 | -4 |

**Haloperidol** **Dopamine** **Phenylephrine**

***Figure 6.15 Diagram of typical plate map for ERK1/2 phosphorylation assays to reduce influence of "edge effect"***
Plate maps such as this were used to assign to different conditions to individual wells of a 96-well plate so as to ensure that no two concentrations of the same drug were at the edge of a plate to minimise any influence of an edge effect. Each shaded value refers to a final drug concentration exposed to cells contained within the corresponding well to the $\log_{10}$ M. 'C' refers to control wells where no drug was added.

- As previously mentioned, high-throughput ERK1/2 phosphorylation assays such as the that provided by the Cellul'erk kit which do not include a step to wash away unbound antibody do not provide a measure of total ERK1/2 contained within each sample. The same amount of

each antibody is added to determine levels of ERK1/2 phosphorylation in a single well. Not only does this limit the amount of data from which to draw more meaningful conclusions based on levels of phosphorylation relative to total quantities of ERK1/2 present, it also removes the possibility of normalising data to account for variations between cultures in individual wells. For $Ca^{2+}$ accumulation assays this was afforded by normalisation data against the internal control of responses provoked through exposure of cultures to a final concentration of 10 µM ionomycin. ERK1/2 phosphorylation – measured as a specific FRET signal (*ΔF%*) – was expressed according to the following equation as defined by Albizu and colleagues [318]:

$$\Delta F\% = \frac{R - R_{Neg}}{R_{Neg}} \times 100$$

Referring to *R* as the 665 nm/620 nm ratio calculated for each individual well/assay, and $R_{Neg}$ as the mean of the same ratio measured for blank controls (donor antibody alone), for which at least 6 were included on each 384-well plate. While this calculation is able to account for some discrepancies between the volumes of antibody added, it cannot normalise values according to the amount of total ERK1/2 present. It is felt that an internal control such as this would greatly enhance both the accuracy and level of information provided by this assay.

- A final consideration with regard to ERK1/2 phosphorylation data presented here is the relatively small *n* numbers provided. The number of repeats for each experiment was unfortunately limited by the still very high cost of these assays, though cheaper alternatives would not have provided the level of throughput required to demonstrate what has been presented above. With respect to experiments that yielded highly variable data such as those making use of antagonists in the presence of agonist or some specific agonists such as 5-HT and histamine, further work would be required to provide more conclusive findings.

Most importantly, data presented here have shown that the effect of a therapeutically relevant concentration of antipsychotic drug can be detected *in vitro* in differentiated CTX0E16/02 cultures. However, this effect could only be detected in the presence of simulation neural, physiological tone. This finding has important implications regarding the way in which we experimentally investigate the mechanism of action of complex drug-receptor interactions. These data suggest that previously attempts to transcriptomically interrogate the mechanism of action of a range of different drugs have been fundamentally flawed, by failing to appreciate the pharmacology of antagonistic compounds.

# *Chapter 7 Discussion*

This thesis provides a detailed phenotypic and pharmacological characterisation of cultures generated through the differentiation of a conditionally immortalised, human cortex derived neural progenitor cell line – CTX0E16/02. Data is presented providing evidence that these progenitor cells can generate differentiated cell-types resembling those that comprise that adult human cortex, namely; glutamatergic and GABAergic neurons, astrocytes and potentially oligodendrocytes. Evidence has also been provided to show that these cultures exhibit markers indicative of synapse formation, and contain cells capable of electrical excitability – based on their ability to mobilise intracellular $Ca^{2+}$ in response to a high $K^{+}$ challenge – and therefore resemble mature neuronal networks. Differentiation of the CTX0E16/02 cell line was accompanied by an increase in the expression of genes encoding proteins associated with neural communication, and those thought to mediate the transduction of signals responsible for the therapeutic efficacy of antipsychotic drugs. Work described here provides the first, detailed pharmacological characterisation of a human neural progenitor cell line and the cultures they generate upon differentiation. As a means of validation, a phenotypic and functional comparison has been made with cultures derived from primary human foetal tissue; demonstrating that these cells reflect the properties of their *in vivo* counterparts. Taken together, these data show that the CTX0E16/02 cell line represents an excellent *in vitro* model with which to investigate the mechanism of action of antipsychotic drugs. Finally – and perhaps most importantly – differentiated CTX0E16/02 cultures have been used to show that the downstream signalling consequences of exposure to an antipsychotic drug can only be detected at clinically relevant concentration, when cultures are additionally exposed to simulated physiological tone. These data have important implications regarding the use of *in vitro* models as a means to understand the pharmacological effects of neuropsychiatric drugs, though has wider relevance to the investigation of any drug *in vitro*.

Human stem cell technology has progressed at a staggering rate over the past decade and advances in this field have made their presence felt in the laboratory, the clinic and within society in general – not least because of the ethical and social issues that their use raises. Indeed, the recent development of iPS cell technology, and the demonstration – at least in animals – that somatic cells can be reprogrammed to an embryonic state and subsequently used to generate adult chimeras though nuclear transfer [513,514], almost questions the nature of life itself. Working within this field at the present moment makes it difficult not to be complacent about what is currently happening, and how these discoveries will change scientific understanding and the nature of health care treatment in the future.

The reason why stem cells represent such an exciting tool for laboratory neuroscientists is that they have the potential to provide a limitless source of the cells that comprise the human brain. Historically, this availability has been a major stumbling block for the study of human neurons – the cells that are responsible for everything from the generation of movement and sensation, to emotion and cognitive ability. While the use of animals and heterologous cell culture systems have proven useful in this endeavour, as we seek to understand the cellular and biochemical mechanisms of arguably uniquely human behaviours, it has become increasing clear that these cannot replace the need to study native

human cells. It is the post-mitotic nature of neurons that makes their study such a challenge. Healthy human neural biopsy material is understandably rare, and even if neuronal cultures are derived from animals – which itself is less than ideal – they cannot be expanded; meaning new animals are required to perform each individual experiment, bringing with them considerable costs and their own ethical implications. In contrast, embryonic stem (ES) cells exhibit self renewal, meaning they can be expanded to suit the needs of almost any experiment, while possessing the potential to form any cell of the mature brain, or indeed any other tissue of the body [515]. ES cells form the inner cell mass of the developing embryo, and are subject to a complex sequence of signalling events as they increase in number and specialisation [50]. Accurate recreation of these developmental signals *in vitro* are far from trivial, and has therefore promoted the use of neural progenitor cells (NPC) as a means to generate cells representative of those that comprise the adult human brain [46,61,328]. NPCs are isolated at a later gestational stage than ES cells, representing specialised cohorts of cells, destined to form distinct regions of the developing brain [51]. Indeed, upon *in vitro* isolation, these cells have been shown to be capable of self renewal in the presence of appropriate trophic stimulation and, upon removal of this trophic stimulation, to spontaneously differentiate into cells representative of their neural region of origin [57-59,61,63,65,66].

The restricted fate of NPC is however accompanied by a concomitant reduction in their self-renewal capacity, when compared to ES cells. Partly to address this issue, Pollock and colleagues demonstrated the utility of controllable ectopic expression of the oncogenic gene – *c*-Myc – within clonally-derived NPCs, as a means to conditionally immortalise these cells [63]. This system allows these NPCs to be maintained under proliferative conditions through 4-OHT-mediated, controlled expression of *c*-Myc, with the subsequent removal facilitating differentiation into both neurons and glia, again representative of their region of origin [63,65-67]. The NPC lines described in this study are all a product of this immortalisation process, including the CTX0E16/02 line, for which a detailed characterisation has been provided.

Recent advances in stem cell technology have identified a range of different means by which human neural cells can be derived, including the differentiation of NPCs, NSCs and ES cells [61,327,334], transdifferentiation of somatic cells into iPS cells prior to differentiation [75], or direct transdifferentiation of somatic cells into neurons [89] – each with their own advantages and weaknesses – and are discussed in detail in ***1.2*** to ***1.4***. However, cells derived through each of these different strategies require considerable characterisation so as to ensure their relevance to the *in vivo* counterparts they have been developed to model, or the application for which they are to be used. A good example of this is provided by the CTX0E03/02 line described above, which has recently entered clinical trial as a potential regenerative therapy in the treatment of stroke in human [111]. As such, this cell line had to be validated with respect to its clinical efficacy in animals, and be shown not to demonstrate tumorigenic properties prior to its use in humans [63,64,108,109].

The purpose of the study described here was to develop an *in vitro* culture system that represented an appropriate model with which to investigate the mechanism of action of currently available

antipsychotic drugs at the cellular and molecular level. In addition, this work had the additional objective of exploring the potential of this culture system as a putative tool for the development of novel antipsychotic medicines. As a starting point, this study began with seven distinct, conditionally immortalised NPC lines derived from diverse regions of the developing human brain, at specifically selected gestational stages to maximise their neurogenic capacity. The differentiation of five of these lines has been described previously [63,65-67,106], while the differentiation of the remaining two – both derived form the developing human cortex (CTX0E03/02 and CTX0E16/02) – has been optimised above. Initially, the expression of genes identified as pivotal to the transduction of the pharmacological effects of antipsychotic drugs was assessed in each of the seven lines under proliferative and differentiated culture conditions (a full list of these genes can be found in Table 3.8). This was used as a means of determining the suitability of each cell line for the prescribed purpose.

Considering the relatively early stage in development that the seven different NPC lines were isolated from (10 – 12 weeks), it was surprising to find that mRNA for many of the neurotransmitter receptors tested was already expressed by proliferating NPCs. This is the first time that the expression of a range of genes, specifically involved in neural communication has been assessed in human NPC cells. However, Hook and colleagues recently demonstrated an increase in the expression of *ADRB1*, encoding the adrenergic $\beta_1$ receptor, in a non-immortalised clonal NPC line derived from 9 – 10 week gestation developing human cortex. This was the only GPCR involved in neurotransmission that the group reported as demonstrating increased expression over a 32 day differentiation period; expression of this gene being absent in proliferative cultures [61]. The expression of this gene was not tested here. These data were obtained using expression microarrays however, and the expression of many GPCRs are known to occur below the limit of detection provided by this platform [516]. It is therefore likely that this group may have missed the expression of many other receptors [516]. From data obtained using whole genome expression arrays, the authors chose to present just seven genes whose expression had intensified over the course of the differentiation period – those that they felt represented 'druggable genes'. Therefore, it is likely that had they detected the expression of any of the genes tested here (which were selected because they are targeted by drugs) they would have been reporte. Another recent study reported by Layden and colleagues investigated the expression of 343 different GPCRs in mouse ES cells and ES cells that had been differentiated for 4 or 20 days as embryoid bodies using quantitative RT-PCR arrays [517]. They surprisingly detected the expression of genes encoding 5-HT (*Htr1b* and *Htr2a*), glutamate (*Grm4* and *Grm6*), GABA (*Gabbr1*), norepinephrine (*Adra1d*) and acetylcholine (*Chrm4*) receptors in undifferentiated ES cells. Of these, *GRM4* and *GRM6* were also found to be ubiquitously expressed in all seven NPC lines described here, while *HTR2A* exhibited limited expression in proliferative cultures, though appeared in all differentiated cultures. This group also found that after just a 4 day expansion as embryoid bodies, the expression of many more different receptors was induced, and showed further increases after 20 days growth as embryoid bodies [517]. Interestingly, while *Adrb1* – the only neurotransmitter GPCR reported to be expressed in cortical NPCs by Hook [61] – was not expressed in ES cells, but this gene was amongst those found to be incrementally induced after a 4 or 20 day expansion as embryoid bodies [517]. The fact that these receptors are expressed at all at such an early

stage in development raises questions about what their possible role could be, though expression was only demonstrated at the message level, and it remains unclear whether they were also expressed as functional receptors at the cell surface. It also raised the question of how early in embryonic development the endogenous ligands that act as agonists at these receptors are present, and what their possible role could be. Evidence has been presented in this thesis to begin to address some of these questions.

The expression of genes encoding neurotransmitter receptors in NPCs derived from 10 – 12 week gestation foetal tissue became less surprising when examining cultures derived from primary neural samples from 7 – 8 week gestation foetal tissue. Even at this early stage, these cultures were shown to be dominated by $MAP2^{+}$ neurons and contained cells capable of fluxing $Ca^{2+}$ in response to a 50 mM $K^{+}$ challenge, suggesting they already possessed the ability to release neurotransmitter. Unfortunately, due to the scarcity of tissue, it was not possible to identify the neurotransmitters these cells may have synthesised. However, the fact that both functional neurons are present and neurotransmitter receptors capable of transducing signals that may emanate from them suggests that neurotransmission – even at this early stage in neurodevelopment – may already have an important role. The function that this signalling performs however remains a neglected area, though this may be attributable to the fact that this represents a novel discovery. Indeed, the earliest stage of human neural development from which provoked electrical currents have been previously recorded is 16 weeks [425], with the first spontaneous firing recorded at 20 weeks [426]. It is unclear from the work presented in this thesis whether spontaneous neuronal firing was also a characteristic of these primary cultures, since the FS3 platform used for these investigations proved insufficiently sensitive to resolve this characteristic. Further work would therefore be required using either single cell $Ca^{2+}$ imaging, or ideally, electrophysiology to establish whether this property is present. A perhaps minor caveat to these findings is that the primary cultures that demonstrated these electrical properties were expanded as adherent cultures prior to investigation. Thus the possibility exists that this observed electrical excitability was not a property of the original primary samples, but only developed upon expansion. However, this seems unlikely when it is consider that the greatest KCl-induced responses were evoked in cultures that had spent the least time exposed to proliferative culture condition. Indeed, detectable electrical excitability became progressively less pronounced the longer primary cultures remained under proliferative culture condition. In addition, cultures that had originally exhibited measurable electrical excitability following sample dissociation, lost this property after further expansion under the proliferative culture conditions used here (see ***Chapter 5***).

A role played by neurotransmitter-mediated communication at this early stage in development (7 – 8 week gestation) is also supported by expression data obtained from these non-expanded primary cultures, as compared to that detected in the seven clonal NPC lines. For instance, proliferating NPCs were characterised by restricted expression with respect to many of the genes tested. Following differentiation, all the investigated NPC lines demonstrated an increase in the range of genes they expressed, while the level of expression increased, in general, for those genes that were already active

(see Table 3.9 and Table 3.10). This change is likely attributable to the emergence of neural phenotypes within these cultures. In short, differentiated NPC cultures were associated with a broader and more intense expression profile than that of their undifferentiated precursors. This trend was reflected in primary cultures when comparing those that had been expanded as proliferative cultures for 28 days – a crude recreation of clonal NPC line cultures, as this would increase the number of NPCs and decrease the number of neurons present – with those that had been differentiated for 28 days (see Figure 5.2, Figure 5.3 and Figure 5.4). Characteristically, restricted and often weak expression of many of the tested genes was found in proliferative cultures, while a broader range and an increase in expression was observed in differentiated cultures – as seen in the NPC lines. However, non-expanded primary cultures exhibited an expression profile indicative of differentiated cultures; with intense expression detected for most of the genes tested. Indeed, the intensity and breadth of genes tested, was for some samples, greater in the initially plated proliferative cultures than was observed in the differentiated cultures. Non-expanded, primary cultures therefore exhibited an expression profile characteristic of differentiated cultures, and was confirmed when assessing their phenotypic characteristics.

Non-expanded, primary cultures contained a high proportion of neurons – a conclusion drawn from the number of $MAP2^{+}$ cells present (Figure 5.1), the detected presence of electrical excitability (Figure 5.10) and a characteristically broad expression profile (Figure 5.2, Figure 5.3 and Figure 5.4) – and was supported further though the nature of observed changes in ligand-induced intracellular $Ca^{2+}$ accumulation (Figure 5.5). This is perhaps best illustrated through responses observed following exposure to acetylcholine or glutamate. Proliferative CTX0E16/02 cultures demonstrated characteristically robust, concentration-dependent responses to acetylcholine, which were consistently attenuated following differentiation. Conversely, glutamate-induced changes in $[Ca^{2+}]_i$ were absent in proliferative cultures though emerged following differentiation (see Figure 4.8 and Figure 4.9). This finding is consistent with a previous report from Hook and colleagues, who – using non-immortalised clonal NPCs lines derived from the developing cortex and hindbrain of 9 – 10 week gestation foetuses – showed that differentiated cells were associated with small cholinergic responses, robust glutamate responses and electrical excitability. This situation was found to be reversed in less differentiated cultures [61]. When compared to observations made in primary cultures here, ligand-induced $Ca^{2+}$ responses in non-expanded primary cultures were characteristic of those expected of differentiated cultures – small cholinergic response and larger glutamatergic response. However, after these cells had been expanded in the presence of mitogens for 28 days, these cells exhibited responses to acetylcholine and glutamate that were strikingly similar to those observed in proliferative CTX0E16/02 cultures. A finding that is likely attributable to a reduction in the number of neurons present and an enrichment in the number of NPCs. Responses from differentiated primary cultures also followed the same trend portrayed by differentiated CTX0E16/02 cells and described previously by Hook and colleagues [61]. Due to differences in the way different primary cultures were treated prior to differentiation, these similarities were more difficult to resolve than they were for proliferative cultures. The reason for this was that, of the four primary cultures tested, while each had remained in culture for the same period of time prior to differentiation, two had been exposed to three passages while the second pair was

exposed to five passages (a measure of the time each culture took to reach confluence, possibly due the differing percentage of progenitor cells present). Interestingly, those exposed to the higher number of passages exhibited responses to acetylcholine and glutamate that were strikingly similar to differentiated CTX0E16/02 cultures, while those exposed to fewer passages exhibited more variable responses. This suggests that with increasing numbers of passages, the primary cultures come to functionally resemble that of the CTX0E16/02 cultures, and is likely attributable to the loss of neurons, that were originally present within these cultures.

Taken together, these data suggest that 7 – 8 week gestation primary foetal tissue already contains functional neurons. In addition, the NPC that coexist with these neurons at this point in development express receptors capable of transducing signals potentially released by these neurons – a property shared with the NPC lines described here. Data described here therefore implicates a likely role for neurotransmitter-mediated signalling, even at these very early stages of neural development, and as such warrants further investigation to elucidate the possible role that this may have in the establishment of neural networks.

The proliferative conditions under which cultures derived from dissociated primary neural embryonic tissues samples were maintained, clearly impacted upon their characteristics with respect to the genes they expressed and their functional properties. These effects were apparent as a product both of the time spent under these culture conditions and as a consequence of passaging the cells. Consistent with the detected presence of a high proportion of $MAP2^+$ cells in non-expanded, proliferative primary cultures, some of these were found upon inspection to exhibit electrical excitability. Interestingly, this property was robustly detected in cultures that took just 6 days to reach confluences – the first time point at which RNA was collected, cells were fixed for staining and functional experiments were performed – though was severely attenuated in a culture that took 9 days and absent in two cultures that took 12 and 16 days respectively to reach confluence. The obvious reason for this was that there were fewer neurons in cultures that did not exhibit electrical excitability, though this did not appear to be the case, as fixed cultures from the five different samples were found to contain comparable numbers of $MAP2^+$ neurons at this stage. This was also reflected in the gene expression profiles and glutamate and acetylcholine-induced $Ca^{2+}$ responses exhibited by these non-expanded proliferative cultures. This therefore suggests that similar numbers of neurons were present in each of the five primary cultures when they were initially established, yet the total number of cells used to seed these cultures was the same. This suggests that the cultures that took longer to reach confluence initially contained a lower proportion of NPC as compared to neurons, as these are the cells expected to be responsible for the proliferative capacity of the cultures. Taken together, these data suggest that the time that these non-expanded cultures spent under proliferative culture conditions, incrementally reduced their capacity to respond to a 50 mM $K^+$ challenge. The mechanism through which this occurred remains unclear though may be due to the internalisation of $Ca_V$ channels or a lack of their *de novo* synthesis.

As mentioned, this time in proliferative culture prior to the first passage did not however appear to reduce levels of expression of the tested genes, see Figure 5.2, Figure 5.3 and Figure 5.4 (time taken to reach confluence was 6, 6, 9, 12 and 16 days respectively for samples 1, 2, 3, 4 and 5). The process of passaging the cells did affect levels of gene expression though – with cultures that had spent 28 days in adherent cultures demonstrating more restricted and weaker expression profiles – characteristic of the clonal NPC lines tested (see Table 3.9 and Table 3.10). This finding is likely attributable to the enrichment of NPCs within these cultures as they proliferate and subsequently outnumber the neurons present, due either to their post-mitotic nature or poor tolerance of passaging. Unfortunately, immunocytochemical staining was not performed at this stage of experimentation, but it is likely that far fewer neurons were present in these expanded proliferative cultures as compared to their non-expanded counterparts. None of the cultures tested at this stage were however capable of elevating $[Ca^{2+}]_i$ to a detectable level in response to 50 mM KCl (see Figure 5.11). Differentiation of primary cultures on the other hand, which resulted in considerable numbers of $MAP2^+$ neurons and a matching gene expression profile, also brought with it robust electrical excitability for all tested samples. Interestingly however, the magnitude of KCl-induced $Ca^{2+}$ responses in differentiated primary cultures was also affected by the number of passages that these cultures underwent prior to differentiation, with cultures exposed to fewer passages (which were also the cultures that took longer to reach confluence initially and did not show excitability at this stage) showing larger KCl-induced responses. Therefore, electrical excitability appeared to be progressively lost with increasing time under proliferative culture conditions prior to expansion, and the capacity to become electrical excitable upon differentiation was progressively reduced with increased numbers of passages. This incremental loss of the ability to become electrically excitable may therefore account for the relative resistance of the CTX0E16/02 line to exhibit this property, as these cells have been exposed to numerous passages and indeed freeze/thaw cycles, which may also affect this property.

The emergence of robust electrical excitability in primary cultures after a 28 day differentiation is in contrast to that observed for CTX0E16/02 cultures, which took 8 weeks before developing this property under similar culture conditions, and was considerably less pronounced than that exhibited by primary cultures after just 4 weeks. A possible reason for the rapid development of electrical excitability in differentiated primary cultures, as compared to the CTX0E16/02 line may have been due to the presence of cells within primary cultures that retained a post mitotic neuronal phenotype during their time in proliferative culture, though lost the capacity to increase $[Ca^{2+}]_i$ in response to KCl. Thus, once exposed to culture conditions that promoted differentiation, these cells were capable of quickly recovering this property. This would be consistent with the fact that primary cultures exposed to fewer passages demonstrated more robust responses to KCl, as they would be expected to contain a higher proportion of these cells. This seems unlikely however, as neurons are known not to tolerate continuous passaging and reseeding [518].

This therefore suggests instead that NPCs within these primary cultures are capable of developing a mature neuronal phenotype more rapidly than CTX0E16/02 cells. The possible reasons that may account

for this are numerous, such as the fact that the CTX0E16/02 cells have been maintained in cultures for a greater period of time, they have been exposed to several freeze/thaw cycles in order to lay down master and working cell banks and have been conditionally immortalised. With respect to the influence of immortalisation, data presented elsewhere would suggest that this procedure does not negatively impact upon the development of electrical excitability. Using non-immortalised cortex and hindbrain derived clonal NPC lines, Hook and colleagues demonstrated that only weak $Ca^{2+}$ responses to 50 mM $K^{+}$ were detected after 8 weeks of differentiation. This group used the same differentiation conditions as described here for primary and CTX0E16/02 cultures (SNBM – which is essentially neurobasal medium supplemented with N2 and B27), though was additionally supplemented with 20 $ngml^{-1}$ BDNF, which has been shown here to promote electrical excitability (though half of this concentration was used in experiments described above). Hook and colleagues found that appreciable levels of electrical excitability were only observed in these cultures after the fourth month [61]. The apparent resistance of the CTX0E16/02 cell line to developing electrical excitability as compared to primary cultures is therefore consistent with previously published work using human clonal NPC lines.

Another factor that may contribute to the rate at which NPCs functionally mature is the region from which they originate. For example, Donato and colleagues found that while NPC lines derived from the developing human cortex (at 14 weeks gestation) remained resistant to the development of electrical excitability, NPCs derived from the ventral mesencephalon (at 10 weeks gestation) were able to develop this property after a two week differentiation period [104]. It should be noted that these experiments were performed using electrophysiological recordings and reported electrical excitability with respect to changes in total intracellular current rather than the ability to flux $Ca^{2+}$ as measured across whole cultures using a FS3 plate reader, as described here. The method described by Donato and colleagues was therefore, considerably more sensitive. Their data suggest that NPCs derived from a phylogenetically more recent region of the brain may require more time to reach functional maturity. Both of the NPC lines described by Donato were conditionally immortalised, in fact, the ventral mesencephalon derived line they used is the VM line described in ***Chapter 3***, above. However, while the cortex derived line was immortalised in exactly the same way as the CTX0E16/02 line, the VM line was not clonally selected, and instead derived as a product of all cells that survived antibiotic selection following immortalisation. Interestingly, the authors of this study suggested that this might ensure that different NPCs with varying neurogenic capacities (or at least the rate at which this develops) may constitute the VM cell line, as would be the case in primary cultures. Data presented here cannot conclusively eliminate any of the possible reasons discussed above to explain the rapid development of electrical excitability in primary culture – or indeed in the VM line as described by Donato and colleagues. This subject definitely warrants further investigation however, as an understanding of the mechanisms that control this property may allow electrically excitable cultures to be generated in a shorter period of time, reducing costs and increasing throughput for any intended downstream experimentation.

Data collected from primary cultures presented here served their initial purpose, in that they reflected the functional properties exhibited by proliferative and differentiated CTX0E16/02 cultures, and therefore demonstrated that they were representative of their *in vivo* counterparts. Indeed, work described previously by Hook and colleagues using a non-immortalised, cortically-derived, clonal NPC line [61], also supported data presented here, with respect to the fact that ectopic expression of the *c*-MycER$^{TAM}$ transgene to maintain the self renewal capacity of these cells does not alter their functional properties, as discussed above. However, the generation of cultures from primary, embryonic neural tissue, also raised several interesting questions, though appears to have partially addressed why the expression of several neurotransmitter receptors is detected in proliferative NPCs. All of the seven, conditionally immortalised NPC lines described above were derived from either 10 or 12 week gestation human foetal tissue samples. Considering the high proportion of neurons that were already present in cultures derived from 7 – 8 week gestation neural foetal tissue, we can quite confidently assume that this was also the case in the primary samples from which the seven NPC lines were originally derived. This would be consistent with a previous report from Bystron and colleagues showing evidence of neurons in the developing human cortex as early as 31 days gestation [423]. Indeed the first synapses are found in the developing cortex at just 9 – 10 weeks gestation [420]. The fact that neurons, capable of forming synapse are already present at this early stage in neural development, and that NPCs present at this stage express receptors – at the message level at least – making them responsive to signals generated by these neurons, implicates a possible role for GPCR-mediated neurotransmission in early neural development. What this role is however remains unclear, with little or no literature currently available relating to this area, and certainly warrants further investigation.

What is clear from data presented here is that CTX0E16/02 cultures are highly plastic with respect to their pharmacological characteristics following differentiation as a result of the culture environment they are exposed to throughout this process. This was first exemplified through the initial optimisation of differentiation conditions for the CTX0E16/02 cell line. These preliminary experiments showed that the culture environment during differentiation bore a considerable impact upon the size and shape of cells produced, the level of survival observed, the relative proportion of different cell types generated and even whether the cultures grew as an adherent monolayer or as clumped groups of cells. Once CTX0E16/02 cultures had been shown to demonstrate robust differentiation in the presence of SNBM, further experimentation to promote electrical excitability and increase functional receptor expression at the plasma membrane showed that the functional characteristics of these cells were also susceptible to manipulation. While extending the period of time that cultures were differentiated for, or exposing them to BDNF were the only conditions that were found to promote electrical excitability, nearly all of the different methods that were explored in an attempt to precipitate this property were found to alter ligand-induced changes in $[Ca^{2+}]_i$ in some way. When we consider that these cells – in their natural *in vivo* environment – must assume their functional role within a complex network as they differentiate, it is perhaps unsurprising that they demonstrate such plasticity with respect to the way in which they respond to external signals. Indeed, a high level of plasticity is likely to be crucial to their ability to functionally integrate into neuronal circuits.

The greatest change observed in ligand-induced intracellular $Ca^{2+}$ accumulation, unsurprisingly occurred as a consequence of differentiation itself. However, due to the fact that the level of expression of every tested gene encoding receptors involved in neurotransmission – with the exception of *HRH1* – was either maintained at levels observed in proliferative cultures, or increased upon differentiation, ligand-induced changes in $[Ca^{2+}]_i$ were expected to rise in response to these receptors' cognate ligands. In contrast, with the exception of an emergence of intracellular $Ca^{2+}$ accumulation in response to glutamate, responses to various ligands observed in proliferative cultures were consistently attenuated upon differentiation. While the expression of every cognate receptor for each of the neurotransmitter ligands investigated was not tested, the overall trend of increased expression led to the hypothesis that the reduction in detected levels of ligand-induced intracellular $Ca^{2+}$ accumulation were attributable to increased cellular heterogeneity within the differentiated cultures. This was of course an anticipated consequence of differentiation, as a relatively homogenous pool of clonal NPCs becomes a heterogeneous pool of neuronal subtypes – as indicated by immunocytochemical staining – and glia. Accordingly, the detected increase in the level of expression of genes encoding receptors was expected to be accounted for by fewer cells within the differentiated cultures capable of responding to these ligands, though the cells that did respond were expected to exhibit high levels of expression, and therefore, considerable more intense responses. This was hypothesised to be detected as a decrease in responsiveness when measured using a plate reader – such as the FS3, used here – that averaged detected levels of fluorescence across a whole cellular field. By measuring intracellular $Ca^{2+}$ accumulation within individual cells, this hypothesis was found to be partly true; that greater heterogeneity was observed with respect to the proportion of cells responding to tested ligands. However, it was found that responding cells did not generate larger responses. On inspection, it was found that proliferative and differentiated cultures contained similar numbers of cells within a given field, though cells within differentiated cultures exhibited comparably smaller cell soma than their NPC precursors, helping to account for a portion of the observed reduction in average fluorescence across the whole culture.

The compromise of detail over throughput paid dividends with respect to the measurement of $Ca^{2+}$ accumulation in individual cells. This strategy provided the means to account for the observed reductions in ligand-induced changes in $[Ca^{2+}]_i$ in differentiated as compared to proliferative cultures, though failed to resolve the paradox posed through concomitant increases in receptor expression. It also demonstrated that not only did differentiation change the magnitude of responses to the same ligand, but in some cases, also changed the nature of these responses. These data highlighted profound changes in the duration of acetylcholine-induced responses between proliferative and differentiated cultures and the heterogeneity in the duration of responses to glutamate within differentiated cultures. Furthermore, the measurement of $Ca^{2+}$ accumulation at the level of single cells was also able to show an apparent induction of spontaneous $Ca^{2+}$ oscillations in cultures exposed to dopamine and that changes in $[Ca^{2+}]_i$ in response to glutamate may be too rapid to accurately resolve using the FS3. Perhaps the most significant contribution this platform made to this study though, was to highlight the need for

more sensitive instrumentation when investigating ligand-induced responses in a native tissue model – as represented by differentiated CTX0E16/02 cultures.

The ability to ectopically express 'druggable' human proteins in robust expression systems such as CHO, HEK or COS-7 cells and demonstrate a desired drug-induced modulation of their activity through the use of transgenic reporter systems revolutionised drug discovery in the 1990's [14,240]. A change that was greatly facilitated by concurrent developments in combinatorial chemistry, miniaturisation, liquid-handling robotics and sensitive, fluorescence-based detection systems [238,240]. These heterologous expression systems ensure robust detection of a desired functional outcome, as defined by the design of the assay itself, and provide effective negative controls through the use of untransfected cells. However, this strategy has come under increasing scrutiny as a means to determine the efficacy of a given molecule [14,452], which has been partly driven by an explosion in our understanding of the most common of drug targets; GPCRs [206,519,520]. Rather than being the simple on/off switches they were once considered as, these molecules represent complex machines capable of a multitude of responses and interactions [521]. Indeed, these interactions with other receptors, signalling molecules and regulatory proteins – which can be cell type specific – reinforce the need to employ native tissues to investigate GPCR pharmacology [14,189,195,336,404].

As discussed previously, due to the seemingly paradoxical attenuation in ligand-induced changes in $[Ca^{2+}]_i$ in the face of increased receptor expression at the message level, it was hypothesised that this may be attributable to a lack of plasma membrane expression, either through a lack of translation or accumulation within the secretory pathway. Experiments were therefore performed to try and improve functional receptor expression at the cell surface, or at least, increase ligand-induced intracellular $Ca^{2+}$ accumulation. These experiments, along with some of those used to provoke electrical excitability in CTX0E16/02 cultures, were found to influence ligand-induced responses. These were often observed as an increase in the maximal response achieved at the highest tested concentration, though were often accompanied by a rightward shift in potency. It is conceivable that for a native tissue cell cultures model – as represented by differentiated CTX0E16/02 cultures – protocols could be developed so as to artificially enrich a specific receptor of interest so as to facilitate its study using currently available, industry standard, high-throughput screening instrumentation, such as FLIPR [242]. However, the point of adopting native *in vitro* tissue culture systems in the first place, is to recreate the 'normal' behaviour of these cells *in vivo*. In attempting to force these cultures to behave in a way that essentially mimics the properties of recombinant systems, so as to facilitate the use of existing technology is perhaps a case of forcing a square peg into a round hole, and defeats the object of the use of these cells in the first place.

The observed increase in receptor expression accompanied by attenuated ligand-induced intracellular $Ca^{2+}$ accumulation in CTX0E16/02 cultures following differentiation may of course be a normal consequence of this process. The most striking difference between proliferative and differentiated CTX0E16/02 cultures is both the size and shape of the cells that comprise them. Proliferative CTX0E16/02 cells have large cell soma and few processes, while differentiated CTX0E16/02 cells exhibit a considerably smaller cell soma, with long, elaborate processes. The formation of these processes,

essentially subdivides the intracellular environment of these cells into compartments, through which the diffusion of signalling molecules such as $Ca^{2+}$ or cAMP would be expected to be restricted as compared to a large, more spherical cell body [522]. In addition, the growth of long neuronal processes would also considerably increase the surface area to volume ratio of these cells, as compared to their NPC precursors. Therefore, a situation could be envisaged whereby neurons are found to express considerably more receptors at their cell surface, yet due to the distal localisation of these receptors within the membrane of processes, these would contribute little to the level of intracellular $Ca^{2+}$ accumulation observed in the cell body, and are therefore difficult to detect using instruments such as fluorescent plate readers. Interestingly, due to the restricted space within a neurite – if we assume that the activation of a given receptor provokes the same level of $Ca^{2+}$ accumulation – this $Ca^{2+}$ would be subject to limited diffusion, and therefore lead to a greater local $Ca^{2+}$ concentration and consequently, a more pronounced $Ca^{2+}$-dependent response [354].

The accumulation of intracellular $Ca^{2+}$ is obviously not the only means through which cells respond to GPCR ligands, and was the rationale behind the experimental measurement of receptor-mediated ERK1/2 phosphorylation, as described in ***Chapter 6***. Another factor that may contribute to the observed reduction in ligand-induced changes in $[Ca^{2+}]_i$ is that cells diversify their signalling repertoire following differentiation. For example, upon differentiation, CTX0E16/02 cultures have been shown to express a broad range of different receptors, as have all the NPC lines described above, which in their natural *in vivo* environment, they may require so as to be capable of responding to a range of neurotransmitter signals from different cells. It might be expected therefore that differentiated neuronal cells may diversify their signalling repertoire, so as to maintain sufficient complexity to allow different extracellular signals to be transduced within cells in different ways. To an extent, this has already been described in the form of receptor dimerisation, functional selectivity, promiscuous receptor coupling and simply through receptor crosstalk [191,192,214,218,221,225,405].

Experimentally, the use of native tissue *in vitro* culture systems are not without their drawbacks. The most obvious being the time these cultures take to mature. Data presented above showed that the earliest time point at which electrical excitability could be provoked in CTX0E16/02 cultures was after 6 weeks, when additionally exposed to trophic stimulation from BDNF. The maintenance of cultures over long period of time increases their susceptibility to infection, which was a particular concern because the CTX0E16/02 cell line are not grown in the presence of antibiotics. Thus, the generation and maintenance of differentiating CTX0E16/02 cultures for further downstream experimentation required considerable amounts of time-consuming work, which was largely attributable to the growth of these cultures in 96-well plates. Another problematic consequence of maintaining cultures over long periods of time is that a considerable level of medium evaporation occurs. While this in itself is not a problem, when the cells are maintained in 96-well plates, it means that wells at the edge of each plate are subject to considerably more evaporation than those located in the middle. Consequently, solutes – such as medium components and excreted factors – become more concentrated in the wells at the edge of the plates. Indeed, it is likely that it was this phenomenon that resulted in the previously mentioned “edge-

effect" that was detected in functional experiments. After a retrospective analysis of all functional data collected, it was also found that this "edge-effect" was most pronounced in cultures maintained for the longest duration, or those exposed to a pharmacological challenge such as exposure to 740 Y-P or DB-cAMP and IBMX. In order to address this issue, while also reducing the time needed to perform medium changes and the risk of infection, it would be very useful if 96-well plates were available that allowed medium to be added at a single point on the plate – perhaps into some kind of reservoir. Once added, the medium should then be able to diffuse between the wells, to ensure each well contains the same volume of medium. However, this system would also have to be capable of isolating each of the wells from each other for downstream applications. This system could perhaps be achieved by simply manufacturing the base, and the vertical walls of the wells as separate pieces. The vertical walls would then be loaded a sufficient height above the base plate to allow free movement of medium between the wells. Ideally, the vertical walls of the wells would also be loaded on springs, so as to enable reversible isolation of the individual wells. This would help to ensure that even numbers of cells are seeded into each well at the outset, though once established, the vertical walls could be lifted, and allow movement of medium between the wells.

The Importance of using native tissues to investigate the signalling consequences of ligand-receptor interactions has been highlighted here in several instances. For example, differentiated CTX0E16/02 cultures were found to demonstrate considerable basal levels of ERK1/2 phosphorylation as compared to their progenitor cells, a property that would provide components of the ERK1/2 signalling cascade a vectorial quality, in that levels of ERK1/2 phosphorylation can be modulated in either direction. In short, the activation of an ERK1/2-specific phosphatase would have little or no influence upon downstream signalling in proliferative CTX0E16/02 cultures under basal condition, though induction of the same phosphatase activity in differentiated cultures would exert a considerable response – as was observed for haloperidol (see Figure 6.14). Another example was illustrated by the activity of TCB-2; a reported 5-$HT_{2A}$-specific full agonist, yet behaved as an inverse agonist in differentiated CTX0E16/02 cultures. Another interesting finding related to the mechanism of intracellular $Ca^{2+}$ accumulation in response to acetylcholine. Date presented here showed that this occurred as a result of muscarinic rather than nicotinic receptor activation, yet rather than being released from intracellular stores, as expected of $G\alpha_q$-coupled receptors, the increase in $[Ca^{2+}]_i$ was found to originate from the extracellular space. In addition, a comparison of detected responses obtained from the same ligand in differentiated CTX0E16/02 cultures using just the three different strategies described here have illustrated the need to approach the concept of ligand efficacy from multiple directions. For example, 1 mM dopamine was found to exert no effect upon intracellular $Ca^{2+}$ accumulation when measured using a plate reader (Figure 4.8), though was shown to provoke asynchronous $Ca^{2+}$ transients when detected at the level of individual cells (Figure 4.12), while demonstrating nanomolar efficacy in its ability to provoke ERK1/2 phosphorylation (Figure 6.7). As another example, while robust changes in $[Ca^{2+}]_i$ were observed in response to acetylcholine, it exerted little effect upon ERK1/2 phosphorylation, while the opposite was true of phenylephrine (see Figure 4.9 and Figure 6.8).

Taken together, these data suggest that if we are to employ native tissue, cell culture models in an attempt to understand the signalling consequences of ligand-receptor interactions, a more holistic approach in how this is detected must be employed [202]. If we are to make optimum use of these culture systems, we must embrace their inherent complexity, and be prepared to evaluate efficacy with respect to a broad range of functional endpoints. The measurement of intracellular $Ca^{2+}$ accumulation remains a cheap, fast and high-throughput means to measure receptor activation. However, kits such as that used in experiments described here to measure ERK1/2 phosphorylation are also relatively high-throughput and are now becoming available to detect the activity of a whole host of different intracellular signalling molecule, such as cAMP, PKA, CREB and histone H3 to name just a few. These remain however particularly expensive, and are still limited to answering only the question that is asked of the assay. These may come into their own in the future however if they can be multiplexed into a single assay, to answer a series of questions from a single experiment – the possibility of which has been recently demonstrated [242]. Instrumentation manufacturers are also stepping up to the mark with respect to providing the sensitivity needed to functionally interrogate native tissues *in vitro*. Confocal laser-based high-content imaging platforms that can be algorithmically programmed now provide the capacity to detect and quantify everything from neurite outgrowth and synapse formation to receptor dimerisation and protein-protein interactions [243,244]. Another approach that represents an exciting means through which native cells can be pharmacologically characterised *in vitro*, are those that do not rely on a fluorescence output at all – so-called label-free experimental platforms as discussed in ***1.10***.

Perhaps the most promising technologies for the investigation of the complexity surrounding cellular responses to drug exposure are those that provide hypothesis-free investigation – proteomics, epigenomics and transcriptomics – as discussed in ***1.8*** and ***1.10***. As we have learned, the activation of a single receptor subtype can provoke a range of different signalling consequences, which themselves can vary depending upon the nature of the interaction of a ligand with that receptor [14]. For example, either through agonism, antagonism, partial agonism, inverse agonism, positive or negative allosteric modulation or functional selectivity [195,196,202,205,206,218,221]. The initial aim of this study was to identify and characterise an *in vitro* platform that could be used to investigate the mechanism of action of antipsychotics – a class of compounds that are known to interact with a whole host of different GPCR subtypes, as discussed previously. Transcriptomics was selected as a means to perform this mechanistic evaluation, as it is able to detect changes that occur as a consequence of the sum of all of the receptor interactions that these compounds exhibit. The use of transcriptomics as a tool to investigate the mechanism of action of antipsychotics is not however a novel approach, though it is felt that previous studies in this area have failed to appreciate the pharmacology of these compounds. Data presented here showed that haloperidol – a first generation antipsychotic – was only capable of effecting levels of ERK1/2 phosphorylation in the micromolar range when added on its own (see Figure 6.14), yet is known to exert its effects *in vivo* at the low nanomolar range, as discussed in ***6.2.9***. However, in the presence of simulated dopaminergic tone, an effect of haloperidol could be detected at therapeutically relevant nanomolar concentrations (see Figure 6.14). Therefore, it is proposed that to obtain biologically meaningful data with respect to the mechanism of action of antipsychotic drugs, physiological tone

should be simultaneously simulated for each of the neurotransmitter systems that these compounds are known to modulate, as described in Figure 1.1, above. This concept was recently highlighted in a study by Brennand and colleagues; who demonstrated the creation of iPS cells from schizophrenic patients and subsequently used these to generate disorder-specific neuronal cultures [75]. By comparing these cells to equivilant cultures from healthy volunteers, they were able to demonstrate both phenotypic and gene expression differences between the cells that comprised these cultures. However, the authors went on to claim that the observed disease-related phenotype could be rescued through exposure of these cultures to 10 µM loxapine (though not 5 µM clozapine, 1 µM olanzapine, 10 µM risperidone, 5 µM thioridazine) during the final stages of differentiation[75]. In light of data presented here showing that physiological tone plays an important role in how antipsychotics exert their effects, the observations in this study should perhaps be treated with some caution, especially when it is considered that the concentration of loxapine that was shown to exert this effect was perhaps 500 times higher than would be expected to achieve clinical efficacy *in vivo* (personal communication from Hugo Geerts).

Differentiated CTX0E16/02 cultures have been shown to represent an ideal cellular platform for the investigation of psychiatric drug function, however, only through providing a physiologically relevant representation of the nature of these compounds' drug-receptor interactions can we hope to understand the molecular mechanism through which they exert their therapeutic effects.

### 7.1.1 Summary of Discovery for CTX0E16/02 Cells

CTX0E16/02 NPCs (nestin$^+$ & KI-67$^+$) differentiate into doublecortin$^+$ neuroblasts/young neurons, tau$^+$ and MAP2$^+$ neurons, S100β$^+$ astrocytes and show some evidence of the expression of the oligodendrocyte marker O4. Both vGluT1$^+$ and vGluT2$^+$ glutamatergic neurons and GABAergic neurons (some of which are calretinin$^+$ or calbindin$^+$) have been detected along with the expression of the synaptic marker VAMP2.

**RNA Expression:**

| | | Proliferative | Differentiated |
|---|---|---|---|
| DRD2 | Dopamine $D_2$ receptor (GPCR) | ✓ | ✓ |
| DRD3 | Dopamine $D_3$ receptor (GPCR) | ✓ | ✓ |
| HTR2A | 5-$HT_{2A}$ receptor (GPCR) | ✗ | ✓ |
| CHRM1 | Cholinergic muscarinic $M_1$ receptor (GPCR) | ✓ | ✓ |
| HRH1 | Histamine $H_1$ receptor (GPCR) | ✓ | ✓ |
| ADRA1A | Adrenergic $\alpha_{1A}$ receptor (GPCR) | ✓ | ✓ |
| TACR3 | Tachykinin $NK_3$ receptor (GPCR) | ✓ | ✓ |
| AVRP1A | Arginine vasopressin $V_{1A}$ receptor (GPCR) | ✗ | ✓ |
| *GRM1-8* | Metabotropic glutamate $mGluR_{1-8}$ receptors (GPCRs) | ✓ | ✓ |
| GRIA2 | Glutamate receptor 2 (AMPA receptor subunit, ionotropic) | ✓ | ✓ |
| GRIN1 | Glutamate receptor, N-methyl D-aspartate (NMDA) 1 (NR1, ionotropic) | ✓ | ✓ |
| GABRA1 | GABA receptor subunit $\alpha_1$ (ionotropic) | ✗ | ✓ |
| SLC6A4 | 5-HT transporter (SERT) | ✓ | ✓ |
| ARRB2 | β-Arrestin 2 (scaffold and signalling protein) | ✓ | ✓ |
| CAV1 | Caveolin-1 (scaffold protein) | ✓ | ✓ |
| DLG4 | Postsynaptic density protein 95 (PSD-95, scaffold protein) | ✓ | ✓ |
| MPDZ | Multiple PDZ domain protein (MUPP1, scaffold protein) | ✓ | ✓ |
| GSK3B | Glycogen synthase kinase 3β (GSK-3β, signalling node) | ✓ | ✓ |

**Functional Responsiveness**

| | Proliferative | Differentiated | |
|---|---|---|---|
| | $Ca^{2+}$ | $Ca^{2+}$ | pERK1/2 |
| Dopamine | ✗ | ✗ | ✓ |
| 5-HT | ✗ | ✗ | ✓ |
| Glutamate | ✗ | ✓ | ✓ |
| GABA | ✗ | ✗ | ✓ |
| Phenylephrine | ✓ | ✓ | ✓ |
| Histamine | ✓ | ✓ | ✓ |
| Acetylcholine | ✓ | ✓ | ✓ |
| Carbamoylcholine | ✓ | ✓ | ✓ |

### 7.1.2 Limitations of Methods

Data presented in this thesis was generated using several different experimental techniques, each with it's own limitations. Immunocytochemisry was used to detect the presence of proteins associated with particular cellular phenotypes found in the human brain, such as the use of antibodies raised against tau or MAP2 as markers of neurons, or S100β-specific antibodies used as a marker for astrocytes. Antibodies used in this study have been widely reported in the existing literature to be specific to their intended

targets. In addition, experiments described above made use of appropriate negative controls to ensure that staining observed was due to a specific interaction between the protein under investigation and the antibody employed. A clear limitation of this approach is that it is a very narrow criterion to distinguish the presence of particular cell types. Immunocytochemisry tells us little or nothing regarding the physiological characteristics of the cultures under investigation, and how it compares to the cells of the adult human brain that they are hoped to model.

Gene expression analysis was used as a means to determine the expression of specific genes at the mRNA level. By definition, this method can only be used as an indication of expression at the protein level and has in this case been used as a surrogate marker for the expression of proteins of interest. It should also be noted that while crude quantitation was applied to expression data for the genes of interest for this study, this was only provided as a means of comparison. The PCR method used here cannot be reliably used as a means to quantify expression, especially between different genes. If required, this could be achieved through the use of quantitative PCR, though for the purposes of this study was considered unnecessary.

In the knowledge that differentiated NPC cultures are heterogeneous with respect to the cell types that comprise them, gene expression analysis, as described above, unfortunately cannot tell us which cell types express each of the investigated genes. The same is true for the functional evaluation of these cultrues with respect to intracellular $Ca^{2+}$ signalling and ERK1/2 phosphorylation. While an average level of gene expression, intracellular $Ca^{2+}$ accumulation or ERK1/2 phosphorylation can be measured across a culture, this does not provide information regarding the contribution of individual cells (or classes of cells) to the average signal observed. There are perhaps a couple of approaches that would facilitate cell type-specific gene expression analysis. Both of which would first involve the use of an antibody to identify the cell type of interest. FACS could then be employed to enrich a particular cell type from a heterogeneous culture before performing gene expression analysis, while laser capture microscopy could be used to select individual cells from a culture for analysis. With respect to identifying cell type-specific signalling, this could again be done with the use of FACS; allowing particular cell types to be enriched prior to experimentation.

Despite the limitations described above, these investigations represent a valuable resource for future work using the CTX0E16/02 NPC line. These cells have been shown to be capable of robust differentiation and to closely resemble the physiological properties of the *in vivo* counterparts we hope them to model.

## *References*


1. Llinás, R.R. The contribution of Santiago Ramón y Cajal to functional neuroscience. *Nat Rev Neurosci* **4**, 77-80 (2003).
2. De Carlos, J.A. & Borrell, J. A historical reflection of the contributions of Cajal and Golgi to the foundations of neuroscience. *Brain Res Rev* **55**, 8-16 (2007).
3. Sacks, O.W. *The man who mistook his wife for a hat*, (Picador, London, 1986).
4. Sacks, O.W. *An anthropologist on Mars : seven paradoxical tales*, (Picador, London, 1995).
5. Ramachandran, V.S. & Blakeslee, S. *Phantoms in the brain : human nature and the architecture of the mind*, (Fourth Estate, London, 1998).
6. Linden, D.E. The challenges and promise of neuroimaging in psychiatry. *Neuron* **73**, 8-22 (2012).
7. Langmoen, I.A. & Apuzzo, M.L. The brain on itself: Nobel laureates and the history of fundamental nervous system function. *Neurosurgery* **61**, 891-907; discussion 907-898 (2007).
8. Livet, J.*, et al.* Transgenic strategies for combinatorial expression of fluorescent proteins in the nervous system. *Nature* **450**, 56-62 (2007).
9. Kola, I. & Landis, J. Can the pharmaceutical industry reduce attrition rates? *Nat Rev Drug Discov* **3**, 711-715 (2004).
10. Kola, I. The state of innovation in drug development. *Clin Pharmacol Ther* **83**, 227-230 (2008).
11. Wong, E.H., Tarazi, F.I. & Shahid, M. The effectiveness of multi-target agents in schizophrenia and mood disorders: Relevance of receptor signature to clinical action. *Pharmacol Ther* **126**, 173-185 (2010).
12. Becker, R.E. & Greig, N.H. Lost in translation: neuropsychiatric drug development. *Sci Transl Med* **2**, 61rv66 (2010).
13. Markou, A., Chiamulera, C., Geyer, M.A., Tricklebank, M. & Steckler, T. Removing obstacles in neuroscience drug discovery: the future path for animal models. *Neuropsychopharmacology* **34**, 74-89 (2009).
14. Kenakin, T.P. Cellular assays as portals to seven-transmembrane receptor-based drug discovery. *Nat Rev Drug Discov* **8**, 617-626 (2009).
15. Conn, P.J. & Roth, B.L. Opportunities and challenges of psychiatric drug discovery: roles for scientists in academic, industry, and government settings. *Neuropsychopharmacology* **33**, 2048-2060 (2008).
16. DiMasi, J.A., Hansen, R.W. & Grabowski, H.G. The price of innovation: new estimates of drug development costs. *J Health Econ* **22**, 151-185 (2003).
17. Kramer, M.S., Last, B., Getson, A. & Reines, S.A. The effects of a selective D4 dopamine receptor antagonist (L-745,870) in acutely psychotic inpatients with schizophrenia. D4 Dopamine Antagonist Group. *Arch Gen Psychiatry* **54**, 567-572 (1997).
18. Truffinet, P.*, et al.* Placebo-controlled study of the D4/5-HT2A antagonist fananserin in the treatment of schizophrenia. *Am J Psychiatry* **156**, 419-425 (1999).

19. Kreienkamp, H.J., Sine, S.M., Maeda, R.K. & Taylor, P. Glycosylation sites selectively interfere with alpha-toxin binding to the nicotinic acetylcholine receptor. *J Biol Chem* **269**, 8108-8114 (1994).
20. Insel, T.R. & Young, L.J. The neurobiology of attachment. *Nat Rev Neurosci* **2**, 129-136 (2001).
21. Hammock, E.A. & Young, L.J. Variation in the vasopressin V1a receptor promoter and expression: implications for inter- and intraspecific variation in social behaviour. *Eur J Neurosci* **16**, 399-402 (2002).
22. Huffaker, S.J.*, et al.* A primate-specific, brain isoform of KCNH2 affects cortical physiology, cognition, neuronal repolarization and risk of schizophrenia. *Nat Med* **15**, 509-518 (2009).
23. Kongsamut, S., Kang, J., Chen, X.L., Roehr, J. & Rampe, D. A comparison of the receptor binding and HERG channel affinities for a series of antipsychotic drugs. *Eur J Pharmacol* **450**, 37-41 (2002).
24. Pouton, C.W. & Haynes, J.M. Embryonic stem cells as a source of models for drug discovery. *Nat Rev Drug Discov* **6**, 605-616 (2007).
25. Luyten, W.H. & Leysen, J.E. Receptor cloning and heterologous expression--towards a new tool for drug discovery. *Trends Biotechnol* **11**, 247-254 (1993).
26. Hakak, Y., Shrestha, D., Goegel, M.C., Behan, D.P. & Chalmers, D.T. Global analysis of G-protein-coupled receptor signaling in human tissues. *FEBS Lett* **550**, 11-17 (2003).
27. Vassilatis, D.K.*, et al.* The G protein-coupled receptor repertoires of human and mouse. *Proc Natl Acad Sci U S A* **100**, 4903-4908 (2003).
28. Noon, L.A.*, et al.* Failed export of the adrenocorticotrophin receptor from the endoplasmic reticulum in non-adrenal cells: evidence in support of a requirement for a specific adrenal accessory factor. *J Endocrinol* **174**, 17-25 (2002).
29. Bulenger, S., Marullo, S. & Bouvier, M. Emerging role of homo- and heterodimerization in G-protein-coupled receptor biosynthesis and maturation. *Trends Pharmacol Sci* **26**, 131-137 (2005).
30. Gimelbrant, A.A., Stoss, T.D., Landers, T.M. & McClintock, T.S. Truncation releases olfactory receptors from the endoplasmic reticulum of heterologous cells. *J Neurochem* **72**, 2301-2311 (1999).
31. Lu, M., Echeverri, F. & Moyer, B.D. Endoplasmic reticulum retention, degradation, and aggregation of olfactory G-protein coupled receptors. *Traffic* **4**, 416-433 (2003).
32. McClintock, T.S.*, et al.* Functional expression of olfactory-adrenergic receptor chimeras and intracellular retention of heterologously expressed olfactory receptors. *Brain Res Mol Brain Res* **48**, 270-278 (1997).
33. Bush, C.F. & Hall, R.A. Olfactory receptor trafficking to the plasma membrane. *Cell Mol Life Sci* **65**, 2289-2295 (2008).
34. Dunham, J.H., Meyer, R.C., Garcia, E.L. & Hall, R.A. GPR37 surface expression enhancement via N-terminal truncation or protein-protein interactions. *Biochemistry* **48**, 10286-10297 (2009).
35. Dunham, J.H. & Hall, R.A. Enhancement of the surface expression of G protein-coupled receptors. *Trends Biotechnol* **27**, 541-545 (2009).

36. Kimple, A.J., Bosch, D.E., Giguere, P.M. & Siderovski, D.P. Regulators of G-protein signaling and their Galpha substrates: promises and challenges in their use as drug discovery targets. *Pharmacol Rev* **63**, 728-749 (2011).
37. Guan, X.M., Kobilka, T.S. & Kobilka, B.K. Enhancement of membrane insertion and function in a type IIIb membrane protein following introduction of a cleavable signal peptide. *J Biol Chem* **267**, 21995-21998 (1992).
38. Marshall, F.H., White, J., Main, M., Green, A. & Wise, A. GABA(B) receptors function as heterodimers. *Biochem Soc Trans* **27**, 530-535 (1999).
39. McLatchie, L.M.*, et al.* RAMPs regulate the transport and ligand specificity of the calcitonin-receptor-like receptor. *Nature* **393**, 333-339 (1998).
40. McNeish, J. Embryonic stem cells in drug discovery. *Nat Rev Drug Discov* **3**, 70-80 (2004).
41. Adamson, D.C., Rasheed, B.A., McLendon, R.E. & Bigner, D.D. Central nervous system. *Cancer Biomark* **9**, 193-210 (2011).
42. Preis, P.N.*, et al.* Neuronal cell differentiation of human neuroblastoma cells by retinoic acid plus herbimycin A. *Cancer Res* **48**, 6530-6534 (1988).
43. Andrews, P.W.*, et al.* Pluripotent embryonal carcinoma clones derived from the human teratocarcinoma cell line Tera-2. Differentiation in vivo and in vitro. *Lab Invest* **50**, 147-162 (1984).
44. Sah, D.W., Ray, J. & Gage, F.H. Bipotent progenitor cell lines from the human CNS. *Nat Biotechnol* **15**, 574-580 (1997).
45. Vescovi, A.L.*, et al.* Isolation and cloning of multipotential stem cells from the embryonic human CNS and establishment of transplantable human neural stem cell lines by epigenetic stimulation. *Exp Neurol* **156**, 71-83 (1999).
46. Carpenter, M.K.*, et al.* In vitro expansion of a multipotent population of human neural progenitor cells. *Exp Neurol* **158**, 265-278 (1999).
47. Flax, J.D.*, et al.* Engraftable human neural stem cells respond to developmental cues, replace neurons, and express foreign genes. *Nat Biotechnol* **16**, 1033-1039 (1998).
48. Lunn, J.S., Sakowski, S.A., Hur, J. & Feldman, E.L. Stem cell technology for neurodegenerative diseases. *Ann Neurol* **70**, 353-361 (2011).
49. Shimada, I.S. & Spees, J.L. Stem and progenitor cells for neurological repair: minor issues, major hurdles, and exciting opportunities for paracrine-based therapeutics. *J Cell Biochem* **112**, 374-380 (2011).
50. Laslett, A.L., Filipczyk, A.A. & Pera, M.F. Characterization and culture of human embryonic stem cells. *Trends Cardiovasc Med* **13**, 295-301 (2003).
51. Price, J. & Williams, B.P. Neural stem cells. *Curr Opin Neurobiol* **11**, 564-567 (2001).
52. Götz, M. & Huttner, W.B. The cell biology of neurogenesis. *Nat Rev Mol Cell Biol* **6**, 777-788 (2005).
53. Zhao, C., Deng, W. & Gage, F.H. Mechanisms and functional implications of adult neurogenesis. *Cell* **132**, 645-660 (2008).

54. Schwartz, P.H.*, et al.* Isolation and characterization of neural progenitor cells from post-mortem human cortex. *J Neurosci Res* **74**, 838-851 (2003).

55. Guillemot, F. Cell fate specification in the mammalian telencephalon. *Prog Neurobiol* **83**, 37-52 (2007).

56. Nat, R. & Dechant, G. Milestones of directed differentiation of mouse and human embryonic stem cells into telencephalic neurons based on neural development in vivo. *Stem Cells Dev* **20**, 947-958 (2011).

57. Storch, A.*, et al.* Long-term proliferation and dopaminergic differentiation of human mesencephalic neural precursor cells. *Exp Neurol* **170**, 317-325 (2001).

58. Jordan, P.M.*, et al.* Generation of spinal motor neurons from human fetal brain-derived neural stem cells: role of basic fibroblast growth factor. *J Neurosci Res* **87**, 318-332 (2009).

59. Rossi, S.L. & Keirstead, H.S. Stem cells and spinal cord regeneration. *Curr Opin Biotechnol* **20**, 552-562 (2009).

60. Bithell, A., Finch, S.E., Hornby, M.F. & Williams, B.P. Fibroblast growth factor 2 maintains the neurogenic capacity of embryonic neural progenitor cells in vitro but changes their neuronal subtype specification. in *Stem Cells*, Vol. 26 1565-1574 (2008).

61. Hook, L.*, et al.* Non-immortalized human neural stem (NS) cells as a scalable platform for cellular assays. *Neurochem Int* **59**, 432-444 (2011).

62. Gray, J.A., Hodges, H. & Sinden, J. Prospects for the clinical application of neural transplantation with the use of conditionally immortalized neuroepithelial stem cells. *Philos Trans R Soc Lond B Biol Sci* **354**, 1407-1421 (1999).

63. Pollock, K.*, et al.* A conditionally immortal clonal stem cell line from human cortical neuroepithelium for the treatment of ischemic stroke. *Exp Neurol* **199**, 143-155 (2006).

64. Stevanato, L.*, et al.* c-MycERTAM transgene silencing in a genetically modified human neural stem cell line implanted into MCAo rodent brain. *BMC Neurosci* **10**, 86 (2009).

65. Anacker, C.*, et al.* Antidepressants increase human hippocampal neurogenesis by activating the glucocorticoid receptor. *Mol Psychiatry* (2011).

66. El-Akabawy, G., Medina, L.M., Jeffries, A., Price, J. & Modo, M. Purmorphamine Increases DARPP-32 Differentiation in Human Striatal Neural Stem Cells Through the Hedgehog Pathway. *Stem Cells Dev* (2011).

67. Cocks, G.*, et al.* Conditionally immortalised stem cell lines from human spinal cord retain regional identity and generate V2a interneurons and motorneurons. (In preparation).

68. Hanna, J.H., Saha, K. & Jaenisch, R. Pluripotency and cellular reprogramming: facts, hypotheses, unresolved issues. *Cell* **143**, 508-525 (2010).

69. Rada-Iglesias, A. & Wysocka, J. Epigenomics of human embryonic stem cells and induced pluripotent stem cells: insights into pluripotency and implications for disease. *Genome Med* **3**, 36 (2011).

70. Takahashi, K. & Yamanaka, S. Induction of pluripotent stem cells from mouse embryonic and adult fibroblast cultures by defined factors. *Cell* **126**, 663-676 (2006).

71. Takahashi, K.*, et al.* Induction of pluripotent stem cells from adult human fibroblasts by defined factors. *Cell* **131**, 861-872 (2007).

72. Park, I.H.*, et al.* Reprogramming of human somatic cells to pluripotency with defined factors. *Nature* **451**, 141-146 (2008).

73. Puri, M.C. & Nagy, A. Concise Review: Embryonic Stem Cells Versus Induced Pluripotent Stem Cells: The Game Is On. *Stem Cells* (2011).

74. Baumann, K. Achieving pluripotency. *Nat Rev Mol Cell Biol* **11**, 677 (2010).

75. Brennand, K.J.*, et al.* Modelling schizophrenia using human induced pluripotent stem cells. *Nature* **473**, 221-225 (2011).

76. Wu, S.M. & Hochedlinger, K. Harnessing the potential of induced pluripotent stem cells for regenerative medicine. *Nat Cell Biol* **13**, 497-505 (2011).

77. Yu, J.*, et al.* Human induced pluripotent stem cells free of vector and transgene sequences. *Science* **324**, 797-801 (2009).

78. Kim, D.*, et al.* Generation of human induced pluripotent stem cells by direct delivery of reprogramming proteins. *Cell Stem Cell* **4**, 472-476 (2009).

79. Aasen, T.*, et al.* Efficient and rapid generation of induced pluripotent stem cells from human keratinocytes. *Nat Biotechnol* **26**, 1276-1284 (2008).

80. Loh, Y.H.*, et al.* Generation of induced pluripotent stem cells from human blood. *Blood* **113**, 5476-5479 (2009).

81. Vierbuchen, T.*, et al.* Direct conversion of fibroblasts to functional neurons by defined factors. *Nature* **463**, 1035-1041 (2010).

82. Nicholas, C.R. & Kriegstein, A.R. Regenerative medicine: Cell reprogramming gets direct. *Nature* **463**, 1031-1032 (2010).

83. Pfisterer, U.*, et al.* Direct conversion of human fibroblasts to dopaminergic neurons. *Proc Natl Acad Sci U S A* **108**, 10343-10348 (2011).

84. Sendtner, M. Regenerative medicine: Bespoke cells for the human brain. *Nature* **476**, 158-159 (2011).

85. Yoo, A.S., Staahl, B.T., Chen, L. & Crabtree, G.R. MicroRNA-mediated switching of chromatin-remodelling complexes in neural development. *Nature* **460**, 642-646 (2009).

86. Yoo, A.S.*, et al.* MicroRNA-mediated conversion of human fibroblasts to neurons. *Nature* **476**, 228-231 (2011).

87. Pang, Z.P.*, et al.* Induction of human neuronal cells by defined transcription factors. *Nature* **476**, 220-223 (2011).

88. Caiazzo, M.*, et al.* Direct generation of functional dopaminergic neurons from mouse and human fibroblasts. *Nature* **476**, 224-227 (2011).

89. Son, E.Y.*, et al.* Conversion of mouse and human fibroblasts into functional spinal motor neurons. *Cell Stem Cell* **9**, 205-218 (2011).

90. Lister, R.*, et al.* Hotspots of aberrant epigenomic reprogramming in human induced pluripotent stem cells. *Nature* **471**, 68-73 (2011).

91. Gore, A.*, et al.* Somatic coding mutations in human induced pluripotent stem cells. *Nature* **471**, 63-67 (2011).

92. Ji, J.*, et al.* Elevated Coding Mutation Rate During the Reprogramming of Human Somatic Cells into Induced Pluripotent Stem Cells. *Stem Cells* (2011).

93. Baker, M. Neurons from reprogrammed cells. *Nat Methods* **8**, 905-909 (2011).

94. Ghosh, Z.*, et al.* Persistent donor cell gene expression among human induced pluripotent stem cells contributes to differences with human embryonic stem cells. *PLoS ONE* **5**, e8975 (2010).

95. Ohi, Y.*, et al.* Incomplete DNA methylation underlies a transcriptional memory of somatic cells in human iPS cells. *Nat Cell Biol* **13**, 541-549 (2011).

96. Pick, M.*, et al.* Clone- and gene-specific aberrations of parental imprinting in human induced pluripotent stem cells. *Stem Cells* **27**, 2686-2690 (2009).

97. Lee, J.H.*, et al.* A robust approach to identifying tissue-specific gene expression regulatory variants using personalized human induced pluripotent stem cells. *PLoS Genet* **5**, e1000718 (2009).

98. Munoz, J.*, et al.* The quantitative proteomes of human-induced pluripotent stem cells and embryonic stem cells. *Mol Syst Biol* **7**, 550 (2011).

99. Chiang, C.H.*, et al.* Integration-free induced pluripotent stem cells derived from schizophrenia patients with a DISC1 mutation. *Mol Psychiatry* **16**, 358-360 (2011).

100. Christopherson, K.S.*, et al.* Thrombospondins are astrocyte-secreted proteins that promote CNS synaptogenesis. *Cell* **120**, 421-433 (2005).

101. Papadeas, S.T., Kraig, S.E., O'Banion, C., Lepore, A.C. & Maragakis, N.J. Astrocytes carrying the superoxide dismutase 1 (SOD1G93A) mutation induce wild-type motor neuron degeneration in vivo. *Proc Natl Acad Sci U S A* **108**, 17803-17808 (2011).

102. Lujan, E., Chanda, S., Ahlenius, H., Südhof, T.C. & Wernig, M. Direct conversion of mouse fibroblasts to self-renewing, tripotent neural precursor cells. *Proceedings of the National Academy of Sciences* (2012).

103. Littlewood, T.D., Hancock, D.C., Danielian, P.S., Parker, M.G. & Evan, G.I. A modified oestrogen receptor ligand-binding domain as an improved switch for the regulation of heterologous proteins. *Nucleic Acids Res* **23**, 1686-1690 (1995).

104. Donato, R.*, et al.* Differential development of neuronal physiological responsiveness in two human neural stem cell lines. *BMC Neurosci* **8**, 36 (2007).

105. Stroemer, P., Hope, A., Patel, S., Pollock, K. & Sinden, J. Development of a human neural stem cell line for use in recovery from disability after stroke. *Front Biosci* **13**, 2290-2292 (2008).

106. Johansson, S., Price, J. & Modo, M. Effect of inflammatory cytokines on major histocompatibility complex expression and differentiation of human neural stem/progenitor cells. *Stem Cells* **26**, 2444-2454 (2008).

107. Miljan, E.A.*, et al.* Implantation of c-mycER TAM immortalized human mesencephalic-derived clonal cell lines ameliorates behavior dysfunction in a rat model of Parkinson's disease. *Stem Cells Dev* **18**, 307-319 (2009).

108. Stroemer, P.*, et al.* The neural stem cell line CTX0E03 promotes behavioral recovery and endogenous neurogenesis after experimental stroke in a dose-dependent fashion. *Neurorehabil Neural Repair* **23**, 895-909 (2009).

109. Smith, E.J.*, et al.* Implantation Site and Lesion Topology Determine Efficacy of a Human Neural Stem Cell Line in a Rat Model of Chronic Stroke. *Stem Cells* (2011).

110. Zunszain, P.A.*, et al.* Interleukin-1beta: A New Regulator of the Kynurenine Pathway Affecting Human Hippocampal Neurogenesis. *Neuropsychopharmacology* (2011).

111. Mack, G.S. ReNeuron and StemCells get green light for neural stem cell trials. *Nat Biotechnol* **29**, 95-97 (2011).

112. Egan, M.F. & Weinberger, D.R. Neurobiology of schizophrenia. *Curr Opin Neurobiol* **7**, 701-707 (1997).

113. Lewis, D.A. & Lieberman, J.A. Catching up on schizophrenia: natural history and neurobiology. *Neuron* **28**, 325-334 (2000).

114. Freedman, R. Schizophrenia. *N Engl J Med* **349**, 1738-1749 (2003).

115. Ross, C.A., Margolis, R.L., Reading, S.A., Pletnikov, M. & Coyle, J.T. Neurobiology of schizophrenia. *Neuron* **52**, 139-153 (2006).

116. World Health Organization. *The ICD-10 classification of mental and behavioural disorders : clinical descriptions and diagnostic guidelines*, (World Health Organization, Geneva, 1992).

117. American Psychiatric Association. *Diagnostic and statistical manual of mental disorders : International version with ICD-10 codes*, (American Psychiatric Association, Washington, D.C., 1995).

118. Siris, S.G. Suicide and schizophrenia. *J Psychopharmacol* **15**, 127-135 (2001).

119. World Health Organization & Srinivasa Murthy, R. *The World health report 2001 : mental health, new understanding, new hope*, (World Health Organization, Geneva, 2001).

120. Rowley, M., Bristow, L.J. & Hutson, P.H. Current and novel approaches to the drug treatment of schizophrenia. *J Med Chem* **44**, 477-501 (2001).

121. Bromet, E.J. & Fennig, S. Epidemiology and natural history of schizophrenia. *Biol Psychiatry* **46**, 871-881 (1999).

122. Lewis, D.A. & Levitt, P. Schizophrenia as a disorder of neurodevelopment. *Annu Rev Neurosci* **25**, 409-432 (2002).

123. Cardno, A.G. & Gottesman, II. Twin studies of schizophrenia: from bow-and-arrow concordances to star wars Mx and functional genomics. *Am J Med Genet* **97**, 12-17 (2000).

124. Gottesman, I.I. & Wolfgram, D.L. *Schizophrenia genesis : the origins of madness*, (Freeman, New York, 1991).

125. Gottesman, II & Shields, J. A polygenic theory of schizophrenia. *Proc Natl Acad Sci U S A* **58**, 199-205 (1967).

126. Mitchell, K.J. & Porteous, D.J. Rethinking the genetic architecture of schizophrenia. *Psychol Med* **41**, 19-32 (2011).

127. Mah, S.*, et al.* Identification of the semaphorin receptor PLXNA2 as a candidate for susceptibility to schizophrenia. *Mol Psychiatry* **11**, 471-478 (2006).

128. Lencz, T.*, et al.* Converging evidence for a pseudoautosomal cytokine receptor gene locus in schizophrenia. *Mol Psychiatry* **12**, 572-580 (2007).

129. Sullivan, P.F.*, et al.* Genomewide association for schizophrenia in the CATIE study: results of stage 1. *Mol Psychiatry* **13**, 570-584 (2008).

130. Dudbridge, F. & Gusnanto, A. Estimation of significance thresholds for genomewide association scans. *Genet Epidemiol* **32**, 227-234 (2008).

131. Sullivan, P.F. The psychiatric GWAS consortium: big science comes to psychiatry. *Neuron* **68**, 182-186 (2010).

132. Stefansson, H.*, et al.* Common variants conferring risk of schizophrenia. *Nature* **460**, 744-747 (2009).

133. Williams, H.J.*, et al.* Fine mapping of ZNF804A and genome-wide significant evidence for its involvement in schizophrenia and bipolar disorder. *Mol Psychiatry* **16**, 429-441 (2011).

134. Ripke, S.*, et al.* Genome-wide association study identifies five new schizophrenia loci. *Nat Genet* **43**, 969-976 (2011).

135. Steinberg, S.*, et al.* Common variants at VRK2 and TCF4 conferring risk of schizophrenia. *Hum Mol Genet* **20**, 4076-4081 (2011).

136. Lee, K.W., Woon, P.S., Teo, Y.Y. & Sim, K. Genome wide association studies (GWAS) and copy number variation (CNV) studies of the major psychoses: what have we learnt? *Neurosci Biobehav Rev* **36**, 556-571 (2012).

137. Hill, M.J., Jeffries, A.R., Dobson, R.J., Price, J. & Bray, N.J. Knockdown of the psychosis susceptibility gene ZNF804A alters expression of genes involved in cell adhesion. *Hum Mol Genet* (2011).

138. Díez-Guerra, F.J. Neurogranin, a link between calcium/calmodulin and protein kinase C signaling in synaptic plasticity. *IUBMB Life* **62**, 597-606 (2010).

139. Flora, A., Garcia, J.J., Thaller, C. & Zoghbi, H.Y. The E-protein Tcf4 interacts with Math1 to regulate differentiation of a specific subset of neuronal progenitors. *Proc Natl Acad Sci U S A* **104**, 15382-15387 (2007).

140. Szulwach, K.E.*, et al.* Cross talk between microRNA and epigenetic regulation in adult neurogenesis. *J Cell Biol* **189**, 127-141 (2010).

141. Smrt, R.D.*, et al.* MicroRNA miR-137 regulates neuronal maturation by targeting ubiquitin ligase mind bomb-1. *Stem Cells* **28**, 1060-1070 (2010).

142. Shi, J.*, et al.* Common variants on chromosome 6p22.1 are associated with schizophrenia. *Nature* **460**, 753-757 (2009).

143. Williams, H.J., Owen, M.J. & O'Donovan, M.C. New findings from genetic association studies of schizophrenia. *J Hum Genet* **54**, 9-14 (2009).

144. Stefansson, H.*, et al.* Large recurrent microdeletions associated with schizophrenia. *Nature* **455**, 232-236 (2008).

145. Stone, J.L.*, et al.* Rare chromosomal deletions and duplications increase risk of schizophrenia. *Nature* **455**, 237-241 (2008).

146. Kirov, G.*, et al.* De novo CNV analysis implicates specific abnormalities of postsynaptic signalling complexes in the pathogenesis of schizophrenia. *Mol Psychiatry* (2011).

147. Owen, M.J., Williams, H.J. & O'Donovan, M.C. Schizophrenia genetics: advancing on two fronts. *Curr Opin Genet Dev* (2009).

148. Esslinger, C.*, et al.* Neural mechanisms of a genome-wide supported psychosis variant. *Science* **324**, 605 (2009).

149. Kirov, G., O'Donovan, M.C. & Owen, M.J. Finding schizophrenia genes. *J Clin Invest* **115**, 1440-1448 (2005).

150. López-Muñoz, F.*, et al.* History of the discovery and clinical introduction of chlorpromazine. *Ann Clin Psychiatry* **17**, 113-135 (2005).

151. Nestler, E.J., Hyman, S.E. & Malenka, R.C. *Molecular neuropharmacology : a foundation for clinical neuroscience*, (McGraw-Hill, Medical Pub. Div., New York, 2001).

152. Carlsson, A. & Lindqvist, M. Effect of chlorpromazine or haloperidol on formation of 3-methoxytyramine and normetanephrine in mouse brain. *Acta Pharmacol Toxicol (Copenh)* **20**, 140-144 (1963).

153. Carlsson, A. Antipsychotic drugs and catecholamine synapses. *J Psychiatr Res* **11**, 57-64 (1974).

154. Seeman, P., Lee, T., Chau-Wong, M. & Wong, K. Antipsychotic drug doses and neuroleptic/dopamine receptors. *Nature* **261**, 717-719 (1976).

155. Creese, I., Burt, D.R. & Snyder, S.H. Dopamine receptor binding predicts clinical and pharmacological potencies of antischizophrenic drugs. *Science* **192**, 481-483 (1976).

156. Kapur, S. & Remington, G. Dopamine D(2) receptors and their role in atypical antipsychotic action: still necessary and may even be sufficient. *Biol Psychiatry* **50**, 873-883 (2001).

157. Agid, O., Kapur, S. & Remington, G. Emerging drugs for schizophrenia. *Expert Opin Emerg Drugs* **13**, 479-495 (2008).

158. Abbas, A.I.*, et al.* Amisulpride is a potent 5-HT7 antagonist: relevance for antidepressant actions in vivo. *Psychopharmacology (Berl)* **205**, 119-128 (2009).

159. Hippius, H. The history of clozapine. *Psychopharmacology (Berl)* **99 Suppl**, S3-5 (1989).

160. Conley, R.R., Tamminga, C.A., Kelly, D.L. & Richardson, C.M. Treatment-resistant schizophrenic patients respond to clozapine after olanzapine non-response. *Biol Psychiatry* **46**, 73-77 (1999).

161. Kane, J., Honigfeld, G., Singer, J. & Meltzer, H. Clozapine for the treatment-resistant schizophrenic. A double-blind comparison with chlorpromazine. *Arch Gen Psychiatry* **45**, 789-796 (1988).

162. Pickar, D.*, et al.* Clinical and biologic response to clozapine in patients with schizophrenia. Crossover comparison with fluphenazine. *Arch Gen Psychiatry* **49**, 345-353 (1992).

163. Aguilar, E.J. & Siris, S.G. Do antipsychotic drugs influence suicidal behavior in schizophrenia? *Psychopharmacol Bull* **40**, 128-142 (2007).

164. Owens, D.G. Adverse effects of antipsychotic agents. Do newer agents offer advantages? *Drugs* **51**, 895-930 (1996).

165. Meltzer, H.Y., Matsubara, S. & Lee, J.C. Classification of typical and atypical antipsychotic drugs on the basis of dopamine D-1, D-2 and serotonin2 pKi values. *J Pharmacol Exp Ther* **251**, 238-246 (1989).

166. Kapur, S. & Seeman, P. Does fast dissociation from the dopamine d(2) receptor explain the action of atypical antipsychotics?: A new hypothesis. *Am J Psychiatry* **158**, 360-369 (2001).

167. Peroutka, S.J. Molecular biology of serotonin (5-HT) receptors. *Synapse* **18**, 241-260 (1994).

168. Richtand, N.M.*, et al.* Dopamine and serotonin receptor binding and antipsychotic efficacy. *Neuropsychopharmacology* **32**, 1715-1726 (2007).

169. Reavill, C., Kettle, A., Holland, V., Riley, G. & Blackburn, T.P. Attenuation of haloperidol-induced catalepsy by a 5-HT2C receptor antagonist. *Br J Pharmacol* **126**, 572-574 (1999).

170. Garzya, V.*, et al.* Studies towards the identification of a new generation of atypical antipsychotic agents. *Bioorg Med Chem Lett* **17**, 400-405 (2007).

171. Kroeze, W.K.*, et al.* H1-histamine receptor affinity predicts short-term weight gain for typical and atypical antipsychotic drugs. *Neuropsychopharmacology* **28**, 519-526 (2003).

172. Carboni, L.*, et al.* Slow dissociation of partial agonists from the D2 receptor is linked to reduced prolactin release. *Int J Neuropsychopharmacol*, 1-12 (2011).

173. Lieberman, J.A. Dopamine partial agonists: a new class of antipsychotic. *CNS Drugs* **18**, 251-267 (2004).

174. Shapiro, D.A.*, et al.* Aripiprazole, a novel atypical antipsychotic drug with a unique and robust pharmacology. *Neuropsychopharmacology* **28**, 1400-1411 (2003).

175. Gray, J.A. & Roth, B.L. The pipeline and future of drug development in schizophrenia. *Mol Psychiatry* **12**, 904-922 (2007).

176. Biedermann, F. & Fleischhacker, W.W. Emerging drugs for schizophrenia. *Expert Opin Emerg Drugs* **16**, 271-282 (2011).

177. Bertolini, A.*, et al.* Paracetamol: new vistas of an old drug. *CNS Drug Rev* **12**, 250-275 (2006).

178. Andersson, D.A.*, et al.* TRPA1 mediates spinal antinociception induced by acetaminophen and the cannabinoid Delta(9)-tetrahydrocannabiorcol. *Nat Commun* **2**, 551 (2011).

179. Lacro, J.P., Dunn, L.B., Dolder, C.R., Leckband, S.G. & Jeste, D.V. Prevalence of and risk factors for medication nonadherence in patients with schizophrenia: a comprehensive review of recent literature. *J Clin Psychiatry* **63**, 892-909 (2002).

180. Arranz, M.J. & Kapur, S. Pharmacogenetics in psychiatry: are we ready for widespread clinical use? *Schizophr Bull* **34**, 1130-1144 (2008).

181. McGlashan, T.H. Early detection and intervention in schizophrenia: research. *Schizophr Bull* **22**, 327-345 (1996).

182. Kirkpatrick, B., Buchanan, R.W., Ross, D.E. & Carpenter, W.T., Jr. A separate disease within the syndrome of schizophrenia. *Arch Gen Psychiatry* **58**, 165-171 (2001).

183. Roth, B.L., Sheffler, D.J. & Kroeze, W.K. Magic shotguns versus magic bullets: selectively non-selective drugs for mood disorders and schizophrenia. *Nat Rev Drug Discov* **3**, 353-359 (2004).

184. Williams, J.B., Mallorga, P.J., Jeffrey Conn, P., Pettibone, D.J. & Sur, C. Effects of typical and atypical antipsychotics on human glycine transporters. *Schizophr Res* **71**, 103-112 (2004).

185. Oldham, W.M. & Hamm, H.E. Heterotrimeric G protein activation by G-protein-coupled receptors. *Nat Rev Mol Cell Biol* **9**, 60-71 (2008).

186. Hewavitharana, T. & Wedegaertner, P.B. Non-canonical signaling and localizations of heterotrimeric G proteins. *Cell Signal* (2011).

187. Ma, Y.C., Huang, J., Ali, S., Lowry, W. & Huang, X.Y. Src tyrosine kinase is a novel direct effector of G proteins. *Cell* **102**, 635-646 (2000).

188. McCudden, C.R., Hains, M.D., Kimple, R.J., Siderovski, D.P. & Willard, F.S. G-protein signaling: back to the future. *Cell Mol Life Sci* **62**, 551-577 (2005).

189. Pierce, K.L., Premont, R.T. & Lefkowitz, R.J. Seven-transmembrane receptors. *Nat Rev Mol Cell Biol* **3**, 639-650 (2002).

190. Marinissen, M.J. & Gutkind, J.S. G-protein-coupled receptors and signaling networks: emerging paradigms. *Trends Pharmacol Sci* **22**, 368-376 (2001).

191. Beaulieu, J.M. & Gainetdinov, R.R. The physiology, signaling, and pharmacology of dopamine receptors. *Pharmacol Rev* **63**, 182-217 (2011).

192. Luttrell, L.M. & Gesty-Palmer, D. Beyond desensitization: physiological relevance of arrestin-dependent signaling. *Pharmacol Rev* **62**, 305-330 (2010).

193. Luttrell, L.M. Composition and function of g protein-coupled receptor signalsomes controlling mitogen-activated protein kinase activity. *J Mol Neurosci* **26**, 253-264 (2005).

194. Luttrell, L.M.*, et al.* Beta-arrestin-dependent formation of beta2 adrenergic receptor-Src protein kinase complexes. *Science* **283**, 655-661 (1999).

195. Urban, J.D.*, et al.* Functional selectivity and classical concepts of quantitative pharmacology. *J Pharmacol Exp Ther* **320**, 1-13 (2007).

196. Mailman, R.B. GPCR functional selectivity has therapeutic impact. *Trends Pharmacol Sci* **28**, 390-396 (2007).

197. Kenakin, T. New concepts in drug discovery: collateral efficacy and permissive antagonism. *Nat Rev Drug Discov* **4**, 919-927 (2005).

198. Gray, J.A. & Roth, B.L. Paradoxical trafficking and regulation of 5-HT(2A) receptors by agonists and antagonists. *Brain Res Bull* **56**, 441-451 (2001).

199. Burris, K.D.*, et al.* Aripiprazole, a novel antipsychotic, is a high-affinity partial agonist at human dopamine D2 receptors. *J Pharmacol Exp Ther* **302**, 381-389 (2002).

200. Lawler, C.P.*, et al.* Interactions of the novel antipsychotic aripiprazole (OPC-14597) with dopamine and serotonin receptor subtypes. *Neuropsychopharmacology* **20**, 612-627 (1999).

201. Urban, J.D., Vargas, G.A., von Zastrow, M. & Mailman, R.B. Aripiprazole has functionally selective actions at dopamine D2 receptor-mediated signaling pathways. *Neuropsychopharmacology* **32**, 67-77 (2007).

202. Kenakin, T. Interrogating 7TM receptors: does texture in the question yield greater texture in the answer? *J Recept Signal Transduct Res* **29**, 132-139 (2009).

203. Allen, J.A.*, et al.* Discovery of beta-arrestin-biased dopamine D2 ligands for probing signal transduction pathways essential for antipsychotic efficacy. *Proc Natl Acad Sci U S A* **108**, 18488-18493 (2011).

204. Christopoulos, A. Allosteric binding sites on cell-surface receptors: novel targets for drug discovery. *Nat Rev Drug Discov* **1**, 198-210 (2002).

205. Christopoulos, A. & Kenakin, T. G protein-coupled receptor allosterism and complexing. *Pharmacol Rev* **54**, 323-374 (2002).

206. Kenakin, T. & Miller, L.J. Seven transmembrane receptors as shapeshifting proteins: the impact of allosteric modulation and functional selectivity on new drug discovery. *Pharmacol Rev* **62**, 265-304 (2010).

207. Macdonald, R.L. & Kelly, K.M. Antiepileptic drug mechanisms of action. *Epilepsia* **36 Suppl 2**, S2-12 (1995).

208. White, H.S. Comparative anticonvulsant and mechanistic profile of the established and newer antiepileptic drugs. *Epilepsia* **40 Suppl 5**, S2-10 (1999).

209. Sur, C.*, et al.* N-desmethylclozapine, an allosteric agonist at muscarinic 1 receptor, potentiates N-methyl-D-aspartate receptor activity. *Proc Natl Acad Sci U S A* **100**, 13674-13679 (2003).

210. Burstein, E.S.*, et al.* Intrinsic efficacy of antipsychotics at human D2, D3, and D4 dopamine receptors: identification of the clozapine metabolite N-desmethylclozapine as a D2/D3 partial agonist. *J Pharmacol Exp Ther* **315**, 1278-1287 (2005).

211. Conn, P.J., Christopoulos, A. & Lindsley, C.W. Allosteric modulators of GPCRs: a novel approach for the treatment of CNS disorders. *Nat Rev Drug Discov* **8**, 41-54 (2009).

212. Romano, C., Yang, W.L. & O'Malley, K.L. Metabotropic glutamate receptor 5 is a disulfide-linked dimer. *J Biol Chem* **271**, 28612-28616 (1996).

213. Kniazeff, J., Prézeau, L., Rondard, P., Pin, J.P. & Goudet, C. Dimers and beyond: The functional puzzles of class C GPCRs. *Pharmacol Ther* **130**, 9-25 (2011).

214. Rives, M.L.*, et al.* Crosstalk between GABAB and mGlu1a receptors reveals new insight into GPCR signal integration. *EMBO J* **28**, 2195-2208 (2009).

215. Albizu, L., Moreno, J.L., González-Maeso, J. & Sealfon, S.C. Heteromerization of G protein-coupled receptors: relevance to neurological disorders and neurotherapeutics. *CNS Neurol Disord Drug Targets* **9**, 636-650 (2010).

216. Perreault, M.L., O'Dowd, B.F. & George, S.R. Dopamine receptor homooligomers and heterooligomers in schizophrenia. *CNS Neurosci Ther* **17**, 52-57 (2011).

217. Ng, G.Y.*, et al.* Dopamine D2 receptor dimers and receptor-blocking peptides. *Biochem Biophys Res Commun* **227**, 200-204 (1996).

218. Łukasiewicz, S.*, et al.* Hetero-dimerization of serotonin 5-HT(2A) and dopamine D(2) receptors. *Biochim Biophys Acta* **1803**, 1347-1358 (2010).

219. Borroto-Escuela, D.O.*, et al.* Dopamine D2 and 5-hydroxytryptamine 5-HT(A) receptors assemble into functionally interacting heteromers. *Biochem Biophys Res Commun* **401**, 605-610 (2010).

220. González-Maeso, J.*, et al.* Identification of a serotonin/glutamate receptor complex implicated in psychosis. *Nature* **452**, 93-97 (2008).

221. Fribourg, M.*, et al.* Decoding the signaling of a GPCR heteromeric complex reveals a unifying mechanism of action of antipsychotic drugs. *Cell* **147**, 1011-1023 (2011).

222. Teitler, M. & Klein, M.T. A new approach for studying GPCR dimers: Drug-induced inactivation and reactivation to reveal GPCR dimer function in vitro, in primary culture, and in vivo. *Pharmacol Ther* (2011).

223. Hasbi, A., O'Dowd, B.F. & George, S.R. Dopamine D1-D2 receptor heteromer signaling pathway in the brain: emerging physiological relevance. *Mol Brain* **4**, 26 (2011).

224. Han, Y., Moreira, I.S., Urizar, E., Weinstein, H. & Javitch, J.A. Allosteric communication between protomers of dopamine class A GPCR dimers modulates activation. *Nat Chem Biol* **5**, 688-695 (2009).

225. Milligan, G. G protein-coupled receptor hetero-dimerization: contribution to pharmacology and function. *Br J Pharmacol* **158**, 5-14 (2009).

226. Pyne, N.J. & Pyne, S. Receptor tyrosine kinase-G-protein-coupled receptor signalling platforms: out of the shadow? *Trends Pharmacol Sci* **32**, 443-450 (2011).

227. Huang, E.J. & Reichardt, L.F. Trk receptors: roles in neuronal signal transduction. *Annu Rev Biochem* **72**, 609-642 (2003).

228. Luttrell, L.M. 'Location, location, location': activation and targeting of MAP kinases by G protein-coupled receptors. *J Mol Endocrinol* **30**, 117-126 (2003).

229. Cervantes, D., Crosby, C. & Xiang, Y. Arrestin orchestrates crosstalk between G protein-coupled receptors to modulate the spatiotemporal activation of ERK MAPK. *Circ Res* **106**, 79-88 (2010).

230. Kukkonen, J.P. A ménage à trois made in heaven: G-protein-coupled receptors, lipids and TRP channels. *Cell Calcium* **50**, 9-26 (2011).

231. Kotecha, S.A*., et al.* A D2 class dopamine receptor transactivates a receptor tyrosine kinase to inhibit NMDA receptor transmission. *Neuron* **35**, 1111-1122 (2002).

232. Fernandez, E., Schiappa, R., Girault, J.A. & Le Novere, N. DARPP-32 is a robust integrator of dopamine and glutamate signals. *PLoS Comput Biol* **2**, e176 (2006).

233. Molteni, R., Calabrese, F., Racagni, G., Fumagalli, F. & Riva, M.A. Antipsychotic drug actions on gene modulation and signaling mechanisms. *Pharmacol Ther* (2009).

234. Lovestone, S., Killick, R., Di Forti, M. & Murray, R. Schizophrenia as a GSK-3 dysregulation disorder. *Trends Neurosci* **30**, 142-149 (2007).

235. Ostrom, R.S. & Insel, P.A. The evolving role of lipid rafts and caveolae in G protein-coupled receptor signaling: implications for molecular pharmacology. *Br J Pharmacol* **143**, 235-245 (2004).

236. Kim, E. & Sheng, M. PDZ domain proteins of synapses. *Nat Rev Neurosci* **5**, 771-781 (2004).

237. Björk, K., Sjögren, B. & Svenningsson, P. Regulation of serotonin receptor function in the nervous system by lipid rafts and adaptor proteins. *Exp Cell Res* **316**, 1351-1356 (2010).

238. Geysen, H.M., Schoenen, F., Wagner, D. & Wagner, R. Combinatorial compound libraries for drug discovery: an ongoing challenge. *Nat Rev Drug Discov* **2**, 222-230 (2003).

239. LaMattina, J.L. The impact of mergers on pharmaceutical R&D. *Nat Rev Drug Discov* **10**, 559-560 (2011).

240. An, W.F. & Tolliday, N. Cell-based assays for high-throughput screening. *Mol Biotechnol* **45**, 180-186 (2010).

241. Evans, N.A*., et al.* Abeta(1-42) reduces synapse number and inhibits neurite outgrowth in primary cortical and hippocampal neurons: a quantitative analysis. *J Neurosci Methods* **175**, 96-103 (2008).

242. Ross, D.A*., et al.* Multiplexed assays by high-content imaging for assessment of GPCR activity. *J Biomol Screen* **13**, 449-455 (2008).

243. Barbaric, I., Gokhale, P.J. & Andrews, P.W. High-content screening of small compounds on human embryonic stem cells. *Biochem Soc Trans* **38**, 1046-1050 (2010).

244. Milligan, G. High-content assays for ligand regulation of G-protein-coupled receptors. *Drug Discov Today* **8**, 579-585 (2003).

245. Fang, Y. & Ferrie, A.M. Optical biosensor differentiates signaling of endogenous PAR1 and PAR2 in A431 cells. *BMC Cell Biol* **8**, 24 (2007).

246. Morse, M., Tran, E., Sun, H., Levenson, R. & Fang, Y. Ligand-directed functional selectivity at the mu opioid receptor revealed by label-free integrative pharmacology on-target. *PLoS ONE* **6**, e25643 (2011).

247. Peters, M.F*., et al.* Evaluation of cellular dielectric spectroscopy, a whole-cell, label-free technology for drug discovery on Gi-coupled GPCRs. *J Biomol Screen* **12**, 312-319 (2007).

248. Qureshi, A.H*., et al.* Proteomic and phospho-proteomic profile of human platelets in basal, resting state: insights into integrin signaling. *PLoS ONE* **4**, e7627 (2009).

249. Phanstiel, D.H*., et al.* Proteomic and phosphoproteomic comparison of human ES and iPS cells. *Nat Methods* **8**, 821-827 (2011).

250. Wang, Z., Gerstein, M. & Snyder, M. RNA-Seq: a revolutionary tool for transcriptomics. *Nat Rev Genet* **10**, 57-63 (2009).

251. Martin, J.A. & Wang, Z. Next-generation transcriptome assembly. *Nat Rev Genet* **12**, 671-682 (2011).

252. Wortzel, I. & Seger, R. The ERK Cascade: Distinct Functions within Various Subcellular Organelles. *Genes Cancer* **2**, 195-209 (2011).

253. Deutch, A.Y., Lee, M.C. & Iadarola, M.J. Regionally specific effects of atypical antipsychotic drugs on striatal Fos expression: The nucleus accumbens shell as a locus of antipsychotic action. *Mol Cell Neurosci* **3**, 332-341 (1992).

254. Deutch, A.Y., Ongür, D. & Duman, R.S. Antipsychotic drugs induce Fos protein in the thalamic paraventricular nucleus: a novel locus of antipsychotic drug action. *Neuroscience* **66**, 337-346 (1995).

255. Fumagalli, F., Frasca, A., Racagni, G. & Riva, M.A. Antipsychotic drugs modulate Arc expression in the rat brain. *Eur Neuropsychopharmacol* **19**, 109-115 (2009).

256. Murphy, L.O. & Blenis, J. MAPK signal specificity: the right place at the right time. *Trends Biochem Sci* **31**, 268-275 (2006).

257. Girgenti, M.J*., et al.* Antipsychotic-induced gene regulation in multiple brain regions. *J Neurochem* **113**, 175-187 (2010).

258. Fernø, J.*, et al.* Antipsychotic drugs activate SREBP-regulated expression of lipid biosynthetic genes in cultured human glioma cells: a novel mechanism of action? *Pharmacogenomics J* **5**, 298-304 (2005).

259. Polymeropoulos, M.H.*, et al.* Common effect of antipsychotics on the biosynthesis and regulation of fatty acids and cholesterol supports a key role of lipid homeostasis in schizophrenia. *Schizophr Res* **108**, 134-142 (2009).

260. Fehér, L.Z.*, et al.* Impact of haloperidol and risperidone on gene expression profile in the rat cortex. *Neurochem Int* **47**, 271-280 (2005).

261. Duncan, C.E., Chetcuti, A.F. & Schofield, P.R. Coregulation of genes in the mouse brain following treatment with clozapine, haloperidol, or olanzapine implicates altered potassium channel subunit expression in the mechanism of antipsychotic drug action. *Psychiatr Genet* **18**, 226-239 (2008).

262. Chong, V.Z., Young, L.T. & Mishra, R.K. cDNA array reveals differential gene expression following chronic neuroleptic administration: implications of synapsin II in haloperidol treatment. *J Neurochem* **82**, 1533-1539 (2002).

263. Cheng, M.C.*, et al.* Chronic treatment with aripiprazole induces differential gene expression in the rat frontal cortex. *Int J Neuropsychopharmacol* **11**, 207-216 (2008).

264. Bahn, S.*, et al.* Gene expression profiling in the post-mortem human brain--no cause for dismay. *J Chem Neuroanat* **22**, 79-94 (2001).

265. Mirnics, K., Levitt, P. & Lewis, D.A. DNA microarray analysis of postmortem brain tissue. *Int Rev Neurobiol* **60**, 153-181 (2004).

266. Iwamoto, K. & Kato, T. Gene expression profiling in schizophrenia and related mental disorders. *Neuroscientist* **12**, 349-361 (2006).

267. Fasulo, W.H. & Hemby, S.E. Time-dependent changes in gene expression profiles of midbrain dopamine neurons following haloperidol administration. *J Neurochem* **87**, 205-219 (2003).

268. Szuchet, S.*, et al.* The genetic signature of perineuronal oligodendrocytes reveals their unique phenotype. *Eur J Neurosci* **34**, 1906-1922 (2011).

269. Thomas, E.A. Molecular profiling of antipsychotic drug function: convergent mechanisms in the pathology and treatment of psychiatric disorders. *Mol Neurobiol* **34**, 109-128 (2006).

270. Middleton, F.A., Mirnics, K., Pierri, J.N., Lewis, D.A. & Levitt, P. Gene expression profiling reveals alterations of specific metabolic pathways in schizophrenia. *J Neurosci* **22**, 2718-2729 (2002).

271. Kapur, S., VanderSpek, S.C., Brownlee, B.A. & Nobrega, J.N. Antipsychotic dosing in preclinical models is often unrepresentative of the clinical condition: a suggested solution based on in vivo occupancy. *J Pharmacol Exp Ther* **305**, 625-631 (2003).

272. Farde, L.*, et al.* Positron emission tomographic analysis of central D1 and D2 dopamine receptor occupancy in patients treated with classical neuroleptics and clozapine. Relation to extrapyramidal side effects. *Arch Gen Psychiatry* **49**, 538-544 (1992).

273. Nordström, A.L.*, et al.* Central D2-dopamine receptor occupancy in relation to antipsychotic drug effects: a double-blind PET study of schizophrenic patients. *Biol Psychiatry* **33**, 227-235 (1993).

274. Kapur, S., Zipursky, R., Jones, C., Remington, G. & Houle, S. Relationship between dopamine D(2) occupancy, clinical response, and side effects: a double-blind PET study of first-episode schizophrenia. *Am J Psychiatry* **157**, 514-520 (2000).

275. Agid, O.*, et al.* Striatal vs extrastriatal dopamine D2 receptors in antipsychotic response--a double-blind PET study in schizophrenia. *Neuropsychopharmacology* **32**, 1209-1215 (2007).

276. Lobo, M.K., Karsten, S.L., Gray, M., Geschwind, D.H. & Yang, X.W. FACS-array profiling of striatal projection neuron subtypes in juvenile and adult mouse brains. *Nat Neurosci* **9**, 443-452 (2006).

277. Samaha, A.N., Seeman, P., Stewart, J., Rajabi, H. & Kapur, S. "Breakthrough" dopamine supersensitivity during ongoing antipsychotic treatment leads to treatment failure over time. *J Neurosci* **27**, 2979-2986 (2007).

278. Branchi, I. The mouse communal nest: investigating the epigenetic influences of the early social environment on brain and behavior development. *Neurosci Biobehav Rev* **33**, 551-559 (2009).

279. Marsden, C.A., King, M.V. & Fone, K.C. Influence of social isolation in the rat on serotonergic function and memory--relevance to models of schizophrenia and the role of 5-HT receptors. *Neuropharmacology* **61**, 400-407 (2011).

280. Gunther, E.C., Stone, D.J., Gerwien, R.W., Bento, P. & Heyes, M.P. Prediction of clinical drug efficacy by classification of drug-induced genomic expression profiles in vitro. *Proc Natl Acad Sci U S A* **100**, 9608-9613 (2003).

281. Lamb, J.*, et al.* The Connectivity Map: using gene-expression signatures to connect small molecules, genes, and disease. *Science* **313**, 1929-1935 (2006).

282. Akslen, L.A., Andersen, K.J. & Bjerkvig, R. Characteristics of human and rat glioma cells grown in a defined medium. *Anticancer Res* **8**, 797-803 (1988).

283. Lum, P.Y.*, et al.* Discovering modes of action for therapeutic compounds using a genome-wide screen of yeast heterozygotes. *Cell* **116**, 121-137 (2004).

284. Kurella, M.*, et al.* DNA microarray analysis of complex biologic processes. *J Am Soc Nephrol* **12**, 1072-1078 (2001).

285. Snyder, S.H. Dopamine receptors, neuroleptics, and schizophrenia. *Am J Psychiatry* **138**, 460-464 (1981).

286. Seeman, P. Atypical antipsychotics: mechanism of action. *Can J Psychiatry* **47**, 27-38 (2002).

287. Stroup, T.S. Heterogeneity of treatment effects in schizophrenia. *Am J Med* **120**, S26-31 (2007).

288. Cutler, A., Ball, S. & Stahl, S.M. Dosing atypical antipsychotics. *CNS Spectr* **13**, 1-16 (2008).

289. Harrison, P.J. & Weinberger, D.R. Schizophrenia genes, gene expression, and neuropathology: on the matter of their convergence. *Mol Psychiatry* **10**, 40-68; image 45 (2005).

290. Okubo, Y.*, et al.* Decreased prefrontal dopamine D1 receptors in schizophrenia revealed by PET. *Nature* **385**, 634-636 (1997).

291. Friedman, J.I., Temporini, H. & Davis, K.L. Pharmacologic strategies for augmenting cognitive performance in schizophrenia. *Biol Psychiatry* **45**, 1-16 (1999).

292. Motulsky, A.G. Drug reactions enzymes, and biochemical genetics. *J Am Med Assoc* **165**, 835-837 (1957).

293. Vogel, F. Moderne problem der humangenetik. *Ergeb Inn Med U Kinderheilk* **12**, 52-125 (1959).

294. Kalow, W. Pharmacogenetics and pharmacogenomics: origin, status, and the hope for personalized medicine. *Pharmacogenomics J* **6**, 162-165 (2006).

295. de Leon, J., Armstrong, S.C. & Cozza, K.L. Clinical guidelines for psychiatrists for the use of pharmacogenetic testing for CYP450 2D6 and CYP450 2C19. *Psychosomatics* **47**, 75-85 (2006).

296. Malhotra, A.K., Zhang, J.P. & Lencz, T. Pharmacogenetics in psychiatry: translating research into clinical practice. *Mol Psychiatry* (2011).

297. de Leon, J. Pharmacogenomics: the promise of personalized medicine for CNS disorders. *Neuropsychopharmacology* **34**, 159-172 (2009).

298. Arranz, M.J*., et al.* Pharmacogenetic prediction of clozapine response. *Lancet* **355**, 1615-1616 (2000).

299. Shi, M.M., Bleavins, M.R. & de la Iglesia, F.A. Pharmacogenetic application in drug development and clinical trials. *Drug Metab Dispos* **29**, 591-595 (2001).

300. Liu, W*., et al.* Pharmacogenetic analysis of the mGlu2/3 agonist LY2140023 monohydrate in the treatment of schizophrenia. *Pharmacogenomics J* (2010).

301. Patil, S.T*., et al.* Activation of mGlu2/3 receptors as a new approach to treat schizophrenia: a randomized Phase 2 clinical trial. *Nat Med* **13**, 1102-1107 (2007).

302. Rawlins, M.D. Cutting the cost of drug development? *Nat Rev Drug Discov* **3**, 360-364 (2004).

303. Guidotti, A*., et al.* Epigenetic GABAergic targets in schizophrenia and bipolar disorder. *Neuropharmacology* **60**, 1007-1016 (2011).

304. Dong, E., Nelson, M., Grayson, D.R., Costa, E. & Guidotti, A. Clozapine and sulpiride but not haloperidol or olanzapine activate brain DNA demethylation. *Proc Natl Acad Sci U S A* **105**, 13614-13619 (2008).

305. Mikami, T., Aoki, M. & Kimura, T. The application of mass spectrometry to proteomics and metabolomics in biomarker discovery and drug development. *Curr Mol Pharmacol* (2011).

306. Napoli, C., de Nigris, F. & Sica, V. New advances in microarrays: finding the genes causally involved in disease. *Methods Mol Med* **108**, 215-233 (2005).

307. Maycox, P.R*., et al.* Analysis of gene expression in two large schizophrenia cohorts identifies multiple changes associated with nerve terminal function. *Mol Psychiatry* (2009).

308. Mill, J*., et al.* Epigenomic profiling reveals DNA-methylation changes associated with major psychosis. *Am J Hum Genet* **82**, 696-711 (2008).

309. Chan, M.K*., et al.* Evidence for disease and antipsychotic medication effects in post-mortem brain from schizophrenia patients. *Mol Psychiatry* **16**, 1189-1202 (2011).

310. Danielian, P.S., White, R., Hoare, S.A., Fawell, S.E. & Parker, M.G. Identification of residues in the estrogen receptor that confer differential sensitivity to estrogen and hydroxytamoxifen. *Mol Endocrinol* **7**, 232-240 (1993).

311. Kubinová, S*., et al.* The use of superporous Ac-CGGASIKVAVS-OH-modified PHEMA scaffolds to promote cell adhesion and the differentiation of human fetal neural precursors. *Biomaterials* **31**, 5966-5975 (2010).

312. Geling, A., Steiner, H., Willem, M., Bally-Cuif, L. & Haass, C. A γ-secretase inhibitor blocks Notch signaling in vivo and causes a severe neurogenic phenotype in zebrafish. *EMBO Rep* **3**, 688-694 (2002).

313. Sinha, S. & Chen, J.K. Purmorphamine activates the Hedgehog pathway by targeting Smoothened. *Nat Chem Biol* **2**, 29-30 (2006).

314. Larkin, M.A*., et al.* Clustal W and Clustal X version 2.0. *Bioinformatics* **23**, 2947-2948 (2007).

315. Untergasser, A*., et al.* Primer3Plus, an enhanced web interface to Primer3. *Nucleic Acids Res* **35**, W71-74 (2007).

316. Rozen, S. & Skaletsky, H. Primer3 on the WWW for general users and for biologist programmers. *Methods Mol Biol* **132**, 365-386 (2000).

317. Liu, C. & Hermann, T.E. Characterization of ionomycin as a calcium ionophore. *J Biol Chem* **253**, 5892-5894 (1978).

318. Albizu, L*., et al.* Time-resolved FRET between GPCR ligands reveals oligomers in native tissues. *Nat Chem Biol* **6**, 587-594 (2010).

319. Verkhratsky, A. & Parpura, V. Recent advances in (patho)physiology of astroglia. *Acta Pharmacol Sin* **31**, 1044-1054 (2010).

320. Cordero-Llana, O*., et al.* Clusterin secreted by astrocytes enhances neuronal differentiation from human neural precursor cells. *Cell Death Differ* **18**, 907-913 (2011).

321. Wierońska, J.M. & Pilc, A. Metabotropic glutamate receptors in the tripartite synapse as a target for new psychotropic drugs. *Neurochem Int* **55**, 85-97 (2009).

322. Vernon, A.C., Smith, E.J., Stevanato, L. & Modo, M. Selective activation of metabotropic glutamate receptor 7 induces inhibition of cellular proliferation and promotes astrocyte differentiation of ventral mesencephalon human neural stem/progenitor cells. *Neurochem Int* **59**, 421-431 (2011).

323. Keshavan, M.S., Tandon, R., Boutros, N.N. & Nasrallah, H.A. Schizophrenia, "just the facts": what we know in 2008 Part 3: neurobiology. *Schizophr Res* **106**, 89-107 (2008).

324. Williams, B.P*., et al.* A PDGF-regulated immediate early gene response initiates neuronal differentiation in ventricular zone progenitor cells. *Neuron* **18**, 553-562 (1997).

325. Park, J.K., Williams, B.P., Alberta, J.A. & Stiles, C.D. Bipotent cortical progenitor cells process conflicting cues for neurons and glia in a hierarchical manner. *J Neurosci* **19**, 10383-10389 (1999).

326. Finch, S.E. The influence of signalling molecules and growth factors on neural progenitor cell specification and fate. (2009).

327. Wichterle, H., Lieberam, I., Porter, J.A. & Jessell, T.M. Directed differentiation of embryonic stem cells into motor neurons. *Cell* **110**, 385-397 (2002).

328. Sun, Y*., et al.* Long-term tripotent differentiation capacity of human neural stem (NS) cells in adherent culture. *Mol Cell Neurosci* **38**, 245-258 (2008).

329. Chanas-Sacre, G., Rogister, B., Moonen, G. & Leprince, P. Radial glia phenotype: origin, regulation, and transdifferentiation. *J Neurosci Res* **61**, 357-363 (2000).

330. Götz, M. & Barde, Y.A. Radial glial cells defined and major intermediates between embryonic stem cells and CNS neurons. *Neuron* **46**, 369-372 (2005).

331. Gupta, A., Tsai, L.H. & Wynshaw-Boris, A. Life is a journey: a genetic look at neocortical development. *Nat Rev Genet* **3**, 342-355 (2002).

332. Rizo, J., Chen, X. & Araç, D. Unraveling the mechanisms of synaptotagmin and SNARE function in neurotransmitter release. *Trends Cell Biol* **16**, 339-350 (2006).

333. Rizo, J. & Rosenmund, C. Synaptic vesicle fusion. *Nat Struct Mol Biol* **15**, 665-674 (2008).

334. Heikkilä, T.J*., et al.* Human embryonic stem cell-derived neuronal cells form spontaneously active neuronal networks in vitro. *Exp Neurol* **218**, 109-116 (2009).

335. Eyles, D.W., McGrath, J.J. & Reynolds, G.P. Neuronal calcium-binding proteins and schizophrenia. *Schizophr Res* **57**, 27-34 (2002).

336. Ritter, S.L. & Hall, R.A. Fine-tuning of GPCR activity by receptor-interacting proteins. *Nat Rev Mol Cell Biol* **10**, 819-830 (2009).

337. Volpicelli, F., Perrone-Capano, C., Da Pozzo, P., Colucci-D'Amato, L. & di Porzio, U. Modulation of nurr1 gene expression in mesencephalic dopaminergic neurones. *J Neurochem* **88**, 1283-1294 (2004).

338. Seeman, P. Targeting the dopamine D2 receptor in schizophrenia. *Expert Opin Ther Targets* **10**, 515-531 (2006).

339. Saiz, P.A*., et al.* An investigation of the alpha1A-adrenergic receptor gene and antipsychotic-induced side-effects. *Hum Psychopharmacol* **23**, 107-114 (2008).

340. Spooren, W., Riemer, C. & Meltzer, H. Opinion: NK3 receptor antagonists: the next generation of antipsychotics? *Nat Rev Drug Discov* **4**, 967-975 (2005).

341. Lefkowitz, R.J. & Shenoy, S.K. Transduction of receptor signals by beta-arrestins. *Science* **308**, 512-517 (2005).

342. Premont, R.T. & Gainetdinov, R.R. Physiological roles of G protein-coupled receptor kinases and arrestins. *Annu Rev Physiol* **69**, 511-534 (2007).

343. Leclerc, P.C*., et al.* A polyaromatic caveolin-binding-like motif in the cytoplasmic tail of the type 1 receptor for angiotensin II plays an important role in receptor trafficking and signaling. *Endocrinology* **143**, 4702-4710 (2002).

344. Cooray, S.N., Chan, L., Webb, T.R., Metherell, L. & Clark, A.J. Accessory proteins are vital for the functional expression of certain G protein-coupled receptors. *Mol Cell Endocrinol* **300**, 17-24 (2009).

345. Xia, Z., Gray, J.A., Compton-Toth, B.A. & Roth, B.L. A direct interaction of PSD-95 with 5-HT2A serotonin receptors regulates receptor trafficking and signal transduction. *J Biol Chem* **278**, 21901-21908 (2003).

346. Sánchez, C. & Hyttel, J. Comparison of the effects of antidepressants and their metabolites on reuptake of biogenic amines and on receptor binding. *Cell Mol Neurobiol* **19**, 467-489 (1999).

347. López-Muñoz, F., Alamo, C. & García-García, P. The discovery of chlordiazepoxide and the clinical introduction of benzodiazepines: half a century of anxiolytic drugs. *J Anxiety Disord* **25**, 554-562 (2011).

348. Ryckmans, T. Modulation of the vasopressin system for the treatment of CNS diseases. *Curr Opin Drug Discov Devel* **13**, 538-547 (2010).
349. Guillemot, F. Cellular and molecular control of neurogenesis in the mammalian telencephalon. *Curr Opin Cell Biol* **17**, 639-647 (2005).
350. Vinson, P.N. & Conn, P.J. Metabotropic glutamate receptors as therapeutic targets for schizophrenia. *Neuropharmacology* **62**, 1461-1472 (2012).
351. Ishihara, M.*, et al.* A new three-dimensional axonal outgrowth assay for central nervous system regeneration. *J Neurosci Methods* **198**, 181-186 (2011).
352. Elliott, N.T. & Yuan, F. A review of three-dimensional in vitro tissue models for drug discovery and transport studies. *J Pharm Sci* **100**, 59-74 (2011).
353. Bota, M., Dong, H.W. & Swanson, L.W. From gene networks to brain networks. *Nat Neurosci* **6**, 795-799 (2003).
354. Petersen, O.H. & Verkhratsky, A. Endoplasmic reticulum calcium tunnels integrate signalling in polarised cells. *Cell Calcium* **42**, 373-378 (2007).
355. Berridge, M.J., Bootman, M.D. & Roderick, H.L. Calcium signalling: dynamics, homeostasis and remodelling. *Nat Rev Mol Cell Biol* **4**, 517-529 (2003).
356. Clapham, D.E. Calcium signaling. *Cell* **131**, 1047-1058 (2007).
357. Kew, J.N. & Kemp, J.A. Ionotropic and metabotropic glutamate receptor structure and pharmacology. *Psychopharmacology (Berl)* **179**, 4-29 (2005).
358. Keramidas, A., Moorhouse, A.J., Schofield, P.R. & Barry, P.H. Ligand-gated ion channels: mechanisms underlying ion selectivity. *Prog Biophys Mol Biol* **86**, 161-204 (2004).
359. Wang, D.D. & Kriegstein, A.R. Defining the role of GABA in cortical development. *J Physiol* **587**, 1873-1879 (2009).
360. Hofmann, T.*, et al.* Direct activation of human TRPC6 and TRPC3 channels by diacylglycerol. *Nature* **397**, 259-263 (1999).
361. Venkatachalam, K., Zheng, F. & Gill, D.L. Regulation of canonical transient receptor potential (TRPC) channel function by diacylglycerol and protein kinase C. *J Biol Chem* **278**, 29031-29040 (2003).
362. Werry, T.D., Wilkinson, G.F. & Willars, G.B. Mechanisms of cross-talk between G-protein-coupled receptors resulting in enhanced release of intracellular Ca2+. *Biochem J* **374**, 281-296 (2003).
363. Hernández-López, S.*, et al.* D2 dopamine receptors in striatal medium spiny neurons reduce L-type Ca2+ currents and excitability via a novel PLC[beta]1-IP3-calcineurin-signaling cascade. *J Neurosci* **20**, 8987-8995 (2000).
364. Barnes, N.M. & Sharp, T. A review of central 5-HT receptors and their function. *Neuropharmacology* **38**, 1083-1152 (1999).
365. Kobilka, B.K. Structural insights into adrenergic receptor function and pharmacology. *Trends Pharmacol Sci* **32**, 213-218 (2011).
366. Felder, C.C. Muscarinic acetylcholine receptors: signal transduction through multiple effectors. *FASEB J* **9**, 619-625 (1995).

367. Tiligada, E., Kyriakidis, K., Chazot, P.L. & Passani, M.B. Histamine pharmacology and new CNS drug targets. *CNS Neurosci Ther* **17**, 620-628 (2011).

368. Fremeau, R.T., Jr., Voglmaier, S., Seal, R.P. & Edwards, R.H. VGLUTs define subsets of excitatory neurons and suggest novel roles for glutamate. *Trends Neurosci* **27**, 98-103 (2004).

369. Bullwinkel, J*., et al.* Ki-67 protein is associated with ribosomal RNA transcription in quiescent and proliferating cells. *J Cell Physiol* **206**, 624-635 (2006).

370. Di Virgilio, F., Steinberg, T.H. & Silverstein, S.C. Inhibition of Fura-2 sequestration and secretion with organic anion transport blockers. *Cell Calcium* **11**, 57-62 (1990).

371. Parker, M.J., Beck, A. & Luetje, C.W. Neuronal nicotinic receptor beta2 and beta4 subunits confer large differences in agonist binding affinity. *Mol Pharmacol* **54**, 1132-1139 (1998).

372. Birdsall, N.J., Hulme, E.C. & Burgen, A. The character of the muscarinic receptors in different regions of the rat brain. *Proc R Soc Lond B Biol Sci* **207**, 1-12 (1980).

373. Cheng, K*., et al.* Lithocholylcholine, a bile acid/acetylcholine hybrid, is a muscarinic receptor antagonist. *J Pharmacol Exp Ther* **303**, 29-35 (2002).

374. Dajas-Bailador, F. & Wonnacott, S. Nicotinic acetylcholine receptors and the regulation of neuronal signalling. *Trends Pharmacol Sci* **25**, 317-324 (2004).

375. Castro-Fernández, C., Maya-Núñez, G. & Conn, P.M. Beyond the signal sequence: protein routing in health and disease. *Endocr Rev* **26**, 479-503 (2005).

376. Conn, P.M., Janovick, J.A., Brothers, S.P. & Knollman, P.E. 'Effective inefficiency': cellular control of protein trafficking as a mechanism of post-translational regulation. *J Endocrinol* **190**, 13-16 (2006).

377. Viard, P*., et al.* Gbetagamma dimers stimulate vascular L-type Ca2+ channels via phosphoinositide 3-kinase. *FASEB J* **13**, 685-694 (1999).

378. Viard, P*., et al.* PI3K promotes voltage-dependent calcium channel trafficking to the plasma membrane. *Nat Neurosci* **7**, 939-946 (2004).

379. Dolphin, A.C. β subunits of voltage-gated calcium channels. *J Bioenerg Biomembr* **35**, 599-620 (2003).

380. Reynolds, B.A. & Weiss, S. Generation of neurons and astrocytes from isolated cells of the adult mammalian central nervous system. *Science* **255**, 1707-1710 (1992).

381. Blair, L.A. & Marshall, J. IGF-1 modulates N and L calcium channels in a PI 3-kinase-dependent manner. *Neuron* **19**, 421-429 (1997).

382. Venkatasubramanian, G*., et al.* Insulin and insulin-like growth factor-1 abnormalities in antipsychotic-naive schizophrenia. *Am J Psychiatry* **164**, 1557-1560 (2007).

383. Venkatasubramanian, G., Chittiprol, S., Neelakantachar, N., Shetty, T. & Gangadhar, B.N. Effect of antipsychotic treatment on Insulin-like Growth Factor-1 and cortisol in schizophrenia: a longitudinal study. *Schizophr Res* **119**, 131-137 (2010).

384. Derossi, D., Williams, E.J., Green, P.J., Dunican, D.J. & Doherty, P. Stimulation of mitogenesis by a cell-permeable PI 3-kinase binding peptide. *Biochem Biophys Res Commun* **251**, 148-152 (1998).

385. Williams, E.J. & Doherty, P. Evidence for and against a pivotal role of PI 3-kinase in a neuronal cell survival pathway. *Mol Cell Neurosci* **13**, 272-280 (1999).

386. Dichter, M.A., Tischler, A.S. & Greene, L.A. Nerve growth factor-induced increase in electrical excitability and acetylcholine sensitivity of a rat pheochromocytoma cell line. *Nature* **268**, 501-504 (1977).

387. Mandel, G., Cooperman, S.S., Maue, R.A., Goodman, R.H. & Brehm, P. Selective induction of brain type II Na+ channels by nerve growth factor. *Proc Natl Acad Sci U S A* **85**, 924-928 (1988).

388. Toledo-Aral, J.J., Brehm, P., Halegoua, S. & Mandel, G. A single pulse of nerve growth factor triggers long-term neuronal excitability through sodium channel gene induction. *Neuron* **14**, 607-611 (1995).

389. Kalman, D., Wong, B., Horvai, A.E., Cline, M.J. & O'Lague, P.H. Nerve growth factor acts through cAMP-dependent protein kinase to increase the number of sodium channels in PC12 cells. *Neuron* **4**, 355-366 (1990).

390. Sharma, N., D'Arcangelo, G., Kleinlaus, A., Halegoua, S. & Trimmer, J.S. Nerve growth factor regulates the abundance and distribution of K+ channels in PC12 cells. *J Cell Biol* **123**, 1835-1843 (1993).

391. Garber, S.S., Hoshi, T. & Aldrich, R.W. Regulation of ionic currents in pheochromocytoma cells by nerve growth factor and dexamethasone. *J Neurosci* **9**, 3976-3987 (1989).

392. Lesser, S.S. & Lo, D.C. Regulation of voltage-gated ion channels by NGF and ciliary neurotrophic factor in SK-N-SH neuroblastoma cells. *J Neurosci* **15**, 253-261 (1995).

393. Fanger, G.R., Jones, J.R. & Maue, R.A. Differential regulation of neuronal sodium channel expression by endogenous and exogenous tyrosine kinase receptors expressed in rat pheochromocytoma cells. *J Neurosci* **15**, 202-213 (1995).

394. Leng, J., Jiang, L., Chen, H. & Zhang, X. Brain-derived neurotrophic factor and electrophysiological properties of voltage-gated ion channels during neuronal stem cell development. *Brain Res* **1272**, 14-24 (2009).

395. Lesser, S.S., Sherwood, N.T. & Lo, D.C. Neurotrophins differentially regulate voltage-gated ion channels. *Mol Cell Neurosci* **10**, 173-183 (1997).

396. Zhang, L., Jiang, H. & Hu, Z. Concentration-dependent effect of nerve growth factor on cell fate determination of neural progenitors. *Stem Cells Dev* **20**, 1723-1731 (2011).

397. Levine, E.S., Dreyfus, C.F., Black, I.B. & Plummer, M.R. Brain-derived neurotrophic factor rapidly enhances synaptic transmission in hippocampal neurons via postsynaptic tyrosine kinase receptors. *Proc Natl Acad Sci U S A* **92**, 8074-8077 (1995).

398. Boulanger, L. & Poo, M.M. Gating of BDNF-induced synaptic potentiation by cAMP. *Science* **284**, 1982-1984 (1999).

399. Lappalainen, R.S.*, et al.* Similarly derived and cultured hESC lines show variation in their developmental potential towards neuronal cells in long-term culture. *Regen Med* **5**, 749-762 (2010).

400. Dvorak, P.*, et al.* Expression and potential role of fibroblast growth factor 2 and its receptors in human embryonic stem cells. *Stem Cells* **23**, 1200-1211 (2005).

401. Eiselleova, L*., et al.* A complex role for FGF-2 in self-renewal, survival, and adhesion of human embryonic stem cells. *Stem Cells* **27**, 1847-1857 (2009).

402. Qian, X., Davis, A.A., Goderie, S.K. & Temple, S. FGF2 concentration regulates the generation of neurons and glia from multipotent cortical stem cells. *Neuron* **18**, 81-93 (1997).

403. Achour, L., Labbé-Jullié, C., Scott, M.G.H. & Marullo, S. An escort for GPCRs: implications for regulation of receptor density at the cell surface. *Trends in Pharmacological Sciences* **29**, 528-535 (2008).

404. Prinster, S.C., Hague, C. & Hall, R.A. Heterodimerization of G protein-coupled receptors: specificity and functional significance. *Pharmacol Rev* **57**, 289-298 (2005).

405. Hermans, E. Biochemical and pharmacological control of the multiplicity of coupling at G-protein-coupled receptors. *Pharmacol Ther* **99**, 25-44 (2003).

406. Nicolson, T.A., Foster, A.F., Bevan, S. & Richards, C.D. Prostaglandin E2 sensitizes primary sensory neurons to histamine. *Neuroscience* **150**, 22-30 (2007).

407. Felder, C.C., Jose, P.A. & Axelrod, J. The dopamine-1 agonist, SKF 82526, stimulates phospholipase-C activity independent of adenylate cyclase. *J Pharmacol Exp Ther* **248**, 171-175 (1989).

408. Dai, R., Ali, M.K., Lezcano, N. & Bergson, C. A crucial role for cAMP and protein kinase A in D1 dopamine receptor regulated intracellular calcium transients. *Neurosignals* **16**, 112-123 (2008).

409. Tang, T.S. & Bezprozvanny, I. Dopamine receptor-mediated Ca(2+) signaling in striatal medium spiny neurons. *J Biol Chem* **279**, 42082-42094 (2004).

410. Ming, Y*., et al.* Modulation of Ca2+ signals by phosphatidylinositol-linked novel D1 dopamine receptor in hippocampal neurons. *J Neurochem* **98**, 1316-1323 (2006).

411. Sahu, A., Tyeryar, K.R., Vongtau, H.O., Sibley, D.R. & Undieh, A.S. D5 dopamine receptors are required for dopaminergic activation of phospholipase C. *Mol Pharmacol* **75**, 447-453 (2009).

412. Lezcano, N. & Bergson, C. D1/D5 dopamine receptors stimulate intracellular calcium release in primary cultures of neocortical and hippocampal neurons. *J Neurophysiol* **87**, 2167-2175 (2002).

413. Lee, S.P*., et al.* Dopamine D1 and D2 receptor Co-activation generates a novel phospholipase C-mediated calcium signal. *J Biol Chem* **279**, 35671-35678 (2004).

414. So, C.H*., et al.* Calcium signaling by dopamine D5 receptor and D5-D2 receptor hetero-oligomers occurs by a mechanism distinct from that for dopamine D1-D2 receptor hetero-oligomers. *Mol Pharmacol* **75**, 843-854 (2009).

415. Hebb, D.O. *The organization of behavior : a neuropsychological theory*, (Wiley, New York, 1949).

416. Palmer, T.D*., et al.* Cell culture. Progenitor cells from human brain after death. *Nature* **411**, 42-43 (2001).

417. Molyneaux, B.J., Arlotta, P., Menezes, J.R.L. & Macklis, J.D. Neuronal subtype specification in the cerebral cortex. *Nat Rev Neurosci* **8**, 427-437 (2007).

418. Hof, P.R., Glezer, II, Nimchinsky, E.A. & Erwin, J.M. Neurochemical and cellular specializations in the mammalian neocortex reflect phylogenetic relationships: evidence from primates, cetaceans, and artiodactyls. *Brain Behav Evol* **55**, 300-310 (2000).

419. Bannister, A.P. Inter- and intra-laminar connections of pyramidal cells in the neocortex. *Neurosci Res* **53**, 95-103 (2005).

420. de Graaf-Peters, V.B. & Hadders-Algra, M. Ontogeny of the human central nervous system: what is happening when? *Early Hum Dev* **82**, 257-266 (2006).

421. Gauduchon, J*., et al.* 4-Hydroxytamoxifen inhibits proliferation of multiple myeloma cells in vitro through down-regulation of c-Myc, up-regulation of p27Kip1, and modulation of Bcl-2 family members. *Clin Cancer Res* **11**, 2345-2354 (2005).

422. Mermelstein, P.G. Membrane-localised oestrogen receptor alpha and beta influence neuronal activity through activation of metabotropic glutamate receptors. *J Neuroendocrinol* **21**, 257-262 (2009).

423. Bystron, I., Rakic, P., Molnar, Z. & Blakemore, C. The first neurons of the human cerebral cortex. *Nat Neurosci* **9**, 880-886 (2006).

424. Boess, F.G. & Martin, I.L. Molecular biology of 5-HT receptors. *Neuropharmacology* **33**, 275-317 (1994).

425. Moore, A.R*., et al.* Electrical excitability of early neurons in the human cerebral cortex during the second trimester of gestation. *Cereb Cortex* **19**, 1795-1805 (2009).

426. Moore, A.R., Zhou, W.L., Jakovcevski, I., Zecevic, N. & Antic, S.D. Spontaneous electrical activity in the human fetal cortex in vitro. *J Neurosci* **31**, 2391-2398 (2011).

427. Wiedehage, J., Schmidtmayer, J. & Buse, E. Development of membrane currents in mammalian neuroventricular cells from the early neural tube stage in vitro: aspects of the neuronal lineage. *Int J Dev Neurosci* **10**, 375-385 (1992).

428. Wojcik-Stanaszek, L., Gregor, A. & Zalewska, T. Regulation of neurogenesis by extracellular matrix and integrins. *Acta Neurobiol Exp (Wars)* **71**, 103-112 (2011).

429. Bjarnadóttir, T.K., Fredriksson, R. & Schiöth, H.B. The adhesion GPCRs: a unique family of G protein-coupled receptors with important roles in both central and peripheral tissues. *Cell Mol Life Sci* **64**, 2104-2119 (2007).

430. Yona, S., Lin, H.H., Siu, W.O., Gordon, S. & Stacey, M. Adhesion-GPCRs: emerging roles for novel receptors. *Trends Biochem Sci* **33**, 491-500 (2008).

431. Karra, D. & Dahm, R. Transfection techniques for neuronal cells. *J Neurosci* **30**, 6171-6177 (2010).

432. Martinez, C.Y. & Hollenbeck, P.J. Transfection of primary central and peripheral nervous system neurons by electroporation. *Methods Cell Biol* **71**, 339-351 (2003).

433. von der Mark, K., Park, J., Bauer, S. & Schmuki, P. Nanoscale engineering of biomimetic surfaces: cues from the extracellular matrix. *Cell Tissue Res* **339**, 131-153 (2010).

434. Lim, S.H., Liu, X.Y., Song, H., Yarema, K.J. & Mao, H.Q. The effect of nanofiber-guided cell alignment on the preferential differentiation of neural stem cells. *Biomaterials* **31**, 9031-9039 (2010).

435. Bakhru, S*., et al.* Direct and cell signaling-based, geometry-induced neuronal differentiation of neural stem cells. *Integr Biol (Camb)* (2011).

436. Wang, Y.*, et al.* The promotion of neural progenitor cells proliferation by aligned and randomly oriented collagen nanofibers through beta1 integrin/MAPK signaling pathway. *Biomaterials* **32**, 6737-6744 (2011).

437. Lam, H.J., Patel, S., Wang, A., Chu, J. & Li, S. In vitro regulation of neural differentiation and axon growth by growth factors and bioactive nanofibers. *Tissue Eng Part A* **16**, 2641-2648 (2010).

438. Herberth, B.*, et al.* Changes of KCl sensitivity of proliferating neural progenitors during in vitro neurogenesis. *J Neurosci Res* **67**, 574-582 (2002).

439. Deisseroth, K.*, et al.* Excitation-neurogenesis coupling in adult neural stem/progenitor cells. *Neuron* **42**, 535-552 (2004).

440. Sohya, K., Kitamura, A. & Akaneya, Y. Chronic membrane depolarization-induced morphological alteration of developing neurons. *Neuroscience* **145**, 232-240 (2007).

441. D'Ascenzo, M.*, et al.* Role of L-type Ca2+ channels in neural stem/progenitor cell differentiation. *Eur J Neurosci* **23**, 935-944 (2006).

442. Grassi, C.*, et al.* Effects of 50 Hz electromagnetic fields on voltage-gated Ca2+ channels and their role in modulation of neuroendocrine cell proliferation and death. *Cell Calcium* **35**, 307-315 (2004).

443. Piacentini, R., Ripoli, C., Mezzogori, D., Azzena, G.B. & Grassi, C. Extremely low-frequency electromagnetic fields promote in vitro neurogenesis via upregulation of Ca(v)1-channel activity. *J Cell Physiol* **215**, 129-139 (2008).

444. Cuccurazzu, B.*, et al.* Exposure to extremely low-frequency (50 Hz) electromagnetic fields enhances adult hippocampal neurogenesis in C57BL/6 mice. *Exp Neurol* **226**, 173-182 (2010).

445. Chang, M.Y., Son, H., Lee, Y.S. & Lee, S.H. Neurons and astrocytes secrete factors that cause stem cells to differentiate into neurons and astrocytes, respectively. *Mol Cell Neurosci* **23**, 414-426 (2003).

446. Ozolek, J.A.*, et al.* In vitro neural differentiation of human embryonic stem cells using a low-density mouse embryonic fibroblast feeder protocol. *Methods Mol Biol* **584**, 71-95 (2010).

447. Gao, X.*, et al.* Human fetal trophonema matrix and uterine endometrium support better human embryonic stem cell growth and neural differentiation than mouse embryonic fibroblasts. *Cell Reprogram* **12**, 295-303 (2010).

448. Osmond, R.I.*, et al.* GPCR screening via ERK 1/2: a novel platform for screening G protein-coupled receptors. *J Biomol Screen* **10**, 730-737 (2005).

449. Dhanasekaran, N. & Premkumar Reddy, E. Signaling by dual specificity kinases. *Oncogene* **17**, 1447-1455 (1998).

450. Hudson, B.D. & Kelly, M.E. Identification of Novel Competing beta(2)AR Phospho-Extracellular Signal Regulated Kinase 1/2 Signaling Pathways in Human Trabecular Meshwork Cells. *J Ocul Pharmacol Ther* (2011).

451. Harvey, C.D.*, et al.* A genetically encoded fluorescent sensor of ERK activity. *Proc Natl Acad Sci U S A* **105**, 19264-19269 (2008).

452. Lodge, A.P., Langmead, C.J., Daniel, G., Anderson, G.W. & Werry, T.D. Performance of mouse neural stem cells as a screening reagent: characterization of PAC1 activity in medium-throughput functional assays. *J Biomol Screen* **15**, 159-168 (2010).

453. Prabakaran, S.*, et al.* Comparative analysis of Erk phosphorylation suggests a mixed strategy for measuring phospho-form distributions. *Mol Syst Biol* **7**, 482 (2011).

454. Crouch, M.F. & Osmond, R.I. New strategies in drug discovery for GPCRs: high throughput detection of cellular ERK phosphorylation. *Comb Chem High Throughput Screen* **11**, 344-356 (2008).

455. Gründer, G., Hippius, H. & Carlsson, A. The 'atypicality' of antipsychotics: a concept re-examined and re-defined. *Nat Rev Drug Discov* **8**, 197-202 (2009).

456. Kapur, S., Zipursky, R.B. & Remington, G. Clinical and theoretical implications of 5-HT2 and D2 receptor occupancy of clozapine, risperidone, and olanzapine in schizophrenia. *Am J Psychiatry* **156**, 286-293 (1999).

457. Davies, M.A., Compton-Toth, B.A., Hufeisen, S.J., Meltzer, H.Y. & Roth, B.L. The highly efficacious actions of N-desmethylclozapine at muscarinic receptors are unique and not a common property of either typical or atypical antipsychotic drugs: is M1 agonism a pre-requisite for mimicking clozapine's actions? *Psychopharmacology (Berl)* **178**, 451-460 (2005).

458. Seeman, P. & Van Tol, H.H. Dopamine receptor pharmacology. *Trends Pharmacol Sci* **15**, 264-270 (1994).

459. Tice, M.A., Hashemi, T., Taylor, L.A., Duffy, R.A. & McQuade, R.D. Characterization of the binding of SCH 39166 to the five cloned dopamine receptor subtypes. *Pharmacol Biochem Behav* **49**, 567-571 (1994).

460. Wu, W.L.*, et al.* Dopamine D1/D5 receptor antagonists with improved pharmacokinetics: design, synthesis, and biological evaluation of phenol bioisosteric analogues of benzazepine D1/D5 antagonists. *J Med Chem* **48**, 680-693 (2005).

461. Briggs, C.A.*, et al.* Activation of the 5-HT1C receptor expressed in Xenopus oocytes by the benzazepines SCH 23390 and SKF 38393. *Br J Pharmacol* **104**, 1038-1044 (1991).

462. Friedman, E.*, et al.* D1-like dopaminergic activation of phosphoinositide hydrolysis is independent of D1A dopamine receptors: evidence from D1A knockout mice. *Mol Pharmacol* **51**, 6-11 (1997).

463. Yan, Z., Song, W.J. & Surmeier, J. D2 dopamine receptors reduce N-type Ca2+ currents in rat neostriatal cholinergic interneurons through a membrane-delimited, protein-kinase-C-insensitive pathway. *J Neurophysiol* **77**, 1003-1015 (1997).

464. McLean, T.H.*, et al.* 1-Aminomethylbenzocycloalkanes: conformationally restricted hallucinogenic phenethylamine analogues as functionally selective 5-HT2A receptor agonists. *J Med Chem* **49**, 5794-5803 (2006).

465. Chang, C.W., Poteet, E., Schetz, J.A., Gumus, Z.H. & Weinstein, H. Towards a quantitative representation of the cell signaling mechanisms of hallucinogens: measurement and mathematical modeling of 5-HT1A and 5-HT2A receptor-mediated ERK1/2 activation. *Neuropharmacology* **56 Suppl 1**, 213-225 (2009).

466. Parker, M.A., Marona-Lewicka, D., Lucaites, V.L., Nelson, D.L. & Nichols, D.E. A novel (benzodifuranyl)aminoalkane with extremely potent activity at the 5-HT2A receptor. *J Med Chem* **41**, 5148-5149 (1998).

467. Fox, M.A., French, H.T., LaPorte, J.L., Blackler, A.R. & Murphy, D.L. The serotonin 5-HT(2A) receptor agonist TCB-2: a behavioral and neurophysiological analysis. *Psychopharmacology (Berl)* **212**, 13-23 (2010).

468. Niebert, M.*, et al.* Expression and function of serotonin 2A and 2B receptors in the mammalian respiratory network. *PLoS ONE* **6**, e21395 (2011).

469. Jensen, A.A., Frølund, B., Liljefors, T. & Krogsgaard-Larsen, P. Neuronal nicotinic acetylcholine receptors: structural revelations, target identifications, and therapeutic inspirations. *J Med Chem* **48**, 4705-4745 (2005).

470. Peters, J.A., Malone, H.M. & Lambert, J.J. Antagonism of 5-HT3 receptor mediated currents in murine N1E-115 neuroblastoma cells by (+)-tubocurarine. *Neurosci Lett* **110**, 107-112 (1990).

471. Wotring, V.E. & Yoon, K.W. The inhibitory effects of nicotinic antagonists on currents elicited by GABA in rat hippocampal neurons. *Neuroscience* **67**, 293-300 (1995).

472. Bolden, C., Cusack, B. & Richelson, E. Antagonism by antimuscarinic and neuroleptic compounds at the five cloned human muscarinic cholinergic receptors expressed in Chinese hamster ovary cells. *J Pharmacol Exp Ther* **260**, 576-580 (1992).

473. Galvan, M., Boer, R. & Schudt, C. Interaction of telenzepine with muscarinic receptors in mammalian sympathetic ganglia. *Eur J Pharmacol* **167**, 1-10 (1989).

474. Pedretti, A., Vistoli, G., Marconi, C. & Testa, B. Muscarinic receptors: A comparative analysis of structural features and binding modes through homology modelling and molecular docking. *Chem Biodivers* **3**, 481-501 (2006).

475. Clapham, D.E. TRP channels as cellular sensors. *Nature* **426**, 517-524 (2003).

476. Harteneck, C. & Gollasch, M. Pharmacological modulation of diacylglycerol-sensitive TRPC3/6/7 channels. *Curr Pharm Biotechnol* **12**, 35-41 (2011).

477. Shi, T.J.*, et al.* Phospholipase C{beta}3 in mouse and human dorsal root ganglia and spinal cord is a possible target for treatment of neuropathic pain. *Proc Natl Acad Sci U S A* **105**, 20004-20008 (2008).

478. Werry, T.D., Gregory, K.J., Sexton, P.M. & Christopoulos, A. Characterization of serotonin 5-HT2C receptor signaling to extracellular signal-regulated kinases 1 and 2. *J Neurochem* **93**, 1603-1615 (2005).

479. Shin, S.H. & Stirling, R. Ascorbic acid potentiates the inhibitory effect of dopamine on prolactin release in primary cultured rat pituitary cells. *J Endocrinol* **118**, 287-294 (1988).

480. Cao, N.*, et al.* Ascorbic acid enhances the cardiac differentiation of induced pluripotent stem cells promoting the proliferation of cardiac progenitor cells. *Cell Res* (2011).

481. Chan, B., Seeman, P., Davis, A. & Madras, B.K. Ascorbate injury and EDTA (or manganese) protection of D2-dopamine receptors. *Eur J Pharmacol* **81**, 111-116 (1982).

482. Heikkila, R.E., Manzino, L., Cabbat, F.S. & Hanly, J.G. Ascorbic acid and the binding of DA agonists to neostriatal membrane preparations. *Neuropharmacology* **22**, 135-137 (1983).

483. Dorris, R.L. Ascorbic acid reduces accumulation of [3H]spiperone in mouse striatum in vivo. *Proc Soc Exp Biol Med* **186**, 13-16 (1987).

484. Shin, S.H., Stirling, R.G., Hanna, S., Lim, M. & Wilson, J.X. Ascorbic acid potentiates the inhibitory effect of dopamine on prolactin release: a putative supplementary agent for PIF. *Endocrinol Exp* **24**, 151-158 (1990).

485. Shin, S.H., Si, F., Chang, A. & Ross, G.M. Dopamine requires ascorbic acid to be the prolactin release-inhibiting factor. *Am J Physiol* **273**, E593-598 (1997).

486. Rebec, G.V., Centore, J.M., White, L.K. & Alloway, K.D. Ascorbic acid and the behavioral response to haloperidol: implications for the action of antipsychotic drugs. *Science* **227**, 438-440 (1985).

487. Heikkila, R.E. & Manzino, L. Ascorbic acid, redox cycling, lipid peroxidation, and the binding of dopamine receptor antagonists. *Ann N Y Acad Sci* **498**, 63-76 (1987).

488. Sibley, D.R., De Lean, A. & Creese, I. Anterior pituitary dopamine receptors. Demonstration of interconvertible high and low affinity states of the D-2 dopamine receptor. *J Biol Chem* **257**, 6351-6361 (1982).

489. Minneman, K.P., Theroux, T.L., Hollinger, S., Han, C. & Esbenshade, T.A. Selectivity of agonists for cloned alpha 1-adrenergic receptor subtypes. *Mol Pharmacol* **46**, 929-936 (1994).

490. Israilova, M., Tanaka, T., Suzuki, F., Morishima, S. & Muramatsu, I. Pharmacological characterization and cross talk of alpha1a- and alpha1b-adrenoceptors coexpressed in human embryonic kidney 293 cells. *J Pharmacol Exp Ther* **309**, 259-266 (2004).

491. Hancock, A.A*., et al.* Antiobesity effects of A-331440, a novel non-imidazole histamine H3 receptor antagonist. *Eur J Pharmacol* **487**, 183-197 (2004).

492. Kamei, A., Mizumoto, Y. & Takehana, M. The relationship between properties of antipsychotic drugs and cataract formation. *Biol Pharm Bull* **17**, 237-242 (1994).

493. Rothbard, A.B., Kuno, E. & Foley, K. Trends in the rate and type of antipsychotic medications prescribed to persons with schizophrenia. *Schizophr Bull* **29**, 531-540 (2003).

494. Divry, P., Bobon, J., Collard, J., Pinchard, A. & Nols, E. [Study & clinical trial of R 1625 or haloperidol, a new neuroleptic & so-called neurodysleptic agent]. *Acta Neurol Psychiatr Belg* **59**, 337-366 (1959).

495. Strange, P.G. Antipsychotic drug action: antagonism, inverse agonism or partial agonism. *Trends Pharmacol Sci* **29**, 314-321 (2008).

496. Heinrich, J.N*., et al.* Aplindore (DAB-452), a high affinity selective dopamine D2 receptor partial agonist. *Eur J Pharmacol* **552**, 36-45 (2006).

497. Neumeyer, J.L., Kula, N.S., Bergman, J. & Baldessarini, R.J. Receptor affinities of dopamine D1 receptor-selective novel phenylbenzazepines. *Eur J Pharmacol* **474**, 137-140 (2003).

498. Terry, P. & Katz, J.L. A comparison of the effects of the D1 receptor antagonists SCH 23390 and SCH 39166 on suppression of feeding behavior by the D1 agonist SKF38393. *Psychopharmacology (Berl)* **113**, 328-333 (1994).

499. Urizar, E*., et al.* CODA-RET reveals functional selectivity as a result of GPCR heteromerization. *Nat Chem Biol* **7**, 624-630 (2011).

500. Moreno, E.*, et al.* Dopamine D1-histamine H3 receptor heteromers provide a selective link to MAPK signaling in GABAergic neurons of the direct striatal pathway. *J Biol Chem* **286**, 5846-5854 (2011).

501. Fernø, J., Skrede, S., Vik-Mo, A.O., Håvik, B. & Steen, V.M. Drug-induced activation of SREBP-controlled lipogenic gene expression in CNS-related cell lines: marked differences between various antipsychotic drugs. *BMC Neurosci* **7**, 69 (2006).

502. Michnick, S.W. The connectivity map. *Nat Chem Biol* **2**, 663-664 (2006).

503. Geerts, H. Of mice and men: bridging the translational disconnect in CNS drug discovery. *CNS Drugs* **23**, 915-926 (2009).

504. Spiros, A., Carr, R. & Geerts, H. Not all partial dopamine D(2) receptor agonists are the same in treating schizophrenia. Exploring the effects of bifeprunox and aripiprazole using a computer model of a primate striatal dopaminergic synapse. *Neuropsychiatr Dis Treat* **6**, 589-603 (2010).

505. Kapur, S.*, et al.* High levels of dopamine D2 receptor occupancy with low-dose haloperidol treatment: a PET study. *Am J Psychiatry* **153**, 948-950 (1996).

506. Bernardo, M.*, et al.* Double-blind olanzapine vs. haloperidol D2 dopamine receptor blockade in schizophrenic patients: a baseline-endpoint. *Psychiatry Res* **107**, 87-97 (2001).

507. MacDonald, M.L.*, et al.* Identifying off-target effects and hidden phenotypes of drugs in human cells. *Nat Chem Biol* **2**, 329-337 (2006).

508. Akam, E. & Strange, P.G. Inverse agonist properties of atypical antipsychotic drugs. *Biochem Pharmacol* **67**, 2039-2045 (2004).

509. Sharrocks, A.D. The ETS-domain transcription factor family. *Nat Rev Mol Cell Biol* **2**, 827-837 (2001).

510. Lisman, J.E. Bursts as a unit of neural information: making unreliable synapses reliable. *Trends Neurosci* **20**, 38-43 (1997).

511. Nilsson, C.L. & Eriksson, E. Haloperidol increases prolactin release and cyclic AMP formation in vitro: inverse agonism at dopamine D2 receptors? *J Neural Transm Gen Sect* **92**, 213-220 (1993).

512. Griffon, N., Pilon, C., Sautel, F., Schwartz, J.C. & Sokoloff, P. Antipsychotics with inverse agonist activity at the dopamine D3 receptor. *J Neural Transm* **103**, 1163-1175 (1996).

513. Okita, K., Ichisaka, T. & Yamanaka, S. Generation of germline-competent induced pluripotent stem cells. *Nature* **448**, 313-317 (2007).

514. Wernig, M.*, et al.* In vitro reprogramming of fibroblasts into a pluripotent ES-cell-like state. *Nature* **448**, 318-324 (2007).

515. Ebert, A.D. & Svendsen, C.N. Human stem cells and drug screening: opportunities and challenges. *Nat Rev Drug Discov* **9**, 367-372 (2010).

516. Maurel, B., Le Digarcher, A., Dantec, C. & Journot, L. Genome-wide profiling of G protein-coupled receptors in cerebellar granule neurons using high-throughput, real-time PCR. *BMC Genomics* **12**, 241 (2011).

517. Layden, B.T., Newman, M., Chen, F., Fisher, A. & Lowe, W.L., Jr. G protein coupled receptors in embryonic stem cells: a role for Gs-alpha signaling. *PLoS ONE* **5**, e9105 (2010).

518. Simón, M.V.*, et al.* Müller glial cells induce stem cell properties in retinal progenitors in vitro and promote their further differentiation into photoreceptors. *J Neurosci Res* **90**, 407-421 (2012).

519. Kenakin, T.P. Pharmacological onomastics: what's in a name? *Br J Pharmacol* **153**, 432-438 (2008).

520. Kenakin, T. Efficacy at G-protein-coupled receptors. *Nat Rev Drug Discov* **1**, 103-110 (2002).

521. Limbird, L.E. The receptor concept: a continuing evolution. *Mol Interv* **4**, 326-336 (2004).

522. Katsuki, T., Joshi, R., Ailani, D. & Hiromi, Y. Compartmentalization within neurites: its mechanisms and implications. *Dev Neurobiol* **71**, 458-473 (2011).

523. Mendez, J.A., Bourque, M.J., Fasano, C., Kortleven, C. & Trudeau, L.E. Somatodendritic dopamine release requires synaptotagmin 4 and 7 and the participation of voltage-gated calcium channels. *J Biol Chem* **286**, 23928-23937 (2011).

524. Smith, R., Klein, P., Koc-Schmitz, Y., Waldvogel, H.J., Faull, R.L., Brundin, P., Plomann, M. & Li, J.Y. Loss of SNAP-25 and rabphilin 3a in sensory-motor cortex in Huntington's disease. *J Neurochem* **103**, 115-123 (2007).

# *Appendices*

## *8.1 Media*

### *8.1.1 Reduced Modified Medium (RMM)*

Dulbecco's modified Eagle's medium F-12 Ham (DMEM:F12) with 15 mM HEPES and sodium bicarbonate (Sigma: D6421) supplemented with 0.03% human serum albumin (PAA: C11-096), 100 $\mu gml^{-1}$ apo-transferrin (Scipac, Sittingbourne, Kent, UK: T100-5), 16.2 $\mu gml^{-1}$ putrescine (Sigma: G5780), 5 $\mu gml^{-1}$ human insulin (Sigma: I9278), 60 $ngml^{-1}$ progesterone (Sigma: P6149), 2 mM L-glutamine (Sigma: G7513) and 40 $ngml^{-1}$ sodium selenite (Sigma, S9133).

### *8.1.2 Human Medium (HM)*

Dulbecco's modified Eagle's medium F-12 Ham with 15 mM HEPES and sodium bicarbonate (Sigma: D6421) supplemented with 0.03% human serum albumin (PAA: C11-096), 100 $\mu gml^{-1}$ apo-transferrin (Scipac, Sittingbourne, Kent, UK: T100-5), 16.2 $\mu gml^{-1}$ putrescine (Sigma: G5780), 5 $\mu gml^{-1}$ human insulin (Sigma: I9278), 60 $ngml^{-1}$ progesterone (Sigma: P6149), 2 mM L-glutamine (Sigma: G7513), 40 $ngml^{-1}$ sodium selenite (Sigma, S9133), 400 $ngml^{-1}$ L-thyroxine ($T_4$, Sigma: T0397), 337 $ngml^{-1}$ 3,3',5-triiodo-L-thyronine ($T_3$, Sigma: T5516), 10 $Uml^{-1}$ heparin (Sigma: H3149) and 40 $ngml^{-1}$ corticosterone (Sigma: C2505).

### *8.1.3 B27 Medium (B27M)*

Dulbecco's modified Eagle's medium F-12 Ham with 15 mM HEPES and sodium bicarbonate (Sigma: D6421) supplemented 2 mM L-glutamine (Sigma: G7513), 10 $Uml^{-1}$ heparin (Sigma: H3149), 50 $\mu gml^{-1}$ Gentamicin (Gibco: 15750) and 1 x B27® serum-free supplement (Gibco: 17504).

### *8.1.4 Supplemented Neurobasal Medium (SNBM)*

Unless otherwise stated, cells were differentiated in Neurobasal® Medium (Gibco: 21103-049) supplemented with 0.03% human serum albumin (PAA: C11-096), 100 $\mu gml^{-1}$, apo-transferrin (Scipac, Sittingbourne, Kent, UK: T100-5), 16.2 $\mu gml^{-1}$ putrescine (Sigma: G5780), 5 $\mu gml^{-1}$ human insulin (Sigma: I9278), 60 $ngml^{-1}$ progesterone (Sigma: P6149), 2 mM L-glutamine (Sigma: G7513), 40 $ngml^{-1}$ sodium selenite (Sigma, S9133) and 1 x B27® serum-free supplement (Gibco: 17504-044).

## 8.2 Primers

| Gene | Primer Name | Sequence (5' – 3') | Fragment Size (bp) |
|---|---|---|---|
| *ADRA1A* | Human ADRA1A_F | GAGAAGAAAGCGGCCAAAAC | 112 |
| | Human ADRA1A_R | AGGGCTTGAAATCAGGGAAG | |
| *ARRB2* | Human ARRB2_F | TGTGGCTCAACTCGAACAAG | 81 |
| | Human ARRB2_R | CTGAGCAGTGGGGTTATGGT | |
| *AVPR1A* | Human AVPR1A_F | TTTGTGATCGTGACGGCTTA | 115 |
| | Human AVPR1A_R | TGGTGATGGTAGGGTTTTCC | |
| *CACNA1C* | Human CACNA1C_F | CCTGAGAATGAGGACGAAGG | 90 |
| | Human CACNA1C_R | GTTTTCGGTGTTGACGGACT | |
| *CAV-1* | Human CAV1_F | GCGACCCTAAACACCTCAAC | 94 |
| | Human CAV1_R | CAAATGCCGTCAAAACTGTG | |
| *CHRM1* | Human CHRM1_F | GGACCCTACAGACCCCTCTT | 116 |
| | Human CHRM1_R | GTGTTCATGGTGGCTAGGTG | |
| *DLG4* | Human DLG4_F | AGGGGGAGATGGAATACGAG | 92 |
| | Human DLG4_R | GATGTGTGGGTTGTCAGTGC | |
| *DRD2* | Human DRD2_F | ATCTCCTGCCCACTCCTCTT | 118 |
| | Human DRD2_R | TGACAATGAAGGGCACGTAG | |
| *DRD3* | Human DRD3-F | TGCCTATGCCTACTCCATCC | 175 |
| | Human DRD3-R | GAGTGCTGCTTTTCCAGCTT | |
| *GABRA1* | Human GABRA1_F | TGGTTATGACAATCGCCTGA | 81 |
| | Human GABRA1_R | CCGAAACTGGTGACGAAGAT | |
| *GRIA2* | Human GRIA2_F | TTCAGATGAGACCCGACCTC | 117 |
| | Human GRIA2_R | GCACAGCTTGCAGTGTTGAT | |
| *GRIN1* | Human GRIN1_F | AGATGGCTCTGTCGGTGTG | 97 |
| | Human GRIN1_R | GTGGGAGTGAAGTGGTCGTT | |
| *GRM1* | Human GRM1_F | CTAGCTGGCATCTTCCTTGG | 231 |
| | Human GRM1_R | TGAGGCAATGATCACCTGAG | |
| *GRM2* | Human GRM2_F | CCGCAGAAGAACGTGGTTAG | 117 |
| | Human GRM2_R | GCAAACAGTGGGGACAAACT | |
| *GRM3* | Human GRM3_F | GGTCTGATCCTGGTGCAAAT | 192 |
| | Human GRM3_R | TTTGAAGGCGTACACAGTGC | |
| *GRM4* | Human GRM4_F | TCTGTCTCCAGCCCTGTCTT | 207 |
| | Human GRM4_R | ACAGGAAAGAAAACGGCAGA | |
| *GRM5* | Human GRM5_F | TCCAGCAGCCTAGTCAACCT | A: 199/B: 203 |
| | Human GRM5_R | GGCTGCTCTTCTCATTCTGG | |
| *GRM6* | Human GRM6_F | ATTGGGCAGTGTGGAAGAAC | 220 |
| | Human GRM6_R | CCCAGTTCCTCAGCTCACTC | |
| *GRM7* | Human GRM7_F | CGGCGCTATGACTTCTTCTC | 169 |
| | Human GRM7_R | CTGCCTCTTTGGAAATCTGC | |
| *GRM8* | Human GRM8_F | GAGGATATTGGAAGCAGCAAA | 153 |
| | Human GRM8_R | TCAATTGATGCTCGTTTGG | |
| *GSK3B* | Human GSK3B_F | AAACTACCAAATGGGCGAGA | 105 |
| | Human GSK3B_R | CCGAGCATGAGGAGGAATAA | |
| *HRH1* | Human HRH1_F | CACACTGAACCCCCTCATCT | 110 |
| | Human HRH1_R | ATTTTGTTGCATCCCCTCAG | |
| *HTR2A* | Human HTR2A_F | CAGAATCCCATCCACCACA | 119 |
| | Human HTR2A_R | TCCTGTAGCCCAAAGACTGG | |
| *MPDZ* | Human MPDZ_F | CCATAGTTTCCCGTTCTCCA | 84 |
| | Human MPDZ_R | CAATCGTTTCCATGTGTTGC | |
| *PPP1R1B* | Human PPP1R1B_F | CTACACACCACCTTCGCTGA | 89 |
| | Human PPP1R1B_R | CTGAGGCCTGGTTCTCATTC | |
| *SLC6A4* | Human SLC6A4_F | GTGATTGGCTATGCTGTGGA | 93 |
| | Human SLC6A4_R | GGTGTAGGGGAGGAGGAATG | |
| *TACR3* | Human TACR3_F | AGGCCGTACTCTCTGCTTTG | 104 |
| | Human TACR3_R | TGATGAGCAATGGGAAACAG | |

## 8.3 Solutions & Buffers

### 8.3.1 $Ca^{2+}$ Release Assay Buffer

HEPES-buffered physiological saline solution containing 140 mM NaCl, 5 mM KCl, 2 mM $CaCl_2$, 1 mM $MgCl_2$, 10 mM HEPES and 10 mM glucose. The solution was buffered to pH 7.4 using 5 M NaOH. Made up in large batches and frozen as 50 ml aliquots. For use it was thawed on day of experiment and only applied to cells after warming to 37°C.

### 8.3.2 $Ca^{2+}$ Release Loading Buffer

$Ca^{2+}$ Release Assay Buffer supplemented with 2.5 µM Fura-2 AM (Invitrogen: F-1201); a $Ca^{2+}$-sensitive ratiometric fluorescent dye and 1 mM probenecid (Sigma: P8761) a non-specific inhibitor of anion transport to prevent the dye from being secreted. Made up directly prior to use and applied to cells at 37°C. Fura-2 AM was made up in DMSO (Sigma: D2650) supplemented with Pluronic® F-127 (Invitrogen: P-3000MP) so as to achieve a final concentration of this nonionic, surfactant polyol of 10%. This was used to increase solubility of the Fura-2 AM dye, and consequently to improve loading.

## 8.4 Test Compounds

| Compound Name | Full Name | Supplier |
|---|---|---|
| Dopamine | 4-(2-Aminoethyl)-1,2-benzenediol hydrochloride | Sigma, H8502 |
| 5-HT | 3-(2-Aminoethyl)-5-hydroxyindole hydrochloride | Sigma, H9523 |
| Glutamate | (*S*)-2-Aminopentanedioic acid | Sigma, G1626 |
| GABA | γ-Aminobutyric Acid | Sigma, A2129 |
| Acetylcholine | Acetylcholine Chloride | Sigma, A6625 |
| Histamine | Histamine Dihydrochloride | Sigma, H7250 |
| Phenylephrine | (R)-(-)-Phenylephrine Hydrochloride | Sigma, A2129 |
| Carbamoylcholine | Carbamoylcholine Chloride | Alfa Aesar, L06674 |
| Raclopride | 3,5-Dichloro-N-[[(2S)-1-ethyl-2-pyrrolidinyl]methyl]-2-hydroxy-6-methoxybenzamide | Tocris, 1810 |
| SCH39166 | (6aS-trans)-11-Chloro-6,6a,7,8,9,13b-hexahydro-7-methyl-5H-benzo[d]naphth[2,1-b]azepin-12-ol hydrobromide | Tocris, 2299 |
| MDL11939 | α-Phenyl-1-(2-phenylethyl)-4-piperidinemethanol | Tocris, 0870 |
| TCB-2 | (4-Bromo-3,6-dimethoxybenzocyclobuten-1-yl)methylamine hydrobromide | Tocris, 2592 |
| Mecamylamine | *N*,2,3,3-Tetramethylbicyclo[2.2.1]heptan-2-amine hydrochloride | Tocris, 2843 |
| Biperiden | α-Bicyclo[2.2.1]hept-5-en-2-yl-α-phenyl-1-piperidinepropanol hydrochloride | Tocris, 2853 |
| Telenzepine | 4,9-Dihydro-3-methyl-4-[(4-methyl-1-piperazinyl)acetyl]-10*H*-thieno[3,4-b][1,5]benzodiazepin-10-one dihydrochloride | Tocris, 1122 |

## 8.5 Supplementary Data

### 8.5.1 Additional Data for Long-Term Continuously Passaged Cultures

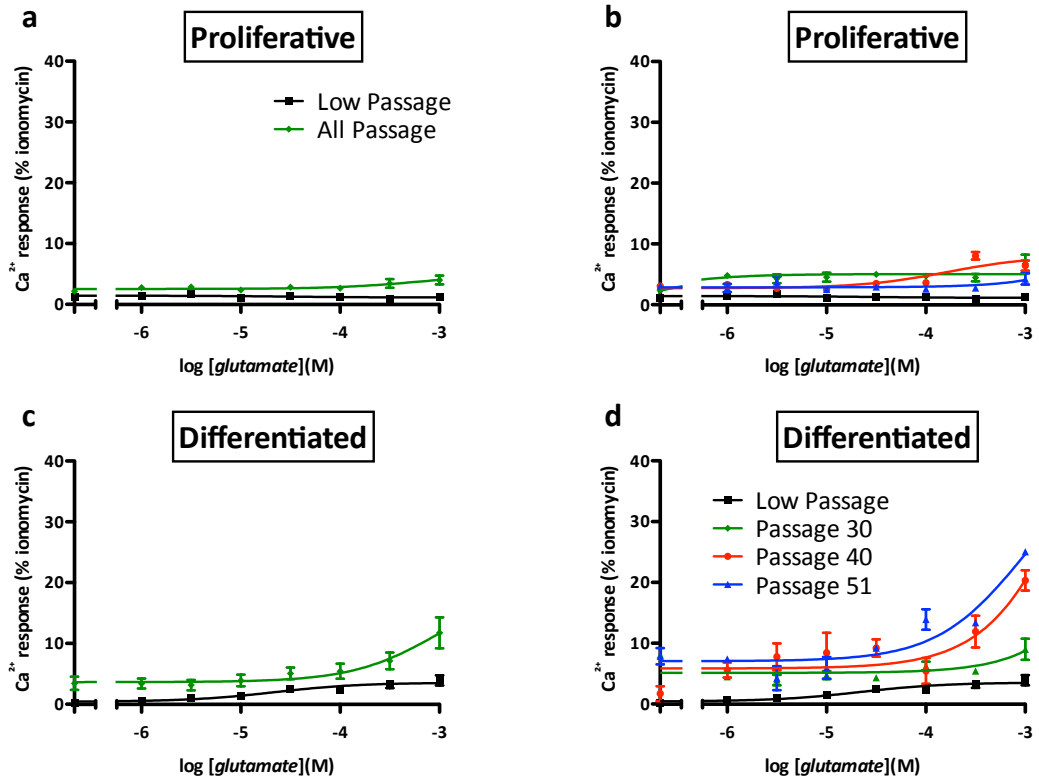


***Figure 8.1 Long-term continuous passage of CTX0E16/02 cells increased glutamate-induced $[Ca^{2+}]_i$ responses in proliferative and differentiated cultures at high concentrations***

Proliferative and differentiated CTX0E16/02 cultures were tested for their ability to respond to glutamate by measuring intracellular $Ca^{2+}$ accumulation. Baseline data or "low passage" (black curves) represents the mean and S.E.M. from two biological replicates (two different frozen cell stocks), each including 3 technical replicates. Higher passage data was the product of continuously expanded CTX0E16/02 cultures with data collected at passage 30 and passage 40. Cells were continuously expanded to passage 50 before being frozen, re-raised and tested at passage 51. Data from all tested passages were pooled to provide the "all passage" category. Concentration-response curves are shown for proliferative (**a** & **b**) and differentiated (**c** & **d**) cultures. Panel **b**, $EC_{50}$ = 0.1 µM and 165.6 µM. Panel **d**, $EC_{50}$ = 22.0 µM. Data points represent mean ± S.E.M. from *n* = 1 (*n* = 2 for "low passage"), with 3 technical replicates and expressed relative to the positive control, ionomycin.

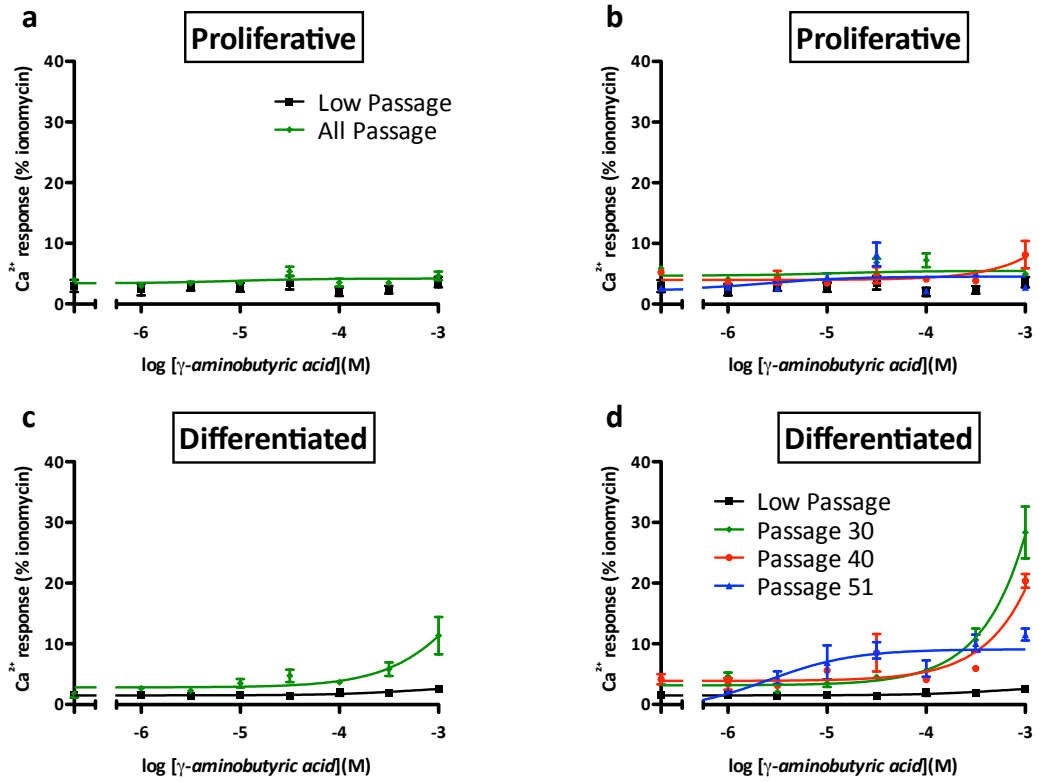


***Figure 8.2 Long-term continuous passage of CTX0E16/02 cells increased GABA-induced $[Ca^{2+}]_i$ responses in differentiated, but not proliferative cultures at high concentrations***

Proliferative and differentiated CTX0E16/02 cultures were tested for their ability to respond to GABA by measuring intracellular $Ca^{2+}$ accumulation. Baseline data or "low passage" (black curves) represents the mean and S.E.M. from two biological replicates (two different frozen cell stocks), each including 3 technical replicates. Higher passage data was the product of continuously expanded CTX0E16/02 cultures with data collected at passage 30 and passage 40. Cells were continuously expanded to passage 50 before being frozen, re-raised and tested at passage 51. Data from all tested passages were pooled to provide the "all passage" category. Concentration-response curves are shown for proliferative (**a** & **b**) and differentiated (**c** & **d**) cultures. Panel **b**, $EC_{50}$ = 11.9 µM and 2.4 µM. Panel **d**, $EC_{50}$ = 2.5 µM. Data points represent mean ± S.E.M. from *n* = 1 (*n* = 2 for "low passage"), with 3 technical replicates and expressed relative to the positive control, ionomycin.

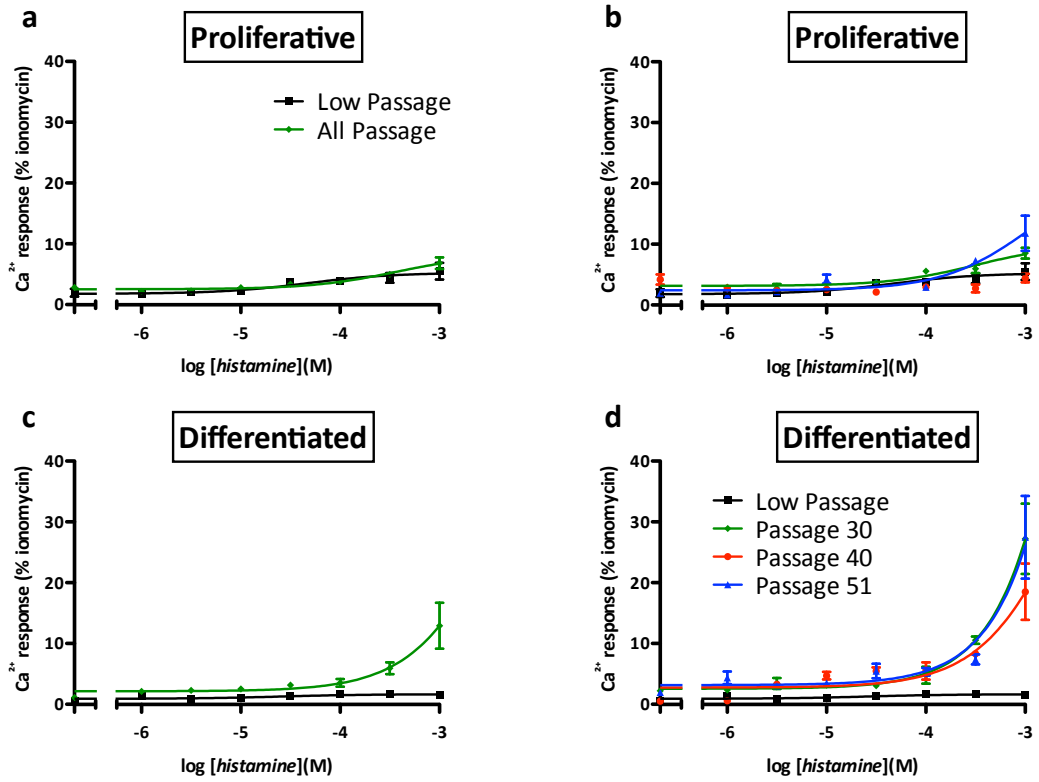


***Figure 8.3 Long-term continuous passage of CTX0E16/02 cells increased histamine-induced $[Ca^{2+}]_i$ responses in proliferative and differentiated cultures at high concentrations***

Proliferative and differentiated CTX0E16/02 cultures were tested for their ability to respond to histamine by measuring intracellular $Ca^{2+}$ accumulation. Baseline data or "low passage" (black curves) represents the mean and S.E.M. from two biological replicates (two different frozen cell stocks), each including 3 technical replicates. Higher passage data was the product of continuously expanded CTX0E16/02 cultures with data collected at passage 30 and passage 40. Cells were continuously expanded to passage 50 before being frozen, re-raised and tested at passage 51. Data from all tested passages were pooled to provide the "all passage" category. Concentration-response curves are shown for proliferative (**a** & **b**) and differentiated (**c** & **d**) cultures. Panel **b**, $EC_{50}$ = 47.0 µM. Data points represent mean ± S.E.M. from *n* = 1 (*n* = 2 for "low passage"), with 3 technical replicates and expressed relative to the positive control, ionomycin.

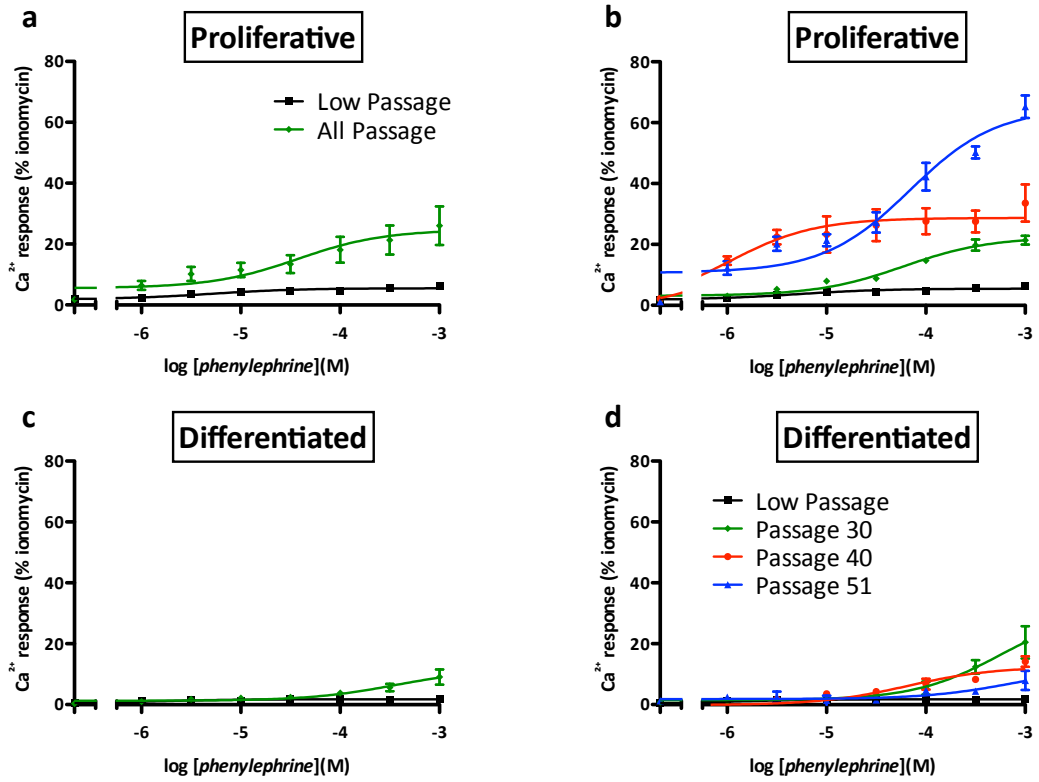


***Figure 8.4 Long-term continuous passage of CTX0E16/02 cells considerably increased the sensitivity of proliferative, but not differentiated cultures to phenylephrine***

Proliferative and differentiated CTX0E16/02 cultures were tested for their ability to respond to phenylephrine by measuring intracellular $Ca^{2+}$ accumulation. Baseline data or "low passage" (black curves) represents the mean and S.E.M. from two biological replicates (two different frozen cell stocks), each including 3 technical replicates. Higher passage data was the product of continuously expanded CTX0E16/02 cultures with data collected at passage 30 and passage 40. Cells were continuously expanded to passage 50 before being frozen, re-raised and tested at passage 51. Data from all tested passages were pooled to provide the "all passage" category. Concentration-response curves are shown for proliferative (**a** & **b**) and differentiated (**c** & **d**) cultures. Panel **a**, $EC_{50}$ = 5.2 µM and 37.7 µM. Panel **b**, $EC_{50}$ = 5.2 µM, 59.7 µM, 1.0 µM and 69.0 µM. Panel **c**, $EC_{50}$ = 1.4 µM and 361.1 µM. Panel **d**, $EC_{50}$ = 1.4 µM, 564.9 µM, 65.4 µM and 735.6 µM. Data points represent mean ± S.E.M. from *n* = 1 (*n* = 2 for "low passage"), with 3 technical replicates and expressed relative to the positive control, ionomycin.

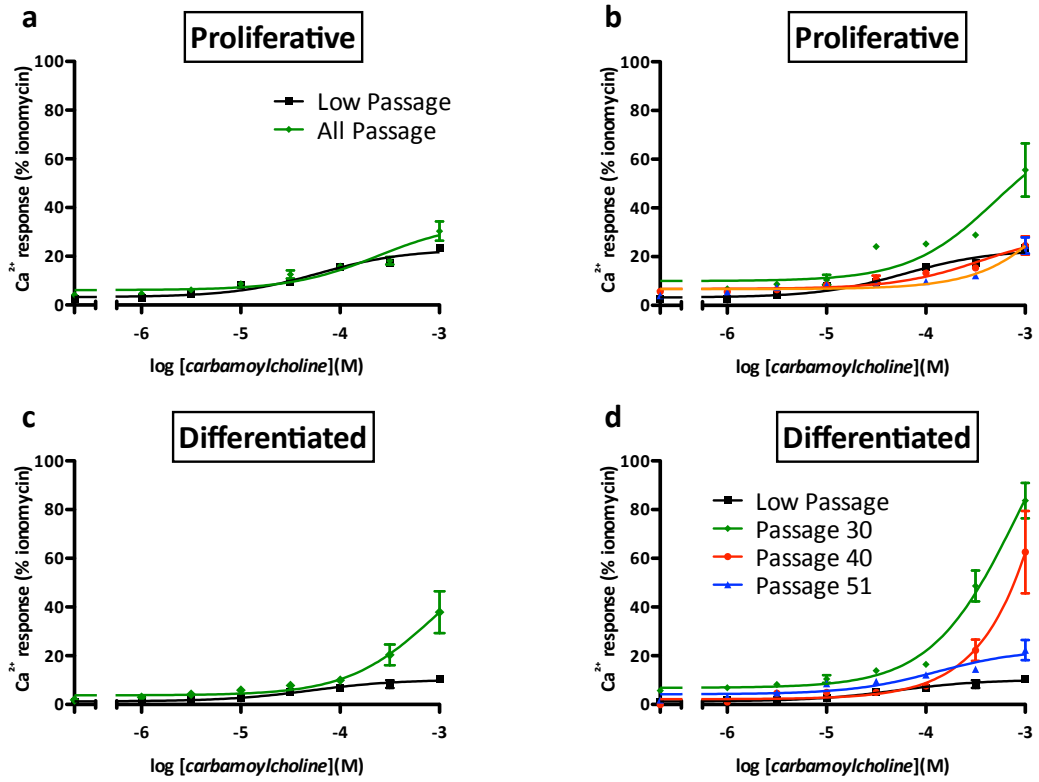


***Figure 8.5 Long-term continuous passage of CTX0E16/02 cells increases carbamoylcholine-induced $[Ca^{2+}]_i$ responses in differentiated, but not proliferative cultures at high concentrations***

Proliferative and differentiated CTX0E16/02 cultures were tested for their ability to respond to carbamoylcholine by measuring intracellular $Ca^{2+}$ accumulation. Baseline data or "low passage" (black curves) represents the mean and S.E.M. from two biological replicates (two different frozen cell stocks), each including 3 technical replicates. Higher passage data was the product of continuously expanded CTX0E16/02 cultures with data collected at passage 30 and passage 40. Cells were continuously expanded to passage 50 before being frozen, re-raised and tested at passage 51. Data from all tested passages were pooled to provide the "all passage" category. Concentration-response curves are shown for proliferative (**a** & **b**) and differentiated (**c** & **d**) cultures. Panel **a**, $EC_{50}$ = 61.4 µM and 237.3 µM. Panel **b**, $EC_{50}$ = 61.3 µM, 502.3 µM, and 361.4 µM. Panel **c**, $EC_{50}$ = 50.6 µM and 867.3 µM. Panel **d**, $EC_{50}$ = 50.6 µM, 838.1 µM, 7843.0 µM and 128.9 µM. Data points represent mean ± S.E.M. from *n* = 1 (*n* = 2 for "low passage"), with 3 technical replicates and expressed relative to the positive control, ionomycin.

## *8.6 Supplementary Information*

### *8.6.1 Personal Communication From Hugo Geerts*

**From:** **Hugo Geerts <Hugo-Geerts@In-Silico-Biosciences.com>**
**Subject:** FW: Neurotransmitter Concentrations
**Date:** 10 July 2011 12:50:12 GMT+01:00
**To:** Greg Anderson <greg.anderson@kcl.ac.uk>

Greg,

Here are the clinically relevant concentrations in nM for the various antipsychotics, derived from PET imaging data in SZ patients:

| | |
|---|---|
| Aripiprazole | 115.0 |
| Asenapine | 13.0 |
| Haloperidol | 8.0 |
| Olanzapine | 90.0 |
| Paliperidone | 60.0 |
| Perphenazine | 9.0 |
| Quetiapine | 800.1 |
| Risperidone | 20.0 |
| Ziprasidone | 32.0 |
| Zotepine | 50.0 |

Note that the risperidone concentration includes the 9-OH metabolite 15 nM and the parent molecule 5 nM. For the different neurotransmitters, this is much more difficult to simulate as this is pulsative because of presynaptic release and clearance through COMT, Ach or transporters. On average, for DA, the free intrasynaptic DA concentration is in the range of 80-100 nM, but can reach peaks of 1250 nM, and in tonic (low-frequency) firing (1-4Hz) can reach almost zero. I don't know if you will be able to pick up effects at such small concentrations…

Let me know if you need anything else,

Good luck,

Hugo